BEHAVIOUR OF FLOW IN OPEN CHANNEL BENDS

BY

D. LEGONO, Ir.

Thesis submitted to The City University
for the award of Degree of Doctor of Philosophy
in the Department of Civil Engineering

September 1986

SYNOPSIS

In this study on behaviour of flow in open channel bends, experimental investigations were carried out in a U-shaped and an S-shaped channel of rectangular cross-section with 180° curvature. The turbulent characteristics were measured by using the Laser Doppler Anemometer (LDA).

Experimental results concerning the distribution of velocity and boundary shear stress together with the distribution of the Reynolds stresses and the instability of secondary flow are presented. The measured velocity distributions in the direction of flow are then compared with those calculated by solving the general equations of motion by the use of finite difference method. The correlation between the velocity and the boundary shear stress distributions is discussed, as well as the distributions of Reynolds stress with the secondary flow.

The growth of the transverse circulation in the U-shaped and S-shaped channels was studied in detail. The striking feature of the instability of flow occurs near the cross-over region of the S-shaped channel, and indicates that the strength of the secondary current produced in the upstream bend is not completely eliminated straight away when the flow enters the downstream bend. The behaviour of the flow patterns in this transition region were studied for three different flow rates and found to be almost identical.

The transverse motion of fluid particles in the cross-section of the bend were observed photographically and compared with the secondary flow pattern revealed by the LDA system.

ACKNOWLEDGEMENTS

The experimental work presented in this thesis was carried out in the Hydraulics Laboratory of the Department of Civil Engineering, The City University, London, under supervision of Dr.K. Arumugam and Mr.K.V. Rao. I am indebted to them for their encouragement throughout the investigation, for their helpful suggestions and criticisms, and for their kindness and understanding.

I wish to thank [redacted], the Head of the Department of Aeronautical Engineering for his help in measuring the Reynolds stresses.

I would also like to thank the Technical Staff of the Hydraulics Laboratory for their assistance throughout the duration of this work. The help of [redacted] in building of the apparatus was highly appreciated. I wish to acknowledge the assistance given to me by [redacted] in connection with the photography.

The financial support of the Indonesian Goverment through the World Bank Education IX Project is gratefully acknowledged.

Last but not the least, I thank [redacted] for her patience and invaluable moral support throughout the course of this research.

NOTATIONS

SYMBOL	MEANING
A	Area of cross-section
A_{τ}	Turbulent or Eddy viscosity
B	Width of a channel
B/h	Aspect ratio
B/Rm	Curvature ratio
C	Chezy coefficient or a constant
d	Distance between fringes
$\eta = z/h$	Relative depth of a point in the cross-section
f	Darcy-Weisbach friction factor
f_s	Frequency shift
F_T	Doppler Frequency
$f_D = f_s + f_T$	Detected frequency
$Fr = \frac{Um}{\sqrt{gh}}$	Froude number
g	Acceleration due to gravity
h	Local depth of flow
i/s, o/s	Inner side and outer side of the wall respectively

I_θ, Ir	Tangential and radial slope of water surface
l	Prandtl mixing length
ln	Natural logarithm
λ	Wave length of the Laser beam
m	Hydraulic radius
n	Manning coefficient
p	Pressure difference
P	Wetted perimeter
Q	Flow rate or discharge
ρ	Fluid density
r_i	Radius of curvature of the inner wall
r_o	Radius of curvature of the outer wall
Rm	Centre line radius of curvature
$Re = \frac{Um\ m}{\nu}$	Reynolds number
SF_b	Shear force near the bed
SF_w	Shear force near the wall
S_{xy}	Strength of the helical flow
$\overline{\tau}_o$	Mean value of boundary shear stress

τ_b	Bed shear stress
τ_w	Wall shear stress
$\tau_{o\theta}, \tau_{or}$	Tangential and radial components of bed shear stress respectively
U	Local mean velocity in the straight channel
Um	Mean velocity over the cross-section
U_*	Friction velocity
v_s	Velocity of the moving fringe
Y	Distance measured from the centre line of the channel, negative towards the inner wall and positive towards the outer wall
θ	Angle of intersection of the Laser beams
x,y,z	Cartesian coordinates x - longitudinal coordinate in the direction of flow the origin taking at the entrance of the straight channel y - lateral coordinate in the direction

	perpendicular to the walls, taking the origin at the inner wall
	z - coordinate perpendicular to x-y plane
r, θ, z	Cylindrical coordinates
u, v, w	Instantaneous velocities respectively in the x,y,z or r, θ, z directions
$\bar{u}, \bar{v}, \bar{w}$	Local mean velocities respectively in the x,y,z or r, θ, z directions
u', v', w'	Fluctuating or temporal velocities respectively in the x,y,z or r, θ, z directions
$\nu = \mu/\rho$	Kinematic viscosity of the fluid
$\nu_\tau = A_\tau/\rho$	Turbulent kinematic viscosity of the fluid
$\gamma = \rho g$	Unit weight of water

CONTENTS

APPENDICES

LIST OF TABLES | Page No.

LIST OF FIGURES Page No.

LIST OF PLATES

CHAPTER 1

INTRODUCTION

1.1 General Introduction

Flow in meandering channels is complicated by several features, including superelevation of the water surface, secondary flow, redistribution of velocity and boundary shear stress, the possibility of flow separation from the banks, and interaction between the flow and the bed topography. The main effect of the bend on the flow passing through it is to induce strong cross-stream motions which lead to asymmetry of the flow thus resulting in a motion known as spiral or helical flow. The simplest possible meander in a river bend consists of two consecutive loops in the shape of a sine curve. However, in any natural river, meandering consists of curved portions of the river connected by the straight portions. It should be noted that the connecting straight portion is the most important part of the meander, because in this region, the maximum velocity crosses the channel from one side of the bank to the other. Then, at the next bend, the helical flow pattern continues downstream and changes the river configuration. The nature of the helical flow is important in the connecting straight and strongly depends upon the pattern of the flow that existed in the upstream bend. Physically, when fluid enters a channel bend, as a result of a stream curvature, there will be a centrifugal force exerted on the fluid, and this centrifugal force will be opposed by transverse pressure gradient. The water surface rises on the outside of the bend, giving rise to a transverse water slope, and the fluid particles close to the channel bed will move towards the inner bank and the fluid particles close to the water surface will move towards the outer bank while moving downstream along the channel. The resulting three-dimensional flow which was previously refered to as spiral or helical flow can be described as a secondary flow perpendicular to and superimposed on the main flow.

Though the existence of secondary flows in curved channels was discovered early in the history of Hydraulics, a complete understanding of the phenomena associated with flow in open channel bends does not seem to have evolved. One reason is, the difficulty in measuring the small secondary components of velocity in the presence of the larger tangential components. The motion at the bed need not always be inwards to satisfy the equations of motion. Indeed flow conditions were reproduced where the motion was outwards in some parts of the bed. The effects of the secondary current and of the resulting helical motion are exhibited in natural streams with erodible boundaries. The movements and the configurations of river beds are intimately interrelated to the secondary currents in the flow. Even in straight channels of non circular cross-section, the secondary currents due to turbulence have a dominant role in the configuration of the channel cross-section. Therefore, secondary currents may occur in straight channels as well as channels of non-uniform plane form. It is still difficult to predict for flows in erodible open channels, whether the interaction of the primary flow with gross open channel features would bring about the presence of the secondary currents, or conversely, the secondary currents would bring about the formation of the channel configuration. Apart from the above question, it is accepted that the secondary currents will affect the process of flow resistance, the sediment transport, the bed and bank erosion, and the development of the channel morphology. However, there is still a lack of knowledge concerning the pattern of the secondary currents particularly near the banks, their variations with time, and their relationship to the boundary shear stress.

Our knowledge of the complex flow at channel bends is still incomplete, one reason being that the small but important secondary currents have proved difficult to measure with conventional techniques. However, the measurement of tangential components of velocity presented very little difficulty, and many experimenters have successfully measured these by using conventional techniques.

1.2 Review of Previous Work

The phenomena associated with flow in open channel bends have been studied for over a century.

In 1876, Thomson appears to have been the first to have pointed out the existence of helical flow in curved channel. In 1944, Mockmore, using two 180^{o} bends, showed that, (1) the tangential components of the forward velocities are greater near the convex bank than the concave bank and vary across the channel in close agreement with the law of free vortex; (2) the angular velocities and accelerations inherent in the spiral motion contribute strongly in the movement of bed load, not only in a downstream direction but toward the inside of the bends; and (3) at about three-fourths of the way around the bend there is a tendency for the development of an eddy or slack water along the inside bank because of the helical or spiral motion which is conducive to the deposition of sediment and the formation of a bar.

In 1949, Shukry studied the problem experimentally, and most of his results agree with those obtained by Mockmore. Shukry developed a new term for the strength of the spiral flow, S_{xy}. This term was defined as the percentage ratio of the mean kinetic energy of the lateral motion to the total kinetic energy of the flow at a given cross-section.

Many of the early laboratory investigations in curved channels (Malouf, 1950; Chacinski, 1956; and Wadekar, 1956 and others) were carried out in rather narrow and sharply curved rectangular flumes over a limited range of flow conditions. Most of the work concerned the measurement of water surface profiles and the tangential velocities. In some instances the obliquity of the flow was recorded using dyes and threads. It was concluded that the obliquity of the flow near the channel bed which measures the intensity of the secondary flow varies directly with the square root of the curvature ratio and inversely with the fourth root of the Reynolds number, whereas Rozovskii (1957), Yen (1965), and Zimmermann (1977) who carried out investigations covering a much wider range of Reynolds numbers in large curved channels, found that the obliquity of the flow varied directly with curvature ratio.

Rozovskii (1957) made a detailed study of the behaviour of flow in bends both theoretically and experimentally. His experimental work included the study of the free surface profiles in the curved stream together with the tangential and radial components of velocity at different depths and radii. Rozovskii's experimental results of tangential velocity components were 1.2 to 1.5 times greater than his theoretical results. He explained that the strength of the secondary flow in a bend gradually increases from the entrance to the exit of the bend and subsequently decays in the straight stretch of the channel. He also concluded that the helical motion does not depend on the boundary roughness of the channel, but the free surface profile will be greatly affected by the roughness of the boundaries.

Chacinski in 1956 measured the velocity in his experiments with a specially designed small pitometer which was carefully calibrated in a straight flume against an ordinary small pitot in order to find its coefficient. Measurements were taken either by chattock manometer with carbon tetrachloride when the velocity was smaller than 15 cm/sec, or by cathatometer and an ordinary water manometer when the velocity was larger than 15 cm/sec. Photographic method was used to measure the bed angles by fixing a thread on the bed in such a way that it was free to move without having any initial twist in it.

In 1959, Chow concluded that the helical flow is caused mainly by (1) friction on the channel walls, which causes lower velocities near the sides of the channel than near the center; (2) centrifugal forces, which depend on the velocity of the fluid particles and the radii of the stream lines; and (3) the vertical velocity distribution which exists in the approach channel flow. He concurred with previous workers that the best formula for calculation of the superelevation in sharp bends was the one based on the law of free vortex.

Sanmuganathan (1966) demonstrated that the secondary cell pattern in a narrow curved channel is unsteady and indicated that the flow phenomena in narrow curved channels involve the combined effect of the bed and the instability of the flow. The unsteady behaviour of the secondary flow was also confirmed by Gotz (1980) for a wide, shallow-curved channel.

In early investigations the mathematical predictions of the curved flow were based on potential flow and ideal rotational flow. Significant contributions to the understanding of flow in curved ducts have been made through ideal rotational flow solutions developed by Hawthorne (1951, 1967) and others. However, inviscid flow solutions have made only a small impact on the understanding of developing flow in curved open channels.

Muramoto (1967) studied the properties of the generating, developing, and fully developed regions of secondary flow in a single bend with respect to the vorticity components. The development of a mathematical model for axisymmetric turbulent flow through open channel bends by Ananyan (1957) and Rozovskii (1957) in USSR was followed by a large number of investigations in wide, shallow bends.

In 1968, Asfari investigated the characteristics of the secondary currents by measuring the velocity distribution and the bed shear stress distribution. The measurements of the velocity distribution were obtained by the photographic method in the case of laminar flow, and by miniature current meter in turbulent flow were then compared with the results obtained from the solution of the general equations of motion from the method of finite differences.

The theoretical models of curved flow developed by Ananyan (1957), Rozovskii (1957), Yen (1965) and De Vriend (1977) were based on a highly simplified representation of turbulence (such as constant eddy viscosity) and on highly restrictive assumptions such as axisymmetry of the curved flow and negligibility of inertia effects. So far, no mathematical model has provided a description of the flow in compound bends where the interaction of the bend components leads to a complex development and decay of water surface slope, transverse circulation and radial asymmetry in the main velocity, and shear stress in the bend.

De Vriend (1981) made an extensive study of the mathematical modelling of curved flow, taking into account the convective influence of the secondary flow as well as the influence of the side walls. He found that the commonly used simplified computational methods which disregard the side wall effects and secondary flow convection are applicable only to very mildly curved flow and that the influence of the steep channel banks is present in a large part of the channel cross-section.

As reported by Humphrey et al. (1981) the numerical uncertainties in the solution of three-dimensional Navier-Stokes equations may be large in comparison with those introduced by the turbulence model. Pressure-driven flow through curved ducts have received considerable attention and, in general, the superior experimental techniques used in duct flows have led to a clearer understanding of the flow mechanism in confined curved duct flow as against that of free-surface flow in bends.

Keerthisena in 1982 investigated the characteristics of flow in S-shaped open channel bends. His work included the measurements of velocity, bed shear stress and free surface profile. The three-tube yaw and pitch probes were introduced to measure the three dimensional velocity field, while the water surface level was obtained with the aid of a static pressure tube. The measurement of bed shear stress was achieved with the aid of a Preston tube. Although his results were not conclusive, owing to a limited range of experiments, lack of reliable measurements, and differences in experimental conditions such as those relating to the inlet and outlet, channel slope, plan geometry and surface finish. His investigation has contributed significantly to a better understanding of the physical processes governing the flow in moderately curved open channel bends and also the general behaviour of the flow in S-bends. It was found from his experiments that the secondary flow pattern did not always give the motion near the bed to be towards the inner bank to satisfy the equations of motion, neither did it give the two cell pattern similar to those found by Thomson (1876) and Wadekar (1956). This is probably due to the influence of important variables such as aspect ratio, Reynolds and Froude numbers of the flow.

Falcon and Kennedy (1983) considered that the radial shear-stress force exerted on a fluid element at any elevation (the vertical distribution of which is the principal determinant of the radial-plane velocity profile) to be equal to the difference between the centrifugal body force and the radial pressure force resulting from the superelevation of the water surface. Even though the integrals of these two forces over the depth are very nearly equal, locally they are grossly out of balance. The radial pressure gradient is very nearly constant over the depth, while the centrifugal force varies from zero at bed level to a maximum near the free surface. It is the difference between the distributions of these two forces that is responsible for the secondary flow.

The secondary flow causes the radial water surface slope to be greater than it would be for a flow with vertically uniform primary velocity (which would not produce a secondary current). This is because the secondary flow produces an inward radial shear force on the bed; the corresponding radial force on the flow must be balanced by part of the radial pressure-gradient force. Thus, in determining the distributions of the three principal radial forces - pressure, shear and centrifugal - exerted on the flow, one is faced with the problem of having two of them - shear and pressure unknown, even if the velocity distribution of the primary flow and hence also the centrifugal force distribution are known. Clearly to proceed with the calculation of these forces, another relation, in addition to the equation expressing the balance of radial forces, is needed.

Falcon and Kennedy developed an analytical model for vertical distributions of radial shear stress and velocity, and radial distributions of depth and streamwise velocity. They used an expression for the conservation of moment-of-momentum as an additional relation required in the formulation of the radial forces. They were able to calculate the radial velocity profile by introducing into the radial momentum equation a linear primary-shear stress distribution and the eddy-viscosity distribution obtained from the power law distribution used for the primary velocity. The streamwise velocity was obtained by using the transverse distribution of local depth of flow. Their analysis was limited to a channel of constant centreline radius which is a good approximation for strongly meandering natural channels. Falcon and Kennedy's analytical model is strictly valid only for uniform flow and at the central regions of the curved channel. However, in the near bank regions, the flow becomes strongly three dimensional and heavily influenced by local bank characteristics (erodibility, slope, roughness, etc.). Analysis of the flow in these regions is correspondingly more difficult than for the central region, and probably must await availability of better experimental data for its guidance.

1.3 Present Investigation

In the present investigation an attempt was made to measure the local mean and fluctuating velocities at different points in the cross-section of an open channel bend. The velocity measurements near to the boundary were successfully carried out by using the Laser Doppler Anemometer (LDA).

In order to achieve a better understanding of the complex flow phenomena in open channel bends, experiments were carried out in U-shaped and S-shaped channels of rectangular cross-section of 180^{o} curvature. The structure of the secondary flow was fully investigated for three different flow rates with uniform depths of flow in the channel. Theoretical results obtained from the equations developed by Rozovskii (1957) and De Vriend (1979) are compared with the experimental results.

The experimental work in this investigation centred in measuring the velocity components in the three coordinates directions, the boundary shear stress, the secondary flow pattern and the Reynold stresses in turbulent flow.

CHAPTER 2

THEORETICAL VELOCITY DISTRIBUTION IN A BEND OF A RECTANGULAR OPEN CHANNEL

2.1 General Introduction

Every flow in a river is in practice a turbulent flow; consequently, any equation of its dynamics, including the flow around bends, must be solved with the aid of the general equations describing the flow of a turbulent stream. Unfortunately, no accurate equations of this kind are known as yet to hydromechanics. It follows that at present it is only possible to speak of an approximate theory in bends by introducing a number of simplifications and hypotheses. Previous workers have made an attempt to formulate an approximate theory of the motion of streams in bends while taking advantage of all available relevant data and verifying the theoretical conclusions under laboratory and field conditions. Though the theory is far from perfect, its form is dictated by the need to solve practical problems. Furthermore, its application can only be proved if it is verified by a sufficiently large amount of experimental data, thus reflecting on the importance of experimental investigations.

The flow phenomena in rivers and artificial channels may vary considerably in magnitude both in time and space. In most cases, however, they have two elements in common: the momentum of water and of sediment. The complexity of mathematical procedure to be used depends strongly on the number of dimensions involved. Flow in rivers is generally variable in time: it is unsteady. For some practical applications however, the variation may be considered so slow that a steady (or quasi-steady) flow situation can be assumed. Considering the spatial distribution of flow, it can be concluded that it is essentially three-dimensional, i.e. the direction and magnitude vary from one point to another. Detailed knowledge of this three-dimensional flow structure in rivers is still very limited, but for many (but not all) engineering applications it is sufficient only to have information about certain mean values. Depending on the type of the mean value required, a number of situations can be identified according to Jansen et al. (1979),

(1) a two-dimensional situation is obtained by averaging over the depth of the river at a particular point; the resulting velocities are still variable in both longitudinal and lateral directions

(2) a quite different two-dimensional situation is obtained by averaging in the lateral direction. The resulting values then depend on longitudinal and vertical coordinates

(3) finally, by far the most important case is the one-dimensional situation, obtained by averaging over an entire cross-section. The resulting values depend only on the longitudinal coordinate. For many practical purposes this is the type of information required.

In the present work an attempt is made to solve the two-dimensional equations for the velocity distribution of flow in open channel bends with the aid of numerical computation techniques. In all practical situations the river flow is turbulent and our knowledge of turbulence is, however, rather limited. Therefore it is thus unavoidable that the solution of the equations can only be obtained through semi-empirical methods.

To analyse the behaviour of flow in a bend of an open channel, it is necessary to describe the movement of the particles of water in the bend of an open channel in three directions. The three-dimensional equations of motion describe the conservation of mass (the continuity equation) and the conservation of momentum as expressed by Newton's second law (Lamb, 1963; Oswattisch, 1959). In the present investigation the equations of motion in cylindrical polar coordinates are used to derive the velocity of flow in the bend, in which u, v and w are the velocity components in the r, θ and z direction respectively as shown in Fig. 2.1.

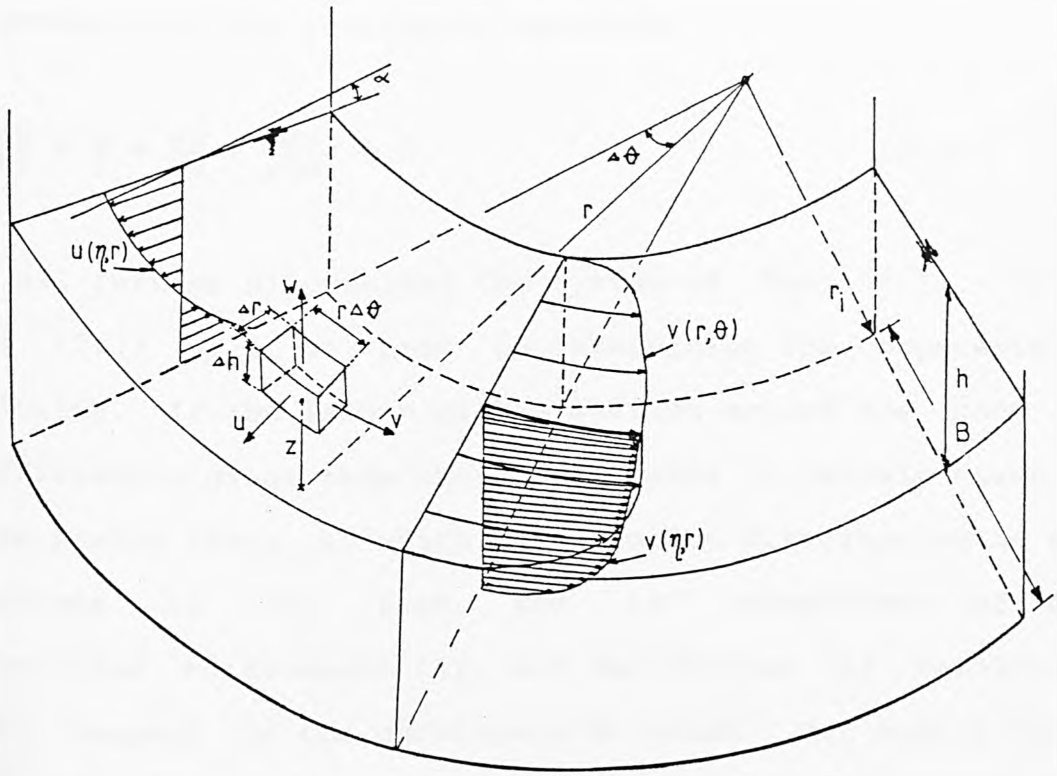

Fig. 2.1 Definition sketch of flow in a bend

Consider a unit mass of fluid element situated near the middle of the channel cross-section where w the vertical component of velocity is very small or negligible. Let the curved element at a distance z from the bed, moving with a velocity v in the tangential direction have a radial inclination of α. Then the system of equations for a steady flow of an incompressible fluid with a free surface in a wide open channel, according to Rozovskii is

$$u\frac{\partial u}{\partial r} + \frac{v\partial u}{r\partial \theta} + w\frac{\partial u}{\partial z} - \frac{v^2}{r} = -gIr + \frac{\partial}{\partial z}(\nu_t \frac{\partial u}{\partial z}) \quad (2.1)$$

$$u\frac{\partial v}{\partial r} + \frac{v\partial v}{r\partial \theta} + w\frac{\partial v}{\partial z} + \frac{vu}{r} = gI_\theta + \frac{\partial}{\partial z}(\nu_t \frac{\partial v}{\partial z}) \quad (2.2)$$

together with the continuity equation

$$\frac{\partial u}{\partial r} + \frac{u}{r} + \frac{\partial w}{\partial z} + \frac{\partial v}{r\partial\theta} = 0 \qquad (2.3)$$

In all further discussions the system of Eqs. (2.1), (2.2) and (2.3) will be used in determining the components of velocity. If the length of the section around the bend is sufficiently great then the stream tends in certain cases to some stable state, at which the velocity distribution in all sections is the same and is independent of the coordinate θ. Consequently, all derivatives of velocities with respect to the coordinate θ vanish. For such a flow, which will henceforth be termed two-dimensional, the above equations assume the form

$$u\frac{\partial u}{\partial r} + w\frac{\partial u}{\partial z} - \frac{v^2}{r} = - gIr + \frac{\partial}{\partial z}(\nu_\tau \frac{\partial u}{\partial z}) \qquad (2.1.a)$$

$$u\frac{\partial v}{\partial r} + w\frac{\partial v}{\partial z} + \frac{vu}{r} = gI_\theta + \frac{\partial}{\partial z}(\nu_\tau \frac{\partial v}{\partial z}) \qquad (2.2.a)$$

and the continuity equation

$$\frac{\partial u}{\partial r} + \frac{u}{r} + \frac{\partial w}{\partial z} = 0 \qquad (2.3.a)$$

In river bends the flow structure is actually three-dimensional, due to the centripetal acceleration. All water particles in a vertical experience the same lateral (radial) pressure gradient. The centripetal acceleration required to keep the particles in a circular path, however, is greater near the surface than near the bottom due to the non-uniform velocity distribution. Near the surface the water particles therefore tend to move outward and near the bottom inward. Thus resulting in a spiral or helical motion. Near the banks compensatory vertical velocity components give upward motion at the inner banks and downward motion at the outer banks.

2.2 Velocity Distribution in an Approach Channel

The velocity distribution along a vertical in an approach channel was obtained by using the concept of mixing length theory proposed by L. Prandtl. The velocity distribution obtained from the above theory is of the form :

$$U = Umax + \frac{1}{\kappa} U_* \ln \eta \qquad (2.4)$$

where $U_* = \sqrt{\tau_o/\rho}$, is the frictional velocity, U is the velocity at a distance z from the boundary, $\eta = z/h$, $\kappa = 0.4$, is the Von-Kármán universal constant, and Umax is the velocity at the water surface.

Using the mean shear stress on the boundary $\tau_o = \rho gmi$ and the Chezy's equation $Um = C\sqrt{mi}$ (where Um is the mean velocity over the cross-section, C the Chezy coefficient, m the hydraulic radius and i the energy gradient), we have

$$U_* = \sqrt{g\ m\ i} = Um \frac{\sqrt{g}}{C} \qquad (2.5)$$

Eq. (2.4) becomes

$$U = Umax + \frac{\sqrt{g}}{\kappa C} \, Um \, \ln\eta \tag{2.4.a}$$

But the mean velocity is given by

$$Um = \int_0^1 U \, d\eta = Umax - \frac{\sqrt{g}}{\kappa C} \, Um$$

and therefore

$$Umax = Um \left(1 + \frac{\sqrt{g}}{\kappa C}\right) \tag{2.6}$$

Now the Eq. (2.4.a) can be written as

$$U = Um \left(1 + \frac{\sqrt{g}}{\kappa C} \left(1 + \ln\eta\right)\right) \tag{2.7}$$

Eq. (2.7) gives the velocity distribution along the vertical near the junction of the approach channel and the bend near the centre line of the stream.

2.3 Radial Velocity Component in a Fully Developed Flow in a Curved Channel

The radial velocity component u can be obtained from the basic Eqs. (2.1.a) and (2.2.a) of two-dimensional turbulent flow in a channel bend using the distribution of tangential velocity v and assuming that the turbulent kinematic viscosity coefficient ν_τ has the same value in the tangential and radial directions.

In what follows, it will be presumed that the turning of the stream takes place along a gentle curve whose radius of curvature is many times greater than the depth of the stream. In such a case, the transverse or radial velocity components will be small and the change in the tangential velocity components at the beginning of the bend will be insignificant. It is therefore permissible to assume in the first approximation that the distribution of the longitudinal or tangential velocity components and the turbulent exchange coefficients in the bend flow will approximately remain initially the same as in the flow upstream of the bend.

Since the radial velocity component (u) and the vertical velocity component (w) are small in comparison with the tangential velocity component (v), the terms ($u\frac{\partial u}{\partial r}$ and $w\frac{\partial u}{\partial z}$) on the left hand side of Eq. (2.1.a) are second order of magnitude and may be ignored.

Eq. (2.1.a) now becomes

$$-\frac{v^2}{r} + g\ Ir = \frac{\partial}{\partial z}\left(\nu_\tau \frac{\partial u}{\partial z} \right) \qquad (2.1.b)$$

substituting $z = \eta h$, we obtain

$$-\frac{v^2}{r} + g\ Ir = \frac{1}{h^2}\frac{\partial}{\partial \eta}\left(\nu_\tau \frac{\partial u}{\partial \eta} \right)$$

Integrating this equation we have

$$\nu_\tau \frac{\partial u}{\partial \eta} = h^2 \int \left(g\ Ir - \frac{v^2}{r} \right) d\eta \qquad (2.8)$$

Substituting Eq. (2.7) into Eq. (2.8) by equating U = v, the tangential velocity, we have

$$\nu_\tau \frac{\partial u}{\partial \eta} = h^2 \int \left(gIr - \frac{Um^2\left(1 + \frac{\sqrt{g}}{\kappa C}(1 + \ln\eta)\right)^2}{r} \right) d\eta$$

Therefore

$$\nu_\tau \frac{\partial u}{\partial \eta} = \frac{h^2 Um^2 g}{C^2 r} \left\{ \left(\frac{rIrC^2}{Um^2} - \frac{(1+\frac{\sqrt{g}}{\kappa C})^2 C^2}{g} \right)\eta - \frac{2}{\kappa} \frac{(1+\frac{\sqrt{g}}{\kappa C})C}{\sqrt{g}} (\eta\ln\eta - \eta) - \frac{1}{\kappa^2}(\eta\ln^2\eta - 2\eta\ln\eta + 2\eta) \right\} + Co \qquad (2.9)$$

The constant of integration Co can be found from the boundary condition that the friction on the free surface is equal to zero. Now applying this boundary condition $(\tau_r/\rho)_{\eta=1} = 0$ gives

$$\nu_\tau \left(\frac{\partial u}{\partial \eta} \right)_{\eta=1} = 0$$

and the value of Co is given by

$$Co = - \frac{h^2 Um^2 g}{C^2 r} \left\{ \left(\frac{rIrC^2}{Um^2} - \frac{(1+\frac{\sqrt{g}}{\kappa C})^2 C^2}{g} \right) + \frac{2C}{\kappa\sqrt{g}}(1+\frac{\sqrt{g}}{\kappa C}) - \frac{2}{\kappa^2} \right\}$$

Substituting the value of Co into Eq. (2.9) we have

$$\nu_\tau \frac{\partial u}{\partial \eta} = \frac{h^2 Um^2 g}{C^2 r} \left\{ \left(\frac{rIrC^2}{Um^2} - \frac{(1+\frac{\sqrt{g}}{\kappa C})^2 C^2}{g} \right) \eta - \frac{1}{\kappa^2}(\eta \ln^2 \eta - 2\eta \ln \eta + 2\eta) - \left(\frac{rIrC^2}{Um^2} - \frac{(1+\frac{\sqrt{g}}{\kappa C})^2 C^2}{g} + \frac{2C}{\kappa\sqrt{g}}(1+\frac{\sqrt{g}}{\kappa C}) - \frac{2}{\kappa^2} \right) \right\} \quad (2.10)$$

The value of turbulent viscosity ν_τ in the Eq. (2.10) can be determined from the condition of equilibrium in different layers of the moving liquid. Now considering the stress distribution, the shear stress at any point in the flow can be determined as

$$\tau = \tau_o (1 - z/h) = \gamma\, h\, i\, (1 - \eta)$$

where $\tau_o = \gamma hi$ is the mean shear stress at the boundary. Therefore, in a uniform turbulent stream, where v = w = 0, the above relation assumes the form

$$\tau = A_\tau \frac{\partial U}{\partial z}$$

where A_τ is the coefficient of eddy viscosity. By using this relationship we arrive at an equation for determining the coefficient A_τ as given below.

$$A_\tau = \frac{\tau}{\frac{\partial U}{\partial z}} = \frac{\gamma\, h\, Um^2\, (1 - \eta)}{C^2 \frac{\partial U}{\partial \eta}} \quad (2.11)$$

From Eq. (2.11) one can now obtain an expression for the coefficient of virtual or eddy kinematic viscosity $\nu_\tau = A_\tau/\rho$ by making use of the velocity distribution obtained in Eq. (2.7). The virtual or eddy kinematic viscosity is given by

$$\nu_\tau = \eta \, h \, Um \frac{\sqrt{g}}{C} \kappa \, (1 - \eta) \tag{2.12}$$

Substituting Eq. (2.12) into (2.10) we have

$$\frac{\partial u}{\partial \eta} = \frac{h^2 Um^2 g}{hUm \frac{\sqrt{g}}{C} (1-\eta)} \Bigg\{ \left(\frac{rIrC^2}{Um^2} - \frac{(1+\frac{\sqrt{g}}{\kappa C})^2 C^2}{g} \right) \eta$$

$$- \frac{2}{\kappa} \frac{(1+\frac{\sqrt{g}}{\kappa C}) C}{g} (\eta \ln \eta - \eta) - \frac{1}{\kappa^2} (\eta \ln^2 \eta - 2\eta \ln \eta + 2\eta)$$

$$- \left(\frac{rIrC^2}{Um^2} - \frac{(1+\frac{\sqrt{g}}{\kappa C})^2 C^2}{g} + \frac{2C}{\kappa\sqrt{g}} (1+\frac{\sqrt{g}}{\kappa C}) - \frac{2}{\kappa^2} \right) \Bigg\}$$

and the radial velocity component is given by

$$u = \frac{hUm\sqrt{g}}{r\kappa C} \Bigg\{ \left(\frac{(1+\frac{\sqrt{g}}{\kappa C})^2 C^2}{g} - \frac{rIrC^2}{Um^2} \right) \int \frac{d\eta}{\eta}$$

$$- \frac{2C}{\kappa\sqrt{g}} (1+\frac{\sqrt{g}}{\kappa C}) \int \frac{\eta \ln \eta - \eta + 1}{\eta (1-\eta)} \, d\eta$$

$$- \frac{1}{\kappa^2} \int \frac{\eta \ln^2 \eta - 2\eta \ln \eta + 2\eta - 2}{(1-\eta)} \, d\eta \Bigg\} \tag{2.13}$$

By introducing

$$f1(\eta) = \int \frac{\eta \ln\eta - \eta + 1}{(1-\eta)} d\eta$$

and

$$f2(\eta) = \int \frac{\eta \ln^2\eta - 2\eta \ln\eta + 2\eta - 2}{(1-\eta)} d\eta$$

the Eq. (2.13) can be written as

$$u = \frac{hUm\sqrt{g}}{r\kappa C}\left(\left(\frac{(1+\frac{\sqrt{g}}{\kappa C})^2 C^2}{g} - \frac{rIrC^2}{Um^2}\right)\ln\eta - \frac{2C}{\kappa\sqrt{g}}(1+\frac{\sqrt{g}}{\kappa C})f1(\eta) - \frac{1}{\kappa^2}f2(\eta)\right) \quad (2.14)$$

where

$$Ir = \alpha_o \frac{Um^2}{gr} + \frac{\tau_{ro}}{gr}$$

As the shear stress in the radial direction is negligibly small, we have

$$Ir = \alpha_o \frac{Um^2}{gr}$$

Since Ir is also given by $Ir = \frac{U^2}{gr}$ at any point in the flow the above equation becomes

$$\frac{U^2}{gr} = \alpha_o \frac{Um^2}{gr}$$

so that

$$\propto_o = \frac{\int_0^1 \frac{U^2}{gr}}{\frac{Um^2}{gr}} = 1 + \frac{g}{\kappa^2 C^2}$$

and thus finally giving the value of Ir as

$$Ir = (1 + \frac{g}{\kappa^2 C^2}) \frac{Um^2}{gr}$$

Now substituting the value of Ir into Eq. (2.14), the radial velocity component can be written as

$$u = \frac{h}{r} Um \frac{1}{\kappa^2} \left(2(\ln\eta - f1(\eta)) - \frac{\sqrt{g}}{\kappa C}(2f1(\eta) + f2(\eta)) \right) \qquad (2.15)$$

Introducing

$$2(\ln\eta - f1(\eta)) = F1(\eta)$$

and

$$2f1(\eta) + f2(\eta) = F2(\eta)$$

Eq. (2.15) can be written as

$$u = \frac{h}{r} Um \frac{1}{\kappa^2} \left(F1(\eta) - \frac{\sqrt{g}}{\kappa C} F2(\eta) \right) \qquad (2.16)$$

where

$$F1(\eta) = 2(\ln\eta - f1(\eta)) = \int \frac{2\ln\eta}{\eta - 1} d\eta$$

and

$$F2(\eta) = 2f1(\eta) + f2(\eta) = - \int \frac{\ln^2\eta}{\eta - 1} d\eta$$

Making use of the fact that the net transverse flow across a vertical must be equal to zero which satisfies the condition that $\int_0^1 u \, d\eta = 0$ the radial velocity distribution in fully developed flow in curved channels can be obtained from the Eq. (2.16). This is achieved by numerical integration method, a brief description of which is illustrated in the following lines.

The functions $F1(\eta)$ and $F2(\eta)$ are solved separately by substituting $0 < \eta < 1$. The values of $F1(\eta)$ and $F2(\eta)$ can be represented as the areas which are formed by the functions in the range $0 < \eta < 1$. In order to achieve a high degree of computational accuracy, the value of η was increased from 0.0001 to 0.9999 with equal increments of 0.0001.

2.4 Distribution of Tangential Velocities Across the Width of a Bend

The distribution of tangential velocity components over the width of a channel bend was investigated by Kozhenikov in 1946. The distribution of velocities according to him must satisfy the equation

$$v = C \times \frac{h}{r} \qquad \text{(C is constant)}$$

Rozovskii (1957) assumed that the distribution of tangential components of velocity v over the width of the channel occurs according to the law of areas, that is

$$v \times r = v_c \times r_c$$

where the values v_c and r_c correspond to the central part of the channel.

Ali (1964) introduced nearly the same equation as Kozhenikov's, suggesting that in the radial direction, it is reasonable to express the tangential velocity variation by the following equation :

$$v = C \times r^m$$

When m has the values of -1 and +1, and the above equation becomes

$$v = \frac{C}{r} \text{ (for free vortex)}$$

$$v = C \times r \text{ (for forced vortex)}$$

2.4.1 Distribution of tangential velocity across the width in the straight channel

Theoretical expression for the velocity distribution across the width for different locations of the U-shaped channel were developed by assuming a velocity distribution in the straight part of the channel upstream of the bend a ; (Rozovskii, 1957) :

$$\frac{U}{Umax} = \left(1 - \left(\frac{2Y}{B}\right)^2\right)^{0.4} \qquad (2.17)$$

where U is the local mean velocity at a distance Y from the mid-point of the channel and B is the width of the channel.

Eq. (2.17) is the basic formula which will be used in determining the tangential velocity distributions across the width of the channel in the regions of the bend entrance, within the bend and the bend exit.

2.4.2 Distribution of tangential velocity across the width at the entrance region of the bend

Rozovskii (1957) and other investigators have developed several expressions to determine the tangential velocity distribution across the width of a curved channel. A simple method of obtaining the expression to depict the tangential velocity distribution across the width of the curved channel is illustrated below.

Considering a very wide stream with free surface superelevation of Δh at the outer wall and applying the Bernoulli's equation, we have

$$\frac{U^2}{2g} = \frac{v^2}{2g} + \Delta h \qquad (2.18)$$

where v is the tangential component of velocity at a distance r from the centre of curvature and U is the local mean velocity as defined in Eq. (2.17).

Therefore the superelevation of the free surface in the channel is given by

$$\Delta h = \int Ir\, dr = \int \frac{v^2}{gr}\, dr + C1 \qquad (2.19)$$

where C1 is a constant of integration.

Substituting the value of Δh into Eq. (2.18) and differentiating with respect to r, we obtain

$$\frac{dv^2}{dr} + 2\,\frac{v^2}{r} - \frac{dU^2}{dr} = 0 \qquad (2.20)$$

Integration of Eq. (2.20) gives the general expression for the tangential velocity distribution across the width at the bend entrance as

$$v = \frac{1}{r}\sqrt{\int r^2 dU^2 + C2} \qquad (2.21)$$

where C2 is the constant of integration which can be evaluated by applying the conservation of mass flowrate in the channel as shown in the equation below.

$$Q = \int_{r_i}^{r_o} v\,h\,dr = \int_{r_i}^{r_o} \frac{h}{r}\sqrt{\int r^2 dU^2 + C2} \qquad (2.22)$$

where r_i, r_o are the radii of the inner and outer banks respectively, h is the depth of flow. Now the tangential velocity distribution at the entrance region of the bend can be obtained by solving the Eqs. (2.21), (2.22) together with the Eq. (2.17) with the aid of finite difference method.

2.4.3 Distribution of tangential velocity across the width within the bend of the channel

As the water enters the bend from the straight portion, the bend brings about a redistribution of velocities over the entire cross-section of the channel. In general, the velocity distribution over the width at the entrance to a bend is represented by the expression given in the Eq. (2.21). Within the bend itself, owing to the exchange of momentum caused by the transverse circulation in radial planes there takes place a redistribution of velocities, thus the maximum velocities gradually moving to the outer bank. In order to obtain the velocity distribution across the width within the bend of the curved channel Rozovskii considered the Eq. (2.2) to represent the bend flow in the cylindrical polar coordinate system, i.e.,

$$u\frac{\partial v}{\partial r} + \frac{v}{r}\frac{\partial v}{\partial \theta} + w\frac{\partial v}{\partial z} + \frac{vu}{r} = gI_\theta + \frac{\partial}{\partial z}\left(\nu_\tau \frac{\partial v}{\partial z}\right) \qquad (2.2)$$

The above Eq. (2.2) can be modified using the following relationship

$$w\frac{\partial v}{\partial z} = \frac{\partial}{\partial z}(vw) - v\frac{\partial w}{\partial z}$$

and together with the equation of continuity

$$\frac{\partial u}{\partial r} + \frac{u}{r} + \frac{\partial v}{r\partial \theta} + \frac{\partial w}{\partial z} = 0 \qquad (2.3)$$

into the form

$$\frac{1}{r^2}\frac{\partial}{\partial z}(r^2 vu) + \frac{\partial v^2}{r\partial\theta} + \frac{\partial vw}{\partial z} = gI_\theta + \frac{1}{\rho}\frac{\partial\tau_\theta}{\partial z} \qquad (2.23)$$

where the tangential shear stress is given by

$$\tau_\theta = A_\tau \frac{\partial v}{\partial z}$$

Since the velocity component in the z direction is equal to zero on the bed and at the free surface (i.e. $w_{z=0} = 0$, $w_{z=h} = 0$) and the tangential shear stress at the free surface is also equal to zero (i.e., $\tau_{\theta\, z=h} = 0$), integrating each term of the above Eq. (2.23) between the limits 0 and h making use of the radial velocity distribution and curved element, Rozovskii obtained an equation for the tangential velocity distribution across the width of the curved channel as

$$0.75\frac{\sqrt{g}}{\kappa^3 C r}\frac{\partial}{r}(rh^2v^2) + \frac{\partial}{\partial\theta}(v^2h) = -\frac{g}{C^2}rv^2 + gI_\theta'h \qquad (2.23.a)$$

where κ is Von-Kármán's universal constant (κ=0.4), C is the Chezy coefficient, h is the depth of flow in the channel and $I_\theta' = I_\theta \times r$, which can be obtained by taking suitable values of I_θ in order to find the tangential velocity by iterative method to satisfy the conservation of mass equation

$$Q = \int_{r_i}^{r_o} vhdr \qquad (2.23.b)$$

Thus, knowing the velocity distribution at the bend entrance, the tangential velocity distribution across the width and at any successive positions within the bend of the channel can be determined by integrating the Eq. (2.23.a) and (2.23.b) with the aid of a step by step numerical calculation method.

2.4.4 Distribution of tangential velocity across the width at the exit region of the bend

To find the tangential velocity distribution at the exit region of the bend, where the transverse slope of the water surface diminishes so that the centrifugal force is negligibly small, we can again use the Bernoulli's equation from the bend to the straight portion of the channel as

$$\frac{U^2}{2g} = \frac{v^2}{2g} + \Delta h \qquad (2.17)$$

where

$$\Delta h = \int \frac{U^2}{gr}\, dr + C2$$

Eq. (2.17) can be written as

$$U^2 = v^2 + 2 \int \frac{v^2}{r}\, dr + C2 \qquad (2.24)$$

where U is the velocity distribution in the straight portion near to the exit region, v is the tangential velocity distribution within the bend near to the exit region and the constant of integration C2 can again be obtained from the principle of the conservation of mass flow rate in the channel

$$Q = \int U \, h \, dr \qquad (2.25)$$

Knowing the tangential velocity distribution across the width of the channel from Eqs. (2.23.a) and (2.23.b) in the region near the exit of the bend, the velocity distribution across the width just downstream of the bend can be computed with the aid of Eqs. (2.24) and (2.25).

2.4.5 Computational procedure by Finite Difference method

The computation of the exact longitudinal flow profile in a bend of an open channel is by no means an easy task. Due to the presence of the centrifugal force, the problem becomes very complex and it is further complicated when the bend is composite, (i.e., when two bends are connected in series in the opposite directions). Bearing in mind the complex nature of the flow in S-shaped channel, the following assumptions are used in solving the Eqs. (2.21), (2.23.a) and (2.24) by using finite difference method.

(i) The longitudinal water surface slope is assumed to be negligible along the channel, (ii) the energy slope and the bed slope of the channel are considered to be very mild, and (iii) the depth of flow is assumed to be uniform along a constant radius.

The Eqs. (2.21), (2.23.a) and (2.24) are used in conjunction with the principle of conservation of mass to determine the tangential velocity distribution across the width of the channel at the bend entrance, within the bend and at the exit region of the bend. Sufficient care is taken in adopting an appropriate sign convention for $\partial\theta$ in the computational procedure in order to determine the tangential velocity distribution across the width beyond the cross-over region of the S-shaped channel. A detailed account of the computational procedure is given in Appendix 1, while its Computer Program is presented in Appendix 2.

CHAPTER 3

THEORETICAL ASPECTS ON THE DEPENDENCE OF SECONDARY CURRENTS ON ANGLE OF TURNING OF THE U-SHAPED CHANNEL

3.1 General Introduction

In Chapter 2, consideration was given to an axi-symmetric two-dimensional steady flow in a bend, where all the derivatives of velocity components with respect to θ vanish from the equations of motion. Owing to the presence of the individual transverse circulation the fluid particles travelling along the curved channel suffer vertical as well as radial displacements, which together with the exchange of momentum between the separate currents alter the characteristic distribution of forward velocity in the curved channel. It has been found by many research workers that the flow becomes axi-symmetric only at some distance from the entrance of the bend where a gradual development of transverse circulation takes place. It is evident that a gradual decay of transverse circulation also takes place when the flow enters the straight length of the channel downstream of the bend thus showing a transition to a rectilinear flow in a straight channel. The question of the growth and decay of this transverse circulation possesses considerable practical interest and accordingly it has attracted the attention of numerous investigators.

Therefore, the theoretical analysis of the dependence of transverse circulation on angle of turning of the U-shaped channel is presented in the following sections.

3.2 Decay of Transverse Circulation Downstream of the Bend

Considering the radial velocity distribution given in Eq. (2.16) and taking the radial component of velocity in the fully developed transverse circulation to be equal to u_o, it can be shown that

$$u_o = \frac{1}{\kappa^2} Um \frac{h}{r} \left(F1(\eta) - \frac{\sqrt{g}}{\kappa C} F2(\eta) \right) \tag{3.1}$$

and similarly Eq. (2.8) can be written as

$$\nu_\tau \frac{\partial u_o}{\partial \eta} = h^2 \int (gIr - \frac{v^2}{r})\, d\eta \tag{3.2}$$

Differentiating Eq. (3.2) with respect to η we have

$$\frac{\partial}{\partial \eta}(\nu_\tau \frac{\partial u_o}{\partial \eta}) = h^2 (gIr - \frac{v^2}{r}) \tag{3.2.a}$$

where

$$Ir = (1 + \frac{g}{\kappa^2 C^2}) \frac{Um^2}{gr}$$

Substituting U from the velocity distribution Eq. (2.7) as equivalent to the tangential velocity component v in the Eq. (3.2.a) and using the above value of Ir, Eq. (3.2.a) reduces to

$$\frac{\partial}{\partial z}(\nu_\tau \frac{\partial u_o}{\partial z}) = - \frac{2\sqrt{g}Um^2}{\kappa C \; r}\left(1 + (1+\frac{\sqrt{g}}{\kappa C})\ln\eta + \frac{\sqrt{g}}{2\kappa C}\ln^2\eta\right) \qquad (3.3)$$

where $\frac{\partial}{\partial z}(\nu_\tau \frac{\partial u}{\partial z})$ varies in proportion with u_o,

giving

$$\frac{\partial}{\partial z}(\nu_\tau \frac{\partial u}{\partial z}) = \frac{u}{u_o}\frac{\partial}{\partial z}(\nu_\tau \frac{\partial u_o}{\partial z}) \qquad (3.4)$$

Substituting Eq. (3.4) into (3.3),

$$\frac{\partial}{\partial z}(\nu_\tau \frac{\partial u}{\partial z}) = \frac{- 2\sqrt{g}uUm\left(1 + (1+\frac{\sqrt{g}}{\kappa C})\ln\eta + \frac{\sqrt{g}}{2\kappa C}\ln^2\eta\right)}{h\,\frac{C}{\kappa}(F1(\eta) - \frac{\sqrt{g}}{\kappa C}F2(\eta))} \qquad (3.5)$$

To solve Eq. (3.5), let us turn to Eq. (2.1), where at the sufficiently small ratio of h/Rm, the terms $u\frac{\partial u}{\partial r}$ and $w\frac{\partial u}{\partial z}$ are very small and can be ignored.

Eq. (2.1) will then become

$$\frac{v\partial u}{r\partial\theta} - \frac{v^2}{r} = - gIr + \frac{\partial}{\partial z}(\nu_\tau \frac{\partial u}{\partial z}) \qquad (2.1.c)$$

Ignoring the inertia forces in the Eq. (2.1.c), and replacing $r\theta = x$ and $v = U$, Eq. (2.1.c) can be written as

$$\frac{U\partial u}{\partial x} = \frac{\partial}{\partial z}(\nu_\tau \frac{\partial u}{\partial z}) \qquad (3.6)$$

Substituting the value of Um from Eq. (2.7) and the value of $\frac{\partial}{\partial z}(\nu_\tau \frac{\partial u}{\partial z})$ from Eq. (3.6) into Eq. (3.5), we obtain

$$U\frac{\partial u}{\partial x} = \frac{-2\sqrt{g}uU\left(1 + (1+\frac{\sqrt{g}}{\kappa C})\ln\eta + \frac{\sqrt{g}}{2\kappa C}\ln^2\eta\right)}{\left(1 + \frac{\sqrt{g}}{\kappa C}(1+\ln\eta)\right)\left(F1(\eta) - \frac{\sqrt{g}}{\kappa C}F2(\eta)\right)\frac{C}{\kappa}h} \quad (3.7)$$

Now introducing the function

$$F(\eta) = \frac{\left(1 + (1+\frac{\sqrt{g}}{\kappa C})\ln\eta + \frac{\sqrt{g}}{2\kappa C}\ln^2\eta\right)}{\left(1 + \frac{\sqrt{g}}{\kappa C}(1+\ln\eta)\right)\left(F1(\eta) - \frac{\sqrt{g}}{\kappa C}F2(\eta)\right)C} \quad (3.7.a)$$

into Eq. (3.7) and integrating with respect to x the radial velocity u can be obtained as

$$u = C1\, e^{-2\sqrt{g}\frac{x}{h}F(\eta)} \quad (3.7.b)$$

If x is measured from the exit region of the bend $u_{(x=0)}$, and hence $C1 = u_o$. Therefore Eq. (3.7.b) now becomes

$$u = u_o\, e^{-2\sqrt{g}\frac{x}{h}F(\eta)}$$

and hence the distance x can be found as

$$x = \frac{h}{2\sqrt{g}F(\eta)}\frac{1}{}\ln\frac{u_o}{u} \quad (3.8)$$

Eq. (3.8) allows the decay of transverse circulation to be determined theoretically, by assuming an average value of $F(\eta)$ for a constant value of κ and C (Chezy coefficient).

3.3 Growth of Transverse Circulation in the Bend

In order to obtain the growth of transverse circulation in the bend, the radial momentum Eq. (2.1.b) is used. For a flow of established circulation, with $u = u_o$, this equation becomes

$$- \frac{v^2}{r} + gIr = \frac{\partial}{\partial z}(\nu_\tau \frac{\partial u_o}{\partial z}) \qquad (2.1.d)$$

where u_o is the transverse velocity in the fully developed flow in a curved channel.

Substituting the left hand side of the Eq. (2.1.d) into Eq. (2.1.c) we have

$$- v \frac{\partial u}{r\partial\theta} = \frac{\partial}{\partial z}(\nu_\tau \frac{\partial(u_o-u)}{\partial z}) \qquad (3.9)$$

Knowing that $\frac{\partial u_o}{\partial\theta} = 0$, the Eq. (3.9) can be written as

$$v \frac{\partial(u_o-u)}{r\partial\theta} = \frac{\partial}{\partial z} (\nu_\tau \frac{\partial(u_o-u)}{\partial z}) \qquad (3.10)$$

On comparing Eqs.(3.10) and (3.6), it can be seen that they possess exactly the same structure, where the magnitude u in Eq. (3.6) corresponds to the magnitude (u_o-u) in Eq. (3.10). This can be interpreted as that the transverse circulation gradually increases from the begining of the bend to reach a fully developed stage at some distance from the entrance of the bend causing the transverse velocity difference of $(u_o - u)$. Subsequently the transverse circulation gradually decreases and consequently obeys the transverse circulation described by the Eq. (3.6). Eq. (3.2) is similar to the Eq. (3.6) with $r\theta = x$ and the solution of the growth of the transverse circulation can be obtained as

$$u_o - u = C1\, e^{-2\sqrt{g}\frac{r\theta}{h}F(\eta)} \qquad (3.11)$$

But at the begining of the bend $C1 = u_o$ and consequently,

$$u = u_o\,(1 - e^{2\sqrt{g}\frac{r\theta}{h}F(\eta)}) \qquad (3.12)$$

This expression determines the growth of transverse circulation in the bend and the growth of transverse circulation will be completed when $u \approx u_o$.

For example $u = 0.9\, u_o$, then θ is called θ_{limit}, which can be attained when

$$\frac{u}{u_o} = 0.9 = (1 - e^{-2\sqrt{g}\frac{r\theta}{h}F(\eta)})$$

which gives

$$\theta_{limit} = \frac{h \ln 0.1}{2r\sqrt{g}F(\eta)}$$

where the growth of transverse circulation is fully developed.

The average value of $F(\eta)$ for $\kappa = 0.4$ and C (Chezy) = 51.0 $m^{1/2}$/sec is given in Fig. 3.1, where according to

Rozovskii (1957) the average value of $F(\eta)$ is assumed to be 0.0082. It is a little different from the average value obtained from the calculation of Eq. (3.7.a) by the author, as shown in Fig. 3.1. The decay and growth of transverse circulation calculated from Eqs. (3.8) and (3.12) are presented in Figs. 3.2 and 3.3 respectively. A Computer Program to solve Eqs. (3.7.a), (3.8) and (3.12) is presented in Appendix 3.

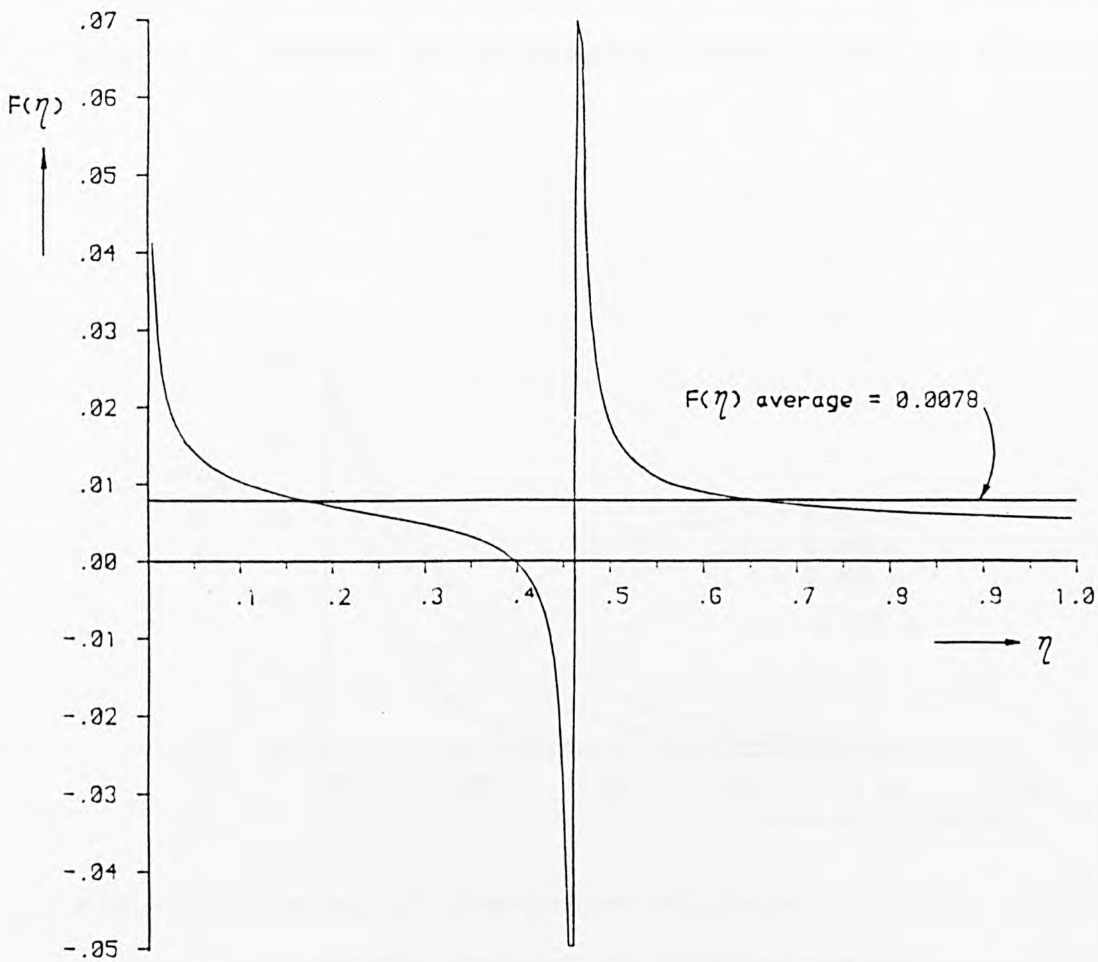

Fig. 3.1 Value of $F(\eta)$ vs η from Eq. (3.7.a)

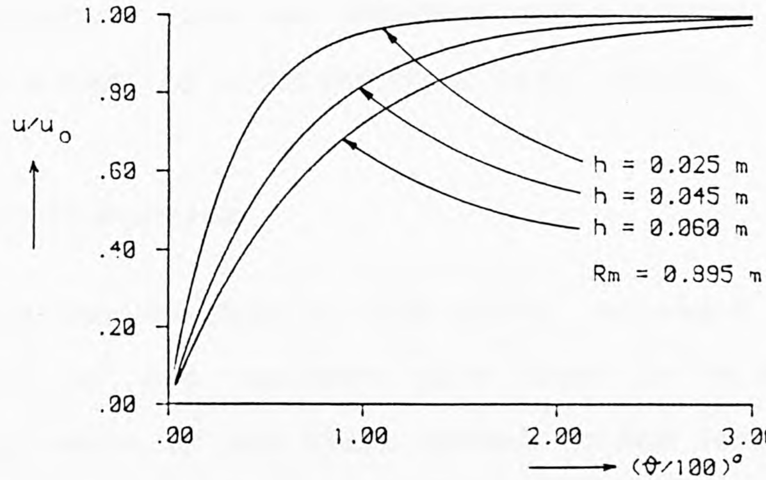

Fig. 3.2 Growth of transverse circulation in a bend

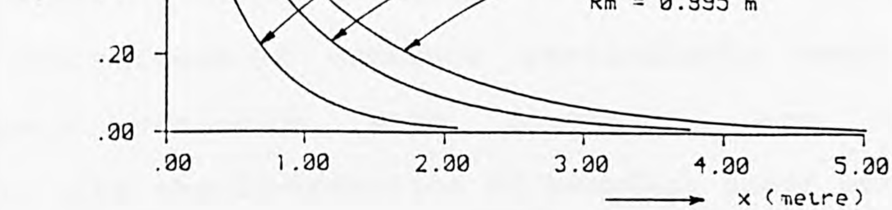

Fig. 3.3 Decay of transverse circulation in straight channel downstream of the bend

CHAPTER 4

SECONDARY FLOW AND BOUNDARY SHEAR STRESS AT A BEND OF A RECTANGULAR OPEN CHANNEL

4.1 General Introduction

Secondary flow can develop in flow along straight channels and channels of non uniform plan form. It is defined as currents that occur in the plane normal to the local axis of the primary flow and is brought about by interaction of the primary flow with gross channel features. Secondary currents are important because they distort the distribution of primary isovels and boundary shear stress from those expected in simple flows. Therefore, they affect the processes of flow resistance, sediment transport, and bed and bank erosion, and influence the development of channel morphology.

Many laboratory investigations of secondary flows have been made. However, there is still a lack of knowledge concerning the pattern of currents particularly near the banks, their variation with discharge, and their relationship with the distribution of boundary shear stress.

In relatively straight, long channels the bed shear stress distribution is normally symmetrical about the channel centre line. In a channel bend the secondary flow originating from streamline curvature leads to an asymmetric bed shear stress distribution. The magnitude and direction of bed shear stress play a decisive role in determining the pattern of movement of bed material in an alluvial channel bend.

The magnitude of the boundary shear stress depends on the velocity gradient near the bed and consequently on the pattern of primary isovels. Peak values of shear stress occur in regions of downwelling where the isovels are compressed and in regions where the primary velocity is relatively high. At a bend the pattern of primary isovels is affected by secondary circulation and so, therefore, are the magnitude and position of the shear stress peaks. At a bend entrance free vortex flow tends to appear, keeping the core of maximum velocity (and the associated shear stress peak) near the inner bank. At the bend itself, secondary circulation develops, thus breaking down the free vortex. At a point that depends on the strength of the circulation and the bend arc angle, the circulation carries the core of maximum velocity across the channel towards the outer bank.

In the work presented here, the secondary flow and boundary shear stress at different cross-sections in U and S-shaped bends in rectangular open channels were studied by direct measurement of velocity near the boundary in the three coordinate directions using the Laser Doppler Anemometer.

The results of the radial and vertical velocity measurements were plotted to depict the secondary flow in the channel while the tangential velocity measurements were used to plot the isovels of the main flow. The boundary shear stress was determined by assuming that the tangential velocity distribution near the boundary will obey the logarithmic law.

4.2 Secondary Flow

The existence of the secondary flow in the cross-section of straight channels has been demonstrated by Nikuradse (1930) who observed that the velocities in the corners of square and triangular cross-sections are relatively large. This can be explained by assuming secondary currents directed towards the corners and has been borne out by experiments with coloured tracers. Little is yet known about the mechanism of these currents. Investigation by Einstein and Li (1958) and Townsend (1956) indicate that the turbulent terms neglected in Eq. (2.1) may be responsible. The velocities have been estimated to be, at maximum, 10 to 20% of the mean velocity. This is the same order of magnitude as the turbulent fluctuations. Variation in channel boundary roughness along the perimeter also gives rise to secondary currents. In this case the secondary flow is directed towards the rougher part of the wall (Hinze, 1967).

In 1876 Thomson gave an explanation for the existence of secondary flow in curved channels. When a river or canal meanders, the velocity of the fluid in a section does not remain tangential. In addition to the tangential motion, much smaller but significant components of velocity are induced in a plane perpendicular to the direction of flow. Thomson used the expression "transverse movement" to describe an important feature of the flow in bends of natural rivers, now generally known as "secondary flows" and they are very noticeable in curved artificial channels. He explained that, owing to centrifugal action in the bend, there exits a pressure gradient from the inner wall to the outer wall. This pressure gradient in the main body of the fluid above the boundary layer is impressed on the boundary below. As the velocity in the boundary layer is less than that in the fluid above it, the boundary layer cannot sustain this pressure gradient, resulting in an inward flow at the base. To ensure continuity, an upward flow at the inner wall, an outward flow at the top, and downward flow at the outer wall exist thus forming a spiral flow caused by transverse or secondary circulation. It is clear that Thomson's theory provides an explanation for the erosion of the outer bank and the accompanying deposition of bed material on the inner bank often observed at the bend of a river. However, his explanation does not answer the question as to whether the existence of the pressure gradient in a section where the velocity is such that the centrifugal force does not balance it, is a sufficient condition to cause spiral flow. It is also clear that though Thomson's mechanism may partly explain the existence of secondary flows, it does not establish whether such flows will die away or alternatively, grow.

Bathurst, Thorne and Hey (1979) studied all the processes at the bends of rivers with coarse alluvial beds. The current knowledge about the subject was introduced, the field measurements of secondary currents and boundary shear stresses were presented and their interrelationship was reviewed.

At the bend entrance the shear field (characterized by the vertical velocity profile) is two-dimensional and contains only the spanwise vorticity of the bend. This is because the primary velocity changes with depth, and the centrifugal force acting on the flow has a different effect at different depths. The shear field therefore becomes skewed and presents a component of its spanwise vorticity in the streamwise direction. The resulting secondary circulation drives surface water towards the outer bank and bed water towards the inner bank.

This single cell of secondary circulation was well understood. However the pattern is sensitive to the presence of any preexisting circulation. In a series of meanders, if the bends are linked by relatively short reaches, the flow cell of one bend can appear as a relict cell at the next bend downstream. Its sense of rotation is then opposite to that of the main cell of the bend. Small cells of reverse circulation have also been observed at the outer banks of single bends in channels and a similar feature may exist in pipes and ducts. The cells are affected by the side wall effect, extending over a region of one or two depths from the bank, but is negligible in bends with large width/depth ratios (aspect ratio).

Secondary flows are typically one order of magnitude smaller than the bulk primary velocity. However, at a bend the strength of the circulation depends on Reynolds number, the cross-section at the bend, the radius of curvature, the ratio of width to depth, and the deflection of the arc angle of the bend. In the channels these parameters vary with discharge as well as between bends.

In deriving Eq. (2.16), no account was given to the inertia terms of the form $u\frac{\partial u}{\partial r} + w\frac{\partial u}{\partial z}$, and the argument was based on the assumption that the flow in a bend follows circular trajectories of constant radii along the depth of the flow. In actual fact, however, the curvature of flow lines changes continuously around the bend and also along the flow depth. Due to velocity changes from bottom to top, the bottom trajectories are of higher curvature than those at the bend. Consideration of the influence of inertia forces due to secondary currents is particularly important in a bend of sharp curvature where (B/Rm) is not much less than one. The parameter r in the right hand term of Eq. (2.16) is actually the central-line radius and may be written as Rm. After considering these inertia terms, Eq. (2.16) is modified by Rozovskii to the following form

$$u = \frac{1}{\kappa^2} Um \frac{h}{Rm} \left(F1(\eta) - \frac{\sqrt{g}}{\kappa C} F2(\eta) + \frac{2.25\ C}{\kappa^3 \sqrt{g}} \left(\frac{h}{Rm}\right)^2 \left(\eta^2 - \eta + \frac{1}{6}\right) \right) \tag{4.1}$$

Further consideration must be given to the derivation of the radial velocity expressed in Eqs. (2.16) and (4.1), in which it was assumed that for a smooth bottom the radial shear stress τ_{ro} near the boundary is equal to zero. In the case of rough boundaries the radial shear stress component τ_{ro} is not negligibly small. For rough boundary the following relationship between the radial and tangential components of shear stress is given by

$$\frac{\tau_{r\delta}}{\tau_{\theta\delta}} = \frac{u_\delta}{v_\delta} \tag{4.2}$$

where $\tau_{r\delta}$ and $\tau_{\theta\delta}$ are the radial and tangential components of the shear stress near the boundary; u_δ and v_δ are the corresponding components of velocity near the boundary; δ is the relative roughness. For rough boundaries the direction of the force with which the stream acts upon it, must apparently coincide with the bottom velocity as sketched in

Fig. 4.1. On resolving the force and velocity vectors into their components in the direction of r and θ, we arrive at Eq. (4.2). By assuming the relation between the stress components and the corresponding velocities to be a linear one, Rozovskii (1957) expressed the relation as

$$\tau_{r\delta} = (A_{\tau}\frac{\partial u}{\partial z}) \quad ; \quad \tau_{\theta\delta} = (A_{\tau}\frac{\partial v}{\partial z}) \qquad (4.3)$$

and Eq. (4.1 can be written as

$$\left\{ \frac{\frac{\partial u}{\partial z}}{\frac{\partial v}{\partial z}} \right\}_{\delta} = \frac{u_{\delta}}{v_{\delta}} \qquad (4.4)$$

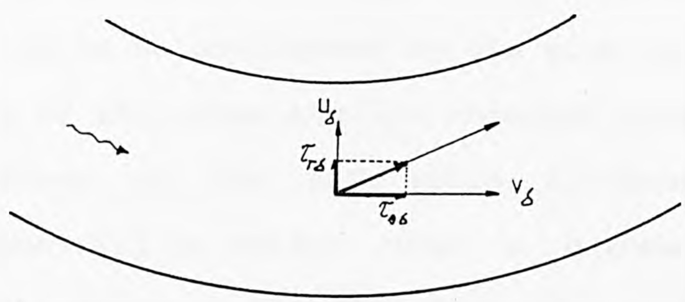

Fig. 4.1 Tangential and radial velocities near the boundary

Furthermore, using the relation of Eq. (4.4) to derive the Eq. (2.14), and utilizing the experimental results in canals with rough bottoms, Rozovskii gave the formula for determining the radial velocity component u in the form

$$u = \frac{1}{\kappa^2}Um\frac{h}{Rm}\left[F1(\eta) - \frac{\sqrt{g}}{\kappa C}\left(F2(\eta) + 0.8(1 + \ln\eta)\right)\right] \qquad (4.5)$$

Bouwmeester (1972) applied the above method for the logarithmic velocity distribution for rough bottom channels, assuming both velocity components v and u, to vanish at level $z = z_o$. The resulting expressions are,

$$u = \frac{1}{\kappa 2} Um \frac{h}{Rm} \left(F1(\eta) + \frac{\sqrt{g}}{\kappa C} F2(\eta) - 2 + 2\frac{g}{\kappa^2 C^2} - 2\frac{\sqrt{g}}{\kappa C}\left(1 - \frac{\sqrt{g}}{\kappa C}\right) \ln \eta \right) \qquad (4.6)$$

The additional term (the last one on the right hand side) in Eq. (4.1) exhibits its effect when h/Rm is not much less than one, and its effects diminish rapidly otherwise.

It should be borne in mind that Eq. (2.16) was derived by assuming the flow to be unaffected by the side walls, due to the large width of the cross-section compared with the flow depth. The effect of the side walls, in these cases, is suggested by Rozovskii to extend over a narrow strip of about twice the depth of the flow from each bank. However, near the side walls of a wide stream and in a flow in a narrow channel, the turbulent stresses neglected in the previous derivation are no longer negligible. Corresponding terms, considering the changes of u and w along r and z must, therefore, be introduced back into the simplified Eq. (2.1.b), Ananyan (1957) then gave the correction factor of distribution of velocity u accross the width of a channel, due to the effect of the side walls for various aspect ratios B/h, as shown in Fig. 4.2.

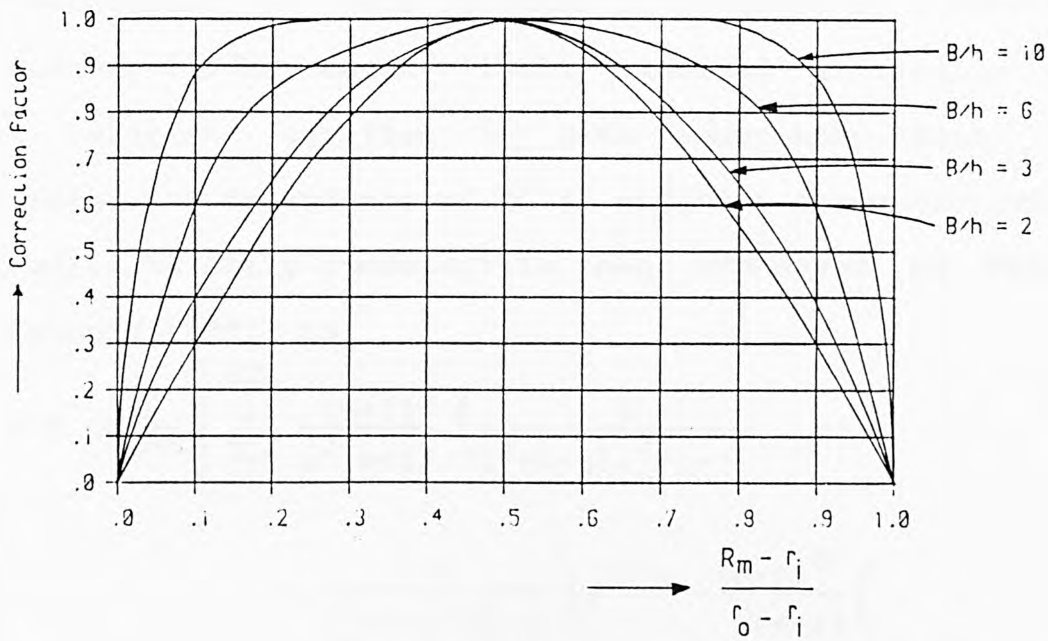

Fig. 4.2 Correction factor of radial velocity component according to Ananyan

In the analytical model developed by Falcon and Kennedy (1983), the primary-flow velocity distribution expressed by the power law,

$$\frac{v}{V} = \frac{n+1}{n} (\eta)^{1/n} \tag{4.7}$$

where v is the vertical distribution of the tangential velocity component, V is the tangential velocity component near the free surface, n is the exponent, which is related to the Darcy-Weisbach friction factor by

$$\frac{1}{n} = \frac{1}{\kappa}\sqrt{f/8} \tag{4.8}$$

where κ = Von-Kármán's universal constant and $f = 8g/C^2$. The background of this relation is reviewed by Zimmermann and Kennedy (1978). Karim (1981) examined critically the above relation, verified it with laboratory data, and formulated the dependence of κ on sediment concentration. The radial velocity component is then expressed by Falcon and Kennedy (1983) as

$$u = 8\,Um\,\frac{h}{Rm}\left\{\sum_{j=0}^{\infty}\frac{(n+1)^4}{n^2(n+1)}\left(\frac{1}{(\frac{3}{n}+2+j)(\frac{3}{n}+1+j)} - \frac{1}{(\frac{1}{n}+1+j)(\frac{1}{n}+j)}\right)\eta^{1/n} - \frac{(n+1)^3}{n(n+2)}\left(\frac{\eta^{(\frac{3}{n}+1+j)}}{(\frac{3}{n}+1+j)} - \frac{\eta^{\frac{1}{n}+j}}{(\frac{1}{n}+j)}\right)\right\} \tag{4.9}$$

Fig. 4.3 shows the non-dimensional relation of $\frac{u}{Um} \times \frac{Rm}{h}$ obtained from Eqs. (2.16), (4.1), (4.5), (4.6) and (4.9), and Computer Programs to solve the above equations are presented in Appendix 4,5,6,7 and 8 respectively.

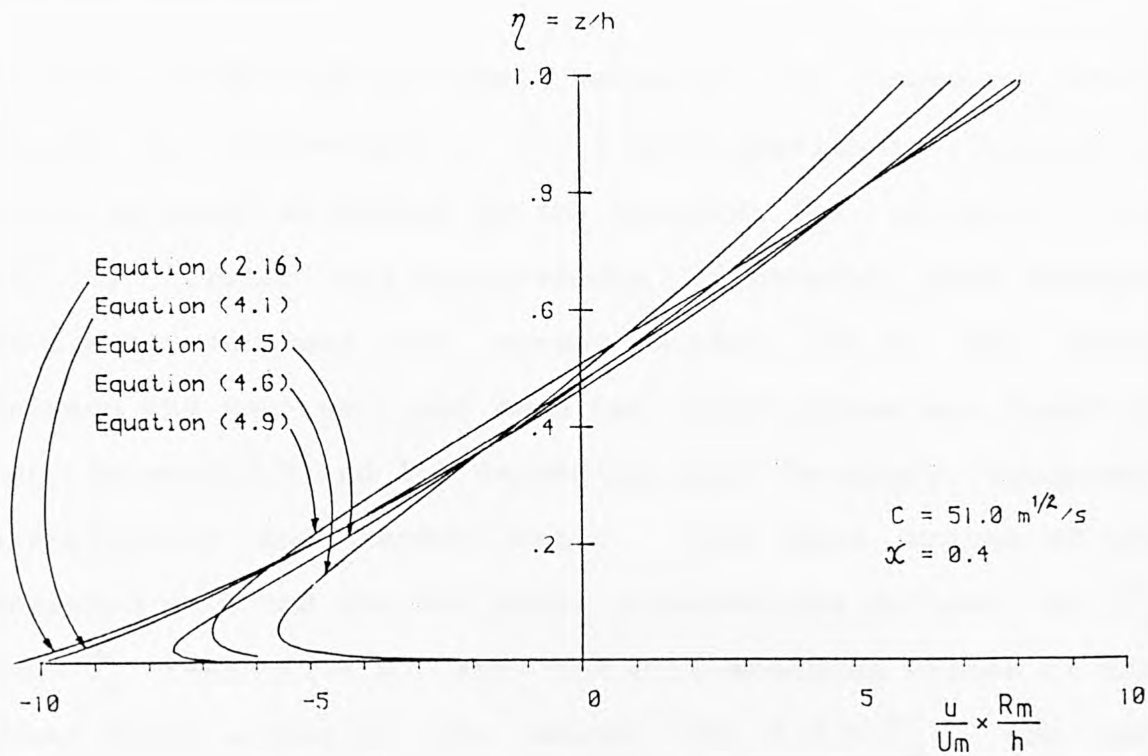

Fig. 4.3 Relation of $\frac{u}{Um} \times \frac{Rm}{h}$ from five different equations of radial velocity component

The experimental results from three different cross-sections in U-shaped and S-shaped channels are observed and compared with the theoretical results. Their deviations are discussed in Chapter 6.

4.3 Boundary Shear Stress

It is well understood that the average shear stress may be readily computed from the hydraulic radius and energy slope, while the distribution of stress around the wetted perimeter cannot be determined successfully by any known theoretical method, particularly for channels of composite roughness and non-uniform shape.

In 1979, Knight and Macdonald measured the boundary shear stress by two methods : (1) A semilogarithmic plotting of velocity profiles normal to the boundary (or isovels); and (2) by Preston tube measurements. In general, both methods gave shear stresses that agreed within 10 %. The ratio between the mean wall and mean bed shear stress was found to vary between 0.2 and 1.2 depending upon boundary roughness distribution and aspect ratio. The mean values of the measured wall and the bed shear stresses are defined by $\bar{\tau}_w$ and $\bar{\tau}_b$ respectively, and the corresponding values of the shear force acting on the walls, $SF_w = 2\ h\ \bar{\tau}_w$, the bed $SF_b = B\ \bar{\tau}_b$, and the wetted perimeter, $SF_p = \bar{\tau}_o\ P = \rho gAi$; in which $\bar{\tau}_o$ = mean boundary shear stress; P = wetted perimeter; ρ = density; g = gravitational acceleration; A = cross-sectional area; and i = energy gradient. As a check of the overall averages, the shear stress distributions were then integrated over the wetted perimeter and the mean value of $\bar{\tau}_{mo}$ obtained. This was then compared with the average shear stress $\bar{\tau}_o$ as derived from energy slope, $\bar{\tau}_o = \rho gmi$, in which m = hydraulic radius. Values of $\bar{\tau}_{mo}/\bar{\tau}_o$ for the 50 experiments obtained and ranged from 0.850 to 1.134 with a mean of 0.976, and indicates that approximately 88 % were within 10 %. This value clearly indicates satisfactory correlation and suggests that calculation of boundary shear stress using the first method is reasonably accurate.

The percentage of the shear force carried by the walls, % SF_w (= SF_w x $100/SF_p$) and bed, % SF_b (= SF_b x $100/SF_p$) were also given. Values of the Nikuradse roughness size for the bed, k_{sb}, were determined from values of the bed friction factor and Reynolds number and were shown in dimensionless form by dividing these by the wall roughness size k_{sw}. The ratio k_{sb}/k_{sw} is then a measure of the differential roughness between the bed and the walls. Finally, Knight arrived at an analytical function, based on various experiments, to describe the variation of % SF_w, $\bar{\tau}_w$ and $\bar{\tau}_b$.

In smooth channel flow, the suggested equation is

$$\% \, SW_w = e^{\alpha}\left(\tanh \pi\beta \; - 0 \; 5(\tanh \pi\beta \; - \beta)^2\right) \qquad (4.11)$$

in which $\alpha = -3.264 \log(B/h + 3) + 6.211$

$\beta = 1 - \gamma/5$

$\gamma = \log\,(k_{sb}/k_{sw})$

The corresponding equations for the mean wall and bed shear stresses are then

$$\frac{\bar{\tau}_w}{\rho g h i} = \frac{\%SF_w}{100} \; \frac{B}{2h} \qquad (4.12)$$

and

$$\frac{\bar{\tau}_b}{\rho g h i} = \frac{\%SF_b}{100} = 1 - 0.01 \; \%SF_w \qquad (4.13)$$

The mean wall and bed shear stress equations above may be related to the overall mean boundary shear stress $\bar{\tau}_o$ by the equation

$$\overline{\tau}_o P = 2h\overline{\tau}_w + B\overline{\tau}_b \tag{4.14}$$

In the case of smooth channels, $k_{sb}=k_{sw}$. Hence $\gamma = 0$, $\beta = 1$, and the right hand side of Eq. (4.11) becomes e^{α}.

Fig. 4.4 shows the variation of % SF_w with B/h obtained from Eq. (4.11) and experimental results on smooth channel flow.

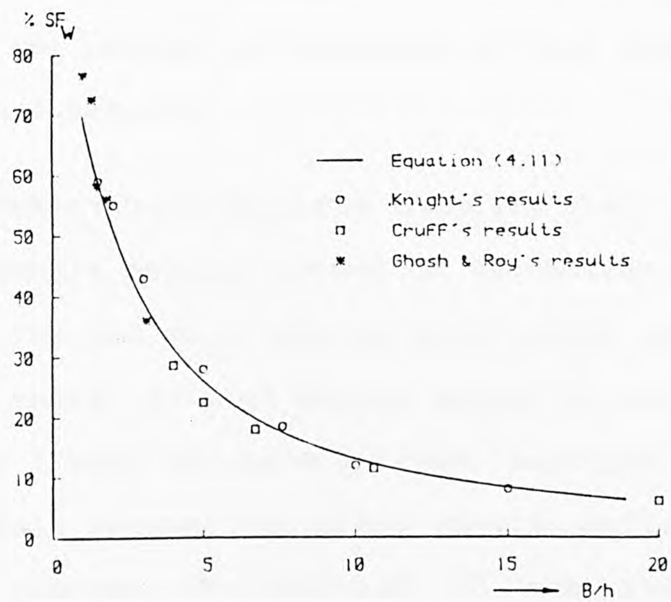

Fig. 4.4 Variation of % SF_w with aspect ratio

A study of the boundary shear stress in symmetrical compound channels was also done by Knight in 1984. He concluded that the boundary shear stress around the wetted perimeter in open channel flow is indeed influenced by the shape of the cross-section, the presence of secondary flows and the lateral distribution of roughness. Although Knight's work was limited to a simple plan form, i.e., uniform plan form, it has given a better understanding of the shear stress distribution near the boundary of flow in open channels.

The major phenomena leading to the asymmetric distribution of bed shear stress in a bend are the secondary circulation and the longitudinal acceleration and deceleration of the main flow. These effects give rise to deformation of the vertical distribution of the main velocity. The bend shear stress depends on the velocity gradient close to the bed and consequently on the pattern of contours of main velocity in a channel cross-section.

Many previous workers have measured boundary shear stress in curved open channels using a number of techniques. In 1950 Malouf obtained the bed shear stress in a curved channel by measuring the speed of sand grains moving in contact with the bed. Wadekar (1956) and Asfari (1968) employed the same method using small perspex and glass spheres rolling on the bed of a curved channel. The relation of the average bed shear stress ($\bar{\tau}_b/\frac{1}{2}\rho u^2$) to the Reynolds number and the curvature ratio (h/Rm) of the bend was obtained. It was noted by Wadekar that particles of large diameter deviate considerably from the direction of the bed shear stress. Apart from that, experimental errors occur due to intermittent inactivity of the movement or due to particles making short jumps, and the method is unwieldly for use in curved channels.

The measurement of boundary shear stress in curved open channels by the use of Preston's technique was initiated by

Ippen et al (1960) and then Ippen and Drinker (1962). The same technique was then used by Yen (1965) in a large trapezoidal meandering channel. The Preston tube was aligned in the flow direction at the bed and the bed shear stress coefficient ($\overline{\tau}_b/\frac{1}{2}\rho u^2$) was found to be independent of the Froude number but dependent on the radius ratio (Rm/B). Yen concluded that erosion and deposition are determined by secondary flow on the bend rather than by bed shear stress. However by measuring bed shear stress and sediment discharge on a sinusoidal meander bend, Hooke (1974) concluded that contrary to the findings of Yen above, it is the sediment distribution rather than the secondary flow which is primarily responsible for the bed geometry of a meandering channel.

The method of point velocity measurement to determine boundary shear stress distribution of logarithmic variation of velocity in the vertical has been reported by Ali (1964), Bathurst et al (1979), and Nouh and Townsend (1979) for movable beds. Bathurst also observed the peak of bed shear stress to be associated with the core of maximum velocity and the uniformity of the bed shear stress distribution was found to be dependent on the Reynolds number and on the strength of secondary circulation. He related that the uniformity increases as the Reynolds number increases. The effect of high Reynolds number and of a subcritical Froude number on the bend characteristics is generally insignificant (Gotz, 1980). Choudhary and Narasimhan (1977) observed that the bed shear ratio, $\tau_b/\overline{\tau}_b$, decreases with an increase in the Froude number and with a decrease in the aspect ratio. They also noted that the position of the maximum shear stress at any section in the strongly curved flow studied tends to occur at lower r/Rm for narrow channels than for wide channels. Several experimental runs obtained from the curved flow studies done by Rozovskii (1957) and Yen (1965) were numerically simulated by De Vriend (1976). He found that the results of the mathematical computations based on the simplified models which disregard the secondary flow convection represent the experimental results rather poorly. However, procedures based on the integration of complete three-dimensional flow equations are very complicated although it gives a proper prediction of the bed shear stress pattern (De Vriend, 1981). Several investigators have predicted bed contours in bends with movable beds on the basis of simplified calculations of radial bed shear stress and found agreement with actual measurements.

Zimmermann and Kennedy (1978) predicted bed contours, using the radial bed shear stress obtained by equating the moment of the radial bed shear stress to the torque induced by centrifugal forces, using a power law distribution for main velocity.

Boundary shear stress is not only affected by the variation of the roughness at the channel boundary itself, but also by the development of the flow circulation. In the work presented here the boundary shear stress is observed along the wetted perimeter of a smooth rectangular open channel for two different plane forms, i.e. a U-shaped channel and an S-shaped channel. Primary isovels patterns are required in order to calculate the boundary shear stress. These were obtained by taking velocity profiles with the aid of the Laser Doppler Anemometer technique using a predetermined grid pattern in the cross-section of the channel as shown in Fig. 5.9. The velocity measurements were taken at 45 points or 54 points for each cross-section, (nine horizontally and five or six vertically). Boundary shear stress was calculated at 19 points around the wetted perimeter of the same cross-section, from the velocity gradient near the bed and near the wall. By establishing the primary velocities of primary isovels near the boundary, the shear stress at a point was determined using the relation

$$U_* = \frac{u_2 - u_1}{5.75 \log(\frac{z_2}{z_1})} \qquad (4.10)$$

in which ρ = density of fluid; $U_* = \sqrt{\tau_o/\rho}$, local shear velocity; and u_1 and u_2 = velocities at two points at distances z_1 and z_2 respectively from the boundary.

It should be noted here that the method, used to calculate the shear stress along the wetted perimeter, described above, is highly dependent on the accuracy of the primary-flow velocity measurement.

CHAPTER 5

EXPERIMENTAL EQUIPMENT AND PROCEDURES

5.1 General Introduction

For many studies of flow, particularly of flow in curved channels, detailed measurements are still very important. The use of the laser Doppler anemometer to measure the mean and the corresponding components of the Reynolds stress-tensor has become very common recently. In contrast to hot-wire instruments and some other conventional techniques, laser anemometers are a non-contact optical instrument which enable the fluid flow structure in gases and liquids to be investigated.

In 1977, Humphrey, Taylor and Whitlaw made use of a laser Doppler anemometer to measure the longitudinal component of mean velocity at a rectangular curved duct. Later in 1981, Humphrey, Whitlaw and Yee provided the basis for the precise measurement of two components of mean velocity and the corresponding Reynolds stresses in the same rectangular curved duct at a Reynolds number corresponding to turbulent flow. As observed by Humphrey the vast majority of the previous investigations of three dimensional curved flow are limited to the determination of the longitudinal main velocity.

Observation of flow in S-shaped open channel bends has been carried out by Keerthisena (1983), who paid special attention to the detailed measurement of flow, using three-tube yaw and pitch probes, and bed shear stress by using a Preston tube. The three components of local mean velocity were measured at the same time for one particular point in the grid framework of the cross-section, but the Reynolds stress-tensor was not discussed. The use of the three-tube yaw and pitch probes made it impossible to measure the velocity field near the boundary.

The purpose of the present investigation is to provide detailed measurements, of quantified and good precision, which will increase present understanding of the physical process governing curved open channel flow. The experimental equipment and experimental techniques used to obtain the measurements are described in the following sections.

5.2 Experimental Equipment

The experimental channels were prepared in two different shapes or planforms. The first channel was a U-shaped channel, made of perspex, consisting of a straight portion of rectangular cross-section (0.15 m by 0.15 m and 1.50 m long), leading to a curved channel of the same cross-section. The radius of the inner wall (r_i) was 0.820 m and that of the outer wall (r_o) was 0.970 m giving a ratio of width to centreline radius (Rm) of 1:6. The curved portion of the channel was extended for 180^{o}, leading to a straight portion of the same cross-section downstream from the bend, thus forming a 'U' shaped channel in plane as shown in Plate 5.1 and Fig. 5.1.

The second channel was an S-shaped channel, prepared by removing the downstream straight portion of the U-shape channel and replacing it with a curved channel of the same cross-section but having a bend in the opposite direction. The curved portion of the downstream channel was also extended for 180^{o}, leading to a straight portion of the same cross-section downstream from the bend, this formed an S-shaped channel as shown in Plate 5.2 and Fig. 5.2.

The base of the channel was 1/2" thick, as were the other parts of the channel (i.e., the base of the inlet and the outlet tank), except the wall part of the channel which was 1/4" thick.

The curvature of the perspex wall was produced initially by warming up the 1/4" thick perspex glass in the water to about 30^{o} C to reduce the ductility of the perspex sheet, which was then bent into the desired shape. The precision of the curvature was considerably high as the process was carried out by a special heavy machine available in the University Work Shop.

A special glue was made to connect the base to the wall part of the channel. This was a mixture of 'Tensol' cement no. 7; 25 parts component A and one-part component B. It must be mixed well before stirring and used within 25 minutes. The hardening process depends on the amount of glue which has been poured into the joint. The thicker the layer, the longer the hardening process. The best result was achieved when the glue was poured layer by layer. Each layer was allowed to dry first before the next layer was poured. This also enable the glue to go into the joint holes properly, so that a water tight joint was obtained.
The main parts of the channel which had to be glued separately were the two straight parts of the channel and the two bend parts of the channel with bends in opposite directions. The other parts of the channel were the inlet and the outlet tank. (The inlet and the outlet tanks are of identical design which enables them to be used interchangeably).

The end of each part of the channel was designed in such a way that the connection between one part and the other was achieved easily by using screws and rubber gaskets. Thus, tight connections were obtained.

The channel bed was arranged so that it was level on a Dexion angle frame for both channel configurations. This was maintained by initially using a micrometer precision level.

Water was then introduced into the channel to a certain level. The water was then allowed to stand over a period of time.
A period of time of 2-3 hours was required to get a still or undisturbed water in the channel, because of its length. At the end of that period of time the channel level was checked by observing the depth of the water along the channel which was supposed to be uniform. Non-uniformity of the still water depth in the channel indicates that the channel is not level. It was made level by adjusting the screws which were available at the bottom of the angle frame. This action may cause the water in the channel to move alternately upstream and downstream. The same procedure was repeated a few times until the still water gave a uniform depth along the entire channel.

Flowrate identification was arranged as follows. First, it had to be managed in such a way that the flow was steady during the experimental run. Because of the uncertainty in obtaining sufficiently steady flow in the channel by directly pumping the water from the sump tank into the inlet tank, a constant head tank was used for the present laboratory investigation. Secondly, to minimise the initial disturbance to the flow, an energy dissipator had to be placed in the inlet tank at the end of the inflow pipe coming out from the constant head tank. Finally to identify the flow rate introduced during the experimental run, a specially designed weir in conjunction with a water depth gauge, mounted on the straight portion downstream from the channel was used. In a uniform flow, a certain flow rate would give a certain depth of flow and thus, a certain weir-crest elevation as well. Calibration was then made to establish the correlation between the flowrate and the depth of flow which is nearly uniform. This flow calibration was required in order to be able to make a quick adjusment of the weir-crest elevation, the water depth gauge and the valve beneath the constant head tank, thus the desired flow rate was obtained. The correlation between weir elevation and uniform depth of flow versus flow rate is presented in Fig. 5.3. Only three different runs were carried out in this investigation. These were 10 l/min, 30 l/min and 50 l/min flowrates corresponding to 0.025 m, 0.045 m and 0.060 m uniform depth of flow respectively.

5.3 Experimental Technique

5.3.1 Laser anemometry

In many cases, flow can only be measured correctly if a non-contact sensor is used. For example, a flow pattern may be of such small dimensions that even the smallest of probes would affect the parameters under investigation, and a flow of chemically active medium would damage a physical probe. Some flow even makes the physical presence of a probe impossible. (For example flows around propellors, flows in turbines, etc.)

In such flows, the Laser Doppler Anemometer (LDA) may be the only possible means of measuring local flow velocity, and in many other flows LDA may be the most practical method of investigating the dynamic properties of flows.
This non-disturbing method of measurement of the velocity field in fully - or semi - transparent flow media has four main features,

i) The creation of "measuring volume", consisting of the crossing point of two monochromatic laser beams which create a local fringe system, which is precisely located within the flow without disturbing the flow.

ii) The generation and introduction into the flow of light-scattering particles, consisting of a small diameter (of the order 1-5 μm) light refracting droplets, preferably of similar density to that of the flow medium.

iii) The method is absolute and requires no calibration. The detection by a photomultiplier, of the variation of light intensity caused by the scattering particles as they pass through the fringe system of the scattering volume.

iv) The processing and interpretation of light intensity signals in terms of time-mean velocities and fluctuation velocities.

5.3.2 Principles

In LDA measurements three modes of operation, the Reference beam Mode, the Differential Doppler Mode and the Dual Scattered Mode have been used, but only the first two have found general acceptance.

A monochromatic coherent beam is produced by the laser which has an extremely high frequency stability. In the Differential Doppler Mode, as used in this experiment, this beam then passes through a beam splitter (see Fig. 5.4). The non-refracted beam then passes through an acousto-optical device known as a Bragg Cell in which ultrasonic energy is propagated transversely to the laser beam to have the frequency of the light waves upshifted or downshifted. The defracted beams have the same optical properties as the incoming beam and cause no deterioration of the performance of the laser Doppler system. The two beams produced then pass through the Beam Displacer, Beam Translater, Beam Expander, and finally pass through a suitable lens arrangement to cross at a convenient position in the fluid flow whose characteristics are to be observed.

The power of the Laser used in this experiment is 10 mW.

At the beam crossing the two laser beams of monochromatic coherent light, each with plane and parallel wave fronts, will form a fringe pattern. The fringes, formed by alternately constructive and destructive superposition of the two beams, define the measuring volume. Frequency shifting may be described as a movement of the fringes in the measuring volume in the velocity of $v_s = f_s \times d$, where f_s is the frequency shift introduced and d is the fringe space

($d = \frac{\lambda}{2 \sin \theta / 2}$), as can be seen in Fig. 5.5.

Movement of the fringe pattern against the flow direction will result in an increase of the frequency of the scattered light from a particle in a measuring volume by an amount f_T, corresponding to an increase in the flow velocity. In other words, the detected frequency is $f_D = f_s + f_T$, taking into account the sign of f_T. Further clarification is presented in section 5.4.2 part a).

5.3.3 Optical components

Laser anemometer measurements can be carried out under conditions which vary considerably. It is thus essential that the optical system can be adopted to the mode and configuration most suited for the particular measurement.

The LDA system adopted for the purposes of the present investigation is LDA mode 8, One-Component Forward Scatter Differential Doppler Mode with Frequency Shifting as shown in figure 5.4, produced by DISA ELEKTRONIK group of companies. The system can facilitate forward scatter flow measurement in both gases and liquids. A range of different front lenses are available for the transmitting optics which enable focal length to be adjusted depending on application.

The scattered light is detected using a photomultiplier which operates in conjunction with a 55N20 Frequency Tracker, and 55N10 Frequency Shifter.

5.3.4 Seeding

The particles responsible for the light scattering at the interference fringe pattern can be considered as being actual velocity measures.
Consequently much importance must be attached to the consideration of such particles if laser anemometry is to be used successfully. The particles should be small enough to track the flow accurately and yet be large enough to scatter sufficient light for the proper operation of the photodetector and the special processor.

Particles which are of most interest in laser anemometry are of a size comparable to the wave length of light (the Lorenz-Mie scatter region) and scatter far more light in a forward direction than in a backward direction. This is particularly marked with the ratio of forward to backscattered light being of the order of 10^2 to 10^3.

A more even scatter is produced with smaller particles whilst larger particles are more unpredictable. Consequently, in general, forward scatter optical arrangements provide better signal to noise ratios. It also means that bigger lasers or better optics should be used for backscatter measurements.

Often the natural concentration of very small particles is much greater than that of particles in the useful range. In some cases, particularly when measuring in liquids, this causes an undesirable shot noise level as a result of incoherent signals from the many small particles.
Whenever possible, therefore, it is wise to control the size and concentration of the seeding particles by means of filtration and the addition of known seeding particles. However, it is not essential to seed while using the LDA system for measurements in water.

5.3.5 Doppler signals

The frequency information relating to the velocity to be measured is picked up by the photomultiplier and translated to a current pulse. This photocurrent also contains noise, the primary source of which is the photodetector shot noise. This however is a fundamental property of the detection process, the interaction between the optical field and the photosensitive material being a quantum process. This unavoidably impresses a certain amount of fluctuation on the mean photocurrent and shot noise, as a consequence undesired light reaching the photodetector this being reflected laser light or merely ambient light.
The best operation of a laser anemometer is achieved if shot noise in the signal is the predominant noise source. Such a performance can only be obtained by proper selection of

laser power, seeding particle size and optical system parameters. In addition selection of the minimum bandwidth needed for measuring the desired velocity range by means of filters should minimise noise. The quality of the signal and performance of the signal processor are dependent upon the number of seeding particles which are simultaneously present in the measuring volume. Should there be an average much less than one particle present in the measuring volume then we speak of a "burst type" Doppler signal. If more particles are present in the measuring volume simultaneously then we speak of a "multi particle" signal. The current from the detector is the sum of the current bursts from each individual particle within the measuring volume. Since the particles are located randomly in space then the individual current contributions are added with random phases. The resulting Doppler signal envelope and phase thus fluctuate.

5.3.6 Signal processing

The Doppler signal contains the velocity information as a frequency modulation of the detector current. The signal processing electronics thus function essentially as a frequency demodulator. The special character of the signal, however, demands a very sophisticated frequency detector. In the multi-particle case the signal is quasi continuous, but the envelope and phase do contain random fluctuations as a result of the random number and positions of the particles in the measuring volumes.

The LDA Tracker is a frequency tracking filter which is able to lock on the Doppler frequency and continue to track the instantaneous frequency provided that the internal servo loop stays locked. The incoming Doppler signal is amplified and filtered by the tracker, with the servo loop implemented as a phase-locked loop. By means of a phase detector the phase difference between the Doppler signal and the output of a voltage controlled oscillator (VCO) is detected. After low-pass filtering, in the loop filter this error signal controls the VCO in such a way that the phase difference is minimised. The high frequency phase noise from the VCO control input is removed by the loop filter which then integrates the error signal over a period of the order of a transit time for a particle through the measuring volume. Providing the loop remains closed, the VCO frequency is then a good measure of the Doppler frequency. However, the correlation between the VCO frequency and the input Doppler frequency is measured by a special circuit the Lock Detector. Should the correlation drop below a preset level, then the locked detector causes the loop to open and the VCO is held as the last value. Following a preset delay of 500 periods, the VCO start to sweep increasingly large frequency bands around the last measured Doppler frequency until lock to the input frequency has been re-established.

Output from the tracker is made available in two analogue forms, the VCO control voltage and the frequency to voltage converter (F/V) output. The F/V output is the more accurate whilst the VCO control voltage is capable of following higher frequencies.

The analog presentation of the Doppler frequency is fed out from the ANALOG OUT connection to the tracker. The detected input frequency f_D is then obtained by connecting to a digital voltmeter from which

$$V_{analog\ out} = \frac{10V}{Range} f_D$$

where Range = maximum frequency in selected range in tracker

$V_{analog\ out}$ originates in a frequency/voltage.

The tracker is designed for continuous signal detection but performs well in the case of relatively short drop-out periods caused by fluctuations in the envelope of the multi-particle signal. The random phase fluctuations of the multi-particle signal cause a small noise signal in the tracker output. This however is unavoidable in any frequency detection system and can be attributed to the random arrival of scattering particles in the measuring volume. This phase noise does not influence mean velocity results although it does add a certain amount to the RMS value. A multi-particle signal is often found when measuring in liquids and under such conditions an LDA system with a tracker processor enables undistorted measurements of highly

turbulent flows to be made. Flows in separated regions, oscillatory motions and reversing flows can also be measured successfully.
A diagram of the LDA signal processing equipment used in the present investigation is shown in Fig. 5.6.

The LDA counter is designed to take care of the burst type Doppler signal where a relatively long period without a signal occurs between burst. Velocities may change appreciably between bursts and hence the LDA counter is neccessarily a wide bandwidth device. In principle the LDA counter acts simply as a timing device which can be programmed to measure time between certain events. The LDA counter systems are most commonly used in situations where low seeding particle concentrations exist such as in wind tunnel measurements.

5.3.7 Traversing mechanism

The optical part of the LDA system, comprising the the Laser Optical Unit and Photomultiplier, was mounted on an optical bench placed on a precision made traversing table capable of moving in three coordinate directions. The table allows 12 cm total traverse in a horizontal (r) direction, 20 cm in a vertical (z) direction and 10 cm in a longitudinal (perpendicular to r-z plane) direction. The accuracy of positioning in each direction was 0.5 mm.

5.4 Experimental Procedure

5.4.1 Initial adjustments

In this section the fundamental steps of initial adjustments of transmitting optics are described paying special attention to the aspects related to the practical use of the Laser Doppler Anemometer. Successful experimental work is quite often influenced by the way in which the instrument used for the experiment is set. Reliable results may be obtained if the instrument is set properly, otherwise considerable errors may arise. Therefore, step by step adjustment of the transmitting optics must be carried out before using it for the experimental work. For more detailed information the experimenter is referred to standard optical textbooks, or the relevant instruction manuals, but the treatment given here should enable the experimenter, with some understanding of optics, to appreciate the design and the limitations of the LDA instruments.

The initial adjustments involve the adjustment of the Laser light beam on its way into its measuring volume, and the determination of calibration factor C which is a function of the Laser wave length (λ) and the angle of the beam intersection (θ).

Firstly, with the transmitting optic consisting of the Laser Adaptor, Beam Splitter, Bragg Cell Section, Beam Displacer and Beam Translator as shown in Fig. 5.4, the adjustments are performed according to the following sequence;

(1) The transmitting optics is mounted on the optical bench, and then the laser is switched on. The Bragg Cell section is connected to its power supply and the frequency of the Laser beam is shifted.

(2) The light beams are positioned properly on the prisms, by making adjustments through small ports located on the Beam Splitter, the Bragg Cell section and the Beam Displacer. The best position is indicated by the brightest image on the screen (a wide screen made of paper is mounted at the front of the system). Adjustments are made by using an Allen key.

(3) In order to ensure that the laser beam is parallel to the top of the optical bench the following procedure is used. The Beam Expander is screwed on the transmitting optics and a special high quality mirror is placed in front of the optics. The reflection from the mirror is aimed back to the Beam Expander. The error in the positions of the reflected and transmitted beams is noted. 50 % of the error is taken out by adjusting small ports on the Beam Translator. The remaining error is taken out by adjusting the screws which are available at the back of the mirror. The transmitting optics is then rotated through 180° and

again the error is corrected in the same way as before until the error disappeared. This can be achieved with 3 to 4 repeated trials.

Secondly, the selected front lens, which in this case has a focal length of 600 mm is screwed on to the Beam Expander. The intersection of the two Laser light beams is checked by placing the test objective lens at the intersection of the two beams. This is done by sliding the test objective lens forward and backward along the axis of the transmitting optic until the images of the two beams are superpositioned, forming a single image on the screen. If a single image cannot be found, it means that the beams do not intersect properly. By making adjustments through ports in the Beam Translator, the beams can be can be made to intersect in such a way so that when the images on the screen are superpositioned, the size of the combined image is the same as the size of the individual beam image.

The initial adjustments described above must be made before any experimental measurements are carried out. Better adjustments may be achieved when the screen is bigger and mounted further away from the transmitting optics. This is because the images of the beams are bigger. However a longer optical bench and a bigger working space are required.

In determining the factor of calibration C, a big screen is located far in front of the transmitting optics. By measuring the distance between the two images on the screen and the distance from the intersection point and the screen, the angle of intersection of the Laser light beams can be determined from the relation

$$\theta = 2 \text{ arc tan } \frac{B}{2L}$$

where

θ = angle of the beams intersection

B = distance between the two images on the screen

L = distance between the intersection point and the screen

For example in one case,

L = 515.50 cm

B = 62.0 cm

giving

$$\theta = 2 \text{ arc tan } \frac{62.0/2}{515.50}$$

$$= 6.8828^{\circ}$$

The calibration factor (C) is defined as ; $C = \frac{\lambda}{2 \sin \theta/2}$, where λ is the Laser wave length ($\lambda = 632.8 \times 10^{-9}$ m). Thus

$$C = \frac{632.8 \times 10^{-9}}{2 \sin \frac{6.8828^{\circ}}{2}}$$

$$= 5.27090 \times 10^{-6} \text{ m/s/Hz}$$

$$= 0.527 \text{ cm/s/KHz (for 600 mm front lens)}$$

L and B were measured to an accuracy of 0.5% and 1%. When L and B were changed by 0.5% and 1% respectively, it was found that C changed by only 0.056%.

For the 310 mm front lens,

$$L = 329.5 \text{ cm}$$

$$B = 78.0 \text{ cm}$$

giving

$$\theta = 2 \arctan \frac{78.0/2}{329.50}$$

$$= 13.500379^{\circ}$$

$$C = \frac{632.8 \times 10^{-9}}{2 \sin \frac{13.500^{\circ}}{2}}$$

and

$$C = 2.69183 \times 10^{-9} \text{ m/s/Hz}$$

$$= 0.269 \text{ cm/s/KHz}$$

5.4.2 Test and measurements

a). Accuracy test of the LDA

The magnitude and direction of the fringe movement was specified by the frequency shift introduced in conjunction with the given alignment of the fringe pattern.

When particles pass through the fringe pattern (measuring volume), the detector measures the sum of the shifted frequency due to the fringe movement and the Doppler frequency.

It was noted that the the frequency shift used during the experimental run was 60 KHz, while the detected input frequency f_D was then obtained by connecting the analog out from the tracker to a digital voltmeter, from which

$$f_D = \frac{\text{Range x } V_{\text{analog out}}}{10}$$

The detected frequency f_D is the sum of f_S and f_T, where f_s is the frequency shift introduced into the system and f_T is the actual frequency of the particle movement which is to be measured.

$$f_D = f_s + f_T$$

where $$f_T = \frac{2 \sin \theta/2}{\lambda} v$$

With the selected setting of the digital voltmeter and the selected frequency shift (= 60 KHz), the accuracy of the digital voltmeter reading was tested by using the LDA in still water. It can be seen from Fig. 5.8 that the average reading of the DC is 6.047 Volts while the average reading of the RMS is 0.436 Volts. These two values are then used as a reference for further data analysis.

As it can be seen in Fig. 5.8, that the test is considered to have a high degree of accuracy because within 465.5 seconds, the 146 DC readings gave the mean value of 6.047. The distribution of the 146 DC readings showed a tendency for normal distribution; with 100% were within 5%, as well as the 108 RMS readings where 80% were within 5%. It was then decided that readings of the DC or RMS would always be taken 20 times and the average value was then obtained. Occasionally, it was also found during the experimental run that the distribution of some DC and RMS readings, at a certain flow and location, were showing a tendency for normal distribution with 100% DC readings were within 5%, and 97-100% RMS readings were within 5%.

In still water, $f_T = 0$, hence, $f_D = f_s = (100000 \times 6.047)/10 = 60.47$ KHz ≈ 60.00 KHz, slightly different with the shift introduced by the frequency shifter.

When water is flowing with a certain velocity and direction, for example, the average reading of DC from this particular situation shows 5.850 Volts, therefore, the actual flow is (5.850 - 6.047) = -0.197 Volts.

$$f_T = \frac{R \times V}{10}$$

$$= \frac{100000 \times (-0.197)}{10}$$

$$f_T = -1.97 \text{ KHz } (f_T < 0)$$

When $f_T < 0$, $f_D < f_S$, the direction of the flow is the same as the direction of the fringe movement.
When $f_T > 0$, $f_D > f_S$, the direction of the flow is against the direction of the fringe movement (see Fig. 5.7).

b). Mean and fluctuating velocity measurements

The mean and fluctuating velocity measurements were made either in the straight portion or at the bend of the channel. The locations of the cross-sections in the U-shaped channel are shown in Fig. 5.1 while in the S-shaped channel are as shown in Fig. 5.2. The grid framework of the measurement points in the cross-section of the channel is shown in Fig. 5.9.

For tangential velocity measurement, the optical bench was mounted on the traversing gear which is able to move in three coordinate directions. The optical bench axis was placed below the channel and maintained perpendicular to the direction of the main flow in such a way that the intersecting beams could be directed to the desired location in the channel where the characteristics of the flow are to be investigated. The axis of the transmitting optics is maintained perpendicular to the longitudinal axis of the channel so that the tangential or forward velocity can be measured.
The mean and fluctuating velocities were measured accordingly by adjusting the DC and RMS button at the front panel of the digital voltmeter.

Initially, a 310 mm front lens was used as this was more convenient due to the limited space available around the channel. Later, a 600 mm front transmitting lens in conjunction with a 300 mm focal length photomultiplier lens was used during the experimental work. However at the straight part of the channel (at sections U-1, U-4, S-1, S-8 for different runs to measure the forward velocity), and U-2 for one particular run to measure the vertical and tangential components of velocity, the 310 mm front transmitting lens in conjunction with the 300 mm focal length photomultiplier lens was used. Consequently, for the first combination mentioned above, the calibration factor C was 0.269 cm/s/KHz, and for the second combination, calibration factor C was 0.527 cm/s/KHz.

The measurements of the mean and fluctuating vertical velocity components were carried out by rotating the optics through 90°. To minimise the time taken, both the mean and the fluctuating components in the tangential and vertical directions were measured at the same time at one measurement point. The procedure was adopted at the next measurement point. Details of this procedure are illustrated in section 5.4.2 d.

The mean and fluctuating radial velocity component measurements were always made after the measurement of the tangential and vertical velocity component characteristics had been made over the whole measurement points in the grid framework of each cross-section.

As it can be seen in Plate 5.2, a specially designed mirror was placed on the optical bench in front of the optic so that the incoming beams could be reflected upwards to enable the radial velocity component to be measured. The optical bench was in the same position as before, when it was used to measure the characteristics of tangential and vertical velocity components. This meant it was unnecessary to make any level adjustment to the traversing gear position.

c). Reynolds stresses measurement

This section gives the detailed procedure for the measurement of Reynolds stresses ($\overline{v'w'}$) and ($\overline{v'u'}$).

From the original position the optical unit is rotated to plus and minus 45^{o} to be able to measure the Reynolds stress $\overline{v'w'}$. Denoting RMS values by σ_+ and σ_-, respectively, we have $\overline{v'w'} = 1/2\ (\sigma_+^{2} - \sigma_-^{2})$.

at +45^{o} : $vw = (\bar{v} + w')(\bar{v} + w')$ (5.1)

at -45^{o} : $vw = (\bar{v} + v')(\bar{w} - w')$ (5.2)

(5.1) $vw = \bar{v}\bar{w} + v'\bar{w} + \bar{v}w' + v'w'$

time averaging,

$$\overline{vw} = \overline{\bar{v}\bar{w}} + \overline{v'\bar{w}} + \overline{\bar{v}w'} + \overline{v'w'}$$

$$\overline{vw} = \overline{\bar{v}\bar{w}} + \overline{v'w'} \qquad (5.1.a)$$

(5.2) $$vw = \bar{v}\bar{w} - v'\bar{w} + \bar{v}w' - v'w'$$

time averaging,

$$\overline{vw} = \overline{\bar{v}\bar{w}} - \overline{v'\bar{w}} + \overline{\bar{v}w'} - \overline{v'w'}$$

$$\overline{vw} = \overline{\bar{v}\bar{w}} - \overline{v'w'} \qquad (5.2.a)$$

from (5.1.a) : $(\overline{v'w'})_1 = \overline{vw} - \overline{\bar{v}\bar{w}}$

from (5.2.a) : $(\overline{v'w'})_2 = -\overline{vw} + \overline{\bar{v}\bar{w}}$

$$(\overline{v'w'})_1 - (\overline{v'w'})_2 = 2\ (\overline{vw} - \overline{\bar{v}\bar{w}})$$
$$= 2\ \overline{v'w'}$$

hence,

$$(\overline{v'w'})_1 - (\overline{v'w'})_2 = 2\ \overline{v'w'}$$

or

$$\overline{v'w'} = 1/2\ ((\overline{v'w'})_1 - (\overline{v'w'})_2)$$
$$= 1/2\ (\sigma_+^2 - \sigma_-^2)$$

where $\sigma_+ = \sqrt{\overline{v'w'}}$ (RMS reading at $+45^{\circ}$)

$\sigma_- = \sqrt{\overline{v'w'}}$ (RMS reading at -45°)

Similarly, the Reynold shear stress formed by the tangential and radial velocity fluctuations $(\overline{v'u'})$, is measured by rotating the optical unit to plus and minus 45° with respect to its original position.

d). Measurement procedure

This section describes the measurement procedure which is essential for the experimental work in order to optimize the time consumption, especially at the bend part of the channel.
The measurements were always made according to the sequential number of cross-sections as shown in Fig. 5.9.

Measurement of vertical and tangential velocities :

Firstly, at one particular point, the mean tangential velocity (DC) with its corresponding fluctuation (RMS) was measured. The optical unit was then rotated through 45^{o} and the fluctuation (RMS) was again measured. The optical unit was again rotated through 90^{o} in order to measure the mean vertical velocity (DC) component and its corresponding fluctuation (RMS) value. Finally, the optical unit was rotated through 135^{o} and the fluctuation (RMS) was measured. These measurements at one particular point give the values of $\bar{v}, \sqrt{v'^2}$, $\bar{w}, \sqrt{w'^2}$ and the $\overline{v'w'}$. The same procedure was followed accordingly for all other measurement points throughout the grid framework.

Measurement of radial velocities :

The next observation was the measurement of the mean radial velocity component with its corresponding fluctuation and the Reynolds stress formed by tangential and radial velocity fluctuations. A specially designed reflecting mirror was placed at the front of the transmitting optics. For this particular situation the photomultiplier was mounted above the channel to enable it to pick up the intersection beam in the flow. The procedure was then repeated, starting from measuring point no. 1 in the grid framework employed in the previous case.

The optical unit was rotated through plus 45° and the beams reflected by the mirror were rotated through plus 45° with respect to radial traverses in the flow. Then the RMS value was measured. The optical unit was rotated through plus 90° for the measurement of mean and fluctuation of radial velocity component. Finally, the optical unit was rotated through 135° and the RMS value was measured. These measurements at one particular point gave the values of $\overline{u}$, $\sqrt{u'^2}$, and $\overline{v'u'}$.

It must be noted here that due to difficulties in maintaining the axis of the optical bench perpendicular to the main flow direction, or perhaps due to slight imperfection of the channel itself, the lens mounted on the P.M. section and the pin hole of the photomultiplier had to be adjusted after every rotation of the transmitting optics. In some situations however, it was impossible to measure the vertical and radial velocity components according to the grids in the cross-section, particularly near the bottom and at the water surface. This was because one of the incoming beams was out of alignment on its way to the measuring volume. The results obtained at various cross-sections for three different runs are discussed in Chapter 6.

e). Secondary flow pattern as observed by photographic technique

The pattern of secondary flow at some cross-sections of the U-shaped and S-shaped channels was observed by photographing the flow by introducing suitable particles.
The particles needed to be of sufficiently small size and representative of the fluid flow itself whilst moving with it. Furthermore the particles needed to be of a density which enabled them to remain suspended within the fluid for a long period. Finally the particles needed to be able to reflect light so that they can be tracked in the flow by photographing them. For the purpose of this investigation, use was therefore made of particles formed from fine filed perspex.

Having obtained suitable particles, the desired flow conditions could be chosen and the particles were introduced into the flow. Initially it was considered that the particles could be introduced directly into the flow as loose powder. It was found, however, that the ground perspex tended to float on the water surface.
The problem was eventually solved by mixing the particles with some water in a bottle prior to introducing them into

the flow. The mixture of particles and water was then introduced into the flow at about 0.5 m upstream from the observation section.

In order to avoid the refractive paths of the light caused by the channel curvature effect, the curved channel was enclosed with a specially designed perpex box (see Plate 5.1), and the box was filled with water, in such a way that the cross-sectional view of the observation section could be clearly seen.

The section under observation was illuminated through a 6 mm slit fixed across the top of the channel. The photographs were then taken using a zoom lens having a focal length of 200 mm and a 27.5 mm extension tube. The distance between the front lens and the illuminated cross-section is about 610 mm.

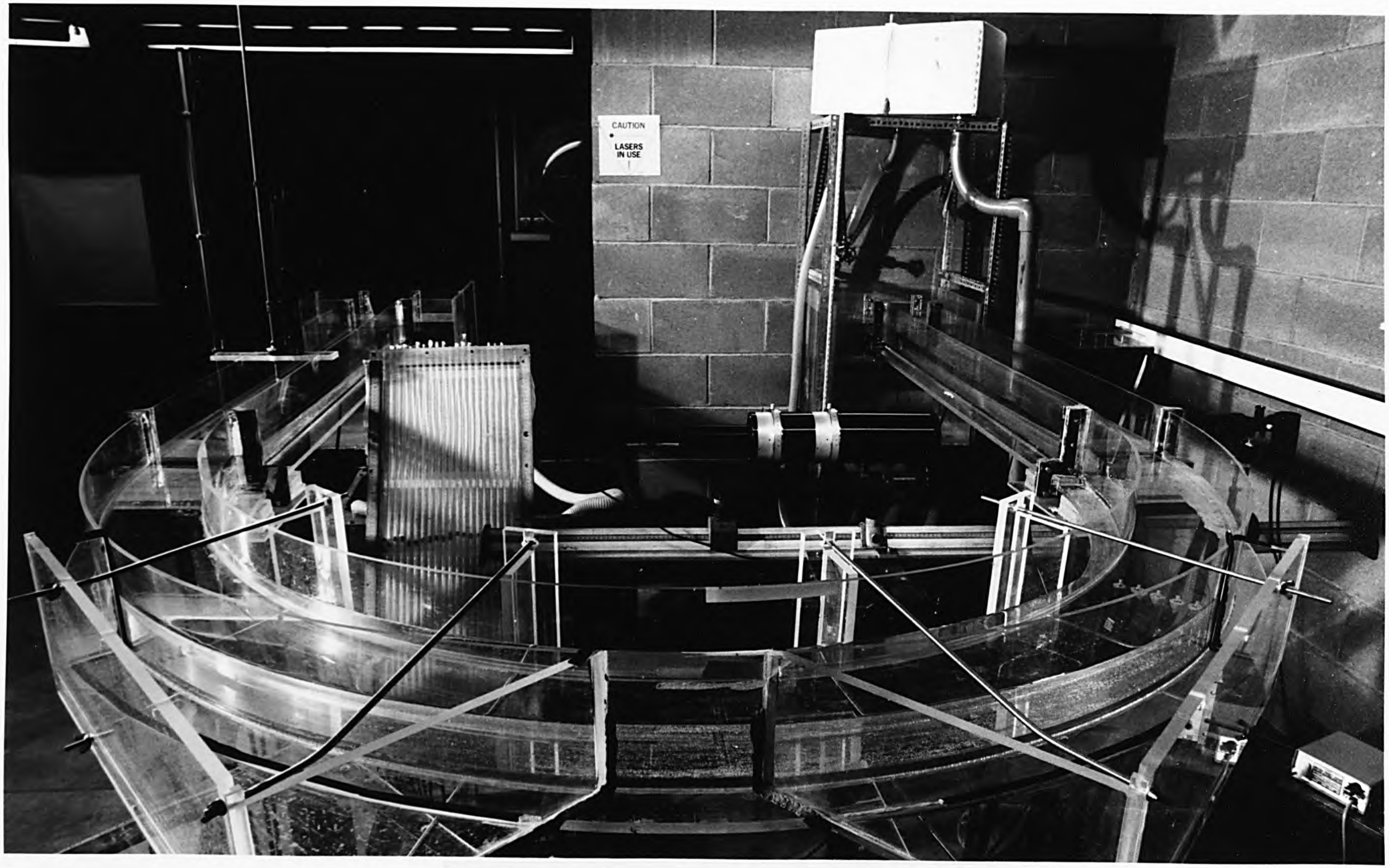

Plate 5.1 U-shaped experimental channel

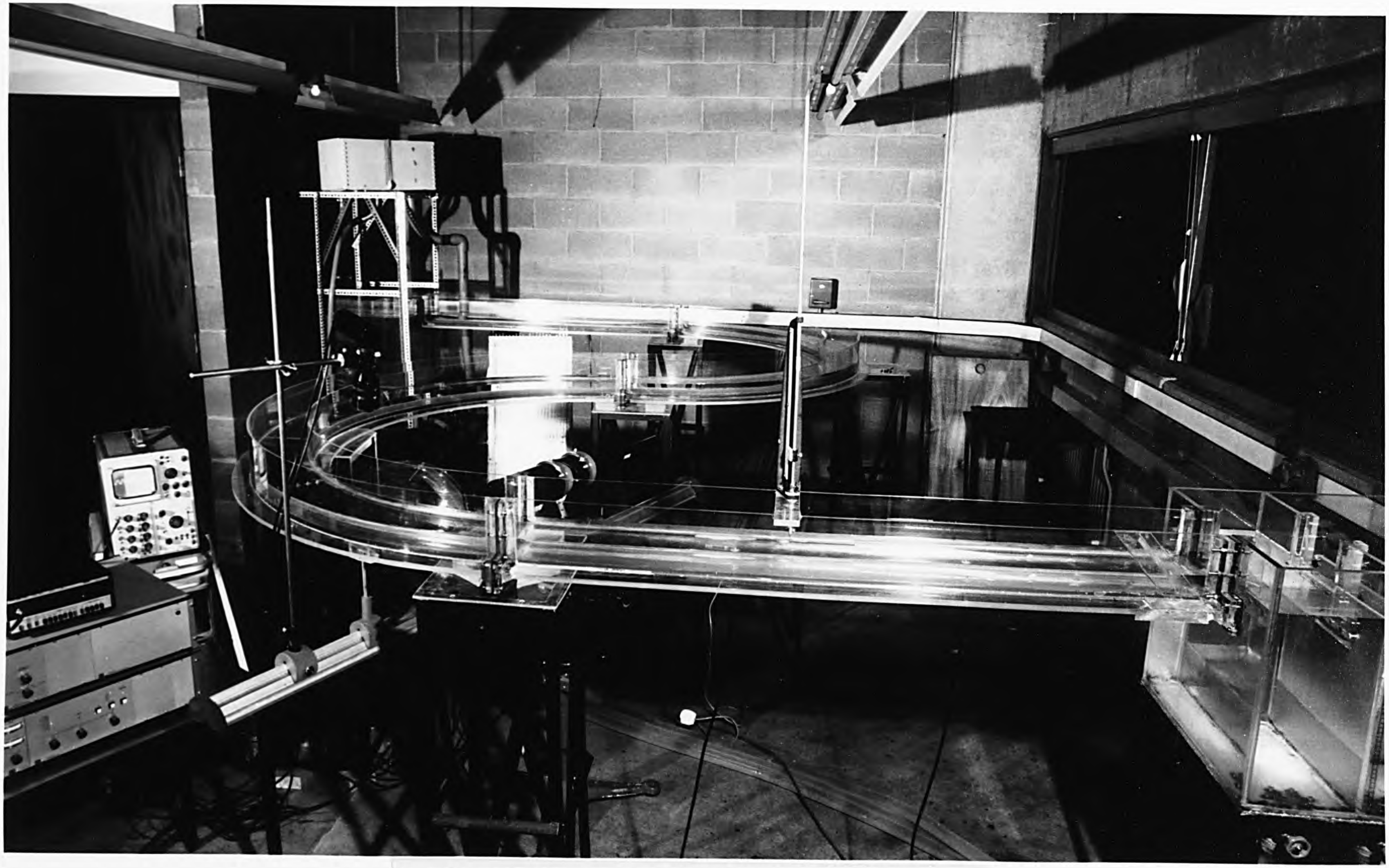

Plate 5.2 S-shaped experimental channel

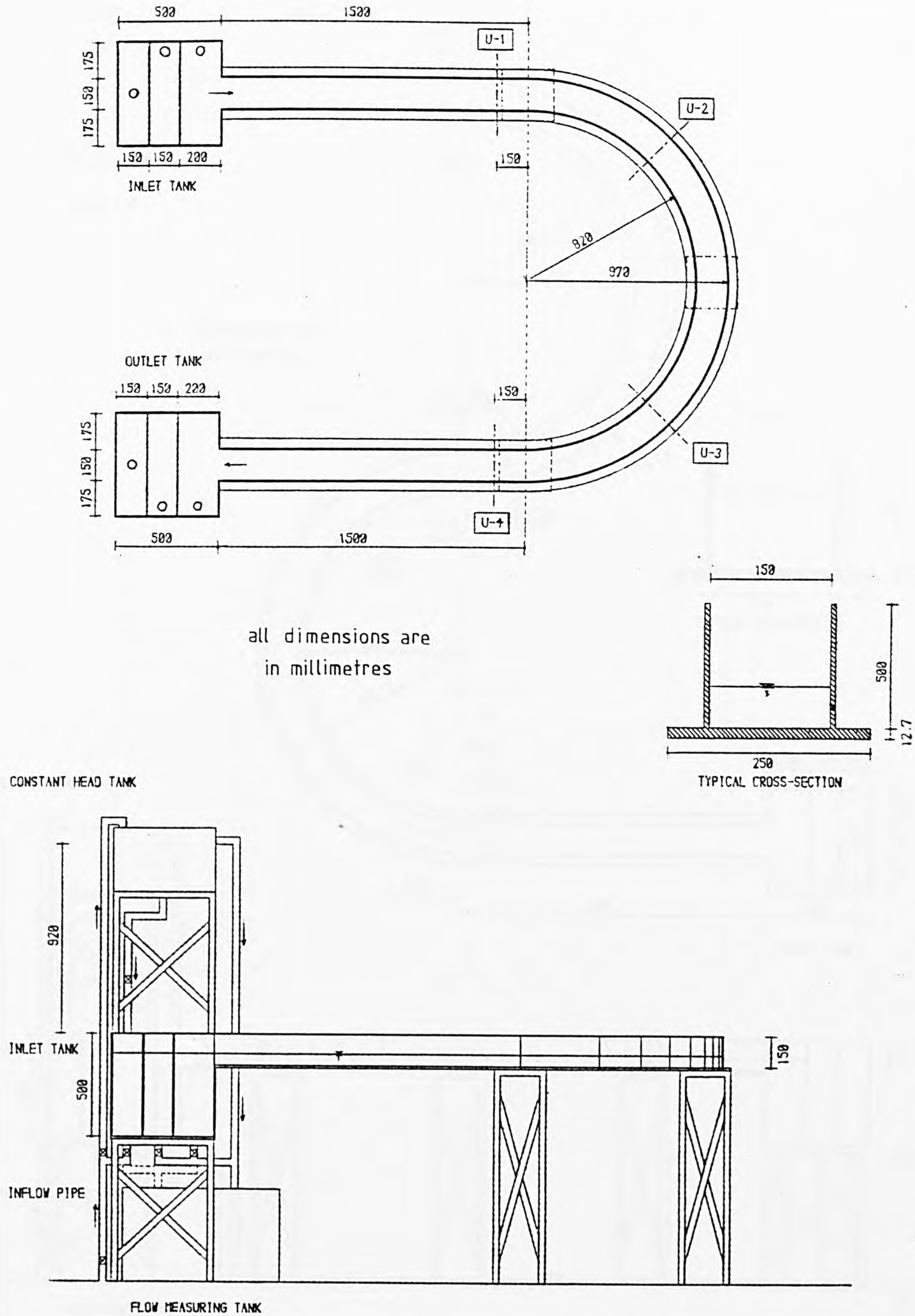

Fig. 5.1 Details of U-shaped experimental channel

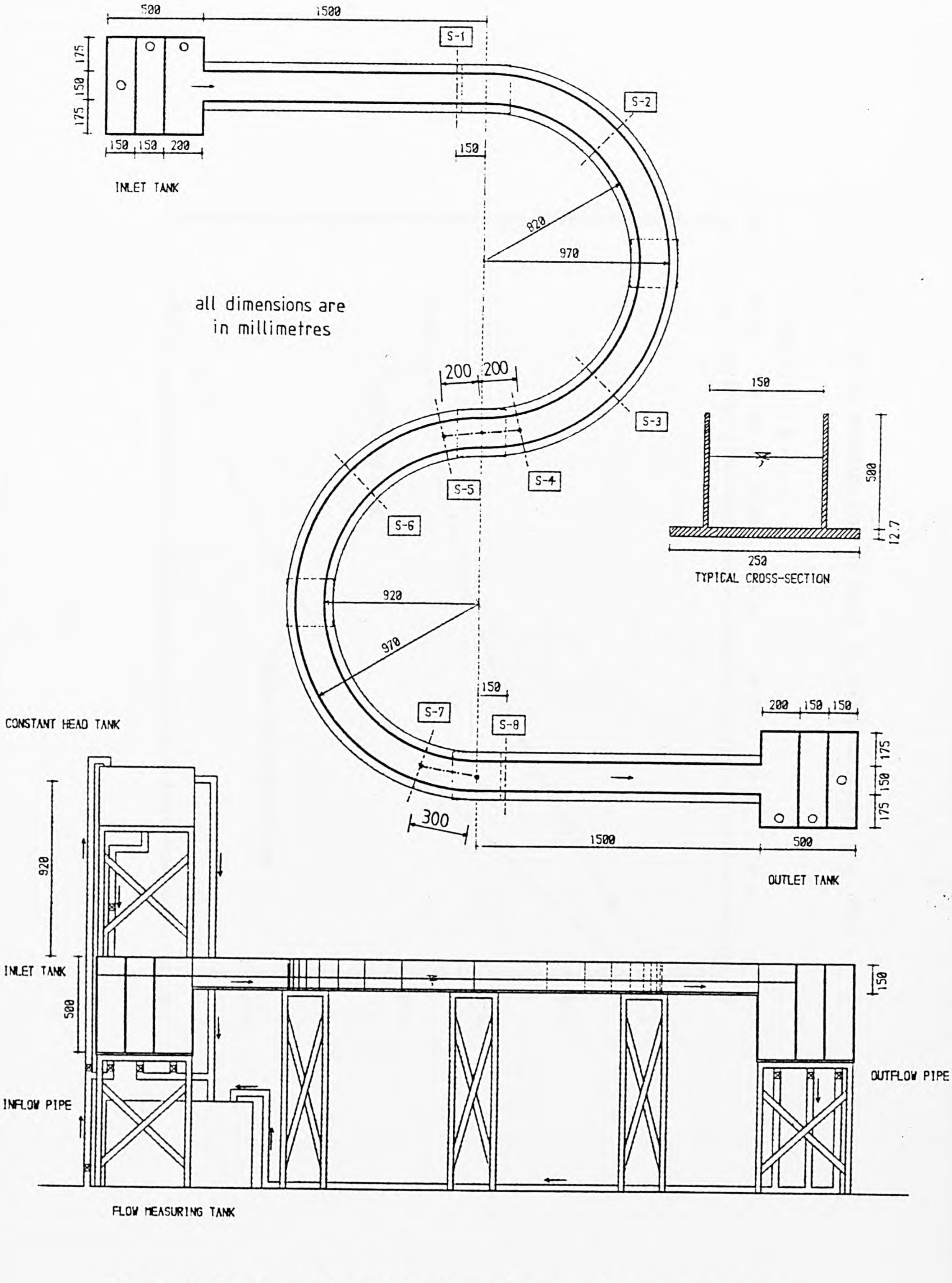

Fig. 5.2 Details of S-shaped experimental channel

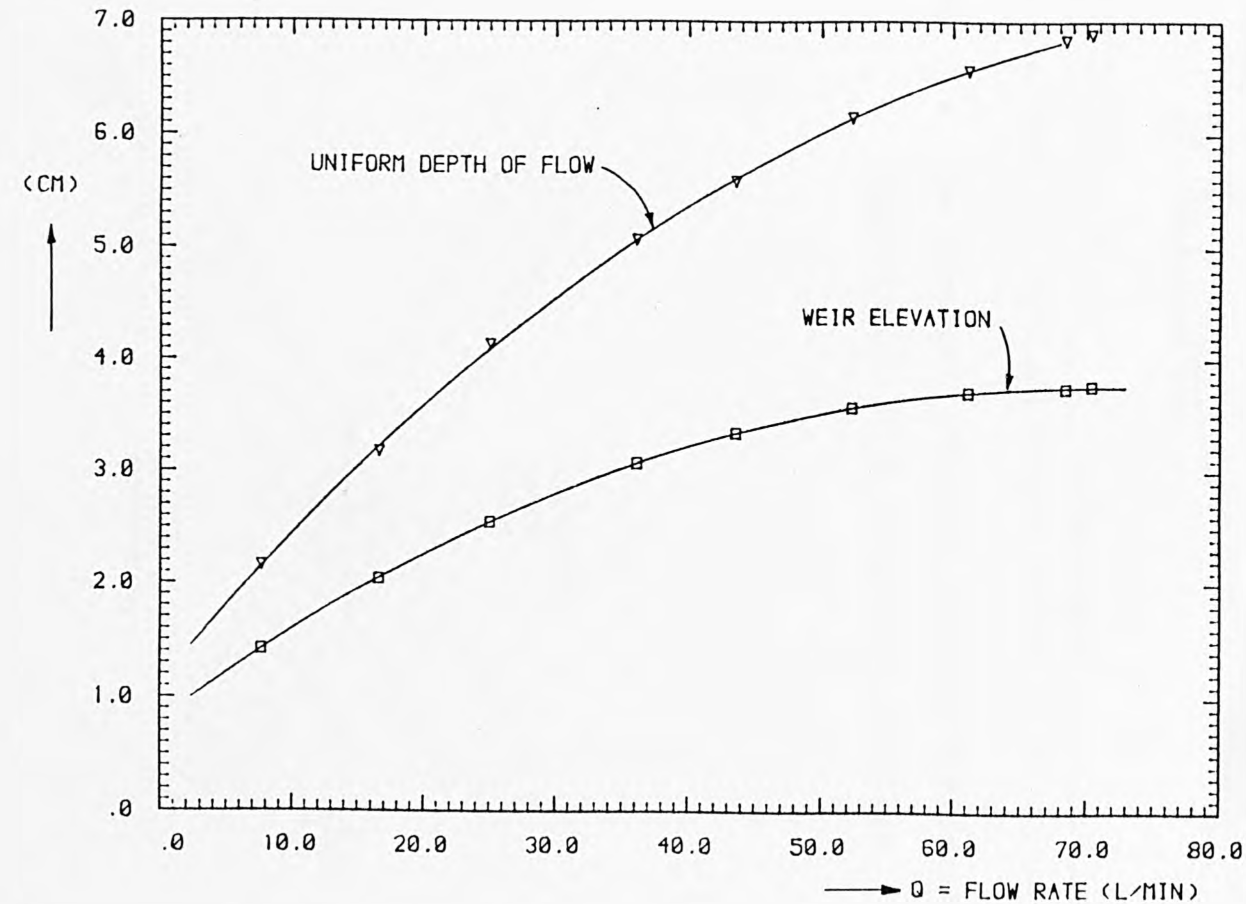

Fig. 5.3 Uniform depth of flow in the channel vs flow rate

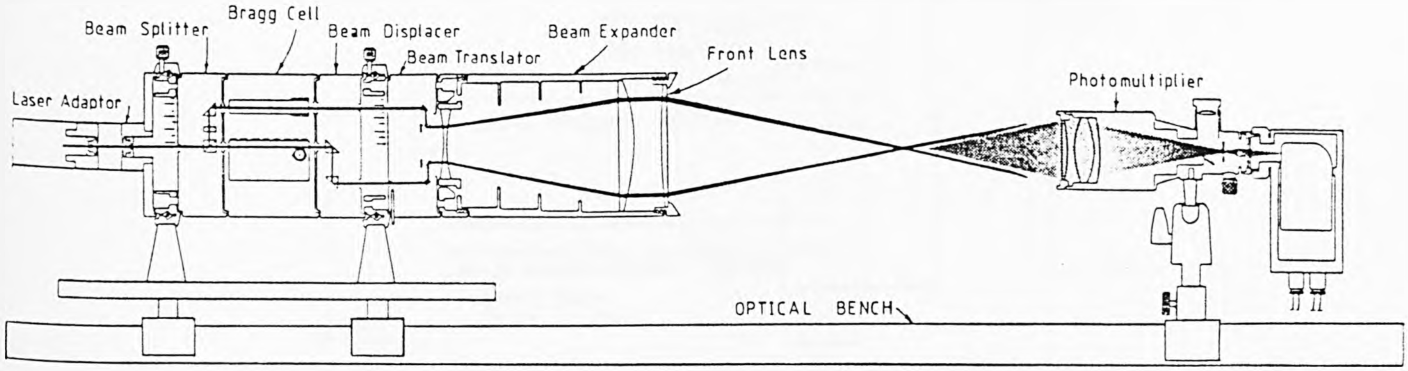

Fig. 5.4 One-component forward scatter differential Doppler mode with frequency shifting

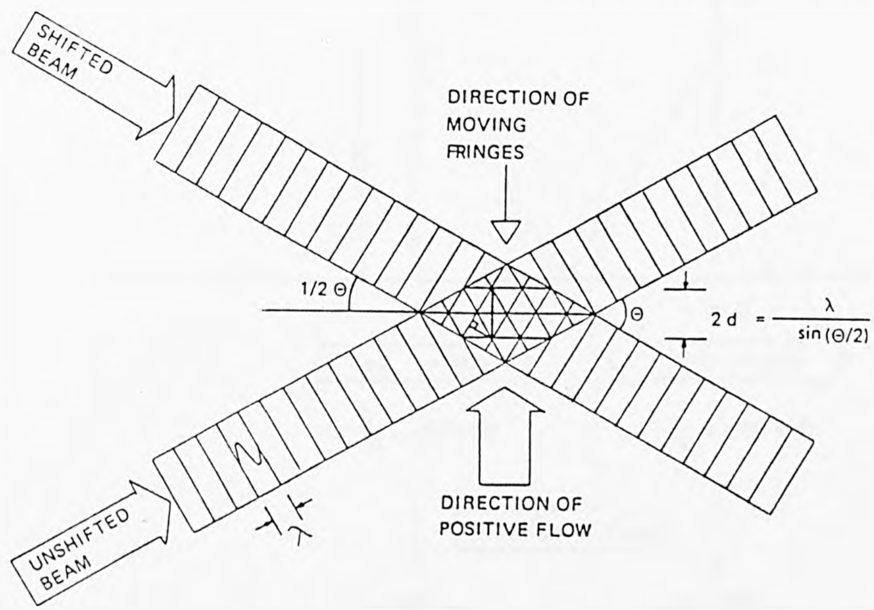

Fig. 5.5 Description of frequency shifting as a movement of the fringes

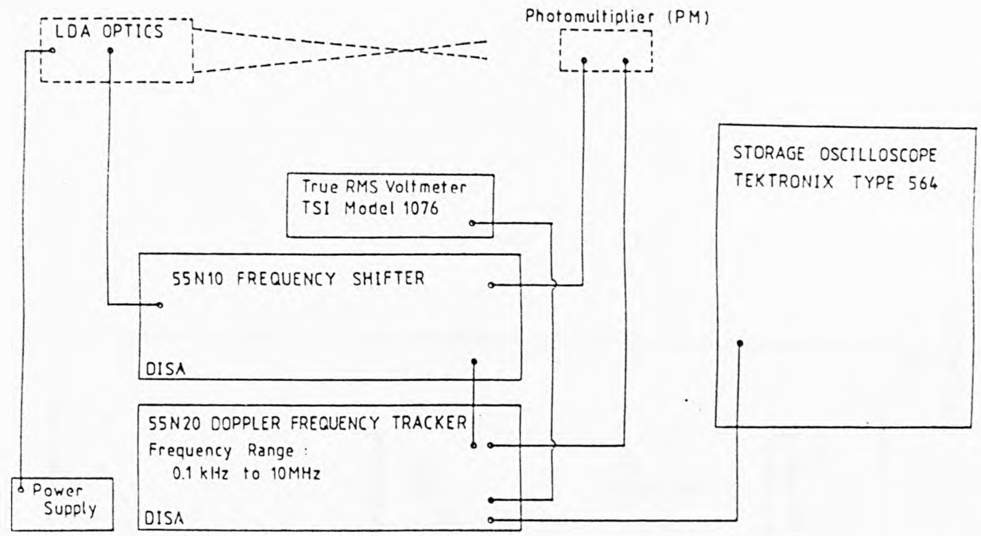

Fig. 5.6 Diagram of LDA signal processing equipments

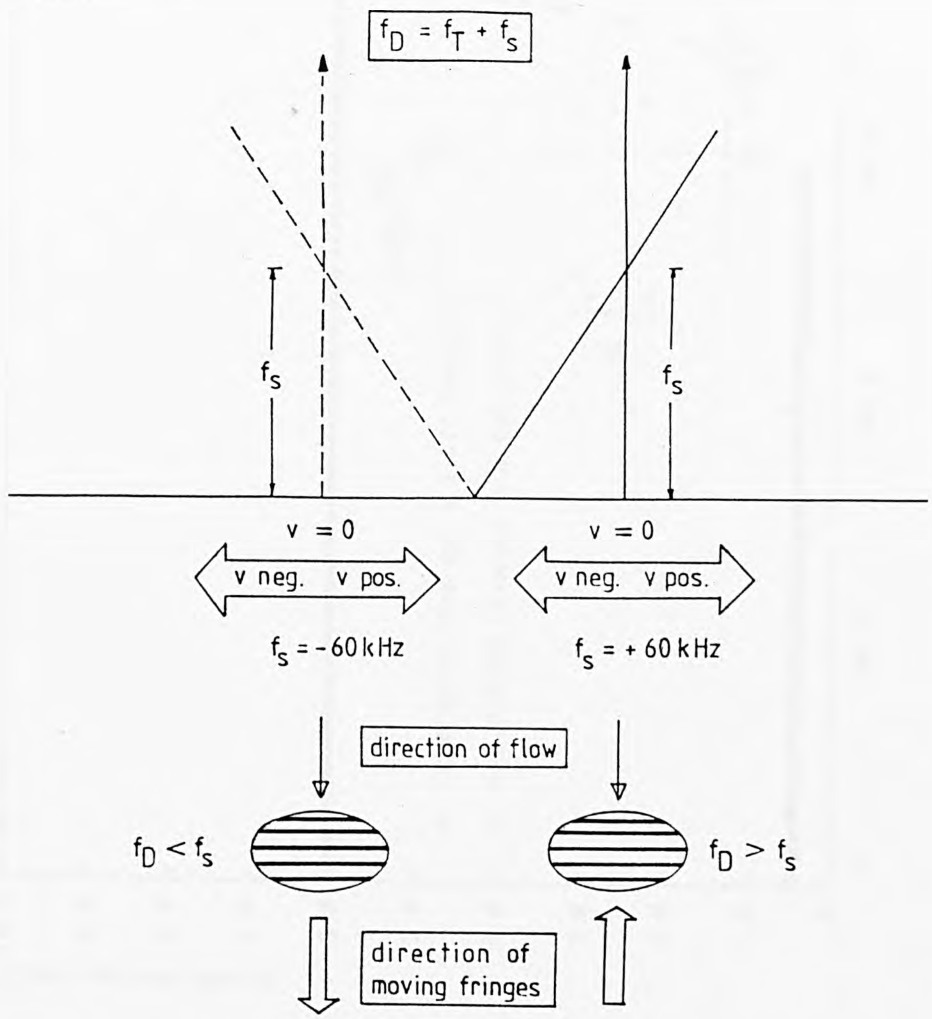

Fig. 5.7 Identification of flow direction by appointing the sign convention of the fringe movement direction

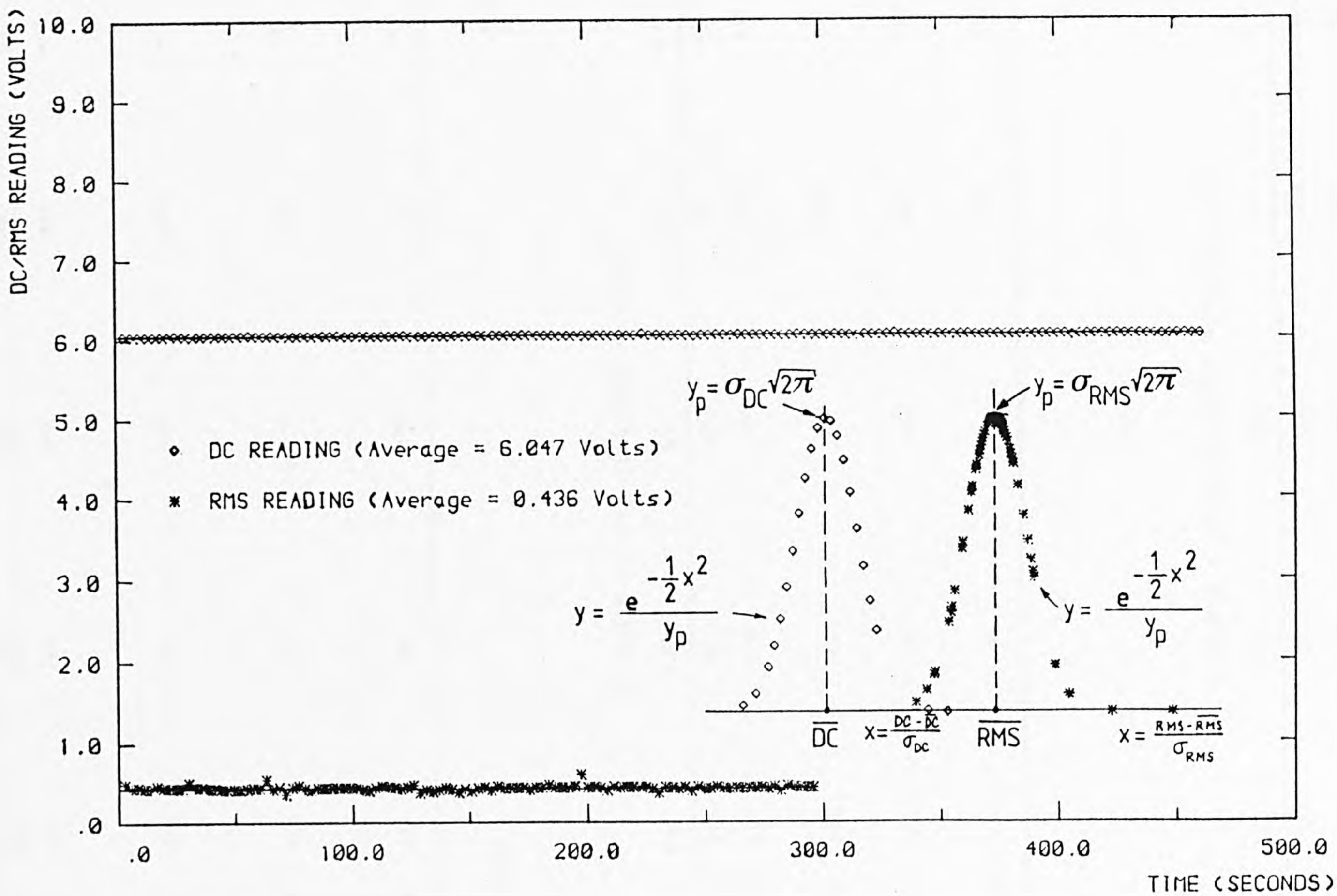

Fiq. 5.8 Accuracy of DC and RMS readings in still water

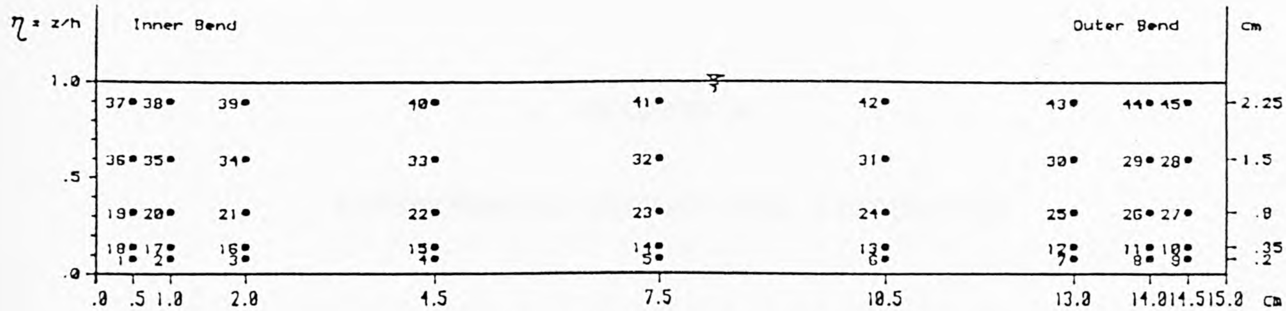

a). Uniform depth of flow = 0.025 M

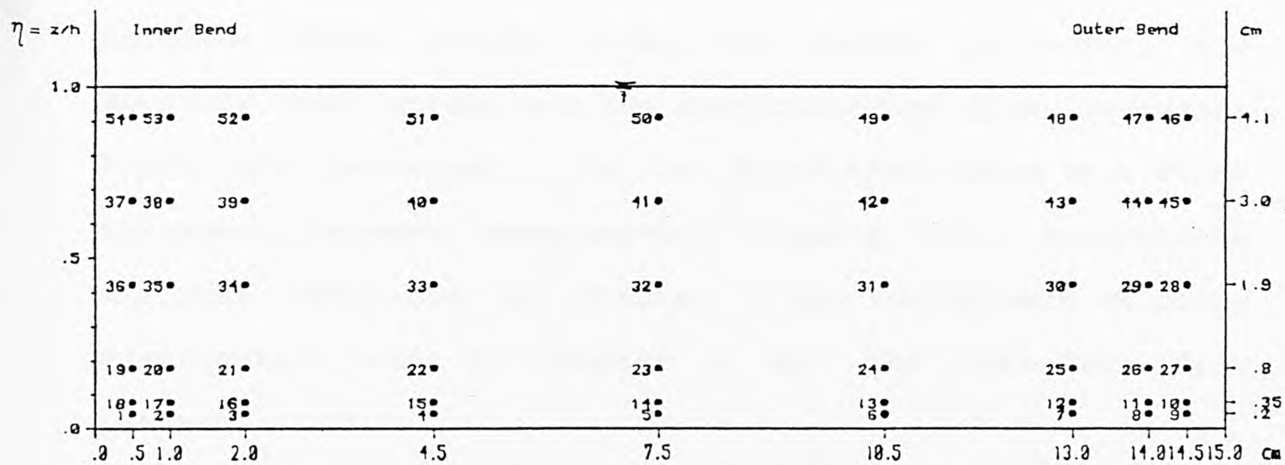

b). Uniform depth of flow = 0.045 M

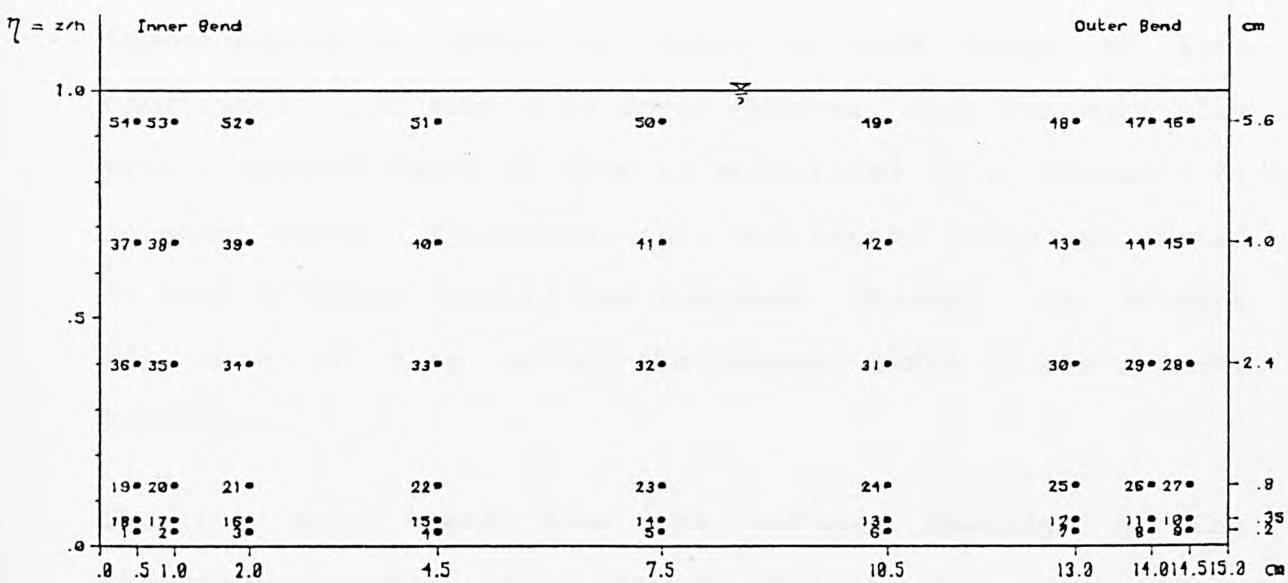

c). Uniform depth of flow = 0.060 M

Fig. 5.9 Grade framework and location of measurement points in the cross-section

CHAPTER 6

EXPERIMENTAL RESULTS AND DISCUSSION

6.1 General Introduction

Experimental results concerning the velocity distribution, boundary shear stress along the wetted perimeter, the Reynolds shear stress and the instability of flow (secondary flow) are presented. It is found that there is a close agreement between experimental results and theoretical analysis described in Chapter 2 for the forward velocity distribution and in Chapter 4 for the secondary flow pattern.

As mentioned earlier in Chapter 5, the experiments were conducted with three different flow rates in the present investigation in order to cover a wide range of flow conditions. It should be noted however, that for each flow rate a uniform depth of flow is maintained in a channel of constant width. Therefore, only the aspect ratio was varied in both U-shaped channel and S-shaped channel. No attempt was made to vary either the channel width or the channel curvature.

The raw data taken from the various readings of the experimental work on U-shaped channel are presented in Tables 6.1 to 6.12, while those on S-shaped channel are presented in Tables 6.13 to 6.36. Using the data presented in Tables 6.1 to 6.36, the velocity and the turbulence intensity distributions in three coordinate directions, the boundary shear stresses, the Reynolds shear stresses and the secondary flows were calculated. The tangential, vertical and radial velocity distributions are tabulated in Tables 6.1.a to 6.36.a, the corresponding intensity of turbulence are tabulated in Tables 6.1.b to 6.36.b, the Reynolds shear stresses are tabulated in Tables 6.1.c to 6.24.c. The results are presented in the graphs shown in Figs. 6.1 to 6.155.

On each graph the particulars relating to the flow are shown separately by specifying the discharge, channel width, uniform depth of flow and the mean velocity over the cross-section (i.e. discharge divided by cross-sectional area).

In most presentations of results, a non-dimensional presentation is preferable to any other as this will clearly show the comparison with a certain value which is considered to be the reference value. The reference value can be the maximum value or the average value of the experimental results. For this reason, the results are normalised by referring to the mean velocity over the cross-section in case of the mean and fluctuation velocity distributions, and referring to the average value of shear stress (obtained from the experimental results) while referring to the boundary shear stress distribution. Especially for the secondary flows, the results are presented in particular magnitude (cm/s) and direction (indicated by arrows). And of course, due to the smallness of their values, the length scale was introduced to enable the secondary flows to be read clearly.

The average values of the shear stress over each boundary, (i.e., the boundary along the inner wall of the channel, along the bottom of the channel and along the outer wall of the channel) were obtained by integrating the results over each boundary.

6.2 Velocity Distribution

Velocity measurements have been carried out by some previous workers on different grid frameworks of the measuring stations (location of measurements). For instance, Asfari (1966) measured the velocity nearest to the boundary at 5 cm from the wall and 10 cm from the bottom. Keerthisena (1983) measured the velocity nearest to the boundary at 5 cm from the wall and 1 cm from the bottom.

In the present investigation the velocity field is mapped in more detail. The author measured the velocity nearest to the boundary at 0.5 cm from the wall and 0.2 cm from the bottom with an accuracy of 0.5 mm.

6.2.1 Tangential velocity distributions and the intensities of turbulence

Measurement of local mean tangential velocities and the corresponding fluctuation velocities was carried out in the manner described in Chapter 5. The results are presented in Figs. 6.1 to 6.12 for the U-shaped channel and in Figs. 6.13 to 6.36 for the S-shaped channel.

a). The U-shaped channel

Figs. 6.1 to 6.3 clearly indicate that the non-uniform distribution of the local mean tangential velocity across the width is not symmetric to the longitudinal axis of the flow in a straight channel. A typical feature of the velocity distributions is that the velocities were smaller in the region near the centre-line of the stream than in the region near the walls, and this occurred for almost every depth of flow at the measuring stations in the cross-section of the channel.

The ratios of $\bar{u}/Um$ range from 0.4 to 1.25 for the value of η = 0.08 to 0.900 with the aspect ratio B/h of 6.00 (run no.1). The range of these ratios become smaller at the smaller aspect ratio, i.e., from 0.4 to 1.05 for the value of η = 0.044 to 0.911 with the aspect ratio of 3.33 (run no.2), and from 0.6 to 1.05 for the value of η = 0.033 to 0.933 with the aspect ratio of 2.50 (run no.3).

The maximum local mean velocity at a particular point is not always near the surface, especially at the region near the wall the value of η ranging from 0.4 - 0.6 has the maximum value of $\bar{u}/Um$ of about 0.8 to 1.1. Thus, at the region near the wall the vertical distribution of tangential velocities did not follow either the Prandtl's mixing length theory or the Power law theory.

The distribution of turbulence intensity seems to be dependent on the value of the Reynolds number. In Fig. 6.1.b, with the Reynolds number of 833 (which is considered to be a low turbulent flow), the turbulence intensities vary from 0.01 to 0.08 times the mean velocity. Figs. 6.2.b and 6.3.b show the decrease of the intensities to 0.05 times the mean velocity for the Reynolds number of 2083 and 3086 respectively.

In section U-2, for the angle of turning (θ) = 45°, due to the presence of the centrifugal force, the local mean velocity across the width is redistributed as shown in Fig. 6.4. Generally at the outer half of the bend the velocity is greater than at the inner half. The effect is more significant in the upper layers than in the lower layers of the cross-section. The range of the local mean velocity is about 0.4 to 1.15 near the centre-line region of the stream, 0.2 to 0.7 near the inner side of the bend and 0.4 to 1.3 at the outer side of the bend as can be seen in Fig. 6.4.a. When the aspect ratio decreases, (as shown in

Figs. 6.5.a and 6.6.a), the presence of the centrifugal force becomes less influential to the development of the flow and it has the tendency of having the greater velocity at the outer half of the bend only in the upper layers of the stream. The turbulence intensity distribution became more irregular with increased value of about 15% of the mean velocity in the range of Re = 833 to 2083, to about 8% of the mean velocity for Re = 3086.

When the flow negotiated 135^{o} of the curved channel, at section U-3 (Figs. 6.7 to 6.9), the distribution of the local mean tangential velocity was very much more developed compared to that at section U-2. Near the top layers (Fig. 6.7.a), shows that the local mean tangential velocities at the inner half of the bend varied from 0.3 to 0.5; in the centre-line region from 1.1 to 1.2; and at the outer half of the bend from 1.3 to 1.4 times the mean velocity. Figs. 6.8.a and 6.9.a reveal that at the lower aspect ratio, the distribution of the tangential velocity brought about by the effect of the channel curvature is weaker. From Figs. 6.7.b, 6.8.b and 6.9.b, one can observe that the turbulence intensities at section U-3 are generally slightly less compared to those at section U-2.

Considering the experimental results at section U-4 downstream of the bend, it can be seen from Figs. 6.10.a, 6.11.a, and 6.12.a that the tangential velocities in the outer half are still greater than those in the inner half of the bend similar to section U-3. This clearly indicates the presence of the residual effect of the strong secondary flows induced in the bend being carried into the straight portion of the channel and the same persists for a considerable length of the straight channel downstream of the bend.

The turbulence intensities seemed to increase considerably, especially in run no.1 at section U-4 (Fig. 6.10.b), where the turbulence intensity at measuring station 13 reached 20% of the mean velocity.

b). The S-shaped channel

The patterns of the tangential velocity distribution across the width of the S-shaped channel are presented in Fig. 6.13 to 6.36. Sections S-1, S-2 and S-3 actually had the same location as sections U-1, U-2 and U-3 of the U-shaped channel. Hence, theoretically, with the same flow rate, the pattern of the velocity field at sections S-1, S-2 and S-3 should be the same as that at sections U-1, U-2 and U-3 of the U-shaped channel. In terms of local mean tangential velocity, it can be seen from Figs. 6.13.a, 6.14.a and 6.15.a that the velocity distributions across the width have more or less similar patterns and magnitudes as those shown in Figs. 6.1 to 6.9. However, there exist some discrepancies which are generally less than 5% and presumably they are due to a small variation of the flow rate.

In section S-4, where the flow had negotiated 167.2^{o} of the curved channel, the distribution of the tangential velocity component became very significant as the flow was aproaching the fully developed phase. The greater velocities occurred in the flow with the highest aspect ratio of 6 (Fig.6.21.a), where the local mean velocities ranged from 0.4 to 0.75 at the inner half of the bend and from 0.7 to 1.49 at the outer half of the bend. Comparing Figs. 6.22 and 6.23 with the aspect ratio of 3.33 and 2.5 respectively, the distribution became less significant when the local mean velocities ranged from 0.5 to 0.80 at the inner half of the bend and from 0.7 to 1.22 at the outer half of the bend.
The turbulence intensities at section S-4 increased considerably in the three flow rates, up to 15% of the mean velocity at Re = 833, 12% at Re = 2083 and 11% at Re = 3086.

In a position symmetrical to section S-4, investigation was carried out at section S-5. The results are presented in Figs. 6.25 to 6.27. It can be observed that on the way to the crossover region, the distribution of the local mean tangential velocity was still developing. As a result, after the centrifugal force changed to the opposite direction, the development of secondary flow in the upstream bend also influenced the development of secondary flow at section S-5. This has produced the local mean velocities at the inner half of the bend from 0.6 to 1.6 times the mean velocity and at the outer half of the bend from 0.1 to 0.7 times the mean velocity (see Fig. 6.25.a).

Considering the experimental results at section S-6, where the flow negotiated 45^{o} of the second curved channel, the distribution of local mean tangential velocity across the width were generally still greater at the inner half of the bend than at the outer half of the bend, but the strength of the non-symmetry was less compared to that at section S-5. Surprisingly, at the higher aspect ratio (Fig .6.28.a), the process of the translocation of the distribution with the greater at the inner half than that at the outer half of the bend was faster at the lower aspect ratio (Figs. 6.29.a and 6.30.a).

The tangential turbulence intensity distributions at section S-6 (Figs. 6.28.b, 6.29.b and 6.30.b) vary from 10-20%, 8-12% and 6-10% with the corresponding aspect ratio of 6, 3.33 and 2.5 respectively, while in general, the turbulence intensities at the inner half of the bend are lower than those at the outer half of the bend.

At the bend of the S-shaped channel at section S-7, where the flow had already negotiated approximately 160.70^{o} of the downstream bend, the distribution of local mean tangential velocities showed greater values at the outer half than at the inner half of the bend. When comparing the experimental results at section S-7 and section S-4, [section S-4 has nearly the same radius of turning as the upstream bend (approximately 167.20^{o})], one can observe that the pattern of the distribution of local mean tangential velocity at section S-7 has deviated considerably. It can be concluded that the centrifugal force in section S-7 was not strong enough to eliminate the residual effect of secondary current induced in the upstream bend. Therefore, the strength of the non-symmetry of the distributions at section S-7 is generally less pronounced than that at section S-4. The same argument can be substantiated by comparing the results plotted in sections S-8 and U-4.

There is no difference in the patterns of turbulence intensity shown at sections S-7 and S-6.

The experimental results at section S-8 plotted in Figs. 6.34, 6.35 and 6.36 indicate the presence of the residual effect of the strong secondary flows induced in the upstream bend being carried into the straight portion of the channel and the same persists for a considerable distance into the straight channel downstream of the bend, showing greater velocities at the outer half of the bend than at the inner half.

The tangential intensity of turbulence at section S-8 (Figs. 6.34.b, 6.35.b and 6.36.b) shows that values of 2-10%, 2-6% and 2-6% for the corresponding aspect ratio of 6, 3.33 and 2.50 are generally smaller than in the upstream sections.

From the various experimental results discussed above, in general, the pattern of the local mean tangential velocity distribution across the width varies directly with the value of the aspect ratio (B/h) as well as the Reynolds number (Re). However, it is difficult to distinguish which one of these two factors has the more influence on the development of the local mean tangential velocity distribution across the width.

The tangential velocity distributions across the width of a channel closely agree with the results obtained by the solution of an equation proposed by Kochenikov (1946) and also Ali (1964) for the forced vortex. Figs. (6.1.a), (6.2.a) and (6.3.a) indicate that at the entry of the bend the flow does not appear symmetrically about the longitudinal axis of the channel. And then Figs. (6.4.a) to (6.12.a) indicate that at the bend of the channel the secondary circulation develops and breaks down the free vortex, providing the maximum velocity near the outer bank.

An approximate solution in the case of three dimensional flow suggests that due to the secondary flow components, the fluid particles travelling along the bend suffer vertical as well as radial displacements. Owing to these displacements, an exchange of momentum between separate currents takes place, and this alters the distribution of forward velocity around the bend. Unless the bend is very long, which is rarely the case in practice, no stable state of flow in curved channels, where it is justifiable to put $\frac{\partial v}{\partial \theta} = 0$, is maintained anywhere around the bend. Such an assumption is only made as a first step to an approximate solution.

The experimental results at the outer half gave speeds generally from 1.2 to 1.5 faster than the theoretical results, thus confirming the findings obtained by Rozovskii (1957). At the inner half of the channel the velocities were 0.6 to 0.8 slower than those obtained in the theoretical results.

Empirically, by introducing the factor F as a function of angle of turning, the radius of turning and the average depth of flow at a given cross-section in the form

$$F = \left[\frac{r_i}{Rm}\right]^{(\alpha - \alpha^2)\frac{r_o}{h}}$$

where $\alpha = \theta/360^\circ$

θ = angle of turning, (which varies from 0 - 360°)

and substituting into the Eq. (2.23.a), a closer agreement is obtained between the results obtained from the experiments and the results obtained from the above modified Eq. (2.23.a). The theoretical and experimental values at several cross-sections are presented in Fig. 6.37.

Another feature that may be seen from the experimental results shown in Figs. 6.1 to 6.36 is the vertical distribution of the tangential velocity in the centre-line of the eight cross-sections of the S-shaped channel. The distributions tend to follow Prandtl's logarithmic theory especially in runs no.2 and 3. The results plotted in Fig. 6.38, indicate that the assumption of the vertical distribution of tangential velocity following the logarithmic law (Eq. (2.4)) can be used in solving the equation of motion at a bend in a rectangular open chanel.

6.2.2 Vertical velocity distributions and the intensities of turbulence

Measurements of the vertical velocity component were not carried out at all frameworks on the grids. The results of local mean vertical velocities with the corresponding turbulence intensity measurements are plotted in Figs. 6.39 to 6.43 for the U-shaped channel, and Figs. 6.44 to 6.61 for the S-shaped channel for the three different flow rates.

a). The U-shaped channel

The existence of the vertical velocity components in curved channel flow when the flow has negotiated 45^{o} of the U-shaped channel is shown in Figs. 6.39.a, 6.40.a and 6.41.a. A general situation can be observed in Fig. 6.39.a where at the inner half of the bend the flow moves upwards, while at the outer half of the bend the flow moves downwards. The magnitude is of the order of 5% of the mean velocity. However, an amazing feature occurred in runs no.2

and 3, in which only a small part of the right side of the bend showed a downward movement of flow. The magnitude of the local mean vertical velocity in run no.2 (Fig. 6.40.a) varied from 3-4% of the mean velocity at the inner half of the bend (with upward motion), 8-10% of the mean velocity in the centre-line region (with upward motion) and 1-2% of the mean velocity at the outer half of the bend (with downward motion). In run no.3 (Fig. 6.41.a), the magnitudes varied 5-12%,10-20% and 2-6% of the mean velocity at the inner half of the bend (with upward motion), near the centre-line region (with upward motion) and at the outer half of the bend (with downward motion) respectively.

The turbulence intensities at this particular cross-section varied from 1-7% of the mean velocity for the three different runs. In general, the further up the layer, the higher the turbulence intensities, except in run no.1 where the lowest layer has the highest turbulence intensity with a magnitude of 9% of the mean velocity.

The local mean vertical velocities with the corresponding turbulence intensities in section U-3 (when the flow had negotiated 135^{o} of the U-shaped channel) are shown in Figs. 6.42 to 6.44. In general, the magnitudes are much smaller compared to those in section U-2, and of the order of 0-2%, 0-8% and 0-9% of the mean velocity for runs no.1, no.2 and no.3 respectively. A special feature can be observed from Figs. 6.43.a and 6.44.a that the vertical velocity is upwards at the inner side of the bend and at the outer side of the bend, while in the region near the centre-line the flow moves downwards. This indicates that there is a two-cell pattern of secondary flow in section U-3.

Having observed the turbulence intensity results at section U-3, the magnitudes are also generally smaller compared to those at section U-2, and they are of the order of 0.5-4% of the mean velocity. The higher values are not always found in the upper layer.

b). The S-shaped channel

In the S-shaped channel, at section S-2, where the flow had negotiated 45^{o} downstream of bend forming the S-shaped channel, a single-cell pattern was formed in the three runs (see Figs. 6.45.a, 6.46.a and 6.47.a). The results of the local mean vertical velocity in run no.1 are much smaller than those in runs no.2 and no.3 with magnitudes in the order of 0-5%, 0-10% and 0-15% of the mean velocity respectively.

The turbulence intensity at section S-2 in run no.1 (Fig. 6.45.b) shows considerably high variation of 12% in the upper layer where $\eta = 0.6$. With a higher flow rate, the turbulence intensity tends to be smaller, as seen in Figs. 4.46.b and 6.47.b which varied from 0-4% of the mean velocity.

Having observed the experimental results obtained in sections S-3 and S-4, when the flow had negotiated 135^{o} and 167.2^{o} respectively in the upstream portion of the S-shaped channel it can be concluded that a two cell pattern of secondary flow generally dominates the situation, with the local mean vertical velocity components of the order of 0-8% of the mean velocity at both sections.

The turbulence intensity in section S-3 has more or less the same magnitude as that in section S-2. In section S-4, which is the cross-over region, the turbulence intensity increased considerably over the three runs, with magnitudes in the order of 0-12%, 0-7% and 0-7.5% for runs no.1, no.2 and no.3 respectively.

When the flow entered the downstream bend of the S-shaped channel, the strength of the secondary flow from the upstream bend was introduced into the downstream bend. As a result, at section S-5, the secondary flow appeared with vertical velocities at the inner side of the bend which were moving downwards, whilst at the outer side of the bend they were moving upwards (see Fig. 6.54.a). A two-cell pattern also appeared at this section during runs no.2 and no.3 (see Figs. 6.55.a and 6.56.a), but the direction had changed compared to that at section S-4. The magnitudes of the local mean vertical velocity components are more or less the same as those at section S-4, i.e. in the order of 0-8% of the mean velocity.

The turbulence intensities in this section are very high, and they are of 4-13%, 1-8% and 1-6.5% of the mean velocity for runs no.1, no.2 and no.3 respectively. It is clear that in the section near the crossover region the turbulence intensity or the fluctuation velocity becomes very high, especially at the higher aspect ratio. It should be noted that section S-5 has an angle of turning of 12.80° of the downstream bend of the S-shaped channel, symmetrical to the crossover region with section S-4 in the upstream bend.

In section S-6 (Figs. 6.57.a, 6.58.a, and 6.59.a), where the strength of the secondary flow introduced from the upstream to the downstream bend was less, in general, the cellular pattern remained the same as in section S-5, but in terms of the magnitudes, the values generally decreased. Surprisingly, the distributions of turbulence intensity in this section remained high during the three different runs, as well as in the section near the crossover region.

Finally, at section S-7, where the flow had negotiated 160.70° of the downstream bend, the cellular pattern was no longer affected by the strength of the secondary flow produced by the upstream bend. As a result, the upward velocity at the inner side of the bend and the downward velocity at the outer side of the bend occurred again (see Figs. 6.60.a, 6.61.a and 6.62.a). The magnitudes of the local mean vertical velocity component varied from 0-10%, 0-5% and 0-5% of the mean velocity in runs no.1, no.2 and no.3 respectively. Only run no.1 had a high turbulence intensity of 1-12%, whilst runs no.2 and no.3 had a turbulence intensity of 2-8% of the mean velocity.

From the above discussion of the experimental results, one can conclude that the vertical velocity distribution across the width is not always symmetrical and that the cellular pattern is not always of single-cell form.

In this investigation, the values of local mean vertical velocity components generally varied from 1-10% and the vertical velocity fluctuation (vertical turbulence intensity) also varied from 1-10%. The breaking down of the strength of the secondary flow induced by the upstream bend took place just after the flow has negotiated 45^{o} of the downstream bend.

6.2.3 Radial velocity distributions and the intensities of turbulence

The results of the local mean radial velocity component measurement of the U-shaped channel are presented in Figs. 6.63 to 6.68, and of the S-shaped channel are presented in Figs. 6.69 to 6.86. The positive flows indicate the outward motion and the negative flow indicate the inward motion.

a) The U-shaped channel

Due to the centripetal acceleration the water particles in a vertical experience the same radial pressure gradient. The centripetal acceleration required to keep the particles following in a circular path, however, is greater near the surface than near the bottom due to the non-uniform velocity distribution. Theoretically, therefore, near the surface the water particles tend to move outwards, while near the bottom they tend to move inwards. The experimental results shown in Figs. 6.63 to 6.68 for the U-shaped channel generally agree with the behaviour of the secondary flow, as described above. The magnitudes of the local mean radial velocity component varied from 0-15% of the mean velocity with a greater radial velocity at the region near the centre-line than in the region away from it. The irregularity of the distribution of local mean radial velocity in a certain layer which has some positive values and some negative values, indicates the presence of a non single cell pattern of secondary flow.

In general, the turbulence intensities varied from 0-5% of the mean velocity, except in section U-2 for runs no.1 and no.2 (Figs. 6.63.b and 6.64.b). At some frameworks on the grids the turbulence intensities increased to 17% of the mean velocity.

Comparing the experimental results at section U-2 and S-2 where the flow had negotiated 45^{o} of the U-shaped channel and the upstream bend of the S-shaped channel, the patterns of the local mean radial velocity distribution were more or less the same in both sections, with the flow moving inwards near the bottom and outwards near the surface. In terms of magnitudes, there were some deviations but these were considered to be minimal (see Figs. 6.63.a, 6.64.a and 6.65.a for section U-2, and Figs. 6.69.a, 6.70.a and 6.71.a for section S-2).
The distributions of radial turbulence intensity in section S-2 are indeed very irregular across the channel width, and the magnitudes varied from 2 to 15% of the mean velocity.

At sections S-3 and S-4, where the flow had negotiated 135^{o} and 167.20^{o} respectively of the upstream bend of the S-shaped channel, despite some deviations, the major feature persists, i.e. the presence of the non single cell pattern is more obvious. Comparing the magnitudes of local mean radial velocity at sections S-3 and S-4 with those at sections S-2, in general, sections S-3 and S-4 had smaller values than those in section S-2.

At the cross-sections in the downstream bend portion of the S-shaped channel, i.e. in sections S-5, S-6 and S-7, the distribution of radial velocity across the channel width was very complex. As the flow passed the crossover region, the centripetal acceleration changed in direction and attempted to cause the water particles to move inwards near the bottom and to move outwards near the surface. At the same time, the influence of the secondary flow resulting from the upstream bend, also contributed to the development of the radial velocity component at sections S-5, S-6 and S-7. As a result, the water particles near the bottom still tend to move outwards while those near the surface tend to move inwards. In section S-5 (Figs. 6.78.a, 6.79.a and 6.80.a), surprisingly, the radial velocity distributions did not follow the above pattern. Even in the layers near the bottom, the water particles tended to move inwards as well as in the layers near the surface, and only in a very small region near the outer wall did the water particles move outwards. Furthermore, the complexity of the local mean radial velocities increased as the flow negotiated 45^{o} of the downstream bend portion of the S-shaped channel, i.e. at section S-6. It can be observed that the water particles moved outwards at almost every position on the grid of the cross-section. By comparing these results to those in section S-5, it can be concluded that from the cross-section after the crossover region up to the cross-section where the flow had negotiated to 45^{o} of the downstream bend portion of the S-shaped channel, there is a gradual transfer of lateral momentum direction. As a result, in this particular region the radial and vertical flows change direction.

Finally, at section S-7, where the flow had negotiated 160.70° of the downstream bend portion of the S-shaped channel, the major feature, that the water particles near the surface move outwards while those near the bottom move inwards occurred again (see Fig. 6.84.a). This indicates that in section S-7, the influence of the secondary flow being induced from the upstream bend portion to the downstream bend portion of the S-shaped channel has been broken down.

A comparison between the experimental results and theoretical results from Eq. (4.1) is presented in Fig. 6.87 by assuming that the development of secondary flow has reached its full stage at sections U-2, U-3 and S-2. S-3 and S-4. Theoretically (according to Eq. (3.12)), in the cross-section where the flow had negotiated 45° and 135° for example, with the uniform depth of flow = 0.025 m (run no.1), the growth of the transverse circulation has only reached 28% and 63% of the full stage. Hence, if this is taken into consideration, the theoretical results should have been multiplied by 0.28 and 0.63 based on the angle of turning of the corresponding cross-sections under investigation. The experimental results of the three different rates of flow for sections U-2, U-3, S-2 and S-3 are compared with the theoretical results.

It can be seen in Fig. 6.87 that in the three different runs there is a close agreement in the values of the $\frac{u}{Um} \times \frac{Rm}{h}$

6.3 Isovels of the Velocity Distribution in the Flow Direction and Boundary Shear Stress

Experimental results of the local mean tangential velocity were plotted in the form of isovels and the boundary shear stresses were calculated from the results obtained from the measurement of local mean tangential velocity at the grid points near the channel boundary according to the method described in Chapter 4 (Eq. (4.10)).

Results from the U-shaped channel were presented in Figs. 6.88 to 6.99 and those from the S-shaped channel were presented in Figs. 6.100 to 6.123. At the straight approach portion (section U-1 of the U-shaped channel, run no.1), the pattern of the isovels provides an explanation for the stable motion over the cross-section. The mean shear stress along the inner wall, the bottom boundary and the outer wall is found to be 0.026 N/m^2, 0.138 N/m^2 and 0.029 N/m^2 respectively (see Fig. 6.88). When the flow rate is increased (runs no.2 and no.3), stable motion changed and some instability near the outer wall was observed. The magnitudes of the mean shear stress increased up to 0.045 N/m^2, 0.194 N/m^2 and 0.053 N/m^2 for run no.2 and up to 0.044 N/m^2, 0.193 N/m^2 and 0.044 N/m^2 for run no.3 along the inner wall, the bottom and the outer wall respectively.

Unstable flow appeared near the outer wall when the flow negotiated 45° of the U-shaped channel. The shear stress at this section also increased and had a greater value at the outer wall than at the inner wall. The distribution of the shear stress along the bottom boundary produced a greater value at the outer side than at the inner side of the bend. If the results obtained from the approach straight channel are compared with section U-2, the overall mean shear stress along the channel boundary increased from 0.110 N/m^2 to 0.124 N/m^2 in run no.1, from 0.140 N/m^2 to 0.232 N/m^2 in run no.2, and from 0.127 N/m^2 to 0.217 N/m^2 in run no.3.
If special attention is given to the isovels formed in section U-2, one can observe that the greatest influence on the creation of unstable motion near the outer wall, occurs in run no.1. This feature is more visible when we observe the results shown in Figs. 6.94, 6.95 and 6.96 of section U-3, where the flow has negotiated 135° of the U-shaped channel.

The overall mean shear stress along the channel boundary in section U-3 is 0.120 N/m^2, 0.127 N/m^2 and 0.195 N/m^2 in runs no.1, no.2 and no.3 respectively, and in comparison with those in section U-2 the deviation is very small. When comparing the experimental results in section U-1 upstream of the bend and section U-4 downstream of the bend of the U-shaped channel, it can be seen that the forward velocity distribution in section U-4 was not symmetrical across the width when compared to that in section U-1. The unstable motion near the outer wall in section U-4 is very obvious especially in run no.1. An overview of all the results from section U-4 in run no.1, no.2 and no.3 indicates reliably the presence of strong secondary currents induced at the bend and carried into the straight portion of the channel. The same persists for a considerable distance in the straight channel downstream of the bend. The overall mean shear stress along the channel boundary in section U-4 is 0.090 N/m^2, 0.205 N/m^2 and 0.318 N/m^2 in runs no.1, no.2 and no.3 respectively.

From the various values of boundary shear stress obtained from the U-shaped channel for the three different runs, it can be said in general, that the greater the flow rate, the greater the overall mean value of shear stress along the channel boundary. The most striking feature of the pattern of the distribution of the shear stress along the boundary is that near the area of stable motion, the shear stress is relatively smaller than that near the area of unstable motion.

The decay of the transverse circulation as expressed in Eq. (3.8) indicates that the helical pattern should disappear in the cross-sections in the straight portion of the channel downstream of the bend at a distance x from the bend, where x approximates to 2.24 m, 4.041 m and 5.39 m in runs no.1, no.2 and no.3 respectively. If the results in section U-4 of the U-shaped channel and section S-8 of the S-shaped channel are compared, it can be seen that the secondary flow in section S-8 in general is less strong than that in section U-4. This is due to the strength of the secondary current in the upstream portion of the bend which is introduced into the downstream bend portion of the S-shaped channel. If section U-4 is considered, where the flow has reached a point 50 cm downstream from the bend, the strength of the secondary current should theoretically (see Eq. 3.33 and Fig. 4.3) have decayed to 35.85%, 56.56% and 65,22% of the fully developed stage of the secondary current in runs no.1, no.2 and no.3 respectively. However, only one cross-section was investigated in the straight portion downstream from the bend, and in any case the length was too short to enable the author to make a comparison between the theoretical and the experimental results of the decay of transverse circulation.

6.4 Secondary Flow Patterns

The experimental results obtained from the local mean radial velocity and local mean vertical velocity measurement were then plotted as resultants of the two components in the r and z directions. Thus the magnitude and direction of the flow at a given cross-section were obtained.

As has already been discussed in Part 6.2.2 and Part 6.2.3 of this chapter, the magnitudes of the local mean vertical velocities varied about 10-15% of the mean velocity as well as the local mean radial velocity. The resultants of the two components accordingly varied about 14-21% of the mean velocity.

Instead of being presented in terms of the ratio to the mean velocity, the secondary flow patterns presented in Figs. 6.124 to 6.131 are given in terms of velocity units, i.e. cm/sec.

In some cross-sections, i.e. cross-sections U-2, U-3 on the three different runs, section S-6 on run no.2 and section S-7 on run no.1, photographs were taken to identify the secondary flow pattern. The results are presented in Plates 6.1, 6.2 and 6.3

Observed results presented in section U-2 of the U-shaped channel, Fig. 6.124, clearly indicate that cellular patterns tend to move inwards near the bottom and outwards near the surface in the three different runs. In run no.1, a small cellular pattern arose at the top right corner of the section with a velocity of about 0.4 cm/s, whilst near the bottom the transverse circulation had a velocity of about 0.8 cm/s. The transverse circulation became very complex in runs no.2 and no.3 because in the region near the central vertical a high vertical velocity of about 1.00 cm/s in run no.2 and 2.00 cm/s in run no.3. If the experimental results of sections U-2 and U-3 are compared, the transverse circulation in section U-3 was generally less complex than that in section U-2, besides the magnitudes were smaller than those in section U-2 with a maximum of 0.3, 0.5 and 0.8 cm/s in runs no.1, no.2 and no.3 respectively. The existence of the second cell pattern can clearly be seen in runs no.2 and no.3 in section U-3, near the top corner of the outer wall of the bend.

Having observed the photographic results in Plates 6.1 and 6.2, the cellular patterns seemed to be of non single-cell form. The second cell always tended to appear near the top corner of the outer wall of the bend. It should be noted here that the experimental results of the transverse component of local mean velocity and photographic observations were carried out at a different times. As a result, there may be some small deviation in the secondary flow pattern obtained in both cases. If a comparison is made between the experimental results in sections U-2 and U-3 and the corresponding photographic results in those sections, one can appreciate that the magnitudes (and also the existence of the secondary cell pattern) of the transverse circulations varied a little over the time.

In section S-2 (Fig. 6.26) of the S-shaped channel the transverse circulation tended to be of a single cell pattern, except in run no.1 where the second cell pattern appeared near the top corner of the outer wall of the channel similar to that in section U-2 of run no.1. By comparing the results in section U-2 and S-2 in run no.1 and no.3, generally, a more sensible pattern can be found in section S-2 as in the region near the central vertical the water particles did not move upwards.

The transverse circulation in section S-3 is rather weaker than that in section S-2, but compared to that at section U-3, the strength of the transverse circulation or secondary current did not deviate very much. The tendency of non single-cell pattern was more obvious in section S-3 than in section S-2. In the last observation section of the upstream bend part of the S-shaped channel (section S-4, Fig. 6.128), the pattern was again not a single cell and the second cell appeared bigger than that in section S-3.

From the above discussion of the experimental results, it can be said that in general, cell patterns of the secondary current in the single bend of a rectangular open channel depend on the angle of turning. The possibility of producing more than one cell pattern increases with the greater angle of turning.

Very complex secondary flow patterns can be seen in sections S-5 and S-6 of the downstream portion of the S-shaped channel (Figs. 6.129 and 6.130). Apparently, the flow tended to circulate toward the inner wall of the bend in section S-5, and then gradually tended to circulate toward the outer wall of the bend. A second cell appeared near the bottom corner of the inner wall of the bend in section S-5 and near the top corner of the outer wall of the bend in section S-6 except in run no.3 where the cellular pattern was very irregular with more than one cell.

The secondary flow patterns, which can be seen in sections S-5 and S-6, are discussed in Part 6.2.3 of this chapter. In the region between sections S-5 and S-6, there took place a gradual change in the flow direction. The photographic results of the secondary flow pattern in section S-6 in runs no.1 and no.2 presented in Plate 6.3 provide a further indication of the complexity of the secondary flow pattern in section S-6.

Finally, at section S-7 (Fig. 6.131), where the flow had negotiated 160.70° of the downstream bend portion of the S-shaped channel, the secondary flow pattern became normal, near the bottom where the water particles moved inwards and near the surface they moved outwards. The second cell pattern was still apparent in this section, and tended to occur near the top corner of the outer wall of the bend. If the results at sections S-7 and U-3 are compared, it can be seen that the secondary currents at section S-7 were rather weaker than those at section S-6, whereas at section U-3 they were much weaker than those at section S-6. This, again, indicates that the strength of the secondary current induced in the upstream bend portion which was subsequently carried into the downstream portion of the S-shaped channel has been broken down on approaching section S-7 and no longer affects the development of secondary flow in the sections thereafter.

6.5 Reynolds Stress Distributions

The Reynolds stresses formed by the tangential and vertical velocity fluctuations ($\overline{v'w'}$) and by the tangential and radial velocity fluctuations ($\overline{v'u'}$) are presented in the form of the ratio with the square of the mean velocity. The results are plotted in Figs. 6.132 to 6.137 for the U-shaped channel and Figs. 6.138 to 6.155 for S-shaped channel.

Figs. 6.132 to 6.137 show that the Reynolds stress patterns in the two sections of the U-shaped channel were very irregular. In general, the values of $\overline{v'w'}/Um^2$ and $\overline{v'u'}/Um^2$ varied from -0.01 to +0.01. Lower values of $\overline{v'w'}/Um^2$ and $\overline{v'u'}/Um^2$ containing positive and negative values appeared in the cross-sections of the S-shaped channel with magnitudes of less than 0.008, except at section S-2 for run no.1 (Fig. 6.138) which had relatively high values of the two Reynolds stresses of about 0.015.

At section S-5 in run no.1 (Fig. 6.147.b), the magnitude of the Reynolds stress is about 0.009 and there were no positive values. Comparing the results of section S-5 with section S-4 (Fig. 6.146.b), it can be noticed that the positive values of the Reynolds stress $\overline{v'u'}$ were present in section S-4, even though they are of small magnitude. From this observation at these two sections, it can be seen that generally the patterns of secondary currents at section S-4 were more regular than at section S-5. The negative and positive values of the Reynolds stresses indicate that the secondary flow is more regular with a tendency to give a single cell pattern. However, such behaviour is weaker at the higher Reynolds number which is evident from Figs. 6.148 and 6.149, and also from Figs. 6.130 and 6.131.

Finally, at sections S-6 and S-7, the negative values of $\overline{v'w'}/Um^2$ (0.00 to -0.01) persisted with lower values occurring at higher Reynolds numbers. On the contrary, the values of $\overline{v'u'}/Um^2$ in sections S-6 and S-7 were dominantly positive, with values less than 0.01, except at section S-7 for runs no.2 and no.3 (Figs. 6.154 and 6.155) the value of $\overline{v'u'}/Um^2$ varied from 0.00 to -0.005.

From the complex nature of the turbulence characteristics discussed above, it can be inferred that the secondary motion in the turbulent case is responsible for the cross-stream convection of Reynolds stress and for high turbulence-energy fluid being driven from the outer side region towards the inner side region of the bend.

CHAPTER 7

CONCLUSIONS AND SUGGESTIONS FOR FURTHER RESEARCH

7.1 Conclusions

A detailed study was made of the velocity distributions at a bend in a rectangular open channel and experiments were carried out on the measurement of mean and fluctuation velocities in three coordinate directions over the various depths of the stream. From the analysis of the results, following conclusions can be drawn :

1. The tangential velocity component distributions across the width of straight approach channels for both U-shape and S-shape channels depend on the the Reynolds number of the flow. A lower Reynolds number indicates that there is a stronger tendency for slower velocity near the boundary than near the midstream region of the flow. The difference is more significant in the upper layers than in the lower layers of the flow.

   The vertical distribution of tangential velocity at different points across the width in the cross-section of the straight approach channel is generally non-uniform but it does not exactly follow the logarithmic velocity distribution law. In a curved plane stream, the maximum tangential velocity at any cross-section does not occur near the surface. This is attributable to the effect of secondary currents developing in the flow. The maximum tangential velocity at any cross-section in any uniform depth of flow occurs near the outer wall of the cross-section of a straight portion downstream of the bend in the U-shaped channel and also near the inner wall of the cross-section downstream from the crossover region of the S-shaped channel. A reasonably accurate numerical solution based on two dimensional flow (depth-averaged main flow) analysis can be obtained by the use of program MFAD1. However, in the region of the side walls of a wide stream, this method fails to give satisfactory results.

2. The distribution of the tangential velocity is inwardly skewed in the transverse direction, giving greater values near the outer wall, and lower values near the inner wall. The effects are less pronounced in the

region near the entrance to the bend in U-shaped and S-shaped channels.

3. The vertical velocity components appear at the bend with the magnitudes of 0-10% of the mean velocity, and generally, with upward motion near the inner wall and downward motion near the outer wall of the bend. In the region near the crossover of the S-shaped channel the distributions occur conversely, with downward motion near the inner wall and upward motion near the outer wall of the bend. Some complex features may occur in the region near the top corner of the outer wall of the bend which contribute to the creation of the second cell pattern. Unlike the vertical velocity component, the radial velocity component produces the greatest magnitudes of the order of 17% of the mean velocity. In general, near the surface the particles move outwards and near the bottom they move inwards, except in the region near the crossover of the S-shaped channel, where the change in direction of transverse velocity occurs. The main cell pattern of secondary flow has magnitude of 21% of the mean velocity, whereas the second cell pattern, which is not always present, has magnitude of 4% of the mean velocity

   Photographs taken of the same flows and locations but at different times showed some differences in the distribution of the cellular pattern over the cross-sections. The photographs taken at some cross-section uphold the suggestion that spiral motion around bends is slightly unstable.

4. In the region near the bend entrances of U-shaped and S-shaped channels the secondary flow is more pronounced near the outer wall than near the inner wall and stronger near the bed than near the free surface. In addition a unidirectional radially inward motion is seen to prevail. Secondary flow gradually develops at the region of the inner wall, leading to a single vortex pattern towards the latter part of the bend. The secondary flow is weaker but the development and decay are delayed at high aspect ratios and Froude numbers.

5. The distribution of the turbulence intensities varies from 2-20% of the mean velocity, and in general, the higher the Reynolds numbers the higher the turbulence intensities. The pattern of the turbulence intensity distribution is very complex, and thus indicates the complex nature of secondary flow. A high turbulence intensity seems to be responsible for the creation of unstable motion due to concave curvature effects at the outer bend of a channel.

6. In a U-shaped channel unstable or agitated motions occur near the outer wall and stable motion near the inner wall. The deformation of the main velocity

distribution is revealed by the rotation of the main velocity isovels, inwards and outwards, corresponding to the effect of stream wise acceleration and secondary flow convections. Shear stress peaks occur near the unstable motions, thus further supporting the fact that agitated motion at the outer part of the wall consequently changes the entire configuration of a natural water course by dislodging material there and eventually transporting and depositing the eroded material at the inner wall downstream of the bend.

The residual effect of the strong secondary current induced in the bend being carried into the straight portion of the channel which persists for a considerable distance along the straight channel downstream of the bend. In the S-shaped channel, strong induced currents at the upstream of the bend are weakened at the downstream of the bend as a result of the change in the direction of centrifugal force. In the region slightly downstream from the crossover the obliquity of the flow is gradually displaced. In addition helical motion and the velocities near the inner wall decrease while near the outer wall they increase. The velocities are greater near the outer wall than near the inner wall. As the flow negotiates about 45^{o} of the upstream bend of the S-shaped channel with the higher aspect ratio the obliquity development process is faster.

7. The shear stress peak is in the order of 1.5 times the overall mean shear stress along the channel boundary of a given section and takes place near the channel bed where the flow motion is unstable. Over the whole length of a channel, the maximum shear stress occurs in the cross-section near the end of the bend of the U-shaped channel, and in the cross-section downstream near the crossover of the S-shaped channel.

8. Secondary flow patterns may exist containing a single-cell pattern and a two-cell pattern (the second cell generally exists in magnitudes which are much smaller than the main cell). The single-cell and main cell of the two-cell pattern have magnitudes of about 14-21% of the mean velocity and may vary with time. Photographic techniques which enabled the secondary flow to be revealed continuously would provide a better understanding of the behaviour of the secondary flow in relation to time variation.

9. The persistence of transverse circulation in a straight channel downstream from the bend is revealed by the streamwise vorticity contour which occurs near the outer wall. It was not revealed whether the transverse circulation occurs in the phase of development or in the phase of decay.

10. The present investigation demonstrates that the LDA system can be used successfully to measure the three components of mean velocity. The results concerning the average velocity can be obtained from the integration of main velocity profiles. These are in good agreement with the mean velocity obtained from the flow rate measurement. The discrepancies are less than 5% of the mean velocity.

A laser anemometer employing frequency shift can be made to respond to the sign of the velocity direction and operate satisfactorily in regions of very low or even zero mean velocity. Therefore, the direction of small secondary components can easily be measured.

Uncertainty arises in the measurement of turbulence flow parameters as the readings always fluctuate greatly. A large number of R.M.S readings need to be taken and analysed using a statistical approach if adequate electronic instrumentation is not available to measure the R.M.S.

7.2 Suggestions for Further Research

A series of experiments, investigating compound bend channels under a wide range of flow conditions and with varying curvature ratios is still needed to remedy the present lack of understanding of the influence of channel configurations, such as curvature ratio and of flow parameters, such aspect ratio and the Reynolds number of the flow. Further investigation of the various cross-sections in the straight channel downstream of the bend will be desirable.

Detailed information is needed on the Reynolds stresses and secondary flows, in order to gain a better understanding of the physical processes governing flow in compound bends. Comprehensive and systematic investigations are important to isolate the effects of parameters such as channel roughness, longitudinal bed slope, transverse bed slope, side wall slope, taken individually, and determine the effect of channel curvature and channel width, before attempting to understand the flow in alluvial meander bends. In this case complex interactions occur between the flow and the bed topography and even the deformation of the channel boundary which may cause the deformation of the channel configuration during the flow process. The characteristics of flow in curved channels in correlation with turbulent flow parameters and Reynolds number is still incomplete. Further study of this subject with a wider range of Reynolds number will also be desirable.

An investigation on idealized meandering flumes can still be conducted by considering the factors which may affect the development of flow in practice. These include the channel boundary roughness, sediment concentration and river engineering works (bridge piers, groynes, checkdams, etc). Such an extensive experimental programme could also provide the much needed data for the verification of computational models which are finding increasing application today.

Engineering Applications.

It is often necessary to build river training works along the banks of a river (e.g. revetment, lining etc.) or in the river across the stream (e.g. groynes, checkdams etc.), not only to improve unfavourable stream patterns but also to stabilize the river. When dealing with a purely meandering type of river, an understanding of the flow is necessary in locating structures such as these. A knowledge of the behaviour of flow in open channel bends as presented in this study may be used as the first guidance in determining the location of the river training works, and also in designing them. When the measurement of the flow velocity in the river cannot be carried out, the estimated flow velocity may be obtained from program 'MFAD1' for determining the distribution of the main flow velocity, and program 'UBOUW' for determining the transverse circulation. Such contribution is also a means as reducing the river investigation works.

REFERENCES

1. Ali, K.S.A.S., 1964, Flow dynamics in trapezoidal open channel bends, Ph.D. Thesis, Colorado State University

2. Ananyan, A.K., 1957, Fluid flow in bends of conduits, Israel Programme of Scientific Translations, Jerusalem

3. Apmann, R.P., 1972, Flow processes in open channel bends, Proc. ASCE, J. Hydr. Div., HY5, p.795

4. Asfari, A.F., 1968, Secondary flow in river bends, Ph.D. Thesis, University of London

5. Bathurst, J.C., Thorne, C.R. and Hey, R.D., 1979, Secondary flow and shear stress at river bends, Proc. ASCE, J. Hydr. Div., HY10, p.1277

6. Boumeester, j., 1972, Basic Principles for the movement of water in natural and artificial water courses, Part II. Delt Univ. of Technol., Internal note.

7. Chacinski, T.M.P., 1956, The secondary flow in meandering channel, Ph.D. Thesis, University of London

8. Choudary, U.K. and Narasimhan, S., 1977, Flow in 180° open channel rigid boundary bends, Proc. ASCE, J. Hydr. Div. HY6, p. 651

9. Chow, V.T., 1959, Open Channel Hydraulics, Mc Graw-Hill Book Co., Inc., New York

10. De Vriend, H.J., 1976, A mathematical model of steady flow in curved shallow channels, Comm. on Hydraulics, Delft Univ. of Technology Rept. No. 76-1

11. De Vriend, H.J., 1977, A mathematical model of a steady flow in curved shallow channels, J. Hydr. Res., 15(1), p.37

12. De Vriend, H.J., 1981a, Velocity redistribution in curved rectangular channels, J. Fluid Mech., 107, p.423

13. Jansen, P.Ph., Bendegom, L.v., Berg, J.v.d, Vries, M.d. and Zanen, A., 1979, Principles of river engineering, Pitman Publishing Ltd.

14. Drain, L.E., 1980, The Laser Doppler technique, John Wiley and Sons

15. Durst, F., Melling, A. and Whitelaw, J.H., 1981, Principles and practice of Laser Doppler Anemometry, second edition, Academic Press Inc., (London) Ltd.

16. Eskinazi, S., An investigation of fully developed turbulent flow in curved channel, A report to the office of Naval Research Mechanics Branch, The Johns Hopkins University

17. Engelund, F., 1975, Instability of flow in a curved alluvial channel, J. Fluid Mechanics, 72, 1, p.145

18. Falcon, M. and Kennedy, J.F., 1983, Flow in alluvial-river curves, J. Fluid Mechanics, Jan.

19. Francis, J.R.D., and Asfari, A.F., 1971, Velocity distributions in wide curved open channel flows, J. Hydr. Res., 9(1), p.73

20. Gotz, W., 1980, Discussion of paper by Bathurst, Thorne and Hey (1979), Proc. ASCE, J. Hydr. Div. HY10, p. 1710

21. Hinze, J.O., 1967, Secondary currents in wall turbulence, In Proc. Int. Symp., Boundary Layers and Turbulence, Kyoto, 1966, also : Physics of Fluids supply., 10, 9, part 2, S122-S125

22. Hooke, R.L., 1974, Shear stress and sediment distribution in a meander bend, UNGI, No.30, University of Uppsala, Sweden

23. Humphrey, J.A.C., Taylor, A.M.K. and Whitlaw, J.H., 1977, Laminar flow in a square duct of strength curvature, J. Fluid Mechanics, 83, 509

24. Humphrey, J.A.C., Whitelaw, J.H. and Yee, G., 198l, Turbulent Flow in a square duct with strong curvature, J. Fluid Mech. 103, p. 443

25. Ippen, A.T., Drinker, P.A., Jobin, W.R. and Noutsopoulus, G.K., 1960, The distribution of boundary shear stress in curved trapezoidal channels, Tech. Reprt No. 43, Hydrodynamics Laboratory, MIT, Cambridge, Mass.

26. Ippen, A.T.and Drinker, P.A., 1962, Boundary shear stress in curved trapezoidal channels, Proc. ASCE, J. Hydr. Div., 88, HY5, p. 143

27. Kalkwijk, J.P. Th and De Vriend, H.J., 1980, Computation of the flow in shallow river bends, J. Hydr. Res., 18(4), p.327

28. Keerthisena, H.H.J., 1982, Flow in S-shaped open channel bends, Ph.D. Thesis, University of Paradeniya, Sri Lanka.

29. Kelly L.G., 1967, Handbook of numerical method and applications, Addison-Wesley Publishing Company

30. Knight, D.W. and Macdonald, J.A., 1979, Open channel flow with varying bed roughness, Proc. ASCE, J. Hydr. Div., 105, HY9, p.1167

31. Knight, D.W., 1981, Boundary shear in smooth and rough channels, Proc. ASCE, J. Hydr. Div., 107, HY7, p.839

32. Knight, D.W. and Hamed, M.E., 1984, Boundary shear in symmetrical compound channels, Proc. ASCE, J. Hydr. Eng., 110, No.10, p.1412

33. Krishnapan, B.G. and Lan, Y.L., 1977, Transverse dispersion in meandering channels, Inland Waters Directorate, Canada Center for Inland Waters, Burlington, Ontario

34. Lawson, C.L. and Hanson, R.J., 1974, Solving Least Squares problems, Prentice-Hall, Inc., Englewood Cliffs, N.J.

35. Leschziner, M.A., and Rodi, N., 1979, Calculation of strong curved open channel flow in shallow river bends, Proc. ASCE, J. Hydr. Div., 105, HY10, p.1297

36. Malouf, K.M., 1950, Movement of detritus in models of river and channel bends, Ph.D. Thesis, University of London

37. Mockmore, C.A., 1944, Flow around bends in stable channels, Transc. ASCE, 109, p.593

38. Muramoto, Y., 1967, Secondary flow in curved open channels, Proc. 12th IAHR Congress, Fort Collins, Colorado, A.53

39. Nikuradse, J., 1930, Investigations on turbulent flows in non circular tubes, Ingenieur-Archiv, 1, 306-322

40. Nouh, M.A. and Townsend, R.D., 1979, Shear stress distribution in stable channel bends, Proc. ASCE, J. Hydr. Div., 105, HY10, p.1233

41. O'Connor, P.D.T., 1985, Practical reliability engineering, second edition, Johns Wiley and Sons

42. Odgaard, A.J., 1981, Transverse bed slope in alluvial channel bends, Proc. ASCE, J. Hydr. Div., 107, HY12, p.1677

43. Perkins, H.J., 1970, The formation of streamwise vorticity in turbulent flow, J. Fluid Mech., Vol. 44, No. 4, United Kingdom, Dec., p.721

44. Prandtl, L., 1952, The essentials of fluid dynamics, Blackie & Sons Limited

45. Quick, M.C., 1974, Mechanism for stream flow meandering, Proc. ASCE, J. Hydr. Div., 100, HY6, p.741

46. Rao, K.V., 1975, Secondary flow in a curved channel as revealed by a Laser Doppler Anemometer, Proceeding of the LDA-Symposium, Copenhagen

47. Rao, K.V. and Legono, D., 1985, Velocity distribution across the width of a rectangular open channel as revealed by the Laser Doppler Anemometer, 21th IAHR Congress, Melbourne, Australia

48. Rozovskii, I.L., 1957, Flow of water in bends of open channels, Israel Programme of Scientific Translations, Jerussalem

49. Sanmuganathan, K., 1966, Secondary flow in curved channels, Ph.D. Thesis, University of London

50. Schlichting, H., 1960, Boundary Layer theory

51. Shukry, A., 1949, Flow around bends in an open flume, Proc. ASCE, 6, p.713

52. Soliman, M.M., and Tinney, E.R., 1968, Flow around 180° bends in open rectangular channels, Proc. ASCE, J. Hydr. Div., 94, HY4, p.893

53. Sovran, G., 1967, Fluid mechanics of internal flow, Proc. of the symposium on a fluid mechanics of internal flow, General motors research laboratories, Warren, Michigan, Elsevier Publishing Company

54. Stanton, R.G., 1961, Numerical methods for science and engineering, Prentice-Hall International Inc.

55. Struiksma, N., Olesen, K.W., Flokstra, C. and De Vriend, H.J., 1985, Bed deformation in alluvial channel bends, J. Hydr. Res., 23(1), pp.57-59

56. Thomson, J., 1876, On the origin and winding of rivers in alluvial plains, with remarks on the flow around bends in pipes, Proc. Royal Soc., 25, p.5

57. Townsend, A.A., 1956, The structure of turbulennce shear flow, Cambridge University Press.

58. Varshney, D.V. and Garde, R.J., 1975, Shear distribution in bends in rectangular channels, J. Hydr. Div., ASCE, HY8, p.1053

59. Vennard and Street, 1982, Elementary fluid mechanics, sixth edition, John Willey and Sons, New York

60. Wadekar, G.T., 1956, Secondary flow in curved channels, Ph.D. Thesis, University of London

61. Wen-Hsing Li, 1983, Fluid mechanics in water resources engineering, Allyn and Bacon, INC.

62. Wright, G., 1973, Elementary experiments with Lasers, Wykenham publications (London) Ltd.

63. Yen, B.C., 1965, Characteristics of subcritical flow in a meandering channel, Report, Iowa Inst. of Hydr. Res., University of Iowa

64. Yen, C.L., 1970, Bed topography effect on flow in a meander, Proc. ASCE, J. Hydr. Div., 96, HY1, p.57

65. Yen, C.L. and Yen, B.C., 1971, Water surface configuration in channel bends, Proc. ASCE, J. Hydr. Div., 97, HY2, p.303

66. Zimmermann, C., 1977, Roughness effects on the flow direction near curved stream beds, J. Hydr. Res., 15(1), p.73

67. Zimmermann, C. and Kennedy, J.F., 1978, Transverse bed slopes in curved alluvial streams, Proc. ASCE, J. Hydr. Div., 104, HY1, p.33

Table 6.1 *Mean and fluctuation velocities and Reynolds shear stress components at section U-1 run no.1*

Loc.no.	Tangential		Vertical		Radial		Reynolds s.s. components				Unit
							v'w'		v'u'		
	DC	RMS	DC	RMS	DC	RMS	+45	-45	+45	-45	
1	6.426	0.398	-	-	-	-	-	-	-	-	Volts
2	6.658	0.387	-	-	-	-	-	-	-	-	Volts
3	6.864	0.380	-	-	-	-	-	-	-	-	Volts
4	6.780	0.385	-	-	-	-	-	-	-	-	Volts
5	6.711	0.399	-	-	-	-	-	-	-	-	Volts
6	6.705	0.379	-	-	-	-	-	-	-	-	Volts
7	6.822	0.366	-	-	-	-	-	-	-	-	Volts
8	6.762	0.407	-	-	-	-	-	-	-	-	Volts
9	6.580	0.400	-	-	-	-	-	-	-	-	Volts
10	7.128	0.444	-	-	-	-	-	-	-	-	Volts
11	7.430	0.404	-	-	-	-	-	-	-	-	Volts
12	7.506	0.429	-	-	-	-	-	-	-	-	Volts
13	7.392	0.425	-	-	-	-	-	-	-	-	Volts
14	7.307	0.364	-	-	-	-	-	-	-	-	Volts
15	7.300	0.370	-	-	-	-	-	-	-	-	Volts
16	7.406	0.357	-	-	-	-	-	-	-	-	Volts
17	7.240	0.340	-	-	-	-	-	-	-	-	Volts
18	6.945	0.354	-	-	-	-	-	-	-	-	Volts
19	7.495	0.390	-	-	-	-	-	-	-	-	Volts
20	7.810	0.331	-	-	-	-	-	-	-	-	Volts
21	8.030	0.384	-	-	-	-	-	-	-	-	Volts
22	7.680	0.393	-	-	-	-	-	-	-	-	Volts
23	7.852	0.370	-	-	-	-	-	-	-	-	Volts
24	7.750	0.383	-	-	-	-	-	-	-	-	Volts
25	7.885	0.432	-	-	-	-	-	-	-	-	Volts
26	7.796	0.333	-	-	-	-	-	-	-	-	Volts
27	7.454	0.490	-	-	-	-	-	-	-	-	Volts
28	7.493	0.391	-	-	-	-	-	-	-	-	Volts
29	7.840	0.370	-	-	-	-	-	-	-	-	Volts
30	8.010	0.310	-	-	-	-	-	-	-	-	Volts
31	7.954	0.352	-	-	-	-	-	-	-	-	Volts
32	7.927	0.325	-	-	-	-	-	-	-	-	Volts
33	7.930	0.302	-	-	-	-	-	-	-	-	Volts
34	7.943	0.316	-	-	-	-	-	-	-	-	Volts
35	7.735	0.340	-	-	-	-	-	-	-	-	Volts
36	7.407	0.360	-	-	-	-	-	-	-	-	Volts
37	6.941	0.376	-	-	-	-	-	-	-	-	Volts
38	7.293	0.356	-	-	-	-	-	-	-	-	Volts
39	7.795	0.350	-	-	-	-	-	-	-	-	Volts
40	8.004	0.301	-	-	-	-	-	-	-	-	Volts
41	8.108	0.313	-	-	-	-	-	-	-	-	Volts
42	8.082	0.320	-	-	-	-	-	-	-	-	Volts
43	7.926	0.320	-	-	-	-	-	-	-	-	Volts
44	7.420	0.354	-	-	-	-	-	-	-	-	Volts
45	7.080	0.370	-	-	-	-	-	-	-	-	Volts

Table 6.2 *Mean and fluctuation velocities and Reynolds shear stress components at section U-1 run no.2*

Loc.no.	Tangential		Vertical		Radial		Reynolds s.s. components				Unit
							v'w'		v'u'		
	DC	RMS	DC	RMS	DC	RMS	+45	-45	+45	-45	
1	7.381	0.420	-	-	-	-	-	-	-	-	Volts
2	7.656	0.412	-	-	-	-	-	-	-	-	Volts
3	7.675	0.403	-	-	-	-	-	-	-	-	Volts
4	7.240	0.460	-	-	-	-	-	-	-	-	Volts
5	7.230	0.480	-	-	-	-	-	-	-	-	Volts
6	7.200	0.430	-	-	-	-	-	-	-	-	Volts
7	7.160	0.443	-	-	-	-	-	-	-	-	Volts
8	7.140	0.410	-	-	-	-	-	-	-	-	Volts
9	7.040	0.379	-	-	-	-	-	-	-	-	Volts
10	7.753	0.408	-	-	-	-	-	-	-	-	Volts
11	8.160	0.462	-	-	-	-	-	-	-	-	Volts
12	8.035	0.455	-	-	-	-	-	-	-	-	Volts
13	8.026	0.453	-	-	-	-	-	-	-	-	Volts
14	7.840	0.486	-	-	-	-	-	-	-	-	Volts
15	7.940	0.467	-	-	-	-	-	-	-	-	Volts
16	8.146	0.471	-	-	-	-	-	-	-	-	Volts
17	8.225	0.408	-	-	-	-	-	-	-	-	Volts
18	7.844	0.439	-	-	-	-	-	-	-	-	Volts
19	8.282	0.430	-	-	-	-	-	-	-	-	Volts
20	8.657	0.331	-	-	-	-	-	-	-	-	Volts
21	8.785	0.340	-	-	-	-	-	-	-	-	Volts
22	8.580	0.394	-	-	-	-	-	-	-	-	Volts
23	8.520	0.405	-	-	-	-	-	-	-	-	Volts
24	8.630	0.401	-	-	-	-	-	-	-	-	Volts
25	8.530	0.419	-	-	-	-	-	-	-	-	Volts
26	8.639	0.424	-	-	-	-	-	-	-	-	Volts
27	8.207	0.382	-	-	-	-	-	-	-	-	Volts
28	8.234	0.364	-	-	-	-	-	-	-	-	Volts
29	8.689	0.360	-	-	-	-	-	-	-	-	Volts
30	8.899	0.358	-	-	-	-	-	-	-	-	Volts
31	8.916	0.335	-	-	-	-	-	-	-	-	Volts
32	8.862	0.340	-	-	-	-	-	-	-	-	Volts
33	8.930	0.345	-	-	-	-	-	-	-	-	Volts
34	8.995	0.350	-	-	-	-	-	-	-	-	Volts
35	8.700	0.390	-	-	-	-	-	-	-	-	Volts
36	8.268	0.418	-	-	-	-	-	-	-	-	Volts
37	8.335	0.454	-	-	-	-	-	-	-	-	Volts
38	8.790	0.448	-	-	-	-	-	-	-	-	Volts
39	9.017	0.312	-	-	-	-	-	-	-	-	Volts
40	9.111	0.310	-	-	-	-	-	-	-	-	Volts
41	8.926	0.305	-	-	-	-	-	-	-	-	Volts
42	9.027	0.323	-	-	-	-	-	-	-	-	Volts
43	8.820	0.349	-	-	-	-	-	-	-	-	Volts
44	8.618	0.366	-	-	-	-	-	-	-	-	Volts
45	8.120	0.505	-	-	-	-	-	-	-	-	Volts
46	8.083	0.445	-	-	-	-	-	-	-	-	Volts
47	8.560	0.420	-	-	-	-	-	-	-	-	Volts
48	8.735	0.380	-	-	-	-	-	-	-	-	Volts
49	9.055	0.340	-	-	-	-	-	-	-	-	Volts
50	9.010	0.306	-	-	-	-	-	-	-	-	Volts
51	9.135	0.305	-	-	-	-	-	-	-	-	Volts
52	8.918	0.313	-	-	-	-	-	-	-	-	Volts
53	8.616	0.345	-	-	-	-	-	-	-	-	Volts
54	8.156	0.406	-	-	-	-	-	-	-	-	Volts

Table 6.3 *Mean and fluctuation velocities and Reynolds shear stress components at section U-1 run no.3*

Loc.no.	Tangential DC	Tangential RMS	Vertical DC	Vertical RMS	Radial DC	Radial RMS	Reynolds s.s. components v'w' +45	v'w' −45	v'u' +45	v'u' −45	Unit
1	7.868	0.460	–	–	–	–	–	–	–	–	Volts
2	8.183	0.465	–	–	–	–	–	–	–	–	Volts
3	8.425	0.472	–	–	–	–	–	–	–	–	Volts
4	8.263	0.492	–	–	–	–	–	–	–	–	Volts
5	8.070	0.523	–	–	–	–	–	–	–	–	Volts
6	8.006	0.535	–	–	–	–	–	–	–	–	Volts
7	7.950	0.540	–	–	–	–	–	–	–	–	Volts
8	7.802	0.487	–	–	–	–	–	–	–	–	Volts
9	7.791	0.471	–	–	–	–	–	–	–	–	Volts
10	8.219	0.451	–	–	–	–	–	–	–	–	Volts
11	8.499	0.462	–	–	–	–	–	–	–	–	Volts
12	8.703	0.498	–	–	–	–	–	–	–	–	Volts
13	8.828	0.522	–	–	–	–	–	–	–	–	Volts
14	8.841	0.513	–	–	–	–	–	–	–	–	Volts
15	8.901	0.535	–	–	–	–	–	–	–	–	Volts
16	9.040	0.407	–	–	–	–	–	–	–	–	Volts
17	8.775	0.432	–	–	–	–	–	–	–	–	Volts
18	8.466	0.452	–	–	–	–	–	–	–	–	Volts
19	8.781	0.432	–	–	–	–	–	–	–	–	Volts
20	9.145	0.435	–	–	–	–	–	–	–	–	Volts
21	9.432	0.340	–	–	–	–	–	–	–	–	Volts
22	9.324	0.452	–	–	–	–	–	–	–	–	Volts
23	9.015	0.387	–	–	–	–	–	–	–	–	Volts
24	9.180	0.417	–	–	–	–	–	–	–	–	Volts
25	9.227	0.350	–	–	–	–	–	–	–	–	Volts
26	9.030	0.383	–	–	–	–	–	–	–	–	Volts
27	8.690	0.397	–	–	–	–	–	–	–	–	Volts
28	8.785	0.420	–	–	–	–	–	–	–	–	Volts
29	9.221	0.416	–	–	–	–	–	–	–	–	Volts
30	9.450	0.380	–	–	–	–	–	–	–	–	Volts
31	9.530	0.323	–	–	–	–	–	–	–	–	Volts
32	9.435	0.358	–	–	–	–	–	–	–	–	Volts
33	9.820	0.360	–	–	–	–	–	–	–	–	Volts
34	9.711	0.325	–	–	–	–	–	–	–	–	Volts
35	9.330	0.425	–	–	–	–	–	–	–	–	Volts
36	8.894	0.480	–	–	–	–	–	–	–	–	Volts
37	9.227	0.459	–	–	–	–	–	–	–	–	Volts
38	9.677	0.383	–	–	–	–	–	–	–	–	Volts
39	9.742	0.304	–	–	–	–	–	–	–	–	Volts
40	9.756	0.320	–	–	–	–	–	–	–	–	Volts
41	9.560	0.314	–	–	–	–	–	–	–	–	Volts
42	9.575	0.313	–	–	–	–	–	–	–	–	Volts
43	9.571	0.355	–	–	–	–	–	–	–	–	Volts
44	9.358	0.480	–	–	–	–	–	–	–	–	Volts
45	8.903	0.488	–	–	–	–	–	–	–	–	Volts
46	8.853	0.487	–	–	–	–	–	–	–	–	Volts
47	9.313	0.450	–	–	–	–	–	–	–	–	Volts
48	9.560	0.420	–	–	–	–	–	–	–	–	Volts
49	9.683	0.353	–	–	–	–	–	–	–	–	Volts
50	9.714	0.290	–	–	–	–	–	–	–	–	Volts
51	9.868	0.295	–	–	–	–	–	–	–	–	Volts
52	9.791	0.300	–	–	–	–	–	–	–	–	Volts
53	9.323	0.392	–	–	–	–	–	–	–	–	Volts
54	8.859	0.420	–	–	–	–	–	–	–	–	Volts

Table 6.4 *Mean and fluctuation velocities and Reynolds shear stress components at section U-2 run no.1*

Loc.no.	Tangential DC	Tangential RMS	Vertical DC	Vertical RMS	Radial DC	Radial RMS	Reynolds s.s. components v'w' +45	v'w' −45	v'u' +45	v'u' −45	Unit
1	6.229	0.476	–	–	–	–	–	–	–	–	Volts
2	6.202	0.485	–	–	–	–	–	–	–	–	Volts
3	6.270	0.450	–	–	–	–	–	–	–	–	Volts
4	6.432	0.445	–	–	–	–	–	–	–	–	Volts
5	6.420	0.425	–	–	–	–	–	–	–	–	Volts
6	6.446	0.432	–	–	–	–	–	–	–	–	Volts
7	6.437	0.433	–	–	–	–	–	–	–	–	Volts
8	6.377	0.460	–	–	–	–	–	–	–	–	Volts
9	6.301	0.515	–	–	–	–	–	–	–	–	Volts
10	6.489	0.570	–	–	6.050	0.576	–	–	–	–	Volts
11	6.637	0.450	–	–	6.044	0.578	–	–	–	–	Volts
12	6.812	0.439	–	–	6.053	0.456	–	–	–	–	Volts
13	6.836	0.453	–	–	6.046	0.445	–	–	–	–	Volts
14	6.800	0.456	–	–	6.051	0.436	–	–	–	–	Volts
15	6.715	0.505	–	–	6.046	0.457	–	–	–	–	Volts
16	6.504	0.460	–	–	6.019	0.454	–	–	–	–	Volts
17	6.390	0.455	–	–	6.004	0.445	–	–	–	–	Volts
18	6.286	0.450	–	–	6.013	0.444	–	–	–	–	Volts
19	6.412	0.407	6.055	0.455	6.000	0.527	0.420	0.452	0.482	0.484	Volts
20	6.547	0.395	6.081	0.458	5.993	0.484	0.387	0.462	0.487	0.453	Volts
21	6.621	0.388	6.051	0.450	5.944	0.525	0.395	0.506	0.476	0.450	Volts
22	6.806	0.510	6.061	0.455	5.888	0.465	0.439	0.515	0.482	0.457	Volts
23	7.031	0.364	6.061	0.369	5.903	0.455	0.367	0.440	0.493	0.424	Volts
24	7.076	0.366	6.040	0.362	5.932	0.453	0.344	0.443	0.487	0.425	Volts
25	7.041	0.353	6.031	0.399	6.005	0.461	0.351	0.427	0.503	0.416	Volts
26	6.953	0.392	6.045	0.376	6.027	0.408	0.374	0.401	0.450	0.372	Volts
27	6.782	0.380	6.047	0.444	6.004	0.462	0.350	0.493	0.520	0.413	Volts
28	6.833	0.372	6.021	0.425	5.995	0.386	0.361	0.495	0.432	0.434	Volts
29	7.027	0.378	6.031	0.441	5.993	0.405	0.351	0.494	0.474	0.411	Volts
30	7.111	0.335	6.025	0.435	6.008	0.444	0.418	0.493	0.502	0.432	Volts
31	7.083	0.330	6.040	0.432	6.076	0.442	0.340	0.489	0.484	0.413	Volts
32	6.903	0.385	6.058	0.415	6.106	0.450	0.379	0.454	0.508	0.413	Volts
33	6.664	0.345	6.029	0.404	6.098	0.450	0.384	0.472	0.455	0.409	Volts
34	6.635	0.395	6.072	0.429	6.046	0.441	0.382	0.446	0.461	0.422	Volts
35	6.539	0.397	6.065	0.417	6.040	0.435	0.439	0.467	0.460	0.420	Volts
36	6.378	0.500	6.066	0.435	6.037	0.476	0.452	0.470	0.490	0.426	Volts
37	6.332	0.467	6.042	0.410	6.055	0.413	0.369	0.394	0.426	0.413	Volts
38	6.503	0.442	6.072	0.430	6.076	0.411	0.383	0.437	0.418	0.415	Volts
39	6.520	0.446	6.063	0.435	6.116	0.490	0.402	0.442	0.518	0.462	Volts
40	6.608	0.416	6.042	0.416	6.081	0.431	0.419	0.474	0.433	0.459	Volts
41	6.714	0.397	6.055	0.406	6.072	0.426	0.376	0.489	0.450	0.397	Volts
42	7.089	0.391	6.028	0.430	6.043	0.442	0.368	0.462	0.483	0.363	Volts
43	7.073	0.405	6.019	0.446	6.005	0.434	0.403	0.466	0.477	0.408	Volts
44	6.936	0.375	6.009	0.451	5.960	0.429	0.415	0.477	0.460	0.403	Volts
45	6.734	0.402	5.992	0.460	5.965	0.396	0.428	0.480	0.467	0.394	Volts

Table 6.5 Mean and fluctuation velocities and Reynolds shear stress components at section U-2 run no.2

Loc.no.	Tangential DC	Tangential RMS	Vertical DC	Vertical RMS	Radial DC	Radial RMS	Reynolds s.s. components v'w' +45	v'w' -45	v'u' +45	v'u' -45	Unit
1	6.400	0.474	-	-	-	-	-	-	-	-	Volts
2	6.548	0.504	-	-	-	-	-	-	-	-	Volts
3	6.713	0.522	-	-	-	-	-	-	-	-	Volts
4	6.826	0.505	-	-	-	-	-	-	-	-	Volts
5	6.838	0.500	-	-	-	-	-	-	-	-	Volts
6	6.800	0.502	-	-	-	-	-	-	-	-	Volts
7	6.810	0.498	-	-	-	-	-	-	-	-	Volts
8	6.784	0.470	-	-	-	-	-	-	-	-	Volts
9	6.604	0.537	-	-	-	-	-	-	-	-	Volts
10	7.036	0.537	-	-	-	-	-	-	-	-	Volts
11	7.280	0.523	-	-	-	-	-	-	-	-	Volts
12	7.330	0.486	-	-	-	-	-	-	-	-	Volts
13	7.359	0.507	-	-	-	-	-	-	-	-	Volts
14	7.361	0.523	-	-	-	-	-	-	-	-	Volts
15	7.297	0.532	-	-	-	-	-	-	-	-	Volts
16	7.092	0.547	-	-	-	-	-	-	-	-	Volts
17	6.800	0.532	-	-	-	-	-	-	-	-	Volts
18	6.646	0.525	-	-	-	-	-	-	-	-	Volts
19	7.033	0.592	6.052	0.498	6.224	0.605	0.406	0.477	0.740	0.590	Volts
20	7.185	0.521	6.072	0.467	6.197	0.672	0.388	0.485	0.743	0.640	Volts
21	7.378	0.523	6.104	0.454	6.171	0.610	0.372	0.503	0.620	0.450	Volts
22	7.536	0.549	6.170	0.452	6.218	0.507	0.355	0.440	0.596	0.475	Volts
23	7.581	0.558	6.167	0.418	6.253	0.474	0.344	0.478	0.580	0.412	Volts
24	7.580	0.561	6.149	0.424	6.180	0.472	0.340	0.525	0.580	0.456	Volts
25	7.482	0.525	6.082	0.388	6.084	0.532	0.356	0.522	0.622	0.470	Volts
26	7.412	0.652	6.049	0.406	6.060	0.515	0.390	0.520	0.572	0.445	Volts
27	7.137	0.656	6.040	0.443	5.985	0.559	0.405	0.578	0.535	0.662	Volts
28	7.145	0.633	6.044	0.406	5.996	0.556	0.458	0.502	0.507	0.640	Volts
29	7.463	0.481	6.036	0.442	6.040	0.547	0.306	0.583	0.530	0.648	Volts
30	7.554	0.471	6.070	0.449	6.077	0.561	0.365	0.580	0.470	0.703	Volts
31	7.623	0.508	6.140	0.473	6.120	0.483	0.360	0.569	0.594	0.420	Volts
32	7.633	0.585	6.206	0.472	6.116	0.542	0.376	0.547	0.625	0.456	Volts
33	7.580	0.553	6.164	0.415	6.070	0.536	0.340	0.560	0.621	0.465	Volts
34	7.404	0.541	6.147	0.440	6.100	0.580	0.413	0.521	0.570	0.449	Volts
35	7.257	0.497	6.100	0.430	6.094	0.519	0.380	0.465	0.611	0.558	Volts
36	7.125	0.542	6.096	0.438	6.110	0.536	0.435	0.455	0.606	0.502	Volts
37	7.070	0.660	6.082	0.358	6.016	0.563	0.690	0.505	0.635	0.537	Volts
38	7.187	0.635	6.088	0.366	6.056	0.543	0.480	0.535	0.626	0.539	Volts
39	7.184	0.194	6.120	0.452	6.008	0.493	0.402	0.526	0.560	0.474	Volts
40	7.442	0.519	6.147	0.470	6.029	0.534	0.380	0.488	0.522	0.414	Volts
41	7.654	0.485	6.211	0.470	6.052	0.456	0.355	0.559	0.670	0.545	Volts
42	7.647	0.485	6.078	0.398	6.038	0.601	0.358	0.590	0.674	0.548	Volts
43	7.536	0.491	6.029	0.390	6.032	0.586	0.325	0.580	0.602	0.509	Volts
44	7.460	0.435	6.034	0.465	6.016	0.547	0.370	0.474	0.624	0.549	Volts
45	7.147	0.462	6.033	0.430	6.022	0.576	0.440	0.560	0.610	0.492	Volts
46	7.019	0.470	-	-	6.007	0.626	-	-	-	-	Volts
47	7.329	0.453	-	-	6.119	0.608	-	-	-	-	Volts
48	7.500	0.467	-	-	6.186	0.500	-	-	-	-	Volts
49	7.653	0.535	-	-	6.006	0.520	-	-	-	-	Volts
50	7.710	0.596	-	-	5.906	0.546	-	-	-	-	Volts
51	7.255	0.569	-	-	5.947	0.530	-	-	-	-	Volts
52	7.060	0.475	-	-	5.868	0.636	-	-	-	-	Volts
53	7.002	0.450	-	-	5.850	0.639	-	-	-	-	Volts
54	6.843	0.485	-	-	5.817	0.646	-	-	-	-	Volts

Table 6.6 Mean and fluctuation velocities and Reynolds shear stress components at section U-2 run no.3

Loc.no.	Tangential DC	Tangential RMS	Vertical DC	Vertical RMS	Radial DC	Radial RMS	Reynolds s.s. components v'w' +45	v'w' -45	v'u' +45	v'u' -45	Unit
1	6.546	0.481	-	-	-	-	-	-	-	-	Volts
2	6.696	0.456	-	-	-	-	-	-	-	-	Volts
3	7.013	0.460	-	-	-	-	-	-	-	-	Volts
4	7.086	0.461	-	-	-	-	-	-	-	-	Volts
5	7.035	0.453	-	-	-	-	-	-	-	-	Volts
6	6.935	0.424	-	-	-	-	-	-	-	-	Volts
7	6.945	0.465	-	-	-	-	-	-	-	-	Volts
8	6.904	0.474	-	-	-	-	-	-	-	-	Volts
9	6.682	0.590	-	-	-	-	-	-	-	-	Volts
10	7.093	0.600	-	-	-	-	-	-	-	-	Volts
11	7.363	0.406	-	-	-	-	-	-	-	-	Volts
12	7.475	0.395	-	-	-	-	-	-	-	-	Volts
13	7.485	0.415	-	-	-	-	-	-	-	-	Volts
14	7.524	0.396	-	-	-	-	-	-	-	-	Volts
15	7.505	0.452	-	-	-	-	-	-	-	-	Volts
16	7.397	0.495	-	-	-	-	-	-	-	-	Volts
17	7.030	0.530	-	-	-	-	-	-	-	-	Volts
18	6.775	0.540	-	-	-	-	-	-	-	-	Volts
19	7.199	0.474	6.108	0.440	5.768	0.513	0.501	0.596	0.607	0.469	Volts
20	7.482	0.487	6.187	0.450	5.767	0.529	0.380	0.607	0.653	0.447	Volts
21	7.670	0.424	6.293	0.455	5.736	0.522	0.333	0.598	0.652	0.469	Volts
22	7.813	0.320	6.262	0.540	5.743	0.527	0.322	0.640	0.648	0.440	Volts
23	7.802	0.325	6.156	0.423	5.772	0.430	0.320	0.548	0.512	0.376	Volts
24	7.777	0.343	6.176	0.485	5.850	0.426	0.379	0.508	0.499	0.382	Volts
25	7.687	0.330	6.036	0.412	5.833	0.473	0.428	0.560	0.585	0.414	Volts
26	7.608	0.360	6.027	0.441	5.890	0.460	0.423	0.570	0.552	0.452	Volts
27	7.296	0.390	6.024	0.445	5.881	0.480	0.450	0.680	0.577	0.427	Volts
28	7.296	0.389	5.950	0.472	5.906	0.480	0.480	0.533	0.606	0.423	Volts
29	7.640	0.364	6.075	0.460	5.920	0.480	0.416	0.540	0.616	0.419	Volts
30	7.830	0.347	6.080	0.400	5.913	0.457	0.388	0.522	0.595	0.390	Volts
31	7.874	0.322	6.141	0.430	5.971	0.423	0.387	0.552	0.512	0.349	Volts
32	7.907	0.333	6.218	0.480	5.972	0.422	0.365	0.527	0.514	0.368	Volts
33	7.950	0.340	6.273	0.498	5.932	0.421	0.378	0.612	0.539	0.358	Volts
34	7.697	0.335	6.184	0.418	6.031	0.416	0.365	0.550	0.506	0.352	Volts
35	7.562	0.370	6.254	0.410	6.003	0.404	0.360	0.596	0.498	0.351	Volts
36	7.325	0.335	6.260	0.440	5.981	0.446	0.408	0.617	0.568	0.367	Volts
37	7.210	0.450	6.147	0.508	6.079	0.448	0.765	0.463	0.528	0.395	Volts
38	7.406	0.370	6.130	0.473	6.085	0.451	0.410	0.482	0.531	0.385	Volts
39	7.479	0.360	6.135	0.460	6.066	0.456	0.380	0.490	0.533	0.408	Volts
40	7.876	0.335	6.200	0.578	6.107	0.452	0.353	0.540	0.509	0.370	Volts
41	7.950	0.309	6.407	0.464	6.104	0.430	0.320	0.535	0.575	0.374	Volts
42	7.839	0.295	6.378	0.439	6.063	0.450	0.345	0.502	0.576	0.370	Volts
43	7.750	0.300	6.140	0.445	5.956	0.444	0.355	0.490	0.550	0.363	Volts
44	7.443	0.614	6.009	0.536	5.955	0.462	0.562	0.630	0.535	0.385	Volts
45	7.033	0.587	5.947	0.580	5.947	0.481	0.607	0.713	0.560	0.404	Volts
46	7.129	0.590	-	-	5.900	0.460	-	-	-	-	Volts
47	7.557	0.386	-	-	5.896	0.484	-	-	-	-	Volts
48	7.692	0.342	-	-	5.902	0.479	-	-	-	-	Volts
49	7.870	0.318	-	-	6.107	0.510	-	-	-	-	Volts
50	7.998	0.308	-	-	6.120	0.455	-	-	-	-	Volts
51	7.672	0.370	-	-	6.158	0.456	-	-	-	-	Volts
52	7.165	0.347	-	-	6.178	0.472	-	-	-	-	Volts
53	7.082	0.400	-	-	6.060	0.472	-	-	-	-	Volts
54	6.890	0.570	-	-	6.057	0.481	-	-	-	-	Volts

Table 6.7 Mean and fluctuation velocities and Reynolds shear stress components at section U-3 run no.1

Loc.no.	Tangential		Vertical		Radial		Reynolds s.s. components v'w'		v'u'		Unit
	DC	RMS	DC	RMS	DC	RMS	+45	-45	+45	-45	
1	6.320	0.410	-	-	-	-	-	-	-	-	Volts
2	6.393	0.393	-	-	-	-	-	-	-	-	Volts
3	6.540	0.409	-	-	-	-	-	-	-	-	Volts
4	6.562	0.386	-	-	-	-	-	-	-	-	Volts
5	6.733	0.436	-	-	-	-	-	-	-	-	Volts
6	6.837	0.426	-	-	-	-	-	-	-	-	Volts
7	7.065	0.365	-	-	-	-	-	-	-	-	Volts
8	7.401	0.380	-	-	-	-	-	-	-	-	Volts
9	7.282	0.400	-	-	-	-	-	-	-	-	Volts
10	7.698	0.412	-	-	6.051	0.474	-	-	-	-	Volts
11	7.875	0.404	-	-	6.046	0.417	-	-	-	-	Volts
12	7.800	0.380	-	-	6.034	0.437	-	-	-	-	Volts
13	7.704	0.467	-	-	6.007	0.450	-	-	-	-	Volts
14	7.439	0.423	-	-	5.967	0.433	-	-	-	-	Volts
15	7.133	0.395	-	-	5.983	0.428	-	-	-	-	Volts
16	6.797	0.460	-	-	5.996	0.440	-	-	-	-	Volts
17	6.556	0.450	-	-	5.996	0.414	-	-	-	-	Volts
18	6.463	0.452	-	-	6.016	0.409	-	-	-	-	Volts
19	6.882	0.423	6.081	0.430	6.057	0.468	0.397	0.450	0.525	0.517	Volts
20	7.099	0.407	6.074	0.364	6.066	0.445	0.351	0.410	0.467	0.474	Volts
21	7.409	0.357	6.057	0.400	6.087	0.490	0.342	0.442	0.508	0.464	Volts
22	7.717	0.354	6.052	0.410	6.087	0.453	0.360	0.460	0.527	0.420	Volts
23	7.967	0.359	6.044	0.382	6.095	0.450	0.379	0.340	0.516	0.430	Volts
24	8.213	0.346	6.029	0.392	6.078	0.444	0.336	0.473	0.541	0.405	Volts
25	8.363	0.347	6.037	0.362	6.098	0.421	0.353	0.475	0.476	0.361	Volts
26	8.297	0.349	6.034	0.387	6.094	0.420	0.337	0.476	0.480	0.380	Volts
27	8.084	0.370	6.015	0.397	6.100	0.419	0.324	0.484	0.476	0.417	Volts
28	7.995	0.362	6.050	0.409	6.120	0.465	0.335	0.461	0.516	0.420	Volts
29	8.225	0.367	6.028	0.410	6.109	0.390	0.374	0.452	0.450	0.386	Volts
30	8.263	0.342	6.012	0.412	6.104	0.420	0.365	0.450	0.480	0.375	Volts
31	8.178	0.340	6.030	0.409	6.109	0.443	0.320	0.400	0.522	0.407	Volts
32	7.843	0.353	6.040	0.408	6.127	0.435	0.342	0.442	0.509	0.380	Volts
33	7.470	0.376	6.044	0.390	6.133	0.430	0.340	0.350	0.479	0.393	Volts
34	7.210	0.480	6.036	0.409	6.100	0.431	0.338	0.422	0.453	0.400	Volts
35	7.028	0.482	6.065	0.395	6.095	0.371	0.338	0.419	0.415	0.401	Volts
36	6.825	0.497	6.082	0.393	6.078	0.410	0.350	0.407	0.477	0.386	Volts
37	6.538	0.530	6.046	0.395	6.067	0.415	0.385	0.420	0.424	0.395	Volts
38	6.647	0.480	6.044	0.393	6.073	0.395	0.372	0.414	0.460	0.360	Volts
39	6.779	0.451	6.042	0.409	6.090	0.383	0.376	0.415	0.389	0.370	Volts
40	7.371	0.354	6.040	0.397	6.110	0.390	0.355	0.413	0.430	0.358	Volts
41	7.875	0.370	6.046	0.400	6.116	0.402	0.326	0.429	0.458	0.355	Volts
42	8.258	0.333	6.038	0.399	6.106	0.423	0.331	0.435	0.469	0.368	Volts
43	8.201	0.386	6.030	0.405	6.038	0.440	0.360	0.408	0.515	0.379	Volts
44	8.009	0.370	6.022	0.410	6.024	0.425	0.370	0.400	0.462	0.379	Volts
45	7.781	0.405	6.011	0.425	6.025	0.452	0.385	0.425	0.520	0.380	Volts

Table 6.8 Mean and fluctuation velocities and Reynolds shear stress components at section U-3 run no.2

Loc.no.	Tangential		Vertical		Radial		Reynolds s.s. components v'w'		v'u'		Unit
	DC	RMS	DC	RMS	DC	RMS	+45	-45	+45	-45	
1	6.385	0.407	-	-	-	-	-	-	-	-	Volts
2	6.631	0.418	-	-	-	-	-	-	-	-	Volts
3	6.666	0.425	-	-	-	-	-	-	-	-	Volts
4	6.760	0.409	-	-	-	-	-	-	-	-	Volts
5	6.896	0.396	-	-	-	-	-	-	-	-	Volts
6	6.867	0.365	-	-	-	-	-	-	-	-	Volts
7	7.077	0.371	-	-	-	-	-	-	-	-	Volts
8	7.277	0.362	-	-	-	-	-	-	-	-	Volts
9	7.023	0.346	-	-	-	-	-	-	-	-	Volts
10	7.333	0.686	-	-	-	-	-	-	-	-	Volts
11	7.617	0.428	-	-	-	-	-	-	-	-	Volts
12	7.470	0.600	-	-	-	-	-	-	-	-	Volts
13	7.237	0.618	-	-	-	-	-	-	-	-	Volts
14	7.221	0.470	-	-	-	-	-	-	-	-	Volts
15	7.058	0.459	-	-	-	-	-	-	-	-	Volts
16	6.925	0.463	-	-	-	-	-	-	-	-	Volts
17	6.875	0.460	-	-	-	-	-	-	-	-	Volts
18	6.621	0.460	-	-	-	-	-	-	-	-	Volts
19	6.927	0.379	6.154	0.425	6.005	0.428	0.398	0.469	0.492	0.383	Volts
20	7.192	0.357	6.100	0.399	5.998	0.448	0.370	0.423	0.540	0.397	Volts
21	7.319	0.355	6.067	0.370	6.009	0.430	0.343	0.420	0.485	0.380	Volts
22	7.454	0.352	6.044	0.460	6.086	0.448	0.347	0.537	0.509	0.420	Volts
23	7.594	0.333	6.043	0.441	6.078	0.460	0.348	0.569	0.566	0.417	Volts
24	7.728	0.355	6.029	0.467	6.100	0.450	0.360	0.596	0.597	0.366	Volts
25	7.783	0.406	6.043	0.440	6.132	0.410	0.490	0.591	0.525	0.345	Volts
26	7.787	0.404	6.020	0.465	6.115	0.433	0.415	0.604	0.547	0.351	Volts
27	7.482	0.389	6.014	0.393	6.089	0.476	0.390	0.614	0.540	0.436	Volts
28	7.433	0.350	6.065	0.452	6.097	0.490	0.346	0.551	0.552	0.357	Volts
29	7.761	0.343	6.058	0.440	6.133	0.457	0.356	0.559	0.550	0.362	Volts
30	7.780	0.340	6.041	0.445	6.163	0.428	0.361	0.555	0.523	0.353	Volts
31	7.728	0.340	6.004	0.452	6.154	0.438	0.348	0.565	0.540	0.373	Volts
32	7.569	0.342	6.030	0.467	6.127	0.462	0.359	0.561	0.515	0.390	Volts
33	7.372	0.357	6.040	0.449	6.131	0.452	0.372	0.539	0.534	0.400	Volts
34	7.237	0.384	6.035	0.460	6.100	0.424	0.385	0.504	0.557	0.425	Volts
35	7.157	0.368	6.087	0.435	6.083	0.459	0.379	0.502	0.473	0.427	Volts
36	6.911	0.385	6.133	0.430	6.084	0.471	0.379	0.460	0.503	0.422	Volts
37	6.729	0.490	6.116	0.449	6.109	0.500	0.440	0.500	0.490	0.422	Volts
38	6.954	0.382	6.113	0.406	6.135	0.420	0.374	0.460	0.485	0.390	Volts
39	6.990	0.392	6.040	0.449	6.112	0.413	0.400	0.520	0.460	0.380	Volts
40	7.273	0.415	6.028	0.448	6.119	0.420	0.394	0.531	0.497	0.356	Volts
41	7.590	0.341	6.040	0.443	6.095	0.414	0.363	0.538	0.512	0.335	Volts
42	7.735	0.350	5.972	0.466	6.080	0.400	0.358	0.530	0.506	0.327	Volts
43	7.745	0.326	6.028	0.465	6.125	0.420	0.344	0.567	0.533	0.348	Volts
44	7.743	0.325	6.100	0.448	6.103	0.444	0.345	0.548	0.540	0.353	Volts
45	7.361	0.333	6.144	0.445	6.070	0.392	0.344	0.554	0.493	0.324	Volts
46	7.271	0.480	-	-	6.012	0.413	-	-	-	-	Volts
47	7.660	0.440	-	-	5.970	0.402	-	-	-	-	Volts
48	7.709	0.402	-	-	5.931	0.413	-	-	-	-	Volts
49	7.670	0.432	-	-	5.990	0.405	-	-	-	-	Volts
50	7.694	0.393	-	-	6.083	0.392	-	-	-	-	Volts
51	7.286	0.409	-	-	6.076	0.388	-	-	-	-	Volts
52	6.939	0.435	-	-	6.096	0.371	-	-	-	-	Volts
53	6.845	0.459	-	-	6.056	0.384	-	-	-	-	Volts
54	6.635	0.462	-	-	6.037	0.378	-	-	-	-	Volts

Table 6.9 *Mean and fluctuation velocities and Reynolds shear stress components at section U-3 run no.3*

Loc.no.	Tangential		Vertical		Radial		Reynolds s.s. components v'w'		v'u'		Unit
	DC	RMS	DC	RMS	DC	RMS	+45	-45	+45	-45	
1	6.717	0.465	-	-	-	-	-	-	-	-	Volts
2	6.908	0.470	-	-	-	-	-	-	-	-	Volts
3	7.046	0.473	-	-	-	-	-	-	-	-	Volts
4	7.070	0.451	-	-	-	-	-	-	-	-	Volts
5	7.117	0.414	-	-	-	-	-	-	-	-	Volts
6	7.243	0.429	-	-	-	-	-	-	-	-	Volts
7	7.380	0.430	-	-	-	-	-	-	-	-	Volts
8	7.480	0.436	-	-	-	-	-	-	-	-	Volts
9	7.196	0.445	-	-	-	-	-	-	-	-	Volts
10	7.590	0.475	-	-	-	-	-	-	-	-	Volts
11	7.942	0.390	-	-	-	-	-	-	-	-	Volts
12	7.906	0.399	-	-	-	-	-	-	-	-	Volts
13	7.753	0.447	-	-	-	-	-	-	-	-	Volts
14	7.576	0.424	-	-	-	-	-	-	-	-	Volts
15	7.444	0.448	-	-	-	-	-	-	-	-	Volts
16	7.315	0.422	-	-	-	-	-	-	-	-	Volts
17	7.145	0.413	-	-	-	-	-	-	-	-	Volts
18	6.901	0.457	-	-	-	-	-	-	-	-	Volts
19	7.149	0.450	6.195	0.462	5.985	0.515	0.453	0.574	0.555	0.570	Volts
20	7.412	0.425	6.120	0.390	5.990	0.470	0.380	0.590	0.534	0.544	Volts
21	7.614	0.360	6.063	0.463	6.000	0.475	0.377	0.560	0.530	0.478	Volts
22	7.743	0.370	6.059	0.443	6.045	0.481	0.345	0.556	0.639	0.546	Volts
23	7.900	0.411	6.037	0.468	6.095	0.532	0.360	0.614	0.555	0.512	Volts
24	8.039	0.350	6.034	0.461	6.075	0.598	0.346	0.608	0.656	0.580	Volts
25	8.051	0.341	6.031	0.445	6.081	0.458	0.351	0.595	0.610	0.352	Volts
26	8.058	0.360	6.013	0.470	6.086	0.444	0.355	0.590	0.583	0.370	Volts
27	7.676	0.384	6.002	0.475	6.060	0.495	0.356	0.585	0.640	0.400	Volts
28	7.621	0.380	6.095	0.467	6.101	0.471	0.345	0.589	0.620	0.421	Volts
29	8.036	0.374	6.059	0.470	6.135	0.444	0.378	0.583	0.575	0.345	Volts
30	8.072	0.365	6.052	0.460	6.149	0.441	0.352	0.600	0.580	0.322	Volts
31	8.042	0.320	6.000	0.455	6.178	0.473	0.335	0.570	0.604	0.428	Volts
32	7.873	0.331	6.001	0.437	6.145	0.476	0.350	0.580	0.597	0.409	Volts
33	7.665	0.340	5.989	0.424	6.130	0.458	0.350	0.555	0.570	0.396	Volts
34	7.540	0.355	6.042	0.460	6.090	0.456	0.380	0.547	0.539	0.423	Volts
35	7.435	0.390	6.119	0.468	6.092	0.442	0.404	0.542	0.538	0.419	Volts
36	7.207	0.457	6.194	0.447	6.092	0.470	0.430	0.503	0.560	0.509	Volts
37	6.862	0.626	6.093	0.450	6.109	0.494	0.404	0.480	0.527	0.404	Volts
38	7.045	0.545	6.120	0.460	6.137	0.500	0.430	0.550	0.527	0.440	Volts
39	7.280	0.409	6.067	0.473	6.125	0.452	0.408	0.551	0.535	0.409	Volts
40	7.645	0.473	6.014	0.453	6.102	0.455	0.432	0.555	0.557	0.380	Volts
41	7.924	0.367	6.022	0.445	6.089	0.450	0.367	0.599	0.560	0.377	Volts
42	8.004	0.385	6.000	0.473	6.138	0.435	0.390	0.650	0.551	0.350	Volts
43	8.016	0.345	6.030	0.525	6.126	0.420	0.480	0.642	0.550	0.346	Volts
44	7.990	0.427	6.070	0.535	6.090	0.452	0.397	0.607	0.555	0.367	Volts
45	7.549	0.443	6.132	0.519	6.090	0.450	0.406	0.617	0.600	0.360	Volts
46	7.399	0.560	-	-	5.727	0.460	-	-	-	-	Volts
47	7.827	0.425	-	-	5.670	0.464	-	-	-	-	Volts
48	7.816	0.370	-	-	5.608	0.479	-	-	-	-	Volts
49	7.960	0.346	-	-	5.604	0.470	-	-	-	-	Volts
50	8.024	0.347	-	-	5.727	0.465	-	-	-	-	Volts
51	7.652	0.388	-	-	5.801	0.444	-	-	-	-	Volts
52	7.333	0.440	-	-	5.879	0.470	-	-	-	-	Volts
53	7.320	0.460	-	-	5.871	0.457	-	-	-	-	Volts
54	7.146	0.627	-	-	5.850	0.447	-	-	-	-	Volts

Table 6.10 *Mean and fluctuation velocities and Reynolds shear stress components at section U-4 run no.1*

Loc.no.	Tangential		Vertical		Radial		Reynolds s.s. components v'w'		v'u'		Unit
	DC	RMS	DC	RMS	DC	RMS	+45	-45	+45	-45	
1	6.286	0.390	-	-	-	-	-	-	-	-	Volts
2	6.375	0.428	-	-	-	-	-	-	-	-	Volts
3	6.443	0.449	-	-	-	-	-	-	-	-	Volts
4	6.605	0.498	-	-	-	-	-	-	-	-	Volts
5	6.684	0.530	-	-	-	-	-	-	-	-	Volts
6	6.659	0.448	-	-	-	-	-	-	-	-	Volts
7	7.022	0.580	-	-	-	-	-	-	-	-	Volts
8	7.286	0.360	-	-	-	-	-	-	-	-	Volts
9	7.075	0.394	-	-	-	-	-	-	-	-	Volts
10	7.575	0.620	-	-	-	-	-	-	-	-	Volts
11	7.811	0.680	-	-	-	-	-	-	-	-	Volts
12	7.650	0.500	-	-	-	-	-	-	-	-	Volts
13	7.336	0.758	-	-	-	-	-	-	-	-	Volts
14	7.252	0.620	-	-	-	-	-	-	-	-	Volts
15	7.070	0.517	-	-	-	-	-	-	-	-	Volts
16	6.883	0.449	-	-	-	-	-	-	-	-	Volts
17	6.651	0.420	-	-	-	-	-	-	-	-	Volts
18	6.471	0.429	-	-	-	-	-	-	-	-	Volts
19	6.770	0.473	-	-	-	-	-	-	-	-	Volts
20	7.012	0.516	-	-	-	-	-	-	-	-	Volts
21	7.327	0.470	-	-	-	-	-	-	-	-	Volts
22	7.573	0.404	-	-	-	-	-	-	-	-	Volts
23	7.895	0.370	-	-	-	-	-	-	-	-	Volts
24	8.230	0.350	-	-	-	-	-	-	-	-	Volts
25	8.376	0.398	-	-	-	-	-	-	-	-	Volts
26	8.297	0.548	-	-	-	-	-	-	-	-	Volts
27	7.957	0.486	-	-	-	-	-	-	-	-	Volts
28	8.036	0.330	-	-	-	-	-	-	-	-	Volts
29	8.438	0.378	-	-	-	-	-	-	-	-	Volts
30	8.422	0.366	-	-	-	-	-	-	-	-	Volts
31	8.230	0.364	-	-	-	-	-	-	-	-	Volts
32	7.797	0.490	-	-	-	-	-	-	-	-	Volts
33	7.482	0.498	-	-	-	-	-	-	-	-	Volts
34	7.282	0.457	-	-	-	-	-	-	-	-	Volts
35	7.215	0.408	-	-	-	-	-	-	-	-	Volts
36	6.937	0.409	-	-	-	-	-	-	-	-	Volts
37	6.524	0.407	-	-	-	-	-	-	-	-	Volts
38	6.725	0.405	-	-	-	-	-	-	-	-	Volts
39	7.017	0.396	-	-	-	-	-	-	-	-	Volts
40	7.540	0.370	-	-	-	-	-	-	-	-	Volts
41	7.973	0.350	-	-	-	-	-	-	-	-	Volts
42	8.311	0.349	-	-	-	-	-	-	-	-	Volts
43	8.271	0.330	-	-	-	-	-	-	-	-	Volts
44	8.120	0.447	-	-	-	-	-	-	-	-	Volts
45	7.725	0.426	-	-	-	-	-	-	-	-	Volts

Table 6.11 Mean and fluctuation velocities and Reynolds shear stress components at section U-4 run no.2

Loc.no.	Tangential		Vertical		Radial		Reynolds s.s. components v'w'		v'u'		Unit
	DC	RMS	DC	RMS	DC	RMS	+45	-45	+45	-45	
1	6.520	0.430	-	-	-	-	-	-	-	-	Volts
2	6.640	0.455	-	-	-	-	-	-	-	-	Volts
3	7.011	0.570	-	-	-	-	-	-	-	-	Volts
4	7.023	0.529	-	-	-	-	-	-	-	-	Volts
5	7.385	0.609	-	-	-	-	-	-	-	-	Volts
6	7.572	0.404	-	-	-	-	-	-	-	-	Volts
7	7.985	0.350	-	-	-	-	-	-	-	-	Volts
8	7.975	0.366	-	-	-	-	-	-	-	-	Volts
9	7.437	0.400	-	-	-	-	-	-	-	-	Volts
10	8.413	0.640	-	-	-	-	-	-	-	-	Volts
11	9.030	0.645	-	-	-	-	-	-	-	-	Volts
12	9.070	0.373	-	-	-	-	-	-	-	-	Volts
13	8.588	0.420	-	-	-	-	-	-	-	-	Volts
14	8.345	0.504	-	-	-	-	-	-	-	-	Volts
15	7.720	0.530	-	-	-	-	-	-	-	-	Volts
16	7.506	0.540	-	-	-	-	-	-	-	-	Volts
17	7.030	0.507	-	-	-	-	-	-	-	-	Volts
18	6.910	0.450	-	-	-	-	-	-	-	-	Volts
19	7.707	0.495	-	-	-	-	-	-	-	-	Volts
20	7.840	0.480	-	-	-	-	-	-	-	-	Volts
21	8.290	0.430	-	-	-	-	-	-	-	-	Volts
22	8.563	0.520	-	-	-	-	-	-	-	-	Volts
23	9.243	0.330	-	-	-	-	-	-	-	-	Volts
24	9.320	0.361	-	-	-	-	-	-	-	-	Volts
25	9.575	0.386	-	-	-	-	-	-	-	-	Volts
26	9.644	0.416	-	-	-	-	-	-	-	-	Volts
27	8.969	0.444	-	-	-	-	-	-	-	-	Volts
28	8.876	0.363	-	-	-	-	-	-	-	-	Volts
29	9.637	0.357	-	-	-	-	-	-	-	-	Volts
30	9.600	0.356	-	-	-	-	-	-	-	-	Volts
31	9.487	0.298	-	-	-	-	-	-	-	-	Volts
32	9.066	0.341	-	-	-	-	-	-	-	-	Volts
33	8.366	0.386	-	-	-	-	-	-	-	-	Volts
34	8.170	0.416	-	-	-	-	-	-	-	-	Volts
35	8.118	0.372	-	-	-	-	-	-	-	-	Volts
36	7.970	0.445	-	-	-	-	-	-	-	-	Volts
37	7.620	0.442	-	-	-	-	-	-	-	-	Volts
38	7.780	0.420	-	-	-	-	-	-	-	-	Volts
39	7.840	0.470	-	-	-	-	-	-	-	-	Volts
40	8.262	0.375	-	-	-	-	-	-	-	-	Volts
41	9.103	0.326	-	-	-	-	-	-	-	-	Volts
42	9.574	0.314	-	-	-	-	-	-	-	-	Volts
43	9.714	0.335	-	-	-	-	-	-	-	-	Volts
44	9.765	0.340	-	-	-	-	-	-	-	-	Volts
45	8.951	0.375	-	-	-	-	-	-	-	-	Volts
46	8.747	0.442	-	-	-	-	-	-	-	-	Volts
47	9.535	0.340	-	-	-	-	-	-	-	-	Volts
48	9.646	0.321	-	-	-	-	-	-	-	-	Volts
49	9.522	0.335	-	-	-	-	-	-	-	-	Volts
50	9.152	0.315	-	-	-	-	-	-	-	-	Volts
51	8.408	0.355	-	-	-	-	-	-	-	-	Volts
52	7.644	0.400	-	-	-	-	-	-	-	-	Volts
53	7.359	0.442	-	-	-	-	-	-	-	-	Volts
54	7.114	0.435	-	-	-	-	-	-	-	-	Volts

Table 6.12 Mean and fluctuation velocities and Reynolds shear stress components at section U-4 run no.3

Loc.no.	Tangential		Vertical		Radial		Reynolds s.s. components v'w'		v'u'		Unit
	DC	RMS	DC	RMS	DC	RMS	+45	-45	+45	-45	
1	6.773	0.560	-	-	-	-	-	-	-	-	Volts
2	6.911	0.640	-	-	-	-	-	-	-	-	Volts
3	7.295	0.603	-	-	-	-	-	-	-	-	Volts
4	7.387	0.670	-	-	-	-	-	-	-	-	Volts
5	7.650	0.870	-	-	-	-	-	-	-	-	Volts
6	7.980	0.375	-	-	-	-	-	-	-	-	Volts
7	8.147	0.440	-	-	-	-	-	-	-	-	Volts
8	8.590	0.454	-	-	-	-	-	-	-	-	Volts
9	8.135	0.457	-	-	-	-	-	-	-	-	Volts
10	9.266	0.520	-	-	-	-	-	-	-	-	Volts
11	9.863	0.450	-	-	-	-	-	-	-	-	Volts
12	9.560	0.445	-	-	-	-	-	-	-	-	Volts
13	9.252	0.480	-	-	-	-	-	-	-	-	Volts
14	8.840	0.620	-	-	-	-	-	-	-	-	Volts
15	8.510	0.532	-	-	-	-	-	-	-	-	Volts
16	8.086	0.670	-	-	-	-	-	-	-	-	Volts
17	7.560	0.605	-	-	-	-	-	-	-	-	Volts
18	7.440	0.536	-	-	-	-	-	-	-	-	Volts
19	8.153	0.505	-	-	-	-	-	-	-	-	Volts
20	8.305	0.520	-	-	-	-	-	-	-	-	Volts
21	8.781	0.467	-	-	-	-	-	-	-	-	Volts
22	9.320	0.446	-	-	-	-	-	-	-	-	Volts
23	9.765	0.333	-	-	-	-	-	-	-	-	Volts
24	10.011	0.338	-	-	-	-	-	-	-	-	Volts
25	10.220	0.320	-	-	-	-	-	-	-	-	Volts
26	10.229	0.320	-	-	-	-	-	-	-	-	Volts
27	9.586	0.390	-	-	-	-	-	-	-	-	Volts
28	9.335	0.456	-	-	-	-	-	-	-	-	Volts
29	10.174	0.350	-	-	-	-	-	-	-	-	Volts
30	10.232	0.280	-	-	-	-	-	-	-	-	Volts
31	10.134	0.307	-	-	-	-	-	-	-	-	Volts
32	9.693	0.315	-	-	-	-	-	-	-	-	Volts
33	8.990	0.405	-	-	-	-	-	-	-	-	Volts
34	8.601	0.380	-	-	-	-	-	-	-	-	Volts
35	8.438	0.368	-	-	-	-	-	-	-	-	Volts
36	8.230	0.430	-	-	-	-	-	-	-	-	Volts
37	7.603	0.486	-	-	-	-	-	-	-	-	Volts
38	7.955	0.423	-	-	-	-	-	-	-	-	Volts
39	8.122	0.355	-	-	-	-	-	-	-	-	Volts
40	8.845	0.340	-	-	-	-	-	-	-	-	Volts
41	9.817	0.297	-	-	-	-	-	-	-	-	Volts
42	10.272	0.290	-	-	-	-	-	-	-	-	Volts
43	10.227	0.370	-	-	-	-	-	-	-	-	Volts
44	10.174	0.365	-	-	-	-	-	-	-	-	Volts
45	9.287	0.545	-	-	-	-	-	-	-	-	Volts
46	9.016	0.510	-	-	-	-	-	-	-	-	Volts
47	9.860	0.420	-	-	-	-	-	-	-	-	Volts
48	10.005	0.330	-	-	-	-	-	-	-	-	Volts
49	10.134	0.305	-	-	-	-	-	-	-	-	Volts
50	9.847	0.298	-	-	-	-	-	-	-	-	Volts
51	8.940	0.306	-	-	-	-	-	-	-	-	Volts
52	8.226	0.322	-	-	-	-	-	-	-	-	Volts
53	8.094	0.325	-	-	-	-	-	-	-	-	Volts
54	7.806	0.380	-	-	-	-	-	-	-	-	Volts

Table 6.13 *Mean and fluctuation velocities and Reynolds shear stress components at section S-1 run no.1*

Loc.no.	Tangential		Vertical		Radial		Reynolds s.s. components v'w'		v'u'		Unit
	DC	RMS	DC	RMS	DC	RMS	+45	-45	+45	-45	
1	6.401	0.445	–	–	–	–	–	–	–	–	Volts
2	6.787	0.365	–	–	–	–	–	–	–	–	Volts
3	6.859	0.509	–	–	–	–	–	–	–	–	Volts
4	6.624	0.469	–	–	–	–	–	–	–	–	Volts
5	6.850	0.401	–	–	–	–	–	–	–	–	Volts
6	6.759	0.363	–	–	–	–	–	–	–	–	Volts
7	6.895	0.394	–	–	–	–	–	–	–	–	Volts
8	6.628	0.387	–	–	–	–	–	–	–	–	Volts
9	6.221	0.453	–	–	–	–	–	–	–	–	Volts
10	6.427	0.450	–	–	–	–	–	–	–	–	Volts
11	7.102	0.443	–	–	–	–	–	–	–	–	Volts
12	7.373	0.350	–	–	–	–	–	–	–	–	Volts
13	7.135	0.380	–	–	–	–	–	–	–	–	Volts
14	7.178	0.372	–	–	–	–	–	–	–	–	Volts
15	7.097	0.383	–	–	–	–	–	–	–	–	Volts
16	7.419	0.349	–	–	–	–	–	–	–	–	Volts
17	7.033	0.367	–	–	–	–	–	–	–	–	Volts
18	6.468	0.512	–	–	–	–	–	–	–	–	Volts
19	7.062	0.547	–	–	–	–	–	–	–	–	Volts
20	7.772	0.325	–	–	–	–	–	–	–	–	Volts
21	7.939	0.345	–	–	–	–	–	–	–	–	Volts
22	7.659	0.414	–	–	–	–	–	–	–	–	Volts
23	7.715	0.319	–	–	–	–	–	–	–	–	Volts
24	7.658	0.349	–	–	–	–	–	–	–	–	Volts
25	7.976	0.325	–	–	–	–	–	–	–	–	Volts
26	7.800	0.375	–	–	–	–	–	–	–	–	Volts
27	6.342	0.589	–	–	–	–	–	–	–	–	Volts
28	6.696	0.441	–	–	–	–	–	–	–	–	Volts
29	7.702	0.369	–	–	–	–	–	–	–	–	Volts
30	8.027	0.354	–	–	–	–	–	–	–	–	Volts
31	7.931	0.331	–	–	–	–	–	–	–	–	Volts
32	7.976	0.303	–	–	–	–	–	–	–	–	Volts
33	7.894	0.332	–	–	–	–	–	–	–	–	Volts
34	7.850	0.342	–	–	–	–	–	–	–	–	Volts
35	7.643	0.334	–	–	–	–	–	–	–	–	Volts
36	6.728	0.512	–	–	–	–	–	–	–	–	Volts
37	6.317	0.452	–	–	–	–	–	–	–	–	Volts
38	7.112	0.426	–	–	–	–	–	–	–	–	Volts
39	7.747	0.410	–	–	–	–	–	–	–	–	Volts
40	8.029	0.372	–	–	–	–	–	–	–	–	Volts
41	8.077	0.307	–	–	–	–	–	–	–	–	Volts
42	8.106	0.301	–	–	–	–	–	–	–	–	Volts
43	7.916	0.309	–	–	–	–	–	–	–	–	Volts
44	7.315	0.367	–	–	–	–	–	–	–	–	Volts
45	6.573	0.388	–	–	–	–	–	–	–	–	Volts

Table 6.14 *Mean and fluctuation velocities and Reynolds shear stress components at section S-1 run no.2*

Loc.no.	Tangential		Vertical		Radial		Reynolds s.s. components v'w'		v'u'		Unit
	DC	RMS	DC	RMS	DC	RMS	+45	-45	+45	-45	
1	6.844	0.506	–	–	–	–	–	–	–	–	Volts
2	7.410	0.448	–	–	–	–	–	–	–	–	Volts
3	7.507	0.461	–	–	–	–	–	–	–	–	Volts
4	7.358	0.543	–	–	–	–	–	–	–	–	Volts
5	7.358	0.481	–	–	–	–	–	–	–	–	Volts
6	7.468	0.462	–	–	–	–	–	–	–	–	Volts
7	7.452	0.444	–	–	–	–	–	–	–	–	Volts
8	7.346	0.409	–	–	–	–	–	–	–	–	Volts
9	6.650	0.460	–	–	–	–	–	–	–	–	Volts
10	7.171	0.480	–	–	–	–	–	–	–	–	Volts
11	8.115	0.425	–	–	–	–	–	–	–	–	Volts
12	7.862	0.452	–	–	–	–	–	–	–	–	Volts
13	8.068	0.460	–	–	–	–	–	–	–	–	Volts
14	7.988	0.444	–	–	–	–	–	–	–	–	Volts
15	8.117	0.467	–	–	–	–	–	–	–	–	Volts
16	8.369	0.402	–	–	–	–	–	–	–	–	Volts
17	8.249	0.381	–	–	–	–	–	–	–	–	Volts
18	7.507	0.395	–	–	–	–	–	–	–	–	Volts
19	7.931	0.472	–	–	–	–	–	–	–	–	Volts
20	8.720	0.358	–	–	–	–	–	–	–	–	Volts
21	8.750	0.362	–	–	–	–	–	–	–	–	Volts
22	8.655	0.411	–	–	–	–	–	–	–	–	Volts
23	8.475	0.417	–	–	–	–	–	–	–	–	Volts
24	8.630	0.424	–	–	–	–	–	–	–	–	Volts
25	8.506	0.365	–	–	–	–	–	–	–	–	Volts
26	8.455	0.349	–	–	–	–	–	–	–	–	Volts
27	7.770	0.536	–	–	–	–	–	–	–	–	Volts
28	7.726	0.559	–	–	–	–	–	–	–	–	Volts
29	8.563	0.401	–	–	–	–	–	–	–	–	Volts
30	8.760	0.343	–	–	–	–	–	–	–	–	Volts
31	8.957	0.406	–	–	–	–	–	–	–	–	Volts
32	8.739	0.341	–	–	–	–	–	–	–	–	Volts
33	8.946	0.358	–	–	–	–	–	–	–	–	Volts
34	8.960	0.322	–	–	–	–	–	–	–	–	Volts
35	8.790	0.404	–	–	–	–	–	–	–	–	Volts
36	8.040	0.511	–	–	–	–	–	–	–	–	Volts
37	7.637	0.571	–	–	–	–	–	–	–	–	Volts
38	8.735	0.379	–	–	–	–	–	–	–	–	Volts
39	9.060	0.323	–	–	–	–	–	–	–	–	Volts
40	9.017	0.294	–	–	–	–	–	–	–	–	Volts
41	8.911	0.297	–	–	–	–	–	–	–	–	Volts
42	9.004	0.276	–	–	–	–	–	–	–	–	Volts
43	8.784	0.362	–	–	–	–	–	–	–	–	Volts
44	8.466	0.388	–	–	–	–	–	–	–	–	Volts
45	6.950	0.969	–	–	–	–	–	–	–	–	Volts
46	7.724	0.444	–	–	–	–	–	–	–	–	Volts
47	8.320	0.403	–	–	–	–	–	–	–	–	Volts
48	8.610	0.352	–	–	–	–	–	–	–	–	Volts
49	9.142	0.298	–	–	–	–	–	–	–	–	Volts
50	9.015	0.293	–	–	–	–	–	–	–	–	Volts
51	9.058	0.292	–	–	–	–	–	–	–	–	Volts
52	8.830	0.322	–	–	–	–	–	–	–	–	Volts
53	8.560	0.397	–	–	–	–	–	–	–	–	Volts
54	6.871	0.997	–	–	–	–	–	–	–	–	Volts

Table 6.15 *Mean and fluctuation velocities and Reynolds shear stress components at section S-1 run no.3*

Loc.no.	Tangential		Vertical		Radial		Reynolds s.s. components v'w'		v'u'		Unit
	DC	RMS	DC	RMS	DC	RMS	+45	-45	+45	-45	
1	7.104	0.489	-	-	-	-	-	-	-	-	Volts
2	7.995	0.502	-	-	-	-	-	-	-	-	Volts
3	8.068	0.572	-	-	-	-	-	-	-	-	Volts
4	8.050	0.561	-	-	-	-	-	-	-	-	Volts
5	7.960	0.565	-	-	-	-	-	-	-	-	Volts
6	7.840	0.522	-	-	-	-	-	-	-	-	Volts
7	7.970	0.514	-	-	-	-	-	-	-	-	Volts
8	7.710	0.483	-	-	-	-	-	-	-	-	Volts
9	6.930	0.678	-	-	-	-	-	-	-	-	Volts
10	7.825	0.454	-	-	-	-	-	-	-	-	Volts
11	8.560	0.449	-	-	-	-	-	-	-	-	Volts
12	8.551	0.498	-	-	-	-	-	-	-	-	Volts
13	8.680	0.521	-	-	-	-	-	-	-	-	Volts
14	8.460	0.500	-	-	-	-	-	-	-	-	Volts
15	8.590	0.513	-	-	-	-	-	-	-	-	Volts
16	8.860	0.483	-	-	-	-	-	-	-	-	Volts
17	8.730	0.463	-	-	-	-	-	-	-	-	Volts
18	8.057	0.487	-	-	-	-	-	-	-	-	Volts
19	8.430	0.694	-	-	-	-	-	-	-	-	Volts
20	9.130	0.550	-	-	-	-	-	-	-	-	Volts
21	9.525	0.381	-	-	-	-	-	-	-	-	Volts
22	9.633	0.386	-	-	-	-	-	-	-	-	Volts
23	9.331	0.387	-	-	-	-	-	-	-	-	Volts
24	9.512	0.361	-	-	-	-	-	-	-	-	Volts
25	9.390	0.365	-	-	-	-	-	-	-	-	Volts
26	9.181	0.419	-	-	-	-	-	-	-	-	Volts
27	8.455	0.585	-	-	-	-	-	-	-	-	Volts
28	8.515	0.590	-	-	-	-	-	-	-	-	Volts
29	9.065	0.458	-	-	-	-	-	-	-	-	Volts
30	9.348	0.369	-	-	-	-	-	-	-	-	Volts
31	9.695	0.339	-	-	-	-	-	-	-	-	Volts
32	9.465	0.355	-	-	-	-	-	-	-	-	Volts
33	9.680	0.327	-	-	-	-	-	-	-	-	Volts
34	9.687	0.349	-	-	-	-	-	-	-	-	Volts
35	9.433	0.412	-	-	-	-	-	-	-	-	Volts
36	8.814	0.559	-	-	-	-	-	-	-	-	Volts
37	9.040	0.485	-	-	-	-	-	-	-	-	Volts
38	9.676	0.323	-	-	-	-	-	-	-	-	Volts
39	9.790	0.298	-	-	-	-	-	-	-	-	Volts
40	9.702	0.308	-	-	-	-	-	-	-	-	Volts
41	9.577	0.301	-	-	-	-	-	-	-	-	Volts
42	9.714	0.319	-	-	-	-	-	-	-	-	Volts
43	9.542	0.364	-	-	-	-	-	-	-	-	Volts
44	9.160	0.405	-	-	-	-	-	-	-	-	Volts
45	8.373	0.629	-	-	-	-	-	-	-	-	Volts
46	8.193	0.834	-	-	-	-	-	-	-	-	Volts
47	9.063	0.628	-	-	-	-	-	-	-	-	Volts
48	9.410	0.419	-	-	-	-	-	-	-	-	Volts
49	9.846	0.320	-	-	-	-	-	-	-	-	Volts
50	9.775	0.333	-	-	-	-	-	-	-	-	Volts
51	9.712	0.339	-	-	-	-	-	-	-	-	Volts
52	9.670	0.342	-	-	-	-	-	-	-	-	Volts
53	9.310	0.399	-	-	-	-	-	-	-	-	Volts
54	8.441	0.495	-	-	-	-	-	-	-	-	Volts

Table 6.16 *Mean and fluctuation velocities and Reynolds shear stress components at section S-2 run no.1*

Loc.no.	Tangential		Vertical		Radial		Reynolds s.s. components v'w'		v'u'		Unit
	DC	RMS	DC	RMS	DC	RMS	+45	-45	+45	-45	
1	6.196	0.423	-	-	-	-	-	-	-	-	Volts
2	6.267	0.399	-	-	-	-	-	-	-	-	Volts
3	6.360	0.379	-	-	-	-	-	-	-	-	Volts
4	6.470	0.376	-	-	-	-	-	-	-	-	Volts
5	6.585	0.360	-	-	-	-	-	-	-	-	Volts
6	6.528	0.372	-	-	-	-	-	-	-	-	Volts
7	6.470	0.354	-	-	-	-	-	-	-	-	Volts
8	6.553	0.341	-	-	-	-	-	-	-	-	Volts
9	6.410	0.435	-	-	-	-	-	-	-	-	Volts
10	6.768	0.582	-	-	5.958	0.485	-	-	-	-	Volts
11	6.849	0.366	-	-	5.965	0.453	-	-	-	-	Volts
12	6.730	0.379	-	-	5.947	0.497	-	-	-	-	Volts
13	6.895	0.344	-	-	5.893	0.521	-	-	-	-	Volts
14	6.850	0.335	-	-	5.861	0.462	-	-	-	-	Volts
15	6.670	0.363	-	-	5.840	0.545	-	-	-	-	Volts
16	6.515	0.381	-	-	5.934	0.559	-	-	-	-	Volts
17	6.440	0.352	-	-	5.991	0.530	-	-	-	-	Volts
18	6.251	0.385	-	-	5.980	0.522	-	-	-	-	Volts
19	6.301	0.471	6.060	0.384	6.015	0.480	0.427	0.527	0.486	0.500	Volts
20	6.576	0.354	6.050	0.409	5.985	0.512	0.490	0.432	0.506	0.546	Volts
21	6.637	0.380	6.049	0.385	5.949	0.505	0.340	0.446	0.487	0.522	Volts
22	6.873	0.360	6.048	0.386	5.972	0.523	0.331	0.446	0.480	0.547	Volts
23	7.049	0.339	6.040	0.397	5.976	0.520	0.353	0.420	0.457	0.555	Volts
24	7.086	0.302	6.023	0.421	5.985	0.510	0.429	0.440	0.480	0.543	Volts
25	7.002	0.338	6.018	0.463	6.048	0.435	0.595	0.565	0.444	0.469	Volts
26	6.952	0.320	6.016	0.418	6.060	0.478	0.661	0.626	0.450	0.466	Volts
27	6.731	0.469	6.007	0.377	6.086	0.420	0.685	0.720	0.401	0.478	Volts
28	6.806	0.489	6.005	0.423	6.066	0.513	0.678	0.634	0.413	0.543	Volts
29	6.979	0.319	6.011	0.415	6.065	0.451	0.630	0.640	0.419	0.554	Volts
30	7.012	0.330	6.012	0.327	6.065	0.486	0.560	0.629	0.456	0.519	Volts
31	7.095	0.309	6.021	0.375	6.045	0.515	0.381	0.518	0.463	0.546	Volts
32	7.020	0.317	6.041	0.350	6.074	0.504	0.358	0.451	0.480	0.535	Volts
33	6.794	0.338	6.060	0.380	6.077	0.527	0.355	0.445	0.520	0.485	Volts
34	6.663	0.339	6.070	0.391	6.030	0.540	0.349	0.405	0.574	0.547	Volts
35	6.625	0.329	6.067	0.420	6.025	0.452	0.380	0.400	0.594	0.527	Volts
36	6.410	0.394	6.075	0.370	6.028	0.500	0.415	0.467	0.555	0.552	Volts
37	6.275	0.412	6.047	0.423	6.031	0.465	0.383	0.466	0.530	0.587	Volts
38	6.504	0.380	6.048	0.402	6.046	0.584	0.379	0.421	0.570	0.544	Volts
39	6.606	0.375	6.048	0.420	6.055	0.614	0.363	0.435	0.507	0.513	Volts
40	6.684	0.357	6.047	0.370	6.060	0.529	0.347	0.402	0.523	0.492	Volts
41	7.007	0.330	6.035	0.407	6.124	0.485	0.369	0.436	0.453	0.512	Volts
42	7.093	0.343	6.026	0.377	6.068	0.506	0.395	0.506	0.441	0.537	Volts
43	6.986	0.353	6.015	0.384	5.997	0.431	0.409	0.508	0.397	0.467	Volts
44	6.846	0.341	5.995	0.395	5.958	0.453	0.415	0.515	0.426	0.521	Volts
45	6.560	0.421	5.981	0.427	5.950	0.476	0.430	0.529	0.445	0.502	Volts

Table 6.17 *Mean and fluctuation velocities and Reynolds shear stress components at section S-2 run no.2*

Loc.no.	Tangential DC	Tangential RMS	Vertical DC	Vertical RMS	Radial DC	Radial RMS	Reynolds s.s. components v'w' +45	v'w' -45	v'u' +45	v'u' -45	Unit
1	6.370	0.423	-	-	-	-	-	-	-	-	Volts
2	6.540	0.406	-	-	-	-	-	-	-	-	Volts
3	6.667	0.410	-	-	-	-	-	-	-	-	Volts
4	6.909	0.349	-	-	-	-	-	-	-	-	Volts
5	6.900	0.364	-	-	-	-	-	-	-	-	Volts
6	6.870	0.343	-	-	-	-	-	-	-	-	Volts
7	6.960	0.457	-	-	-	-	-	-	-	-	Volts
8	6.850	0.346	-	-	-	-	-	-	-	-	Volts
9	6.690	0.510	-	-	-	-	-	-	-	-	Volts
10	6.962	0.587	-	-	-	-	-	-	-	-	Volts
11	7.245	0.419	-	-	-	-	-	-	-	-	Volts
12	7.294	0.317	-	-	-	-	-	-	-	-	Volts
13	7.290	0.354	-	-	-	-	-	-	-	-	Volts
14	7.286	0.338	-	-	-	-	-	-	-	-	Volts
15	7.240	0.351	-	-	-	-	-	-	-	-	Volts
16	6.960	0.396	-	-	-	-	-	-	-	-	Volts
17	6.705	0.377	-	-	-	-	-	-	-	-	Volts
18	6.506	0.429	-	-	-	-	-	-	-	-	Volts
19	6.805	0.389	6.102	0.432	5.960	0.500	0.432	0.466	0.610	0.602	Volts
20	7.000	0.388	6.146	0.442	5.825	0.564	0.409	0.492	0.557	0.601	Volts
21	7.257	0.366	6.077	0.421	5.850	0.545	0.406	0.524	0.495	0.585	Volts
22	7.497	0.298	6.035	0.448	5.858	0.542	0.393	0.500	0.511	0.605	Volts
23	7.516	0.307	6.025	0.403	5.874	0.537	0.358	0.531	0.537	0.633	Volts
24	7.560	0.282	6.017	0.378	5.902	0.520	0.335	0.491	0.508	0.597	Volts
25	7.473	0.314	6.000	0.401	5.937	0.496	0.334	0.511	0.458	0.563	Volts
26	7.440	0.309	5.972	0.404	5.990	0.520	0.360	0.493	0.446	0.560	Volts
27	7.090	0.471	5.995	0.409	6.007	0.505	0.363	0.525	0.466	0.575	Volts
28	7.170	0.492	6.037	0.426	6.028	0.479	0.370	0.522	0.445	0.554	Volts
29	7.490	0.335	6.037	0.428	6.050	0.541	0.360	0.527	0.460	0.539	Volts
30	7.500	0.306	5.991	0.393	6.050	0.528	0.358	0.504	0.447	0.545	Volts
31	7.585	0.298	6.001	0.411	6.052	0.510	0.350	0.551	0.497	0.563	Volts
32	7.563	0.323	6.029	0.384	6.060	0.556	0.333	0.501	0.524	0.590	Volts
33	7.515	0.330	6.047	0.418	6.080	0.517	0.336	0.521	0.521	0.555	Volts
34	7.310	0.326	6.075	0.410	6.034	0.556	0.358	0.520	0.554	0.603	Volts
35	7.181	0.334	6.179	0.466	5.977	0.559	0.362	0.549	0.562	0.597	Volts
36	6.957	0.383	6.191	0.435	6.003	0.586	0.417	0.466	0.634	0.531	Volts
37	6.910	0.409	6.195	0.412	6.106	0.508	0.415	0.500	0.496	0.587	Volts
38	7.133	0.362	6.180	0.456	6.107	0.529	0.424	0.473	0.513	0.554	Volts
39	7.184	0.334	6.084	0.430	6.124	0.500	0.390	0.582	0.457	0.552	Volts
40	7.400	0.314	6.035	0.410	6.135	0.520	0.372	0.500	0.491	0.570	Volts
41	7.609	0.284	6.023	0.413	6.163	0.521	0.343	0.532	0.452	0.592	Volts
42	7.564	0.281	5.973	0.448	6.091	0.465	0.348	0.564	0.415	0.517	Volts
43	7.450	0.317	6.014	0.449	6.040	0.475	0.355	0.556	0.481	0.555	Volts
44	7.404	0.319	6.010	0.440	6.089	0.480	0.386	0.525	0.441	0.534	Volts
45	6.910	0.747	6.017	0.421	6.094	0.475	0.417	0.523	0.446	0.544	Volts
46	6.836	0.468	-	-	5.990	0.490	-	-	-	-	Volts
47	7.217	0.338	-	-	5.973	0.512	-	-	-	-	Volts
48	7.330	0.312	-	-	5.995	0.457	-	-	-	-	Volts
49	7.607	0.336	-	-	6.140	0.492	-	-	-	-	Volts
50	7.604	0.361	-	-	6.192	0.503	-	-	-	-	Volts
51	7.217	0.344	-	-	6.169	0.555	-	-	-	-	Volts
52	6.985	0.318	-	-	6.178	0.512	-	-	-	-	Volts
53	6.855	0.320	-	-	6.126	0.527	-	-	-	-	Volts
54	6.615	0.409	-	-	6.070	0.503	-	-	-	-	Volts

Table 6.18 *Mean and fluctuation velocities and Reynolds shear stress components at section S-2 run no.3*

Loc.no.	Tangential DC	Tangential RMS	Vertical DC	Vertical RMS	Radial DC	Radial RMS	Reynolds s.s. components v'w' +45	v'w' -45	v'u' +45	v'u' -45	Unit
1	6.291	0.521	-	-	-	-	-	-	-	-	Volts
2	6.664	0.405	-	-	-	-	-	-	-	-	Volts
3	6.853	0.459	-	-	-	-	-	-	-	-	Volts
4	7.083	0.380	-	-	-	-	-	-	-	-	Volts
5	7.080	0.371	-	-	-	-	-	-	-	-	Volts
6	7.041	0.352	-	-	-	-	-	-	-	-	Volts
7	7.010	0.347	-	-	-	-	-	-	-	-	Volts
8	7.070	0.347	-	-	-	-	-	-	-	-	Volts
9	6.597	0.495	-	-	-	-	-	-	-	-	Volts
10	7.210	0.437	-	-	-	-	-	-	-	-	Volts
11	7.413	0.382	-	-	-	-	-	-	-	-	Volts
12	7.401	0.462	-	-	-	-	-	-	-	-	Volts
13	7.425	0.341	-	-	-	-	-	-	-	-	Volts
14	7.515	0.357	-	-	-	-	-	-	-	-	Volts
15	7.460	0.356	-	-	-	-	-	-	-	-	Volts
16	7.273	0.459	-	-	-	-	-	-	-	-	Volts
17	6.860	0.520	-	-	-	-	-	-	-	-	Volts
18	6.599	0.565	-	-	-	-	-	-	-	-	Volts
19	7.010	0.510	6.193	0.471	5.884	0.593	0.544	0.528	0.551	0.605	Volts
20	7.280	0.454	6.189	0.468	5.810	0.620	0.472	0.558	0.575	0.680	Volts
21	7.652	0.439	6.115	0.458	5.790	0.640	0.430	0.560	0.520	0.615	Volts
22	7.800	0.364	6.044	0.450	5.825	0.546	0.435	0.588	0.487	0.662	Volts
23	7.804	0.320	6.021	0.437	5.850	0.535	0.390	0.567	0.480	0.632	Volts
24	7.740	0.312	6.012	0.435	5.874	0.534	0.473	0.565	0.476	0.604	Volts
25	7.636	0.324	5.990	0.445	5.992	0.525	0.442	0.569	0.510	0.529	Volts
26	7.533	0.365	5.959	0.410	6.022	0.457	0.368	0.503	0.395	0.545	Volts
27	7.080	0.618	5.980	0.418	6.040	0.470	0.380	0.520	0.459	0.500	Volts
28	7.350	0.443	5.997	0.390	6.042	0.526	0.362	0.547	0.487	0.607	Volts
29	7.607	0.319	5.939	0.445	6.048	0.468	0.380	0.565	0.406	0.550	Volts
30	7.705	0.311	5.975	0.444	6.087	0.497	0.360	0.568	0.459	0.579	Volts
31	7.890	0.321	5.985	0.433	6.023	0.524	0.354	0.569	0.450	0.586	Volts
32	7.898	0.318	6.022	0.382	6.049	0.533	0.331	0.495	0.484	0.584	Volts
33	7.963	0.314	6.047	0.412	6.043	0.510	0.333	0.563	0.485	0.609	Volts
34	7.717	0.315	6.104	0.422	6.014	0.546	0.377	0.529	0.470	0.590	Volts
35	7.539	0.414	6.206	0.490	6.031	0.522	0.397	0.499	0.460	0.582	Volts
36	7.145	0.471	6.326	0.422	6.037	0.515	0.356	0.486	0.524	0.545	Volts
37	6.992	0.478	6.310	0.454	6.126	0.553	0.411	0.494	0.540	0.609	Volts
38	7.390	0.354	6.246	0.452	6.030	0.619	0.420	0.568	0.573	0.610	Volts
39	7.552	0.439	6.102	0.422	6.061	0.627	0.386	0.512	0.540	0.615	Volts
40	7.865	0.342	6.007	0.427	6.135	0.590	0.367	0.514	0.580	0.657	Volts
41	7.994	0.305	6.027	0.440	6.160	0.572	0.367	0.575	0.602	0.647	Volts
42	7.950	0.309	5.946	0.445	6.101	0.588	0.362	0.580	0.525	0.660	Volts
43	7.702	0.318	5.981	0.449	6.083	0.483	0.350	0.568	0.450	0.560	Volts
44	7.640	0.387	6.030	0.438	6.100	0.470	0.342	0.487	0.426	0.567	Volts
45	7.283	0.522	6.030	0.395	6.086	0.466	0.361	0.503	0.442	0.579	Volts
46	6.975	0.565	-	-	5.990	0.462	-	-	-	-	Volts
47	7.459	0.341	-	-	5.968	0.490	-	-	-	-	Volts
48	7.620	0.318	-	-	6.007	0.487	-	-	-	-	Volts
49	7.860	0.322	-	-	6.144	0.546	-	-	-	-	Volts
50	7.993	0.309	-	-	6.248	0.545	-	-	-	-	Volts
51	7.660	0.362	-	-	6.143	0.685	-	-	-	-	Volts
52	7.168	0.342	-	-	6.120	0.697	-	-	-	-	Volts
53	7.109	0.385	-	-	6.103	0.562	-	-	-	-	Volts
54	6.673	0.497	-	-	6.023	0.513	-	-	-	-	Volts

Table 6.19 *Mean and fluctuation velocities and Reynolds shear stress components at section S-3 run no.1*

Loc.no.	Tangential		Vertical		Radial		Reynolds s.s. components v'w'		v'u'		Unit
	DC	RMS	DC	RMS	DC	RMS	+45	-45	+45	-45	
1	6.096	0.590	-	-	-	-	-	-	-	-	Volts
2	6.175	0.456	-	-	-	-	-	-	-	-	Volts
3	6.303	0.436	-	-	-	-	-	-	-	-	Volts
4	6.350	0.486	-	-	-	-	-	-	-	-	Volts
5	6.441	0.506	-	-	-	-	-	-	-	-	Volts
6	6.550	0.390	-	-	-	-	-	-	-	-	Volts
7	6.593	0.412	-	-	-	-	-	-	-	-	Volts
8	6.620	0.564	-	-	-	-	-	-	-	-	Volts
9	6.504	0.588	-	-	-	-	-	-	-	-	Volts
10	6.888	0.594	-	-	6.023	0.411	-	-	-	-	Volts
11	7.001	0.360	-	-	6.006	0.463	-	-	-	-	Volts
12	6.950	0.354	-	-	5.979	0.426	-	-	-	-	Volts
13	6.890	0.351	-	-	5.963	0.404	-	-	-	-	Volts
14	6.690	0.376	-	-	5.953	0.470	-	-	-	-	Volts
15	6.560	0.373	-	-	5.943	0.435	-	-	-	-	Volts
16	6.400	0.367	-	-	5.965	0.421	-	-	-	-	Volts
17	6.269	0.386	-	-	6.000	0.428	-	-	-	-	Volts
18	6.176	0.446	-	-	6.019	0.410	-	-	-	-	Volts
19	6.330	0.418	6.072	0.400	6.018	0.428	0.428	0.510	0.371	0.344	Volts
20	6.514	0.451	6.061	0.425	6.017	0.415	0.417	0.443	0.396	0.404	Volts
21	6.621	0.380	6.054	0.444	6.023	0.439	0.408	0.467	0.362	0.412	Volts
22	6.848	0.365	6.043	0.425	6.046	0.413	0.404	0.437	0.381	0.418	Volts
23	6.994	0.375	6.031	0.450	6.042	0.384	0.405	0.473	0.338	0.398	Volts
24	7.120	0.382	6.026	0.388	6.036	0.429	0.347	0.474	0.344	0.419	Volts
25	7.193	0.421	6.021	0.418	6.038	0.378	0.370	0.507	0.335	0.431	Volts
26	7.189	0.435	6.027	0.441	6.035	0.371	0.394	0.485	0.315	0.436	Volts
27	7.063	0.410	6.017	0.422	6.047	0.387	0.400	0.472	0.323	0.435	Volts
28	7.080	0.383	6.063	0.423	6.061	0.363	0.373	0.480	0.295	0.420	Volts
29	7.160	0.422	6.028	0.427	6.060	0.339	0.414	0.482	0.307	0.422	Volts
30	7.163	0.423	6.018	0.425	6.046	0.375	0.375	0.483	0.296	0.409	Volts
31	7.105	0.396	6.026	0.451	6.057	0.362	0.381	0.440	0.333	0.431	Volts
32	6.896	0.402	6.040	0.426	6.076	0.350	0.385	0.442	0.347	0.410	Volts
33	6.681	0.403	6.027	0.436	6.091	0.348	0.398	0.467	0.356	0.390	Volts
34	6.585	0.397	6.056	0.412	6.070	0.380	0.389	0.449	0.368	0.434	Volts
35	6.461	0.480	6.060	0.438	6.056	0.400	0.396	0.448	0.386	0.408	Volts
36	6.396	0.450	6.070	0.438	6.046	0.437	0.462	0.515	0.364	0.396	Volts
37	6.283	0.527	6.060	0.480	6.041	0.463	0.459	0.547	0.435	0.419	Volts
38	6.325	0.520	6.048	0.485	6.053	0.446	0.452	0.500	0.376	0.403	Volts
39	6.462	0.498	6.037	0.442	6.094	0.436	0.421	0.440	0.399	0.428	Volts
40	6.636	0.447	6.039	0.431	6.044	0.390	0.426	0.493	0.336	0.422	Volts
41	6.915	0.357	6.033	0.410	6.047	0.380	0.366	0.442	0.361	0.426	Volts
42	7.125	0.423	6.032	0.415	6.054	0.372	0.364	0.470	0.341	0.422	Volts
43	7.094	0.436	6.030	0.418	5.986	0.350	0.377	0.475	0.331	0.439	Volts
44	7.086	0.369	6.028	0.422	5.921	0.374	0.385	0.485	0.317	0.448	Volts
45	6.974	0.420	6.025	0.435	5.948	0.371	0.395	0.490	0.330	0.451	Volts

Table 6.20 *Mean and fluctuation velocities and Reynolds shear stress components at section S-3 run no.2*

Loc.no.	Tangential		Vertical		Radial		Reynolds s.s. components v'w'		v'u'		Unit
	DC	RMS	DC	RMS	DC	RMS	+45	-45	+45	-45	
1	6.251	0.485	-	-	-	-	-	-	-	-	Volts
2	6.454	0.418	-	-	-	-	-	-	-	-	Volts
3	6.625	0.393	-	-	-	-	-	-	-	-	Volts
4	6.766	0.384	-	-	-	-	-	-	-	-	Volts
5	6.821	0.375	-	-	-	-	-	-	-	-	Volts
6	6.882	0.369	-	-	-	-	-	-	-	-	Volts
7	6.889	0.358	-	-	-	-	-	-	-	-	Volts
8	6.993	0.364	-	-	-	-	-	-	-	-	Volts
9	6.625	0.444	-	-	-	-	-	-	-	-	Volts
10	7.308	0.635	-	-	-	-	-	-	-	-	Volts
11	7.633	0.361	-	-	-	-	-	-	-	-	Volts
12	7.565	0.359	-	-	-	-	-	-	-	-	Volts
13	7.395	0.345	-	-	-	-	-	-	-	-	Volts
14	7.240	0.384	-	-	-	-	-	-	-	-	Volts
15	7.126	0.415	-	-	-	-	-	-	-	-	Volts
16	6.999	0.423	-	-	-	-	-	-	-	-	Volts
17	6.704	0.421	-	-	-	-	-	-	-	-	Volts
18	6.546	0.440	-	-	-	-	-	-	-	-	Volts
19	6.799	0.439	6.123	0.492	5.988	0.464	0.455	0.524	0.429	0.496	Volts
20	7.050	0.402	6.109	0.431	5.958	0.413	0.404	0.552	0.373	0.516	Volts
21	7.205	0.392	6.069	0.433	5.975	0.377	0.381	0.470	0.367	0.502	Volts
22	7.333	0.354	6.040	0.415	5.985	0.450	0.367	0.492	0.403	0.533	Volts
23	7.508	0.336	6.021	0.440	5.934	0.426	0.371	0.513	0.405	0.523	Volts
24	7.660	0.326	6.016	0.407	5.970	0.468	0.375	0.537	0.340	0.595	Volts
25	7.712	0.327	6.023	0.472	6.045	0.423	0.383	0.519	0.356	0.511	Volts
26	7.747	0.311	6.010	0.478	6.035	0.400	0.367	0.541	0.332	0.529	Volts
27	7.416	0.479	5.995	0.445	6.014	0.398	0.363	0.517	0.345	0.575	Volts
28	7.442	0.466	6.067	0.425	6.051	0.398	0.362	0.506	0.376	0.513	Volts
29	7.727	0.323	6.061	0.432	6.072	0.405	0.365	0.510	0.337	0.462	Volts
30	7.703	0.320	6.036	0.418	6.080	0.407	0.367	0.498	0.361	0.537	Volts
31	7.660	0.319	5.997	0.431	6.065	0.415	0.371	0.494	0.384	0.464	Volts
32	7.497	0.331	6.018	0.412	6.035	0.398	0.343	0.482	0.406	0.502	Volts
33	7.282	0.343	6.025	0.454	6.047	0.376	0.416	0.492	0.317	0.465	Volts
34	7.072	0.372	6.066	0.430	6.023	0.437	0.399	0.480	0.362	0.532	Volts
35	7.021	0.390	6.113	0.403	6.004	0.375	0.397	0.468	0.357	0.503	Volts
36	6.792	0.414	6.158	0.461	6.018	0.510	0.438	0.490	0.411	0.489	Volts
37	6.543	0.460	6.095	0.416	6.053	0.466	0.487	0.506	0.395	0.491	Volts
38	6.777	0.442	6.116	0.477	6.076	0.348	0.451	0.511	0.351	0.406	Volts
39	6.958	0.386	6.046	0.430	6.035	0.367	0.407	0.506	0.354	0.439	Volts
40	7.237	0.354	6.020	0.411	6.063	0.398	0.403	0.526	0.373	0.450	Volts
41	7.487	0.333	6.027	0.426	6.080	0.441	0.391	0.499	0.430	0.473	Volts
42	7.680	0.356	5.992	0.444	6.044	0.401	0.340	0.509	0.361	0.504	Volts
43	7.677	0.330	6.012	0.417	5.982	0.429	0.342	0.490	0.352	0.534	Volts
44	7.698	0.323	6.082	0.410	6.003	0.420	0.371	0.487	0.348	0.540	Volts
45	7.411	0.508	6.109	0.403	6.000	0.438	0.379	0.469	0.353	0.539	Volts
46	7.204	0.430	-	-	5.914	0.421	-	-	-	-	Volts
47	7.582	0.344	-	-	5.862	0.446	-	-	-	-	Volts
48	7.670	0.332	-	-	5.959	0.413	-	-	-	-	Volts
49	7.680	0.337	-	-	5.991	0.367	-	-	-	-	Volts
50	7.578	0.375	-	-	6.083	0.436	-	-	-	-	Volts
51	7.260	0.355	-	-	6.081	0.318	-	-	-	-	Volts
52	6.936	0.377	-	-	6.100	0.418	-	-	-	-	Volts
53	6.705	0.420	-	-	6.095	0.377	-	-	-	-	Volts
54	6.540	0.416	-	-	6.032	0.412	-	-	-	-	Volts

Table 6.21 Mean and fluctuation velocities and Reynolds shear stress components at section S-3 run no.3

Loc.no.	Tangential		Vertical		Radial		Reynolds s.s. components v'w'		v'u'		Unit
	DC	RMS	DC	RMS	DC	RMS	+45	-45	+45	-45	
1	6.575	0.445	-	-	-	-	-	-	-	-	Volts
2	6.785	0.436	-	-	-	-	-	-	-	-	Volts
3	6.909	0.393	-	-	-	-	-	-	-	-	Volts
4	7.083	0.358	-	-	-	-	-	-	-	-	Volts
5	7.113	0.403	-	-	-	-	-	-	-	-	Volts
6	7.139	0.420	-	-	-	-	-	-	-	-	Volts
7	7.375	0.448	-	-	-	-	-	-	-	-	Volts
8	7.365	0.450	-	-	-	-	-	-	-	-	Volts
9	7.140	0.435	-	-	-	-	-	-	-	-	Volts
10	7.530	0.399	-	-	-	-	-	-	-	-	Volts
11	7.917	0.374	-	-	-	-	-	-	-	-	Volts
12	7.842	0.372	-	-	-	-	-	-	-	-	Volts
13	7.750	0.388	-	-	-	-	-	-	-	-	Volts
14	7.615	0.392	-	-	-	-	-	-	-	-	Volts
15	7.367	0.402	-	-	-	-	-	-	-	-	Volts
16	7.305	0.418	-	-	-	-	-	-	-	-	Volts
17	7.147	0.459	-	-	-	-	-	-	-	-	Volts
18	6.841	0.496	-	-	-	-	-	-	-	-	Volts
19	6.857	0.608	6.147	0.486	6.064	0.650	0.527	0.617	0.613	0.523	Volts
20	7.297	0.430	6.103	0.464	6.076	0.581	0.431	0.604	0.609	0.508	Volts
21	7.555	0.450	6.071	0.435	5.974	0.614	0.405	0.531	0.445	0.601	Volts
22	7.637	0.390	6.047	0.449	5.990	0.547	0.385	0.518	0.478	0.572	Volts
23	7.812	0.323	6.027	0.440	6.000	0.612	0.374	0.535	0.485	0.526	Volts
24	7.913	0.325	6.017	0.410	6.020	0.523	0.335	0.500	0.460	0.652	Volts
25	8.007	0.314	6.007	0.421	6.009	0.404	0.348	0.497	0.341	0.573	Volts
26	7.970	0.350	5.999	0.437	6.045	0.408	0.340	0.564	0.316	0.531	Volts
27	7.670	0.476	5.987	0.410	6.013	0.442	0.352	0.547	0.448	0.491	Volts
28	7.565	0.469	6.052	0.463	6.031	0.447	0.424	0.476	0.427	0.575	Volts
29	8.015	0.301	6.073	0.381	6.065	0.397	0.318	0.438	0.336	0.535	Volts
30	8.002	0.307	6.036	0.383	6.110	0.446	0.328	0.474	0.324	0.481	Volts
31	7.942	0.308	6.003	0.422	6.098	0.440	0.343	0.490	0.354	0.629	Volts
32	7.845	0.326	6.005	0.382	6.083	0.425	0.303	0.510	0.330	0.551	Volts
33	7.684	0.332	6.017	0.397	6.065	0.376	0.330	0.465	0.364	0.477	Volts
34	7.506	0.345	6.038	0.378	6.061	0.423	0.316	0.472	0.367	0.522	Volts
35	7.364	0.353	6.111	0.449	6.037	0.434	0.368	0.478	0.371	0.522	Volts
36	6.933	0.587	6.180	0.388	6.043	0.393	0.380	0.575	0.359	0.450	Volts
37	6.740	0.438	6.083	0.433	6.057	0.391	0.411	0.502	0.430	0.435	Volts
38	7.090	0.377	6.162	0.463	6.090	0.399	0.378	0.454	0.353	0.472	Volts
39	7.222	0.325	6.066	0.396	6.091	0.384	0.366	0.491	0.371	0.491	Volts
40	7.561	0.295	6.002	0.408	6.042	0.415	0.329	0.469	0.348	0.482	Volts
41	7.906	0.286	6.025	0.427	6.055	0.417	0.322	0.492	0.349	0.511	Volts
42	8.023	0.305	5.978	0.374	6.070	0.446	0.305	0.388	0.378	0.544	Volts
43	8.013	0.290	6.099	0.354	6.037	0.418	0.292	0.492	0.391	0.525	Volts
44	7.975	0.298	6.103	0.401	6.027	0.371	0.335	0.457	0.352	0.470	Volts
45	7.547	0.462	6.171	0.390	5.990	0.440	0.357	0.480	0.362	0.578	Volts
46	7.449	0.405	-	-	5.927	0.404	-	-	-	-	Volts
47	7.796	0.321	-	-	5.871	0.427	-	-	-	-	Volts
48	7.854	0.306	-	-	5.868	0.402	-	-	-	-	Volts
49	7.938	0.298	-	-	5.988	0.383	-	-	-	-	Volts
50	7.960	0.306	-	-	6.019	0.446	-	-	-	-	Volts
51	7.662	0.327	-	-	6.057	0.424	-	-	-	-	Volts
52	7.253	0.402	-	-	6.090	0.532	-	-	-	-	Volts
53	7.165	0.532	-	-	6.053	0.385	-	-	-	-	Volts
54	6.913	0.561	-	-	6.037	0.473	-	-	-	-	Volts

Table 6.22 Mean and fluctuation velocities and Reynolds shear stress components at section S-4 run no.1

Loc.no.	Tangential		Vertical		Radial		Reynolds s.s. components v'w'		v'u'		Unit
	DC	RMS	DC	RMS	DC	RMS	+45	-45	+45	-45	
1	6.201	0.457	-	-	-	-	-	-	-	-	Volts
2	6.280	0.407	-	-	-	-	-	-	-	-	Volts
3	6.387	0.402	-	-	-	-	-	-	-	-	Volts
4	6.433	0.391	-	-	-	-	-	-	-	-	Volts
5	6.506	0.367	-	-	-	-	-	-	-	-	Volts
6	6.580	0.335	-	-	-	-	-	-	-	-	Volts
7	6.648	0.321	-	-	-	-	-	-	-	-	Volts
8	6.770	0.348	-	-	-	-	-	-	-	-	Volts
9	6.685	0.363	-	-	-	-	-	-	-	-	Volts
10	6.906	0.387	-	-	6.040	0.517	-	-	-	-	Volts
11	7.085	0.304	-	-	6.020	0.516	-	-	-	-	Volts
12	7.013	0.325	-	-	6.010	0.385	-	-	-	-	Volts
13	6.920	0.317	-	-	6.014	0.484	-	-	-	-	Volts
14	6.774	0.334	-	-	5.984	0.436	-	-	-	-	Volts
15	6.635	0.367	-	-	5.986	0.500	-	-	-	-	Volts
16	6.550	0.371	-	-	5.990	0.417	-	-	-	-	Volts
17	6.407	0.362	-	-	6.005	0.453	-	-	-	-	Volts
18	6.308	0.411	-	-	6.012	0.439	-	-	-	-	Volts
19	6.446	0.411	6.066	0.438	6.032	0.430	0.482	0.453	0.479	0.567	Volts
20	6.559	0.368	6.071	0.419	6.031	0.435	0.407	0.456	0.489	0.514	Volts
21	6.711	0.356	6.052	0.441	6.018	0.480	0.452	0.428	0.492	0.460	Volts
22	6.851	0.354	6.053	0.414	6.009	0.537	0.454	0.450	0.459	0.462	Volts
23	7.013	0.346	6.052	0.393	6.040	0.461	0.348	0.457	0.473	0.495	Volts
24	7.172	0.336	6.040	0.397	6.030	0.410	0.374	0.495	0.443	0.459	Volts
25	7.256	0.312	6.036	0.450	6.074	0.415	0.368	0.414	0.440	0.451	Volts
26	7.257	0.321	6.047	0.356	6.073	0.419	0.330	0.456	0.403	0.477	Volts
27	6.933	0.396	6.040	0.414	6.072	0.425	0.328	0.496	0.417	0.480	Volts
28	7.077	0.377	6.072	0.385	6.048	0.465	0.375	0.469	0.418	0.485	Volts
29	7.217	0.322	6.025	0.407	6.049	0.468	0.342	0.489	0.418	0.483	Volts
30	7.216	0.317	6.024	0.401	6.059	0.466	0.324	0.485	0.386	0.468	Volts
31	7.119	0.325	6.038	0.395	6.051	0.449	0.331	0.475	0.431	0.509	Volts
32	6.930	0.334	6.046	0.386	6.062	0.466	0.342	0.418	0.483	0.471	Volts
33	6.768	0.333	6.043	0.340	6.048	0.541	0.357	0.408	0.486	0.461	Volts
34	6.650	0.310	6.052	0.358	6.058	0.479	0.322	0.405	0.490	0.455	Volts
35	6.570	0.341	6.065	0.388	6.059	0.469	0.348	0.422	0.520	0.485	Volts
36	6.463	0.424	6.087	0.430	6.037	0.468	0.415	0.436	0.441	0.586	Volts
37	6.356	0.454	6.051	0.385	6.026	0.495	0.469	0.465	0.470	0.490	Volts
38	6.435	0.460	6.050	0.363	6.050	0.460	0.426	0.466	0.471	0.505	Volts
39	6.572	0.399	6.037	0.382	6.053	0.438	0.422	0.384	0.500	0.449	Volts
40	6.737	0.386	6.042	0.384	6.031	0.503	0.401	0.399	0.436	0.473	Volts
41	6.958	0.316	6.043	0.383	6.053	0.415	0.332	0.450	0.476	0.493	Volts
42	7.159	0.303	6.041	0.399	6.060	0.430	0.308	0.424	0.441	0.471	Volts
43	7.184	0.309	6.035	0.402	6.011	0.387	0.300	0.412	0.408	0.441	Volts
44	7.150	0.315	6.028	0.419	5.996	0.420	0.288	0.389	0.451	0.482	Volts
45	7.044	0.336	6.010	0.439	5.977	0.435	0.277	0.380	0.460	0.490	Volts

Table 6.23 Mean and fluctuation velocities and Reynolds shear stress components at section S-4 run no.2

Loc.no.	Tangential DC	Tangential RMS	Vertical DC	Vertical RMS	Radial DC	Radial RMS	Reynolds s.s. v'w' +45	v'w' -45	v'u' +45	v'u' -45	Unit
1	6.353	0.433	-	-	-	-	-	-	-	-	Volts
2	6.510	0.385	-	-	-	-	-	-	-	-	Volts
3	6.700	0.418	-	-	-	-	-	-	-	-	Volts
4	6.783	0.393	-	-	-	-	-	-	-	-	Volts
5	6.833	0.334	-	-	-	-	-	-	-	-	Volts
6	6.897	0.329	-	-	-	-	-	-	-	-	Volts
7	7.169	0.314	-	-	-	-	-	-	-	-	Volts
8	7.217	0.296	-	-	-	-	-	-	-	-	Volts
9	6.992	0.369	-	-	-	-	-	-	-	-	Volts
10	7.340	0.386	-	-	-	-	-	-	-	-	Volts
11	7.681	0.313	-	-	-	-	-	-	-	-	Volts
12	7.605	0.330	-	-	-	-	-	-	-	-	Volts
13	7.489	0.317	-	-	-	-	-	-	-	-	Volts
14	7.266	0.364	-	-	-	-	-	-	-	-	Volts
15	7.065	0.352	-	-	-	-	-	-	-	-	Volts
16	6.914	0.379	-	-	-	-	-	-	-	-	Volts
17	6.710	0.408	-	-	-	-	-	-	-	-	Volts
18	6.504	0.531	-	-	-	-	-	-	-	-	Volts
19	6.717	0.446	6.107	0.439	5.999	0.470	0.480	0.486	0.481	0.495	Volts
20	7.000	0.391	6.111	0.387	6.012	0.481	0.478	0.473	0.430	0.462	Volts
21	7.150	0.357	6.074	0.400	6.031	0.441	0.356	0.434	0.469	0.497	Volts
22	7.385	0.329	6.046	0.397	6.042	0.477	0.351	0.484	0.452	0.455	Volts
23	7.570	0.303	6.050	0.368	6.037	0.398	0.314	0.490	0.388	0.474	Volts
24	7.674	0.295	6.043	0.407	6.080	0.456	0.304	0.459	0.397	0.451	Volts
25	7.714	0.283	6.044	0.369	6.108	0.432	0.312	0.436	0.457	0.518	Volts
26	7.738	0.318	6.030	0.427	6.086	0.416	0.339	0.478	0.410	0.506	Volts
27	7.436	0.421	6.025	0.407	6.080	0.418	0.475	0.480	0.411	0.500	Volts
28	7.459	0.399	6.072	0.370	6.072	0.450	0.408	0.473	0.420	0.499	Volts
29	7.736	0.287	6.059	0.375	6.087	0.466	0.303	0.481	0.426	0.497	Volts
30	7.714	0.278	6.056	0.330	6.107	0.380	0.289	0.493	0.351	0.432	Volts
31	7.698	0.272	6.010	0.391	6.070	0.420	0.301	0.471	0.411	0.467	Volts
32	7.508	0.282	6.046	0.334	6.037	0.454	0.292	0.444	0.381	0.483	Volts
33	7.209	0.301	6.054	0.356	6.053	0.447	0.300	0.410	0.405	0.486	Volts
34	7.134	0.306	6.066	0.398	6.037	0.424	0.351	0.385	0.406	0.468	Volts
35	7.056	0.330	6.112	0.375	6.030	0.494	0.366	0.392	0.415	0.477	Volts
36	6.872	0.378	6.140	0.402	6.046	0.410	0.370	0.410	0.453	0.451	Volts
37	6.716	0.374	6.137	0.399	6.071	0.415	0.345	0.410	0.428	0.434	Volts
38	6.926	0.332	6.117	0.346	6.075	0.414	0.324	0.398	0.421	0.457	Volts
39	7.020	0.335	6.069	0.340	6.060	0.389	0.314	0.400	0.471	0.418	Volts
40	7.174	0.291	6.051	0.379	6.052	0.426	0.313	0.410	0.414	0.487	Volts
41	7.507	0.280	6.049	0.345	6.043	0.413	0.297	0.414	0.443	0.498	Volts
42	7.729	0.274	6.000	0.339	6.031	0.402	0.280	0.428	0.439	0.450	Volts
43	7.725	0.271	6.053	0.358	6.054	0.429	0.311	0.422	0.367	0.454	Volts
44	7.767	0.264	6.111	0.333	6.050	0.388	0.279	0.422	0.378	0.435	Volts
45	7.500	0.363	6.124	0.351	6.049	0.400	0.327	0.432	0.375	0.450	Volts
46	7.433	0.305	-	-	6.000	0.400	-	-	-	-	Volts
47	7.642	0.277	-	-	5.976	0.381	-	-	-	-	Volts
48	7.655	0.267	-	-	5.944	0.361	-	-	-	-	Volts
49	7.720	0.281	-	-	5.961	0.404	-	-	-	-	Volts
50	7.540	0.293	-	-	6.062	0.410	-	-	-	-	Volts
51	7.196	0.328	-	-	6.039	0.409	-	-	-	-	Volts
52	6.931	0.392	-	-	6.062	0.433	-	-	-	-	Volts
53	6.835	0.369	-	-	6.053	0.434	-	-	-	-	Volts
54	6.636	0.400	-	-	6.030	0.437	-	-	-	-	Volts

Table 6.24 Mean and fluctuation velocities and Reynolds shear stress components at section S-4 run no.3

Loc.no.	Tangential DC	Tangential RMS	Vertical DC	Vertical RMS	Radial DC	Radial RMS	Reynolds s.s. v'w' +45	v'w' -45	v'u' +45	v'u' -45	Unit
1	6.412	0.470	-	-	-	-	-	-	-	-	Volts
2	6.702	0.419	-	-	-	-	-	-	-	-	Volts
3	6.822	0.406	-	-	-	-	-	-	-	-	Volts
4	7.037	0.362	-	-	-	-	-	-	-	-	Volts
5	7.153	0.310	-	-	-	-	-	-	-	-	Volts
6	7.143	0.290	-	-	-	-	-	-	-	-	Volts
7	7.298	0.305	-	-	-	-	-	-	-	-	Volts
8	7.267	0.346	-	-	-	-	-	-	-	-	Volts
9	6.969	0.393	-	-	-	-	-	-	-	-	Volts
10	7.375	0.426	-	-	-	-	-	-	-	-	Volts
11	7.871	0.280	-	-	-	-	-	-	-	-	Volts
12	7.890	0.289	-	-	-	-	-	-	-	-	Volts
13	7.720	0.305	-	-	-	-	-	-	-	-	Volts
14	7.515	0.316	-	-	-	-	-	-	-	-	Volts
15	7.345	0.322	-	-	-	-	-	-	-	-	Volts
16	7.200	0.360	-	-	-	-	-	-	-	-	Volts
17	6.990	0.411	-	-	-	-	-	-	-	-	Volts
18	6.553	0.492	-	-	-	-	-	-	-	-	Volts
19	6.786	0.554	6.122	0.439	5.914	0.492	0.415	0.439	0.450	0.547	Volts
20	7.202	0.340	6.139	0.346	5.884	0.506	0.340	0.411	0.477	0.530	Volts
21	7.480	0.342	6.097	0.380	5.859	0.491	0.362	0.441	0.457	0.521	Volts
22	7.643	0.305	6.058	0.355	5.870	0.494	0.354	0.448	0.440	0.491	Volts
23	7.821	0.287	6.043	0.333	5.874	0.449	0.313	0.470	0.451	0.468	Volts
24	7.933	0.284	6.041	0.336	5.980	0.469	0.307	0.443	0.452	0.459	Volts
25	8.030	0.286	6.051	0.336	6.055	0.402	0.280	0.442	0.374	0.472	Volts
26	8.012	0.271	6.041	0.310	6.044	0.399	0.274	0.424	0.378	0.474	Volts
27	7.505	0.474	6.029	0.324	6.070	0.400	0.334	0.466	0.380	0.480	Volts
28	7.565	0.464	6.092	0.310	6.060	0.420	0.316	0.467	0.390	0.485	Volts
29	7.996	0.265	6.073	0.315	6.082	0.455	0.285	0.419	0.405	0.489	Volts
30	8.016	0.259	6.067	0.297	6.094	0.406	0.261	0.411	0.368	0.494	Volts
31	7.965	0.269	6.015	0.303	6.106	0.437	0.277	0.417	0.417	0.478	Volts
32	7.833	0.263	6.042	0.317	6.035	0.545	0.290	0.433	0.444	0.587	Volts
33	7.615	0.281	6.053	0.331	5.998	0.565	0.310	0.411	0.528	0.588	Volts
34	7.423	0.319	6.075	0.373	6.034	0.509	0.306	0.459	0.480	0.511	Volts
35	7.300	0.300	6.140	0.363	6.052	0.432	0.313	0.450	0.520	0.497	Volts
36	6.903	0.445	6.220	0.373	6.056	0.464	0.384	0.455	0.559	0.553	Volts
37	6.662	0.484	6.106	0.413	6.060	0.470	0.358	0.435	0.591	0.552	Volts
38	7.069	0.318	6.150	0.376	6.083	0.484	0.326	0.441	0.485	0.496	Volts
39	7.220	0.283	6.070	0.317	6.064	0.487	0.314	0.408	0.528	0.495	Volts
40	7.576	0.281	6.044	0.325	6.007	0.520	0.295	0.387	0.430	0.522	Volts
41	7.912	0.257	6.034	0.310	6.040	0.432	0.275	0.405	0.445	0.532	Volts
42	7.985	0.261	5.988	0.314	6.037	0.451	0.263	0.426	0.405	0.548	Volts
43	8.010	0.262	6.099	0.327	6.046	0.448	0.284	0.418	0.540	0.480	Volts
44	8.006	0.320	6.114	0.306	6.015	0.461	0.279	0.419	0.391	0.485	Volts
45	7.626	0.471	6.100	0.400	6.000	0.472	0.336	0.432	0.400	0.487	Volts
46	7.499	0.394	-	-	5.942	0.420	-	-	-	-	Volts
47	7.800	0.287	-	-	5.959	0.406	-	-	-	-	Volts
48	7.921	0.256	-	-	5.926	0.405	-	-	-	-	Volts
49	8.005	0.254	-	-	5.884	0.492	-	-	-	-	Volts
50	7.925	0.266	-	-	6.022	0.488	-	-	-	-	Volts
51	7.591	0.277	-	-	6.036	0.495	-	-	-	-	Volts
52	7.260	0.293	-	-	6.043	0.505	-	-	-	-	Volts
53	7.181	0.350	-	-	6.013	0.452	-	-	-	-	Volts
54	6.823	0.427	-	-	5.976	0.520	-	-	-	-	Volts

Table 6.25 Mean and fluctuation velocities and Reynolds shear stress components at section S-5 run no.1

Loc.no.	Tangential		Vertical		Radial		Reynolds s.s. components v'w'		v'u'		Unit
	DC	RMS	DC	RMS	DC	RMS	+45	-45	+45	-45	
1	6.275	0.341	-	-	-	-	-	-	-	-	Volts
2	6.471	0.319	-	-	-	-	-	-	-	-	Volts
3	6.555	0.343	-	-	-	-	-	-	-	-	Volts
4	6.491	0.329	-	-	-	-	-	-	-	-	Volts
5	6.388	0.335	-	-	-	-	-	-	-	-	Volts
6	6.292	0.348	-	-	-	-	-	-	-	-	Volts
7	6.149	0.394	-	-	-	-	-	-	-	-	Volts
8	6.098	0.394	-	-	-	-	-	-	-	-	Volts
9	6.084	0.508	-	-	-	-	-	-	-	-	Volts
10	6.066	0.398	-	-	6.042	0.432	-	-	-	-	Volts
11	6.158	0.394	-	-	6.021	0.420	-	-	-	-	Volts
12	6.276	0.371	-	-	6.008	0.422	-	-	-	-	Volts
13	6.486	0.333	-	-	5.991	0.361	-	-	-	-	Volts
14	6.659	0.314	-	-	5.988	0.386	-	-	-	-	Volts
15	6.886	0.303	-	-	5.987	0.383	-	-	-	-	Volts
16	6.898	0.356	-	-	5.980	0.385	-	-	-	-	Volts
17	6.816	0.382	-	-	5.957	0.392	-	-	-	-	Volts
18	6.588	0.374	-	-	5.998	0.393	-	-	-	-	Volts
19	6.962	0.451	6.023	0.407	5.983	0.375	0.450	0.504	0.440	0.331	Volts
20	7.284	0.338	6.037	0.412	5.975	0.409	0.425	0.360	0.471	0.345	Volts
21	7.308	0.311	6.050	0.330	5.994	0.380	0.398	0.344	0.440	0.340	Volts
22	7.255	0.296	6.053	0.353	6.000	0.363	0.391	0.324	0.425	0.324	Volts
23	7.015	0.336	6.048	0.345	6.010	0.393	0.397	0.314	0.399	0.339	Volts
24	6.806	0.288	6.041	0.357	5.989	0.392	0.405	0.337	0.420	0.374	Volts
25	6.607	0.328	6.034	0.337	5.981	0.419	0.394	0.338	0.421	0.383	Volts
26	6.546	0.333	6.028	0.366	5.972	0.404	0.377	0.345	0.424	0.380	Volts
27	6.445	0.334	6.046	0.347	5.989	0.424	0.385	0.391	0.418	0.399	Volts
28	6.600	0.336	6.030	0.353	5.977	0.425	0.405	0.349	0.434	0.381	Volts
29	6.693	0.317	6.018	0.359	5.986	0.433	0.386	0.370	0.417	0.376	Volts
30	6.636	0.317	6.037	0.355	6.014	0.392	0.373	0.328	0.431	0.362	Volts
31	6.784	0.303	6.054	0.361	6.035	0.386	0.379	0.315	0.397	0.332	Volts
32	6.974	0.292	6.054	0.340	6.037	0.379	0.388	0.306	0.419	0.319	Volts
33	7.225	0.298	6.046	0.365	6.010	0.381	0.406	0.308	0.438	0.327	Volts
34	7.359	0.305	6.035	0.369	5.972	0.360	0.419	0.285	0.421	0.340	Volts
35	7.347	0.325	6.023	0.342	5.961	0.368	0.397	0.288	0.414	0.333	Volts
36	7.028	0.365	6.017	0.357	5.974	0.389	0.451	0.362	0.439	0.352	Volts
37	6.831	0.382	6.030	0.334	6.011	0.390	0.423	0.366	0.487	0.360	Volts
38	7.141	0.335	6.023	0.326	5.959	0.405	0.385	0.287	0.483	0.366	Volts
39	7.310	0.306	6.049	0.344	5.961	0.398	0.460	0.297	0.482	0.350	Volts
40	7.280	0.285	6.033	0.334	6.000	0.394	0.405	0.282	0.485	0.356	Volts
41	7.034	0.290	6.043	0.320	6.009	0.389	0.400	0.295	0.477	0.336	Volts
42	6.784	0.308	6.048	0.350	6.043	0.377	0.386	0.298	0.436	0.368	Volts
43	6.374	0.353	6.050	0.371	6.060	0.375	0.384	0.300	0.440	0.366	Volts
44	6.529	0.350	6.058	0.383	6.055	0.382	0.380	0.320	0.423	0.364	Volts
45	6.441	0.339	6.065	0.390	6.052	0.428	0.375	0.335	0.444	0.372	Volts

Table 6.26 Mean and fluctuation velocities and Reynolds shear stress components at section S-5 run no.2

Loc.no.	Tangential		Vertical		Radial		Reynolds s.s. components v'w'		v'u'		Unit
	DC	RMS	DC	RMS	DC	RMS	+45	-45	+45	-45	
1	6.661	0.440	-	-	-	-	-	-	-	-	Volts
2	6.834	0.355	-	-	-	-	-	-	-	-	Volts
3	6.814	0.349	-	-	-	-	-	-	-	-	Volts
4	6.885	0.341	-	-	-	-	-	-	-	-	Volts
5	6.838	0.342	-	-	-	-	-	-	-	-	Volts
6	6.624	0.350	-	-	-	-	-	-	-	-	Volts
7	6.394	0.374	-	-	-	-	-	-	-	-	Volts
8	6.446	0.365	-	-	-	-	-	-	-	-	Volts
9	6.302	0.369	-	-	-	-	-	-	-	-	Volts
10	6.444	0.352	-	-	-	-	-	-	-	-	Volts
11	6.653	0.320	-	-	-	-	-	-	-	-	Volts
12	6.620	0.343	-	-	-	-	-	-	-	-	Volts
13	6.953	0.326	-	-	-	-	-	-	-	-	Volts
14	7.254	0.306	-	-	-	-	-	-	-	-	Volts
15	7.344	0.300	-	-	-	-	-	-	-	-	Volts
16	7.377	0.323	-	-	-	-	-	-	-	-	Volts
17	7.405	0.318	-	-	-	-	-	-	-	-	Volts
18	7.122	0.431	-	-	-	-	-	-	-	-	Volts
19	7.664	0.450	6.010	0.369	5.970	0.382	0.495	0.363	0.425	0.328	Volts
20	8.028	0.364	6.047	0.374	5.988	0.370	0.498	0.336	0.441	0.312	Volts
21	7.944	0.319	6.043	0.350	6.006	0.354	0.438	0.315	0.450	0.310	Volts
22	7.850	0.301	6.066	0.340	6.031	0.355	0.432	0.311	0.456	0.299	Volts
23	7.611	0.304	6.058	0.346	6.016	0.370	0.409	0.290	0.466	0.305	Volts
24	7.288	0.306	6.056	0.337	5.982	0.387	0.419	0.310	0.424	0.336	Volts
25	6.915	0.320	6.027	0.360	5.930	0.395	0.406	0.318	0.477	0.369	Volts
26	6.884	0.328	6.043	0.336	5.914	0.405	0.402	0.332	0.461	0.365	Volts
27	6.640	0.422	6.099	0.363	5.953	0.409	0.421	0.348	0.468	0.369	Volts
28	6.708	0.391	5.994	0.379	5.940	0.435	0.427	0.350	0.460	0.364	Volts
29	7.020	0.311	6.011	0.407	5.960	0.388	0.421	0.320	0.454	0.370	Volts
30	7.040	0.306	6.024	0.346	5.972	0.377	0.400	0.333	0.467	0.364	Volts
31	7.180	0.295	6.070	0.337	6.015	0.398	0.450	0.312	0.438	0.340	Volts
32	7.519	0.284	6.074	0.322	6.036	0.385	0.415	0.315	0.440	0.348	Volts
33	7.878	0.302	6.087	0.351	6.012	0.407	0.483	0.307	0.474	0.347	Volts
34	7.985	0.298	6.032	0.373	6.018	0.411	0.452	0.346	0.462	0.352	Volts
35	8.014	0.391	6.000	0.420	5.991	0.423	0.460	0.343	0.478	0.356	Volts
36	7.632	0.503	5.996	0.430	5.973	0.422	0.571	0.496	0.461	0.365	Volts
37	7.656	0.399	5.970	0.373	5.954	0.439	0.511	0.338	0.490	0.373	Volts
38	8.030	0.289	5.977	0.356	5.964	0.385	0.460	0.283	0.480	0.377	Volts
39	7.994	0.266	6.012	0.331	5.963	0.395	0.429	0.272	0.467	0.355	Volts
40	7.887	0.283	6.089	0.330	5.974	0.394	0.432	0.284	0.484	0.385	Volts
41	7.525	0.308	6.045	0.388	6.030	0.386	0.441	0.272	0.460	0.330	Volts
42	7.050	0.292	6.079	0.370	6.062	0.389	0.418	0.303	0.431	0.373	Volts
43	6.837	0.297	6.045	0.362	6.091	0.393	0.376	0.304	0.427	0.346	Volts
44	6.794	0.301	5.959	0.379	6.038	0.399	0.422	0.330	0.413	0.355	Volts
45	6.545	0.403	5.939	0.378	6.047	0.432	0.416	0.338	0.438	0.397	Volts
46	6.426	0.365	-	-	6.095	0.447	-	-	-	-	Volts
47	6.639	0.312	-	-	6.105	0.430	-	-	-	-	Volts
48	6.716	0.320	-	-	6.105	0.404	-	-	-	-	Volts
49	7.230	0.292	-	-	6.047	0.451	-	-	-	-	Volts
50	7.580	0.285	-	-	6.011	0.387	-	-	-	-	Volts
51	7.878	0.293	-	-	5.960	0.386	-	-	-	-	Volts
52	7.955	0.295	-	-	5.900	0.363	-	-	-	-	Volts
53	7.906	0.310	-	-	5.944	0.390	-	-	-	-	Volts
54	7.569	0.369	-	-	6.003	0.395	-	-	-	-	Volts

Table 6.27 Mean and fluctuation velocities and Reynolds shear stress components at section S-5 run no.3

Loc.no.	Tangential		Vertical		Radial		Reynolds s.s. components				Unit
							v'w'		v'u'		
	DC	RMS	DC	RMS	DC	RMS	+45	-45	+45	-45	
1	6.814	0.397	-	-	-	-	-	-	-	-	Volts
2	7.070	0.356	-	-	-	-	-	-	-	-	Volts
3	6.936	0.344	-	-	-	-	-	-	-	-	Volts
4	6.990	0.339	-	-	-	-	-	-	-	-	Volts
5	6.893	0.347	-	-	-	-	-	-	-	-	Volts
6	6.820	0.328	-	-	-	-	-	-	-	-	Volts
7	6.603	0.365	-	-	-	-	-	-	-	-	Volts
8	6.666	0.347	-	-	-	-	-	-	-	-	Volts
9	6.565	0.368	-	-	-	-	-	-	-	-	Volts
10	6.745	0.341	-	-	-	-	-	-	-	-	Volts
11	6.874	0.334	-	-	-	-	-	-	-	-	Volts
12	6.948	0.332	-	-	-	-	-	-	-	-	Volts
13	7.283	0.327	-	-	-	-	-	-	-	-	Volts
14	7.510	0.303	-	-	-	-	-	-	-	-	Volts
15	7.700	0.295	-	-	-	-	-	-	-	-	Volts
16	7.740	0.335	-	-	-	-	-	-	-	-	Volts
17	7.811	0.398	-	-	-	-	-	-	-	-	Volts
18	7.474	0.399	-	-	-	-	-	-	-	-	Volts
19	7.917	0.420	5.990	0.352	5.964	0.422	0.463	0.359	0.500	0.350	Volts
20	8.303	0.291	6.053	0.350	5.971	0.404	0.453	0.301	0.507	0.313	Volts
21	8.258	0.287	6.046	0.333	5.999	0.383	0.483	0.279	0.507	0.345	Volts
22	8.100	0.272	6.059	0.333	6.018	0.406	0.458	0.282	0.501	0.390	Volts
23	7.852	0.269	6.065	0.334	5.965	0.346	0.428	0.275	0.449	0.320	Volts
24	7.551	0.278	6.062	0.335	5.923	0.357	0.426	0.288	0.453	0.349	Volts
25	7.272	0.289	6.027	0.332	5.910	0.368	0.389	0.306	0.482	0.350	Volts
26	7.161	0.290	6.041	0.336	5.915	0.444	0.407	0.318	0.457	0.352	Volts
27	7.014	0.312	6.070	0.325	5.946	0.464	0.393	0.315	0.440	0.369	Volts
28	7.140	0.320	5.959	0.363	5.962	0.492	0.445	0.326	0.458	0.377	Volts
29	7.296	0.315	5.987	0.340	5.958	0.388	0.422	0.293	0.456	0.334	Volts
30	7.340	0.278	6.034	0.333	5.982	0.390	0.402	0.299	0.501	0.341	Volts
31	7.473	0.278	6.083	0.322	6.014	0.376	0.394	0.283	0.457	0.346	Volts
32	7.911	0.273	6.076	0.326	6.000	0.357	0.407	0.273	0.466	0.294	Volts
33	8.188	0.268	6.076	0.364	6.028	0.374	0.448	0.284	0.511	0.321	Volts
34	8.305	0.264	6.018	0.341	6.026	0.381	0.453	0.272	0.502	0.379	Volts
35	8.319	0.272	6.002	0.361	6.005	0.389	0.442	0.284	0.507	0.337	Volts
36	7.904	0.438	5.988	0.331	5.981	0.384	0.482	0.345	0.520	0.343	Volts
37	7.818	0.496	5.985	0.417	5.972	0.372	0.524	0.415	0.477	0.314	Volts
38	8.252	0.292	5.980	0.419	5.980	0.357	0.442	0.295	0.495	0.298	Volts
39	8.288	0.282	6.006	0.378	5.981	0.390	0.481	0.278	0.478	0.319	Volts
40	8.221	0.255	6.090	0.323	6.013	0.364	0.424	0.279	0.523	0.306	Volts
41	7.945	0.274	6.062	0.326	6.005	0.361	0.438	0.283	0.471	0.313	Volts
42	7.319	0.290	6.086	0.328	6.060	0.328	0.385	0.306	0.422	0.322	Volts
43	6.994	0.285	6.081	0.345	6.101	0.397	0.348	0.312	0.430	0.345	Volts
44	7.021	0.300	5.953	0.369	6.100	0.377	0.382	0.316	0.426	0.333	Volts
45	6.847	0.304	5.884	0.345	6.078	0.421	0.408	0.312	0.435	0.402	Volts
46	6.655	0.366	-	-	6.139	0.376	-	-	-	-	Volts
47	6.839	0.327	-	-	6.135	0.378	-	-	-	-	Volts
48	6.942	0.314	-	-	6.114	0.371	-	-	-	-	Volts
49	7.300	0.325	-	-	6.050	0.364	-	-	-	-	Volts
50	7.853	0.335	-	-	6.031	0.382	-	-	-	-	Volts
51	8.175	0.311	-	-	5.942	0.398	-	-	-	-	Volts
52	8.239	0.389	-	-	5.924	0.343	-	-	-	-	Volts
53	8.120	0.470	-	-	5.972	0.381	-	-	-	-	Volts
54	7.698	0.500	-	-	5.997	0.359	-	-	-	-	Volts

Table 6.28 Mean and fluctuation velocities and Reynolds shear stress components at section S-6 run no.1

Loc.no.	Tangential		Vertical		Radial		Reynolds s.s. components				Unit
							v'w'		v'u'		
	DC	RMS	DC	RMS	DC	RMS	+45	-45	+45	-45	
1	6.245	0.382	-	-	-	-	-	-	-	-	Volts
2	6.379	0.371	-	-	-	-	-	-	-	-	Volts
3	6.458	0.355	-	-	-	-	-	-	-	-	Volts
4	6.522	0.345	-	-	-	-	-	-	-	-	Volts
5	6.480	0.352	-	-	-	-	-	-	-	-	Volts
6	6.307	0.372	-	-	-	-	-	-	-	-	Volts
7	6.317	0.369	-	-	-	-	-	-	-	-	Volts
8	6.336	0.358	-	-	-	-	-	-	-	-	Volts
9	6.242	0.372	-	-	-	-	-	-	-	-	Volts
10	6.330	0.351	-	-	6.048	0.393	-	-	-	-	Volts
11	6.508	0.329	-	-	6.046	0.371	-	-	-	-	Volts
12	6.489	0.335	-	-	6.029	0.388	-	-	-	-	Volts
13	6.473	0.332	-	-	6.041	0.372	-	-	-	-	Volts
14	6.739	0.315	-	-	6.092	0.359	-	-	-	-	Volts
15	6.860	0.302	-	-	6.087	0.373	-	-	-	-	Volts
16	6.760	0.333	-	-	6.012	0.394	-	-	-	-	Volts
17	6.595	0.359	-	-	5.993	0.394	-	-	-	-	Volts
18	6.380	0.419	-	-	6.006	0.388	-	-	-	-	Volts
19	6.426	0.363	5.998	0.385	6.014	0.437	0.410	0.356	0.391	0.430	Volts
20	6.663	0.357	5.997	0.370	6.035	0.378	0.425	0.348	0.375	0.412	Volts
21	6.803	0.313	6.033	0.373	6.030	0.364	0.397	0.331	0.370	0.404	Volts
22	7.164	0.283	6.037	0.322	6.116	0.347	0.382	0.295	0.342	0.420	Volts
23	7.127	0.289	6.062	0.321	6.100	0.399	0.373	0.315	0.321	0.410	Volts
24	6.730	0.319	6.034	0.341	6.025	0.389	0.346	0.312	0.331	0.404	Volts
25	6.597	0.321	6.052	0.357	6.089	0.391	0.379	0.326	0.365	0.416	Volts
26	6.610	0.317	6.061	0.382	6.086	0.384	0.446	0.337	0.377	0.401	Volts
27	6.416	0.309	6.056	0.446	6.077	0.420	0.455	0.354	0.346	0.393	Volts
28	6.413	0.347	6.046	0.452	6.090	0.412	0.437	0.330	0.390	0.409	Volts
29	6.593	0.321	6.063	0.360	6.083	0.380	0.353	0.328	0.386	0.405	Volts
30	6.640	0.310	6.076	0.360	6.047	0.373	0.368	0.330	0.368	0.407	Volts
31	6.850	0.288	6.031	0.327	6.060	0.369	0.371	0.304	0.369	0.416	Volts
32	7.192	0.271	6.062	0.331	6.118	0.364	0.376	0.309	0.335	0.389	Volts
33	6.870	0.305	6.019	0.380	6.180	0.360	0.401	0.320	0.337	0.371	Volts
34	6.670	0.339	6.042	0.347	6.133	0.371	0.456	0.346	0.351	0.400	Volts
35	6.637	0.332	5.986	0.411	6.049	0.388	0.468	0.349	0.366	0.407	Volts
36	6.424	0.415	6.001	0.441	6.063	0.384	0.474	0.419	0.352	0.409	Volts
37	6.260	0.444	5.995	0.373	6.104	0.415	0.452	0.378	0.385	0.406	Volts
38	6.482	0.358	6.000	0.376	6.112	0.387	0.407	0.341	0.391	0.417	Volts
39	6.590	0.347	6.057	0.384	6.151	0.386	0.398	0.352	0.377	0.402	Volts
40	7.005	0.346	6.024	0.360	6.142	0.351	0.401	0.325	0.364	0.410	Volts
41	7.250	0.300	6.035	0.352	6.150	0.340	0.383	0.304	0.341	0.399	Volts
42	7.009	0.365	6.053	0.344	6.174	0.341	0.376	0.310	0.334	0.409	Volts
43	6.766	0.351	6.063	0.322	6.103	0.384	0.380	0.320	0.365	0.419	Volts
44	6.553	0.333	6.070	0.323	6.028	0.407	0.390	0.325	0.371	0.408	Volts
45	6.397	0.363	6.062	0.334	6.031	0.431	0.405	0.322	0.378	0.415	Volts

Table 6.29 *Mean and fluctuation velocities and Reynolds shear stress components at section S-6 run no.2*

Loc.no.	Tangential DC	Tangential RMS	Vertical DC	Vertical RMS	Radial DC	Radial RMS	Reynolds s.s. components v'w' +45	v'w' −45	v'u' +45	v'u' −45	Unit
1	6.518	0.422	–	–	–	–	–	–	–	–	Volts
2	6.789	0.394	–	–	–	–	–	–	–	–	Volts
3	7.064	0.316	–	–	–	–	–	–	–	–	Volts
4	7.129	0.297	–	–	–	–	–	–	–	–	Volts
5	6.900	0.332	–	–	–	–	–	–	–	–	Volts
6	6.720	0.331	–	–	–	–	–	–	–	–	Volts
7	6.580	0.352	–	–	–	–	–	–	–	–	Volts
8	6.561	0.324	–	–	–	–	–	–	–	–	Volts
9	6.394	0.394	–	–	–	–	–	–	–	–	Volts
10	6.612	0.361	–	–	–	–	–	–	–	–	Volts
11	6.807	0.328	–	–	–	–	–	–	–	–	Volts
12	6.794	0.325	–	–	–	–	–	–	–	–	Volts
13	6.948	0.328	–	–	–	–	–	–	–	–	Volts
14	7.214	0.311	–	–	–	–	–	–	–	–	Volts
15	7.540	0.326	–	–	–	–	–	–	–	–	Volts
16	7.614	0.302	–	–	–	–	–	–	–	–	Volts
17	7.370	0.324	–	–	–	–	–	–	–	–	Volts
18	6.988	0.369	–	–	–	–	–	–	–	–	Volts
19	7.030	0.416	5.940	0.378	6.070	0.352	0.443	0.353	0.323	0.427	Volts
20	7.458	0.311	5.956	0.358	6.071	0.362	0.426	0.312	0.324	0.440	Volts
21	7.852	0.308	6.035	0.352	6.121	0.366	0.409	0.285	0.307	0.464	Volts
22	7.802	0.301	6.049	0.342	6.075	0.340	0.426	0.287	0.296	0.442	Volts
23	7.536	0.290	6.059	0.332	6.083	0.393	0.402	0.304	0.314	0.427	Volts
24	7.105	0.303	6.045	0.330	6.084	0.356	0.413	0.313	0.315	0.420	Volts
25	6.968	0.325	6.011	0.347	6.070	0.360	0.401	0.317	0.378	0.402	Volts
26	6.957	0.311	6.058	0.333	6.107	0.391	0.400	0.319	0.397	0.436	Volts
27	6.748	0.344	6.088	0.354	6.094	0.421	0.411	0.328	0.399	0.425	Volts
28	6.770	0.362	6.050	0.334	6.097	0.387	0.402	0.318	0.359	0.402	Volts
29	6.980	0.331	6.054	0.337	6.136	0.432	0.393	0.326	0.339	0.421	Volts
30	7.030	0.311	6.056	0.356	6.095	0.357	0.404	0.313	0.330	0.386	Volts
31	7.175	0.309	6.044	0.346	6.070	0.394	0.412	0.298	0.332	0.414	Volts
32	7.545	0.296	6.048	0.335	6.047	0.418	0.415	0.288	0.305	0.413	Volts
33	7.920	0.272	6.035	0.336	6.136	0.352	0.441	0.272	0.286	0.419	Volts
34	7.670	0.288	5.991	0.349	6.125	0.340	0.413	0.286	0.302	0.429	Volts
35	7.370	0.308	6.000	0.357	6.111	0.402	0.440	0.300	0.320	0.417	Volts
36	6.934	0.445	5.916	0.379	6.107	0.404	0.456	0.341	0.319	0.427	Volts
37	6.769	0.406	5.897	0.412	6.104	0.382	0.475	0.375	0.372	0.457	Volts
38	7.170	0.352	5.975	0.350	6.080	0.392	0.456	0.301	0.371	0.452	Volts
39	7.336	0.307	6.010	0.332	6.110	0.346	0.434	0.295	0.358	0.463	Volts
40	7.922	0.277	6.041	0.326	6.100	0.349	0.418	0.274	0.322	0.435	Volts
41	7.653	0.276	6.044	0.328	6.104	0.345	0.412	0.273	0.318	0.445	Volts
42	7.267	0.304	6.073	0.341	6.061	0.391	0.413	0.288	0.340	0.408	Volts
43	7.056	0.323	6.084	0.333	6.059	0.378	0.401	0.310	0.329	0.392	Volts
44	7.012	0.357	6.032	0.331	6.053	0.360	0.408	0.325	0.312	0.410	Volts
45	6.818	0.329	6.000	0.341	6.047	0.363	0.412	0.354	0.353	0.412	Volts
46	6.670	0.332	–	–	6.018	0.383	–	–	–	–	Volts
47	6.857	0.331	–	–	6.029	0.402	–	–	–	–	Volts
48	6.984	0.323	–	–	6.056	0.360	–	–	–	–	Volts
49	7.423	0.290	–	–	6.163	0.355	–	–	–	–	Volts
50	7.704	0.307	–	–	6.149	0.427	–	–	–	–	Volts
51	7.887	0.301	–	–	6.193	0.403	–	–	–	–	Volts
52	7.240	0.381	–	–	6.135	0.378	–	–	–	–	Volts
53	7.060	0.369	–	–	6.090	0.372	–	–	–	–	Volts
54	6.716	0.419	–	–	6.054	0.406	–	–	–	–	Volts

Table 6.30 *Mean and fluctuation velocities and Reynolds shear stress components at section S-6 run no.3*

Loc.no.	Tangential DC	Tangential RMS	Vertical DC	Vertical RMS	Radial DC	Radial RMS	Reynolds s.s. components v'w' +45	v'w' −45	v'u' +45	v'u' −45	Unit
1	6.660	0.437	–	–	–	–	–	–	–	–	Volts
2	7.006	0.338	–	–	–	–	–	–	–	–	Volts
3	7.193	0.316	–	–	–	–	–	–	–	–	Volts
4	7.256	0.300	–	–	–	–	–	–	–	–	Volts
5	7.000	0.313	–	–	–	–	–	–	–	–	Volts
6	6.870	0.328	–	–	–	–	–	–	–	–	Volts
7	6.863	0.324	–	–	–	–	–	–	–	–	Volts
8	6.818	0.309	–	–	–	–	–	–	–	–	Volts
9	6.614	0.322	–	–	–	–	–	–	–	–	Volts
10	6.800	0.341	–	–	–	–	–	–	–	–	Volts
11	7.129	0.303	–	–	–	–	–	–	–	–	Volts
12	7.199	0.320	–	–	–	–	–	–	–	–	Volts
13	7.248	0.291	–	–	–	–	–	–	–	–	Volts
14	7.510	0.284	–	–	–	–	–	–	–	–	Volts
15	7.850	0.293	–	–	–	–	–	–	–	–	Volts
16	7.771	0.300	–	–	–	–	–	–	–	–	Volts
17	7.550	0.328	–	–	–	–	–	–	–	–	Volts
18	7.161	0.412	–	–	–	–	–	–	–	–	Volts
19	7.418	0.415	5.873	0.388	5.880	0.419	0.508	0.374	0.405	0.492	Volts
20	7.824	0.332	5.925	0.366	5.935	0.428	0.495	0.334	0.397	0.487	Volts
21	8.135	0.322	6.035	0.365	6.015	0.407	0.466	0.284	0.392	0.480	Volts
22	8.092	0.270	6.046	0.341	6.018	0.379	0.453	0.287	0.358	0.476	Volts
23	7.880	0.279	6.066	0.332	6.070	0.415	0.456	0.282	0.353	0.455	Volts
24	7.464	0.294	6.050	0.325	6.126	0.416	0.404	0.292	0.372	0.442	Volts
25	7.170	0.306	6.035	0.346	6.180	0.421	0.414	0.320	0.421	0.456	Volts
26	7.254	0.288	6.071	0.345	6.170	0.404	0.390	0.314	0.422	0.432	Volts
27	6.894	0.362	6.113	0.331	6.123	0.425	0.458	0.292	0.410	0.465	Volts
28	6.987	0.349	6.012	0.348	6.129	0.407	0.408	0.302	0.497	0.457	Volts
29	7.344	0.291	6.012	0.344	6.115	0.448	0.424	0.296	0.426	0.443	Volts
30	7.390	0.289	6.053	0.343	6.085	0.490	0.401	0.288	0.469	0.432	Volts
31	7.492	0.261	6.087	0.343	6.080	0.398	0.403	0.280	0.371	0.445	Volts
32	7.815	0.257	6.085	0.325	6.106	0.388	0.393	0.281	0.447	0.489	Volts
33	8.190	0.270	6.047	0.322	6.123	0.394	0.407	0.277	0.391	0.454	Volts
34	7.990	0.282	6.014	0.350	6.157	0.386	0.444	0.282	0.366	0.451	Volts
35	7.742	0.311	5.997	0.358	6.127	0.356	0.453	0.315	0.343	0.422	Volts
36	7.327	0.400	5.864	0.375	6.110	0.399	0.511	0.354	0.337	0.462	Volts
37	7.000	0.424	5.875	0.397	6.130	0.431	0.465	0.371	0.378	0.457	Volts
38	7.389	0.331	5.904	0.406	6.092	0.421	0.447	0.342	0.423	0.467	Volts
39	7.705	0.336	6.045	0.380	6.137	0.403	0.439	0.332	0.336	0.478	Volts
40	8.249	0.264	6.056	0.342	6.158	0.347	0.464	0.268	0.326	0.474	Volts
41	7.870	0.277	6.060	0.333	6.090	0.408	0.448	0.283	0.459	0.486	Volts
42	7.515	0.321	6.111	0.325	6.034	0.404	0.433	0.294	0.452	0.456	Volts
43	7.257	0.307	6.090	0.352	6.023	0.398	0.465	0.303	0.458	0.459	Volts
44	7.315	0.304	6.008	0.346	6.030	0.444	0.459	0.309	0.473	0.424	Volts
45	6.974	0.424	5.911	0.353	6.044	0.465	0.514	0.308	0.493	0.435	Volts
46	6.754	0.377	–	–	6.000	0.428	–	–	–	–	Volts
47	7.081	0.317	–	–	6.003	0.441	–	–	–	–	Volts
48	7.222	0.317	–	–	6.026	0.416	–	–	–	–	Volts
49	7.585	0.285	–	–	6.040	0.414	–	–	–	–	Volts
50	8.040	0.270	–	–	6.186	0.425	–	–	–	–	Volts
51	8.236	0.271	–	–	6.208	0.386	–	–	–	–	Volts
52	7.800	0.312	–	–	6.201	0.366	–	–	–	–	Volts
53	7.442	0.340	–	–	6.158	0.424	–	–	–	–	Volts
54	7.158	0.480	–	–	6.097	0.394	–	–	–	–	Volts

Table 6.31 *Mean and fluctuation velocities and Reynolds shear stress components at section S-7 run no.1*

Loc.no.	Tangential DC	Tangential RMS	Vertical DC	Vertical RMS	Radial DC	Radial RMS	Reynolds s.s. components v'w' +45	v'w' -45	v'u' +45	v'u' -45	Unit
1	6.246	0.353	-	-	-	-	-	-	-	-	Volts
2	6.290	0.363	-	-	-	-	-	-	-	-	Volts
3	6.349	0.349	-	-	-	-	-	-	-	-	Volts
4	6.395	0.355	-	-	-	-	-	-	-	-	Volts
5	6.434	0.343	-	-	-	-	-	-	-	-	Volts
6	6.541	0.330	-	-	-	-	-	-	-	-	Volts
7	6.590	0.327	-	-	-	-	-	-	-	-	Volts
8	6.616	0.320	-	-	-	-	-	-	-	-	Volts
9	6.402	0.354	-	-	-	-	-	-	-	-	Volts
10	6.782	0.382	-	-	6.091	0.438	-	-	-	-	Volts
11	7.027	0.312	-	-	6.098	0.386	-	-	-	-	Volts
12	6.983	0.320	-	-	6.087	0.351	-	-	-	-	Volts
13	6.866	0.319	-	-	6.055	0.394	-	-	-	-	Volts
14	6.749	0.331	-	-	6.010	0.373	-	-	-	-	Volts
15	6.601	0.342	-	-	6.002	0.376	-	-	-	-	Volts
16	6.454	0.362	-	-	6.016	0.379	-	-	-	-	Volts
17	6.400	0.375	-	-	6.025	0.379	-	-	-	-	Volts
18	6.369	0.366	-	-	6.026	0.459	-	-	-	-	Volts
19	6.495	0.357	6.013	0.448	6.038	0.424	0.457	0.392	0.376	0.446	Volts
20	6.594	0.358	6.020	0.386	6.033	0.386	0.412	0.347	0.379	0.423	Volts
21	6.671	0.346	6.033	0.371	6.037	0.396	0.384	0.312	0.355	0.437	Volts
22	6.847	0.327	6.031	0.371	6.023	0.383	0.384	0.313	0.371	0.432	Volts
23	6.943	0.317	6.044	0.373	6.039	0.378	0.401	0.305	0.336	0.419	Volts
24	7.057	0.302	6.043	0.347	6.070	0.369	0.385	0.291	0.337	0.397	Volts
25	7.093	0.295	6.044	0.326	6.106	0.344	0.379	0.289	0.339	0.379	Volts
26	7.157	0.297	6.053	0.357	6.116	0.352	0.389	0.298	0.335	0.400	Volts
27	6.837	0.413	6.059	0.372	6.103	0.406	0.430	0.312	0.362	0.448	Volts
28	6.730	0.418	6.019	0.360	6.107	0.422	0.405	0.325	0.399	0.451	Volts
29	7.122	0.278	6.032	0.326	6.124	0.334	0.376	0.296	0.351	0.403	Volts
30	7.089	0.294	6.056	0.345	6.110	0.336	0.382	0.307	0.304	0.383	Volts
31	7.014	0.304	6.049	0.335	6.094	0.351	0.407	0.299	0.337	0.423	Volts
32	6.875	0.304	6.040	0.362	6.110	0.394	0.397	0.310	0.356	0.416	Volts
33	6.766	0.324	6.040	0.373	6.099	0.372	0.402	0.324	0.397	0.435	Volts
34	6.637	0.336	6.037	0.357	6.074	0.423	0.404	0.357	0.400	0.408	Volts
35	6.564	0.365	6.030	0.389	6.069	0.407	0.434	0.362	0.435	0.434	Volts
36	6.465	0.373	6.020	0.383	6.060	0.416	0.444	0.358	0.414	0.449	Volts
37	6.413	0.422	6.033	0.370	6.042	0.476	0.407	0.362	0.415	0.453	Volts
38	6.479	0.358	6.030	0.411	6.064	0.396	0.490	0.370	0.387	0.411	Volts
39	6.575	0.380	6.034	0.380	6.078	0.409	0.411	0.348	0.382	0.429	Volts
40	6.713	0.385	6.040	0.364	6.110	0.388	0.412	0.330	0.373	0.430	Volts
41	6.915	0.330	6.045	0.357	6.101	0.380	0.410	0.318	0.371	0.391	Volts
42	7.079	0.318	6.048	0.368	6.079	0.401	0.410	0.314	0.331	0.376	Volts
43	7.036	0.334	6.051	0.372	6.052	0.364	0.415	0.320	0.317	0.409	Volts
44	7.032	0.337	6.060	0.381	5.995	0.402	0.420	0.325	0.376	0.406	Volts
45	6.635	0.417	6.059	0.383	6.000	0.493	0.425	0.345	0.426	0.410	Volts

Table 6.32 *Mean and fluctuation velocities and Reynolds shear stress components at section S-7 run no.2*

Loc.no.	Tangential DC	Tangential RMS	Vertical DC	Vertical RMS	Radial DC	Radial RMS	Reynolds s.s. components v'w' +45	v'w' -45	v'u' +45	v'u' -45	Unit
1	6.586	0.359	-	-	-	-	-	-	-	-	Volts
2	6.795	0.351	-	-	-	-	-	-	-	-	Volts
3	6.751	0.342	-	-	-	-	-	-	-	-	Volts
4	6.794	0.330	-	-	-	-	-	-	-	-	Volts
5	6.826	0.311	-	-	-	-	-	-	-	-	Volts
6	6.882	0.310	-	-	-	-	-	-	-	-	Volts
7	7.008	0.310	-	-	-	-	-	-	-	-	Volts
8	7.075	0.299	-	-	-	-	-	-	-	-	Volts
9	6.972	0.361	-	-	-	-	-	-	-	-	Volts
10	7.224	0.396	-	-	-	-	-	-	-	-	Volts
11	7.527	0.288	-	-	-	-	-	-	-	-	Volts
12	7.497	0.278	-	-	-	-	-	-	-	-	Volts
13	7.356	0.276	-	-	-	-	-	-	-	-	Volts
14	7.270	0.347	-	-	-	-	-	-	-	-	Volts
15	7.192	0.325	-	-	-	-	-	-	-	-	Volts
16	7.104	0.333	-	-	-	-	-	-	-	-	Volts
17	6.964	0.335	-	-	-	-	-	-	-	-	Volts
18	6.733	0.358	-	-	-	-	-	-	-	-	Volts
19	6.970	0.345	5.980	0.375	6.021	0.404	0.454	0.321	0.410	0.392	Volts
20	7.215	0.299	5.991	0.353	6.008	0.394	0.438	0.317	0.426	0.334	Volts
21	7.260	0.271	6.023	0.348	6.015	0.386	0.411	0.303	0.438	0.314	Volts
22	7.360	0.279	6.031	0.332	5.994	0.369	0.399	0.300	0.444	0.302	Volts
23	7.520	0.278	6.041	0.325	5.970	0.358	0.414	0.271	0.421	0.308	Volts
24	7.599	0.278	6.050	0.317	5.936	0.355	0.415	0.275	0.414	0.304	Volts
25	7.666	0.324	6.055	0.329	5.962	0.348	0.396	0.268	0.421	0.300	Volts
26	7.665	0.276	6.077	0.343	5.958	0.326	0.429	0.286	0.412	0.290	Volts
27	7.328	0.435	6.075	0.351	6.012	0.348	0.446	0.323	0.424	0.293	Volts
28	7.283	0.444	6.040	0.347	5.973	0.332	0.466	0.340	0.426	0.307	Volts
29	7.657	0.268	6.030	0.347	5.959	0.370	0.450	0.275	0.432	0.299	Volts
30	7.661	0.261	6.060	0.345	5.954	0.331	0.434	0.268	0.416	0.298	Volts
31	7.639	0.262	6.071	0.340	6.003	0.362	0.426	0.274	0.438	0.301	Volts
32	7.461	0.284	6.060	0.320	5.999	0.330	0.417	0.275	0.422	0.292	Volts
33	7.384	0.299	6.031	0.360	5.996	0.359	0.420	0.293	0.444	0.303	Volts
34	7.242	0.293	6.025	0.356	6.003	0.352	0.416	0.290	0.445	0.324	Volts
35	7.232	0.317	5.993	0.354	6.014	0.379	0.433	0.298	0.416	0.337	Volts
36	6.952	0.333	5.956	0.378	6.000	0.391	0.441	0.311	0.414	0.339	Volts
37	6.720	0.383	5.959	0.394	5.970	0.387	0.513	0.315	0.423	0.334	Volts
38	6.973	0.329	5.990	0.385	5.964	0.360	0.480	0.303	0.414	0.353	Volts
39	7.100	0.294	6.046	0.365	5.954	0.375	0.467	0.308	0.408	0.339	Volts
40	7.232	0.278	6.062	0.354	5.958	0.373	0.422	0.269	0.405	0.301	Volts
41	7.460	0.282	6.056	0.337	5.947	0.360	0.417	0.264	0.404	0.318	Volts
42	7.600	0.278	6.076	0.320	5.971	0.347	0.401	0.272	0.405	0.331	Volts
43	7.630	0.278	6.031	0.317	6.011	0.362	0.425	0.285	0.432	0.324	Volts
44	7.646	0.282	5.988	0.349	5.996	0.392	0.451	0.293	0.431	0.334	Volts
45	7.257	0.471	5.955	0.347	5.995	0.402	0.459	0.302	0.491	0.369	Volts
46	7.115	0.436	-	-	6.032	0.326	-	-	-	-	Volts
47	7.528	0.304	-	-	6.068	0.359	-	-	-	-	Volts
48	7.619	0.287	-	-	6.081	0.368	-	-	-	-	Volts
49	7.652	0.298	-	-	6.035	0.381	-	-	-	-	Volts
50	7.449	0.287	-	-	5.979	0.389	-	-	-	-	Volts
51	7.294	0.312	-	-	5.962	0.360	-	-	-	-	Volts
52	7.028	0.407	-	-	5.963	0.353	-	-	-	-	Volts
53	6.989	0.404	-	-	6.013	0.407	-	-	-	-	Volts
54	6.767	0.474	-	-	6.023	0.403	-	-	-	-	Volts

Table 6.33 Mean and fluctuation velocities and Reynolds shear stress components at section S-7 run no.3

Loc.no.	Tangential		Vertical		Radial		Reynolds s.s. components v'w'		v'u'		Unit
	DC	RMS	DC	RMS	DC	RMS	+45	-45	+45	-45	
1	6.756	0.389	-	-	-	-	-	-	-	-	Volts
2	6.997	0.367	-	-	-	-	-	-	-	-	Volts
3	7.121	0.356	-	-	-	-	-	-	-	-	Volts
4	7.064	0.372	-	-	-	-	-	-	-	-	Volts
5	7.085	0.359	-	-	-	-	-	-	-	-	Volts
6	7.146	0.348	-	-	-	-	-	-	-	-	Volts
7	7.219	0.343	-	-	-	-	-	-	-	-	Volts
8	7.385	0.359	-	-	-	-	-	-	-	-	Volts
9	7.230	0.427	-	-	-	-	-	-	-	-	Volts
10	7.420	0.442	-	-	-	-	-	-	-	-	Volts
11	7.681	0.321	-	-	-	-	-	-	-	-	Volts
12	7.649	0.308	-	-	-	-	-	-	-	-	Volts
13	7.619	0.303	-	-	-	-	-	-	-	-	Volts
14	7.551	0.324	-	-	-	-	-	-	-	-	Volts
15	7.445	0.336	-	-	-	-	-	-	-	-	Volts
16	7.420	0.330	-	-	-	-	-	-	-	-	Volts
17	7.220	0.375	-	-	-	-	-	-	-	-	Volts
18	6.960	0.409	-	-	-	-	-	-	-	-	Volts
19	7.142	0.441	5.964	0.342	6.075	0.413	0.513	0.331	0.496	0.417	Volts
20	7.407	0.362	5.996	0.334	6.086	0.430	0.493	0.321	0.485	0.386	Volts
21	7.505	0.352	6.041	0.347	6.095	0.397	0.458	0.300	0.458	0.397	Volts
22	7.599	0.301	6.058	0.341	6.078	0.379	0.426	0.288	0.455	0.357	Volts
23	7.771	0.279	6.058	0.315	6.047	0.348	0.440	0.289	0.448	0.355	Volts
24	7.844	0.315	6.041	0.334	6.020	0.389	0.445	0.306	0.433	0.328	Volts
25	7.871	0.297	6.090	0.314	5.982	0.366	0.437	0.279	0.461	0.302	Volts
26	7.853	0.292	6.013	0.326	5.997	0.361	0.450	0.284	0.457	0.294	Volts
27	7.516	0.454	6.072	0.358	5.999	0.359	0.475	0.339	0.448	0.298	Volts
28	7.539	0.447	6.051	0.346	5.955	0.369	0.426	0.311	0.457	0.299	Volts
29	7.913	0.286	6.065	0.315	5.954	0.377	0.429	0.273	0.443	0.302	Volts
30	7.950	0.292	6.055	0.321	5.925	0.364	0.446	0.260	0.455	0.303	Volts
31	7.926	0.262	6.058	0.326	5.924	0.413	0.440	0.268	0.450	0.352	Volts
32	7.863	0.293	6.053	0.336	5.950	0.429	0.425	0.265	0.497	0.349	Volts
33	7.686	0.307	6.040	0.322	5.976	0.417	0.422	0.272	0.496	0.381	Volts
34	7.589	0.317	6.025	0.323	6.004	0.410	0.402	0.287	0.482	0.379	Volts
35	7.523	0.329	5.980	0.319	5.952	0.477	0.411	0.312	0.471	0.397	Volts
36	7.259	0.376	5.914	0.337	5.940	0.476	0.412	0.311	0.461	0.414	Volts
37	7.080	0.423	5.920	0.401	5.998	0.443	0.474	0.310	0.440	0.400	Volts
38	7.307	0.346	5.990	0.352	5.945	0.441	0.420	0.301	0.467	0.401	Volts
39	7.411	0.300	6.014	0.311	5.968	0.443	0.408	0.273	0.456	0.407	Volts
40	7.601	0.288	6.051	0.320	5.984	0.480	0.418	0.273	0.458	0.375	Volts
41	7.791	0.276	6.070	0.320	5.985	0.440	0.395	0.274	0.483	0.368	Volts
42	7.928	0.272	6.075	0.313	5.958	0.440	0.393	0.268	0.468	0.331	Volts
43	7.923	0.271	6.052	0.310	5.983	0.350	0.426	0.273	0.446	0.295	Volts
44	7.922	0.353	6.016	0.329	5.988	0.335	0.428	0.283	0.438	0.301	Volts
45	7.549	0.446	5.991	0.348	5.989	0.322	0.467	0.371	0.435	0.293	Volts
46	7.373	0.428	-	-	6.080	0.351	-	-	-	-	Volts
47	7.721	0.341	-	-	6.092	0.355	-	-	-	-	Volts
48	7.820	0.287	-	-	6.100	0.366	-	-	-	-	Volts
49	7.896	0.285	-	-	6.102	0.348	-	-	-	-	Volts
50	7.882	0.278	-	-	6.016	0.391	-	-	-	-	Volts
51	7.640	0.290	-	-	5.985	0.419	-	-	-	-	Volts
52	7.390	0.302	-	-	5.986	0.418	-	-	-	-	Volts
53	7.335	0.344	-	-	6.049	0.369	-	-	-	-	Volts
54	7.114	0.430	-	-	6.053	0.375	-	-	-	-	Volts

Table 6.34 Mean and fluctuation velocities and Reynolds shear stress components at section S-8 run no.1

Loc.no.	Tangential		Vertical		Radial		Reynolds s.s. components v'w'		v'u'		Unit
	DC	RMS	DC	RMS	DC	RMS	+45	-45	+45	-45	
1	6.289	0.420	-	-	-	-	-	-	-	-	Volts
2	6.375	0.390	-	-	-	-	-	-	-	-	Volts
3	6.455	0.398	-	-	-	-	-	-	-	-	Volts
4	6.549	0.392	-	-	-	-	-	-	-	-	Volts
5	6.651	0.384	-	-	-	-	-	-	-	-	Volts
6	6.870	0.353	-	-	-	-	-	-	-	-	Volts
7	6.791	0.336	-	-	-	-	-	-	-	-	Volts
8	6.825	0.357	-	-	-	-	-	-	-	-	Volts
9	6.467	0.415	-	-	-	-	-	-	-	-	Volts
10	7.200	0.388	-	-	-	-	-	-	-	-	Volts
11	7.753	0.327	-	-	-	-	-	-	-	-	Volts
12	7.609	0.320	-	-	-	-	-	-	-	-	Volts
13	7.606	0.329	-	-	-	-	-	-	-	-	Volts
14	7.276	0.313	-	-	-	-	-	-	-	-	Volts
15	7.040	0.319	-	-	-	-	-	-	-	-	Volts
16	6.852	0.327	-	-	-	-	-	-	-	-	Volts
17	6.585	0.338	-	-	-	-	-	-	-	-	Volts
18	6.430	0.422	-	-	-	-	-	-	-	-	Volts
19	6.797	0.416	-	-	-	-	-	-	-	-	Volts
20	7.035	0.353	-	-	-	-	-	-	-	-	Volts
21	7.387	0.322	-	-	-	-	-	-	-	-	Volts
22	7.606	0.293	-	-	-	-	-	-	-	-	Volts
23	7.895	0.278	-	-	-	-	-	-	-	-	Volts
24	8.184	0.265	-	-	-	-	-	-	-	-	Volts
25	8.314	0.258	-	-	-	-	-	-	-	-	Volts
26	8.370	0.244	-	-	-	-	-	-	-	-	Volts
27	7.760	0.355	-	-	-	-	-	-	-	-	Volts
28	7.763	0.373	-	-	-	-	-	-	-	-	Volts
29	8.384	0.276	-	-	-	-	-	-	-	-	Volts
30	8.350	0.284	-	-	-	-	-	-	-	-	Volts
31	8.177	0.264	-	-	-	-	-	-	-	-	Volts
32	7.812	0.268	-	-	-	-	-	-	-	-	Volts
33	7.530	0.263	-	-	-	-	-	-	-	-	Volts
34	7.270	0.298	-	-	-	-	-	-	-	-	Volts
35	7.184	0.352	-	-	-	-	-	-	-	-	Volts
36	6.990	0.330	-	-	-	-	-	-	-	-	Volts
37	6.501	0.389	-	-	-	-	-	-	-	-	Volts
38	6.705	0.366	-	-	-	-	-	-	-	-	Volts
39	6.857	0.367	-	-	-	-	-	-	-	-	Volts
40	7.520	0.347	-	-	-	-	-	-	-	-	Volts
41	7.887	0.272	-	-	-	-	-	-	-	-	Volts
42	8.210	0.258	-	-	-	-	-	-	-	-	Volts
43	8.267	0.283	-	-	-	-	-	-	-	-	Volts
44	8.151	0.290	-	-	-	-	-	-	-	-	Volts
45	7.560	0.354	-	-	-	-	-	-	-	-	Volts

Table 6.35 *Mean and fluctuation velocities and Reynolds shear stress components at section S-8 run no.2*

Loc.no.	Tangential		Vertical		Radial		Reynolds s.s. components v'w'		v'u'		Unit
	DC	RMS	DC	RMS	DC	RMS	+45	-45	+45	-45	
1	6.691	0.424	-	-	-	-	-	-	-	-	Volts
2	6.774	0.400	-	-	-	-	-	-	-	-	Volts
3	6.940	0.419	-	-	-	-	-	-	-	-	Volts
4	6.980	0.414	-	-	-	-	-	-	-	-	Volts
5	6.986	0.369	-	-	-	-	-	-	-	-	Volts
6	7.063	0.344	-	-	-	-	-	-	-	-	Volts
7	7.219	0.338	-	-	-	-	-	-	-	-	Volts
8	7.523	0.351	-	-	-	-	-	-	-	-	Volts
9	7.005	0.385	-	-	-	-	-	-	-	-	Volts
10	8.310	0.432	-	-	-	-	-	-	-	-	Volts
11	8.860	0.288	-	-	-	-	-	-	-	-	Volts
12	8.594	0.346	-	-	-	-	-	-	-	-	Volts
13	8.335	0.328	-	-	-	-	-	-	-	-	Volts
14	8.063	0.350	-	-	-	-	-	-	-	-	Volts
15	7.769	0.367	-	-	-	-	-	-	-	-	Volts
16	7.581	0.316	-	-	-	-	-	-	-	-	Volts
17	7.221	0.400	-	-	-	-	-	-	-	-	Volts
18	7.075	0.464	-	-	-	-	-	-	-	-	Volts
19	7.623	0.412	-	-	-	-	-	-	-	-	Volts
20	7.920	0.334	-	-	-	-	-	-	-	-	Volts
21	8.198	0.299	-	-	-	-	-	-	-	-	Volts
22	8.540	0.296	-	-	-	-	-	-	-	-	Volts
23	8.904	0.271	-	-	-	-	-	-	-	-	Volts
24	9.206	0.256	-	-	-	-	-	-	-	-	Volts
25	9.366	0.271	-	-	-	-	-	-	-	-	Volts
26	9.445	0.273	-	-	-	-	-	-	-	-	Volts
27	8.835	0.356	-	-	-	-	-	-	-	-	Volts
28	8.731	0.347	-	-	-	-	-	-	-	-	Volts
29	9.400	0.256	-	-	-	-	-	-	-	-	Volts
30	9.417	0.257	-	-	-	-	-	-	-	-	Volts
31	9.254	0.261	-	-	-	-	-	-	-	-	Volts
32	8.880	0.263	-	-	-	-	-	-	-	-	Volts
33	8.593	0.271	-	-	-	-	-	-	-	-	Volts
34	8.164	0.298	-	-	-	-	-	-	-	-	Volts
35	8.129	0.279	-	-	-	-	-	-	-	-	Volts
36	7.782	0.316	-	-	-	-	-	-	-	-	Volts
37	7.220	0.411	-	-	-	-	-	-	-	-	Volts
38	7.560	0.367	-	-	-	-	-	-	-	-	Volts
39	7.874	0.352	-	-	-	-	-	-	-	-	Volts
40	8.416	0.286	-	-	-	-	-	-	-	-	Volts
41	8.871	0.256	-	-	-	-	-	-	-	-	Volts
42	9.300	0.262	-	-	-	-	-	-	-	-	Volts
43	9.390	0.263	-	-	-	-	-	-	-	-	Volts
44	9.392	0.317	-	-	-	-	-	-	-	-	Volts
45	8.702	0.376	-	-	-	-	-	-	-	-	Volts
46	8.350	0.373	-	-	-	-	-	-	-	-	Volts
47	8.970	0.276	-	-	-	-	-	-	-	-	Volts
48	9.250	0.272	-	-	-	-	-	-	-	-	Volts
49	9.314	0.237	-	-	-	-	-	-	-	-	Volts
50	8.990	0.267	-	-	-	-	-	-	-	-	Volts
51	8.528	0.297	-	-	-	-	-	-	-	-	Volts
52	7.854	0.352	-	-	-	-	-	-	-	-	Volts
53	7.540	0.335	-	-	-	-	-	-	-	-	Volts
54	7.220	0.406	-	-	-	-	-	-	-	-	Volts

Table 6.36 *Mean and fluctuation velocities and Reynolds shear stress components at section S-8 run no.3*

Loc.no.	Tangential		Vertical		Radial		Reynolds s.s. components v'w'		v'u'		Unit
	DC	RMS	DC	RMS	DC	RMS	+45	-45	+45	-45	
1	7.060	0.363	-	-	-	-	-	-	-	-	Volts
2	7.170	0.387	-	-	-	-	-	-	-	-	Volts
3	7.442	0.439	-	-	-	-	-	-	-	-	Volts
4	7.727	0.360	-	-	-	-	-	-	-	-	Volts
5	7.800	0.374	-	-	-	-	-	-	-	-	Volts
6	7.658	0.337	-	-	-	-	-	-	-	-	Volts
7	7.727	0.348	-	-	-	-	-	-	-	-	Volts
8	7.856	0.361	-	-	-	-	-	-	-	-	Volts
9	7.480	0.417	-	-	-	-	-	-	-	-	Volts
10	8.855	0.366	-	-	-	-	-	-	-	-	Volts
11	9.465	0.286	-	-	-	-	-	-	-	-	Volts
12	9.328	0.281	-	-	-	-	-	-	-	-	Volts
13	9.033	0.279	-	-	-	-	-	-	-	-	Volts
14	8.860	0.321	-	-	-	-	-	-	-	-	Volts
15	8.503	0.336	-	-	-	-	-	-	-	-	Volts
16	8.035	0.323	-	-	-	-	-	-	-	-	Volts
17	7.605	0.335	-	-	-	-	-	-	-	-	Volts
18	7.466	0.418	-	-	-	-	-	-	-	-	Volts
19	8.067	0.371	-	-	-	-	-	-	-	-	Volts
20	8.281	0.308	-	-	-	-	-	-	-	-	Volts
21	8.706	0.279	-	-	-	-	-	-	-	-	Volts
22	9.037	0.263	-	-	-	-	-	-	-	-	Volts
23	9.404	0.269	-	-	-	-	-	-	-	-	Volts
24	9.685	0.256	-	-	-	-	-	-	-	-	Volts
25	9.824	0.262	-	-	-	-	-	-	-	-	Volts
26	9.800	0.287	-	-	-	-	-	-	-	-	Volts
27	9.012	0.358	-	-	-	-	-	-	-	-	Volts
28	8.942	0.345	-	-	-	-	-	-	-	-	Volts
29	9.831	0.265	-	-	-	-	-	-	-	-	Volts
30	9.901	0.251	-	-	-	-	-	-	-	-	Volts
31	9.792	0.245	-	-	-	-	-	-	-	-	Volts
32	9.500	0.241	-	-	-	-	-	-	-	-	Volts
33	8.976	0.246	-	-	-	-	-	-	-	-	Volts
34	8.701	0.268	-	-	-	-	-	-	-	-	Volts
35	8.535	0.277	-	-	-	-	-	-	-	-	Volts
36	8.262	0.303	-	-	-	-	-	-	-	-	Volts
37	7.695	0.334	-	-	-	-	-	-	-	-	Volts
38	7.950	0.324	-	-	-	-	-	-	-	-	Volts
39	8.080	0.310	-	-	-	-	-	-	-	-	Volts
40	8.795	0.249	-	-	-	-	-	-	-	-	Volts
41	9.503	0.245	-	-	-	-	-	-	-	-	Volts
42	9.821	0.258	-	-	-	-	-	-	-	-	Volts
43	9.836	0.266	-	-	-	-	-	-	-	-	Volts
44	9.628	0.280	-	-	-	-	-	-	-	-	Volts
45	8.746	0.431	-	-	-	-	-	-	-	-	Volts
46	8.523	0.368	-	-	-	-	-	-	-	-	Volts
47	9.337	0.310	-	-	-	-	-	-	-	-	Volts
48	9.680	0.313	-	-	-	-	-	-	-	-	Volts
49	9.811	0.275	-	-	-	-	-	-	-	-	Volts
50	9.523	0.246	-	-	-	-	-	-	-	-	Volts
51	8.940	0.256	-	-	-	-	-	-	-	-	Volts
52	8.338	0.271	-	-	-	-	-	-	-	-	Volts
53	8.039	0.413	-	-	-	-	-	-	-	-	Volts
54	7.806	0.385	-	-	-	-	-	-	-	-	Volts

Table 6.1 a). The tangential, vertical and radial mean velocity distribution at section U-1 run no.1 Um = 0.04444 m/s

Loc. no.	η = z/h	2Y/B	Tangential v [m/s]	Tangential v/Um	Vertical w [m/s]	Vertical w/Um	Radial u [m/s]	Radial u/Um
1	0.080	-0.93	0.01020	0.2294	-	-	-	-
2	0.080	-0.87	0.01644	0.3698	-	-	-	-
3	0.080	-0.73	0.02198	0.4945	-	-	-	-
4	0.080	-0.40	0.01972	0.4436	-	-	-	-
5	0.080	0.	0.01786	0.4019	-	-	-	-
6	0.080	0.40	0.01770	0.3983	-	-	-	-
7	0.080	0.73	0.02085	0.4691	-	-	-	-
8	0.080	0.87	0.01923	0.4328	-	-	-	-
9	0.080	0.93	0.01434	0.3226	-	-	-	-
10	0.140	0.93	0.02908	0.6543	-	-	-	-
11	0.140	0.87	0.03720	0.8371	-	-	-	-
12	0.140	0.73	0.03925	0.8831	-	-	-	-
13	0.140	0.40	0.03618	0.8141	-	-	-	-
14	0.140	0.	0.03389	0.7626	-	-	-	-
15	0.140	-0.40	0.03371	0.7584	-	-	-	-
16	0.140	-0.73	0.03656	0.8225	-	-	-	-
17	0.140	-0.87	0.03209	0.7221	-	-	-	-
18	0.140	-0.93	0.02416	0.5435	-	-	-	-
19	0.320	-0.93	0.03895	0.8764	-	-	-	-
20	0.320	-0.87	0.04742	1.0671	-	-	-	-
21	0.320	-0.73	0.05334	1.2002	-	-	-	-
22	0.320	-0.40	0.04393	0.9884	-	-	-	-
23	0.320	0.	0.04855	1.0925	-	-	-	-
24	0.320	0.40	0.04581	1.0307	-	-	-	-
25	0.320	0.73	0.04944	1.1124	-	-	-	-
26	0.320	0.87	0.04705	1.0586	-	-	-	-
27	0.320	0.93	0.03785	0.8516	-	-	-	-
28	0.600	0.93	0.03890	0.8752	-	-	-	-
29	0.600	0.87	0.04823	1.0852	-	-	-	-
30	0.600	0.73	0.05280	1.1881	-	-	-	-
31	0.600	0.40	0.05130	1.1542	-	-	-	-
32	0.600	0.	0.05057	1.1379	-	-	-	-
33	0.600	-0.40	0.05065	1.1397	-	-	-	-
34	0.600	-0.73	0.05100	1.1476	-	-	-	-
35	0.600	-0.87	0.04541	1.0217	-	-	-	-
36	0.600	-0.93	0.03658	0.8231	-	-	-	-
37	0.900	-0.93	0.02405	0.5411	-	-	-	-
38	0.900	-0.87	0.03352	0.7541	-	-	-	-
39	0.900	-0.73	0.04702	1.0580	-	-	-	-
40	0.900	-0.40	0.05264	1.1845	-	-	-	-
41	0.900	0.	0.05544	1.2474	-	-	-	-
42	0.900	0.40	0.05474	1.2317	-	-	-	-
43	0.900	0.73	0.05055	1.1373	-	-	-	-
44	0.900	0.87	0.03693	0.8310	-	-	-	-
45	0.900	0.93	0.02779	0.6252	-	-	-	-

Table 6.2 a). The tangential, vertical and radial mean velocity distribution at section U-1 run no.2 Um = 0.07407 m/s

Loc. no.	η = z/h	2Y/B	Tangential v [m/s]	Tangential v/Um	Vertical w [m/s]	Vertical w/Um	Radial u [m/s]	Radial u/Um
1	0.044	-0.93	0.03588	0.4844	-	-	-	-
2	0.044	-0.87	0.04328	0.5843	-	-	-	-
3	0.044	-0.73	0.04379	0.5912	-	-	-	-
4	0.044	-0.40	0.03209	0.4332	-	-	-	-
5	0.044	0.	0.03182	0.4296	-	-	-	-
6	0.044	0.40	0.03102	0.4187	-	-	-	-
7	0.044	0.73	0.02994	0.4042	-	-	-	-
8	0.044	0.87	0.02940	0.3969	-	-	-	-
9	0.044	0.93	0.02671	0.3606	-	-	-	-
10	0.078	0.93	0.04589	0.6195	-	-	-	-
11	0.078	0.87	0.05684	0.7673	-	-	-	-
12	0.078	0.73	0.05348	0.7219	-	-	-	-
13	0.078	0.40	0.05324	0.7187	-	-	-	-
14	0.078	0.	0.04823	0.6511	-	-	-	-
15	0.078	-0.40	0.05092	0.6874	-	-	-	-
16	0.078	-0.73	0.05646	0.7623	-	-	-	-
17	0.078	-0.87	0.05859	0.7909	-	-	-	-
18	0.078	-0.93	0.04834	0.6526	-	-	-	-
19	0.178	-0.93	0.06012	0.8116	-	-	-	-
20	0.178	-0.87	0.07021	0.9478	-	-	-	-
21	0.178	-0.73	0.07365	0.9943	-	-	-	-
22	0.178	-0.40	0.06814	0.9199	-	-	-	-
23	0.178	0.	0.06652	0.8981	-	-	-	-
24	0.178	0.40	0.06948	0.9380	-	-	-	-
25	0.178	0.73	0.06679	0.9017	-	-	-	-
26	0.178	0.87	0.06972	0.9413	-	-	-	-
27	0.178	0.93	0.05810	0.7844	-	-	-	-
28	0.422	0.93	0.05883	0.7942	-	-	-	-
29	0.422	0.87	0.07107	0.9594	-	-	-	-
30	0.422	0.73	0.07672	1.0357	-	-	-	-
31	0.422	0.40	0.07718	1.0419	-	-	-	-
32	0.422	0.	0.07572	1.0223	-	-	-	-
33	0.422	-0.40	0.07755	1.0470	-	-	-	-
34	0.422	-0.73	0.07930	1.0706	-	-	-	-
35	0.422	-0.87	0.07137	0.9634	-	-	-	-
36	0.422	-0.93	0.05974	0.8066	-	-	-	-
37	0.667	-0.93	0.06155	0.8309	-	-	-	-
38	0.667	-0.87	0.07379	0.9961	-	-	-	-
39	0.667	-0.73	0.07989	1.0786	-	-	-	-
40	0.667	-0.40	0.08242	1.1127	-	-	-	-
41	0.667	0.	0.07745	1.0455	-	-	-	-
42	0.667	0.40	0.08016	1.0822	-	-	-	-
43	0.667	0.73	0.07459	1.0070	-	-	-	-
44	0.667	0.87	0.06916	0.9337	-	-	-	-
45	0.667	0.93	0.05576	0.7528	-	-	-	-
46	0.911	0.93	0.05477	0.7394	-	-	-	-
47	0.911	0.87	0.06760	0.9126	-	-	-	-
48	0.911	0.73	0.07231	0.9761	-	-	-	-
49	0.911	0.40	0.08092	1.0924	-	-	-	-
50	0.911	0.	0.07970	1.0760	-	-	-	-
51	0.911	-0.40	0.08307	1.1214	-	-	-	-
52	0.911	-0.73	0.07723	1.0426	-	-	-	-
53	0.911	-0.87	0.06911	0.9329	-	-	-	-
54	0.911	-0.93	0.05673	0.7659	-	-	-	-

Table 6.3 a). The tangential, vertical and radial mean velocity distribution at section U-1 run no.3 Um = 0.09259 m/s

Loc. no.	η = z/h	2Y/B	Tangential v [m/s]	Tangential v/Um	Vertical w [m/s]	Vertical w/Um	Radial u [m/s]	Radial u/Um
1	0.033	-0.93	0.04898	0.5290	-	-	-	-
2	0.033	-0.87	0.05746	0.6206	-	-	-	-
3	0.033	-0.73	0.06397	0.6909	-	-	-	-
4	0.033	-0.40	0.05961	0.6438	-	-	-	-
5	0.033	0.	0.05442	0.5877	-	-	-	-
6	0.033	0.40	0.05270	0.5691	-	-	-	-
7	0.033	0.73	0.05119	0.5529	-	-	-	-
8	0.033	0.87	0.04721	0.5099	-	-	-	-
9	0.033	0.93	0.04691	0.5067	-	-	-	-
10	0.058	0.93	0.05843	0.6310	-	-	-	-
11	0.058	0.87	0.06596	0.7124	-	-	-	-
12	0.058	0.73	0.07145	0.7716	-	-	-	-
13	0.058	0.40	0.07481	0.8079	-	-	-	-
14	0.058	0.	0.07516	0.8117	-	-	-	-
15	0.058	-0.40	0.07677	0.8291	-	-	-	-
16	0.058	-0.73	0.08051	0.8695	-	-	-	-
17	0.058	-0.87	0.07338	0.7925	-	-	-	-
18	0.058	-0.93	0.06507	0.7028	-	-	-	-
19	0.133	-0.93	0.07354	0.7943	-	-	-	-
20	0.133	-0.87	0.08334	0.9000	-	-	-	-
21	0.133	-0.73	0.09106	0.9834	-	-	-	-
22	0.133	-0.40	0.08815	0.9520	-	-	-	-
23	0.133	0.	0.07984	0.8623	-	-	-	-
24	0.133	0.40	0.08428	0.9102	-	-	-	-
25	0.133	0.73	0.08554	0.9239	-	-	-	-
26	0.133	0.87	0.08024	0.8666	-	-	-	-
27	0.133	0.93	0.07110	0.7678	-	-	-	-
28	0.400	0.93	0.07365	0.7954	-	-	-	-
29	0.400	0.87	0.08538	0.9221	-	-	-	-
30	0.400	0.73	0.09154	0.9886	-	-	-	-
31	0.400	0.40	0.09369	1.0119	-	-	-	-
32	0.400	0.	0.09114	0.9843	-	-	-	-
33	0.400	-0.40	0.10149	1.0961	-	-	-	-
34	0.400	-0.73	0.09856	1.0645	-	-	-	-
35	0.400	-0.87	0.08831	0.9538	-	-	-	-
36	0.400	-0.93	0.07658	0.8271	-	-	-	-
37	0.667	-0.93	0.08554	0.9239	-	-	-	-
38	0.667	-0.87	0.09765	1.0546	-	-	-	-
39	0.667	-0.73	0.09940	1.0735	-	-	-	-
40	0.667	-0.40	0.09977	1.0775	-	-	-	-
41	0.667	0.	0.09450	1.0206	-	-	-	-
42	0.667	0.40	0.09490	1.0250	-	-	-	-
43	0.667	0.73	0.09480	1.0238	-	-	-	-
44	0.667	0.87	0.08907	0.9619	-	-	-	-
45	0.667	0.93	0.07683	0.8297	-	-	-	-
46	0.933	0.93	0.07548	0.8152	-	-	-	-
47	0.933	0.87	0.08786	0.9488	-	-	-	-
48	0.933	0.73	0.09450	1.0206	-	-	-	-
49	0.933	0.40	0.09781	1.0563	-	-	-	-
50	0.933	0.	0.09864	1.0653	-	-	-	-
51	0.933	-0.40	0.10278	1.1101	-	-	-	-
52	0.933	-0.73	0.10071	1.0877	-	-	-	-
53	0.933	-0.87	0.08812	0.9517	-	-	-	-
54	0.933	-0.93	0.07564	0.8169	-	-	-	-

Table 6.4 a). The tangential, vertical and radial mean velocity distribution at section U-2 run no.1 Um = 0.04444 m/s

Loc. no.	η = z/h	2Y/B	Tangential v [m/s]	Tangential v/Um	Vertical w [m/s]	Vertical w/Um	Radial u [m/s]	Radial u/Um
1	0.080	-0.93	0.00959	0.2158	-	-	-	-
2	0.080	-0.87	0.00817	0.1838	-	-	-	-
3	0.080	-0.73	0.01175	0.2644	-	-	-	-
4	0.080	-0.40	0.02029	0.4565	-	-	-	-
5	0.080	0.	0.01966	0.4423	-	-	-	-
6	0.080	0.40	0.02103	0.4731	-	-	-	-
7	0.080	0.73	0.02055	0.4624	-	-	-	-
8	0.080	0.87	0.01739	0.3913	-	-	-	-
9	0.080	0.93	0.01339	0.3012	-	-	-	-
10	0.140	0.93	0.02329	0.5241	-	-	0.00016	0.0036
11	0.140	0.87	0.03109	0.6996	-	-	-0.00016	-0.0036
12	0.140	0.73	0.04032	0.9071	-	-	0.00032	0.0071
13	0.140	0.40	0.04158	0.9356	-	-	-0.00005	-0.0012
14	0.140	0.	0.03968	0.8929	-	-	0.00021	0.0047
15	0.140	-0.40	0.03520	0.7921	-	-	-0.00005	-0.0012
16	0.140	-0.73	0.02408	0.5419	-	-	-0.00148	-0.0332
17	0.140	-0.87	0.01808	0.4067	-	-	-0.00227	-0.0510
18	0.140	-0.93	0.01260	0.2834	-	-	-0.00179	-0.0403
19	0.320	-0.93	0.01924	0.4328	0.00042	0.0095	-0.00248	-0.0557
20	0.320	-0.87	0.02635	0.5929	0.00179	0.0403	-0.00285	-0.0640
21	0.320	-0.73	0.03025	0.6806	0.00021	0.0047	-0.00543	-0.1221
22	0.320	-0.40	0.04000	0.9000	0.00074	0.0166	-0.00838	-0.1885
23	0.320	0.	0.05186	1.1668	0.00074	0.0166	-0.00759	-0.1707
24	0.320	0.40	0.05423	1.2201	-0.00037	-0.0083	-0.00606	-0.1364
25	0.320	0.73	0.05238	1.1786	-0.00084	-0.0190	-0.00221	-0.0498
26	0.320	0.87	0.04775	1.0743	-0.00011	-0.0024	-0.00105	-0.0237
27	0.320	0.93	0.03873	0.8715	0.	0.	-0.00227	-0.0510
28	0.600	0.93	0.04142	0.9320	-0.00137	-0.0308	-0.00274	-0.0617
29	0.600	0.87	0.05165	1.1620	-0.00084	-0.0190	-0.00285	-0.0640
30	0.600	0.73	0.05607	1.2616	-0.00116	-0.0261	-0.00206	-0.0462
31	0.600	0.40	0.05460	1.2284	-0.00037	-0.0083	0.00153	0.0344
32	0.600	0.	0.04511	1.0150	0.00058	0.0130	0.00311	0.0700
33	0.600	-0.40	0.03252	0.7316	-0.00095	-0.0213	0.00269	0.0605
34	0.600	-0.73	0.03099	0.6972	0.00132	0.0296	-0.00005	-0.0012
35	0.600	-0.87	0.02593	0.5834	0.00095	0.0213	-0.00037	-0.0083
36	0.600	-0.93	0.01744	0.3925	0.00100	0.0225	-0.00053	-0.0119
37	0.900	-0.93	0.01502	0.3379	-0.00026	-0.0059	0.00042	0.0095
38	0.900	-0.87	0.02403	0.5407	0.00132	0.0296	0.00153	0.0344
39	0.900	-0.73	0.02493	0.5609	0.00084	0.0190	0.00364	0.0818
40	0.900	-0.40	0.02956	0.6652	-0.00026	-0.0059	0.00179	0.0403
41	0.900	0.	0.03515	0.7909	0.00042	0.0095	0.00132	0.0296
42	0.900	0.40	0.05491	1.2356	-0.00100	-0.0225	-0.00021	-0.0047
43	0.900	0.73	0.05407	1.2166	-0.00148	-0.0332	-0.00221	-0.0498
44	0.900	0.87	0.04685	1.0541	-0.00200	-0.0451	-0.00458	-0.1032
45	0.900	0.93	0.03620	0.8146	-0.00290	-0.0652	-0.00432	-0.0972

Table 6.5 a). The tangential, vertical and radial mean velocity distribution at section U-2 run no.2 Um = 0.07407 m/s

Loc. no.	η = z/h	2Y/B	Tangential v [m/s]	Tangential v/Um	Vertical w [m/s]	Vertical w/Um	Radial u [m/s]	Radial u/Um
1	0.044	−0.93	0.01860	0.2511	–	–	–	–
2	0.044	−0.87	0.02640	0.3564	–	–	–	–
3	0.044	−0.73	0.03510	0.4738	–	–	–	–
4	0.044	−0.40	0.04105	0.5542	–	–	–	–
5	0.044	0.	0.04169	0.5628	–	–	–	–
6	0.044	0.40	0.03968	0.5357	–	–	–	–
7	0.044	0.73	0.04021	0.5428	–	–	–	–
8	0.044	0.87	0.03884	0.5243	–	–	–	–
9	0.044	0.93	0.02935	0.3963	–	–	–	–
10	0.078	0.93	0.05212	0.7036	–	–	–	–
11	0.078	0.87	0.06498	0.8772	–	–	–	–
12	0.078	0.73	0.06761	0.9128	–	–	–	–
13	0.078	0.40	0.06914	0.9334	–	–	–	–
14	0.078	0.	0.06925	0.9348	–	–	–	–
15	0.078	−0.40	0.06587	0.8893	–	–	–	–
16	0.078	−0.73	0.05507	0.7435	–	–	–	–
17	0.078	−0.87	0.03968	0.5357	–	–	–	–
18	0.078	−0.93	0.03157	0.4262	–	–	–	–
19	0.178	−0.93	0.05196	0.7015	0.00026	0.0036	−0.00933	−0.1259
20	0.178	−0.87	0.05997	0.8096	0.00132	0.0178	−0.00791	−0.1067
21	0.178	−0.73	0.07014	0.9469	0.00300	0.0406	−0.00653	−0.0882
22	0.178	−0.40	0.07847	1.0593	0.00648	0.0875	−0.00901	−0.1217
23	0.178	0.	0.08084	1.0914	0.00632	0.0854	−0.01086	−0.1466
24	0.178	0.40	0.08079	1.0907	0.00538	0.0726	−0.00701	−0.0946
25	0.178	0.73	0.07562	1.0209	0.00184	0.0249	−0.00195	−0.0263
26	0.178	0.87	0.07194	0.9711	0.00011	0.0014	−0.00069	−0.0092
27	0.178	0.93	0.05744	0.7755	−0.00037	−0.0050	0.00327	0.0441
28	0.422	0.93	0.05786	0.7812	−0.00016	−0.0021	0.00269	0.0363
29	0.422	0.87	0.07462	1.0074	−0.00058	−0.0078	0.00037	0.0050
30	0.422	0.73	0.07942	1.0722	0.00121	0.0164	−0.00158	−0.0213
31	0.422	0.40	0.08306	1.1212	0.00490	0.0662	−0.00385	−0.0519
32	0.422	0.	0.08358	1.1284	0.00838	0.1131	−0.00364	−0.0491
33	0.422	−0.40	0.08079	1.0907	0.00617	0.0832	−0.00121	−0.0164
34	0.422	−0.73	0.07151	0.9654	0.00527	0.0711	−0.00279	−0.0377
35	0.422	−0.87	0.06377	0.8609	0.00279	0.0377	−0.00248	−0.0334
36	0.422	−0.93	0.05681	0.7669	0.00258	0.0349	−0.00332	−0.0448
37	0.667	−0.93	0.05391	0.7278	0.00184	0.0249	0.00163	0.0221
38	0.667	−0.87	0.06008	0.8111	0.00216	0.0292	−0.00047	−0.0064
39	0.667	−0.73	0.05992	0.8089	0.00385	0.0519	0.00206	0.0277
40	0.667	−0.40	0.07352	0.9925	0.00527	0.0711	0.00095	0.0128
41	0.667	0.	0.08469	1.1433	0.00864	0.1167	−0.00026	−0.0036
42	0.667	0.40	0.08432	1.1383	0.00163	0.0221	0.00047	0.0064
43	0.667	0.73	0.07847	1.0593	−0.00095	−0.0128	0.00079	0.0107
44	0.667	0.87	0.07447	1.0053	−0.00069	−0.0092	0.00163	0.0221
45	0.667	0.93	0.05797	0.7826	−0.00074	−0.0100	0.00132	0.0178
46	0.911	0.93	0.05122	0.6915	–	–	0.00211	0.0285
47	0.911	0.87	0.06756	0.9121	–	–	−0.00379	−0.0512
48	0.911	0.73	0.07657	1.0337	–	–	−0.00733	−0.0989
49	0.911	0.40	0.08464	1.1426	–	–	0.00216	0.0292
50	0.911	0.	0.08764	1.1831	–	–	0.00743	0.1003
51	0.911	−0.40	0.06366	0.8594	–	–	0.00527	0.0711
52	0.911	−0.73	0.05339	0.7207	–	–	0.00943	0.1273
53	0.911	−0.87	0.05033	0.6794	–	–	0.01038	0.1402
54	0.911	−0.93	0.04195	0.5663	–	–	0.01212	0.1636

Table 6.6 a). The tangential, vertical and radial mean velocity distribution at section U-2 run no.3 Um = 0.09259 m/s

Loc. no.	η = z/h	2Y/B	Tangential v [m/s]	Tangential v/Um	Vertical w [m/s]	Vertical w/Um	Radial u [m/s]	Radial u/Um
1	0.033	−0.93	0.02630	0.2840	–	–	–	–
2	0.033	−0.87	0.03420	0.3694	–	–	–	–
3	0.033	−0.73	0.05091	0.5498	–	–	–	–
4	0.033	−0.40	0.05476	0.5914	–	–	–	–
5	0.033	0.	0.05207	0.5623	–	–	–	–
6	0.033	0.40	0.04680	0.5054	–	–	–	–
7	0.033	0.73	0.04732	0.5111	–	–	–	–
8	0.033	0.87	0.04516	0.4878	–	–	–	–
9	0.033	0.93	0.03346	0.3614	–	–	–	–
10	0.058	0.93	0.05512	0.5953	–	–	–	–
11	0.058	0.87	0.06935	0.7490	–	–	–	–
12	0.058	0.73	0.07526	0.8128	–	–	–	–
13	0.058	0.40	0.07578	0.8185	–	–	–	–
14	0.058	0.	0.07784	0.8406	–	–	–	–
15	0.058	−0.40	0.07684	0.8298	–	–	–	–
16	0.058	−0.73	0.07115	0.7684	–	–	–	–
17	0.058	−0.87	0.05180	0.5595	–	–	–	–
18	0.058	−0.93	0.03837	0.4143	–	–	–	–
19	0.133	−0.93	0.06071	0.6557	0.00321	0.0347	−0.01470	−0.1588
20	0.133	−0.87	0.07562	0.8167	0.00738	0.0797	−0.01476	−0.1594
21	0.133	−0.73	0.08553	0.9237	0.01296	0.1400	−0.01639	−0.1770
22	0.133	−0.40	0.09307	1.0051	0.01133	0.1224	−0.01602	−0.1730
23	0.133	0.	0.09249	0.9989	0.00574	0.0620	−0.01449	−0.1565
24	0.133	0.40	0.09117	0.9846	0.00680	0.0734	−0.01038	−0.1121
25	0.133	0.73	0.08643	0.9334	−0.00058	−0.0063	−0.01128	−0.1218
26	0.133	0.87	0.08226	0.8885	−0.00105	−0.0114	−0.00827	−0.0894
27	0.133	0.93	0.06582	0.7109	−0.00121	−0.0131	−0.00875	−0.0945
28	0.400	0.93	0.06582	0.7109	−0.00511	−0.0552	−0.00743	−0.0803
29	0.400	0.87	0.08395	0.9067	0.00148	0.0159	−0.00669	−0.0723
30	0.400	0.73	0.09396	1.0148	0.00174	0.0188	−0.00706	−0.0763
31	0.400	0.40	0.09628	1.0399	0.00495	0.0535	−0.00401	−0.0433
32	0.400	0.	0.09802	1.0586	0.00901	0.0973	−0.00395	−0.0427
33	0.400	−0.40	0.10029	1.0831	0.01191	0.1286	−0.00606	−0.0655
34	0.400	−0.73	0.08696	0.9391	0.00722	0.0780	−0.00084	−0.0091
35	0.400	−0.87	0.07984	0.8623	0.01091	0.1178	−0.00232	−0.0250
36	0.400	−0.93	0.06735	0.7274	0.01123	0.1212	−0.00348	−0.0376
37	0.667	−0.93	0.06129	0.6619	0.00527	0.0569	0.00169	0.0182
38	0.667	−0.87	0.07162	0.7735	0.00437	0.0472	0.00200	0.0216
39	0.667	−0.73	0.07547	0.8150	0.00464	0.0501	0.00100	0.0108
40	0.667	−0.40	0.09639	1.0410	0.00806	0.0871	0.00316	0.0341
41	0.667	0.	0.10029	1.0831	0.01897	0.2049	0.00300	0.0324
42	0.667	0.40	0.09444	1.0199	0.01744	0.1884	0.00084	0.0091
43	0.667	0.73	0.08975	0.9693	0.00490	0.0529	−0.00480	−0.0518
44	0.667	0.87	0.07357	0.7945	−0.00200	−0.0216	−0.00485	−0.0524
45	0.667	0.93	0.05196	0.5612	−0.00527	−0.0569	−0.00527	−0.0569
46	0.933	0.93	0.05702	0.6158	–	–	−0.00775	−0.0837
47	0.933	0.87	0.07958	0.8594	–	–	−0.00796	−0.0859
48	0.933	0.73	0.08669	0.9363	–	–	−0.00764	−0.0825
49	0.933	0.40	0.09607	1.0376	–	–	0.00316	0.0341
50	0.933	0.	0.10282	1.1104	–	–	0.00385	0.0415
51	0.933	−0.40	0.08564	0.9249	–	–	0.00585	0.0632
52	0.933	−0.73	0.05892	0.6363	–	–	0.00690	0.0746
53	0.933	−0.87	0.05454	0.5891	–	–	0.00069	0.0074
54	0.933	−0.93	0.04443	0.4798	–	–	0.00053	0.0057

Table 6.7 a). The tangential, vertical and radial mean velocity distribution at section U-3 run no.1 Um = 0.04444 m/s

Loc. no.	η = z/h	2Y/B	Tangential v [m/s]	v/Um	Vertical w [m/s]	w/Um	Radial u [m/s]	u/Um
1	0.080	-0.93	0.01439	0.3237	-	-	-	-
2	0.080	-0.87	0.01823	0.4103	-	-	-	-
3	0.080	-0.73	0.02598	0.5846	-	-	-	-
4	0.080	-0.40	0.02714	0.6107	-	-	-	-
5	0.080	0.	0.03615	0.8134	-	-	-	-
6	0.080	0.40	0.04163	0.9367	-	-	-	-
7	0.080	0.73	0.05365	1.2071	-	-	-	-
8	0.080	0.87	0.07136	1.6055	-	-	-	-
9	0.080	0.93	0.06508	1.4644	-	-	-	-
10	0.140	0.93	0.08701	1.9577	-	-	0.00021	0.0047
11	0.140	0.87	0.09634	2.1676	-	-	-0.00005	-0.0012
12	0.140	0.73	0.09238	2.0786	-	-	-0.00069	-0.0154
13	0.140	0.40	0.08732	1.9648	-	-	-0.00211	-0.0474
14	0.140	0.	0.07336	1.6506	-	-	-0.00422	-0.0949
15	0.140	-0.40	0.05723	1.2877	-	-	-0.00337	-0.0759
16	0.140	-0.73	0.03952	0.8893	-	-	-0.00269	-0.0605
17	0.140	-0.87	0.02682	0.6035	-	-	-0.00269	-0.0605
18	0.140	-0.93	0.02192	0.4933	-	-	-0.00163	-0.0368
19	0.320	-0.93	0.04400	0.9901	0.00179	0.0403	0.00053	0.0119
20	0.320	-0.87	0.05544	1.2474	0.00142	0.0320	0.00100	0.0225
21	0.320	-0.73	0.07178	1.6150	0.00053	0.0119	0.00211	0.0474
22	0.320	-0.40	0.08801	1.9802	0.00026	0.0059	0.00211	0.0474
23	0.320	0.	0.10118	2.2766	-0.00016	-0.0036	0.00253	0.0569
24	0.320	0.40	0.11415	2.5683	-0.00095	-0.0213	0.00163	0.0368
25	0.320	0.73	0.12205	2,7462	-0.00053	-0.0119	0.00269	0.0605
26	0.320	0.87	0.11858	2.6679	-0.00069	-0.0154	0.00248	0.0557
27	0.320	0.93	0.10735	2.4154	-0.00169	-0.0379	0.00279	0.0628
28	0.600	0.93	0.10266	2.3098	0.00016	0.0036	0.00385	0.0866
29	0.600	0.87	0.11478	2.5826	-0.00100	-0.0225	0.00327	0.0735
30	0.600	0.73	0.11678	2.6276	-0.00184	-0.0415	0.00300	0.0676
31	0.600	0.40	0.11230	2.5268	-0.00090	-0.0202	0.00327	0.0735
32	0.600	0.	0.09465	2.1296	-0.00037	-0.0083	0.00422	0.0949
33	0.600	-0.40	0.07499	1.6873	-0.00016	-0.0036	0.00453	0.1020
34	0.600	-0.73	0.06129	1.3790	-0.00058	-0.0130	0.00279	0.0628
35	0.600	-0.87	0.05170	1.1632	0.00095	0.0213	0.00253	0.0569
36	0.600	-0.93	0.04100	0.9225	0.00184	0.0415	0.00163	0.0368
37	0.900	-0.93	0.02588	0.5822	-0.00005	-0.0012	0.00105	0.0237
38	0.900	-0.87	0.03162	0.7115	-0.00016	-0.0036	0.00137	0.0308
39	0.900	-0.73	0.03858	0.8680	-0.00026	-0.0059	0.00227	0.0510
40	0.900	-0.40	0.06977	1.5699	-0.00037	-0.0083	0.00332	0.0747
41	0.900	0.	0.09634	2.1676	-0.00005	-0.0012	0.00364	0.0818
42	0.900	0.40	0.11652	2.6217	-0.00047	-0.0107	0.00311	0.0700
43	0.900	0.73	0.11352	2.5541	-0.00090	-0.0202	-0.00047	-0.0107
44	0.900	0.87	0.10340	2.3264	-0.00132	-0.0296	-0.00121	-0.0273
45	0.900	0.93	0.09138	2.0561	-0.00190	-0.0427	-0.00116	-0.0261

Table 6.8 a). The tangential, vertical and radial mean velocity distribution at section U-3 run no.2 Um = 0.07407 m/s

Loc. no.	η = z/h	2Y/B	Tangential v [m/s]	v/Um	Vertical w [m/s]	w/Um	Radial u [m/s]	u/Um
1	0.044	-0.93	0.01781	0.2405	-	-	-	-
2	0.044	-0.87	0.03078	0.4155	-	-	-	-
3	0.044	-0.73	0.03262	0.4404	-	-	-	-
4	0.044	-0.40	0.03758	0.5073	-	-	-	-
5	0.044	0.	0.04474	0.6040	-	-	-	-
6	0.044	0.40	0.04321	0.5834	-	-	-	-
7	0.044	0.73	0.05428	0.7328	-	-	-	-
8	0.044	0.87	0.06482	0.8751	-	-	-	-
9	0.044	0.93	0.05144	0.6944	-	-	-	-
10	0.078	0.93	0.06777	0.9149	-	-	-	-
11	0.078	0.87	0.08274	1.1170	-	-	-	-
12	0.078	0.73	0.07499	1.0124	-	-	-	-
13	0.078	0.40	0.06271	0.8466	-	-	-	-
14	0.078	0.	0.06187	0.8352	-	-	-	-
15	0.078	-0.40	0.05328	0.7193	-	-	-	-
16	0.078	-0.73	0.04627	0.6247	-	-	-	-
17	0.078	-0.87	0.04364	0.5891	-	-	-	-
18	0.078	-0.93	0.03025	0.4084	-	-	-	-
19	0.178	-0.93	0.04638	0.6261	0.00564	0.0761	-0.00221	-0.0299
20	0.178	-0.87	0.06034	0.8146	0.00279	0.0377	-0.00258	-0.0349
21	0.178	-0.73	0.06703	0.9050	0.00105	0.0142	-0.00200	-0.0270
22	0.178	-0.40	0.07415	1.0010	-0.00016	-0.0021	0.00206	0.0277
23	0.178	0.	0.08153	1.1006	-0.00021	-0.0028	0.00163	0.0221
24	0.178	0.40	0.08859	1.1959	-0.00095	-0.0128	0.00279	0.0377
25	0.178	0.73	0.09149	1.2351	-0.00021	-0.0028	0.00448	0.0605
26	0.178	0.87	0.09170	1.2379	-0.00142	-0.0192	0.00358	0.0484
27	0.178	0.93	0.07562	1.0209	-0.00174	-0.0235	0.00221	0.0299
28	0.422	0.93	0.07304	0.9861	0.00095	0.0128	0.00264	0.0356
29	0.422	0.87	0.09033	1.2194	0.00058	0.0078	0.00453	0.0612
30	0.422	0.73	0.09133	1.2329	-0.00032	-0.0043	0.00611	0.0825
31	0.422	0.40	0.08859	1.1959	-0.00227	-0.0306	0.00564	0.0761
32	0.422	0.	0.08021	1.0828	-0.00090	-0.0121	0.00422	0.0569
33	0.422	-0.40	0.06983	0.9427	-0.00037	-0.0050	0.00443	0.0598
34	0.422	-0.73	0.06271	0.8466	-0.00063	-0.0085	0.00279	0.0377
35	0.422	-0.87	0.05850	0.7897	0.00211	0.0285	0.00190	0.0256
36	0.422	-0.93	0.04553	0.6147	0.00453	0.0612	0.00195	0.0263
37	0.667	-0.93	0.03594	0.4852	0.00364	0.0491	0.00327	0.0441
38	0.667	-0.87	0.04780	0.6453	0.00348	0.0470	0.00464	0.0626
39	0.667	-0.73	0.04970	0.6709	-0.00037	-0.0050	0.00343	0.0462
40	0.667	-0.40	0.06461	0.8722	-0.00100	-0.0135	0.00379	0.0512
41	0.667	0.	0.08132	1.0978	-0.00037	-0.0050	0.00253	0.0341
42	0.667	0.40	0.08896	1.2009	-0.00395	-0.0534	0.00174	0.0235
43	0.667	0.73	0.08948	1.2080	-0.00100	-0.0135	0.00411	0.0555
44	0.667	0.87	0.08938	1.2066	0.00279	0.0377	0.00295	0.0398
45	0.667	0.93	0.06925	0.9348	0.00511	0.0690	0.00121	0.0164
46	0.911	0.93	0.06450	0.8708	-	-	-0.00184	-0.0249
47	0.911	0.87	0.08501	1.1476	-	-	-0.00406	-0.0548
48	0.911	0.73	0.08759	1.1824	-	-	-0.00611	-0.0825
49	0.911	0.40	0.08553	1.1547	-	-	-0.00300	-0.0406
50	0.911	0.	0.08680	1.1718	-	-	0.00190	0.0256
51	0.911	-0.40	0.06530	0.8815	-	-	0.00153	0.0206
52	0.911	-0.73	0.04701	0.6346	-	-	0.00258	0.0349
53	0.911	-0.87	0.04205	0.5677	-	-	0.00047	0.0064
54	0.911	-0.93	0.03099	0.4183	-	-	-0.00053	-0.0071

Table 6.9 a). The tangential, vertical and radial mean velocity distribution at section U-3 run no.3 Um = 0.09259 m/s

Loc. no.	η = z/h	2Y/B	Tangential v [m/s]	Tangential v/Um	Vertical w [m/s]	Vertical w/Um	Radial u [m/s]	Radial u/Um
1	0.033	−0.93	0.03531	0.3813	−	−	−	−
2	0.033	−0.87	0.04537	0.4900	−	−	−	−
3	0.033	−0.73	0.05265	0.5686	−	−	−	−
4	0.033	−0.40	0.05391	0.5823	−	−	−	−
5	0.033	0.	0.05639	0.6090	−	−	−	−
6	0.033	0.40	0.06303	0.6807	−	−	−	−
7	0.033	0.73	0.07025	0.7587	−	−	−	−
8	0.033	0.87	0.07552	0.8156	−	−	−	−
9	0.033	0.93	0.06055	0.6540	−	−	−	−
10	0.058	0.93	0.08132	0.8782	−	−	−	−
11	0.058	0.87	0.09987	1.0786	−	−	−	−
12	0.058	0.73	0.09797	1.0581	−	−	−	−
13	0.058	0.40	0.08991	0.9710	−	−	−	−
14	0.058	0.	0.08058	0.8702	−	−	−	−
15	0.058	−0.40	0.07362	0.7951	−	−	−	−
16	0.058	−0.73	0.06682	0.7217	−	−	−	−
17	0.058	−0.87	0.05786	0.6249	−	−	−	−
18	0.058	−0.93	0.04501	0.4861	−	−	−	−
19	0.133	−0.93	0.05808	0.6272	0.00780	0.0842	−0.00327	−0.0353
20	0.133	−0.87	0.07194	0.7769	0.00385	0.0415	−0.00300	−0.0324
21	0.133	−0.73	0.08258	0.8919	0.00084	0.0091	−0.00248	−0.0268
22	0.133	−0.40	0.08938	0.9653	0.00063	0.0068	−0.00011	−0.0011
23	0.133	0.	0.09765	1.0547	−0.00053	−0.0057	0.00253	0.0273
24	0.133	0.40	0.10498	1.1338	−0.00069	−0.0074	0.00148	0.0159
25	0.133	0.73	0.10561	1.1406	−0.00084	−0.0091	0.00179	0.0194
26	0.133	0.87	0.10598	1.1446	−0.00179	−0.0194	0.00206	0.0222
27	0.133	0.93	0.08585	0.9272	−0.00237	−0.0256	0.00069	0.0074
28	0.400	0.93	0.08295	0.8959	0.00253	0.0273	0.00285	0.0307
29	0.400	0.87	0.10482	1.1321	0.00063	0.0068	0.00464	0.0501
30	0.400	0.73	0.10672	1.1525	0.00026	0.0028	0.00538	0.0581
31	0.400	0.40	0.10514	1.1355	−0.00248	−0.0268	0.00690	0.0746
32	0.400	0.	0.09623	1.0393	−0.00242	−0.0262	0.00516	0.0558
33	0.400	−0.40	0.08527	0.9209	−0.00306	−0.0330	0.00437	0.0472
34	0.400	−0.73	0.07868	0.8498	−0.00026	−0.0028	0.00227	0.0245
35	0.400	−0.87	0.07315	0.7900	0.00379	0.0410	0.00237	0.0256
36	0.400	−0.93	0.06113	0.6602	0.00775	0.0837	0.00237	0.0256
37	0.667	−0.93	0.04295	0.4639	0.00242	0.0262	0.00327	0.0353
38	0.667	−0.87	0.05259	0.5680	0.00385	0.0415	0.00474	0.0512
39	0.667	−0.73	0.06498	0.7018	0.00105	0.0114	0.00411	0.0444
40	0.667	−0.40	0.08421	0.9095	−0.00174	−0.0188	0.00290	0.0313
41	0.667	0.	0.09892	1.0683	−0.00132	−0.0142	0.00221	0.0239
42	0.667	0.40	0.10313	1.1138	−0.00248	−0.0268	0.00480	0.0518
43	0.667	0.73	0.10377	1.1207	−0.00090	−0.0097	0.00416	0.0450
44	0.667	0.87	0.10240	1.1059	0.00121	0.0131	0.00227	0.0245
45	0.667	0.93	0.07916	0.8549	0.00448	0.0484	0.00227	0.0245
46	0.933	0.93	0.07125	0.7695	−	−	−0.01686	−0.1821
47	0.933	0.87	0.09381	1.0131	−	−	−0.01987	−0.2146
48	0.933	0.73	0.09323	1.0068	−	−	−0.02314	−0.2499
49	0.933	0.40	0.10082	1.0888	−	−	−0.02335	−0.2521
50	0.933	0.	0.10419	1.1252	−	−	−0.01686	−0.1821
51	0.933	−0.40	0.08458	0.9135	−	−	−0.01296	−0.1400
52	0.933	−0.73	0.06777	0.7319	−	−	−0.00885	−0.0956
53	0.933	−0.87	0.06709	0.7245	−	−	−0.00928	−0.1002
54	0.933	−0.93	0.05792	0.6255	−	−	−0.01038	−0.1121

Table 6.10 a). The tangential, vertical and radial mean velocity distribution at section U-4 run no.1 Um = 0.04444 m/s

Loc. no.	η = z/h	2Y/B	Tangential v [m/s]	Tangential v/Um	Vertical w [m/s]	Vertical w/Um	Radial u [m/s]	Radial u/Um
1	0.080	−0.93	0.00643	0.1447	−	−	−	−
2	0.080	−0.87	0.00882	0.1985	−	−	−	−
3	0.080	−0.73	0.01065	0.2397	−	−	−	−
4	0.080	−0.40	0.01501	0.3377	−	−	−	−
5	0.080	0.	0.01714	0.3855	−	−	−	−
6	0.080	0.40	0.01646	0.3704	−	−	−	−
7	0.080	0.73	0.02623	0.5901	−	−	−	−
8	0.080	0.87	0.03333	0.7499	−	−	−	−
9	0.080	0.93	0.02765	0.6222	−	−	−	−
10	0.140	0.93	0.04110	0.9248	−	−	−	−
11	0.140	0.87	0.04745	1.0677	−	−	−	−
12	0.140	0.73	0.04312	0.9702	−	−	−	−
13	0.140	0.40	0.03467	0.7802	−	−	−	−
14	0.140	0.	0.03241	0.7293	−	−	−	−
15	0.140	−0.40	0.02752	0.6192	−	−	−	−
16	0.140	−0.73	0.02249	0.5060	−	−	−	−
17	0.140	−0.87	0.01625	0.3656	−	−	−	−
18	0.140	−0.93	0.01141	0.2566	−	−	−	−
19	0.320	−0.93	0.01945	0.4376	−	−	−	−
20	0.320	−0.87	0.02596	0.5841	−	−	−	−
21	0.320	−0.73	0.03443	0.7747	−	−	−	−
22	0.320	−0.40	0.04105	0.9236	−	−	−	−
23	0.320	0.	0.04971	1.1185	−	−	−	−
24	0.320	0.40	0.05872	1.3213	−	−	−	−
25	0.320	0.73	0.06265	1.4096	−	−	−	−
26	0.320	0.87	0.06053	1.3618	−	−	−	−
27	0.320	0.93	0.05138	1.1560	−	−	−	−
28	0.600	0.93	0.05350	1.2038	−	−	−	−
29	0.600	0.87	0.06432	1.4472	−	−	−	−
30	0.600	0.73	0.06389	1.4375	−	−	−	−
31	0.600	0.40	0.05872	1.3213	−	−	−	−
32	0.600	0.	0.04708	1.0592	−	−	−	−
33	0.600	−0.40	0.03860	0.8685	−	−	−	−
34	0.600	−0.73	0.03322	0.7475	−	−	−	−
35	0.600	−0.87	0.03142	0.7069	−	−	−	−
36	0.600	−0.93	0.02394	0.5387	−	−	−	−
37	0.900	−0.93	0.01283	0.2887	−	−	−	−
38	0.900	−0.87	0.01824	0.4104	−	−	−	−
39	0.900	−0.73	0.02609	0.5871	−	−	−	−
40	0.900	−0.40	0.04016	0.9036	−	−	−	−
41	0.900	0.	0.05181	1.1657	−	−	−	−
42	0.900	0.40	0.06090	1.3703	−	−	−	−
43	0.900	0.73	0.05983	1.3461	−	−	−	−
44	0.900	0.87	0.05576	1.2547	−	−	−	−
45	0.900	0.93	0.04514	1.0156	−	−	−	−

Table 6.11 a). The tangential, vertical and radial mean velocity distribution at section U-4 run no.2 Um = 0.07407 m/s

Loc. no.	η = z/h	2Y/B	Tangential v [m/s]	Tangential v/Um	Vertical w [m/s]	Vertical w/Um	Radial u [m/s]	Radial u/Um
1	0.044	-0.93	0.01272	0.1718	-	-	-	-
2	0.044	-0.87	0.01595	0.2153	-	-	-	-
3	0.044	-0.73	0.02593	0.3501	-	-	-	-
4	0.044	-0.40	0.02625	0.3544	-	-	-	-
5	0.044	0.	0.03599	0.4859	-	-	-	-
6	0.044	0.40	0.04102	0.5538	-	-	-	-
7	0.044	0.73	0.05213	0.7038	-	-	-	-
8	0.044	0.87	0.05186	0.7002	-	-	-	-
9	0.044	0.93	0.03739	0.5048	-	-	-	-
10	0.078	0.93	0.06365	0.8592	-	-	-	-
11	0.078	0.87	0.08024	1.0833	-	-	-	-
12	0.078	0.73	0.08132	1.0978	-	-	-	-
13	0.078	0.40	0.06835	0.9228	-	-	-	-
14	0.078	0.	0.06182	0.8345	-	-	-	-
15	0.078	-0.40	0.04500	0.6075	-	-	-	-
16	0.078	-0.73	0.03925	0.5298	-	-	-	-
17	0.078	-0.87	0.02644	0.3570	-	-	-	-
18	0.078	-0.93	0.02321	0.3134	-	-	-	-
19	0.178	-0.93	0.04465	0.6028	-	-	-	-
20	0.178	-0.87	0.04823	0.6511	-	-	-	-
21	0.178	-0.73	0.06034	0.8145	-	-	-	-
22	0.178	-0.40	0.06768	0.9137	-	-	-	-
23	0.178	0.	0.08597	1.1606	-	-	-	-
24	0.178	0.40	0.08804	1.1886	-	-	-	-
25	0.178	0.73	0.09490	1.2812	-	-	-	-
26	0.178	0.87	0.09676	1.3063	-	-	-	-
27	0.178	0.93	0.07860	1.0611	-	-	-	-
28	0.422	0.93	0.07610	1.0274	-	-	-	-
29	0.422	0.87	0.09657	1.3037	-	-	-	-
30	0.422	0.73	0.09558	1.2903	-	-	-	-
31	0.422	0.40	0.09254	1.2492	-	-	-	-
32	0.422	0.	0.08121	1.0963	-	-	-	-
33	0.422	-0.40	0.06238	0.8421	-	-	-	-
34	0.422	-0.73	0.05711	0.7710	-	-	-	-
35	0.422	-0.87	0.05571	0.7521	-	-	-	-
36	0.422	-0.93	0.05173	0.6983	-	-	-	-
37	0.667	-0.93	0.04231	0.5712	-	-	-	-
38	0.667	-0.87	0.04662	0.6293	-	-	-	-
39	0.667	-0.73	0.04823	0.6511	-	-	-	-
40	0.667	-0.40	0.05958	0.8044	-	-	-	-
41	0.667	0.	0.08221	1.1098	-	-	-	-
42	0.667	0.40	0.09488	1.2808	-	-	-	-
43	0.667	0.73	0.09864	1.3317	-	-	-	-
44	0.667	0.87	0.10001	1.3502	-	-	-	-
45	0.667	0.93	0.07812	1.0546	-	-	-	-
46	0.911	0.93	0.07263	0.9805	-	-	-	-
47	0.911	0.87	0.09383	1.2667	-	-	-	-
48	0.911	0.73	0.09681	1.3070	-	-	-	-
49	0.911	0.40	0.09348	1.2619	-	-	-	-
50	0.911	0.	0.08352	1.1276	-	-	-	-
51	0.911	-0.40	0.06351	0.8574	-	-	-	-
52	0.911	-0.73	0.04296	0.5800	-	-	-	-
53	0.911	-0.87	0.03529	0.4765	-	-	-	-
54	0.911	-0.93	0.02870	0.3875	-	-	-	-

Table 6.12 a). The tangential, vertical and radial mean velocity distribution at section U-4 run no.3 Um = 0.09259 m/s

Loc. no.	η = z/h	2Y/B	Tangential v [m/s]	Tangential v/Um	Vertical w [m/s]	Vertical w/Um	Radial u [m/s]	Radial u/Um
1	0.033	-0.93	0.01953	0.2109	-	-	-	-
2	0.033	-0.87	0.02324	0.2510	-	-	-	-
3	0.033	-0.73	0.03357	0.3626	-	-	-	-
4	0.033	-0.40	0.03605	0.3893	-	-	-	-
5	0.033	0.	0.04312	0.4657	-	-	-	-
6	0.033	0.40	0.05200	0.5616	-	-	-	-
7	0.033	0.73	0.05649	0.6101	-	-	-	-
8	0.033	0.87	0.06841	0.7388	-	-	-	-
9	0.033	0.93	0.05617	0.6066	-	-	-	-
10	0.058	0.93	0.08659	0.9352	-	-	-	-
11	0.058	0.87	0.10265	1.1086	-	-	-	-
12	0.058	0.73	0.09450	1.0206	-	-	-	-
13	0.058	0.40	0.08621	0.9311	-	-	-	-
14	0.058	0.	0.07513	0.8114	-	-	-	-
15	0.058	-0.40	0.06625	0.7156	-	-	-	-
16	0.058	-0.73	0.05485	0.5924	-	-	-	-
17	0.058	-0.87	0.04070	0.4396	-	-	-	-
18	0.058	-0.93	0.03747	0.4047	-	-	-	-
19	0.133	-0.93	0.05665	0.6118	-	-	-	-
20	0.133	-0.87	0.06074	0.6560	-	-	-	-
21	0.133	-0.73	0.07354	0.7943	-	-	-	-
22	0.133	-0.40	0.08804	0.9509	-	-	-	-
23	0.133	0.	0.10001	1.0802	-	-	-	-
24	0.133	0.40	0.10663	1.1516	-	-	-	-
25	0.133	0.73	0.11225	1.2123	-	-	-	-
26	0.133	0.87	0.11250	1.2150	-	-	-	-
27	0.133	0.93	0.09520	1.0282	-	-	-	-
28	0.400	0.93	0.08845	0.9552	-	-	-	-
29	0.400	0.87	0.11102	1.1990	-	-	-	-
30	0.400	0.73	0.11258	1.2158	-	-	-	-
31	0.400	0.40	0.10994	1.1874	-	-	-	-
32	0.400	0.	0.09808	1.0592	-	-	-	-
33	0.400	-0.40	0.07917	0.8550	-	-	-	-
34	0.400	-0.73	0.06870	0.7420	-	-	-	-
35	0.400	-0.87	0.06432	0.6946	-	-	-	-
36	0.400	-0.93	0.05872	0.6342	-	-	-	-
37	0.667	-0.93	0.04186	0.4520	-	-	-	-
38	0.667	-0.87	0.05133	0.5543	-	-	-	-
39	0.667	-0.73	0.05582	0.6028	-	-	-	-
40	0.667	-0.40	0.07527	0.8129	-	-	-	-
41	0.667	0.	0.10141	1.0953	-	-	-	-
42	0.667	0.40	0.11365	1.2274	-	-	-	-
43	0.667	0.73	0.11244	1.2144	-	-	-	-
44	0.667	0.87	0.11102	1.1990	-	-	-	-
45	0.667	0.93	0.08716	0.9413	-	-	-	-
46	0.933	0.93	0.07987	0.8626	-	-	-	-
47	0.933	0.87	0.10257	1.1078	-	-	-	-
48	0.933	0.73	0.10647	1.1499	-	-	-	-
49	0.933	0.40	0.10994	1.1874	-	-	-	-
50	0.933	0.	0.10222	1.1040	-	-	-	-
51	0.933	-0.40	0.07782	0.8405	-	-	-	-
52	0.933	-0.73	0.05862	0.6330	-	-	-	-
53	0.933	-0.87	0.05506	0.5947	-	-	-	-
54	0.933	-0.93	0.04732	0.5110	-	-	-	-

Table 6.13 a). The tangential, vertical and radial mean velocity distribution at section S-1 run no.1 Um = 0.04444 m/s

Loc. no.	η = z/h	2Y/B	Tangential v [m/s]	v/Um	Vertical w [m/s]	w/Um	Radial u [m/s]	u/Um
1	0.080	-0.93	0.00952	0.2143	-	-	-	-
2	0.080	-0.87	0.01991	0.4479	-	-	-	-
3	0.080	-0.73	0.02184	0.4915	-	-	-	-
4	0.080	-0.40	0.01552	0.3492	-	-	-	-
5	0.080	0.	0.02160	0.4860	-	-	-	-
6	0.080	0.40	0.01915	0.4309	-	-	-	-
7	0.080	0.73	0.02281	0.5133	-	-	-	-
8	0.080	0.87	0.01563	0.3517	-	-	-	-
9	0.080	0.93	0.00468	0.1053	-	-	-	-
10	0.140	0.93	0.01022	0.2300	-	-	-	-
11	0.140	0.87	0.02838	0.6385	-	-	-	-
12	0.140	0.73	0.03567	0.8026	-	-	-	-
13	0.140	0.40	0.02927	0.6585	-	-	-	-
14	0.140	0.	0.03042	0.6845	-	-	-	-
15	0.140	-0.40	0.02825	0.6355	-	-	-	-
16	0.140	-0.73	0.03691	0.8304	-	-	-	-
17	0.140	-0.87	0.02652	0.5968	-	-	-	-
18	0.140	-0.93	0.01132	0.2548	-	-	-	-
19	0.320	-0.93	0.02730	0.6143	-	-	-	-
20	0.320	-0.87	0.04640	1.0441	-	-	-	-
21	0.320	-0.73	0.05089	1.1451	-	-	-	-
22	0.320	-0.40	0.04336	0.9757	-	-	-	-
23	0.320	0.	0.04487	1.0096	-	-	-	-
24	0.320	0.40	0.04334	0.9751	-	-	-	-
25	0.320	0.73	0.05189	1.1675	-	-	-	-
26	0.320	0.87	0.04716	1.0610	-	-	-	-
27	0.320	0.93	0.00794	0.1785	-	-	-	-
28	0.600	0.93	0.01746	0.3928	-	-	-	-
29	0.600	0.87	0.04452	1.0017	-	-	-	-
30	0.600	0.73	0.05326	1.1984	-	-	-	-
31	0.600	0.40	0.05068	1.1403	-	-	-	-
32	0.600	0.	0.05189	1.1675	-	-	-	-
33	0.600	-0.40	0.04968	1.1179	-	-	-	-
34	0.600	-0.73	0.04850	1.0913	-	-	-	-
35	0.600	-0.87	0.04293	0.9660	-	-	-	-
36	0.600	-0.93	0.01832	0.4122	-	-	-	-
37	0.900	-0.93	0.00726	0.1634	-	-	-	-
38	0.900	-0.87	0.02865	0.6446	-	-	-	-
39	0.900	-0.73	0.04573	1.0289	-	-	-	-
40	0.900	-0.40	0.05332	1.1996	-	-	-	-
41	0.900	0.	0.05461	1.2287	-	-	-	-
42	0.900	0.40	0.05539	1.2462	-	-	-	-
43	0.900	0.73	0.05028	1.1312	-	-	-	-
44	0.900	0.87	0.03411	0.7675	-	-	-	-
45	0.900	0.93	0.01415	0.3184	-	-	-	-

Table 6.14 a). The tangential, vertical and radial mean velocity distribution at section S-1 run no.2 Um = 0.07407 m/s

Loc. no.	η = z/h	2Y/B	Tangential v [m/s]	v/Um	Vertical w [m/s]	w/Um	Radial u [m/s]	u/Um
1	0.044	-0.93	0.02144	0.2894	-	-	-	-
2	0.044	-0.87	0.03666	0.4950	-	-	-	-
3	0.044	-0.73	0.03927	0.5302	-	-	-	-
4	0.044	-0.40	0.03527	0.4761	-	-	-	-
5	0.044	0.	0.03527	0.4761	-	-	-	-
6	0.044	0.40	0.03822	0.5160	-	-	-	-
7	0.044	0.73	0.03779	0.5102	-	-	-	-
8	0.044	0.87	0.03494	0.4717	-	-	-	-
9	0.044	0.93	0.01622	0.2190	-	-	-	-
10	0.078	0.93	0.03024	0.4082	-	-	-	-
11	0.078	0.87	0.05563	0.7510	-	-	-	-
12	0.078	0.73	0.04882	0.6591	-	-	-	-
13	0.078	0.40	0.05436	0.7339	-	-	-	-
14	0.078	0.	0.05221	0.7049	-	-	-	-
15	0.078	-0.40	0.05568	0.7517	-	-	-	-
16	0.078	-0.73	0.06246	0.8432	-	-	-	-
17	0.078	-0.87	0.05923	0.7997	-	-	-	-
18	0.078	-0.93	0.03927	0.5302	-	-	-	-
19	0.178	-0.93	0.05068	0.6842	-	-	-	-
20	0.178	-0.87	0.07190	0.9707	-	-	-	-
21	0.178	-0.73	0.07271	0.9816	-	-	-	-
22	0.178	-0.40	0.07016	0.9471	-	-	-	-
23	0.178	0.	0.06531	0.8817	-	-	-	-
24	0.178	0.40	0.06948	0.9380	-	-	-	-
25	0.178	0.73	0.06615	0.8930	-	-	-	-
26	0.178	0.87	0.06478	0.8745	-	-	-	-
27	0.178	0.93	0.04635	0.6257	-	-	-	-
28	0.422	0.93	0.04517	0.6097	-	-	-	-
29	0.422	0.87	0.06768	0.9137	-	-	-	-
30	0.422	0.73	0.07298	0.9852	-	-	-	-
31	0.422	0.40	0.07828	1.0568	-	-	-	-
32	0.422	0.	0.07241	0.9776	-	-	-	-
33	0.422	-0.40	0.07798	1.0528	-	-	-	-
34	0.422	-0.73	0.07836	1.0579	-	-	-	-
35	0.422	-0.87	0.07379	0.9961	-	-	-	-
36	0.422	-0.93	0.05361	0.7238	-	-	-	-
37	0.667	-0.93	0.04277	0.5774	-	-	-	-
38	0.667	-0.87	0.07231	0.9761	-	-	-	-
39	0.667	-0.73	0.08105	1.0942	-	-	-	-
40	0.667	-0.40	0.07989	1.0786	-	-	-	-
41	0.667	0.	0.07704	1.0401	-	-	-	-
42	0.667	0.40	0.07954	1.0738	-	-	-	-
43	0.667	0.73	0.07363	0.9939	-	-	-	-
44	0.667	0.87	0.06507	0.8785	-	-	-	-
45	0.667	0.93	0.02429	0.3279	-	-	-	-
46	0.911	0.93	0.04511	0.6090	-	-	-	-
47	0.911	0.87	0.06114	0.8254	-	-	-	-
48	0.911	0.73	0.06894	0.9308	-	-	-	-
49	0.911	0.40	0.08326	1.1239	-	-	-	-
50	0.911	0.	0.07984	1.0778	-	-	-	-
51	0.911	-0.40	0.08100	1.0934	-	-	-	-
52	0.911	-0.73	0.07486	1.0106	-	-	-	-
53	0.911	-0.87	0.06760	0.9126	-	-	-	-
54	0.911	-0.93	0.02217	0.2992	-	-	-	-

Table 6.15 a). The tangential, vertical and radial mean velocity distribution at section S-1 run no.3 Um = 0.09259 m/s

Loc. no.	η = z/h	2Y/B	Tangential v [m/s]	Tangential v/Um	Vertical w [m/s]	Vertical w/Um	Radial u [m/s]	Radial u/Um
1	0.033	-0.93	0.02843	0.3071	-	-	-	-
2	0.033	-0.87	0.05240	0.5659	-	-	-	-
3	0.033	-0.73	0.05436	0.5871	-	-	-	-
4	0.033	-0.40	0.05388	0.5819	-	-	-	-
5	0.033	0.	0.05146	0.5558	-	-	-	-
6	0.033	0.40	0.04823	0.5209	-	-	-	-
7	0.033	0.73	0.05173	0.5587	-	-	-	-
8	0.033	0.87	0.04473	0.4831	-	-	-	-
9	0.033	0.93	0.02375	0.2565	-	-	-	-
10	0.058	0.93	0.04783	0.5165	-	-	-	-
11	0.058	0.87	0.06760	0.7301	-	-	-	-
12	0.058	0.73	0.06736	0.7275	-	-	-	-
13	0.058	0.40	0.07083	0.7649	-	-	-	-
14	0.058	0.	0.06491	0.7010	-	-	-	-
15	0.058	-0.40	0.06841	0.7388	-	-	-	-
16	0.058	-0.73	0.07567	0.8172	-	-	-	-
17	0.058	-0.87	0.07217	0.7795	-	-	-	-
18	0.058	-0.93	0.05407	0.5839	-	-	-	-
19	0.133	-0.93	0.06410	0.6923	-	-	-	-
20	0.133	-0.87	0.08293	0.8957	-	-	-	-
21	0.133	-0.73	0.09356	1.0104	-	-	-	-
22	0.133	-0.40	0.09646	1.0418	-	-	-	-
23	0.133	0.	0.08834	0.9541	-	-	-	-
24	0.133	0.40	0.09321	1.0067	-	-	-	-
25	0.133	0.73	0.08993	0.9712	-	-	-	-
26	0.133	0.87	0.08430	0.9105	-	-	-	-
27	0.133	0.93	0.06478	0.6996	-	-	-	-
28	0.400	0.93	0.06639	0.7170	-	-	-	-
29	0.400	0.87	0.08118	0.8768	-	-	-	-
30	0.400	0.73	0.08880	0.9590	-	-	-	-
31	0.400	0.40	0.09813	1.0598	-	-	-	-
32	0.400	0.	0.09194	0.9930	-	-	-	-
33	0.400	-0.40	0.09773	1.0555	-	-	-	-
34	0.400	-0.73	0.09792	1.0575	-	-	-	-
35	0.400	-0.87	0.09108	0.9837	-	-	-	-
36	0.400	-0.93	0.07443	0.8039	-	-	-	-
37	0.667	-0.93	0.08051	0.8695	-	-	-	-
38	0.667	-0.87	0.09762	1.0543	-	-	-	-
39	0.667	-0.73	0.10069	1.0874	-	-	-	-
40	0.667	-0.40	0.09832	1.0619	-	-	-	-
41	0.667	0.	0.09496	1.0255	-	-	-	-
42	0.667	0.40	0.09864	1.0653	-	-	-	-
43	0.667	0.73	0.09402	1.0154	-	-	-	-
44	0.667	0.87	0.08374	0.9044	-	-	-	-
45	0.667	0.93	0.06257	0.6757	-	-	-	-
46	0.933	0.93	0.05773	0.6235	-	-	-	-
47	0.933	0.87	0.08113	0.8762	-	-	-	-
48	0.933	0.73	0.09046	0.9770	-	-	-	-
49	0.933	0.40	0.10219	1.1037	-	-	-	-
50	0.933	0.	0.10028	1.0831	-	-	-	-
51	0.933	-0.40	0.09859	1.0648	-	-	-	-
52	0.933	-0.73	0.09746	1.0526	-	-	-	-
53	0.933	-0.87	0.08777	0.9480	-	-	-	-
54	0.933	-0.93	0.06440	0.6955	-	-	-	-

Table 6.16 a). The tangential, vertical and radial mean velocity distribution at section S-2 run no.1 Um = 0.04444 m/s

Loc. no.	η = z/h	2Y/B	Tangential v [m/s]	Tangential v/Um	Vertical w [m/s]	Vertical w/Um	Radial u [m/s]	Radial u/Um
1	0.080	-0.93	0.00785	0.1767	-	-	-	-
2	0.080	-0.87	0.01159	0.2609	-	-	-	-
3	0.080	-0.73	0.01650	0.3711	-	-	-	-
4	0.080	-0.40	0.02229	0.5016	-	-	-	-
5	0.080	0.	0.02835	0.6379	-	-	-	-
6	0.080	0.40	0.02535	0.5703	-	-	-	-
7	0.080	0.73	0.02229	0.5016	-	-	-	-
8	0.080	0.87	0.02667	0.6000	-	-	-	-
9	0.080	0.93	0.01913	0.4304	-	-	-	-
10	0.140	0.93	0.03800	0.8549	-	-	-0.00469	-0.1055
11	0.140	0.87	0.04227	0.9510	-	-	-0.00432	-0.0972
12	0.140	0.73	0.03599	0.8099	-	-	-0.00527	-0.1186
13	0.140	0.40	0.04469	1.0055	-	-	-0.00812	-0.1826
14	0.140	0.	0.04232	0.9522	-	-	-0.00980	-0.2205
15	0.140	-0.40	0.03283	0.7387	-	-	-0.01091	-0.2455
16	0.140	-0.73	0.02466	0.5549	-	-	-0.00596	-0.1340
17	0.140	-0.87	0.02071	0.4660	-	-	-0.00295	-0.0664
18	0.140	-0.93	0.01075	0.2419	-	-	-0.00353	-0.0794
19	0.320	-0.93	0.01339	0.3012	0.00069	0.0154	-0.00169	-0.0379
20	0.320	-0.87	0.02788	0.6273	0.00016	0.0036	-0.00327	-0.0735
21	0.320	-0.73	0.03109	0.6996	0.00011	0.0024	-0.00516	-0.1162
22	0.320	-0.40	0.04353	0.9794	0.00005	0.0012	-0.00395	-0.0889
23	0.320	0.	0.05281	1.1881	-0.00037	-0.0083	-0.00374	-0.0842
24	0.320	0.40	0.05476	1.2320	-0.00126	-0.0285	-0.00327	-0.0735
25	0.320	0.73	0.05033	1.1324	-0.00153	-0.0344	0.00005	0.0012
26	0.320	0.87	0.04769	1.0731	-0.00163	-0.0368	0.00069	0.0154
27	0.320	0.93	0.03605	0.8111	-0.00211	-0.0474	0.00206	0.0462
28	0.600	0.93	0.04000	0.9000	-0.00221	-0.0498	0.00100	0.0225
29	0.600	0.87	0.04912	1.1051	-0.00190	-0.0427	0.00095	0.0213
30	0.600	0.73	0.05086	1.1442	-0.00184	-0.0415	0.00095	0.0213
31	0.600	0.40	0.05523	1.2427	-0.00137	-0.0308	-0.00011	-0.0024
32	0.600	0.	0.05128	1.1537	-0.00032	-0.0071	0.00142	0.0320
33	0.600	-0.40	0.03937	0.8858	0.00069	0.0154	0.00158	0.0356
34	0.600	-0.73	0.03246	0.7304	0.00121	0.0273	-0.00090	-0.0202
35	0.600	-0.87	0.03046	0.6854	0.00105	0.0237	-0.00116	-0.0261
36	0.600	-0.93	0.01913	0.4304	0.00148	0.0332	-0.00100	-0.0225
37	0.900	-0.93	0.01202	0.2704	0.	0.	-0.00084	-0.0190
38	0.900	-0.87	0.02408	0.5419	0.00005	0.0012	-0.00005	-0.0012
39	0.900	-0.73	0.02946	0.6628	0.00005	0.0012	0.00042	0.0095
40	0.900	-0.40	0.03357	0.7553	0.	0.	0.00069	0.0154
41	0.900	0.	0.05059	1.1383	-0.00063	-0.0142	0.00406	0.0913
42	0.900	0.40	0.05512	1.2403	-0.00111	-0.0249	0.00111	0.0249
43	0.900	0.73	0.04949	1.1134	-0.00169	-0.0379	-0.00264	-0.0593
44	0.900	0.87	0.04211	0.9474	-0.00274	-0.0617	-0.00469	-0.1055
45	0.900	0.93	0.02704	0.6083	-0.00348	-0.0783	-0.00511	-0.1150

Table 6.17 a). The tangential, vertical and radial mean velocity distribution at section S-2 run no.2 Um = 0.07407 m/s

Loc. no.	η = z/h	2Y/B	Tangential v [m/s]	Tangential v/Um	Vertical w [m/s]	Vertical w/Um	Radial u [m/s]	Radial u/Um
1	0.044	−0.93	0.01702	0.2298	–	–	–	–
2	0.044	−0.87	0.02598	0.3507	–	–	–	–
3	0.044	−0.73	0.03267	0.4411	–	–	–	–
4	0.044	−0.40	0.04543	0.6133	–	–	–	–
5	0.044	0.	0.04495	0.6069	–	–	–	–
6	0.044	0.40	0.04337	0.5855	–	–	–	–
7	0.044	0.73	0.04812	0.6496	–	–	–	–
8	0.044	0.87	0.04232	0.5713	–	–	–	–
9	0.044	0.93	0.03389	0.4575	–	–	–	–
10	0.078	0.93	0.04822	0.6510	–	–	–	–
11	0.078	0.87	0.06313	0.8523	–	–	–	–
12	0.078	0.73	0.06572	0.8872	–	–	–	–
13	0.078	0.40	0.06551	0.8843	–	–	–	–
14	0.078	0.	0.06530	0.8815	–	–	–	–
15	0.078	−0.40	0.06287	0.8488	–	–	–	–
16	0.078	−0.73	0.04812	0.6496	–	–	–	–
17	0.078	−0.87	0.03468	0.4681	–	–	–	–
18	0.078	−0.93	0.02419	0.3266	–	–	–	–
19	0.178	−0.93	0.03995	0.5393	0.00290	0.0391	−0.00458	−0.0619
20	0.178	−0.87	0.05022	0.6780	0.00522	0.0704	−0.01170	−0.1579
21	0.178	−0.73	0.06377	0.8609	0.00158	0.0213	−0.01038	−0.1402
22	0.178	−0.40	0.07641	1.0316	−0.00063	−0.0085	−0.00996	−0.1345
23	0.178	0.	0.07742	1.0451	−0.00116	−0.0157	−0.00912	−0.1231
24	0.178	0.40	0.07974	1.0764	−0.00158	−0.0213	−0.00764	−0.1032
25	0.178	0.73	0.07515	1.0145	−0.00248	−0.0334	−0.00580	−0.0783
26	0.178	0.87	0.07341	0.9910	−0.00395	−0.0534	−0.00300	−0.0406
27	0.178	0.93	0.05497	0.7420	−0.00274	−0.0370	−0.00211	−0.0285
28	0.422	0.93	0.05918	0.7990	−0.00053	−0.0071	−0.00100	−0.0135
29	0.422	0.87	0.07605	1.0266	−0.00053	−0.0071	0.00016	0.0021
30	0.422	0.73	0.07657	1.0337	−0.00295	−0.0398	0.00016	0.0021
31	0.422	0.40	0.08105	1.0942	−0.00242	−0.0327	0.00026	0.0036
32	0.422	0.	0.07989	1.0786	−0.00095	−0.0128	0.00069	0.0092
33	0.422	−0.40	0.07736	1.0444	0.	0.	0.00174	0.0235
34	0.422	−0.73	0.06656	0.8986	0.00148	0.0199	−0.00069	−0.0092
35	0.422	−0.87	0.05976	0.8068	0.00696	0.0939	−0.00369	−0.0498
36	0.422	−0.93	0.04796	0.6474	0.00759	0.1024	−0.00232	−0.0313
37	0.667	−0.93	0.04548	0.6140	0.00780	0.1053	0.00311	0.0420
38	0.667	−0.87	0.05723	0.7726	0.00701	0.0946	0.00316	0.0427
39	0.667	−0.73	0.05992	0.8089	0.00195	0.0263	0.00406	0.0548
40	0.667	−0.40	0.07130	0.9626	−0.00063	−0.0085	0.00464	0.0626
41	0.667	0.	0.08232	1.1113	−0.00126	−0.0171	0.00611	0.0825
42	0.667	0.40	0.07995	1.0793	−0.00390	−0.0526	0.00232	0.0313
43	0.667	0.73	0.07394	0.9982	−0.00174	−0.0235	−0.00037	−0.0050
44	0.667	0.87	0.07151	0.9654	−0.00195	−0.0263	0.00221	0.0299
45	0.667	0.93	0.04548	0.6140	−0.00158	−0.0213	0.00248	0.0334
46	0.911	0.93	0.04158	0.5613	–	–	−0.00300	−0.0406
47	0.911	0.87	0.06166	0.8324	–	–	−0.00390	−0.0526
48	0.911	0.73	0.06761	0.9128	–	–	−0.00274	−0.0370
49	0.911	0.40	0.08221	1.1099	–	–	0.00490	0.0662
50	0.911	0.	0.08205	1.1077	–	–	0.00764	0.1032
51	0.911	−0.40	0.06166	0.8324	–	–	0.00643	0.0868
52	0.911	−0.73	0.04943	0.6673	–	–	0.00690	0.0932
53	0.911	−0.87	0.04258	0.5749	–	–	0.00416	0.0562
54	0.911	−0.93	0.02993	0.4041	–	–	0.00121	0.0164

Table 6.18 a). The tangential, vertical and radial mean velocity distribution at section S-2 run no.3 Um = 0.09259 m/s

Loc. no.	η = z/h	2Y/B	Tangential v [m/s]	Tangential v/Um	Vertical w [m/s]	Vertical w/Um	Radial u [m/s]	Radial u/Um
1	0.033	−0.93	0.01286	0.1389	–	–	–	–
2	0.033	−0.87	0.03252	0.3512	–	–	–	–
3	0.033	−0.73	0.04248	0.4587	–	–	–	–
4	0.033	−0.40	0.05460	0.5896	–	–	–	–
5	0.033	0.	0.05444	0.5879	–	–	–	–
6	0.033	0.40	0.05238	0.5657	–	–	–	–
7	0.033	0.73	0.05075	0.5481	–	–	–	–
8	0.033	0.87	0.05391	0.5823	–	–	–	–
9	0.033	0.93	0.02899	0.3130	–	–	–	–
10	0.058	0.93	0.06129	0.6619	–	–	–	–
11	0.058	0.87	0.07199	0.7775	–	–	–	–
12	0.058	0.73	0.07136	0.7706	–	–	–	–
13	0.058	0.40	0.07262	0.7843	–	–	–	–
14	0.058	0.	0.07736	0.8355	–	–	–	–
15	0.058	−0.40	0.07447	0.8042	–	–	–	–
16	0.058	−0.73	0.06461	0.6978	–	–	–	–
17	0.058	−0.87	0.04285	0.4627	–	–	–	–
18	0.058	−0.93	0.02909	0.3142	–	–	–	–
19	0.133	−0.93	0.05075	0.5481	0.00769	0.0831	−0.00859	−0.0928
20	0.133	−0.87	0.06498	0.7018	0.00748	0.0808	−0.01249	−0.1349
21	0.133	−0.73	0.08458	0.9135	0.00358	0.0387	−0.01354	−0.1463
22	0.133	−0.40	0.09238	0.9977	−0.00016	−0.0017	−0.01170	−0.1264
23	0.133	0.	0.09259	1.0000	−0.00137	−0.0148	−0.01038	−0.1121
24	0.133	0.40	0.08922	0.9636	−0.00184	−0.0199	−0.00912	−0.0985
25	0.133	0.73	0.08374	0.9044	−0.00300	−0.0324	−0.00290	−0.0313
26	0.133	0.87	0.07831	0.8458	−0.00464	−0.0501	−0.00132	−0.0142
27	0.133	0.93	0.05444	0.5879	−0.00353	−0.0381	−0.00037	−0.0040
28	0.400	0.93	0.06867	0.7416	−0.00264	−0.0285	−0.00026	−0.0028
29	0.400	0.87	0.08221	0.8879	−0.00569	−0.0615	0.00005	0.0006
30	0.400	0.73	0.08738	0.9437	−0.00379	−0.0410	0.00211	0.0228
31	0.400	0.40	0.09713	1.0490	−0.00327	−0.0353	−0.00126	−0.0137
32	0.400	0.	0.09755	1.0535	−0.00132	−0.0142	0.00011	0.0011
33	0.400	−0.40	0.10097	1.0905	0.	0.	−0.00021	−0.0023
34	0.400	−0.73	0.08801	0.9505	0.00300	0.0324	−0.00174	−0.0188
35	0.400	−0.87	0.07863	0.8492	0.00838	0.0905	−0.00084	−0.0091
36	0.400	−0.93	0.05786	0.6249	0.01470	0.1588	−0.00053	−0.0057
37	0.667	−0.93	0.04980	0.5379	0.01386	0.1497	0.00416	0.0450
38	0.667	−0.87	0.07078	0.7644	0.01049	0.1133	−0.00090	−0.0097
39	0.667	−0.73	0.07931	0.8566	0.00290	0.0313	0.00074	0.0080
40	0.667	−0.40	0.09581	1.0347	−0.00211	−0.0228	0.00464	0.0501
41	0.667	0.	0.10261	1.1082	−0.00105	−0.0114	0.00596	0.0643
42	0.667	0.40	0.10029	1.0831	−0.00532	−0.0575	0.00285	0.0307
43	0.667	0.73	0.08722	0.9420	−0.00348	−0.0376	0.00190	0.0205
44	0.667	0.87	0.08395	0.9067	−0.00090	−0.0097	0.00279	0.0302
45	0.667	0.93	0.06514	0.7035	−0.00090	−0.0097	0.00206	0.0222
46	0.933	0.93	0.04891	0.5282	–	–	−0.00300	−0.0324
47	0.933	0.87	0.07441	0.8037	–	–	−0.00416	−0.0450
48	0.933	0.73	0.08290	0.8953	–	–	−0.00211	−0.0228
49	0.933	0.40	0.09555	1.0319	–	–	0.00511	0.0552
50	0.933	0.	0.10255	1.1076	–	–	0.01059	0.1144
51	0.933	−0.40	0.08501	0.9181	–	–	0.00506	0.0546
52	0.933	−0.73	0.05908	0.6380	–	–	0.00385	0.0415
53	0.933	−0.87	0.05597	0.6044	–	–	0.00295	0.0319
54	0.933	−0.93	0.03299	0.3563	–	–	−0.00126	−0.0137

Table 6.19 a). The tangential, vertical and radial mean velocity distribution at section S-3 run no.1 Um = 0.04444 m/s

Loc. no.	η = z/h	2Y/B	Tangential v [m/s]	Tangential v/Um	Vertical w [m/s]	Vertical w/Um	Radial u [m/s]	Radial u/Um
1	0.080	-0.93	0.00258	0.0581	-	-	-	-
2	0.080	-0.87	0.00675	0.1518	-	-	-	-
3	0.080	-0.73	0.01349	0.3036	-	-	-	-
4	0.080	-0.40	0.01597	0.3593	-	-	-	-
5	0.080	0.	0.02076	0.4672	-	-	-	-
6	0.080	0.40	0.02651	0.5964	-	-	-	-
7	0.080	0.73	0.02877	0.6474	-	-	-	-
8	0.080	0.87	0.03020	0.6794	-	-	-	-
9	0.080	0.93	0.02408	0.5419	-	-	-	-
10	0.140	0.93	0.04432	0.9972	-	-	-0.00126	-0.0285
11	0.140	0.87	0.05028	1.1312	-	-	-0.00216	-0.0486
12	0.140	0.73	0.04759	1.0707	-	-	-0.00358	-0.0806
13	0.140	0.40	0.04443	0.9996	-	-	-0.00443	-0.0996
14	0.140	0.	0.03389	0.7624	-	-	-0.00495	-0.1115
15	0.140	-0.40	0.02704	0.6083	-	-	-0.00548	-0.1233
16	0.140	-0.73	0.01860	0.4186	-	-	-0.00432	-0.0972
17	0.140	-0.87	0.01170	0.2632	-	-	-0.00248	-0.0557
18	0.140	-0.93	0.00680	0.1530	-	-	-0.00148	-0.0332
19	0.320	-0.93	0.01491	0.3356	0.00132	0.0296	-0.00153	-0.0344
20	0.320	-0.87	0.02461	0.5537	0.00074	0.0166	-0.00158	-0.0356
21	0.320	-0.73	0.03025	0.6806	0.00037	0.0083	-0.00126	-0.0285
22	0.320	-0.40	0.04221	0.9498	-0.00021	-0.0047	-0.00005	-0.0012
23	0.320	0.	0.04991	1.1229	-0.00084	-0.0190	-0.00026	-0.0059
24	0.320	0.40	0.05655	1.2723	-0.00111	-0.0249	-0.00058	-0.0130
25	0.320	0.73	0.06039	1.3589	-0.00137	-0.0308	-0.00047	-0.0107
26	0.320	0.87	0.06018	1.3541	-0.00105	-0.0237	-0.00063	-0.0142
27	0.320	0.93	0.05354	1.2047	-0.00158	-0.0356	0.	0.
28	0.600	0.93	0.05444	1.2249	0.00084	0.0190	0.00074	0.0166
29	0.600	0.87	0.05866	1.3197	-0.00100	-0.0225	0.00069	0.0154
30	0.600	0.73	0.05881	1.3233	-0.00153	-0.0344	-0.00005	-0.0012
31	0.600	0.40	0.05576	1.2545	-0.00111	-0.0249	0.00053	0.0119
32	0.600	0.	0.04474	1.0067	-0.00037	-0.0083	0.00153	0.0344
33	0.600	-0.40	0.03341	0.7518	-0.00105	-0.0237	0.00232	0.0522
34	0.600	-0.73	0.02835	0.6379	0.00047	0.0107	0.00121	0.0273
35	0.600	-0.87	0.02182	0.4909	0.00069	0.0154	0.00047	0.0107
36	0.600	-0.93	0.01839	0.4138	0.00121	0.0273	-0.00005	-0.0012
37	0.900	-0.93	0.01244	0.2798	0.00069	0.0154	-0.00032	-0.0071
38	0.900	-0.87	0.01465	0.3296	0.00005	0.0012	0.00032	0.0071
39	0.900	-0.73	0.02187	0.4921	-0.00053	-0.0119	0.00248	0.0557
40	0.900	-0.40	0.03104	0.6984	-0.00042	-0.0095	-0.00016	-0.0036
41	0.900	0.	0.04574	1.0292	-0.00074	-0.0166	0.	0.
42	0.900	0.40	0.05681	1.2782	-0.00079	-0.0178	0.00037	0.0083
43	0.900	0.73	0.05518	1.2415	-0.00090	-0.0202	-0.00321	-0.0723
44	0.900	0.87	0.05476	1.2320	-0.00100	-0.0225	-0.00664	-0.1494
45	0.900	0.93	0.04885	1.0992	-0.00116	-0.0261	-0.00522	-0.1174

Table 6.20 a). The tangential, vertical and radial mean velocity distribution at section S-3 run no.2 Um = 0.07407 m/s

Loc. no.	η = z/h	2Y/B	Tangential v [m/s]	Tangential v/Um	Vertical w [m/s]	Vertical w/Um	Radial u [m/s]	Radial u/Um
1	0.044	-0.93	0.01075	0.1451	-	-	-	-
2	0.044	-0.87	0.02145	0.2896	-	-	-	-
3	0.044	-0.73	0.03046	0.4112	-	-	-	-
4	0.044	-0.40	0.03789	0.5115	-	-	-	-
5	0.044	0.	0.04079	0.5507	-	-	-	-
6	0.044	0.40	0.04400	0.5941	-	-	-	-
7	0.044	0.73	0.04437	0.5990	-	-	-	-
8	0.044	0.87	0.04985	0.6730	-	-	-	-
9	0.044	0.93	0.03046	0.4112	-	-	-	-
10	0.078	0.93	0.06645	0.8971	-	-	-	-
11	0.078	0.87	0.08358	1.1284	-	-	-	-
12	0.078	0.73	0.08000	1.0800	-	-	-	-
13	0.078	0.40	0.07104	0.9590	-	-	-	-
14	0.078	0.	0.06287	0.8488	-	-	-	-
15	0.078	-0.40	0.05686	0.7677	-	-	-	-
16	0.078	-0.73	0.05017	0.6773	-	-	-	-
17	0.078	-0.87	0.03462	0.4674	-	-	-	-
18	0.078	-0.93	0.02630	0.3550	-	-	-	-
19	0.178	-0.93	0.03963	0.5350	0.00401	0.0541	-0.00311	-0.0420
20	0.178	-0.87	0.05286	0.7136	0.00327	0.0441	-0.00469	-0.0633
21	0.178	-0.73	0.06103	0.8239	0.00116	0.0157	-0.00379	-0.0512
22	0.178	-0.40	0.06777	0.9149	-0.00037	-0.0050	-0.00327	-0.0441
23	0.178	0.	0.07699	1.0394	-0.00137	-0.0185	-0.00596	-0.0804
24	0.178	0.40	0.08501	1.1476	-0.00163	-0.0221	-0.00406	-0.0548
25	0.178	0.73	0.08775	1.1846	-0.00126	-0.0171	-0.00011	-0.0014
26	0.178	0.87	0.08959	1.2095	-0.00195	-0.0263	-0.00063	-0.0085
27	0.178	0.93	0.07215	0.9740	-0.00274	-0.0370	-0.00174	-0.0235
28	0.422	0.93	0.07352	0.9925	0.00105	0.0142	0.00021	0.0028
29	0.422	0.87	0.08854	1.1952	0.00074	0.0100	0.00132	0.0178
30	0.422	0.73	0.08727	1.1782	-0.00058	-0.0078	0.00174	0.0235
31	0.422	0.40	0.08501	1.1476	-0.00264	-0.0356	0.00095	0.0128
32	0.422	0.	0.07641	1.0316	-0.00153	-0.0206	-0.00063	-0.0085
33	0.422	-0.40	0.06508	0.8786	-0.00116	-0.0157	0.	0.
34	0.422	-0.73	0.05402	0.7292	0.00100	0.0135	-0.00126	-0.0171
35	0.422	-0.87	0.05133	0.6930	0.00348	0.0470	-0.00227	-0.0306
36	0.422	-0.93	0.03926	0.5300	0.00585	0.0790	-0.00153	-0.0206
37	0.667	-0.93	0.02614	0.3529	0.00253	0.0341	0.00032	0.0043
38	0.667	-0.87	0.03847	0.5194	0.00364	0.0491	0.00153	0.0206
39	0.667	-0.73	0.04801	0.6481	-0.00005	-0.0007	-0.00063	-0.0085
40	0.667	-0.40	0.06271	0.8466	-0.00142	-0.0192	0.00084	0.0114
41	0.667	0.	0.07589	1.0245	-0.00105	-0.0142	0.00174	0.0235
42	0.667	0.40	0.08606	1.1618	-0.00290	-0.0391	-0.00016	-0.0021
43	0.667	0.73	0.08590	1.1597	-0.00184	-0.0249	-0.00343	-0.0462
44	0.667	0.87	0.08701	1.1746	0.00184	0.0249	-0.00232	-0.0313
45	0.667	0.93	0.07188	0.9704	0.00327	0.0441	-0.00248	-0.0334
46	0.911	0.93	0.06097	0.8231	-	-	-0.00701	-0.0946
47	0.911	0.87	0.08089	1.0921	-	-	-0.00975	-0.1316
48	0.911	0.73	0.08553	1.1547	-	-	-0.00464	-0.0626
49	0.911	0.40	0.08606	1.1618	-	-	-0.00295	-0.0398
50	0.911	0.	0.08068	1.0892	-	-	0.00190	0.0256
51	0.911	-0.40	0.06393	0.8630	-	-	0.00179	0.0242
52	0.911	-0.73	0.04685	0.6325	-	-	0.00279	0.0377
53	0.911	-0.87	0.03468	0.4681	-	-	0.00253	0.0341
54	0.911	-0.93	0.02598	0.3507	-	-	-0.00079	-0.0107

Table 6.21 a). The tangential, vertical and radial mean velocity distribution at section S-3 run no.3 Um = 0.09259 m/s

Loc. no.	η = z/h	2Y/B	Tangential v [m/s]	Tangential v/Um	Vertical w [m/s]	Vertical w/Um	Radial u [m/s]	Radial u/Um
1	0.033	-0.93	0.02783	0.3005	-	-	-	-
2	0.033	-0.87	0.03889	0.4200	-	-	-	-
3	0.033	-0.73	0.04543	0.4906	-	-	-	-
4	0.033	-0.40	0.05460	0.5896	-	-	-	-
5	0.033	0.	0.05618	0.6067	-	-	-	-
6	0.033	0.40	0.05755	0.6215	-	-	-	-
7	0.033	0.73	0.06999	0.7558	-	-	-	-
8	0.033	0.87	0.06946	0.7502	-	-	-	-
9	0.033	0.93	0.05760	0.6221	-	-	-	-
10	0.058	0.93	0.07815	0.8441	-	-	-	-
11	0.058	0.87	0.09855	1.0643	-	-	-	-
12	0.058	0.73	0.09460	1.0216	-	-	-	-
13	0.058	0.40	0.08975	0.9693	-	-	-	-
14	0.058	0.	0.08263	0.8924	-	-	-	-
15	0.058	-0.40	0.06956	0.7513	-	-	-	-
16	0.058	-0.73	0.06630	0.7160	-	-	-	-
17	0.058	-0.87	0.05797	0.6261	-	-	-	-
18	0.058	-0.93	0.04184	0.4519	-	-	-	-
19	0.133	-0.93	0.04269	0.4610	0.00527	0.0569	0.00090	0.0097
20	0.133	-0.87	0.06587	0.7114	0.00295	0.0319	0.00153	0.0165
21	0.133	-0.73	0.07947	0.8583	0.00126	0.0137	-0.00385	-0.0415
22	0.133	-0.40	0.08379	0.9050	0.	0.	-0.00300	-0.0324
23	0.133	0.	0.09302	1.0046	-0.00105	-0.0114	-0.00248	-0.0268
24	0.133	0.40	0.09834	1.0621	-0.00158	-0.0171	-0.00142	-0.0154
25	0.133	0.73	0.10329	1.1156	-0.00211	-0.0228	-0.00200	-0.0216
26	0.133	0.87	0.10134	1.0945	-0.00253	-0.0273	-0.00011	-0.0011
27	0.133	0.93	0.08553	0.9237	-0.00316	-0.0341	-0.00179	-0.0194
28	0.400	0.93	0.08000	0.8640	0.00026	0.0028	-0.00084	-0.0091
29	0.400	0.87	0.10371	1.1201	0.00137	0.0148	0.00095	0.0102
30	0.400	0.73	0.10303	1.1127	-0.00058	-0.0063	0.00332	0.0359
31	0.400	0.40	0.09987	1.0786	-0.00232	-0.0250	0.00269	0.0290
32	0.400	0.	0.09475	1.0233	-0.00221	-0.0239	0.00190	0.0205
33	0.400	-0.40	0.08627	0.9317	-0.00158	-0.0171	0.00095	0.0102
34	0.400	-0.73	0.07689	0.8304	-0.00047	-0.0051	0.00074	0.0080
35	0.400	-0.87	0.06941	0.7496	0.00337	0.0364	-0.00053	-0.0057
36	0.400	-0.93	0.04669	0.5043	0.00701	0.0757	-0.00021	-0.0023
37	0.667	-0.93	0.03652	0.3944	0.00190	0.0205	0.00053	0.0057
38	0.667	-0.87	0.05497	0.5936	0.00606	0.0655	0.00227	0.0245
39	0.667	-0.73	0.06192	0.6688	0.00100	0.0108	0.00232	0.0250
40	0.667	-0.40	0.07979	0.8617	-0.00237	-0.0256	-0.00026	-0.0028
41	0.667	0.	0.09797	1.0581	-0.00116	-0.0125	0.00042	0.0046
42	0.667	0.40	0.10414	1.1247	-0.00364	-0.0393	0.00121	0.0131
43	0.667	0.73	0.10361	1.1190	0.00274	0.0296	-0.00053	-0.0057
44	0.667	0.87	0.10161	1.0973	0.00295	0.0319	-0.00105	-0.0114
45	0.667	0.93	0.07905	0.8537	0.00653	0.0706	-0.00300	-0.0324
46	0.933	0.93	0.07389	0.7980	-	-	-0.00632	-0.0683
47	0.933	0.87	0.09217	0.9955	-	-	-0.00928	-0.1002
48	0.933	0.73	0.09523	1.0285	-	-	-0.00943	-0.1019
49	0.933	0.40	0.09966	1.0763	-	-	-0.00311	-0.0336
50	0.933	0.	0.10082	1.0888	-	-	-0.00148	-0.0159
51	0.933	-0.40	0.08511	0.9192	-	-	0.00053	0.0057
52	0.933	-0.73	0.06356	0.6864	-	-	0.00227	0.0245
53	0.933	-0.87	0.05892	0.6363	-	-	0.00032	0.0034
54	0.933	-0.93	0.04564	0.4929	-	-	-0.00053	-0.0057

Table 6.22 a). The tangential, vertical and radial mean velocity distribution at section S-4 run no.1 Um = 0.04444 m/s

Loc. no.	η = z/h	2Y/B	Tangential v [m/s]	Tangential v/Um	Vertical w [m/s]	Vertical w/Um	Radial u [m/s]	Radial u/Um
1	0.080	-0.93	0.00812	0.1826	-	-	-	-
2	0.080	-0.87	0.01228	0.2763	-	-	-	-
3	0.080	-0.73	0.01792	0.4032	-	-	-	-
4	0.080	-0.40	0.02034	0.4577	-	-	-	-
5	0.080	0.	0.02419	0.5443	-	-	-	-
6	0.080	0.40	0.02809	0.6320	-	-	-	-
7	0.080	0.73	0.03167	0.7126	-	-	-	-
8	0.080	0.87	0.03810	0.8573	-	-	-	-
9	0.080	0.93	0.03362	0.7565	-	-	-	-
10	0.140	0.93	0.04527	1.0186	-	-	-0.00037	-0.0083
11	0.140	0.87	0.05470	1.2308	-	-	-0.00142	-0.0320
12	0.140	0.73	0.05091	1.1454	-	-	-0.00195	-0.0439
13	0.140	0.40	0.04601	1.0352	-	-	-0.00174	-0.0391
14	0.140	0.	0.03831	0.8620	-	-	-0.00332	-0.0747
15	0.140	-0.40	0.03099	0.6972	-	-	-0.00321	-0.0723
16	0.140	-0.73	0.02651	0.5964	-	-	-0.00300	-0.0676
17	0.140	-0.87	0.01897	0.4269	-	-	-0.00221	-0.0498
18	0.140	-0.93	0.01375	0.3095	-	-	-0.00184	-0.0415
19	0.320	-0.93	0.02103	0.4731	0.00100	0.0225	-0.00079	-0.0178
20	0.320	-0.87	0.02698	0.6071	0.00126	0.0285	-0.00084	-0.0190
21	0.320	-0.73	0.03499	0.7873	0.00026	0.0059	-0.00153	-0.0344
22	0.320	-0.40	0.04237	0.9533	0.00032	0.0071	-0.00200	-0.0451
23	0.320	0.	0.05091	1.1454	0.00026	0.0059	-0.00037	-0.0083
24	0.320	0.40	0.05929	1.3340	-0.00037	-0.0083	-0.00090	-0.0202
25	0.320	0.73	0.06371	1.4336	-0.00058	-0.0130	0.00142	0.0320
26	0.320	0.87	0.06377	1.4348	0.	0.	0.00137	0.0308
27	0.320	0.93	0.04669	1.0506	-0.00037	-0.0083	0.00132	0.0296
28	0.600	0.93	0.05428	1.2213	0.00132	0.0296	0.00005	0.0012
29	0.600	0.87	0.06166	1.3873	-0.00116	-0.0261	0.00011	0.0024
30	0.600	0.73	0.06161	1.3861	-0.00121	-0.0273	0.00063	0.0142
31	0.600	0.40	0.05649	1.2711	-0.00047	-0.0107	0.00021	0.0047
32	0.600	0.	0.04653	1.0470	-0.00005	-0.0012	0.00079	0.0178
33	0.600	-0.40	0.03800	0.8549	-0.00021	-0.0047	0.00005	0.0012
34	0.600	-0.73	0.03178	0.7150	0.00026	0.0059	0.00058	0.0130
35	0.600	-0.87	0.02756	0.6201	0.00095	0.0213	0.00063	0.0142
36	0.600	-0.93	0.02192	0.4933	0.00211	0.0474	-0.00053	-0.0119
37	0.900	-0.93	0.01628	0.3664	0.00021	0.0047	-0.00111	-0.0249
38	0.900	-0.87	0.02045	0.4601	0.00016	0.0036	0.00016	0.0036
39	0.900	-0.73	0.02767	0.6225	-0.00053	-0.0119	0.00032	0.0071
40	0.900	-0.40	0.03636	0.8182	-0.00026	-0.0059	-0.00084	-0.0190
41	0.900	0.	0.04801	1.0802	-0.00021	-0.0047	0.00032	0.0071
42	0.900	0.40	0.05860	1.3186	-0.00032	-0.0071	0.00069	0.0154
43	0.900	0.73	0.05992	1.3482	-0.00063	-0.0142	-0.00190	-0.0427
44	0.900	0.87	0.05813	1.3079	-0.00100	-0.0225	-0.00269	-0.0605
45	0.900	0.93	0.05254	1.1822	-0.00195	-0.0439	-0.00369	-0.0830

Table 6.23 a). The tangential, vertical and radial mean velocity distribution at section S-4 run no.2 Um = 0.07407 m/s

Loc. no.	η = z/h	2Y/B	Tangential v [m/s]	Tangential v/Um	Vertical w [m/s]	Vertical w/Um	Radial u [m/s]	Radial u/Um
1	0.044	-0.93	0.01613	0.2177	-	-	-	-
2	0.044	-0.87	0.02440	0.3294	-	-	-	-
3	0.044	-0.73	0.03441	0.4646	-	-	-	-
4	0.044	-0.40	0.03879	0.5236	-	-	-	-
5	0.044	0.	0.04142	0.5592	-	-	-	-
6	0.044	0.40	0.04480	0.6047	-	-	-	-
7	0.044	0.73	0.05913	0.7982	-	-	-	-
8	0.044	0.87	0.06166	0.8324	-	-	-	-
9	0.044	0.93	0.04980	0.6723	-	-	-	-
10	0.078	0.93	0.06814	0.9199	-	-	-	-
11	0.078	0.87	0.08611	1.1625	-	-	-	-
12	0.078	0.73	0.08211	1.1084	-	-	-	-
13	0.078	0.40	0.07599	1.0259	-	-	-	-
14	0.078	0.	0.06424	0.8673	-	-	-	-
15	0.078	-0.40	0.05365	0.7243	-	-	-	-
16	0.078	-0.73	0.04569	0.6168	-	-	-	-
17	0.078	-0.87	0.03494	0.4717	-	-	-	-
18	0.078	-0.93	0.02408	0.3251	-	-	-	-
19	0.178	-0.93	0.03531	0.4767	0.00316	0.0427	-0.00253	-0.0341
20	0.178	-0.87	0.05022	0.6780	0.00337	0.0455	-0.00184	-0.0249
21	0.178	-0.73	0.05813	0.7847	0.00142	0.0192	-0.00084	-0.0114
22	0.178	-0.40	0.07051	0.9519	-0.00005	-0.0007	-0.00026	-0.0036
23	0.178	0.	0.08026	1.0835	0.00016	0.0021	-0.00053	-0.0071
24	0.178	0.40	0.08574	1.1575	-0.00021	-0.0028	0.00174	0.0235
25	0.178	0.73	0.08785	1.1860	-0.00016	-0.0021	0.00321	0.0434
26	0.178	0.87	0.08912	1.2031	-0.00090	-0.0121	0.00206	0.0277
27	0.178	0.93	0.07320	0.9882	-0.00116	-0.0157	0.00174	0.0235
28	0.422	0.93	0.07441	1.0046	0.00132	0.0178	0.00132	0.0178
29	0.422	0.87	0.08901	1.2016	0.00063	0.0085	0.00211	0.0285
30	0.422	0.73	0.08785	1.1860	0.00047	0.0064	0.00316	0.0427
31	0.422	0.40	0.08701	1.1746	-0.00195	-0.0263	0.00121	0.0164
32	0.422	0.	0.07699	1.0394	-0.00005	-0.0007	-0.00053	-0.0071
33	0.422	-0.40	0.06124	0.8267	0.00037	0.0050	0.00032	0.0043
34	0.422	-0.73	0.05728	0.7733	0.00100	0.0135	-0.00053	-0.0071
35	0.422	-0.87	0.05317	0.7179	0.00343	0.0462	-0.00090	-0.0121
36	0.422	-0.93	0.04348	0.5869	0.00490	0.0662	-0.00005	-0.0007
37	0.667	-0.93	0.03526	0.4760	0.00474	0.0640	0.00126	0.0171
38	0.667	-0.87	0.04632	0.6254	0.00369	0.0498	0.00148	0.0199
39	0.667	-0.73	0.05128	0.6922	0.00116	0.0157	0.00069	0.0092
40	0.667	-0.40	0.05939	0.8018	0.00021	0.0028	0.00026	0.0036
41	0.667	0.	0.07694	1.0387	0.00011	0.0014	-0.00021	-0.0028
42	0.667	0.40	0.08864	1.1967	-0.00248	-0.0334	-0.00084	-0.0114
43	0.667	0.73	0.08843	1.1938	0.00032	0.0043	0.00037	0.0050
44	0.667	0.87	0.09064	1.2237	0.00337	0.0455	0.00016	0.0021
45	0.667	0.93	0.07657	1.0337	0.00406	0.0548	0.00011	0.0014
46	0.911	0.93	0.07304	0.9861	-	-	-0.00248	-0.0334
47	0.911	0.87	0.08406	1.1348	-	-	-0.00374	-0.0505
48	0.911	0.73	0.08474	1.1440	-	-	-0.00543	-0.0733
49	0.911	0.40	0.08817	1.1903	-	-	-0.00453	-0.0612
50	0.911	0.	0.07868	1.0622	-	-	0.00079	0.0107
51	0.911	-0.40	0.06055	0.8175	-	-	-0.00042	-0.0057
52	0.911	-0.73	0.04659	0.6289	-	-	0.00079	0.0107
53	0.911	-0.87	0.04153	0.5606	-	-	0.00032	0.0043
54	0.911	-0.93	0.03104	0.4190	-	-	-0.00090	-0.0121

Table 6.24 a). The tangential, vertical and radial mean velocity distribution at section S-4 run no.3 Um = 0.09259 m/s

Loc. no.	η = z/h	2Y/B	Tangential v [m/s]	Tangential v/Um	Vertical w [m/s]	Vertical w/Um	Radial u [m/s]	Radial u/Um
1	0.033	-0.93	0.01924	0.2077	-	-	-	-
2	0.033	-0.87	0.03452	0.3728	-	-	-	-
3	0.033	-0.73	0.04084	0.4411	-	-	-	-
4	0.033	-0.40	0.05217	0.5635	-	-	-	-
5	0.033	0.	0.05829	0.6295	-	-	-	-
6	0.033	0.40	0.05776	0.6238	-	-	-	-
7	0.033	0.73	0.06593	0.7120	-	-	-	-
8	0.033	0.87	0.06429	0.6944	-	-	-	-
9	0.033	0.93	0.04859	0.5248	-	-	-	-
10	0.058	0.93	0.06999	0.7558	-	-	-	-
11	0.058	0.87	0.09612	1.0381	-	-	-	-
12	0.058	0.73	0.09713	1.0490	-	-	-	-
13	0.058	0.40	0.08817	0.9522	-	-	-	-
14	0.058	0.	0.07736	0.8355	-	-	-	-
15	0.058	-0.40	0.06840	0.7388	-	-	-	-
16	0.058	-0.73	0.06076	0.6562	-	-	-	-
17	0.058	-0.87	0.04970	0.5367	-	-	-	-
18	0.058	-0.93	0.02667	0.2880	-	-	-	-
19	0.133	-0.93	0.03895	0.4206	0.00395	0.0427	-0.00701	-0.0757
20	0.133	-0.87	0.06087	0.6574	0.00485	0.0524	-0.00859	-0.0928
21	0.133	-0.73	0.07552	0.8156	0.00264	0.0285	-0.00991	-0.1070
22	0.133	-0.40	0.08411	0.9084	0.00058	0.0063	-0.00933	-0.1007
23	0.133	0.	0.09349	1.0097	-0.00021	-0.0023	-0.00912	-0.0985
24	0.133	0.40	0.09939	1.0734	-0.00032	-0.0034	-0.00353	-0.0381
25	0.133	0.73	0.10450	1.1286	0.00021	0.0023	0.00042	0.0046
26	0.133	0.87	0.10356	1.1184	-0.00032	-0.0034	-0.00016	-0.0017
27	0.133	0.93	0.07684	0.8298	-0.00095	-0.0102	0.00121	0.0131
28	0.400	0.93	0.08000	0.8640	0.00237	0.0256	0.00174	0.0188
29	0.400	0.87	0.10271	1.1093	0.00137	0.0148	0.00184	0.0199
30	0.400	0.73	0.10377	1.1207	0.00105	0.0114	0.00248	0.0268
31	0.400	0.40	0.10108	1.0916	-0.00169	-0.0182	0.00311	0.0336
32	0.400	0.	0.09412	1.0165	-0.00026	-0.0028	-0.00063	-0.0068
33	0.400	-0.40	0.08263	0.8924	0.00032	0.0034	-0.00258	-0.0279
34	0.400	-0.73	0.07252	0.7832	0.00148	0.0159	-0.00069	-0.0074
35	0.400	-0.87	0.06603	0.7132	0.00490	0.0529	0.00026	0.0028
36	0.400	-0.93	0.04511	0.4872	0.00912	0.0985	0.00047	0.0051
37	0.667	-0.93	0.03241	0.3500	0.00311	0.0336	0.00069	0.0074
38	0.667	-0.87	0.05386	0.5817	0.00543	0.0586	0.00190	0.0205
39	0.667	-0.73	0.06182	0.6676	0.00121	0.0131	0.00090	0.0097
40	0.667	-0.40	0.08058	0.8702	-0.00016	-0.0017	-0.00211	-0.0228
41	0.667	0.	0.09829	1.0615	-0.00069	-0.0074	-0.00037	-0.0040
42	0.667	0.40	0.10213	1.1030	-0.00311	-0.0336	-0.00053	-0.0057
43	0.667	0.73	0.10345	1.1173	0.00274	0.0296	-0.00005	-0.0006
44	0.667	0.87	0.10324	1.1150	0.00353	0.0381	-0.00169	-0.0182
45	0.667	0.93	0.08321	0.8987	0.00279	0.0302	-0.00248	-0.0268
46	0.933	0.93	0.07652	0.8264	-	-	-0.00553	-0.0598
47	0.933	0.87	0.09238	0.9977	-	-	-0.00464	-0.0501
48	0.933	0.73	0.09876	1.0666	-	-	-0.00638	-0.0689
49	0.933	0.40	0.10319	1.1144	-	-	-0.00859	-0.0928
50	0.933	0.	0.09897	1.0689	-	-	-0.00132	-0.0142
51	0.933	-0.40	0.08137	0.8788	-	-	-0.00058	-0.0063
52	0.933	-0.73	0.06393	0.6904	-	-	-0.00021	-0.0023
53	0.933	-0.87	0.05976	0.6454	-	-	-0.00179	-0.0194
54	0.933	-0.93	0.04090	0.4417	-	-	-0.00374	-0.0404

Table 6.25 a). The tangential, vertical and radial mean velocity distribution at section S-5 run no.1 U_m = 0.04444 m/s

Loc. no.	η = z/h	2Y/B	Tangential v [m/s]	v/Um	Vertical w [m/s]	w/Um	Radial u [m/s]	u/Um
1	0.080	-0.93	0.01202	0.2704	-	-	-	-
2	0.080	-0.87	0.02234	0.5028	-	-	-	-
3	0.080	-0.73	0.02677	0.6024	-	-	-	-
4	0.080	-0.40	0.02340	0.5265	-	-	-	-
5	0.080	0.	0.01797	0.4043	-	-	-	-
6	0.080	0.40	0.01291	0.2905	-	-	-	-
7	0.080	0.73	0.00538	0.1209	-	-	-	-
8	0.080	0.87	0.00269	0.0605	-	-	-	-
9	0.080	0.93	0.00195	0.0439	-	-	-	-
10	0.140	0.93	0.00100	0.0225	-	-	-0.00026	-0.0059
11	0.140	0.87	0.00585	0.1316	-	-	-0.00137	-0.0308
12	0.140	0.73	0.01207	0.2715	-	-	-0.00206	-0.0462
13	0.140	0.40	0.02314	0.5205	-	-	-0.00295	-0.0664
14	0.140	0.	0.03225	0.7257	-	-	-0.00311	-0.0700
15	0.140	-0.40	0.04422	0.9948	-	-	-0.00316	-0.0711
16	0.140	-0.73	0.04485	1.0091	-	-	-0.00353	-0.0794
17	0.140	-0.87	0.04053	0.9118	-	-	-0.00474	-0.1067
18	0.140	-0.93	0.02851	0.6415	-	-	-0.00258	-0.0581
19	0.320	-0.93	0.04822	1.0850	-0.00126	-0.0285	-0.00337	-0.0759
20	0.320	-0.87	0.06519	1.4668	-0.00053	-0.0119	-0.00379	-0.0854
21	0.320	-0.73	0.06645	1.4952	0.00016	0.0036	-0.00279	-0.0628
22	0.320	-0.40	0.06366	1.4324	0.00032	0.0071	-0.00248	-0.0557
23	0.320	0.	0.05101	1.1478	0.00005	0.0012	-0.00195	-0.0439
24	0.320	0.40	0.04000	0.9000	-0.00032	-0.0071	-0.00306	-0.0688
25	0.320	0.73	0.02951	0.6640	-0.00069	-0.0154	-0.00348	-0.0783
26	0.320	0.87	0.02630	0.5917	-0.00100	-0.0225	-0.00395	-0.0889
27	0.320	0.93	0.02097	0.4719	-0.00005	-0.0012	-0.00306	-0.0688
28	0.600	0.93	0.02914	0.6557	-0.00090	-0.0202	-0.00369	-0.0830
29	0.600	0.87	0.03404	0.7660	-0.00153	-0.0344	-0.00321	-0.0723
30	0.600	0.73	0.03104	0.6984	-0.00053	-0.0119	-0.00174	-0.0391
31	0.600	0.40	0.03884	0.8739	0.00037	0.0083	-0.00063	-0.0142
32	0.600	0.	0.04885	1.0992	0.00037	0.0083	-0.00053	-0.0119
33	0.600	-0.40	0.06208	1.3968	-0.00005	-0.0012	-0.00195	-0.0439
34	0.600	-0.73	0.06914	1.5557	-0.00063	-0.0142	-0.00395	-0.0889
35	0.600	-0.87	0.06851	1.5415	-0.00126	-0.0285	-0.00453	-0.1020
36	0.600	-0.93	0.05170	1.1632	-0.00158	-0.0356	-0.00385	-0.0866
37	0.900	-0.93	0.04132	0.9296	-0.00090	-0.0202	-0.00190	-0.0427
38	0.900	-0.87	0.05765	1.2972	-0.00126	-0.0285	-0.00464	-0.1043
39	0.900	-0.73	0.06656	1.4976	0.00011	0.0024	-0.00453	-0.1020
40	0.900	-0.40	0.06498	1.4620	-0.00074	-0.0166	-0.00248	-0.0557
41	0.900	0.	0.05201	1.1703	-0.00021	-0.0047	-0.00200	-0.0451
42	0.900	0.40	0.03884	0.8739	0.00005	0.0012	-0.00021	-0.0047
43	0.900	0.73	0.01723	0.3877	0.00016	0.0036	0.00069	0.0154
44	0.900	0.87	0.02540	0.5715	0.00058	0.0130	0.00042	0.0095
45	0.900	0.93	0.02076	0.4672	0.00095	0.0213	0.00026	0.0059

Table 6.26 a). The tangential, vertical and radial mean velocity distribution at section S-5 run no.2 U_m = 0.07407 m/s

Loc. no.	η = z/h	2Y/B	Tangential v [m/s]	v/Um	Vertical w [m/s]	w/Um	Radial u [m/s]	u/Um
1	0.044	-0.93	0.03236	0.4368	-	-	-	-
2	0.044	-0.87	0.04147	0.5599	-	-	-	-
3	0.044	-0.73	0.04042	0.5457	-	-	-	-
4	0.044	-0.40	0.04416	0.5962	-	-	-	-
5	0.044	0.	0.04169	0.5628	-	-	-	-
6	0.044	0.40	0.03041	0.4105	-	-	-	-
7	0.044	0.73	0.01829	0.2469	-	-	-	-
8	0.044	0.87	0.02103	0.2839	-	-	-	-
9	0.044	0.93	0.01344	0.1814	-	-	-	-
10	0.078	0.93	0.02092	0.2824	-	-	-	-
11	0.078	0.87	0.03194	0.4311	-	-	-	-
12	0.078	0.73	0.03020	0.4077	-	-	-	-
13	0.078	0.40	0.04775	0.6446	-	-	-	-
14	0.078	0.	0.06361	0.8587	-	-	-	-
15	0.078	-0.40	0.06835	0.9228	-	-	-	-
16	0.078	-0.73	0.07009	0.9462	-	-	-	-
17	0.078	-0.87	0.07157	0.9661	-	-	-	-
18	0.078	-0.93	0.05665	0.7648	-	-	-	-
19	0.178	-0.93	0.08522	1.1504	-0.00195	-0.0263	-0.00406	-0.0548
20	0.178	-0.87	0.10440	1.4094	0.	0.	-0.00311	-0.0420
21	0.178	-0.73	0.09997	1.3496	-0.00021	-0.0028	-0.00216	-0.0292
22	0.178	-0.40	0.09502	1.2827	0.00100	0.0135	-0.00084	-0.0114
23	0.178	0.	0.08242	1.1127	0.00058	0.0078	-0.00163	-0.0221
24	0.178	0.40	0.06540	0.8829	0.00047	0.0064	-0.00343	-0.0462
25	0.178	0.73	0.04574	0.6175	-0.00105	-0.0142	-0.00617	-0.0832
26	0.178	0.87	0.04411	0.5955	-0.00021	-0.0028	-0.00701	-0.0946
27	0.178	0.93	0.03125	0.4219	0.00274	0.0370	-0.00495	-0.0669
28	0.422	0.93	0.03483	0.4703	-0.00279	-0.0377	-0.00564	-0.0761
29	0.422	0.87	0.05128	0.6922	-0.00190	-0.0256	-0.00458	-0.0619
30	0.422	0.73	0.05233	0.7065	-0.00121	-0.0164	-0.00395	-0.0534
31	0.422	0.40	0.05971	0.8061	0.00121	0.0164	-0.00169	-0.0228
32	0.422	0.	0.07757	1.0473	0.00142	0.0192	-0.00058	-0.0078
33	0.422	-0.40	0.09649	1.3027	0.00211	0.0285	-0.00184	-0.0249
34	0.422	-0.73	0.10213	1.3788	-0.00079	-0.0107	-0.00153	-0.0206
35	0.422	-0.87	0.10366	1.3994	-0.00248	-0.0334	-0.00295	-0.0398
36	0.422	-0.93	0.08353	1.1276	-0.00269	-0.0363	-0.00390	-0.0526
37	0.667	-0.93	0.08479	1.1447	-0.00406	-0.0548	-0.00490	-0.0662
38	0.667	-0.87	0.10450	1.4108	-0.00369	-0.0498	-0.00437	-0.0591
39	0.667	-0.73	0.10261	1.3852	-0.00184	-0.0249	-0.00443	-0.0598
40	0.667	-0.40	0.09697	1.3091	0.00221	0.0299	-0.00385	-0.0519
41	0.667	0.	0.07789	1.0515	-0.00011	-0.0014	-0.00090	-0.0121
42	0.667	0.40	0.05286	0.7136	0.00169	0.0228	0.00079	0.0107
43	0.667	0.73	0.04163	0.5620	-0.00011	-0.0014	0.00232	0.0313
44	0.667	0.87	0.03937	0.5315	-0.00464	-0.0626	-0.00047	-0.0064
45	0.667	0.93	0.02624	0.3543	-0.00569	-0.0768	0.	0.
46	0.911	0.93	0.01997	0.2696	-	-	0.00253	0.0341
47	0.911	0.87	0.03120	0.4212	-	-	0.00306	0.0413
48	0.911	0.73	0.03526	0.4760	-	-	0.00306	0.0413
49	0.911	0.40	0.06234	0.8416	-	-	0.	0.
50	0.911	0.	0.08079	1.0907	-	-	-0.00190	-0.0256
51	0.911	-0.40	0.09649	1.3027	-	-	-0.00458	-0.0619
52	0.911	-0.73	0.10055	1.3574	-	-	-0.00775	-0.1046
53	0.911	-0.87	0.09797	1.3226	-	-	-0.00543	-0.0733
54	0.911	-0.93	0.08021	1.0828	-	-	-0.00232	-0.0313

Table 6.27 a). The tangential, vertical and radial mean velocity distribution at section S-5 run no.3 Um = 0.09259 m/s

Loc. no.	η = z/h	2Y/B	Tangential v [m/s]	Tangential v/Um	Vertical w [m/s]	Vertical w/Um	Radial u [m/s]	Radial u/Um
1	0.033	−0.93	0.04042	0.4365	–	–	–	–
2	0.033	−0.87	0.05391	0.5823	–	–	–	–
3	0.033	−0.73	0.04685	0.5060	–	–	–	–
4	0.033	−0.40	0.04970	0.5367	–	–	–	–
5	0.033	0.	0.04458	0.4815	–	–	–	–
6	0.033	0.40	0.04074	0.4400	–	–	–	–
7	0.033	0.73	0.02930	0.3165	–	–	–	–
8	0.033	0.87	0.03262	0.3523	–	–	–	–
9	0.033	0.93	0.02730	0.2948	–	–	–	–
10	0.058	0.93	0.03678	0.3973	–	–	–	–
11	0.058	0.87	0.04358	0.4707	–	–	–	–
12	0.058	0.73	0.04748	0.5128	–	–	–	–
13	0.058	0.40	0.06514	0.7035	–	–	–	–
14	0.058	0.	0.07710	0.8327	–	–	–	–
15	0.058	−0.40	0.08711	0.9408	–	–	–	–
16	0.058	−0.73	0.08922	0.9636	–	–	–	–
17	0.058	−0.87	0.09296	1.0040	–	–	–	–
18	0.058	−0.93	0.07520	0.8122	–	–	–	–
19	0.133	−0.93	0.09855	1.0643	−0.00300	−0.0324	−0.00437	−0.0472
20	0.133	−0.87	0.11889	1.2840	0.00032	0.0034	−0.00401	−0.0433
21	0.133	−0.73	0.11652	1.2584	−0.00005	−0.0006	−0.00253	−0.0273
22	0.133	−0.40	0.10819	1.1685	0.00063	0.0068	−0.00153	−0.0165
23	0.133	0.	0.09512	1.0273	0.00095	0.0102	−0.00432	−0.0467
24	0.133	0.40	0.07926	0.8560	0.00079	0.0085	−0.00653	−0.0706
25	0.133	0.73	0.06456	0.6972	−0.00105	−0.0114	−0.00722	−0.0780
26	0.133	0.87	0.05871	0.6340	−0.00032	−0.0034	−0.00696	−0.0751
27	0.133	0.93	0.05096	0.5504	0.00121	0.0131	−0.00532	−0.0575
28	0.400	0.93	0.05760	0.6221	−0.00464	−0.0501	−0.00448	−0.0484
29	0.400	0.87	0.06582	0.7109	−0.00316	−0.0341	−0.00469	−0.0507
30	0.400	0.73	0.06814	0.7359	−0.00069	−0.0074	−0.00343	−0.0370
31	0.400	0.40	0.07515	0.8116	0.00190	0.0205	−0.00174	−0.0188
32	0.400	0.	0.09823	1.0609	0.00153	0.0165	−0.00248	−0.0268
33	0.400	−0.40	0.11283	1.2186	0.00153	0.0165	−0.00100	−0.0108
34	0.400	−0.73	0.11900	1.2852	−0.00153	−0.0165	−0.00111	−0.0120
35	0.400	−0.87	0.11973	1.2931	−0.00237	−0.0256	−0.00221	−0.0239
36	0.400	−0.93	0.09786	1.0569	−0.00311	−0.0336	−0.00348	−0.0376
37	0.667	−0.93	0.09333	1.0080	−0.00327	−0.0353	−0.00395	−0.0427
38	0.667	−0.87	0.11620	1.2550	−0.00353	−0.0381	−0.00353	−0.0381
39	0.667	−0.73	0.11810	1.2755	−0.00216	−0.0233	−0.00348	−0.0376
40	0.667	−0.40	0.11457	1.2374	0.00227	0.0245	−0.00179	−0.0194
41	0.667	0.	0.10002	1.0803	0.00079	0.0085	−0.00221	−0.0239
42	0.667	0.40	0.06703	0.7240	0.00206	0.0222	0.00069	0.0074
43	0.667	0.73	0.04991	0.5390	0.00179	0.0194	0.00285	0.0307
44	0.667	0.87	0.05133	0.5544	−0.00495	−0.0535	0.00279	0.0302
45	0.667	0.93	0.04216	0.4553	−0.00859	−0.0928	0.00163	0.0176
46	0.933	0.93	0.03204	0.3460	–	–	0.00485	0.0524
47	0.933	0.87	0.04174	0.4508	–	–	0.00464	0.0501
48	0.933	0.73	0.04717	0.5094	–	–	0.00353	0.0381
49	0.933	0.40	0.06603	0.7132	–	–	0.00016	0.0017
50	0.933	0.	0.09518	1.0279	–	–	−0.00084	−0.0091
51	0.933	−0.40	0.11215	1.2112	–	–	−0.00553	−0.0598
52	0.933	−0.73	0.11552	1.2476	–	–	−0.00648	−0.0700
53	0.933	−0.87	0.10925	1.1799	–	–	−0.00395	−0.0427
54	0.933	−0.93	0.08701	0.9397	–	–	−0.00264	−0.0285

Table 6.28 a). The tangential, vertical and radial mean velocity distribution at section S-6 run no.1 Um = 0.04444 m/s

Loc. no.	η = z/h	2Y/B	Tangential v [m/s]	Tangential v/Um	Vertical w [m/s]	Vertical w/Um	Radial u [m/s]	Radial u/Um
1	0.080	−0.93	0.01043	0.2348	–	–	–	–
2	0.080	−0.87	0.01750	0.3937	–	–	–	–
3	0.080	−0.73	0.02166	0.4873	–	–	–	–
4	0.080	−0.40	0.02503	0.5632	–	–	–	–
5	0.080	0.	0.02282	0.5134	–	–	–	–
6	0.080	0.40	0.01370	0.3083	–	–	–	–
7	0.080	0.73	0.01423	0.3202	–	–	–	–
8	0.080	0.87	0.01523	0.3427	–	–	–	–
9	0.080	0.93	0.01028	0.2312	–	–	–	–
10	0.140	0.93	0.01491	0.3356	–	–	0.00005	0.0012
11	0.140	0.87	0.02429	0.5466	–	–	−0.00005	−0.0012
12	0.140	0.73	0.02329	0.5241	–	–	−0.00095	−0.0213
13	0.140	0.40	0.02245	0.5051	–	–	−0.00032	−0.0071
14	0.140	0.	0.03647	0.8205	–	–	0.00237	0.0534
15	0.140	−0.40	0.04285	0.9640	–	–	0.00211	0.0474
16	0.140	−0.73	0.03758	0.8454	–	–	−0.00184	−0.0415
17	0.140	−0.87	0.02888	0.6498	–	–	−0.00285	−0.0640
18	0.140	−0.93	0.01755	0.3949	–	–	−0.00216	−0.0486
19	0.320	−0.93	0.01997	0.4494	−0.00258	−0.0581	−0.00174	−0.0391
20	0.320	−0.87	0.03246	0.7304	−0.00264	−0.0593	−0.00063	−0.0142
21	0.320	−0.73	0.03984	0.8964	−0.00074	−0.0166	−0.00090	−0.0202
22	0.320	−0.40	0.05887	1.3245	−0.00053	−0.0119	0.00364	0.0818
23	0.320	0.	0.05692	1.2806	0.00079	0.0178	0.00279	0.0628
24	0.320	0.40	0.03599	0.8099	−0.00069	−0.0154	−0.00116	−0.0261
25	0.320	0.73	0.02899	0.6522	0.00026	0.0059	0.00221	0.0498
26	0.320	0.87	0.02967	0.6676	0.00074	0.0166	0.00206	0.0462
27	0.320	0.93	0.01945	0.4375	0.00047	0.0107	0.00158	0.0356
28	0.600	0.93	0.01929	0.4340	−0.00005	−0.0012	0.00227	0.0510
29	0.600	0.87	0.02877	0.6474	0.00084	0.0190	0.00190	0.0427
30	0.600	0.73	0.03125	0.7031	0.00153	0.0344	0.	0.
31	0.600	0.40	0.04232	0.9522	−0.00084	−0.0190	0.00069	0.0154
32	0.600	0.	0.06034	1.3577	0.00079	0.0178	0.00374	0.0842
33	0.600	−0.40	0.04337	0.9759	−0.00148	−0.0332	0.00701	0.1577
34	0.600	−0.73	0.03283	0.7387	−0.00026	−0.0059	0.00453	0.1020
35	0.600	−0.87	0.03109	0.6996	−0.00321	−0.0723	0.00011	0.0024
36	0.600	−0.93	0.01987	0.4470	−0.00242	−0.0545	0.00084	0.0190
37	0.900	−0.93	0.01123	0.2526	−0.00274	−0.0617	0.00300	0.0676
38	0.900	−0.87	0.02292	0.5158	−0.00248	−0.0557	0.00343	0.0771
39	0.900	−0.73	0.02862	0.6439	0.00053	0.0119	0.00548	0.1233
40	0.900	−0.40	0.05049	1.1359	−0.00121	−0.0273	0.00501	0.1126
41	0.900	0.	0.06340	1.4265	−0.00063	−0.0142	0.00543	0.1221
42	0.900	0.40	0.05070	1.1407	0.00032	0.0071	0.00669	0.1506
43	0.900	0.73	0.03789	0.8526	0.00084	0.0190	0.00295	0.0664
44	0.900	0.87	0.02667	0.6000	0.00121	0.0273	−0.00100	−0.0225
45	0.900	0.93	0.01845	0.4150	0.00079	0.0178	−0.00084	−0.0190

Table 6.29 a). The tangential, vertical and radial mean velocity distribution at section S-6 run no.2 Um = 0.07407 m/s

Loc. no.	η = z/h	2Y/B	Tangential v [m/s]	Tangential v/Um	Vertical w [m/s]	Vertical w/Um	Radial u [m/s]	Radial u/Um
1	0.044	−0.93	0.02482	0.3351	–	–	–	–
2	0.044	−0.87	0.03910	0.5279	–	–	–	–
3	0.044	−0.73	0.05360	0.7235	–	–	–	–
4	0.044	−0.40	0.05702	0.7698	–	–	–	–
5	0.044	0.	0.04495	0.6069	–	–	–	–
6	0.044	0.40	0.03547	0.4788	–	–	–	–
7	0.044	0.73	0.02809	0.3792	–	–	–	–
8	0.044	0.87	0.02709	0.3657	–	–	–	–
9	0.044	0.93	0.01829	0.2469	–	–	–	–
10	0.078	0.93	0.02978	0.4020	–	–	–	–
11	0.078	0.87	0.04005	0.5407	–	–	–	–
12	0.078	0.73	0.03937	0.5315	–	–	–	–
13	0.078	0.40	0.04748	0.6410	–	–	–	–
14	0.078	0.	0.06150	0.8303	–	–	–	–
15	0.078	−0.40	0.07868	1.0622	–	–	–	–
16	0.078	−0.73	0.08258	1.1148	–	–	–	–
17	0.078	−0.87	0.06972	0.9412	–	–	–	–
18	0.078	−0.93	0.04959	0.6695	–	–	–	–
19	0.178	−0.93	0.05180	0.6994	−0.00564	−0.0761	0.00121	0.0164
20	0.178	−0.87	0.07436	1.0039	−0.00480	−0.0647	0.00126	0.0171
21	0.178	−0.73	0.09512	1.2842	−0.00063	−0.0085	0.00390	0.0526
22	0.178	−0.40	0.09249	1.2486	0.00011	0.0014	0.00148	0.0199
23	0.178	0.	0.07847	1.0593	0.00063	0.0085	0.00190	0.0256
24	0.178	0.40	0.05576	0.7527	−0.00011	−0.0014	0.00195	0.0263
25	0.178	0.73	0.04854	0.6552	−0.00190	−0.0256	0.00121	0.0164
26	0.178	0.87	0.04796	0.6474	0.00058	0.0078	0.00316	0.0427
27	0.178	0.93	0.03694	0.4987	0.00216	0.0292	0.00248	0.0334
28	0.422	0.93	0.03810	0.5144	0.00016	0.0021	0.00264	0.0356
29	0.422	0.87	0.04917	0.6638	0.00037	0.0050	0.00469	0.0633
30	0.422	0.73	0.05180	0.6994	0.00047	0.0064	0.00253	0.0341
31	0.422	0.40	0.05945	0.8025	−0.00016	−0.0021	0.00121	0.0164
32	0.422	0.	0.07894	1.0658	0.00005	0.0007	0.	0.
33	0.422	−0.40	0.09871	1.3325	−0.00063	−0.0085	0.00469	0.0633
34	0.422	−0.73	0.08553	1.1547	−0.00295	−0.0398	0.00411	0.0555
35	0.422	−0.87	0.06972	0.9412	−0.00248	−0.0334	0.00337	0.0455
36	0.422	−0.93	0.04674	0.6311	−0.00690	−0.0932	0.00316	0.0427
37	0.667	−0.93	0.03805	0.5137	−0.00790	−0.1067	0.00300	0.0406
38	0.667	−0.87	0.05918	0.7990	−0.00379	−0.0512	0.00174	0.0235
39	0.667	−0.73	0.06793	0.9171	−0.00195	−0.0263	0.00332	0.0448
40	0.667	−0.40	0.09881	1.3340	−0.00032	−0.0043	0.00279	0.0377
41	0.667	0.	0.08464	1.1426	−0.00016	−0.0021	0.00300	0.0406
42	0.667	0.40	0.06429	0.8680	0.00137	0.0185	0.00074	0.0100
43	0.667	0.73	0.05317	0.7179	0.00195	0.0263	0.00063	0.0085
44	0.667	0.87	0.05086	0.6865	−0.00079	−0.0107	0.00032	0.0043
45	0.667	0.93	0.04063	0.5485	−0.00248	−0.0334	0.	0.
46	0.911	0.93	0.03283	0.4432	–	–	−0.00153	−0.0206
47	0.911	0.87	0.04269	0.5763	–	–	−0.00095	−0.0128
48	0.911	0.73	0.04938	0.6666	–	–	0.00047	0.0064
49	0.911	0.40	0.07252	0.9790	–	–	0.00611	0.0825
50	0.911	0.	0.08732	1.1789	–	–	0.00538	0.0726
51	0.911	−0.40	0.09697	1.3091	–	–	0.00769	0.1039
52	0.911	−0.73	0.06287	0.8488	–	–	0.00464	0.0626
53	0.911	−0.87	0.05339	0.7207	–	–	0.00227	0.0306
54	0.911	−0.93	0.03526	0.4760	–	–	0.00037	0.0050

Table 6.30 a). The tangential, vertical and radial mean velocity distribution at section S-6 run no.3 Um = 0.09259 m/s

Loc. no.	η = z/h	2Y/B	Tangential v [m/s]	Tangential v/Um	Vertical w [m/s]	Vertical w/Um	Radial u [m/s]	Radial u/Um
1	0.033	−0.93	0.03231	0.3489	–	–	–	–
2	0.033	−0.87	0.05054	0.5458	–	–	–	–
3	0.033	−0.73	0.06039	0.6523	–	–	–	–
4	0.033	−0.40	0.06371	0.6881	–	–	–	–
5	0.033	0.	0.05022	0.5424	–	–	–	–
6	0.033	0.40	0.04337	0.4684	–	–	–	–
7	0.033	0.73	0.04300	0.4644	–	–	–	–
8	0.033	0.87	0.04063	0.4388	–	–	–	–
9	0.033	0.93	0.02988	0.3227	–	–	–	–
10	0.058	0.93	0.03968	0.4286	–	–	–	–
11	0.058	0.87	0.05702	0.6158	–	–	–	–
12	0.058	0.73	0.06071	0.6557	–	–	–	–
13	0.058	0.40	0.06329	0.6836	–	–	–	–
14	0.058	0.	0.07710	0.8327	–	–	–	–
15	0.058	−0.40	0.09502	1.0262	–	–	–	–
16	0.058	−0.73	0.09085	0.9812	–	–	–	–
17	0.058	−0.87	0.07921	0.8554	–	–	–	–
18	0.058	−0.93	0.05871	0.6340	–	–	–	–
19	0.133	−0.93	0.07225	0.7803	−0.00917	−0.0990	−0.00880	−0.0950
20	0.133	−0.87	0.09365	1.0114	−0.00643	−0.0694	−0.00590	−0.0637
21	0.133	−0.73	0.11004	1.1884	−0.00063	−0.0068	−0.00169	−0.0182
22	0.133	−0.40	0.10777	1.1639	−0.00005	−0.0006	−0.00153	−0.0165
23	0.133	0.	0.09660	1.0433	0.00100	0.0108	0.00121	0.0131
24	0.133	0.40	0.07468	0.8065	0.00016	0.0017	0.00416	0.0450
25	0.133	0.73	0.05918	0.6392	−0.00063	−0.0068	0.00701	0.0757
26	0.133	0.87	0.06361	0.6870	0.00126	0.0137	0.00648	0.0700
27	0.133	0.93	0.04464	0.4821	0.00348	0.0376	0.00401	0.0433
28	0.400	0.93	0.04954	0.5350	−0.00184	−0.0199	0.00432	0.0467
29	0.400	0.87	0.06835	0.7382	−0.00184	−0.0199	0.00358	0.0387
30	0.400	0.73	0.07078	0.7644	0.00032	0.0034	0.00200	0.0216
31	0.400	0.40	0.07615	0.8224	0.00211	0.0228	0.00174	0.0188
32	0.400	0.	0.09317	1.0063	0.00200	0.0216	0.00311	0.0336
33	0.400	−0.40	0.11294	1.2197	0.	0.	0.00401	0.0433
34	0.400	−0.73	0.10240	1.1059	−0.00174	−0.0188	0.00580	0.0626
35	0.400	−0.87	0.08933	0.9647	−0.00264	−0.0285	0.00422	0.0455
36	0.400	−0.93	0.06746	0.7285	−0.00964	−0.1042	0.00332	0.0359
37	0.667	−0.93	0.05022	0.5424	−0.00906	−0.0979	0.00437	0.0472
38	0.667	−0.87	0.07072	0.7638	−0.00754	−0.0814	0.00237	0.0256
39	0.667	−0.73	0.08738	0.9437	−0.00011	−0.0011	0.00474	0.0512
40	0.667	−0.40	0.11605	1.2533	0.00047	0.0051	0.00585	0.0632
41	0.667	0.	0.09607	1.0376	0.00069	0.0074	0.00227	0.0245
42	0.667	0.40	0.07736	0.8355	0.00337	0.0364	−0.00069	−0.0074
43	0.667	0.73	0.06377	0.6887	0.00227	0.0245	−0.00126	−0.0137
44	0.667	0.87	0.06682	0.7217	−0.00206	−0.0222	−0.00090	−0.0097
45	0.667	0.93	0.04885	0.5276	−0.00717	−0.0774	−0.00016	−0.0017
46	0.933	0.93	0.03726	0.4024	–	–	−0.00248	−0.0268
47	0.933	0.87	0.05449	0.5885	–	–	−0.00232	−0.0250
48	0.933	0.73	0.06192	0.6688	–	–	−0.00111	−0.0120
49	0.933	0.40	0.08105	0.8754	–	–	−0.00037	−0.0040
50	0.933	0.	0.10503	1.1343	–	–	0.00733	0.0791
51	0.933	−0.40	0.11536	1.2459	–	–	0.00848	0.0916
52	0.933	−0.73	0.09238	0.9977	–	–	0.00812	0.0877
53	0.933	−0.87	0.07352	0.7940	–	–	0.00585	0.0632
54	0.933	−0.93	0.05855	0.6323	–	–	0.00264	0.0285

Table 6.31 a). *The tangential, vertical and radial mean velocity distribution at section S-7 run no.1* Um = 0.04444 m/s

Loc. no.	η = z/h	2Y/B	Tangential v [m/s]	Tangential v/Um	Vertical w [m/s]	Vertical w/Um	Radial u [m/s]	Radial u/Um
1	0.080	−0.93	0.01049	0.2360	–	–	–	–
2	0.080	−0.87	0.01281	0.2881	–	–	–	–
3	0.080	−0.73	0.01592	0.3581	–	–	–	–
4	0.080	−0.40	0.01834	0.4126	–	–	–	–
5	0.080	0.	0.02039	0.4589	–	–	–	–
6	0.080	0.40	0.02603	0.5858	–	–	–	–
7	0.080	0.73	0.02862	0.6439	–	–	–	–
8	0.080	0.87	0.02999	0.6747	–	–	–	–
9	0.080	0.93	0.01871	0.4209	–	–	–	–
10	0.140	0.93	0.03873	0.8715	–	–	0.00232	0.0522
11	0.140	0.87	0.05165	1.1620	–	–	0.00269	0.0605
12	0.140	0.73	0.04933	1.1099	–	–	0.00211	0.0474
13	0.140	0.40	0.04316	0.9711	–	–	0.00042	0.0095
14	0.140	0.	0.03700	0.8324	–	–	−0.00195	−0.0439
15	0.140	−0.40	0.02920	0.6569	–	–	−0.00237	−0.0534
16	0.140	−0.73	0.02145	0.4826	–	–	−0.00163	−0.0368
17	0.140	−0.87	0.01860	0.4186	–	–	−0.00116	−0.0261
18	0.140	−0.93	0.01697	0.3818	–	–	−0.00111	−0.0249
19	0.320	−0.93	0.02361	0.5312	−0.00179	−0.0403	−0.00047	−0.0107
20	0.320	−0.87	0.02883	0.6486	−0.00142	−0.0320	−0.00074	−0.0166
21	0.320	−0.73	0.03288	0.7399	−0.00074	−0.0166	−0.00053	−0.0119
22	0.320	−0.40	0.04216	0.9486	−0.00084	−0.0190	−0.00126	−0.0285
23	0.320	0.	0.04722	1.0624	−0.00016	−0.0036	−0.00042	−0.0095
24	0.320	0.40	0.05323	1.1976	−0.00021	−0.0047	0.00121	0.0273
25	0.320	0.73	0.05512	1.2403	−0.00016	−0.0036	0.00311	0.0700
26	0.320	0.87	0.05850	1.3162	0.00032	0.0071	0.00364	0.0818
27	0.320	0.93	0.04163	0.9367	0.00063	0.0142	0.00295	0.0664
28	0.600	0.93	0.03599	0.8099	−0.00148	−0.0332	0.00316	0.0711
29	0.600	0.87	0.05665	1.2747	−0.00079	−0.0178	0.00406	0.0913
30	0.600	0.73	0.05491	1.2356	0.00047	0.0107	0.00332	0.0747
31	0.600	0.40	0.05096	1.1466	0.00011	0.0024	0.00248	0.0557
32	0.600	0.	0.04364	0.9818	−0.00037	−0.0083	0.00332	0.0747
33	0.600	−0.40	0.03789	0.8526	−0.00037	−0.0083	0.00274	0.0617
34	0.600	−0.73	0.03109	0.6996	−0.00053	−0.0119	0.00142	0.0320
35	0.600	−0.87	0.02725	0.6130	−0.00090	−0.0202	0.00116	0.0261
36	0.600	−0.93	0.02203	0.4956	−0.00142	−0.0320	0.00069	0.0154
37	0.900	−0.93	0.01929	0.4340	−0.00074	−0.0166	−0.00026	−0.0059
38	0.900	−0.87	0.02277	0.5122	−0.00090	−0.0202	0.00090	0.0202
39	0.900	−0.73	0.02783	0.6261	−0.00069	−0.0154	0.00163	0.0368
40	0.900	−0.40	0.03510	0.7897	−0.00037	−0.0083	0.00332	0.0747
41	0.900	0.	0.04574	1.0292	−0.00011	−0.0024	0.00285	0.0640
42	0.900	0.40	0.05439	1.2237	0.00005	0.0012	0.00169	0.0379
43	0.900	0.73	0.05212	1.1727	0.00021	0.0047	0.00026	0.0059
44	0.900	0.87	0.05191	1.1680	0.00069	0.0154	−0.00274	−0.0617
45	0.900	0.93	0.03099	0.6972	0.00063	0.0142	−0.00248	−0.0557

Table 6.32 a). *The tangential, vertical and radial mean velocity distribution at section S-7 run no.2* Um = 0.07407 m/s

Loc. no.	η = z/h	2Y/B	Tangential v [m/s]	Tangential v/Um	Vertical w [m/s]	Vertical w/Um	Radial u [m/s]	Radial u/Um
1	0.044	−0.93	0.02841	0.3835	–	–	–	–
2	0.044	−0.87	0.03942	0.5322	–	–	–	–
3	0.044	−0.73	0.03710	0.5009	–	–	–	–
4	0.044	−0.40	0.03937	0.5315	–	–	–	–
5	0.044	0.	0.04105	0.5542	–	–	–	–
6	0.044	0.40	0.04400	0.5941	–	–	–	–
7	0.044	0.73	0.05064	0.6837	–	–	–	–
8	0.044	0.87	0.05418	0.7314	–	–	–	–
9	0.044	0.93	0.04875	0.6581	–	–	–	–
10	0.078	0.93	0.06203	0.8374	–	–	–	–
11	0.078	0.87	0.07800	1.0529	–	–	–	–
12	0.078	0.73	0.07641	1.0316	–	–	–	–
13	0.078	0.40	0.06898	0.9313	–	–	–	–
14	0.078	0.	0.06445	0.8701	–	–	–	–
15	0.078	−0.40	0.06034	0.8146	–	–	–	–
16	0.078	−0.73	0.05570	0.7520	–	–	–	–
17	0.078	−0.87	0.04833	0.6524	–	–	–	–
18	0.078	−0.93	0.03615	0.4881	–	–	–	–
19	0.178	−0.93	0.04864	0.6567	−0.00353	−0.0477	−0.00137	−0.0185
20	0.178	−0.87	0.06155	0.8310	−0.00295	−0.0398	−0.00206	−0.0277
21	0.178	−0.73	0.06393	0.8630	−0.00126	−0.0171	−0.00169	−0.0228
22	0.178	−0.40	0.06920	0.9341	−0.00084	−0.0114	−0.00279	−0.0377
23	0.178	0.	0.07763	1.0480	−0.00032	−0.0043	−0.00406	−0.0548
24	0.178	0.40	0.08179	1.1042	0.00016	0.0021	−0.00585	−0.0790
25	0.178	0.73	0.08532	1.1518	0.00042	0.0057	−0.00448	−0.0605
26	0.178	0.87	0.08527	1.1511	0.00158	0.0213	−0.00469	−0.0633
27	0.178	0.93	0.06751	0.9114	0.00148	0.0199	−0.00184	−0.0249
28	0.422	0.93	0.06514	0.8794	−0.00037	−0.0050	−0.00390	−0.0526
29	0.422	0.87	0.08485	1.1454	−0.00090	−0.0121	−0.00464	−0.0626
30	0.422	0.73	0.08506	1.1483	0.00069	0.0092	−0.00490	−0.0662
31	0.422	0.40	0.08390	1.1326	0.00126	0.0171	−0.00232	−0.0313
32	0.422	0.	0.07452	1.0060	0.00069	0.0092	−0.00253	−0.0341
33	0.422	−0.40	0.07046	0.9512	−0.00084	−0.0114	−0.00269	−0.0363
34	0.422	−0.73	0.06298	0.8502	−0.00116	−0.0157	−0.00232	−0.0313
35	0.422	−0.87	0.06245	0.8431	−0.00285	−0.0384	−0.00174	−0.0235
36	0.422	−0.93	0.04769	0.6439	−0.00480	−0.0647	−0.00248	−0.0334
37	0.667	−0.93	0.03547	0.4788	−0.00464	−0.0626	−0.00406	−0.0548
38	0.667	−0.87	0.04880	0.6588	−0.00300	−0.0406	−0.00437	−0.0591
39	0.667	−0.73	0.05549	0.7492	−0.00005	−0.0007	−0.00490	−0.0662
40	0.667	−0.40	0.06245	0.8431	0.00079	0.0107	−0.00469	−0.0633
41	0.667	0.	0.07447	1.0053	0.00047	0.0064	−0.00527	−0.0711
42	0.667	0.40	0.08184	1.1049	0.00153	0.0206	−0.00401	−0.0541
43	0.667	0.73	0.08342	1.1262	−0.00084	−0.0114	−0.00190	−0.0256
44	0.667	0.87	0.08427	1.1376	−0.00311	−0.0420	−0.00269	−0.0363
45	0.667	0.93	0.06377	0.8609	−0.00485	−0.0655	−0.00274	−0.0370
46	0.911	0.93	0.05628	0.7598	–	–	−0.00079	−0.0107
47	0.911	0.87	0.07805	1.0537	–	–	0.00111	0.0149
48	0.911	0.73	0.08284	1.1184	–	–	0.00179	0.0242
49	0.911	0.40	0.08458	1.1419	–	–	−0.00063	−0.0085
50	0.911	0.	0.07389	0.9975	–	–	−0.00358	−0.0484
51	0.911	−0.40	0.06572	0.8872	–	–	−0.00448	−0.0605
52	0.911	−0.73	0.05170	0.6979	–	–	−0.00443	−0.0598
53	0.911	−0.87	0.04964	0.6702	–	–	−0.00179	−0.0242
54	0.911	−0.93	0.03794	0.5122	–	–	−0.00126	−0.0171

Table 6.33 a). The tangential, vertical and radial mean velocity distribution at section S-7 run no.3 Um = 0.09259 m/s

Loc. no.	η = z/h	2Y/B	Tangential v [m/s]	Tangential v/Um	Vertical w [m/s]	Vertical w/Um	Radial u [m/s]	Radial u/Um
1	0.033	−0.93	0.03736	0.4035	–	–	–	–
2	0.033	−0.87	0.05006	0.5407	–	–	–	–
3	0.033	−0.73	0.05660	0.6113	–	–	–	–
4	0.033	−0.40	0.05360	0.5788	–	–	–	–
5	0.033	0.	0.05470	0.5908	–	–	–	–
6	0.033	0.40	0.05792	0.6255	–	–	–	–
7	0.033	0.73	0.06176	0.6671	–	–	–	–
8	0.033	0.87	0.07051	0.7615	–	–	–	–
9	0.033	0.93	0.06234	0.6733	–	–	–	–
10	0.058	0.93	0.07236	0.7815	–	–	–	–
11	0.058	0.87	0.08611	0.9300	–	–	–	–
12	0.058	0.73	0.08443	0.9118	–	–	–	–
13	0.058	0.40	0.08284	0.8947	–	–	–	–
14	0.058	0.	0.07926	0.8560	–	–	–	–
15	0.058	−0.40	0.07367	0.7957	–	–	–	–
16	0.058	−0.73	0.07236	0.7815	–	–	–	–
17	0.058	−0.87	0.06182	0.6676	–	–	–	–
18	0.058	−0.93	0.04812	0.5196	–	–	–	–
19	0.133	−0.93	0.05771	0.6232	−0.00437	−0.0472	0.00148	0.0159
20	0.133	−0.87	0.07167	0.7741	−0.00269	−0.0290	0.00206	0.0222
21	0.133	−0.73	0.07684	0.8298	−0.00032	−0.0034	0.00253	0.0273
22	0.133	−0.40	0.08179	0.8833	0.00058	0.0063	0.00163	0.0176
23	0.133	0.	0.09085	0.9812	0.00058	0.0063	0.	0.
24	0.133	0.40	0.09470	1.0228	−0.00032	−0.0034	−0.00142	−0.0154
25	0.133	0.73	0.09612	1.0381	0.00227	0.0245	−0.00343	−0.0370
26	0.133	0.87	0.09518	1.0279	−0.00179	−0.0194	−0.00264	−0.0285
27	0.133	0.93	0.07742	0.8361	0.00132	0.0142	−0.00253	−0.0273
28	0.400	0.93	0.07863	0.8492	0.00021	0.0023	−0.00485	−0.0524
29	0.400	0.87	0.09834	1.0621	0.00095	0.0102	−0.00490	−0.0529
30	0.400	0.73	0.10029	1.0831	0.00042	0.0046	−0.00643	−0.0694
31	0.400	0.40	0.09902	1.0695	0.00058	0.0063	−0.00648	−0.0700
32	0.400	0.	0.09570	1.0336	0.00032	0.0034	−0.00511	−0.0552
33	0.400	−0.40	0.08638	0.9329	−0.00037	−0.0040	−0.00374	−0.0404
34	0.400	−0.73	0.08126	0.8776	−0.00116	−0.0125	−0.00227	−0.0245
35	0.400	−0.87	0.07779	0.8401	−0.00353	−0.0381	−0.00501	−0.0541
36	0.400	−0.93	0.06387	0.6898	−0.00701	−0.0757	−0.00564	−0.0609
37	0.667	−0.93	0.05444	0.5879	−0.00669	−0.0723	−0.00258	−0.0279
38	0.667	−0.87	0.06640	0.7171	−0.00300	−0.0324	−0.00538	−0.0581
39	0.667	−0.73	0.07188	0.7763	−0.00174	−0.0188	−0.00416	−0.0450
40	0.667	−0.40	0.08190	0.8845	0.00021	0.0023	−0.00332	−0.0359
41	0.667	0.	0.09191	0.9926	0.00121	0.0131	−0.00327	−0.0353
42	0.667	0.40	0.09913	1.0706	0.00148	0.0159	−0.00469	−0.0507
43	0.667	0.73	0.09887	1.0677	0.00026	0.0028	−0.00337	−0.0364
44	0.667	0.87	0.09881	1.0672	−0.00163	−0.0176	−0.00311	−0.0336
45	0.667	0.93	0.07916	0.8549	−0.00295	−0.0319	−0.00306	−0.0330
46	0.933	0.93	0.06988	0.7547	–	–	0.00174	0.0188
47	0.933	0.87	0.08822	0.9528	–	–	0.00237	0.0256
48	0.933	0.73	0.09344	1.0091	–	–	0.00279	0.0302
49	0.933	0.40	0.09744	1.0524	–	–	0.00290	0.0313
50	0.933	0.	0.09670	1.0444	–	–	−0.00163	−0.0176
51	0.933	−0.40	0.08395	0.9067	–	–	−0.00327	−0.0353
52	0.933	−0.73	0.07078	0.7644	–	–	−0.00321	−0.0347
53	0.933	−0.87	0.06788	0.7331	–	–	0.00011	0.0011
54	0.933	−0.93	0.05623	0.6073	–	–	0.00032	0.0034

Table 6.34 a). The tangential, vertical and radial mean velocity distribution at section S-8 run no.1 Um = 0.04444 m/s

Loc. no.	η = z/h	2Y/B	Tangential v [m/s]	Tangential v/Um	Vertical w [m/s]	Vertical w/Um	Radial u [m/s]	Radial u/Um
1	0.080	−0.93	0.00651	0.1465	–	–	–	–
2	0.080	−0.87	0.00882	0.1985	–	–	–	–
3	0.080	−0.73	0.01098	0.2469	–	–	–	–
4	0.080	−0.40	0.01350	0.3038	–	–	–	–
5	0.080	0.	0.01625	0.3656	–	–	–	–
6	0.080	0.40	0.02214	0.4981	–	–	–	–
7	0.080	0.73	0.02001	0.4503	–	–	–	–
8	0.080	0.87	0.02093	0.4709	–	–	–	–
9	0.080	0.93	0.01130	0.2542	–	–	–	–
10	0.140	0.93	0.03102	0.6979	–	–	–	–
11	0.140	0.87	0.04589	1.0326	–	–	–	–
12	0.140	0.73	0.04202	0.9454	–	–	–	–
13	0.140	0.40	0.04194	0.9436	–	–	–	–
14	0.140	0.	0.03306	0.7439	–	–	–	–
15	0.140	−0.40	0.02671	0.6010	–	–	–	–
16	0.140	−0.73	0.02165	0.4872	–	–	–	–
17	0.140	−0.87	0.01447	0.3256	–	–	–	–
18	0.140	−0.93	0.01030	0.2318	–	–	–	–
19	0.320	−0.93	0.02017	0.4539	–	–	–	–
20	0.320	−0.87	0.02658	0.5980	–	–	–	–
21	0.320	−0.73	0.03605	0.8110	–	–	–	–
22	0.320	−0.40	0.04194	0.9436	–	–	–	–
23	0.320	0.	0.04971	1.1185	–	–	–	–
24	0.320	0.40	0.05749	1.2934	–	–	–	–
25	0.320	0.73	0.06098	1.3721	–	–	–	–
26	0.320	0.87	0.06249	1.4060	–	–	–	–
27	0.320	0.93	0.04608	1.0368	–	–	–	–
28	0.600	0.93	0.04616	1.0386	–	–	–	–
29	0.600	0.87	0.06287	1.4145	–	–	–	–
30	0.600	0.73	0.06195	1.3939	–	–	–	–
31	0.600	0.40	0.05730	1.2892	–	–	–	–
32	0.600	0.	0.04748	1.0683	–	–	–	–
33	0.600	−0.40	0.03989	0.8976	–	–	–	–
34	0.600	−0.73	0.03290	0.7402	–	–	–	–
35	0.600	−0.87	0.03059	0.6882	–	–	–	–
36	0.600	−0.93	0.02537	0.5708	–	–	–	–
37	0.900	−0.93	0.01221	0.2748	–	–	–	–
38	0.900	−0.87	0.01770	0.3983	–	–	–	–
39	0.900	−0.73	0.02179	0.4903	–	–	–	–
40	0.900	−0.40	0.03962	0.8915	–	–	–	–
41	0.900	0.	0.04950	1.1137	–	–	–	–
42	0.900	0.40	0.05818	1.3092	–	–	–	–
43	0.900	0.73	0.05972	1.3437	–	–	–	–
44	0.900	0.87	0.05660	1.2734	–	–	–	–
45	0.900	0.93	0.04070	0.9157	–	–	–	–

Table 6.35 a). The tangential, vertical and radial mean velocity distribution at section S-8 run no.2 Um = 0.07407 m/s

Loc. no.	η = z/h	2Y/B	Tangential v [m/s]	Tangential v/Um	Vertical w [m/s]	Vertical w/Um	Radial u [m/s]	Radial u/Um
1	0.044	-0.93	0.01732	0.2339	-	-	-	-
2	0.044	-0.87	0.01956	0.2640	-	-	-	-
3	0.044	-0.73	0.02402	0.3243	-	-	-	-
4	0.044	-0.40	0.02510	0.3388	-	-	-	-
5	0.044	0.	0.02526	0.3410	-	-	-	-
6	0.044	0.40	0.02733	0.3690	-	-	-	-
7	0.044	0.73	0.03153	0.4256	-	-	-	-
8	0.044	0.87	0.03970	0.5360	-	-	-	-
9	0.044	0.93	0.02577	0.3479	-	-	-	-
10	0.078	0.93	0.06087	0.8218	-	-	-	-
11	0.078	0.87	0.07567	1.0215	-	-	-	-
12	0.078	0.73	0.06851	0.9249	-	-	-	-
13	0.078	0.40	0.06155	0.8309	-	-	-	-
14	0.078	0.	0.05423	0.7321	-	-	-	-
15	0.078	-0.40	0.04632	0.6253	-	-	-	-
16	0.078	-0.73	0.04126	0.5571	-	-	-	-
17	0.078	-0.87	0.03158	0.4263	-	-	-	-
18	0.078	-0.93	0.02765	0.3733	-	-	-	-
19	0.178	-0.93	0.04239	0.5723	-	-	-	-
20	0.178	-0.87	0.05038	0.6802	-	-	-	-
21	0.178	-0.73	0.05786	0.7811	-	-	-	-
22	0.178	-0.40	0.06706	0.9053	-	-	-	-
23	0.178	0.	0.07685	1.0375	-	-	-	-
24	0.178	0.40	0.08498	1.1472	-	-	-	-
25	0.178	0.73	0.08928	1.2053	-	-	-	-
26	0.178	0.87	0.09141	1.2340	-	-	-	-
27	0.178	0.93	0.07500	1.0125	-	-	-	-
28	0.422	0.93	0.07220	0.9747	-	-	-	-
29	0.422	0.87	0.09020	1.2176	-	-	-	-
30	0.422	0.73	0.09065	1.2238	-	-	-	-
31	0.422	0.40	0.08627	1.1646	-	-	-	-
32	0.422	0.	0.07621	1.0288	-	-	-	-
33	0.422	-0.40	0.06849	0.9246	-	-	-	-
34	0.422	-0.73	0.05695	0.7688	-	-	-	-
35	0.422	-0.87	0.05601	0.7561	-	-	-	-
36	0.422	-0.93	0.04667	0.6301	-	-	-	-
37	0.667	-0.93	0.03155	0.4260	-	-	-	-
38	0.667	-0.87	0.04070	0.5494	-	-	-	-
39	0.667	-0.73	0.04915	0.6635	-	-	-	-
40	0.667	-0.40	0.06373	0.8603	-	-	-	-
41	0.667	0.	0.07597	1.0255	-	-	-	-
42	0.667	0.40	0.08751	1.1813	-	-	-	-
43	0.667	0.73	0.08993	1.2140	-	-	-	-
44	0.667	0.87	0.08998	1.2147	-	-	-	-
45	0.667	0.93	0.07142	0.9642	-	-	-	-
46	0.911	0.93	0.06195	0.8363	-	-	-	-
47	0.911	0.87	0.07863	1.0615	-	-	-	-
48	0.911	0.73	0.08616	1.1632	-	-	-	-
49	0.911	0.40	0.08788	1.1864	-	-	-	-
50	0.911	0.	0.07917	1.0688	-	-	-	-
51	0.911	-0.40	0.06674	0.9010	-	-	-	-
52	0.911	-0.73	0.04861	0.6562	-	-	-	-
53	0.911	-0.87	0.04016	0.5422	-	-	-	-
54	0.911	-0.93	0.03155	0.4260	-	-	-	-

Table 6.36 a). The tangential, vertical and radial mean velocity distribution at section S-8 run no.3 Um = 0.09259 m/s

Loc. no.	η = z/h	2Y/B	Tangential v [m/s]	Tangential v/Um	Vertical w [m/s]	Vertical w/Um	Radial u [m/s]	Radial u/Um
1	0.033	-0.93	0.02725	0.2943	-	-	-	-
2	0.033	-0.87	0.03021	0.3263	-	-	-	-
3	0.033	-0.73	0.03753	0.4053	-	-	-	-
4	0.033	-0.40	0.04519	0.4881	-	-	-	-
5	0.033	0.	0.04716	0.5093	-	-	-	-
6	0.033	0.40	0.04334	0.4680	-	-	-	-
7	0.033	0.73	0.04519	0.4881	-	-	-	-
8	0.033	0.87	0.04866	0.5256	-	-	-	-
9	0.033	0.93	0.03855	0.4163	-	-	-	-
10	0.058	0.93	0.07554	0.8158	-	-	-	-
11	0.058	0.87	0.09194	0.9930	-	-	-	-
12	0.058	0.73	0.08826	0.9532	-	-	-	-
13	0.058	0.40	0.08032	0.8675	-	-	-	-
14	0.058	0.	0.07567	0.8172	-	-	-	-
15	0.058	-0.40	0.06607	0.7135	-	-	-	-
16	0.058	-0.73	0.05348	0.5776	-	-	-	-
17	0.058	-0.87	0.04191	0.4526	-	-	-	-
18	0.058	-0.93	0.03817	0.4122	-	-	-	-
19	0.133	-0.93	0.05434	0.5869	-	-	-	-
20	0.133	-0.87	0.06009	0.6490	-	-	-	-
21	0.133	-0.73	0.07153	0.7725	-	-	-	-
22	0.133	-0.40	0.08043	0.8687	-	-	-	-
23	0.133	0.	0.09030	0.9753	-	-	-	-
24	0.133	0.40	0.09786	1.0569	-	-	-	-
25	0.133	0.73	0.10160	1.0973	-	-	-	-
26	0.133	0.87	0.10096	1.0903	-	-	-	-
27	0.133	0.93	0.07976	0.8614	-	-	-	-
28	0.400	0.93	0.07788	0.8411	-	-	-	-
29	0.400	0.87	0.10179	1.0993	-	-	-	-
30	0.400	0.73	0.10367	1.1197	-	-	-	-
31	0.400	0.40	0.10074	1.0880	-	-	-	-
32	0.400	0.	0.09289	1.0032	-	-	-	-
33	0.400	-0.40	0.07879	0.8509	-	-	-	-
34	0.400	-0.73	0.07139	0.7710	-	-	-	-
35	0.400	-0.87	0.06693	0.7228	-	-	-	-
36	0.400	-0.93	0.05958	0.6435	-	-	-	-
37	0.667	-0.93	0.04433	0.4788	-	-	-	-
38	0.667	-0.87	0.05119	0.5529	-	-	-	-
39	0.667	-0.73	0.05469	0.5906	-	-	-	-
40	0.667	-0.40	0.07392	0.7983	-	-	-	-
41	0.667	0.	0.09297	1.0040	-	-	-	-
42	0.667	0.40	0.10152	1.0964	-	-	-	-
43	0.667	0.73	0.10192	1.1008	-	-	-	-
44	0.667	0.87	0.09633	1.0404	-	-	-	-
45	0.667	0.93	0.07260	0.7841	-	-	-	-
46	0.933	0.93	0.06660	0.7193	-	-	-	-
47	0.933	0.87	0.08850	0.9558	-	-	-	-
48	0.933	0.73	0.09773	1.0555	-	-	-	-
49	0.933	0.40	0.10125	1.0935	-	-	-	-
50	0.933	0.	0.09350	1.0098	-	-	-	-
51	0.933	-0.40	0.07782	0.8405	-	-	-	-
52	0.933	-0.73	0.06163	0.6656	-	-	-	-
53	0.933	-0.87	0.05358	0.5787	-	-	-	-
54	0.933	-0.93	0.04732	0.5110	-	-	-	-

Table 6.1 *b). The tangential, vertical and radial turbulence intensity distribution at section U-1 run no.1* *Um = 0.04444 m/s*

Loc. no.	η = z/h	2Y/B	Tangential $\sqrt{\overline{v'^2}}$ [m/s]	$\sqrt{\overline{v'^2}}$/Um	Vertical $\sqrt{\overline{w'^2}}$ [m/s]	$\sqrt{\overline{w'^2}}$/Um	Radial $\sqrt{\overline{u'^2}}$ [m/s]	$\sqrt{\overline{u'^2}}$/Um
1	0.080	-0.93	0.00102	0.0230	-	-	-	-
2	0.080	-0.87	0.00132	0.0297	-	-	-	-
3	0.080	-0.73	0.00151	0.0339	-	-	-	-
4	0.080	-0.40	0.00137	0.0309	-	-	-	-
5	0.080	0.	0.00100	0.0224	-	-	-	-
6	0.080	0.40	0.00153	0.0345	-	-	-	-
7	0.080	0.73	0.00188	0.0424	-	-	-	-
8	0.080	0.87	0.00078	0.0176	-	-	-	-
9	0.080	0.93	0.00097	0.0218	-	-	-	-
10	0.140	0.93	0.00022	0.0048	-	-	-	-
11	0.140	0.87	0.00086	0.0194	-	-	-	-
12	0.140	0.73	0.00019	0.0042	-	-	-	-
13	0.140	0.40	0.00030	0.0067	-	-	-	-
14	0.140	0.	0.00194	0.0436	-	-	-	-
15	0.140	-0.40	0.00178	0.0399	-	-	-	-
16	0.140	-0.73	0.00213	0.0478	-	-	-	-
17	0.140	-0.87	0.00258	0.0581	-	-	-	-
18	0.140	-0.93	0.00221	0.0496	-	-	-	-
19	0.320	-0.93	0.00124	0.0278	-	-	-	-
20	0.320	-0.87	0.00282	0.0636	-	-	-	-
21	0.320	-0.73	0.00140	0.0315	-	-	-	-
22	0.320	-0.40	0.00116	0.0260	-	-	-	-
23	0.320	0.	0.00178	0.0399	-	-	-	-
24	0.320	0.40	0.00143	0.0321	-	-	-	-
25	0.320	0.73	0.00011	0.0024	-	-	-	-
26	0.320	0.87	0.00277	0.0623	-	-	-	-
27	0.320	0.93	0.00145	0.0327	-	-	-	-
28	0.600	0.93	0.00121	0.0272	-	-	-	-
29	0.600	0.87	0.00178	0.0399	-	-	-	-
30	0.600	0.73	0.00339	0.0763	-	-	-	-
31	0.600	0.40	0.00226	0.0508	-	-	-	-
32	0.600	0.	0.00299	0.0672	-	-	-	-
33	0.600	-0.40	0.00360	0.0811	-	-	-	-
34	0.600	-0.73	0.00323	0.0726	-	-	-	-
35	0.600	-0.87	0.00258	0.0581	-	-	-	-
36	0.600	-0.93	0.00204	0.0460	-	-	-	-
37	0.900	-0.93	0.00161	0.0363	-	-	-	-
38	0.900	-0.87	0.00215	0.0484	-	-	-	-
39	0.900	-0.73	0.00231	0.0521	-	-	-	-
40	0.900	-0.40	0.00363	0.0817	-	-	-	-
41	0.900	0.	0.00331	0.0744	-	-	-	-
42	0.900	0.40	0.00312	0.0702	-	-	-	-
43	0.900	0.73	0.00312	0.0702	-	-	-	-
44	0.900	0.87	0.00221	0.0496	-	-	-	-
45	0.900	0.93	0.00178	0.0399	-	-	-	-

Table 6.2 *b). The tangential, vertical and radial turbulence intensity distribution at section U-1 run no.2* *Um = 0.07407 m/s*

Loc. no.	η = z/h	2Y/B	Tangential $\sqrt{\overline{v'^2}}$ [m/s]	$\sqrt{\overline{v'^2}}$/Um	Vertical $\sqrt{\overline{w'^2}}$ [m/s]	$\sqrt{\overline{w'^2}}$/Um	Radial $\sqrt{\overline{u'^2}}$ [m/s]	$\sqrt{\overline{u'^2}}$/Um
1	0.044	-0.93	0.00043	0.0058	-	-	-	-
2	0.044	-0.87	0.00065	0.0087	-	-	-	-
3	0.044	-0.73	0.00089	0.0120	-	-	-	-
4	0.044	-0.40	0.00065	0.0087	-	-	-	-
5	0.044	0.	0.00118	0.0160	-	-	-	-
6	0.044	0.40	0.00016	0.0022	-	-	-	-
7	0.044	0.73	0.00019	0.0025	-	-	-	-
8	0.044	0.87	0.00070	0.0094	-	-	-	-
9	0.044	0.93	0.00153	0.0207	-	-	-	-
10	0.078	0.93	0.00075	0.0102	-	-	-	-
11	0.078	0.87	0.00070	0.0094	-	-	-	-
12	0.078	0.73	0.00051	0.0069	-	-	-	-
13	0.078	0.40	0.00046	0.0062	-	-	-	-
14	0.078	0.	0.00135	0.0182	-	-	-	-
15	0.078	-0.40	0.00083	0.0113	-	-	-	-
16	0.078	-0.73	0.00094	0.0127	-	-	-	-
17	0.078	-0.87	0.00075	0.0102	-	-	-	-
18	0.078	-0.93	0.00008	0.0011	-	-	-	-
19	0.178	-0.93	0.00016	0.0022	-	-	-	-
20	0.178	-0.87	0.00282	0.0381	-	-	-	-
21	0.178	-0.73	0.00258	0.0349	-	-	-	-
22	0.178	-0.40	0.00113	0.0153	-	-	-	-
23	0.178	0.	0.00083	0.0113	-	-	-	-
24	0.178	0.40	0.00094	0.0127	-	-	-	-
25	0.178	0.73	0.00046	0.0062	-	-	-	-
26	0.178	0.87	0.00032	0.0044	-	-	-	-
27	0.178	0.93	0.00145	0.0196	-	-	-	-
28	0.422	0.93	0.00194	0.0261	-	-	-	-
29	0.422	0.87	0.00204	0.0276	-	-	-	-
30	0.422	0.73	0.00210	0.0283	-	-	-	-
31	0.422	0.40	0.00272	0.0367	-	-	-	-
32	0.422	0.	0.00258	0.0349	-	-	-	-
33	0.422	-0.40	0.00245	0.0330	-	-	-	-
34	0.422	-0.73	0.00231	0.0312	-	-	-	-
35	0.422	-0.87	0.00124	0.0167	-	-	-	-
36	0.422	-0.93	0.00048	0.0065	-	-	-	-
37	0.667	-0.93	0.00048	0.0065	-	-	-	-
38	0.667	-0.87	0.00032	0.0044	-	-	-	-
39	0.667	-0.73	0.00334	0.0450	-	-	-	-
40	0.667	-0.40	0.00339	0.0458	-	-	-	-
41	0.667	0.	0.00352	0.0476	-	-	-	-
42	0.667	0.40	0.00304	0.0410	-	-	-	-
43	0.667	0.73	0.00234	0.0316	-	-	-	-
44	0.667	0.87	0.00188	0.0254	-	-	-	-
45	0.667	0.93	0.00186	0.0251	-	-	-	-
46	0.911	0.93	0.00024	0.0033	-	-	-	-
47	0.911	0.87	0.00043	0.0058	-	-	-	-
48	0.911	0.73	0.00151	0.0203	-	-	-	-
49	0.911	0.40	0.00258	0.0349	-	-	-	-
50	0.911	0.	0.00350	0.0472	-	-	-	-
51	0.911	-0.40	0.00352	0.0476	-	-	-	-
52	0.911	-0.73	0.00331	0.0447	-	-	-	-
53	0.911	-0.87	0.00245	0.0330	-	-	-	-
54	0.911	-0.93	0.00081	0.0109	-	-	-	-

Table 6.3 *b). The tangential, vertical and radial turbulence intensity distribution at section U-1 run no.3* *Um = 0.09259 m/s*

Loc. no.	η = z/h	2Y/B	Tangential $\sqrt{\overline{v'^2}}$ [m/s]	Tangential $\sqrt{\overline{v'^2}}$/Um	Vertical $\sqrt{\overline{w'^2}}$ [m/s]	Vertical $\sqrt{\overline{w'^2}}$/Um	Radial $\sqrt{\overline{u'^2}}$ [m/s]	Radial $\sqrt{\overline{u'^2}}$/Um
1	0.033	-0.93	0.00065	0.0070	-	-	-	-
2	0.033	-0.87	0.00078	0.0084	-	-	-	-
3	0.033	-0.73	0.00097	0.0105	-	-	-	-
4	0.033	-0.40	0.00151	0.0163	-	-	-	-
5	0.033	0.	0.00234	0.0253	-	-	-	-
6	0.033	0.40	0.00266	0.0288	-	-	-	-
7	0.033	0.73	0.00280	0.0302	-	-	-	-
8	0.033	0.87	0.00137	0.0148	-	-	-	-
9	0.033	0.93	0.00094	0.0102	-	-	-	-
10	0.058	0.93	0.00040	0.0044	-	-	-	-
11	0.058	0.87	0.00070	0.0076	-	-	-	-
12	0.058	0.73	0.00167	0.0180	-	-	-	-
13	0.058	0.40	0.00231	0.0250	-	-	-	-
14	0.058	0.	0.00207	0.0224	-	-	-	-
15	0.058	-0.40	0.00266	0.0288	-	-	-	-
16	0.058	-0.73	0.00078	0.0084	-	-	-	-
17	0.058	-0.87	0.00011	0.0012	-	-	-	-
18	0.058	-0.93	0.00043	0.0046	-	-	-	-
19	0.133	-0.93	0.00011	0.0012	-	-	-	-
20	0.133	-0.87	0.00003	0.0003	-	-	-	-
21	0.133	-0.73	0.00258	0.0279	-	-	-	-
22	0.133	-0.40	0.00043	0.0046	-	-	-	-
23	0.133	0.	0.00132	0.0142	-	-	-	-
24	0.133	0.40	0.00051	0.0055	-	-	-	-
25	0.133	0.73	0.00231	0.0250	-	-	-	-
26	0.133	0.87	0.00143	0.0154	-	-	-	-
27	0.133	0.93	0.00105	0.0113	-	-	-	-
28	0.400	0.93	0.00043	0.0046	-	-	-	-
29	0.400	0.87	0.00054	0.0058	-	-	-	-
30	0.400	0.73	0.00151	0.0163	-	-	-	-
31	0.400	0.40	0.00304	0.0328	-	-	-	-
32	0.400	0.	0.00210	0.0227	-	-	-	-
33	0.400	-0.40	0.00204	0.0221	-	-	-	-
34	0.400	-0.73	0.00299	0.0322	-	-	-	-
35	0.400	-0.87	0.00030	0.0032	-	-	-	-
36	0.400	-0.93	0.00118	0.0128	-	-	-	-
37	0.667	-0.93	0.00062	0.0067	-	-	-	-
38	0.667	-0.87	0.00143	0.0154	-	-	-	-
39	0.667	-0.73	0.00355	0.0383	-	-	-	-
40	0.667	-0.40	0.00312	0.0337	-	-	-	-
41	0.667	0.	0.00328	0.0354	-	-	-	-
42	0.667	0.40	0.00331	0.0357	-	-	-	-
43	0.667	0.73	0.00218	0.0235	-	-	-	-
44	0.667	0.87	0.00118	0.0128	-	-	-	-
45	0.667	0.93	0.00140	0.0151	-	-	-	-
46	0.933	0.93	0.00137	0.0148	-	-	-	-
47	0.933	0.87	0.00038	0.0041	-	-	-	-
48	0.933	0.73	0.00043	0.0046	-	-	-	-
49	0.933	0.40	0.00223	0.0241	-	-	-	-
50	0.933	0.	0.00393	0.0424	-	-	-	-
51	0.933	-0.40	0.00379	0.0410	-	-	-	-
52	0.933	-0.73	0.00366	0.0395	-	-	-	-
53	0.933	-0.87	0.00118	0.0128	-	-	-	-
54	0.933	-0.93	0.00043	0.0046	-	-	-	-

Table 6.4 *b). The tangential, vertical and radial turbulence intensity distribution at section U-2 run no.1* *Um = 0.04444 m/s*

Loc. no.	η = z/h	2Y/B	Tangential $\sqrt{\overline{v'^2}}$ [m/s]	Tangential $\sqrt{\overline{v'^2}}$/Um	Vertical $\sqrt{\overline{w'^2}}$ [m/s]	Vertical $\sqrt{\overline{w'^2}}$/Um	Radial $\sqrt{\overline{u'^2}}$ [m/s]	Radial $\sqrt{\overline{u'^2}}$/Um
1	0.080	-0.93	0.00211	0.0474	-	-	-	-
2	0.080	-0.87	0.00258	0.0581	-	-	-	-
3	0.080	-0.73	0.00074	0.0166	-	-	-	-
4	0.080	-0.40	0.00047	0.0107	-	-	-	-
5	0.080	0.	0.00058	0.0130	-	-	-	-
6	0.080	0.40	0.00021	0.0047	-	-	-	-
7	0.080	0.73	0.00016	0.0036	-	-	-	-
8	0.080	0.87	0.00126	0.0285	-	-	-	-
9	0.080	0.93	0.00416	0.0937	-	-	-	-
10	0.140	0.93	0.00706	0.1589	-	-	0.00738	0.1660
11	0.140	0.87	0.00074	0.0166	-	-	0.00748	0.1684
12	0.140	0.73	0.00016	0.0036	-	-	0.00105	0.0237
13	0.140	0.40	0.00090	0.0202	-	-	0.00047	0.0107
14	0.140	0.	0.00105	0.0237	-	-	0.	0.
15	0.140	-0.40	0.00364	0.0818	-	-	0.00111	0.0249
16	0.140	-0.73	0.00126	0.0285	-	-	0.00095	0.0213
17	0.140	-0.87	0.00100	0.0225	-	-	0.00047	0.0107
18	0.140	-0.93	0.00074	0.0166	-	-	0.00042	0.0095
19	0.320	-0.93	0.00153	0.0344	0.00100	0.0225	0.00480	0.1079
20	0.320	-0.87	0.00216	0.0486	0.00116	0.0261	0.00253	0.0569
21	0.320	-0.73	0.00253	0.0569	0.00074	0.0166	0.00469	0.1055
22	0.320	-0.40	0.00390	0.0877	0.00100	0.0225	0.00153	0.0344
23	0.320	0.	0.00379	0.0854	0.00353	0.0794	0.00100	0.0225
24	0.320	0.40	0.00369	0.0830	0.00390	0.0877	0.00090	0.0202
25	0.320	0.73	0.00437	0.0984	0.00195	0.0439	0.00132	0.0296
26	0.320	0.87	0.00232	0.0522	0.00316	0.0711	0.00148	0.0332
27	0.320	0.93	0.00295	0.0664	0.00042	0.0095	0.00137	0.0308
28	0.600	0.93	0.00337	0.0759	0.00058	0.0130	0.00264	0.0593
29	0.600	0.87	0.00306	0.0688	0.00026	0.0059	0.00163	0.0368
30	0.600	0.73	0.00532	0.1198	0.00005	0.0012	0.00042	0.0095
31	0.600	0.40	0.00559	0.1257	0.00021	0.0047	0.00032	0.0071
32	0.600	0.	0.00269	0.0605	0.00111	0.0249	0.00074	0.0166
33	0.600	-0.40	0.00480	0.1079	0.00169	0.0379	0.00074	0.0166
34	0.600	-0.73	0.00216	0.0486	0.00037	0.0083	0.00026	0.0059
35	0.600	-0.87	0.00206	0.0462	0.00100	0.0225	0.00005	0.0012
36	0.600	-0.93	0.00337	0.0759	0.00005	0.0012	0.00211	0.0474
37	0.900	-0.93	0.00163	0.0368	0.00137	0.0308	0.00121	0.0273
38	0.900	-0.87	0.00032	0.0071	0.00032	0.0071	0.00132	0.0296
39	0.900	-0.73	0.00053	0.0119	0.00005	0.0012	0.00285	0.0640
40	0.900	-0.40	0.00105	0.0237	0.00105	0.0237	0.00026	0.0059
41	0.900	0.	0.00206	0.0462	0.00158	0.0356	0.00053	0.0119
42	0.900	0.40	0.00237	0.0534	0.00032	0.0071	0.00032	0.0071
43	0.900	0.73	0.00163	0.0368	0.00053	0.0119	0.00011	0.0024
44	0.900	0.87	0.00321	0.0723	0.00079	0.0178	0.00037	0.0083
45	0.900	0.93	0.00179	0.0403	0.00126	0.0285	0.00211	0.0474

Table 6.5 *b). The tangential, vertical and radial turbulence intensity distribution at section U-2 run no.2* Um = 0.07407 m/s

Loc. no.	η = z/h	2Y/B	Tangential $\sqrt{v'^2}$ [m/s]	Tangential $\sqrt{v'^2}$/Um	Vertical $\sqrt{w'^2}$ [m/s]	Vertical $\sqrt{w'^2}$/Um	Radial $\sqrt{u'^2}$ [m/s]	Radial $\sqrt{u'^2}$/Um
1	0.044	-0.93	0.00200	0.0270	-	-	-	-
2	0.044	-0.87	0.00358	0.0484	-	-	-	-
3	0.044	-0.73	0.00453	0.0612	-	-	-	-
4	0.044	-0.40	0.00364	0.0491	-	-	-	-
5	0.044	0.	0.00337	0.0455	-	-	-	-
6	0.044	0.40	0.00348	0.0470	-	-	-	-
7	0.044	0.73	0.00327	0.0441	-	-	-	-
8	0.044	0.87	0.00179	0.0242	-	-	-	-
9	0.044	0.93	0.00532	0.0719	-	-	-	-
10	0.078	0.93	0.00532	0.0719	-	-	-	-
11	0.078	0.87	0.00458	0.0619	-	-	-	-
12	0.078	0.73	0.00264	0.0356	-	-	-	-
13	0.078	0.40	0.00374	0.0505	-	-	-	-
14	0.078	0.	0.00458	0.0619	-	-	-	-
15	0.078	-0.40	0.00506	0.0683	-	-	-	-
16	0.078	-0.73	0.00585	0.0790	-	-	-	-
17	0.078	-0.87	0.00506	0.0683	-	-	-	-
18	0.078	-0.93	0.00469	0.0633	-	-	-	-
19	0.178	-0.93	0.00822	0.1110	0.00327	0.0441	0.00891	0.1202
20	0.178	-0.87	0.00448	0.0605	0.00163	0.0221	0.01244	0.1679
21	0.178	-0.73	0.00458	0.0619	0.00095	0.0128	0.00917	0.1238
22	0.178	-0.40	0.00596	0.0804	0.00084	0.0114	0.00374	0.0505
23	0.178	0.	0.00643	0.0868	0.00095	0.0128	0.00200	0.0270
24	0.178	0.40	0.00659	0.0889	0.00063	0.0085	0.00190	0.0256
25	0.178	0.73	0.00469	0.0633	0.00253	0.0341	0.00506	0.0683
26	0.178	0.87	0.01138	0.1537	0.00158	0.0213	0.00416	0.0562
27	0.178	0.93	0.01159	0.1565	0.00037	0.0050	0.00648	0.0875
28	0.422	0.93	0.01038	0.1402	0.00158	0.0213	0.00632	0.0854
29	0.422	0.87	0.00237	0.0320	0.00032	0.0043	0.00585	0.0790
30	0.422	0.73	0.00184	0.0249	0.00069	0.0092	0.00659	0.0889
31	0.422	0.40	0.00379	0.0512	0.00195	0.0263	0.00248	0.0334
32	0.422	0.	0.00785	0.1060	0.00190	0.0256	0.00559	0.0754
33	0.422	-0.40	0.00617	0.0832	0.00111	0.0149	0.00527	0.0711
34	0.422	-0.73	0.00553	0.0747	0.00021	0.0028	0.00759	0.1024
35	0.422	-0.87	0.00321	0.0434	0.00032	0.0043	0.00437	0.0591
36	0.422	-0.93	0.00559	0.0754	0.00011	0.0014	0.00527	0.0711
37	0.667	-0.93	0.01180	0.1594	0.00411	0.0555	0.00669	0.0904
38	0.667	-0.87	0.01049	0.1416	0.00369	0.0498	0.00564	0.0761
39	0.667	-0.73	0.01275	0.1722	0.00084	0.0114	0.00300	0.0406
40	0.667	-0.40	0.00437	0.0591	0.00179	0.0242	0.00516	0.0697
41	0.667	0.	0.00258	0.0349	0.00179	0.0242	0.00105	0.0142
42	0.667	0.40	0.00258	0.0349	0.00200	0.0270	0.00870	0.1174
43	0.667	0.73	0.00290	0.0391	0.00242	0.0327	0.00791	0.1067
44	0.667	0.87	0.00005	0.0007	0.00153	0.0206	0.00585	0.0790
45	0.667	0.93	0.00137	0.0185	0.00032	0.0043	0.00738	0.0996
46	0.911	0.93	0.00179	0.0242	-	-	0.01001	0.1352
47	0.911	0.87	0.00090	0.0121	-	-	0.00906	0.1224
48	0.911	0.73	0.00163	0.0221	-	-	0.00337	0.0455
49	0.911	0.40	0.00522	0.0704	-	-	0.00443	0.0598
50	0.911	0.	0.00843	0.1138	-	-	0.00580	0.0783
51	0.911	-0.40	0.00701	0.0946	-	-	0.00495	0.0669
52	0.911	-0.73	0.00206	0.0277	-	-	0.01054	0.1423
53	0.911	-0.87	0.00074	0.0100	-	-	0.01070	0.1444
54	0.911	-0.93	0.00258	0.0349	-	-	0.01107	0.1494

Table 6.6 *b). The tangential, vertical and radial turbulence intensity distribution at section U-2 run no.3* Um = 0.09259 m/s

Loc. no.	η = z/h	2Y/B	Tangential $\sqrt{v'^2}$ [m/s]	Tangential $\sqrt{v'^2}$/Um	Vertical $\sqrt{w'^2}$ [m/s]	Vertical $\sqrt{w'^2}$/Um	Radial $\sqrt{u'^2}$ [m/s]	Radial $\sqrt{u'^2}$/Um
1	0.033	-0.93	0.00237	0.0256	-	-	-	-
2	0.033	-0.87	0.00105	0.0114	-	-	-	-
3	0.033	-0.73	0.00126	0.0137	-	-	-	-
4	0.033	-0.40	0.00132	0.0142	-	-	-	-
5	0.033	0.	0.00090	0.0097	-	-	-	-
6	0.033	0.40	0.00063	0.0068	-	-	-	-
7	0.033	0.73	0.00153	0.0165	-	-	-	-
8	0.033	0.87	0.00200	0.0216	-	-	-	-
9	0.033	0.93	0.00812	0.0877	-	-	-	-
10	0.058	0.93	0.00864	0.0933	-	-	-	-
11	0.058	0.87	0.00158	0.0171	-	-	-	-
12	0.058	0.73	0.00216	0.0233	-	-	-	-
13	0.058	0.40	0.00111	0.0120	-	-	-	-
14	0.058	0.	0.00211	0.0228	-	-	-	-
15	0.058	-0.40	0.00084	0.0091	-	-	-	-
16	0.058	-0.73	0.00311	0.0336	-	-	-	-
17	0.058	-0.87	0.00495	0.0535	-	-	-	-
18	0.058	-0.93	0.00548	0.0592	-	-	-	-
19	0.133	-0.93	0.00200	0.0216	0.00021	0.0023	0.00406	0.0438
20	0.133	-0.87	0.00269	0.0290	0.00074	0.0080	0.00490	0.0529
21	0.133	-0.73	0.00063	0.0068	0.00100	0.0108	0.00453	0.0489
22	0.133	-0.40	0.00611	0.0660	0.00548	0.0592	0.00480	0.0518
23	0.133	0.	0.00585	0.0632	0.00069	0.0074	0.00032	0.0034
24	0.133	0.40	0.00490	0.0529	0.00258	0.0279	0.00053	0.0057
25	0.133	0.73	0.00559	0.0603	0.00126	0.0137	0.00195	0.0211
26	0.133	0.87	0.00401	0.0433	0.00026	0.0028	0.00126	0.0137
27	0.133	0.93	0.00242	0.0262	0.00047	0.0051	0.00232	0.0250
28	0.400	0.93	0.00248	0.0268	0.00190	0.0205	0.00232	0.0250
29	0.400	0.87	0.00379	0.0410	0.00126	0.0137	0.00232	0.0250
30	0.400	0.73	0.00469	0.0507	0.00190	0.0205	0.00111	0.0120
31	0.400	0.40	0.00601	0.0649	0.00032	0.0034	0.00069	0.0074
32	0.400	0.	0.00543	0.0586	0.00232	0.0250	0.00074	0.0080
33	0.400	-0.40	0.00506	0.0546	0.00327	0.0353	0.00079	0.0085
34	0.400	-0.73	0.00532	0.0575	0.00095	0.0102	0.00105	0.0114
35	0.400	-0.87	0.00348	0.0376	0.00137	0.0148	0.00169	0.0182
36	0.400	-0.93	0.00532	0.0575	0.00021	0.0023	0.00053	0.0057
37	0.667	-0.93	0.00074	0.0080	0.00379	0.0410	0.00063	0.0068
38	0.667	-0.87	0.00348	0.0376	0.00195	0.0211	0.00079	0.0085
39	0.667	-0.73	0.00401	0.0433	0.00126	0.0137	0.00105	0.0114
40	0.667	-0.40	0.00532	0.0575	0.00748	0.0808	0.00084	0.0091
41	0.667	0.	0.00669	0.0723	0.00148	0.0159	0.00032	0.0034
42	0.667	0.40	0.00743	0.0803	0.00016	0.0017	0.00074	0.0080
43	0.667	0.73	0.00717	0.0774	0.00047	0.0051	0.00042	0.0046
44	0.667	0.87	0.00938	0.1013	0.00527	0.0569	0.00137	0.0148
45	0.667	0.93	0.00796	0.0859	0.00759	0.0820	0.00237	0.0256
46	0.933	0.93	0.00812	0.0877	-	-	0.00126	0.0137
47	0.933	0.87	0.00264	0.0285	-	-	0.00253	0.0273
48	0.933	0.73	0.00495	0.0535	-	-	0.00227	0.0245
49	0.933	0.40	0.00622	0.0672	-	-	0.00390	0.0421
50	0.933	0.	0.00675	0.0729	-	-	0.00100	0.0108
51	0.933	-0.40	0.00348	0.0376	-	-	0.00105	0.0114
52	0.933	-0.73	0.00469	0.0507	-	-	0.00190	0.0205
53	0.933	-0.87	0.00190	0.0205	-	-	0.00190	0.0205
54	0.933	-0.93	0.00706	0.0763	-	-	0.00237	0.0256

Table 6.7 *b). The tangential, vertical and radial turbulence intensity distribution at section U-3 run no.1* *Um = 0.04444 m/s*

Loc. no.	η = z/h	2Y/B	Tangential		Vertical		Radial	
			$\sqrt{\overline{v'^2}}$ [m/s]	$\sqrt{\overline{v'^2}}$/Um	$\sqrt{\overline{w'^2}}$ [m/s]	$\sqrt{\overline{w'^2}}$/Um	$\sqrt{\overline{u'^2}}$ [m/s]	$\sqrt{\overline{u'^2}}$/Um
1	0.080	−0.93	0.00137	0.0308	–	–	–	–
2	0.080	−0.87	0.00227	0.0510	–	–	–	–
3	0.080	−0.73	0.00142	0.0320	–	–	–	–
4	0.080	−0.40	0.00264	0.0593	–	–	–	–
5	0.080	0.	0.	0.	–	–	–	–
6	0.080	0.40	0.00053	0.0119	–	–	–	–
7	0.080	0.73	0.00374	0.0842	–	–	–	–
8	0.080	0.87	0.00295	0.0664	–	–	–	–
9	0.080	0.93	0.00190	0.0427	–	–	–	–
10	0.140	0.93	0.00126	0.0285	–	–	0.00200	0.0451
11	0.140	0.87	0.00169	0.0379	–	–	0.00100	0.0225
12	0.140	0.73	0.00295	0.0664	–	–	0.00005	0.0012
13	0.140	0.40	0.00163	0.0368	–	–	0.00074	0.0166
14	0.140	0.	0.00069	0.0154	–	–	0.00016	0.0036
15	0.140	−0.40	0.00216	0.0486	–	–	0.00042	0.0095
16	0.140	−0.73	0.00126	0.0285	–	–	0.00021	0.0047
17	0.140	−0.87	0.00074	0.0166	–	–	0.00116	0.0261
18	0.140	−0.93	0.00084	0.0190	–	–	0.00142	0.0320
19	0.320	−0.93	0.00069	0.0154	0.00032	0.0071	0.00169	0.0379
20	0.320	−0.87	0.00153	0.0344	0.00379	0.0854	0.00047	0.0107
21	0.320	−0.73	0.00416	0.0937	0.00190	0.0427	0.00285	0.0640
22	0.320	−0.40	0.00432	0.0972	0.00137	0.0308	0.00090	0.0202
23	0.320	0.	0.00406	0.0913	0.00285	0.0640	0.00074	0.0166
24	0.320	0.40	0.00474	0.1067	0.00232	0.0522	0.00042	0.0095
25	0.320	0.73	0.00469	0.1055	0.00390	0.0877	0.00079	0.0178
26	0.320	0.87	0.00458	0.1032	0.00258	0.0581	0.00084	0.0190
27	0.320	0.93	0.00348	0.0783	0.00206	0.0462	0.00090	0.0202
28	0.600	0.93	0.00390	0.0877	0.00142	0.0320	0.00153	0.0344
29	0.600	0.87	0.00364	0.0818	0.00137	0.0308	0.00242	0.0545
30	0.600	0.73	0.00495	0.1115	0.00126	0.0285	0.00084	0.0190
31	0.600	0.40	0.00506	0.1138	0.00142	0.0320	0.00037	0.0083
32	0.600	0.	0.00437	0.0984	0.00148	0.0332	0.00005	0.0012
33	0.600	−0.40	0.00316	0.0711	0.00242	0.0545	0.00032	0.0071
34	0.600	−0.73	0.00232	0.0522	0.00142	0.0320	0.00026	0.0059
35	0.600	−0.87	0.00242	0.0545	0.00216	0.0486	0.00343	0.0771
36	0.600	−0.93	0.00321	0.0723	0.00227	0.0510	0.00137	0.0308
37	0.900	−0.93	0.00495	0.1115	0.00216	0.0486	0.00111	0.0249
38	0.900	−0.87	0.00232	0.0522	0.00227	0.0510	0.00216	0.0486
39	0.900	−0.73	0.00079	0.0178	0.00142	0.0320	0.00279	0.0628
40	0.900	−0.40	0.00432	0.0972	0.00206	0.0462	0.00242	0.0545
41	0.900	0.	0.00348	0.0783	0.00190	0.0427	0.00179	0.0403
42	0.900	0.40	0.00543	0.1221	0.00195	0.0439	0.00069	0.0154
43	0.900	0.73	0.00264	0.0593	0.00163	0.0368	0.00021	0.0047
44	0.900	0.87	0.00348	0.0783	0.00137	0.0308	0.00058	0.0130
45	0.900	0.93	0.00163	0.0368	0.00058	0.0130	0.00084	0.0190

Table 6.8 *b). The tangential, vertical and radial turbulence intensity distribution at section U-3 run no.2* *Um = 0.07407 m/s*

Loc. no.	η = z/h	2Y/B	Tangential		Vertical		Radial	
			$\sqrt{\overline{v'^2}}$ [m/s]	$\sqrt{\overline{v'^2}}$/Um	$\sqrt{\overline{w'^2}}$ [m/s]	$\sqrt{\overline{w'^2}}$/Um	$\sqrt{\overline{u'^2}}$ [m/s]	$\sqrt{\overline{u'^2}}$/Um
1	0.044	−0.93	0.00153	0.0206	–	–	–	–
2	0.044	−0.87	0.00095	0.0128	–	–	–	–
3	0.044	−0.73	0.00058	0.0078	–	–	–	–
4	0.044	−0.40	0.00142	0.0192	–	–	–	–
5	0.044	0.	0.00211	0.0285	–	–	–	–
6	0.044	0.40	0.00374	0.0505	–	–	–	–
7	0.044	0.73	0.00343	0.0462	–	–	–	–
8	0.044	0.87	0.00390	0.0526	–	–	–	–
9	0.044	0.93	0.00474	0.0640	–	–	–	–
10	0.078	0.93	0.01317	0.1779	–	–	–	–
11	0.078	0.87	0.00042	0.0057	–	–	–	–
12	0.078	0.73	0.00864	0.1167	–	–	–	–
13	0.078	0.40	0.00959	0.1295	–	–	–	–
14	0.078	0.	0.00179	0.0242	–	–	–	–
15	0.078	−0.40	0.00121	0.0164	–	–	–	–
16	0.078	−0.73	0.00142	0.0192	–	–	–	–
17	0.078	−0.87	0.00126	0.0171	–	–	–	–
18	0.078	−0.93	0.00126	0.0171	–	–	–	–
19	0.178	−0.93	0.00300	0.0406	0.00058	0.0078	0.00042	0.0057
20	0.178	−0.87	0.00416	0.0562	0.00195	0.0263	0.00063	0.0085
21	0.178	−0.73	0.00427	0.0576	0.00348	0.0470	0.00032	0.0043
22	0.178	−0.40	0.00443	0.0598	0.00126	0.0171	0.00063	0.0085
23	0.178	0.	0.00543	0.0733	0.00026	0.0036	0.00126	0.0171
24	0.178	0.40	0.00427	0.0576	0.00163	0.0221	0.00074	0.0100
25	0.178	0.73	0.00158	0.0213	0.00021	0.0028	0.00137	0.0185
26	0.178	0.87	0.00169	0.0228	0.00153	0.0206	0.00016	0.0021
27	0.178	0.93	0.00248	0.0334	0.00227	0.0306	0.00211	0.0285
28	0.422	0.93	0.00453	0.0612	0.00084	0.0114	0.00285	0.0384
29	0.422	0.87	0.00490	0.0662	0.00021	0.0028	0.00111	0.0149
30	0.422	0.73	0.00506	0.0683	0.00047	0.0064	0.00042	0.0057
31	0.422	0.40	0.00506	0.0683	0.00084	0.0114	0.00011	0.0014
32	0.422	0.	0.00495	0.0669	0.00163	0.0221	0.00137	0.0185
33	0.422	−0.40	0.00416	0.0562	0.00069	0.0092	0.00084	0.0114
34	0.422	−0.73	0.00274	0.0370	0.00126	0.0171	0.00063	0.0085
35	0.422	−0.87	0.00358	0.0484	0.00005	0.0007	0.00121	0.0164
36	0.422	−0.93	0.00269	0.0363	0.00032	0.0043	0.00184	0.0249
37	0.667	−0.93	0.00285	0.0384	0.00069	0.0092	0.00337	0.0455
38	0.667	−0.87	0.00285	0.0384	0.00158	0.0213	0.00084	0.0114
39	0.667	−0.73	0.00232	0.0313	0.00069	0.0092	0.00121	0.0164
40	0.667	−0.40	0.00111	0.0149	0.00063	0.0085	0.00084	0.0114
41	0.667	0.	0.00501	0.0676	0.00037	0.0050	0.00116	0.0157
42	0.667	0.40	0.00453	0.0612	0.00158	0.0213	0.00190	0.0256
43	0.667	0.73	0.00580	0.0783	0.00153	0.0206	0.00084	0.0114
44	0.667	0.87	0.00585	0.0790	0.00063	0.0085	0.00042	0.0057
45	0.667	0.93	0.00543	0.0733	0.00047	0.0064	0.00232	0.0313
46	0.911	0.93	0.00232	0.0313	–	–	0.00121	0.0164
47	0.911	0.87	0.00021	0.0028	–	–	0.00179	0.0242
48	0.911	0.73	0.00179	0.0242	–	–	0.00121	0.0164
49	0.911	0.40	0.00021	0.0028	–	–	0.00163	0.0221
50	0.911	0.	0.00227	0.0306	–	–	0.00232	0.0313
51	0.911	−0.40	0.00142	0.0192	–	–	0.00253	0.0341
52	0.911	−0.73	0.00005	0.0007	–	–	0.00343	0.0462
53	0.911	−0.87	0.00121	0.0164	–	–	0.00274	0.0370
54	0.911	−0.93	0.00137	0.0185	–	–	0.00306	0.0413

Table 6.9 *b). The tangential, vertical and radial turbulence intensity distribution at section U-3 run no.3* *Um = 0.09259 m/s*

Loc. no.	η = z/h	2Y/B	Tangential $\sqrt{\overline{v'^2}}$ [m/s]	Tangential $\sqrt{\overline{v'^2}}$/Um	Vertical $\sqrt{\overline{w'^2}}$ [m/s]	Vertical $\sqrt{\overline{w'^2}}$/Um	Radial $\sqrt{\overline{u'^2}}$ [m/s]	Radial $\sqrt{\overline{u'^2}}$/Um
1	0.033	-0.93	0.00153	0.0165	-	-	-	-
2	0.033	-0.87	0.00179	0.0194	-	-	-	-
3	0.033	-0.73	0.00195	0.0211	-	-	-	-
4	0.033	-0.40	0.00079	0.0085	-	-	-	-
5	0.033	0.	0.00116	0.0125	-	-	-	-
6	0.033	0.40	0.00037	0.0040	-	-	-	-
7	0.033	0.73	0.00032	0.0034	-	-	-	-
8	0.033	0.87	0.	0.	-	-	-	-
9	0.033	0.93	0.00047	0.0051	-	-	-	-
10	0.058	0.93	0.00206	0.0222	-	-	-	-
11	0.058	0.87	0.00242	0.0262	-	-	-	-
12	0.058	0.73	0.00195	0.0211	-	-	-	-
13	0.058	0.40	0.00058	0.0063	-	-	-	-
14	0.058	0.	0.00063	0.0068	-	-	-	-
15	0.058	-0.40	0.00063	0.0068	-	-	-	-
16	0.058	-0.73	0.00074	0.0080	-	-	-	-
17	0.058	-0.87	0.00121	0.0131	-	-	-	-
18	0.058	-0.93	0.00111	0.0120	-	-	-	-
19	0.133	-0.93	0.00074	0.0080	0.00137	0.0148	0.00416	0.0450
20	0.133	-0.87	0.00058	0.0063	0.00242	0.0262	0.00179	0.0194
21	0.133	-0.73	0.00401	0.0433	0.00142	0.0154	0.00206	0.0222
22	0.133	-0.40	0.00348	0.0376	0.00037	0.0040	0.00237	0.0256
23	0.133	0.	0.00132	0.0142	0.00169	0.0182	0.00506	0.0546
24	0.133	0.40	0.00453	0.0489	0.00132	0.0142	0.00854	0.0922
25	0.133	0.73	0.00501	0.0541	0.00047	0.0051	0.00116	0.0125
26	0.133	0.87	0.00401	0.0433	0.00179	0.0194	0.00042	0.0046
27	0.133	0.93	0.00274	0.0296	0.00206	0.0222	0.00311	0.0336
28	0.400	0.93	0.00295	0.0319	0.00163	0.0176	0.00184	0.0199
29	0.400	0.87	0.00327	0.0353	0.00179	0.0194	0.00042	0.0046
30	0.400	0.73	0.00374	0.0404	0.00126	0.0137	0.00026	0.0028
31	0.400	0.40	0.00611	0.0660	0.00100	0.0108	0.00195	0.0211
32	0.400	0.	0.00553	0.0598	0.00005	0.0006	0.00211	0.0228
33	0.400	-0.40	0.00506	0.0546	0.00063	0.0068	0.00116	0.0125
34	0.400	-0.73	0.00427	0.0461	0.00126	0.0137	0.00105	0.0114
35	0.400	-0.87	0.00242	0.0262	0.00169	0.0182	0.00032	0.0034
36	0.400	-0.93	0.00111	0.0120	0.00058	0.0063	0.00179	0.0194
37	0.667	-0.93	0.01001	0.1081	0.00074	0.0080	0.00306	0.0330
38	0.667	-0.87	0.00574	0.0620	0.00126	0.0137	0.00337	0.0364
39	0.667	-0.73	0.00142	0.0154	0.00195	0.0211	0.00084	0.0091
40	0.667	-0.40	0.00195	0.0211	0.00090	0.0097	0.00100	0.0108
41	0.667	0.	0.00364	0.0393	0.00047	0.0051	0.00074	0.0080
42	0.667	0.40	0.00269	0.0290	0.00195	0.0211	0.00005	0.0006
43	0.667	0.73	0.00480	0.0518	0.00469	0.0507	0.00084	0.0091
44	0.667	0.87	0.00047	0.0051	0.00522	0.0563	0.00084	0.0091
45	0.667	0.93	0.00037	0.0040	0.00437	0.0472	0.00074	0.0080
46	0.933	0.93	0.00653	0.0706	-	-	0.00126	0.0137
47	0.933	0.87	0.00058	0.0063	-	-	0.00148	0.0159
48	0.933	0.73	0.00348	0.0376	-	-	0.00227	0.0245
49	0.933	0.40	0.00474	0.0512	-	-	0.00179	0.0194
50	0.933	0.	0.00469	0.0507	-	-	0.00153	0.0165
51	0.933	-0.40	0.00253	0.0273	-	-	0.00042	0.0046
52	0.933	-0.73	0.00021	0.0023	-	-	0.00179	0.0194
53	0.933	-0.87	0.00126	0.0137	-	-	0.00111	0.0120
54	0.933	-0.93	0.01007	0.1087	-	-	0.00058	0.0063

Table 6.10 *b). The tangential, vertical and radial turbulence intensity distribution at section U-4 run no.1* *Um = 0.04444 m/s*

Loc. no.	η = z/h	2Y/B	Tangential $\sqrt{\overline{v'^2}}$ [m/s]	Tangential $\sqrt{\overline{v'^2}}$/Um	Vertical $\sqrt{\overline{w'^2}}$ [m/s]	Vertical $\sqrt{\overline{w'^2}}$/Um	Radial $\sqrt{\overline{u'^2}}$ [m/s]	Radial $\sqrt{\overline{u'^2}}$/Um
1	0.080	-0.93	0.00124	0.0278	-	-	-	-
2	0.080	-0.87	0.00022	0.0048	-	-	-	-
3	0.080	-0.73	0.00035	0.0079	-	-	-	-
4	0.080	-0.40	0.00167	0.0375	-	-	-	-
5	0.080	0.	0.00253	0.0569	-	-	-	-
6	0.080	0.40	0.00032	0.0073	-	-	-	-
7	0.080	0.73	0.00387	0.0872	-	-	-	-
8	0.080	0.87	0.00204	0.0460	-	-	-	-
9	0.080	0.93	0.00113	0.0254	-	-	-	-
10	0.140	0.93	0.00495	0.1114	-	-	-	-
11	0.140	0.87	0.00656	0.1477	-	-	-	-
12	0.140	0.73	0.00172	0.0387	-	-	-	-
13	0.140	0.40	0.00866	0.1949	-	-	-	-
14	0.140	0.	0.00495	0.1114	-	-	-	-
15	0.140	-0.40	0.00218	0.0490	-	-	-	-
16	0.140	-0.73	0.00035	0.0079	-	-	-	-
17	0.140	-0.87	0.00043	0.0097	-	-	-	-
18	0.140	-0.93	0.00019	0.0042	-	-	-	-
19	0.320	-0.93	0.00100	0.0224	-	-	-	-
20	0.320	-0.87	0.00215	0.0484	-	-	-	-
21	0.320	-0.73	0.00091	0.0206	-	-	-	-
22	0.320	-0.40	0.00086	0.0194	-	-	-	-
23	0.320	0.	0.00178	0.0399	-	-	-	-
24	0.320	0.40	0.00231	0.0521	-	-	-	-
25	0.320	0.73	0.00102	0.0230	-	-	-	-
26	0.320	0.87	0.00301	0.0678	-	-	-	-
27	0.320	0.93	0.00135	0.0303	-	-	-	-
28	0.600	0.93	0.00285	0.0642	-	-	-	-
29	0.600	0.87	0.00156	0.0351	-	-	-	-
30	0.600	0.73	0.00188	0.0424	-	-	-	-
31	0.600	0.40	0.00194	0.0436	-	-	-	-
32	0.600	0.	0.00145	0.0327	-	-	-	-
33	0.600	-0.40	0.00167	0.0375	-	-	-	-
34	0.600	-0.73	0.00056	0.0127	-	-	-	-
35	0.600	-0.87	0.00075	0.0169	-	-	-	-
36	0.600	-0.93	0.00073	0.0163	-	-	-	-
37	0.900	-0.93	0.00078	0.0176	-	-	-	-
38	0.900	-0.87	0.00083	0.0188	-	-	-	-
39	0.900	-0.73	0.00108	0.0242	-	-	-	-
40	0.900	-0.40	0.00178	0.0399	-	-	-	-
41	0.900	0.	0.00231	0.0521	-	-	-	-
42	0.900	0.40	0.00234	0.0527	-	-	-	-
43	0.900	0.73	0.00285	0.0642	-	-	-	-
44	0.900	0.87	0.00030	0.0067	-	-	-	-
45	0.900	0.93	0.00027	0.0061	-	-	-	-

Table 6.11 b). The tangential, vertical and radial turbulence intensity distribution at section U-4 run no.2 Um = 0.07407 m/s

Loc. no.	η = z/h	2Y/B	Tangential $\sqrt{v'^2}$ [m/s]	Tangential $\sqrt{v'^2}$/Um	Vertical $\sqrt{w'^2}$ [m/s]	Vertical $\sqrt{w'^2}$/Um	Radial $\sqrt{u'^2}$ [m/s]	Radial $\sqrt{u'^2}$/Um
1	0.044	-0.93	0.00016	0.0022	-	-	-	-
2	0.044	-0.87	0.00051	0.0069	-	-	-	-
3	0.044	-0.73	0.00360	0.0487	-	-	-	-
4	0.044	-0.40	0.00250	0.0338	-	-	-	-
5	0.044	0.	0.00465	0.0628	-	-	-	-
6	0.044	0.40	0.00086	0.0116	-	-	-	-
7	0.044	0.73	0.00231	0.0312	-	-	-	-
8	0.044	0.87	0.00188	0.0254	-	-	-	-
9	0.044	0.93	0.00097	0.0131	-	-	-	-
10	0.078	0.93	0.00549	0.0741	-	-	-	-
11	0.078	0.87	0.00562	0.0759	-	-	-	-
12	0.078	0.73	0.00169	0.0229	-	-	-	-
13	0.078	0.40	0.00043	0.0058	-	-	-	-
14	0.078	0.	0.00183	0.0247	-	-	-	-
15	0.078	-0.40	0.00253	0.0341	-	-	-	-
16	0.078	-0.73	0.00280	0.0378	-	-	-	-
17	0.078	-0.87	0.00191	0.0258	-	-	-	-
18	0.078	-0.93	0.00038	0.0051	-	-	-	-
19	0.178	-0.93	0.00159	0.0214	-	-	-	-
20	0.178	-0.87	0.00118	0.0160	-	-	-	-
21	0.178	-0.73	0.00016	0.0022	-	-	-	-
22	0.178	-0.40	0.00226	0.0305	-	-	-	-
23	0.178	0.	0.00285	0.0385	-	-	-	-
24	0.178	0.40	0.00202	0.0272	-	-	-	-
25	0.178	0.73	0.00135	0.0182	-	-	-	-
26	0.178	0.87	0.00054	0.0073	-	-	-	-
27	0.178	0.93	0.00022	0.0029	-	-	-	-
28	0.422	0.93	0.00196	0.0265	-	-	-	-
29	0.422	0.87	0.00213	0.0287	-	-	-	-
30	0.422	0.73	0.00215	0.0291	-	-	-	-
31	0.422	0.40	0.00371	0.0501	-	-	-	-
32	0.422	0.	0.00256	0.0345	-	-	-	-
33	0.422	-0.40	0.00135	0.0182	-	-	-	-
34	0.422	-0.73	0.00054	0.0073	-	-	-	-
35	0.422	-0.87	0.00172	0.0232	-	-	-	-
36	0.422	-0.93	0.00024	0.0033	-	-	-	-
37	0.667	-0.93	0.00016	0.0022	-	-	-	-
38	0.667	-0.87	0.00043	0.0058	-	-	-	-
39	0.667	-0.73	0.00091	0.0123	-	-	-	-
40	0.667	-0.40	0.00164	0.0222	-	-	-	-
41	0.667	0.	0.00296	0.0399	-	-	-	-
42	0.667	0.40	0.00328	0.0443	-	-	-	-
43	0.667	0.73	0.00272	0.0367	-	-	-	-
44	0.667	0.87	0.00258	0.0349	-	-	-	-
45	0.667	0.93	0.00164	0.0222	-	-	-	-
46	0.911	0.93	0.00016	0.0022	-	-	-	-
47	0.911	0.87	0.00258	0.0349	-	-	-	-
48	0.911	0.73	0.00309	0.0418	-	-	-	-
49	0.911	0.40	0.00272	0.0367	-	-	-	-
50	0.911	0.	0.00325	0.0439	-	-	-	-
51	0.911	-0.40	0.00218	0.0294	-	-	-	-
52	0.911	-0.73	0.00097	0.0131	-	-	-	-
53	0.911	-0.87	0.00016	0.0022	-	-	-	-
54	0.911	-0.93	0.00003	0.0004	-	-	-	-

Table 6.12 b). The tangential, vertical and radial turbulence intensity distribution at section U-4 run no.3 Um = 0.09259 m/s

Loc. no.	η = z/h	2Y/B	Tangential $\sqrt{v'^2}$ [m/s]	Tangential $\sqrt{v'^2}$/Um	Vertical $\sqrt{w'^2}$ [m/s]	Vertical $\sqrt{w'^2}$/Um	Radial $\sqrt{u'^2}$ [m/s]	Radial $\sqrt{u'^2}$/Um
1	0.033	-0.93	0.00334	0.0360	-	-	-	-
2	0.033	-0.87	0.00549	0.0593	-	-	-	-
3	0.033	-0.73	0.00449	0.0485	-	-	-	-
4	0.033	-0.40	0.00629	0.0680	-	-	-	-
5	0.033	0.	0.01167	0.1261	-	-	-	-
6	0.033	0.40	0.00164	0.0177	-	-	-	-
7	0.033	0.73	0.00011	0.0012	-	-	-	-
8	0.033	0.87	0.00048	0.0052	-	-	-	-
9	0.033	0.93	0.00056	0.0061	-	-	-	-
10	0.058	0.93	0.00226	0.0244	-	-	-	-
11	0.058	0.87	0.00038	0.0041	-	-	-	-
12	0.058	0.73	0.00024	0.0026	-	-	-	-
13	0.058	0.40	0.00118	0.0128	-	-	-	-
14	0.058	0.	0.00495	0.0535	-	-	-	-
15	0.058	-0.40	0.00258	0.0279	-	-	-	-
16	0.058	-0.73	0.00629	0.0680	-	-	-	-
17	0.058	-0.87	0.00455	0.0491	-	-	-	-
18	0.058	-0.93	0.00269	0.0291	-	-	-	-
19	0.133	-0.93	0.00186	0.0200	-	-	-	-
20	0.133	-0.87	0.00226	0.0244	-	-	-	-
21	0.133	-0.73	0.00083	0.0090	-	-	-	-
22	0.133	-0.40	0.00027	0.0029	-	-	-	-
23	0.133	0.	0.00277	0.0299	-	-	-	-
24	0.133	0.40	0.00264	0.0285	-	-	-	-
25	0.133	0.73	0.00312	0.0337	-	-	-	-
26	0.133	0.87	0.00312	0.0337	-	-	-	-
27	0.133	0.93	0.00124	0.0134	-	-	-	-
28	0.400	0.93	0.00054	0.0058	-	-	-	-
29	0.400	0.87	0.00231	0.0250	-	-	-	-
30	0.400	0.73	0.00420	0.0453	-	-	-	-
31	0.400	0.40	0.00347	0.0375	-	-	-	-
32	0.400	0.	0.00325	0.0352	-	-	-	-
33	0.400	-0.40	0.00083	0.0090	-	-	-	-
34	0.400	-0.73	0.00151	0.0163	-	-	-	-
35	0.400	-0.87	0.00183	0.0198	-	-	-	-
36	0.400	-0.93	0.00016	0.0017	-	-	-	-
37	0.667	-0.93	0.00135	0.0145	-	-	-	-
38	0.667	-0.87	0.00035	0.0038	-	-	-	-
39	0.667	-0.73	0.00218	0.0235	-	-	-	-
40	0.667	-0.40	0.00258	0.0279	-	-	-	-
41	0.667	0.	0.00374	0.0404	-	-	-	-
42	0.667	0.40	0.00393	0.0424	-	-	-	-
43	0.667	0.73	0.00178	0.0192	-	-	-	-
44	0.667	0.87	0.00191	0.0206	-	-	-	-
45	0.667	0.93	0.00293	0.0317	-	-	-	-
46	0.933	0.93	0.00199	0.0215	-	-	-	-
47	0.933	0.87	0.00043	0.0046	-	-	-	-
48	0.933	0.73	0.00285	0.0308	-	-	-	-
49	0.933	0.40	0.00352	0.0381	-	-	-	-
50	0.933	0.	0.00371	0.0401	-	-	-	-
51	0.933	-0.40	0.00350	0.0378	-	-	-	-
52	0.933	-0.73	0.00307	0.0331	-	-	-	-
53	0.933	-0.87	0.00299	0.0322	-	-	-	-
54	0.933	-0.93	0.00151	0.0163	-	-	-	-

Table 6.13 b). *The tangential, vertical and radial turbulence intensity distribution at section S-1 run no.1* $U_m = 0.04444$ m/s

Loc. no.	η = z/h	2Y/B	Tangential $\sqrt{\overline{v'^2}}$ [m/s]	Tangential $\sqrt{\overline{v'^2}}/U_m$	Vertical $\sqrt{\overline{w'^2}}$ [m/s]	Vertical $\sqrt{\overline{w'^2}}/U_m$	Radial $\sqrt{\overline{u'^2}}$ [m/s]	Radial $\sqrt{\overline{u'^2}}/U_m$
1	0.080	-0.93	0.00013	0.0030	-	-	-	-
2	0.080	-0.87	0.00202	0.0454	-	-	-	-
3	0.080	-0.73	0.00186	0.0418	-	-	-	-
4	0.080	-0.40	0.00078	0.0176	-	-	-	-
5	0.080	0.	0.00105	0.0236	-	-	-	-
6	0.080	0.40	0.00207	0.0466	-	-	-	-
7	0.080	0.73	0.00124	0.0278	-	-	-	-
8	0.080	0.87	0.00143	0.0321	-	-	-	-
9	0.080	0.93	0.00035	0.0079	-	-	-	-
10	0.140	0.93	0.00027	0.0061	-	-	-	-
11	0.140	0.87	0.00008	0.0018	-	-	-	-
12	0.140	0.73	0.00242	0.0545	-	-	-	-
13	0.140	0.40	0.00161	0.0363	-	-	-	-
14	0.140	0.	0.00183	0.0412	-	-	-	-
15	0.140	-0.40	0.00153	0.0345	-	-	-	-
16	0.140	-0.73	0.00245	0.0551	-	-	-	-
17	0.140	-0.87	0.00196	0.0442	-	-	-	-
18	0.140	-0.93	0.00194	0.0436	-	-	-	-
19	0.320	-0.93	0.00288	0.0648	-	-	-	-
20	0.320	-0.87	0.00309	0.0696	-	-	-	-
21	0.320	-0.73	0.00256	0.0575	-	-	-	-
22	0.320	-0.40	0.00070	0.0157	-	-	-	-
23	0.320	0.	0.00325	0.0732	-	-	-	-
24	0.320	0.40	0.00245	0.0551	-	-	-	-
25	0.320	0.73	0.00309	0.0696	-	-	-	-
26	0.320	0.87	0.00175	0.0393	-	-	-	-
27	0.320	0.93	0.00401	0.0902	-	-	-	-
28	0.600	0.93	0.00003	0.0006	-	-	-	-
29	0.600	0.87	0.00191	0.0430	-	-	-	-
30	0.600	0.73	0.00231	0.0521	-	-	-	-
31	0.600	0.40	0.00293	0.0660	-	-	-	-
32	0.600	0.	0.00369	0.0829	-	-	-	-
33	0.600	-0.40	0.00291	0.0654	-	-	-	-
34	0.600	-0.73	0.00264	0.0593	-	-	-	-
35	0.600	-0.87	0.00285	0.0642	-	-	-	-
36	0.600	-0.93	0.00194	0.0436	-	-	-	-
37	0.900	-0.93	0.00032	0.0073	-	-	-	-
38	0.900	-0.87	0.00038	0.0085	-	-	-	-
39	0.900	-0.73	0.00081	0.0182	-	-	-	-
40	0.900	-0.40	0.00183	0.0412	-	-	-	-
41	0.900	0.	0.00358	0.0805	-	-	-	-
42	0.900	0.40	0.00374	0.0841	-	-	-	-
43	0.900	0.73	0.00352	0.0793	-	-	-	-
44	0.900	0.87	0.00196	0.0442	-	-	-	-
45	0.900	0.93	0.00140	0.0315	-	-	-	-

Table 6.14 b). *The tangential, vertical and radial turbulence intensity distribution at section S-1 run no.2* $U_m = 0.07407$ m/s

Loc. no.	η = z/h	2Y/B	Tangential $\sqrt{\overline{v'^2}}$ [m/s]	Tangential $\sqrt{\overline{v'^2}}/U_m$	Vertical $\sqrt{\overline{w'^2}}$ [m/s]	Vertical $\sqrt{\overline{w'^2}}/U_m$	Radial $\sqrt{\overline{u'^2}}$ [m/s]	Radial $\sqrt{\overline{u'^2}}/U_m$
1	0.044	-0.93	0.00178	0.0240	-	-	-	-
2	0.044	-0.87	0.00022	0.0029	-	-	-	-
3	0.044	-0.73	0.00056	0.0076	-	-	-	-
4	0.044	-0.40	0.00277	0.0374	-	-	-	-
5	0.044	0.	0.00110	0.0149	-	-	-	-
6	0.044	0.40	0.00059	0.0080	-	-	-	-
7	0.044	0.73	0.00011	0.0015	-	-	-	-
8	0.044	0.87	0.00083	0.0113	-	-	-	-
9	0.044	0.93	0.00054	0.0073	-	-	-	-
10	0.078	0.93	0.00108	0.0145	-	-	-	-
11	0.078	0.87	0.00040	0.0054	-	-	-	-
12	0.078	0.73	0.00032	0.0044	-	-	-	-
13	0.078	0.40	0.00054	0.0073	-	-	-	-
14	0.078	0.	0.00011	0.0015	-	-	-	-
15	0.078	-0.40	0.00073	0.0098	-	-	-	-
16	0.078	-0.73	0.00102	0.0138	-	-	-	-
17	0.078	-0.87	0.00159	0.0214	-	-	-	-
18	0.078	-0.93	0.00121	0.0163	-	-	-	-
19	0.178	-0.93	0.00086	0.0116	-	-	-	-
20	0.178	-0.87	0.00221	0.0298	-	-	-	-
21	0.178	-0.73	0.00210	0.0283	-	-	-	-
22	0.178	-0.40	0.00078	0.0105	-	-	-	-
23	0.178	0.	0.00062	0.0084	-	-	-	-
24	0.178	0.40	0.00043	0.0058	-	-	-	-
25	0.178	0.73	0.00202	0.0272	-	-	-	-
26	0.178	0.87	0.00245	0.0330	-	-	-	-
27	0.178	0.93	0.00258	0.0349	-	-	-	-
28	0.422	0.93	0.00320	0.0432	-	-	-	-
29	0.422	0.87	0.00105	0.0142	-	-	-	-
30	0.422	0.73	0.00261	0.0352	-	-	-	-
31	0.422	0.40	0.00091	0.0123	-	-	-	-
32	0.422	0.	0.00266	0.0360	-	-	-	-
33	0.422	-0.40	0.00221	0.0298	-	-	-	-
34	0.422	-0.73	0.00317	0.0429	-	-	-	-
35	0.422	-0.87	0.00097	0.0131	-	-	-	-
36	0.422	-0.93	0.00191	0.0258	-	-	-	-
37	0.667	-0.93	0.00352	0.0476	-	-	-	-
38	0.667	-0.87	0.00164	0.0222	-	-	-	-
39	0.667	-0.73	0.00315	0.0425	-	-	-	-
40	0.667	-0.40	0.00393	0.0530	-	-	-	-
41	0.667	0.	0.00385	0.0519	-	-	-	-
42	0.667	0.40	0.00441	0.0596	-	-	-	-
43	0.667	0.73	0.00210	0.0283	-	-	-	-
44	0.667	0.87	0.00140	0.0189	-	-	-	-
45	0.667	0.93	0.01423	0.1921	-	-	-	-
46	0.911	0.93	0.00011	0.0015	-	-	-	-
47	0.911	0.87	0.00100	0.0134	-	-	-	-
48	0.911	0.73	0.00237	0.0320	-	-	-	-
49	0.911	0.40	0.00382	0.0516	-	-	-	-
50	0.911	0.	0.00395	0.0534	-	-	-	-
51	0.911	-0.40	0.00398	0.0537	-	-	-	-
52	0.911	-0.73	0.00317	0.0429	-	-	-	-
53	0.911	-0.87	0.00116	0.0156	-	-	-	-
54	0.911	-0.93	0.01498	0.2023	-	-	-	-

Table 6.15 *b). The tangential, vertical and radial turbulence intensity distribution at section S-1 run no.3* *Um = 0.09259 m/s*

Loc. no.	η = z/h	2Y/B	Tangential		Vertical		Radial	
			$\sqrt{\overline{v'^2}}$ [m/s]	$\sqrt{\overline{v'^2}}$/Um	$\sqrt{\overline{w'^2}}$ [m/s]	$\sqrt{\overline{w'^2}}$/Um	$\sqrt{\overline{u'^2}}$ [m/s]	$\sqrt{\overline{u'^2}}$/Um
1	0.033	-0.93	0.00132	0.0142	-	-	-	-
2	0.033	-0.87	0.00167	0.0180	-	-	-	-
3	0.033	-0.73	0.00355	0.0383	-	-	-	-
4	0.033	-0.40	0.00325	0.0352	-	-	-	-
5	0.033	0.	0.00336	0.0363	-	-	-	-
6	0.033	0.40	0.00221	0.0238	-	-	-	-
7	0.033	0.73	0.00199	0.0215	-	-	-	-
8	0.033	0.87	0.00116	0.0125	-	-	-	-
9	0.033	0.93	0.00640	0.0691	-	-	-	-
10	0.058	0.93	0.00038	0.0041	-	-	-	-
11	0.058	0.87	0.00024	0.0026	-	-	-	-
12	0.058	0.73	0.00156	0.0169	-	-	-	-
13	0.058	0.40	0.00218	0.0235	-	-	-	-
14	0.058	0.	0.00161	0.0174	-	-	-	-
15	0.058	-0.40	0.00196	0.0212	-	-	-	-
16	0.058	-0.73	0.00116	0.0125	-	-	-	-
17	0.058	-0.87	0.00062	0.0067	-	-	-	-
18	0.058	-0.93	0.00126	0.0137	-	-	-	-
19	0.133	-0.93	0.00683	0.0738	-	-	-	-
20	0.133	-0.87	0.00296	0.0320	-	-	-	-
21	0.133	-0.73	0.00159	0.0171	-	-	-	-
22	0.133	-0.40	0.00145	0.0157	-	-	-	-
23	0.133	0.	0.00143	0.0154	-	-	-	-
24	0.133	0.40	0.00213	0.0230	-	-	-	-
25	0.133	0.73	0.00202	0.0218	-	-	-	-
26	0.133	0.87	0.00056	0.0061	-	-	-	-
27	0.133	0.93	0.00390	0.0421	-	-	-	-
28	0.400	0.93	0.00404	0.0436	-	-	-	-
29	0.400	0.87	0.00048	0.0052	-	-	-	-
30	0.400	0.73	0.00191	0.0206	-	-	-	-
31	0.400	0.40	0.00272	0.0293	-	-	-	-
32	0.400	0.	0.00229	0.0247	-	-	-	-
33	0.400	-0.40	0.00304	0.0328	-	-	-	-
34	0.400	-0.73	0.00245	0.0264	-	-	-	-
35	0.400	-0.87	0.00075	0.0081	-	-	-	-
36	0.400	-0.93	0.00320	0.0346	-	-	-	-
37	0.667	-0.93	0.00121	0.0131	-	-	-	-
38	0.667	-0.87	0.00315	0.0340	-	-	-	-
39	0.667	-0.73	0.00382	0.0413	-	-	-	-
40	0.667	-0.40	0.00355	0.0383	-	-	-	-
41	0.667	0.	0.00374	0.0404	-	-	-	-
42	0.667	0.40	0.00325	0.0352	-	-	-	-
43	0.667	0.73	0.00204	0.0221	-	-	-	-
44	0.667	0.87	0.00094	0.0102	-	-	-	-
45	0.667	0.93	0.00508	0.0549	-	-	-	-
46	0.933	0.93	0.01060	0.1145	-	-	-	-
47	0.933	0.87	0.00506	0.0546	-	-	-	-
48	0.933	0.73	0.00056	0.0061	-	-	-	-
49	0.933	0.40	0.00323	0.0349	-	-	-	-
50	0.933	0.	0.00288	0.0311	-	-	-	-
51	0.933	-0.40	0.00272	0.0293	-	-	-	-
52	0.933	-0.73	0.00264	0.0285	-	-	-	-
53	0.933	-0.87	0.00110	0.0119	-	-	-	-
54	0.933	-0.93	0.00148	0.0160	-	-	-	-

Table 6.16 *b). The tangential, vertical and radial turbulence intensity distribution at section S-2 run no.1* *Um = 0.04444 m/s*

Loc. no.	η = z/h	2Y/B	Tangential		Vertical		Radial	
			$\sqrt{\overline{v'^2}}$ [m/s]	$\sqrt{\overline{v'^2}}$/Um	$\sqrt{\overline{w'^2}}$ [m/s]	$\sqrt{\overline{w'^2}}$/Um	$\sqrt{\overline{u'^2}}$ [m/s]	$\sqrt{\overline{u'^2}}$/Um
1	0.080	-0.93	0.00090	0.0202	-	-	-	-
2	0.080	-0.87	0.00216	0.0486	-	-	-	-
3	0.080	-0.73	0.00321	0.0723	-	-	-	-
4	0.080	-0.40	0.00337	0.0759	-	-	-	-
5	0.080	0.	0.00422	0.0949	-	-	-	-
6	0.080	0.40	0.00358	0.0806	-	-	-	-
7	0.080	0.73	0.00453	0.1020	-	-	-	-
8	0.080	0.87	0.00522	0.1174	-	-	-	-
9	0.080	0.93	0.00026	0.0059	-	-	-	-
10	0.140	0.93	0.00748	0.1684	-	-	0.00237	0.0534
11	0.140	0.87	0.00390	0.0877	-	-	0.00069	0.0154
12	0.140	0.73	0.00321	0.0723	-	-	0.00300	0.0676
13	0.140	0.40	0.00506	0.1138	-	-	0.00427	0.0960
14	0.140	0.	0.00553	0.1245	-	-	0.00116	0.0261
15	0.140	-0.40	0.00406	0.0913	-	-	0.00553	0.1245
16	0.140	-0.73	0.00311	0.0700	-	-	0.00627	0.1411
17	0.140	-0.87	0.00464	0.1043	-	-	0.00474	0.1067
18	0.140	-0.93	0.00290	0.0652	-	-	0.00432	0.0972
19	0.320	-0.93	0.00163	0.0368	0.00295	0.0664	0.00211	0.0474
20	0.320	-0.87	0.00453	0.1020	0.00163	0.0368	0.00379	0.0854
21	0.320	-0.73	0.00316	0.0711	0.00290	0.0652	0.00343	0.0771
22	0.320	-0.40	0.00422	0.0949	0.00285	0.0640	0.00437	0.0984
23	0.320	0.	0.00532	0.1198	0.00227	0.0510	0.00422	0.0949
24	0.320	0.40	0.00727	0.1636	0.00100	0.0225	0.00369	0.0830
25	0.320	0.73	0.00538	0.1209	0.00121	0.0273	0.00026	0.0059
26	0.320	0.87	0.00632	0.1423	0.00116	0.0261	0.00200	0.0451
27	0.320	0.93	0.00153	0.0344	0.00332	0.0747	0.00105	0.0237
28	0.600	0.93	0.00258	0.0581	0.00090	0.0202	0.00385	0.0866
29	0.600	0.87	0.00638	0.1435	0.00132	0.0296	0.00058	0.0130
30	0.600	0.73	0.00580	0.1304	0.00596	0.1340	0.00242	0.0545
31	0.600	0.40	0.00690	0.1553	0.00343	0.0771	0.00395	0.0889
32	0.600	0.	0.00648	0.1458	0.00474	0.1067	0.00337	0.0759
33	0.600	-0.40	0.00538	0.1209	0.00316	0.0711	0.00458	0.1032
34	0.600	-0.73	0.00532	0.1198	0.00258	0.0581	0.00527	0.1186
35	0.600	-0.87	0.00585	0.1316	0.00105	0.0237	0.00063	0.0142
36	0.600	-0.93	0.00242	0.0545	0.00369	0.0830	0.00316	0.0711
37	0.900	-0.93	0.00148	0.0332	0.00090	0.0202	0.00132	0.0296
38	0.900	-0.87	0.00316	0.0711	0.00200	0.0451	0.00759	0.1707
39	0.900	-0.73	0.00343	0.0771	0.00105	0.0237	0.00917	0.2063
40	0.900	-0.40	0.00437	0.0984	0.00369	0.0830	0.00469	0.1055
41	0.900	0.	0.00580	0.1304	0.00174	0.0391	0.00237	0.0534
42	0.900	0.40	0.00511	0.1150	0.00332	0.0747	0.00348	0.0783
43	0.900	0.73	0.00458	0.1032	0.00295	0.0664	0.00047	0.0107
44	0.900	0.87	0.00522	0.1174	0.00237	0.0534	0.00069	0.0154
45	0.900	0.93	0.00100	0.0225	0.00069	0.0154	0.00190	0.0427

Table 6.17 *b). The tangential, vertical and radial turbulence intensity distribution at section S-2 run no.2* *Um = 0.07407 m/s*

Loc. no.	η = z/h	2Y/B	Tangential $\sqrt{v'^2}$ [m/s]	Tangential $\sqrt{v'^2}$/Um	Vertical $\sqrt{w'^2}$ [m/s]	Vertical $\sqrt{w'^2}$/Um	Radial $\sqrt{u'^2}$ [m/s]	Radial $\sqrt{u'^2}$/Um
1	0.044	-0.93	0.00090	0.0121	-	-	-	-
2	0.044	-0.87	0.00179	0.0242	-	-	-	-
3	0.044	-0.73	0.00158	0.0213	-	-	-	-
4	0.044	-0.40	0.00480	0.0647	-	-	-	-
5	0.044	0.	0.00401	0.0541	-	-	-	-
6	0.044	0.40	0.00511	0.0690	-	-	-	-
7	0.044	0.73	0.00090	0.0121	-	-	-	-
8	0.044	0.87	0.00495	0.0669	-	-	-	-
9	0.044	0.93	0.00369	0.0498	-	-	-	-
10	0.078	0.93	0.00775	0.1046	-	-	-	-
11	0.078	0.87	0.00111	0.0149	-	-	-	-
12	0.078	0.73	0.00648	0.0875	-	-	-	-
13	0.078	0.40	0.00453	0.0612	-	-	-	-
14	0.078	0.	0.00538	0.0726	-	-	-	-
15	0.078	-0.40	0.00469	0.0633	-	-	-	-
16	0.078	-0.73	0.00232	0.0313	-	-	-	-
17	0.078	-0.87	0.00332	0.0448	-	-	-	-
18	0.078	-0.93	0.00058	0.0078	-	-	-	-
19	0.178	-0.93	0.00269	0.0363	0.00042	0.0057	0.00316	0.0427
20	0.178	-0.87	0.00274	0.0370	0.00011	0.0014	0.00653	0.0882
21	0.178	-0.73	0.00390	0.0526	0.00100	0.0135	0.00553	0.0747
22	0.178	-0.40	0.00748	0.1010	0.00042	0.0057	0.00538	0.0726
23	0.178	0.	0.00701	0.0946	0.00195	0.0263	0.00511	0.0690
24	0.178	0.40	0.00833	0.1124	0.00327	0.0441	0.00422	0.0569
25	0.178	0.73	0.00664	0.0896	0.00206	0.0277	0.00295	0.0398
26	0.178	0.87	0.00690	0.0932	0.00190	0.0256	0.00422	0.0569
27	0.178	0.93	0.00163	0.0221	0.00163	0.0221	0.00343	0.0462
28	0.422	0.93	0.00274	0.0370	0.00074	0.0100	0.00206	0.0277
29	0.422	0.87	0.00553	0.0747	0.00063	0.0085	0.00532	0.0719
30	0.422	0.73	0.00706	0.0953	0.00248	0.0334	0.00464	0.0626
31	0.422	0.40	0.00748	0.1010	0.00153	0.0206	0.00369	0.0498
32	0.422	0.	0.00617	0.0832	0.00295	0.0398	0.00611	0.0825
33	0.422	-0.40	0.00580	0.0783	0.00116	0.0157	0.00406	0.0548
34	0.422	-0.73	0.00601	0.0811	0.00158	0.0213	0.00611	0.0825
35	0.422	-0.87	0.00559	0.0754	0.00137	0.0185	0.00627	0.0847
36	0.422	-0.93	0.00300	0.0406	0.00026	0.0036	0.00769	0.1039
37	0.667	-0.93	0.00163	0.0221	0.00148	0.0199	0.00358	0.0484
38	0.667	-0.87	0.00411	0.0555	0.00084	0.0114	0.00469	0.0633
39	0.667	-0.73	0.00559	0.0754	0.00053	0.0071	0.00316	0.0427
40	0.667	-0.40	0.00664	0.0896	0.00158	0.0213	0.00422	0.0569
41	0.667	0.	0.00822	0.1110	0.00142	0.0192	0.00427	0.0576
42	0.667	0.40	0.00838	0.1131	0.00042	0.0057	0.00132	0.0178
43	0.667	0.73	0.00648	0.0875	0.00047	0.0064	0.00184	0.0249
44	0.667	0.87	0.00638	0.0861	0.	0.	0.00211	0.0285
45	0.667	0.93	0.01618	0.2184	0.00100	0.0135	0.00184	0.0249
46	0.911	0.93	0.00148	0.0199	-	-	0.00263	0.0356
47	0.911	0.87	0.00538	0.0726	-	-	0.00379	0.0512
48	0.911	0.73	0.00675	0.0911	-	-	0.00090	0.0121
49	0.911	0.40	0.00548	0.0740	-	-	0.00274	0.0370
50	0.911	0.	0.00416	0.0562	-	-	0.00332	0.0448
51	0.911	-0.40	0.00506	0.0683	-	-	0.00606	0.0818
52	0.911	-0.73	0.00643	0.0868	-	-	0.00379	0.0512
53	0.911	-0.87	0.00632	0.0854	-	-	0.00458	0.0619
54	0.911	-0.93	0.00163	0.0221	-	-	0.00332	0.0448

Table 6.18 *b). The tangential, vertical and radial turbulence intensity distribution at section S-2 run no.3* *Um = 0.09259 m/s*

Loc. no.	η = z/h	2Y/B	Tangential $\sqrt{v'^2}$ [m/s]	Tangential $\sqrt{v'^2}$/Um	Vertical $\sqrt{w'^2}$ [m/s]	Vertical $\sqrt{w'^2}$/Um	Radial $\sqrt{u'^2}$ [m/s]	Radial $\sqrt{u'^2}$/Um
1	0.033	-0.93	0.00427	0.0461	-	-	-	-
2	0.033	-0.87	0.00184	0.0199	-	-	-	-
3	0.033	-0.73	0.00100	0.0108	-	-	-	-
4	0.033	-0.40	0.00316	0.0341	-	-	-	-
5	0.033	0.	0.00364	0.0393	-	-	-	-
6	0.033	0.40	0.00464	0.0501	-	-	-	-
7	0.033	0.73	0.00490	0.0529	-	-	-	-
8	0.033	0.87	0.00490	0.0529	-	-	-	-
9	0.033	0.93	0.00290	0.0313	-	-	-	-
10	0.058	0.93	0.00016	0.0017	-	-	-	-
11	0.058	0.87	0.00306	0.0330	-	-	-	-
12	0.058	0.73	0.00116	0.0125	-	-	-	-
13	0.058	0.40	0.00522	0.0563	-	-	-	-
14	0.058	0.	0.00437	0.0472	-	-	-	-
15	0.058	-0.40	0.00443	0.0478	-	-	-	-
16	0.058	-0.73	0.00100	0.0108	-	-	-	-
17	0.058	-0.87	0.00422	0.0455	-	-	-	-
18	0.058	-0.93	0.00659	0.0711	-	-	-	-
19	0.133	-0.93	0.00369	0.0398	0.00163	0.0176	0.00806	0.0871
20	0.133	-0.87	0.00074	0.0080	0.00148	0.0159	0.00949	0.1024
21	0.133	-0.73	0.00005	0.0006	0.00095	0.0102	0.01054	0.1138
22	0.133	-0.40	0.00401	0.0433	0.00053	0.0057	0.00559	0.0603
23	0.133	0.	0.00632	0.0683	0.00016	0.0017	0.00501	0.0541
24	0.133	0.40	0.00675	0.0729	0.00026	0.0028	0.00495	0.0535
25	0.133	0.73	0.00611	0.0660	0.00026	0.0028	0.00448	0.0484
26	0.133	0.87	0.00395	0.0427	0.00158	0.0171	0.00090	0.0097
27	0.133	0.93	0.00938	0.1013	0.00116	0.0125	0.00158	0.0171
28	0.400	0.93	0.00016	0.0017	0.00264	0.0285	0.00453	0.0489
29	0.400	0.87	0.00638	0.0689	0.00026	0.0028	0.00148	0.0159
30	0.400	0.73	0.00680	0.0734	0.00021	0.0023	0.00300	0.0324
31	0.400	0.40	0.00627	0.0677	0.00037	0.0040	0.00443	0.0478
32	0.400	0.	0.00643	0.0694	0.00306	0.0330	0.00490	0.0529
33	0.400	-0.40	0.00664	0.0717	0.00148	0.0159	0.00369	0.0398
34	0.400	-0.73	0.00659	0.0711	0.00095	0.0102	0.00559	0.0603
35	0.400	-0.87	0.00137	0.0148	0.00263	0.0285	0.00432	0.0467
36	0.400	-0.93	0.00163	0.0176	0.00095	0.0102	0.00395	0.0427
37	0.667	-0.93	0.00200	0.0216	0.00074	0.0080	0.00596	0.0643
38	0.667	-0.87	0.00453	0.0489	0.00063	0.0068	0.00943	0.1019
39	0.667	-0.73	0.00005	0.0006	0.00095	0.0102	0.00985	0.1064
40	0.667	-0.40	0.00516	0.0558	0.00069	0.0074	0.00791	0.0854
41	0.667	0.	0.00711	0.0768	0.	0.	0.00696	0.0751
42	0.667	0.40	0.00690	0.0746	0.00026	0.0028	0.00780	0.0842
43	0.667	0.73	0.00643	0.0694	0.00047	0.0051	0.00227	0.0245
44	0.667	0.87	0.00279	0.0302	0.00011	0.0011	0.00158	0.0171
45	0.667	0.93	0.00432	0.0467	0.00237	0.0256	0.00137	0.0148
46	0.933	0.93	0.00659	0.0711	-	-	0.00116	0.0125
47	0.933	0.87	0.00522	0.0563	-	-	0.00263	0.0285
48	0.933	0.73	0.00643	0.0694	-	-	0.00248	0.0268
49	0.933	0.40	0.00622	0.0672	-	-	0.00559	0.0603
50	0.933	0.	0.00690	0.0746	-	-	0.00553	0.0598
51	0.933	-0.40	0.00411	0.0444	-	-	0.01291	0.1394
52	0.933	-0.73	0.00516	0.0558	-	-	0.01354	0.1463
53	0.933	-0.87	0.00290	0.0313	-	-	0.00643	0.0694
54	0.933	-0.93	0.00300	0.0324	-	-	0.00385	0.0415

Table 6.19 *b). The tangential, vertical and radial turbulence intensity distribution at section S-3 run no.1* Um = 0.04444 m/s

Loc. no.	η = z/h	2Y/B	Tangential $\sqrt{v'^2}$ [m/s]	Tangential $\sqrt{v'^2}$/Um	Vertical $\sqrt{w'^2}$ [m/s]	Vertical $\sqrt{w'^2}$/Um	Radial $\sqrt{u'^2}$ [m/s]	Radial $\sqrt{u'^2}$/Um
1	0.080	-0.93	0.00791	0.1779	-	-	-	-
2	0.080	-0.87	0.00084	0.0190	-	-	-	-
3	0.080	-0.73	0.00021	0.0047	-	-	-	-
4	0.080	-0.40	0.00242	0.0545	-	-	-	-
5	0.080	0.	0.00348	0.0783	-	-	-	-
6	0.080	0.40	0.00264	0.0593	-	-	-	-
7	0.080	0.73	0.00148	0.0332	-	-	-	-
8	0.080	0.87	0.00653	0.1470	-	-	-	-
9	0.080	0.93	0.00780	0.1755	-	-	-	-
10	0.140	0.93	0.00812	0.1826	-	-	0.00153	0.0344
11	0.140	0.87	0.00422	0.0949	-	-	0.00121	0.0273
12	0.140	0.73	0.00453	0.1020	-	-	0.00074	0.0166
13	0.140	0.40	0.00469	0.1055	-	-	0.00190	0.0427
14	0.140	0.	0.00337	0.0759	-	-	0.00158	0.0356
15	0.140	-0.40	0.00353	0.0794	-	-	0.00026	0.0059
16	0.140	-0.73	0.00385	0.0866	-	-	0.00100	0.0225
17	0.140	-0.87	0.00285	0.0640	-	-	0.00063	0.0142
18	0.140	-0.93	0.00032	0.0071	-	-	0.00158	0.0356
19	0.320	-0.93	0.00116	0.0261	0.00211	0.0474	0.00063	0.0142
20	0.320	-0.87	0.00058	0.0130	0.00079	0.0178	0.00132	0.0296
21	0.320	-0.73	0.00316	0.0711	0.00021	0.0047	0.00005	0.0012
22	0.320	-0.40	0.00395	0.0889	0.00079	0.0178	0.00142	0.0320
23	0.320	0.	0.00343	0.0771	0.00053	0.0119	0.00295	0.0664
24	0.320	0.40	0.00306	0.0688	0.00274	0.0617	0.00058	0.0130
25	0.320	0.73	0.00100	0.0225	0.00116	0.0261	0.00327	0.0735
26	0.320	0.87	0.00026	0.0059	0.00005	0.0012	0.00364	0.0818
27	0.320	0.93	0.00158	0.0356	0.00095	0.0213	0.00279	0.0628
28	0.600	0.93	0.00300	0.0676	0.00090	0.0202	0.00406	0.0913
29	0.600	0.87	0.00095	0.0213	0.00069	0.0154	0.00532	0.1198
30	0.600	0.73	0.00090	0.0202	0.00079	0.0178	0.00343	0.0771
31	0.600	0.40	0.00232	0.0522	0.00058	0.0130	0.00411	0.0925
32	0.600	0.	0.00200	0.0451	0.00074	0.0166	0.00474	0.1067
33	0.600	-0.40	0.00195	0.0439	0.00021	0.0047	0.00485	0.1091
34	0.600	-0.73	0.00227	0.0510	0.00148	0.0332	0.00316	0.0711
35	0.600	-0.87	0.00211	0.0474	0.00011	0.0024	0.00211	0.0474
36	0.600	-0.93	0.00053	0.0119	0.00011	0.0024	0.00016	0.0036
37	0.900	-0.93	0.00458	0.1032	0.00211	0.0474	0.00121	0.0273
38	0.900	-0.87	0.00422	0.0949	0.00237	0.0534	0.00032	0.0071
39	0.900	-0.73	0.00306	0.0688	0.00011	0.0024	0.00021	0.0047
40	0.900	-0.40	0.00037	0.0083	0.00047	0.0107	0.00264	0.0593
41	0.900	0.	0.00437	0.0984	0.00158	0.0356	0.00316	0.0711
42	0.900	0.40	0.00090	0.0202	0.00132	0.0296	0.00358	0.0806
43	0.900	0.73	0.00021	0.0047	0.00116	0.0261	0.00474	0.1067
44	0.900	0.87	0.00374	0.0842	0.00095	0.0213	0.00348	0.0783
45	0.900	0.93	0.00105	0.0237	0.00026	0.0059	0.00364	0.0818

Table 6.20 *b). The tangential, vertical and radial turbulence intensity distribution at section S-3 run no.2* Um = 0.07407 m/s

Loc. no.	η = z/h	2Y/B	Tangential $\sqrt{v'^2}$ [m/s]	Tangential $\sqrt{v'^2}$/Um	Vertical $\sqrt{w'^2}$ [m/s]	Vertical $\sqrt{w'^2}$/Um	Radial $\sqrt{u'^2}$ [m/s]	Radial $\sqrt{u'^2}$/Um
1	0.044	-0.93	0.00237	0.0320	-	-	-	-
2	0.044	-0.87	0.00116	0.0157	-	-	-	-
3	0.044	-0.73	0.00248	0.0334	-	-	-	-
4	0.044	-0.40	0.00295	0.0398	-	-	-	-
5	0.044	0.	0.00343	0.0462	-	-	-	-
6	0.044	0.40	0.00374	0.0505	-	-	-	-
7	0.044	0.73	0.00432	0.0583	-	-	-	-
8	0.044	0.87	0.00401	0.0541	-	-	-	-
9	0.044	0.93	0.00021	0.0028	-	-	-	-
10	0.078	0.93	0.01028	0.1387	-	-	-	-
11	0.078	0.87	0.00416	0.0562	-	-	-	-
12	0.078	0.73	0.00427	0.0576	-	-	-	-
13	0.078	0.40	0.00501	0.0676	-	-	-	-
14	0.078	0.	0.00295	0.0398	-	-	-	-
15	0.078	-0.40	0.00132	0.0178	-	-	-	-
16	0.078	-0.73	0.00090	0.0121	-	-	-	-
17	0.078	-0.87	0.00100	0.0135	-	-	-	-
18	0.078	-0.93	0.	0.	-	-	-	-
19	0.178	-0.93	0.00005	0.0007	0.00274	0.0370	0.00126	0.0171
20	0.178	-0.87	0.00200	0.0270	0.00047	0.0064	0.00142	0.0192
21	0.178	-0.73	0.00253	0.0341	0.00037	0.0050	0.00332	0.0448
22	0.178	-0.40	0.00453	0.0612	0.00132	0.0178	0.00053	0.0071
23	0.178	0.	0.00548	0.0740	0.	0.	0.00074	0.0100
24	0.178	0.40	0.00601	0.0811	0.00174	0.0235	0.00148	0.0199
25	0.178	0.73	0.00596	0.0804	0.00169	0.0228	0.00090	0.0121
26	0.178	0.87	0.00680	0.0918	0.00200	0.0270	0.00211	0.0285
27	0.178	0.93	0.00206	0.0277	0.00026	0.0036	0.00221	0.0299
28	0.422	0.93	0.00137	0.0185	0.00079	0.0107	0.00221	0.0299
29	0.422	0.87	0.00617	0.0832	0.00042	0.0057	0.00184	0.0249
30	0.422	0.73	0.00632	0.0854	0.00116	0.0157	0.00174	0.0235
31	0.422	0.40	0.00638	0.0861	0.00047	0.0064	0.00132	0.0178
32	0.422	0.	0.00574	0.0775	0.00148	0.0199	0.00221	0.0299
33	0.422	-0.40	0.00511	0.0690	0.00074	0.0100	0.00337	0.0455
34	0.422	-0.73	0.00358	0.0484	0.00053	0.0071	0.00016	0.0021
35	0.422	-0.87	0.00264	0.0356	0.00195	0.0263	0.00343	0.0462
36	0.422	-0.93	0.00137	0.0185	0.00111	0.0149	0.00369	0.0498
37	0.667	-0.93	0.00105	0.0142	0.00126	0.0171	0.00137	0.0185
38	0.667	-0.87	0.00011	0.0014	0.00195	0.0263	0.00485	0.0655
39	0.667	-0.73	0.00285	0.0384	0.00053	0.0071	0.00385	0.0519
40	0.667	-0.40	0.00453	0.0612	0.00153	0.0206	0.00221	0.0299
41	0.667	0.	0.00564	0.0761	0.00074	0.0100	0.00005	0.0007
42	0.667	0.40	0.00443	0.0598	0.00021	0.0028	0.00206	0.0277
43	0.667	0.73	0.00580	0.0783	0.00121	0.0164	0.00058	0.0078
44	0.667	0.87	0.00617	0.0832	0.00158	0.0213	0.00105	0.0142
45	0.667	0.93	0.00358	0.0484	0.00195	0.0263	0.00011	0.0014
46	0.911	0.93	0.00053	0.0071	-	-	0.00100	0.0135
47	0.911	0.87	0.00506	0.0683	-	-	0.00032	0.0043
48	0.911	0.73	0.00569	0.0768	-	-	0.00142	0.0192
49	0.911	0.40	0.00543	0.0733	-	-	0.00385	0.0519
50	0.911	0.	0.00343	0.0462	-	-	0.00021	0.0028
51	0.911	-0.40	0.00448	0.0605	-	-	0.00643	0.0868
52	0.911	-0.73	0.00332	0.0448	-	-	0.00116	0.0157
53	0.911	-0.87	0.00105	0.0142	-	-	0.00332	0.0448
54	0.911	-0.93	0.00126	0.0171	-	-	0.00148	0.0199

Table 6.21 b). The tangential, vertical and radial turbulence intensity distribution at section S-3 run no.3 Um = 0.09259 m/s

Loc. no.	η = z/h	2Y/B	Tangential $\sqrt{v'^2}$ [m/s]	Tangential $\sqrt{v'^2}$/Um	Vertical $\sqrt{w'^2}$ [m/s]	Vertical $\sqrt{w'^2}$/Um	Radial $\sqrt{u'^2}$ [m/s]	Radial $\sqrt{u'^2}$/Um
1	0.033	-0.93	0.00026	0.0028	-	-	-	-
2	0.033	-0.87	0.00021	0.0023	-	-	-	-
3	0.033	-0.73	0.00248	0.0268	-	-	-	-
4	0.033	-0.40	0.00432	0.0467	-	-	-	-
5	0.033	0.	0.00195	0.0211	-	-	-	-
6	0.033	0.40	0.00105	0.0114	-	-	-	-
7	0.033	0.73	0.00042	0.0046	-	-	-	-
8	0.033	0.87	0.00053	0.0057	-	-	-	-
9	0.033	0.93	0.00026	0.0028	-	-	-	-
10	0.058	0.93	0.00216	0.0233	-	-	-	-
11	0.058	0.87	0.00348	0.0376	-	-	-	-
12	0.058	0.73	0.00358	0.0387	-	-	-	-
13	0.058	0.40	0.00274	0.0296	-	-	-	-
14	0.058	0.	0.00253	0.0273	-	-	-	-
15	0.058	-0.40	0.00200	0.0216	-	-	-	-
16	0.058	-0.73	0.00116	0.0125	-	-	-	-
17	0.058	-0.87	0.00100	0.0108	-	-	-	-
18	0.058	-0.93	0.00295	0.0319	-	-	-	-
19	0.133	-0.93	0.00885	0.0956	0.00242	0.0262	0.01107	0.1195
20	0.133	-0.87	0.00053	0.0057	0.00126	0.0137	0.00743	0.0803
21	0.133	-0.73	0.00053	0.0057	0.00026	0.0028	0.00917	0.0990
22	0.133	-0.40	0.00264	0.0285	0.00047	0.0051	0.00564	0.0609
23	0.133	0.	0.00617	0.0666	0.	0.	0.00906	0.0979
24	0.133	0.40	0.00606	0.0655	0.00158	0.0171	0.00437	0.0472
25	0.133	0.73	0.00664	0.0717	0.00100	0.0108	0.00190	0.0205
26	0.133	0.87	0.00474	0.0512	0.00016	0.0017	0.00169	0.0182
27	0.133	0.93	0.00190	0.0205	0.00158	0.0171	0.00011	0.0011
28	0.400	0.93	0.00153	0.0165	0.00121	0.0131	0.00037	0.0040
29	0.400	0.87	0.00733	0.0791	0.00311	0.0336	0.00227	0.0245
30	0.400	0.73	0.00701	0.0757	0.00300	0.0324	0.00032	0.0034
31	0.400	0.40	0.00696	0.0751	0.00095	0.0102	0.	0.
32	0.400	0.	0.00601	0.0649	0.00306	0.0330	0.00079	0.0085
33	0.400	-0.40	0.00569	0.0615	0.00227	0.0245	0.00337	0.0364
34	0.400	-0.73	0.00501	0.0541	0.00327	0.0353	0.00090	0.0097
35	0.400	-0.87	0.00458	0.0495	0.00047	0.0051	0.00032	0.0034
36	0.400	-0.93	0.00775	0.0837	0.00274	0.0296	0.00248	0.0268
37	0.667	-0.93	0.00011	0.0011	0.00037	0.0040	0.00258	0.0279
38	0.667	-0.87	0.00332	0.0359	0.00121	0.0131	0.00216	0.0233
39	0.667	-0.73	0.00606	0.0655	0.00232	0.0250	0.00295	0.0319
40	0.667	-0.40	0.00764	0.0825	0.00169	0.0182	0.00132	0.0142
41	0.667	0.	0.00812	0.0877	0.00069	0.0074	0.00121	0.0131
42	0.667	0.40	0.00711	0.0768	0.00348	0.0376	0.00032	0.0034
43	0.667	0.73	0.00791	0.0854	0.00453	0.0489	0.00116	0.0125
44	0.667	0.87	0.00748	0.0808	0.00206	0.0222	0.00364	0.0393
45	0.667	0.93	0.00116	0.0125	0.00264	0.0285	0.	0.
46	0.933	0.93	0.00184	0.0199	-	-	0.00190	0.0205
47	0.933	0.87	0.00627	0.0677	-	-	0.00069	0.0074
48	0.933	0.73	0.00706	0.0763	-	-	0.00200	0.0216
49	0.933	0.40	0.00748	0.0808	-	-	0.00300	0.0324
50	0.933	0.	0.00706	0.0763	-	-	0.00032	0.0034
51	0.933	-0.40	0.00596	0.0643	-	-	0.00084	0.0091
52	0.933	-0.73	0.00200	0.0216	-	-	0.00485	0.0524
53	0.933	-0.87	0.00485	0.0524	-	-	0.00290	0.0313
54	0.933	-0.93	0.00638	0.0689	-	-	0.00174	0.0188

Table 6.22 b). The tangential, vertical and radial turbulence intensity distribution at section S-4 run no.1 Um = 0.04444 m/s

Loc. no.	η = z/h	2Y/B	Tangential $\sqrt{v'^2}$ [m/s]	Tangential $\sqrt{v'^2}$/Um	Vertical $\sqrt{w'^2}$ [m/s]	Vertical $\sqrt{w'^2}$/Um	Radial $\sqrt{u'^2}$ [m/s]	Radial $\sqrt{u'^2}$/Um
1	0.080	-0.93	0.00090	0.0202	-	-	-	-
2	0.080	-0.87	0.00174	0.0391	-	-	-	-
3	0.080	-0.73	0.00200	0.0451	-	-	-	-
4	0.080	-0.40	0.00258	0.0581	-	-	-	-
5	0.080	0.	0.00385	0.0866	-	-	-	-
6	0.080	0.40	0.00553	0.1245	-	-	-	-
7	0.080	0.73	0.00627	0.1411	-	-	-	-
8	0.080	0.87	0.00485	0.1091	-	-	-	-
9	0.080	0.93	0.00406	0.0913	-	-	-	-
10	0.140	0.93	0.00279	0.0628	-	-	0.00406	0.0913
11	0.140	0.87	0.00717	0.1613	-	-	0.00401	0.0901
12	0.140	0.73	0.00606	0.1364	-	-	0.00290	0.0652
13	0.140	0.40	0.00648	0.1458	-	-	0.00232	0.0522
14	0.140	0.	0.00559	0.1257	-	-	0.00021	0.0047
15	0.140	-0.40	0.00385	0.0866	-	-	0.00316	0.0711
16	0.140	-0.73	0.00364	0.0818	-	-	0.00121	0.0273
17	0.140	-0.87	0.00411	0.0925	-	-	0.00069	0.0154
18	0.140	-0.93	0.00153	0.0344	-	-	0.00005	0.0012
19	0.320	-0.93	0.00153	0.0344	0.00011	0.0024	0.00053	0.0119
20	0.320	-0.87	0.00379	0.0854	0.00111	0.0249	0.00026	0.0059
21	0.320	-0.73	0.00443	0.0996	0.00005	0.0012	0.00211	0.0474
22	0.320	-0.40	0.00453	0.1020	0.00137	0.0308	0.00511	0.1150
23	0.320	0.	0.00495	0.1115	0.00248	0.0557	0.00111	0.0249
24	0.320	0.40	0.00548	0.1233	0.00227	0.0510	0.00158	0.0356
25	0.320	0.73	0.00675	0.1518	0.00053	0.0119	0.00132	0.0296
26	0.320	0.87	0.00627	0.1411	0.00443	0.0996	0.00111	0.0249
27	0.320	0.93	0.00232	0.0522	0.00137	0.0308	0.00079	0.0178
28	0.600	0.93	0.00332	0.0747	0.00290	0.0652	0.00132	0.0296
29	0.600	0.87	0.00622	0.1399	0.00174	0.0391	0.00148	0.0332
30	0.600	0.73	0.00648	0.1458	0.00206	0.0462	0.00137	0.0308
31	0.600	0.40	0.00606	0.1364	0.00237	0.0534	0.00047	0.0107
32	0.600	0.	0.00559	0.1257	0.00285	0.0640	0.00137	0.0308
33	0.600	-0.40	0.00564	0.1269	0.00527	0.1186	0.00532	0.1198
34	0.600	-0.73	0.00685	0.1541	0.00432	0.0972	0.00206	0.0462
35	0.600	-0.87	0.00522	0.1174	0.00274	0.0617	0.00153	0.0344
36	0.600	-0.93	0.00084	0.0190	0.00053	0.0119	0.00148	0.0332
37	0.900	-0.93	0.00074	0.0166	0.00290	0.0652	0.00290	0.0652
38	0.900	-0.87	0.00105	0.0237	0.00406	0.0913	0.00105	0.0237
39	0.900	-0.73	0.00216	0.0486	0.00306	0.0688	0.00011	0.0024
40	0.900	-0.40	0.00285	0.0640	0.00295	0.0664	0.00332	0.0747
41	0.900	0.	0.00653	0.1470	0.00300	0.0676	0.00132	0.0296
42	0.900	0.40	0.00722	0.1624	0.00216	0.0486	0.00053	0.0119
43	0.900	0.73	0.00690	0.1553	0.00200	0.0451	0.00279	0.0628
44	0.900	0.87	0.00659	0.1482	0.00111	0.0249	0.00105	0.0237
45	0.900	0.93	0.00548	0.1233	0.00005	0.0012	0.00026	0.0059

Table 6.23 *b). The tangential, vertical and radial turbulence intensity distribution at section S-4 run no.2* Um = 0.07407 m/s

Loc. no.	η = z/h	2Y/B	Tangential $\sqrt{\overline{v'^2}}$ [m/s]	Tangential $\sqrt{\overline{v'^2}}$/Um	Vertical $\sqrt{\overline{w'^2}}$ [m/s]	Vertical $\sqrt{\overline{w'^2}}$/Um	Radial $\sqrt{\overline{u'^2}}$ [m/s]	Radial $\sqrt{\overline{u'^2}}$/Um
1	0.044	-0.93	0.00037	0.0050	-	-	-	-
2	0.044	-0.87	0.00290	0.0391	-	-	-	-
3	0.044	-0.73	0.00116	0.0157	-	-	-	-
4	0.044	-0.40	0.00248	0.0334	-	-	-	-
5	0.044	0.	0.00559	0.0754	-	-	-	-
6	0.044	0.40	0.00585	0.0790	-	-	-	-
7	0.044	0.73	0.00664	0.0896	-	-	-	-
8	0.044	0.87	0.00759	0.1024	-	-	-	-
9	0.044	0.93	0.00374	0.0505	-	-	-	-
10	0.078	0.93	0.00285	0.0384	-	-	-	-
11	0.078	0.87	0.00669	0.0904	-	-	-	-
12	0.078	0.73	0.00580	0.0783	-	-	-	-
13	0.078	0.40	0.00648	0.0875	-	-	-	-
14	0.078	0.	0.00401	0.0541	-	-	-	-
15	0.078	-0.40	0.00464	0.0626	-	-	-	-
16	0.078	-0.73	0.00321	0.0434	-	-	-	-
17	0.078	-0.87	0.00169	0.0228	-	-	-	-
18	0.078	-0.93	0.00480	0.0647	-	-	-	-
19	0.178	-0.93	0.00032	0.0043	0.00005	0.0007	0.00158	0.0213
20	0.178	-0.87	0.00258	0.0349	0.00279	0.0377	0.00216	0.0292
21	0.178	-0.73	0.00437	0.0591	0.00211	0.0285	0.00005	0.0007
22	0.178	-0.40	0.00585	0.0790	0.00227	0.0306	0.00195	0.0263
23	0.178	0.	0.00722	0.0975	0.00379	0.0512	0.00221	0.0299
24	0.178	0.40	0.00764	0.1032	0.00174	0.0235	0.00084	0.0114
25	0.178	0.73	0.00827	0.1117	0.00374	0.0505	0.00042	0.0057
26	0.178	0.87	0.00643	0.0868	0.00069	0.0092	0.00126	0.0171
27	0.178	0.93	0.00100	0.0135	0.00174	0.0235	0.00116	0.0157
28	0.422	0.93	0.00216	0.0292	0.00369	0.0498	0.00053	0.0071
29	0.422	0.87	0.00806	0.1089	0.00343	0.0462	0.00137	0.0185
30	0.422	0.73	0.00854	0.1153	0.00580	0.0783	0.00316	0.0427
31	0.422	0.40	0.00885	0.1195	0.00258	0.0349	0.00105	0.0142
32	0.422	0.	0.00833	0.1124	0.00559	0.0754	0.00074	0.0100
33	0.422	-0.40	0.00733	0.0989	0.00443	0.0598	0.00037	0.0050
34	0.422	-0.73	0.00706	0.0953	0.00221	0.0299	0.00084	0.0114
35	0.422	-0.87	0.00580	0.0783	0.00343	0.0462	0.00285	0.0384
36	0.422	-0.93	0.00327	0.0441	0.00200	0.0270	0.00158	0.0213
37	0.667	-0.93	0.00348	0.0470	0.00216	0.0292	0.00132	0.0178
38	0.667	-0.87	0.00569	0.0768	0.00495	0.0669	0.00137	0.0185
39	0.667	-0.73	0.00553	0.0747	0.00527	0.0711	0.00269	0.0363
40	0.667	-0.40	0.00785	0.1060	0.00321	0.0434	0.00074	0.0100
41	0.667	0.	0.00843	0.1138	0.00501	0.0676	0.00142	0.0192
42	0.667	0.40	0.00875	0.1181	0.00532	0.0719	0.00200	0.0270
43	0.667	0.73	0.00891	0.1202	0.00432	0.0583	0.00058	0.0078
44	0.667	0.87	0.00928	0.1252	0.00564	0.0761	0.00274	0.0370
45	0.667	0.93	0.00406	0.0548	0.00469	0.0633	0.00211	0.0285
46	0.911	0.93	0.00711	0.0960	-	-	0.00211	0.0285
47	0.911	0.87	0.00859	0.1160	-	-	0.00311	0.0420
48	0.911	0.73	0.00912	0.1231	-	-	0.00416	0.0562
49	0.911	0.40	0.00838	0.1131	-	-	0.00190	0.0256
50	0.911	0.	0.00775	0.1046	-	-	0.00158	0.0213
51	0.911	-0.40	0.00590	0.0797	-	-	0.00163	0.0221
52	0.911	-0.73	0.00253	0.0341	-	-	0.00037	0.0050
53	0.911	-0.87	0.00374	0.0505	-	-	0.00032	0.0043
54	0.911	-0.93	0.00211	0.0285	-	-	0.00016	0.0021

Table 6.24 *b). The tangential, vertical and radial turbulence intensity distribution at section S-4 run no.3* Um = 0.09259 m/s

Loc. no.	η = z/h	2Y/B	Tangential $\sqrt{\overline{v'^2}}$ [m/s]	Tangential $\sqrt{\overline{v'^2}}$/Um	Vertical $\sqrt{\overline{w'^2}}$ [m/s]	Vertical $\sqrt{\overline{w'^2}}$/Um	Radial $\sqrt{\overline{u'^2}}$ [m/s]	Radial $\sqrt{\overline{u'^2}}$/Um
1	0.033	-0.93	0.00158	0.0171	-	-	-	-
2	0.033	-0.87	0.00111	0.0120	-	-	-	-
3	0.033	-0.73	0.00179	0.0194	-	-	-	-
4	0.033	-0.40	0.00411	0.0444	-	-	-	-
5	0.033	0.	0.00685	0.0740	-	-	-	-
6	0.033	0.40	0.00791	0.0854	-	-	-	-
7	0.033	0.73	0.00711	0.0768	-	-	-	-
8	0.033	0.87	0.00495	0.0535	-	-	-	-
9	0.033	0.93	0.00248	0.0268	-	-	-	-
10	0.058	0.93	0.00074	0.0080	-	-	-	-
11	0.058	0.87	0.00843	0.0911	-	-	-	-
12	0.058	0.73	0.00796	0.0859	-	-	-	-
13	0.058	0.40	0.00711	0.0768	-	-	-	-
14	0.058	0.	0.00653	0.0706	-	-	-	-
15	0.058	-0.40	0.00622	0.0672	-	-	-	-
16	0.058	-0.73	0.00422	0.0455	-	-	-	-
17	0.058	-0.87	0.00153	0.0165	-	-	-	-
18	0.058	-0.93	0.00274	0.0296	-	-	-	-
19	0.133	-0.93	0.00601	0.0649	0.00005	0.0006	0.00274	0.0296
20	0.133	-0.87	0.00527	0.0569	0.00495	0.0535	0.00348	0.0376
21	0.133	-0.73	0.00516	0.0558	0.00316	0.0341	0.00269	0.0290
22	0.133	-0.40	0.00711	0.0768	0.00448	0.0484	0.00285	0.0307
23	0.133	0.	0.00806	0.0871	0.00564	0.0609	0.00047	0.0051
24	0.133	0.40	0.00822	0.0888	0.00548	0.0592	0.00153	0.0165
25	0.133	0.73	0.00812	0.0877	0.00548	0.0592	0.00200	0.0216
26	0.133	0.87	0.00891	0.0962	0.00685	0.0740	0.00216	0.0233
27	0.133	0.93	0.00179	0.0194	0.00611	0.0660	0.00211	0.0228
28	0.400	0.93	0.00126	0.0137	0.00685	0.0740	0.00105	0.0114
29	0.400	0.87	0.00922	0.0996	0.00659	0.0711	0.00079	0.0085
30	0.400	0.73	0.00954	0.1030	0.00754	0.0814	0.00179	0.0194
31	0.400	0.40	0.00901	0.0973	0.00722	0.0780	0.00016	0.0017
32	0.400	0.	0.00933	0.1007	0.00648	0.0700	0.00553	0.0598
33	0.400	-0.40	0.00838	0.0905	0.00574	0.0620	0.00659	0.0711
34	0.400	-0.73	0.00638	0.0689	0.00353	0.0381	0.00364	0.0393
35	0.400	-0.87	0.00738	0.0797	0.00406	0.0438	0.00042	0.0046
36	0.400	-0.93	0.00026	0.0028	0.00353	0.0381	0.00126	0.0137
37	0.667	-0.93	0.00232	0.0250	0.00142	0.0154	0.00158	0.0171
38	0.667	-0.87	0.00643	0.0694	0.00337	0.0364	0.00232	0.0250
39	0.667	-0.73	0.00827	0.0894	0.00648	0.0700	0.00248	0.0268
40	0.667	-0.40	0.00838	0.0905	0.00606	0.0655	0.00422	0.0455
41	0.667	0.	0.00964	0.1042	0.00685	0.0740	0.00042	0.0046
42	0.667	0.40	0.00943	0.1019	0.00664	0.0717	0.00058	0.0063
43	0.667	0.73	0.00938	0.1013	0.00596	0.0643	0.00042	0.0046
44	0.667	0.87	0.00632	0.0683	0.00706	0.0763	0.00111	0.0120
45	0.667	0.93	0.00163	0.0176	0.00211	0.0228	0.00169	0.0182
46	0.933	0.93	0.00242	0.0262	-	-	0.00105	0.0114
47	0.933	0.87	0.00806	0.0871	-	-	0.00179	0.0194
48	0.933	0.73	0.00970	0.1047	-	-	0.00184	0.0199
49	0.933	0.40	0.00980	0.1059	-	-	0.00274	0.0296
50	0.933	0.	0.00917	0.0990	-	-	0.00253	0.0273
51	0.933	-0.40	0.00859	0.0928	-	-	0.00290	0.0313
52	0.933	-0.73	0.00775	0.0837	-	-	0.00343	0.0370
53	0.933	-0.87	0.00474	0.0512	-	-	0.00063	0.0068
54	0.933	-0.93	0.00069	0.0074	-	-	0.00422	0.0455

Table 6.25 b). The tangential, vertical and radial turbulence intensity distribution at section S-5 run no.1 Um = 0.04444 m/s

Loc. no.	η = z/h	2Y/B	Tangential $\sqrt{\overline{v'^2}}$ [m/s]	Tangential $\sqrt{\overline{v'^2}}$/Um	Vertical $\sqrt{\overline{w'^2}}$ [m/s]	Vertical $\sqrt{\overline{w'^2}}$/Um	Radial $\sqrt{\overline{u'^2}}$ [m/s]	Radial $\sqrt{\overline{u'^2}}$/Um
1	0.080	-0.93	0.00501	0.1126	-	-	-	-
2	0.080	-0.87	0.00617	0.1387	-	-	-	-
3	0.080	-0.73	0.00490	0.1103	-	-	-	-
4	0.080	-0.40	0.00564	0.1269	-	-	-	-
5	0.080	0.	0.00532	0.1198	-	-	-	-
6	0.080	0.40	0.00464	0.1043	-	-	-	-
7	0.080	0.73	0.00221	0.0498	-	-	-	-
8	0.080	0.87	0.00221	0.0498	-	-	-	-
9	0.080	0.93	0.00379	0.0854	-	-	-	-
10	0.140	0.93	0.00200	0.0451	-	-	0.00021	0.0047
11	0.140	0.87	0.00221	0.0498	-	-	0.00084	0.0190
12	0.140	0.73	0.00343	0.0771	-	-	0.00074	0.0166
13	0.140	0.40	0.00543	0.1221	-	-	0.00395	0.0889
14	0.140	0.	0.00643	0.1447	-	-	0.00264	0.0593
15	0.140	-0.40	0.00701	0.1577	-	-	0.00279	0.0628
16	0.140	-0.73	0.00422	0.0949	-	-	0.00269	0.0605
17	0.140	-0.87	0.00285	0.0640	-	-	0.00232	0.0522
18	0.140	-0.93	0.00327	0.0735	-	-	0.00227	0.0510
19	0.320	-0.93	0.00079	0.0178	0.00153	0.0344	0.00321	0.0723
20	0.320	-0.87	0.00516	0.1162	0.00126	0.0285	0.00142	0.0320
21	0.320	-0.73	0.00659	0.1482	0.00559	0.1257	0.00295	0.0664
22	0.320	-0.40	0.00738	0.1660	0.00437	0.0984	0.00385	0.0866
23	0.320	0.	0.00527	0.1186	0.00480	0.1079	0.00227	0.0510
24	0.320	0.40	0.00780	0.1755	0.00416	0.0937	0.00232	0.0522
25	0.320	0.73	0.00569	0.1281	0.00522	0.1174	0.00090	0.0202
26	0.320	0.87	0.00543	0.1221	0.00369	0.0830	0.00169	0.0379
27	0.320	0.93	0.00538	0.1209	0.00469	0.1055	0.00063	0.0142
28	0.600	0.93	0.00527	0.1186	0.00437	0.0984	0.00058	0.0130
29	0.600	0.87	0.00627	0.1411	0.00406	0.0913	0.00016	0.0036
30	0.600	0.73	0.00627	0.1411	0.00427	0.0960	0.00232	0.0522
31	0.600	0.40	0.00701	0.1577	0.00395	0.0889	0.00264	0.0593
32	0.600	0.	0.00759	0.1707	0.00506	0.1138	0.00300	0.0676
33	0.600	-0.40	0.00727	0.1636	0.00374	0.0842	0.00290	0.0652
34	0.600	-0.73	0.00690	0.1553	0.00353	0.0794	0.00401	0.0901
35	0.600	-0.87	0.00585	0.1316	0.00495	0.1115	0.00358	0.0806
36	0.600	-0.93	0.00374	0.0842	0.00416	0.0937	0.00248	0.0557
37	0.900	-0.93	0.00285	0.0640	0.00538	0.1209	0.00242	0.0545
38	0.900	-0.87	0.00532	0.1198	0.00580	0.1304	0.00163	0.0368
39	0.900	-0.73	0.00685	0.1541	0.00485	0.1091	0.00200	0.0451
40	0.900	-0.40	0.00796	0.1790	0.00538	0.1209	0.00221	0.0498
41	0.900	0.	0.00769	0.1731	0.00611	0.1375	0.00248	0.0557
42	0.900	0.40	0.00675	0.1518	0.00453	0.1020	0.00311	0.0700
43	0.900	0.73	0.00437	0.0984	0.00343	0.0771	0.00321	0.0723
44	0.900	0.87	0.00453	0.1020	0.00279	0.0628	0.00285	0.0640
45	0.900	0.93	0.00511	0.1150	0.00242	0.0545	0.00042	0.0095

Table 6.26 b). The tangential, vertical and radial turbulence intensity distribution at section S-5 run no.2 Um = 0.07407 m/s

Loc. no.	η = z/h	2Y/B	Tangential $\sqrt{\overline{v'^2}}$ [m/s]	Tangential $\sqrt{\overline{v'^2}}$/Um	Vertical $\sqrt{\overline{w'^2}}$ [m/s]	Vertical $\sqrt{\overline{w'^2}}$/Um	Radial $\sqrt{\overline{u'^2}}$ [m/s]	Radial $\sqrt{\overline{u'^2}}$/Um
1	0.044	-0.93	0.00021	0.0028	-	-	-	-
2	0.044	-0.87	0.00427	0.0576	-	-	-	-
3	0.044	-0.73	0.00458	0.0619	-	-	-	-
4	0.044	-0.40	0.00501	0.0676	-	-	-	-
5	0.044	0.	0.00495	0.0669	-	-	-	-
6	0.044	0.40	0.00453	0.0612	-	-	-	-
7	0.044	0.73	0.00327	0.0441	-	-	-	-
8	0.044	0.87	0.00374	0.0505	-	-	-	-
9	0.044	0.93	0.00353	0.0477	-	-	-	-
10	0.078	0.93	0.00443	0.0598	-	-	-	-
11	0.078	0.87	0.00611	0.0825	-	-	-	-
12	0.078	0.73	0.00490	0.0662	-	-	-	-
13	0.078	0.40	0.00580	0.0783	-	-	-	-
14	0.078	0.	0.00685	0.0925	-	-	-	-
15	0.078	-0.40	0.00717	0.0968	-	-	-	-
16	0.078	-0.73	0.00596	0.0804	-	-	-	-
17	0.078	-0.87	0.00622	0.0840	-	-	-	-
18	0.078	-0.93	0.00026	0.0036	-	-	-	-
19	0.178	-0.93	0.00074	0.0100	0.00353	0.0477	0.00285	0.0384
20	0.178	-0.87	0.00379	0.0512	0.00327	0.0441	0.00348	0.0470
21	0.178	-0.73	0.00617	0.0832	0.00453	0.0612	0.00432	0.0583
22	0.178	-0.40	0.00711	0.0960	0.00506	0.0683	0.00427	0.0576
23	0.178	0.	0.00696	0.0939	0.00474	0.0640	0.00348	0.0470
24	0.178	0.40	0.00685	0.0925	0.00522	0.0704	0.00258	0.0349
25	0.178	0.73	0.00611	0.0825	0.00401	0.0541	0.00216	0.0292
26	0.178	0.87	0.00569	0.0768	0.00527	0.0711	0.00163	0.0221
27	0.178	0.93	0.00074	0.0100	0.00385	0.0519	0.00142	0.0192
28	0.422	0.93	0.00237	0.0320	0.00300	0.0406	0.00005	0.0007
29	0.422	0.87	0.00659	0.0889	0.00153	0.0206	0.00253	0.0341
30	0.422	0.73	0.00685	0.0925	0.00474	0.0640	0.00311	0.0420
31	0.422	0.40	0.00743	0.1003	0.00522	0.0704	0.00200	0.0270
32	0.422	0.	0.00801	0.1081	0.00601	0.0811	0.00269	0.0363
33	0.422	-0.40	0.00706	0.0953	0.00448	0.0605	0.00153	0.0206
34	0.422	-0.73	0.00727	0.0982	0.00332	0.0448	0.00132	0.0178
35	0.422	-0.87	0.00237	0.0320	0.00084	0.0114	0.00069	0.0092
36	0.422	-0.93	0.00353	0.0477	0.00032	0.0043	0.00074	0.0100
37	0.667	-0.93	0.00195	0.0263	0.00332	0.0448	0.00016	0.0021
38	0.667	-0.87	0.00775	0.1046	0.00422	0.0569	0.00269	0.0363
39	0.667	-0.73	0.00896	0.1209	0.00553	0.0747	0.00216	0.0292
40	0.667	-0.40	0.00806	0.1089	0.00559	0.0754	0.00221	0.0299
41	0.667	0.	0.00675	0.0911	0.00253	0.0341	0.00264	0.0356
42	0.667	0.40	0.00759	0.1024	0.00348	0.0470	0.00248	0.0334
43	0.667	0.73	0.00733	0.0989	0.00390	0.0526	0.00227	0.0306
44	0.667	0.87	0.00711	0.0960	0.00300	0.0406	0.00195	0.0263
45	0.667	0.93	0.00174	0.0235	0.00306	0.0413	0.00021	0.0028
46	0.911	0.93	0.00374	0.0505	-	-	0.00058	0.0078
47	0.911	0.87	0.00653	0.0882	-	-	0.00032	0.0043
48	0.911	0.73	0.00611	0.0825	-	-	0.00169	0.0228
49	0.911	0.40	0.00759	0.1024	-	-	0.00079	0.0107
50	0.911	0.	0.00796	0.1074	-	-	0.00258	0.0349
51	0.911	-0.40	0.00754	0.1017	-	-	0.00264	0.0356
52	0.911	-0.73	0.00743	0.1003	-	-	0.00385	0.0519
53	0.911	-0.87	0.00664	0.0896	-	-	0.00242	0.0327
54	0.911	-0.93	0.00353	0.0477	-	-	0.00216	0.0292

Table 6.27 *b). The tangential, vertical and radial turbulence intensity distribution at section S-5 run no.3* Um = 0.09259 m/s

Loc. no.	η = z/h	2Y/B	Tangential $\sqrt{\overline{v'^2}}$ [m/s]	Tangential $\sqrt{\overline{v'^2}}$/Um	Vertical $\sqrt{\overline{w'^2}}$ [m/s]	Vertical $\sqrt{\overline{w'^2}}$/Um	Radial $\sqrt{\overline{u'^2}}$ [m/s]	Radial $\sqrt{\overline{u'^2}}$/Um
1	0.033	-0.93	0.00206	0.0222	-	-	-	-
2	0.033	-0.87	0.00422	0.0455	-	-	-	-
3	0.033	-0.73	0.00485	0.0524	-	-	-	-
4	0.033	-0.40	0.00511	0.0552	-	-	-	-
5	0.033	0.	0.00469	0.0507	-	-	-	-
6	0.033	0.40	0.00569	0.0615	-	-	-	-
7	0.033	0.73	0.00374	0.0404	-	-	-	-
8	0.033	0.87	0.00469	0.0507	-	-	-	-
9	0.033	0.93	0.00358	0.0387	-	-	-	-
10	0.058	0.93	0.00501	0.0541	-	-	-	-
11	0.058	0.87	0.00538	0.0581	-	-	-	-
12	0.058	0.73	0.00548	0.0592	-	-	-	-
13	0.058	0.40	0.00574	0.0620	-	-	-	-
14	0.058	0.	0.00701	0.0757	-	-	-	-
15	0.058	-0.40	0.00743	0.0803	-	-	-	-
16	0.058	-0.73	0.00532	0.0575	-	-	-	-
17	0.058	-0.87	0.00200	0.0216	-	-	-	-
18	0.058	-0.93	0.00195	0.0211	-	-	-	-
19	0.133	-0.93	0.00084	0.0091	0.00443	0.0478	0.00074	0.0080
20	0.133	-0.87	0.00764	0.0825	0.00453	0.0489	0.00169	0.0182
21	0.133	-0.73	0.00785	0.0848	0.00543	0.0586	0.00279	0.0302
22	0.133	-0.40	0.00864	0.0933	0.00543	0.0586	0.00158	0.0171
23	0.133	0.	0.00880	0.0950	0.00538	0.0581	0.00474	0.0512
24	0.133	0.40	0.00833	0.0899	0.00532	0.0575	0.00416	0.0450
25	0.133	0.73	0.00775	0.0837	0.00548	0.0592	0.00358	0.0387
26	0.133	0.87	0.00769	0.0831	0.00527	0.0569	0.00042	0.0046
27	0.133	0.93	0.00653	0.0706	0.00585	0.0632	0.00148	0.0159
28	0.400	0.93	0.00611	0.0660	0.00385	0.0415	0.00295	0.0319
29	0.400	0.87	0.00638	0.0689	0.00506	0.0546	0.00253	0.0273
30	0.400	0.73	0.00833	0.0899	0.00543	0.0586	0.00242	0.0262
31	0.400	0.40	0.00833	0.0899	0.00601	0.0649	0.00316	0.0341
32	0.400	0.	0.00859	0.0928	0.00580	0.0626	0.00416	0.0450
33	0.400	-0.40	0.00885	0.0956	0.00379	0.0410	0.00327	0.0353
34	0.400	-0.73	0.00906	0.0979	0.00501	0.0541	0.00290	0.0313
35	0.400	-0.87	0.00864	0.0933	0.00395	0.0427	0.00248	0.0268
36	0.400	-0.93	0.00011	0.0011	0.00553	0.0598	0.00274	0.0296
37	0.667	-0.93	0.00316	0.0341	0.00100	0.0108	0.00337	0.0364
38	0.667	-0.87	0.00759	0.0820	0.00090	0.0097	0.00416	0.0450
39	0.667	-0.73	0.00812	0.0877	0.00306	0.0330	0.00242	0.0262
40	0.667	-0.40	0.00954	0.1030	0.00596	0.0643	0.00379	0.0410
41	0.667	0.	0.00854	0.0922	0.00580	0.0626	0.00395	0.0427
42	0.667	0.40	0.00769	0.0831	0.00569	0.0615	0.00569	0.0615
43	0.667	0.73	0.00796	0.0859	0.00480	0.0518	0.00206	0.0222
44	0.667	0.87	0.00717	0.0774	0.00353	0.0381	0.00311	0.0336
45	0.667	0.93	0.00696	0.0751	0.00480	0.0518	0.00079	0.0085
46	0.933	0.93	0.00369	0.0398	-	-	0.00316	0.0341
47	0.933	0.87	0.00574	0.0620	-	-	0.00306	0.0330
48	0.933	0.73	0.00643	0.0694	-	-	0.00343	0.0370
49	0.933	0.40	0.00585	0.0632	-	-	0.00379	0.0410
50	0.933	0.	0.00532	0.0575	-	-	0.00285	0.0307
51	0.933	-0.40	0.00659	0.0711	-	-	0.00200	0.0216
52	0.933	-0.73	0.00248	0.0268	-	-	0.00490	0.0529
53	0.933	-0.87	0.00179	0.0194	-	-	0.00290	0.0313
54	0.933	-0.93	0.00337	0.0364	-	-	0.00406	0.0438

Table 6.28 *b). The tangential, vertical and radial turbulence intensity distribution at section S-6 run no.1* Um = 0.04444 m/s

Loc. no.	η = z/h	2Y/B	Tangential $\sqrt{\overline{v'^2}}$ [m/s]	Tangential $\sqrt{\overline{v'^2}}$/Um	Vertical $\sqrt{\overline{w'^2}}$ [m/s]	Vertical $\sqrt{\overline{w'^2}}$/Um	Radial $\sqrt{\overline{u'^2}}$ [m/s]	Radial $\sqrt{\overline{u'^2}}$/Um
1	0.080	-0.93	0.00285	0.0640	-	-	-	-
2	0.080	-0.87	0.00343	0.0771	-	-	-	-
3	0.080	-0.73	0.00427	0.0960	-	-	-	-
4	0.080	-0.40	0.00480	0.1079	-	-	-	-
5	0.080	0.	0.00443	0.0996	-	-	-	-
6	0.080	0.40	0.00337	0.0759	-	-	-	-
7	0.080	0.73	0.00353	0.0794	-	-	-	-
8	0.080	0.87	0.00411	0.0925	-	-	-	-
9	0.080	0.93	0.00337	0.0759	-	-	-	-
10	0.140	0.93	0.00448	0.1008	-	-	0.00227	0.0510
11	0.140	0.87	0.00564	0.1269	-	-	0.00343	0.0771
12	0.140	0.73	0.00532	0.1198	-	-	0.00253	0.0569
13	0.140	0.40	0.00548	0.1233	-	-	0.00337	0.0759
14	0.140	0.	0.00638	0.1435	-	-	0.00406	0.0913
15	0.140	-0.40	0.00706	0.1589	-	-	0.00332	0.0747
16	0.140	-0.73	0.00543	0.1221	-	-	0.00221	0.0498
17	0.140	-0.87	0.00406	0.0913	-	-	0.00221	0.0498
18	0.140	-0.93	0.00090	0.0202	-	-	0.00253	0.0569
19	0.320	-0.93	0.00385	0.0866	0.00269	0.0605	0.00005	0.0012
20	0.320	-0.87	0.00416	0.0937	0.00348	0.0783	0.00306	0.0688
21	0.320	-0.73	0.00648	0.1458	0.00332	0.0747	0.00379	0.0854
22	0.320	-0.40	0.00806	0.1814	0.00601	0.1352	0.00469	0.1055
23	0.320	0.	0.00775	0.1743	0.00606	0.1364	0.00195	0.0439
24	0.320	0.40	0.00617	0.1387	0.00501	0.1126	0.00248	0.0557
25	0.320	0.73	0.00606	0.1364	0.00416	0.0937	0.00237	0.0534
26	0.320	0.87	0.00627	0.1411	0.00285	0.0640	0.00274	0.0617
27	0.320	0.93	0.00669	0.1506	0.00053	0.0119	0.00084	0.0190
28	0.600	0.93	0.00469	0.1055	0.00084	0.0190	0.00126	0.0285
29	0.600	0.87	0.00606	0.1364	0.00401	0.0901	0.00295	0.0664
30	0.600	0.73	0.00664	0.1494	0.00401	0.0901	0.00332	0.0747
31	0.600	0.40	0.00780	0.1755	0.00574	0.1292	0.00353	0.0794
32	0.600	0.	0.00870	0.1956	0.00553	0.1245	0.00379	0.0854
33	0.600	-0.40	0.00690	0.1553	0.00295	0.0664	0.00401	0.0901
34	0.600	-0.73	0.00511	0.1150	0.00469	0.1055	0.00343	0.0771
35	0.600	-0.87	0.00548	0.1233	0.00132	0.0296	0.00253	0.0569
36	0.600	-0.93	0.00111	0.0249	0.00026	0.0059	0.00274	0.0617
37	0.900	-0.93	0.00042	0.0095	0.00332	0.0747	0.00111	0.0249
38	0.900	-0.87	0.00411	0.0925	0.00316	0.0711	0.00258	0.0581
39	0.900	-0.73	0.00469	0.1055	0.00274	0.0617	0.00264	0.0593
40	0.900	-0.40	0.00474	0.1067	0.00401	0.0901	0.00448	0.1008
41	0.900	0.	0.00717	0.1613	0.00443	0.0996	0.00506	0.1138
42	0.900	0.40	0.00374	0.0842	0.00485	0.1091	0.00501	0.1126
43	0.900	0.73	0.00448	0.1008	0.00601	0.1352	0.00274	0.0617
44	0.900	0.87	0.00543	0.1221	0.00596	0.1340	0.00153	0.0344
45	0.900	0.93	0.00385	0.0866	0.00538	0.1209	0.00026	0.0059

Table 6.29 b). The tangential, vertical and radial turbulence intensity distribution at section S-6 run no.2 Um = 0.07407 m/s

Loc. no.	η = z/h	2Y/B	Tangential $\sqrt{v'^2}$ [m/s]	Tangential $\sqrt{v'^2}$/Um	Vertical $\sqrt{w'^2}$ [m/s]	Vertical $\sqrt{w'^2}$/Um	Radial $\sqrt{u'^2}$ [m/s]	Radial $\sqrt{u'^2}$/Um
1	0.044	-0.93	0.00074	0.0100	-	-	-	-
2	0.044	-0.87	0.00221	0.0299	-	-	-	-
3	0.044	-0.73	0.00632	0.0854	-	-	-	-
4	0.044	-0.40	0.00733	0.0989	-	-	-	-
5	0.044	0.	0.00548	0.0740	-	-	-	-
6	0.044	0.40	0.00553	0.0747	-	-	-	-
7	0.044	0.73	0.00443	0.0598	-	-	-	-
8	0.044	0.87	0.00590	0.0797	-	-	-	-
9	0.044	0.93	0.00221	0.0299	-	-	-	-
10	0.078	0.93	0.00395	0.0534	-	-	-	-
11	0.078	0.87	0.00569	0.0768	-	-	-	-
12	0.078	0.73	0.00585	0.0790	-	-	-	-
13	0.078	0.40	0.00569	0.0768	-	-	-	-
14	0.078	0.	0.00659	0.0889	-	-	-	-
15	0.078	-0.40	0.00580	0.0783	-	-	-	-
16	0.078	-0.73	0.00706	0.0953	-	-	-	-
17	0.078	-0.87	0.00590	0.0797	-	-	-	-
18	0.078	-0.93	0.00353	0.0477	-	-	-	-
19	0.178	-0.93	0.00105	0.0142	0.00306	0.0413	0.00443	0.0598
20	0.178	-0.87	0.00659	0.0889	0.00411	0.0555	0.00390	0.0526
21	0.178	-0.73	0.00675	0.0911	0.00443	0.0598	0.00369	0.0498
22	0.178	-0.40	0.00711	0.0960	0.00495	0.0669	0.00506	0.0683
23	0.178	0.	0.00769	0.1039	0.00548	0.0740	0.00227	0.0306
24	0.178	0.40	0.00701	0.0946	0.00559	0.0754	0.00422	0.0569
25	0.178	0.73	0.00585	0.0790	0.00469	0.0633	0.00401	0.0541
26	0.178	0.87	0.00659	0.0889	0.00543	0.0733	0.00237	0.0320
27	0.178	0.93	0.00485	0.0655	0.00432	0.0583	0.00079	0.0107
28	0.422	0.93	0.00390	0.0526	0.00538	0.0726	0.00258	0.0349
29	0.422	0.87	0.00553	0.0747	0.00522	0.0704	0.00021	0.0028
30	0.422	0.73	0.00659	0.0889	0.00422	0.0569	0.00416	0.0562
31	0.422	0.40	0.00669	0.0904	0.00474	0.0640	0.00221	0.0299
32	0.422	0.	0.00738	0.0996	0.00532	0.0719	0.00095	0.0128
33	0.422	-0.40	0.00864	0.1167	0.00527	0.0711	0.00443	0.0598
34	0.422	-0.73	0.00780	0.1053	0.00458	0.0619	0.00506	0.0683
35	0.422	-0.87	0.00675	0.0911	0.00416	0.0562	0.00179	0.0242
36	0.422	-0.93	0.00047	0.0064	0.00300	0.0406	0.00169	0.0228
37	0.667	-0.93	0.00158	0.0213	0.00126	0.0171	0.00285	0.0384
38	0.667	-0.87	0.00443	0.0598	0.00453	0.0612	0.00232	0.0313
39	0.667	-0.73	0.00680	0.0918	0.00548	0.0740	0.00474	0.0640
40	0.667	-0.40	0.00838	0.1131	0.00580	0.0783	0.00458	0.0619
41	0.667	0.	0.00843	0.1138	0.00569	0.0768	0.00480	0.0647
42	0.667	0.40	0.00696	0.0939	0.00501	0.0676	0.00237	0.0320
43	0.667	0.73	0.00596	0.0804	0.00543	0.0733	0.00306	0.0413
44	0.667	0.87	0.00416	0.0562	0.00553	0.0747	0.00401	0.0541
45	0.667	0.93	0.00564	0.0761	0.00501	0.0676	0.00385	0.0519
46	0.911	0.93	0.00548	0.0740	-	-	0.00279	0.0377
47	0.911	0.87	0.00553	0.0747	-	-	0.00179	0.0242
48	0.911	0.73	0.00596	0.0804	-	-	0.00401	0.0541
49	0.911	0.40	0.00769	0.1039	-	-	0.00427	0.0576
50	0.911	0.	0.00680	0.0918	-	-	0.00047	0.0064
51	0.911	-0.40	0.00711	0.0960	-	-	0.00174	0.0235
52	0.911	-0.73	0.00290	0.0391	-	-	0.00306	0.0413
53	0.911	-0.87	0.00353	0.0477	-	-	0.00337	0.0455
54	0.911	-0.93	0.00090	0.0121	-	-	0.00158	0.0213

Table 6.30 b). The tangential, vertical and radial turbulence intensity distribution at section S-6 run no.3 Um = 0.09259 m/s

Loc. no.	η = z/h	2Y/B	Tangential $\sqrt{v'^2}$ [m/s]	Tangential $\sqrt{v'^2}$/Um	Vertical $\sqrt{w'^2}$ [m/s]	Vertical $\sqrt{w'^2}$/Um	Radial $\sqrt{u'^2}$ [m/s]	Radial $\sqrt{u'^2}$/Um
1	0.033	-0.93	0.00005	0.0006	-	-	-	-
2	0.033	-0.87	0.00516	0.0558	-	-	-	-
3	0.033	-0.73	0.00632	0.0683	-	-	-	-
4	0.033	-0.40	0.00717	0.0774	-	-	-	-
5	0.033	0.	0.00648	0.0700	-	-	-	-
6	0.033	0.40	0.00569	0.0615	-	-	-	-
7	0.033	0.73	0.00590	0.0637	-	-	-	-
8	0.033	0.87	0.00669	0.0723	-	-	-	-
9	0.033	0.93	0.00601	0.0649	-	-	-	-
10	0.058	0.93	0.00501	0.0541	-	-	-	-
11	0.058	0.87	0.00701	0.0757	-	-	-	-
12	0.058	0.73	0.00611	0.0660	-	-	-	-
13	0.058	0.40	0.00764	0.0825	-	-	-	-
14	0.058	0.	0.00801	0.0865	-	-	-	-
15	0.058	-0.40	0.00754	0.0814	-	-	-	-
16	0.058	-0.73	0.00717	0.0774	-	-	-	-
17	0.058	-0.87	0.00569	0.0615	-	-	-	-
18	0.058	-0.93	0.00126	0.0137	-	-	-	-
19	0.133	-0.93	0.00111	0.0120	0.00253	0.0273	0.00090	0.0097
20	0.133	-0.87	0.00548	0.0592	0.00369	0.0398	0.00042	0.0046
21	0.133	-0.73	0.00601	0.0649	0.00374	0.0404	0.00153	0.0165
22	0.133	-0.40	0.00875	0.0945	0.00501	0.0541	0.00300	0.0324
23	0.133	0.	0.00827	0.0894	0.00548	0.0592	0.00111	0.0120
24	0.133	0.40	0.00748	0.0808	0.00585	0.0632	0.00105	0.0114
25	0.133	0.73	0.00685	0.0740	0.00474	0.0512	0.00079	0.0085
26	0.133	0.87	0.00780	0.0842	0.00480	0.0518	0.00169	0.0182
27	0.133	0.93	0.00390	0.0421	0.00553	0.0598	0.00058	0.0063
28	0.400	0.93	0.00458	0.0495	0.00464	0.0501	0.00153	0.0165
29	0.400	0.87	0.00764	0.0825	0.00485	0.0524	0.00063	0.0068
30	0.400	0.73	0.00775	0.0837	0.00490	0.0529	0.00285	0.0307
31	0.400	0.40	0.00922	0.0996	0.00490	0.0529	0.00200	0.0216
32	0.400	0.	0.00943	0.1019	0.00585	0.0632	0.00253	0.0273
33	0.400	-0.40	0.00875	0.0945	0.00601	0.0649	0.00221	0.0239
34	0.400	-0.73	0.00812	0.0877	0.00453	0.0489	0.00264	0.0285
35	0.400	-0.87	0.00659	0.0711	0.00411	0.0444	0.00422	0.0455
36	0.400	-0.93	0.00190	0.0205	0.00321	0.0347	0.00195	0.0211
37	0.667	-0.93	0.00063	0.0068	0.00206	0.0222	0.00026	0.0028
38	0.667	-0.87	0.00553	0.0598	0.00158	0.0171	0.00079	0.0085
39	0.667	-0.73	0.00527	0.0569	0.00295	0.0319	0.00174	0.0188
40	0.667	-0.40	0.00906	0.0979	0.00495	0.0535	0.00469	0.0507
41	0.667	0.	0.00838	0.0905	0.00543	0.0586	0.00148	0.0159
42	0.667	0.40	0.00606	0.0655	0.00585	0.0632	0.00169	0.0182
43	0.667	0.73	0.00680	0.0734	0.00443	0.0478	0.00200	0.0216
44	0.667	0.87	0.00696	0.0751	0.00474	0.0512	0.00042	0.0046
45	0.667	0.93	0.00063	0.0068	0.00437	0.0472	0.00153	0.0165
46	0.933	0.93	0.00311	0.0336	-	-	0.00042	0.0046
47	0.933	0.87	0.00627	0.0677	-	-	0.00026	0.0028
48	0.933	0.73	0.00627	0.0677	-	-	0.00105	0.0114
49	0.933	0.40	0.00796	0.0859	-	-	0.00116	0.0125
50	0.933	0.	0.00875	0.0945	-	-	0.00058	0.0063
51	0.933	-0.40	0.00870	0.0939	-	-	0.00264	0.0285
52	0.933	-0.73	0.00653	0.0706	-	-	0.00369	0.0398
53	0.933	-0.87	0.00506	0.0546	-	-	0.00063	0.0068
54	0.933	-0.93	0.00232	0.0250	-	-	0.00221	0.0239

Table 6.31 b). The tangential, vertical and radial turbulence intensity distribution at section S-7 run no.1 Um = 0.04444 m/s

Loc. no.	η = z/h	2Y/B	Tangential $\sqrt{v'^2}$ [m/s]	Tangential $\sqrt{v'^2}$/Um	Vertical $\sqrt{w'^2}$ [m/s]	Vertical $\sqrt{w'^2}$/Um	Radial $\sqrt{u'^2}$ [m/s]	Radial $\sqrt{u'^2}$/Um
1	0.080	-0.93	0.00437	0.0984	-	-	-	-
2	0.080	-0.87	0.00385	0.0866	-	-	-	-
3	0.080	-0.73	0.00458	0.1032	-	-	-	-
4	0.080	-0.40	0.00427	0.0960	-	-	-	-
5	0.080	0.	0.00490	0.1103	-	-	-	-
6	0.080	0.40	0.00559	0.1257	-	-	-	-
7	0.080	0.73	0.00574	0.1292	-	-	-	-
8	0.080	0.87	0.00611	0.1375	-	-	-	-
9	0.080	0.93	0.00432	0.0972	-	-	-	-
10	0.140	0.93	0.00285	0.0640	-	-	0.00011	0.0024
11	0.140	0.87	0.00653	0.1470	-	-	0.00264	0.0593
12	0.140	0.73	0.00611	0.1375	-	-	0.00448	0.1008
13	0.140	0.40	0.00617	0.1387	-	-	0.00221	0.0498
14	0.140	0.	0.00553	0.1245	-	-	0.00332	0.0747
15	0.140	-0.40	0.00495	0.1115	-	-	0.00316	0.0711
16	0.140	-0.73	0.00390	0.0877	-	-	0.00300	0.0676
17	0.140	-0.87	0.00321	0.0723	-	-	0.00300	0.0676
18	0.140	-0.93	0.00369	0.0830	-	-	0.00121	0.0273
19	0.320	-0.93	0.00416	0.0937	0.00063	0.0142	0.00063	0.0142
20	0.320	-0.87	0.00411	0.0925	0.00264	0.0593	0.00264	0.0593
21	0.320	-0.73	0.00474	0.1067	0.00343	0.0771	0.00211	0.0474
22	0.320	-0.40	0.00574	0.1292	0.00343	0.0771	0.00279	0.0628
23	0.320	0.	0.00627	0.1411	0.00332	0.0747	0.00306	0.0688
24	0.320	0.40	0.00706	0.1589	0.00469	0.1055	0.00353	0.0794
25	0.320	0.73	0.00743	0.1672	0.00580	0.1304	0.00485	0.1091
26	0.320	0.87	0.00733	0.1648	0.00416	0.0937	0.00443	0.0996
27	0.320	0.93	0.00121	0.0273	0.00337	0.0759	0.00158	0.0356
28	0.600	0.93	0.00095	0.0213	0.00401	0.0901	0.00074	0.0166
29	0.600	0.87	0.00833	0.1873	0.00580	0.1304	0.00538	0.1209
30	0.600	0.73	0.00748	0.1684	0.00480	0.1079	0.00527	0.1186
31	0.600	0.40	0.00696	0.1565	0.00532	0.1198	0.00448	0.1008
32	0.600	0.	0.00696	0.1565	0.00390	0.0877	0.00221	0.0498
33	0.600	-0.40	0.00590	0.1328	0.00332	0.0747	0.00337	0.0759
34	0.600	-0.73	0.00527	0.1186	0.00416	0.0937	0.00069	0.0154
35	0.600	-0.87	0.00374	0.0842	0.00248	0.0557	0.00153	0.0344
36	0.600	-0.93	0.00332	0.0747	0.00279	0.0628	0.00105	0.0237
37	0.900	-0.93	0.00074	0.0166	0.00348	0.0783	0.00211	0.0474
38	0.900	-0.87	0.00411	0.0925	0.00132	0.0296	0.00211	0.0474
39	0.900	-0.73	0.00295	0.0664	0.00295	0.0664	0.00142	0.0320
40	0.900	-0.40	0.00269	0.0605	0.00379	0.0854	0.00253	0.0569
41	0.900	0.	0.00559	0.1257	0.00416	0.0937	0.00295	0.0664
42	0.900	0.40	0.00622	0.1399	0.00358	0.0806	0.00184	0.0415
43	0.900	0.73	0.00538	0.1209	0.00337	0.0759	0.00379	0.0854
44	0.900	0.87	0.00522	0.1174	0.00290	0.0652	0.00179	0.0403
45	0.900	0.93	0.00100	0.0225	0.00279	0.0628	0.00300	0.0676

Table 6.32 b). The tangential, vertical and radial turbulence intensity distribution at section S-7 run no.2 Um = 0.07407 m/s

Loc. no.	η = z/h	2Y/B	Tangential $\sqrt{v'^2}$ [m/s]	Tangential $\sqrt{v'^2}$/Um	Vertical $\sqrt{w'^2}$ [m/s]	Vertical $\sqrt{w'^2}$/Um	Radial $\sqrt{u'^2}$ [m/s]	Radial $\sqrt{u'^2}$/Um
1	0.044	-0.93	0.00406	0.0548	-	-	-	-
2	0.044	-0.87	0.00448	0.0605	-	-	-	-
3	0.044	-0.73	0.00495	0.0669	-	-	-	-
4	0.044	-0.40	0.00559	0.0754	-	-	-	-
5	0.044	0.	0.00659	0.0889	-	-	-	-
6	0.044	0.40	0.00664	0.0896	-	-	-	-
7	0.044	0.73	0.00664	0.0896	-	-	-	-
8	0.044	0.87	0.00722	0.0975	-	-	-	-
9	0.044	0.93	0.00395	0.0534	-	-	-	-
10	0.078	0.93	0.00211	0.0285	-	-	-	-
11	0.078	0.87	0.00780	0.1053	-	-	-	-
12	0.078	0.73	0.00833	0.1124	-	-	-	-
13	0.078	0.40	0.00843	0.1138	-	-	-	-
14	0.078	0.	0.00469	0.0633	-	-	-	-
15	0.078	-0.40	0.00585	0.0790	-	-	-	-
16	0.078	-0.73	0.00543	0.0733	-	-	-	-
17	0.078	-0.87	0.00532	0.0719	-	-	-	-
18	0.078	-0.93	0.00411	0.0555	-	-	-	-
19	0.178	-0.93	0.00480	0.0647	0.00321	0.0434	0.00169	0.0228
20	0.178	-0.87	0.00722	0.0975	0.00437	0.0591	0.00221	0.0299
21	0.178	-0.73	0.00870	0.1174	0.00464	0.0626	0.00264	0.0356
22	0.178	-0.40	0.00827	0.1117	0.00548	0.0740	0.00353	0.0477
23	0.178	0.	0.00833	0.1124	0.00585	0.0790	0.00411	0.0555
24	0.178	0.40	0.00833	0.1124	0.00627	0.0847	0.00427	0.0576
25	0.178	0.73	0.00590	0.0797	0.00564	0.0761	0.00464	0.0626
26	0.178	0.87	0.00843	0.1138	0.00490	0.0662	0.00580	0.0783
27	0.178	0.93	0.00005	0.0007	0.00448	0.0605	0.00464	0.0626
28	0.422	0.93	0.00042	0.0057	0.00469	0.0633	0.00548	0.0740
29	0.422	0.87	0.00885	0.1195	0.00469	0.0633	0.00348	0.0470
30	0.422	0.73	0.00922	0.1245	0.00480	0.0647	0.00553	0.0747
31	0.422	0.40	0.00917	0.1238	0.00506	0.0683	0.00390	0.0526
32	0.422	0.	0.00801	0.1081	0.00611	0.0825	0.00559	0.0754
33	0.422	-0.40	0.00722	0.0975	0.00401	0.0541	0.00406	0.0548
34	0.422	-0.73	0.00754	0.1017	0.00422	0.0569	0.00443	0.0598
35	0.422	-0.87	0.00627	0.0847	0.00432	0.0583	0.00300	0.0406
36	0.422	-0.93	0.00543	0.0733	0.00306	0.0413	0.00237	0.0320
37	0.667	-0.93	0.00279	0.0377	0.00221	0.0299	0.00258	0.0349
38	0.667	-0.87	0.00564	0.0761	0.00269	0.0363	0.00401	0.0541
39	0.667	-0.73	0.00748	0.1010	0.00374	0.0505	0.00321	0.0434
40	0.667	-0.40	0.00833	0.1124	0.00432	0.0583	0.00332	0.0448
41	0.667	0.	0.00812	0.1096	0.00522	0.0704	0.00401	0.0541
42	0.667	0.40	0.00833	0.1124	0.00611	0.0825	0.00469	0.0633
43	0.667	0.73	0.00833	0.1124	0.00627	0.0847	0.00390	0.0526
44	0.667	0.87	0.00812	0.1096	0.00458	0.0619	0.00232	0.0313
45	0.667	0.93	0.00184	0.0249	0.00469	0.0633	0.00179	0.0242
46	0.911	0.93	0.	0.	-	-	0.00580	0.0783
47	0.911	0.87	0.00696	0.0939	-	-	0.00406	0.0548
48	0.911	0.73	0.00785	0.1060	-	-	0.00358	0.0484
49	0.911	0.40	0.00727	0.0982	-	-	0.00290	0.0391
50	0.911	0.	0.00785	0.1060	-	-	0.00248	0.0334
51	0.911	-0.40	0.00653	0.0882	-	-	0.00401	0.0541
52	0.911	-0.73	0.00153	0.0206	-	-	0.00437	0.0591
53	0.911	-0.87	0.00169	0.0228	-	-	0.00153	0.0206
54	0.911	-0.93	0.00200	0.0270	-	-	0.00174	0.0235

Table 6.33 *b). The tangential, vertical and radial turbulence intensity distribution at section S-7 run no.3* Um = 0.09259 m/s

Loc. no.	η = z/h	2Y/B	Tangential $\sqrt{\overline{v'^2}}$ [m/s]	Tangential $\sqrt{\overline{v'^2}}$/Um	Vertical $\sqrt{\overline{w'^2}}$ [m/s]	Vertical $\sqrt{\overline{w'^2}}$/Um	Radial $\sqrt{\overline{u'^2}}$ [m/s]	Radial $\sqrt{\overline{u'^2}}$/Um
1	0.033	−0.93	0.00248	0.0268	–	–	–	–
2	0.033	−0.87	0.00364	0.0393	–	–	–	–
3	0.033	−0.73	0.00422	0.0455	–	–	–	–
4	0.033	−0.40	0.00337	0.0364	–	–	–	–
5	0.033	0.	0.00406	0.0438	–	–	–	–
6	0.033	0.40	0.00464	0.0501	–	–	–	–
7	0.033	0.73	0.00490	0.0529	–	–	–	–
8	0.033	0.87	0.00406	0.0438	–	–	–	–
9	0.033	0.93	0.00047	0.0051	–	–	–	–
10	0.058	0.93	0.00032	0.0034	–	–	–	–
11	0.058	0.87	0.00606	0.0655	–	–	–	–
12	0.058	0.73	0.00675	0.0729	–	–	–	–
13	0.058	0.40	0.00701	0.0757	–	–	–	–
14	0.058	0.	0.00590	0.0637	–	–	–	–
15	0.058	−0.40	0.00527	0.0569	–	–	–	–
16	0.058	−0.73	0.00559	0.0603	–	–	–	–
17	0.058	−0.87	0.00321	0.0347	–	–	–	–
18	0.058	−0.93	0.00142	0.0154	–	–	–	–
19	0.133	−0.93	0.00026	0.0028	0.00495	0.0535	0.00121	0.0131
20	0.133	−0.87	0.00390	0.0421	0.00538	0.0581	0.00032	0.0034
21	0.133	−0.73	0.00443	0.0478	0.00469	0.0507	0.00206	0.0222
22	0.133	−0.40	0.00711	0.0768	0.00501	0.0541	0.00300	0.0324
23	0.133	0.	0.00827	0.0894	0.00638	0.0689	0.00464	0.0501
24	0.133	0.40	0.00638	0.0689	0.00538	0.0581	0.00248	0.0268
25	0.133	0.73	0.00733	0.0791	0.00643	0.0694	0.00369	0.0398
26	0.133	0.87	0.00759	0.0820	0.00580	0.0626	0.00395	0.0427
27	0.133	0.93	0.00095	0.0102	0.00411	0.0444	0.00406	0.0438
28	0.400	0.93	0.00058	0.0063	0.00474	0.0512	0.00353	0.0381
29	0.400	0.87	0.00791	0.0854	0.00638	0.0689	0.00311	0.0336
30	0.400	0.73	0.00759	0.0820	0.00606	0.0655	0.00379	0.0410
31	0.400	0.40	0.00917	0.0990	0.00580	0.0626	0.00121	0.0131
32	0.400	0.	0.00754	0.0814	0.00527	0.0569	0.00037	0.0040
33	0.400	−0.40	0.00680	0.0734	0.00601	0.0649	0.00100	0.0108
34	0.400	−0.73	0.00627	0.0677	0.00596	0.0643	0.00137	0.0148
35	0.400	−0.87	0.00564	0.0609	0.00617	0.0666	0.00216	0.0233
36	0.400	−0.93	0.00316	0.0341	0.00522	0.0563	0.00211	0.0228
37	0.667	−0.93	0.00069	0.0074	0.00184	0.0199	0.00037	0.0040
38	0.667	−0.87	0.00474	0.0512	0.00443	0.0478	0.00026	0.0028
39	0.667	−0.73	0.00717	0.0774	0.00659	0.0711	0.00037	0.0040
40	0.667	−0.40	0.00780	0.0842	0.00611	0.0660	0.00232	0.0250
41	0.667	0.	0.00843	0.0911	0.00611	0.0660	0.00021	0.0023
42	0.667	0.40	0.00864	0.0933	0.00648	0.0700	0.00021	0.0023
43	0.667	0.73	0.00870	0.0939	0.00664	0.0717	0.00453	0.0489
44	0.667	0.87	0.00437	0.0472	0.00564	0.0609	0.00532	0.0575
45	0.667	0.93	0.00053	0.0057	0.00464	0.0501	0.00601	0.0649
46	0.933	0.93	0.00042	0.0046	–	–	0.00448	0.0484
47	0.933	0.87	0.00501	0.0541	–	–	0.00427	0.0461
48	0.933	0.73	0.00785	0.0848	–	–	0.00369	0.0398
49	0.933	0.40	0.00796	0.0859	–	–	0.00464	0.0501
50	0.933	0.	0.00833	0.0899	–	–	0.00237	0.0256
51	0.933	−0.40	0.00769	0.0831	–	–	0.00090	0.0097
52	0.933	−0.73	0.00706	0.0763	–	–	0.00095	0.0102
53	0.933	−0.87	0.00485	0.0524	–	–	0.00353	0.0381
54	0.933	−0.93	0.00032	0.0034	–	–	0.00321	0.0347

Table 6.34 *b). The tangential, vertical and radial turbulence intensity distribution at section S-8 run no.1* Um = 0.04444 m/s

Loc. no.	η = z/h	2Y/B	Tangential $\sqrt{\overline{v'^2}}$ [m/s]	Tangential $\sqrt{\overline{v'^2}}$/Um	Vertical $\sqrt{\overline{w'^2}}$ [m/s]	Vertical $\sqrt{\overline{w'^2}}$/Um	Radial $\sqrt{\overline{u'^2}}$ [m/s]	Radial $\sqrt{\overline{u'^2}}$/Um
1	0.080	−0.93	0.00043	0.0097	–	–	–	–
2	0.080	−0.87	0.00124	0.0278	–	–	–	–
3	0.080	−0.73	0.00102	0.0230	–	–	–	–
4	0.080	−0.40	0.00118	0.0266	–	–	–	–
5	0.080	0.	0.00140	0.0315	–	–	–	–
6	0.080	0.40	0.00223	0.0502	–	–	–	–
7	0.080	0.73	0.00269	0.0605	–	–	–	–
8	0.080	0.87	0.00213	0.0478	–	–	–	–
9	0.080	0.93	0.00056	0.0127	–	–	–	–
10	0.140	0.93	0.00129	0.0291	–	–	–	–
11	0.140	0.87	0.00293	0.0660	–	–	–	–
12	0.140	0.73	0.00312	0.0702	–	–	–	–
13	0.140	0.40	0.00288	0.0648	–	–	–	–
14	0.140	0.	0.00331	0.0744	–	–	–	–
15	0.140	−0.40	0.00315	0.0708	–	–	–	–
16	0.140	−0.73	0.00293	0.0660	–	–	–	–
17	0.140	−0.87	0.00264	0.0593	–	–	–	–
18	0.140	−0.93	0.00038	0.0085	–	–	–	–
19	0.320	−0.93	0.00054	0.0121	–	–	–	–
20	0.320	−0.87	0.00223	0.0502	–	–	–	–
21	0.320	−0.73	0.00307	0.0690	–	–	–	–
22	0.320	−0.40	0.00385	0.0866	–	–	–	–
23	0.320	0.	0.00425	0.0956	–	–	–	–
24	0.320	0.40	0.00460	0.1035	–	–	–	–
25	0.320	0.73	0.00479	0.1077	–	–	–	–
26	0.320	0.87	0.00516	0.1162	–	–	–	–
27	0.320	0.93	0.00218	0.0490	–	–	–	–
28	0.600	0.93	0.00169	0.0381	–	–	–	–
29	0.600	0.87	0.00430	0.0968	–	–	–	–
30	0.600	0.73	0.00409	0.0920	–	–	–	–
31	0.600	0.40	0.00463	0.1041	–	–	–	–
32	0.600	0.	0.00452	0.1017	–	–	–	–
33	0.600	−0.40	0.00465	0.1047	–	–	–	–
34	0.600	−0.73	0.00371	0.0835	–	–	–	–
35	0.600	−0.87	0.00226	0.0508	–	–	–	–
36	0.600	−0.93	0.00285	0.0642	–	–	–	–
37	0.900	−0.93	0.00126	0.0284	–	–	–	–
38	0.900	−0.87	0.00188	0.0424	–	–	–	–
39	0.900	−0.73	0.00186	0.0418	–	–	–	–
40	0.900	−0.40	0.00239	0.0539	–	–	–	–
41	0.900	0.	0.00441	0.0993	–	–	–	–
42	0.900	0.40	0.00479	0.1077	–	–	–	–
43	0.900	0.73	0.00412	0.0926	–	–	–	–
44	0.900	0.87	0.00393	0.0884	–	–	–	–
45	0.900	0.93	0.00221	0.0496	–	–	–	–

Table 6.35 b). The tangential, vertical and radial turbulence intensity distribution at section S-8 run no.2 Um = 0.07407 m/s

Loc. no.	η = z/h	2Y/B	Tangential $\sqrt{v'^2}$ [m/s]	Tangential $\sqrt{v'^2}$/Um	Vertical $\sqrt{w'^2}$ [m/s]	Vertical $\sqrt{w'^2}$/Um	Radial $\sqrt{u'^2}$ [m/s]	Radial $\sqrt{u'^2}$/Um
1	0.044	-0.93	0.00032	0.0044	-	-	-	-
2	0.044	-0.87	0.00097	0.0131	-	-	-	-
3	0.044	-0.73	0.00046	0.0062	-	-	-	-
4	0.044	-0.40	0.00059	0.0080	-	-	-	-
5	0.044	0.	0.00180	0.0243	-	-	-	-
6	0.044	0.40	0.00247	0.0334	-	-	-	-
7	0.044	0.73	0.00264	0.0356	-	-	-	-
8	0.044	0.87	0.00229	0.0309	-	-	-	-
9	0.044	0.93	0.00137	0.0185	-	-	-	-
10	0.078	0.93	0.00011	0.0015	-	-	-	-
11	0.078	0.87	0.00398	0.0537	-	-	-	-
12	0.078	0.73	0.00242	0.0327	-	-	-	-
13	0.078	0.40	0.00291	0.0392	-	-	-	-
14	0.078	0.	0.00231	0.0312	-	-	-	-
15	0.078	-0.40	0.00186	0.0251	-	-	-	-
16	0.078	-0.73	0.00323	0.0436	-	-	-	-
17	0.078	-0.87	0.00097	0.0131	-	-	-	-
18	0.078	-0.93	0.00075	0.0102	-	-	-	-
19	0.178	-0.93	0.00065	0.0087	-	-	-	-
20	0.178	-0.87	0.00274	0.0370	-	-	-	-
21	0.178	-0.73	0.00369	0.0498	-	-	-	-
22	0.178	-0.40	0.00377	0.0508	-	-	-	-
23	0.178	0.	0.00444	0.0599	-	-	-	-
24	0.178	0.40	0.00484	0.0654	-	-	-	-
25	0.178	0.73	0.00444	0.0599	-	-	-	-
26	0.178	0.87	0.00438	0.0592	-	-	-	-
27	0.178	0.93	0.00215	0.0291	-	-	-	-
28	0.422	0.93	0.00239	0.0323	-	-	-	-
29	0.422	0.87	0.00484	0.0654	-	-	-	-
30	0.422	0.73	0.00482	0.0650	-	-	-	-
31	0.422	0.40	0.00471	0.0636	-	-	-	-
32	0.422	0.	0.00465	0.0628	-	-	-	-
33	0.422	-0.40	0.00444	0.0599	-	-	-	-
34	0.422	-0.73	0.00371	0.0501	-	-	-	-
35	0.422	-0.87	0.00422	0.0570	-	-	-	-
36	0.422	-0.93	0.00323	0.0436	-	-	-	-
37	0.667	-0.93	0.00067	0.0091	-	-	-	-
38	0.667	-0.87	0.00186	0.0251	-	-	-	-
39	0.667	-0.73	0.00226	0.0305	-	-	-	-
40	0.667	-0.40	0.00404	0.0545	-	-	-	-
41	0.667	0.	0.00484	0.0654	-	-	-	-
42	0.667	0.40	0.00468	0.0632	-	-	-	-
43	0.667	0.73	0.00465	0.0628	-	-	-	-
44	0.667	0.87	0.00320	0.0432	-	-	-	-
45	0.667	0.93	0.00161	0.0218	-	-	-	-
46	0.911	0.93	0.00169	0.0229	-	-	-	-
47	0.911	0.87	0.00430	0.0581	-	-	-	-
48	0.911	0.73	0.00441	0.0596	-	-	-	-
49	0.911	0.40	0.00535	0.0723	-	-	-	-
50	0.911	0.	0.00455	0.0614	-	-	-	-
51	0.911	-0.40	0.00374	0.0505	-	-	-	-
52	0.911	-0.73	0.00226	0.0305	-	-	-	-
53	0.911	-0.87	0.00272	0.0367	-	-	-	-
54	0.911	-0.93	0.00081	0.0109	-	-	-	-

Table 6.36 b). The tangential, vertical and radial turbulence intensity distribution at section S-8 run no.3 Um = 0.09259 m/s

Loc. no.	η = z/h	2Y/B	Tangential $\sqrt{v'^2}$ [m/s]	Tangential $\sqrt{v'^2}$/Um	Vertical $\sqrt{w'^2}$ [m/s]	Vertical $\sqrt{w'^2}$/Um	Radial $\sqrt{u'^2}$ [m/s]	Radial $\sqrt{u'^2}$/Um
1	0.033	-0.93	0.00196	0.0212	-	-	-	-
2	0.033	-0.87	0.00132	0.0142	-	-	-	-
3	0.033	-0.73	0.00008	0.0009	-	-	-	-
4	0.033	-0.40	0.00204	0.0221	-	-	-	-
5	0.033	0.	0.00167	0.0180	-	-	-	-
6	0.033	0.40	0.00266	0.0288	-	-	-	-
7	0.033	0.73	0.00237	0.0256	-	-	-	-
8	0.033	0.87	0.00202	0.0218	-	-	-	-
9	0.033	0.93	0.00051	0.0055	-	-	-	-
10	0.058	0.93	0.00188	0.0203	-	-	-	-
11	0.058	0.87	0.00404	0.0436	-	-	-	-
12	0.058	0.73	0.00417	0.0450	-	-	-	-
13	0.058	0.40	0.00422	0.0456	-	-	-	-
14	0.058	0.	0.00309	0.0334	-	-	-	-
15	0.058	-0.40	0.00269	0.0291	-	-	-	-
16	0.058	-0.73	0.00304	0.0328	-	-	-	-
17	0.058	-0.87	0.00272	0.0293	-	-	-	-
18	0.058	-0.93	0.00048	0.0052	-	-	-	-
19	0.133	-0.93	0.00175	0.0189	-	-	-	-
20	0.133	-0.87	0.00344	0.0372	-	-	-	-
21	0.133	-0.73	0.00422	0.0456	-	-	-	-
22	0.133	-0.40	0.00465	0.0503	-	-	-	-
23	0.133	0.	0.00449	0.0485	-	-	-	-
24	0.133	0.40	0.00484	0.0523	-	-	-	-
25	0.133	0.73	0.00468	0.0506	-	-	-	-
26	0.133	0.87	0.00401	0.0433	-	-	-	-
27	0.133	0.93	0.00210	0.0227	-	-	-	-
28	0.400	0.93	0.00245	0.0264	-	-	-	-
29	0.400	0.87	0.00460	0.0497	-	-	-	-
30	0.400	0.73	0.00498	0.0537	-	-	-	-
31	0.400	0.40	0.00514	0.0555	-	-	-	-
32	0.400	0.	0.00525	0.0567	-	-	-	-
33	0.400	-0.40	0.00511	0.0552	-	-	-	-
34	0.400	-0.73	0.00452	0.0488	-	-	-	-
35	0.400	-0.87	0.00428	0.0462	-	-	-	-
36	0.400	-0.93	0.00358	0.0386	-	-	-	-
37	0.667	-0.93	0.00274	0.0296	-	-	-	-
38	0.667	-0.87	0.00301	0.0325	-	-	-	-
39	0.667	-0.73	0.00339	0.0366	-	-	-	-
40	0.667	-0.40	0.00503	0.0543	-	-	-	-
41	0.667	0.	0.00514	0.0555	-	-	-	-
42	0.667	0.40	0.00479	0.0517	-	-	-	-
43	0.667	0.73	0.00457	0.0494	-	-	-	-
44	0.667	0.87	0.00420	0.0453	-	-	-	-
45	0.667	0.93	0.00013	0.0015	-	-	-	-
46	0.933	0.93	0.00183	0.0198	-	-	-	-
47	0.933	0.87	0.00339	0.0366	-	-	-	-
48	0.933	0.73	0.00331	0.0357	-	-	-	-
49	0.933	0.40	0.00433	0.0468	-	-	-	-
50	0.933	0.	0.00511	0.0552	-	-	-	-
51	0.933	-0.40	0.00484	0.0523	-	-	-	-
52	0.933	-0.73	0.00444	0.0479	-	-	-	-
53	0.933	-0.87	0.00062	0.0067	-	-	-	-
54	0.933	-0.93	0.00137	0.0148	-	-	-	-

Table 6.1 c). Reynolds shear stress distribution at section U-2 run no.1 Um = 0.04444 m/s

Loc. no.	η = z/h	2Y/B	Rey.s.s. formed by v' and w': $\overline{vw}[m^2/s^2]$ [x100]	$-\rho\overline{vw}[N/m^2]$	$\overline{vw}/Um^2$ [x100]	Rey.s.s. formed by v' and u': $\overline{vu}[m^2/s^2]$ [x100]	$-\rho\overline{vu}[N/m^2]$	$\overline{vu}/Um^2$ [x100]
1	0.044	-0.93	-	-	-	-	-	-
2	0.044	-0.87	-	-	-	-	-	-
3	0.044	-0.73	-	-	-	-	-	-
4	0.044	-0.40	-	-	-	-	-	-
5	0.044	0.	-	-	-	-	-	-
6	0.044	0.40	-	-	-	-	-	-
7	0.044	0.73	-	-	-	-	-	-
8	0.044	0.87	-	-	-	-	-	-
9	0.044	0.93	-	-	-	-	-	-
10	0.078	0.93	-	-	-	-	-	-
11	0.078	0.87	-	-	-	-	-	-
12	0.078	0.73	-	-	-	-	-	-
13	0.078	0.40	-	-	-	-	-	-
14	0.078	0.	-	-	-	-	-	-
15	0.078	-0.40	-	-	-	-	-	-
16	0.078	-0.73	-	-	-	-	-	-
17	0.078	-0.87	-	-	-	-	-	-
18	0.078	-0.93	-	-	-	-	-	-
19	0.178	-0.93	0.00000	-0.00000	0.0000	-0.00003	0.00026	-0.0132
20	0.178	-0.87	-0.00024	0.00240	-0.1213	0.00032	-0.00321	0.1625
21	0.178	-0.73	0.00045	-0.00447	0.2263	0.00019	-0.00195	0.0987
22	0.178	-0.40	0.00087	-0.00865	0.4381	0.00023	-0.00233	0.1178
23	0.178	0.	-0.00066	0.00659	-0.3336	0.00043	-0.00431	0.2183
24	0.178	0.40	-0.00117	0.01169	-0.5916	0.00034	-0.00344	0.1743
25	0.178	0.73	-0.00099	0.00992	-0.5022	0.00057	-0.00568	0.2875
26	0.178	0.87	-0.00036	0.00364	-0.1841	-0.00054	0.00542	-0.2742
27	0.178	0.93	-0.00058	0.00576	-0.2915	0.00091	-0.00906	0.4588
28	0.422	0.93	-0.00030	0.00298	-0.1507	0.00000	-0.00002	0.0008
29	0.422	0.87	-0.00054	0.00536	-0.2714	0.00011	-0.00114	0.0576
30	0.422	0.73	0.00041	-0.00406	0.2056	0.00060	-0.00603	0.3051
31	0.422	0.40	-0.00089	0.00890	-0.4504	0.00025	-0.00246	0.1248
32	0.422	0.	-0.00041	0.00406	-0.2056	0.00065	-0.00646	0.3272
33	0.422	-0.40	-0.00020	0.00196	-0.0990	-0.00005	0.00051	-0.0259
34	0.422	-0.73	-0.00039	0.00391	-0.1980	0.00006	-0.00060	0.0302
35	0.422	-0.87	0.00013	-0.00132	0.0669	0.00004	-0.00044	0.0225
36	0.422	-0.93	0.00012	-0.00125	0.0633	0.00039	-0.00391	0.1980
37	0.667	-0.93	-0.00038	0.00378	-0.1916	-0.00006	0.00060	-0.0302
38	0.667	-0.87	-0.00039	0.00390	-0.1974	-0.00002	0.00016	-0.0082
39	0.667	-0.73	-0.00016	0.00156	-0.0787	0.00084	-0.00840	0.4252
40	0.667	-0.40	0.00016	-0.00160	0.0812	-0.00007	0.00072	-0.0366
41	0.667	0.	-0.00011	0.00110	-0.0556	-0.00018	0.00184	-0.0931
42	0.667	0.40	-0.00055	0.00548	-0.2775	-0.00043	0.00433	-0.2193
43	0.667	0.73	-0.00003	0.00026	-0.0133	0.00012	-0.00125	0.0631
44	0.667	0.87	0.00017	-0.00172	0.0872	-0.00007	0.00071	-0.0361
45	0.667	0.93	0.00026	-0.00260	0.1316	-0.00011	0.00112	-0.0565

Table 6.2 c). Reynolds shear stress distribution at section U-2 run no.2 Um = 0.07407 m/s

Loc. no.	η = z/h	2Y/B	Rey.s.s. formed by v' and w': $\overline{vw}[m^2/s^2]$ [x100]	$-\rho\overline{vw}[N/m^2]$	$\overline{vw}/Um$ [x100]	Rey.s.s. formed by v' and u': $\overline{vu}[m^2/s^2]$ [x100]	$-\rho\overline{vu}[N/m^2]$	$\overline{vu}/Um$ [x100]
1	0.033	-0.93	-	-	-	-	-	-
2	0.033	-0.87	-	-	-	-	-	-
3	0.033	-0.73	-	-	-	-	-	-
4	0.033	-0.40	-	-	-	-	-	-
5	0.033	0.	-	-	-	-	-	-
6	0.033	0.40	-	-	-	-	-	-
7	0.033	0.73	-	-	-	-	-	-
8	0.033	0.87	-	-	-	-	-	-
9	0.033	0.93	-	-	-	-	-	-
10	0.058	0.93	-	-	-	-	-	-
11	0.058	0.87	-	-	-	-	-	-
12	0.058	0.73	-	-	-	-	-	-
13	0.058	0.40	-	-	-	-	-	-
14	0.058	0.	-	-	-	-	-	-
15	0.058	-0.40	-	-	-	-	-	-
16	0.058	-0.73	-	-	-	-	-	-
17	0.058	-0.87	-	-	-	-	-	-
18	0.058	-0.93	-	-	-	-	-	-
19	0.133	-0.93	-0.00011	0.00108	-0.0198	0.00954	-0.09540	1.7387
20	0.133	-0.87	-0.00001	0.00013	-0.0025	0.00731	-0.07309	1.3320
21	0.133	-0.73	-0.00005	0.00055	-0.0099	0.00467	-0.04674	0.8519
22	0.133	-0.40	0.00091	-0.00909	0.1656	0.00334	-0.03344	0.6094
23	0.133	0.	0.00093	-0.00930	0.1696	0.00280	-0.02800	0.5102
24	0.133	0.40	0.00018	-0.00180	0.0328	0.00282	-0.02824	0.5147
25	0.133	0.73	-0.00014	0.00138	-0.0252	0.00464	-0.04644	0.8463
26	0.133	0.87	-0.00069	0.00686	-0.1250	0.00256	-0.02557	0.4660
27	0.133	0.93	-0.00267	0.02667	-0.4860	-0.00573	0.05732	-1.0446
28	0.400	0.93	-0.00054	0.00538	-0.0980	-0.00508	0.05079	-0.9256
29	0.400	0.87	-0.00065	0.00654	-0.1192	-0.00501	0.05014	-0.9138
30	0.400	0.73	-0.00218	0.02179	-0.3972	-0.00974	0.09739	-1.7749
31	0.400	0.40	-0.00165	0.01654	-0.3015	0.00343	-0.03431	0.6253
32	0.400	0.	-0.00121	0.01211	-0.2207	0.00490	-0.04905	0.8939
33	0.400	-0.40	-0.00086	0.00855	-0.1559	0.00464	-0.04636	0.8449
34	0.400	-0.73	-0.00093	0.00930	-0.1695	0.00247	-0.02470	0.4502
35	0.400	-0.87	0.00032	-0.00319	0.0581	0.00219	-0.02186	0.3984
36	0.400	-0.93	-0.00005	0.00050	-0.0091	0.00341	-0.03408	0.6212
37	0.667	-0.93	0.00830	-0.08298	1.5123	0.00408	-0.04083	0.7441
38	0.667	-0.87	-0.00109	0.01092	-0.1990	0.00354	-0.03540	0.6451
39	0.667	-0.73	-0.00096	0.00964	-0.1757	0.00193	-0.01935	0.3526
40	0.667	-0.40	0.00006	-0.00060	0.0109	0.00096	-0.00960	0.1749
41	0.667	0.	-0.00119	0.01190	-0.2168	0.00595	-0.05954	1.0851
42	0.667	0.40	-0.00245	0.02448	-0.4462	0.00612	-0.06124	1.1161
43	0.667	0.73	-0.00117	0.01169	-0.2130	0.00309	-0.03087	0.5625
44	0.667	0.87	0.00040	-0.00404	0.0737	0.00313	-0.03135	0.5713
45	0.667	0.93	-0.00213	0.02133	-0.3887	0.00377	-0.03769	0.6869
46	0.933	0.93	-	-	-	-	-	-
47	0.933	0.87	-	-	-	-	-	-
48	0.933	0.73	-	-	-	-	-	-
49	0.933	0.40	-	-	-	-	-	-
50	0.933	0.	-	-	-	-	-	-
51	0.933	-0.40	-	-	-	-	-	-
52	0.933	-0.73	-	-	-	-	-	-
53	0.933	-0.87	-	-	-	-	-	-
54	0.933	-0.93	-	-	-	-	-	-

Table 6.3 c). Reynolds shear stress distribution at section U-2 run no.3 Um = 0.09259 m/s

Loc. no.	η = z/h	2Y/B	Rey.s.s. formed by v' and w': $\overline{vw}$[m²/s²] [x100]	$-\rho\overline{vw}$[N/m²]	$\overline{vw}/Um^2$ [x100]	Rey.s.s. formed by v' and u': $\overline{vu}$[m²/s²] [x100]	$-\rho\overline{vu}$[N/m²]	$\overline{vu}/Um^2$ [x100]
1	0.033	-0.93	-	-	-	-	-	-
2	0.033	-0.87	-	-	-	-	-	-
3	0.033	-0.73	-	-	-	-	-	-
4	0.033	-0.40	-	-	-	-	-	-
5	0.033	0.	-	-	-	-	-	-
6	0.033	0.40	-	-	-	-	-	-
7	0.033	0.73	-	-	-	-	-	-
8	0.033	0.87	-	-	-	-	-	-
9	0.033	0.93	-	-	-	-	-	-
10	0.058	0.93	-	-	-	-	-	-
11	0.058	0.87	-	-	-	-	-	-
12	0.058	0.73	-	-	-	-	-	-
13	0.058	0.40	-	-	-	-	-	-
14	0.058	0.	-	-	-	-	-	-
15	0.058	-0.40	-	-	-	-	-	-
16	0.058	-0.73	-	-	-	-	-	-
17	0.058	-0.87	-	-	-	-	-	-
18	0.058	-0.93	-	-	-	-	-	-
19	0.133	-0.93	-0.00297	0.02968	-0.3462	0.00391	-0.03909	0.4560
20	0.133	-0.87	-0.00363	0.03625	-0.4228	0.00652	-0.06522	0.7607
21	0.133	-0.73	-0.00217	0.02171	-0.2532	0.00633	-0.06328	0.7381
22	0.133	-0.40	-0.00397	0.03974	-0.4636	0.00624	-0.06239	0.7277
23	0.133	0.	0.00013	-0.00127	0.0148	0.00030	-0.00302	0.0352
24	0.133	0.40	-0.00027	0.00269	-0.0313	0.00015	-0.00146	0.0171
25	0.133	0.73	-0.00213	0.02126	-0.2480	0.00302	-0.03016	0.3518
26	0.133	0.87	-0.00247	0.02470	-0.2881	0.00183	-0.01833	0.2138
27	0.133	0.93	-0.00824	0.08240	-0.9611	0.00275	-0.02750	0.3207
28	0.400	0.93	-0.00104	0.01038	-0.1210	0.00399	-0.03990	0.4654
29	0.400	0.87	-0.00145	0.01446	-0.1687	0.00446	-0.04459	0.5201
30	0.400	0.73	-0.00071	0.00707	-0.0825	0.00322	-0.03217	0.3752
31	0.400	0.40	-0.00154	0.01535	-0.1791	-0.00025	0.00249	-0.0290
32	0.400	0.	-0.00045	0.00450	-0.0525	0.00020	-0.00203	0.0236
33	0.400	-0.40	-0.00383	0.03834	-0.4472	0.00063	-0.00628	0.0733
34	0.400	-0.73	-0.00110	0.01105	-0.1288	-0.00030	0.00299	-0.0349
35	0.400	-0.87	-0.00275	0.02753	-0.3211	-0.00047	0.00470	-0.0548
36	0.400	-0.93	-0.00444	0.04440	-0.5179	0.00176	-0.01758	0.2051
37	0.667	-0.93	0.01493	-0.14930	1.7414	0.00094	-0.00942	0.1099
38	0.667	-0.87	-0.00020	0.00200	-0.0233	0.00089	-0.00892	0.1041
39	0.667	-0.73	0.00003	-0.00031	0.0036	0.00120	-0.01198	0.1397
40	0.667	-0.40	-0.00055	0.00545	-0.0636	0.00014	-0.00135	0.0158
41	0.667	0.	0.00051	-0.00508	0.0592	0.00215	-0.02149	0.2507
42	0.667	0.40	0.00055	-0.00545	0.0636	0.00212	-0.02117	0.2469
43	0.667	0.73	0.00051	-0.00506	0.0590	0.00106	-0.01065	0.1242
44	0.667	0.87	-0.00302	0.03022	-0.3525	0.00100	-0.01000	0.1166
45	0.667	0.93	-0.00659	0.06594	-0.7692	0.00199	-0.01993	0.2325
46	0.933	0.93	-	-	-	-	-	-
47	0.933	0.87	-	-	-	-	-	-
48	0.933	0.73	-	-	-	-	-	-
49	0.933	0.40	-	-	-	-	-	-
50	0.933	0.	-	-	-	-	-	-
51	0.933	-0.40	-	-	-	-	-	-
52	0.933	-0.73	-	-	-	-	-	-
53	0.933	-0.87	-	-	-	-	-	-
54	0.933	-0.93	-	-	-	-	-	-

Table 6.4 c). Reynolds shear stress distribution at section U-3 run no.1 Um = 0.04444 m/s

Loc. no.	η = z/h	2Y/B	Rey.s.s. formed by v' and w': $\overline{vw}$[m²/s²] [x100]	$-\rho\overline{vw}$[N/m²]	$\overline{vw}/Um^2$ [x100]	Rey.s.s. formed by v' and u': $\overline{vu}$[m²/s²] [x100]	$-\rho\overline{vu}$[N/m²]	$\overline{vu}/Um^2$ [x100]
1	0.044	-0.93	-	-	-	-	-	-
2	0.044	-0.87	-	-	-	-	-	-
3	0.044	-0.73	-	-	-	-	-	-
4	0.044	-0.40	-	-	-	-	-	-
5	0.044	0.	-	-	-	-	-	-
6	0.044	0.40	-	-	-	-	-	-
7	0.044	0.73	-	-	-	-	-	-
8	0.044	0.87	-	-	-	-	-	-
9	0.044	0.93	-	-	-	-	-	-
10	0.078	0.93	-	-	-	-	-	-
11	0.078	0.87	-	-	-	-	-	-
12	0.078	0.73	-	-	-	-	-	-
13	0.078	0.40	-	-	-	-	-	-
14	0.078	0.	-	-	-	-	-	-
15	0.078	-0.40	-	-	-	-	-	-
16	0.078	-0.73	-	-	-	-	-	-
17	0.078	-0.87	-	-	-	-	-	-
18	0.078	-0.93	-	-	-	-	-	-
19	0.178	-0.93	0.00018	-0.00184	0.0931	0.00019	-0.00189	0.0956
20	0.178	-0.87	0.00091	-0.00909	0.4604	-0.00007	0.00067	-0.0340
21	0.178	-0.73	0.00122	-0.01222	0.6186	0.00061	-0.00611	0.3093
22	0.178	-0.40	0.00072	-0.00722	0.3656	0.00111	-0.01114	0.5642
23	0.178	0.	-0.00083	0.00829	-0.4195	0.00088	-0.00884	0.4474
24	0.178	0.40	0.00120	-0.01199	0.6068	0.00140	-0.01398	0.7075
25	0.178	0.73	0.00075	-0.00745	0.3774	-0.00056	0.00559	-0.2830
26	0.178	0.87	0.00114	-0.01139	0.5765	-0.00017	0.00167	-0.0844
27	0.178	0.93	0.00142	-0.01422	0.7199	0.00017	-0.00172	0.0871
28	0.422	0.93	0.00133	-0.01330	0.6732	0.00085	-0.00853	0.4319
29	0.422	0.87	0.00050	-0.00498	0.2522	-0.00032	0.00320	-0.1620
30	0.422	0.73	0.00067	-0.00673	0.3406	-0.00025	0.00248	-0.1255
31	0.422	0.40	0.00169	-0.01689	0.8548	0.00091	-0.00910	0.4608
32	0.422	0.	0.00122	-0.01222	0.6186	0.00030	-0.00305	0.1542
33	0.422	-0.40	0.00025	-0.00253	0.1279	-0.00000	0.00000	-0.0000
34	0.422	-0.73	0.00131	-0.01306	0.6614	-0.00014	0.00140	-0.0708
35	0.422	-0.87	0.00129	-0.01294	0.6548	-0.00011	0.00109	-0.0551
36	0.422	-0.93	0.00091	-0.00910	0.4608	-0.00011	0.00114	-0.0576
37	0.667	-0.93	0.00033	-0.00326	0.1649	-0.00021	0.00213	-0.1081
38	0.667	-0.87	0.00050	-0.00502	0.2539	-0.00072	0.00722	-0.3656
39	0.667	-0.73	0.00044	-0.00439	0.2221	-0.00030	0.00298	-0.1509
40	0.667	-0.40	0.00084	-0.00838	0.4241	-0.00084	0.00840	-0.4252
41	0.667	0.	0.00167	-0.01673	0.8472	-0.00084	0.00844	-0.4272
42	0.667	0.40	0.00153	-0.01531	0.7750	-0.00049	0.00491	-0.2485
43	0.667	0.73	0.00069	-0.00693	0.3509	0.00042	-0.00415	0.2103
44	0.667	0.87	0.00042	-0.00425	0.2151	-0.00036	0.00357	-0.1809
45	0.667	0.93	0.00034	-0.00344	0.1743	0.00054	-0.00544	0.2756

Table 6.5 c). Reynolds shear stress distribution at section U-3 run no.2 Um = 0.07407 m/s

Loc. no.	η = z/h	2Y/B	Rey.s.s. formed by v' and w': $\overline{vw}$[m²/s²] [x100]	$-\rho\overline{vw}$[N/m²]	$\overline{vw}/Um^2$ [x100]	Rey.s.s. formed by v' and u': $\overline{vu}$[m²/s²] [x100]	$-\rho\overline{vu}$[N/m²]	$\overline{vu}/Um^2$ [x100]
1	0.033	-0.93	-	-	-	-	-	-
2	0.033	-0.87	-	-	-	-	-	-
3	0.033	-0.73	-	-	-	-	-	-
4	0.033	-0.40	-	-	-	-	-	-
5	0.033	0.	-	-	-	-	-	-
6	0.033	0.40	-	-	-	-	-	-
7	0.033	0.73	-	-	-	-	-	-
8	0.033	0.87	-	-	-	-	-	-
9	0.033	0.93	-	-	-	-	-	-
10	0.058	0.93	-	-	-	-	-	-
11	0.058	0.87	-	-	-	-	-	-
12	0.058	0.73	-	-	-	-	-	-
13	0.058	0.40	-	-	-	-	-	-
14	0.058	0.	-	-	-	-	-	-
15	0.058	-0.40	-	-	-	-	-	-
16	0.058	-0.73	-	-	-	-	-	-
17	0.058	-0.87	-	-	-	-	-	-
18	0.058	-0.93	-	-	-	-	-	-
19	0.133	-0.93	0.00005	-0.00049	0.0090	0.00005	-0.00045	0.0083
20	0.133	-0.87	0.00058	-0.00581	0.1060	0.00129	-0.01291	0.2352
21	0.133	-0.73	0.00117	-0.01165	0.2124	-0.00010	0.00102	-0.0186
22	0.133	-0.40	-0.00032	0.00317	-0.0577	0.00070	-0.00704	0.1284
23	0.133	0.	-0.00138	0.01381	-0.2517	0.00230	-0.02297	0.4186
24	0.133	0.40	-0.00275	0.02753	-0.5017	0.00292	-0.02919	0.5320
25	0.133	0.73	-0.00293	0.02931	-0.5342	-0.00005	0.00050	-0.0091
26	0.133	0.87	-0.00386	0.03858	-0.7031	0.00071	-0.00708	0.1290
27	0.133	0.93	-0.00411	0.04106	-0.7483	0.00150	-0.01502	0.2737
28	0.400	0.93	-0.00071	0.00712	-0.1297	0.00100	-0.01002	0.1826
29	0.400	0.87	-0.00121	0.01212	-0.2209	0.00104	-0.01044	0.1903
30	0.400	0.73	-0.00119	0.01185	-0.2160	0.00009	-0.00094	0.0172
31	0.400	0.40	-0.00124	0.01235	-0.2252	0.00095	-0.00951	0.1733
32	0.400	0.	-0.00135	0.01346	-0.2454	0.00057	-0.00573	0.1044
33	0.400	-0.40	-0.00090	0.00904	-0.1648	0.00115	-0.01154	0.2103
34	0.400	-0.73	-0.00028	0.00281	-0.0512	0.00202	-0.02016	0.3675
35	0.400	-0.87	-0.00015	0.00154	-0.0280	0.00018	-0.00179	0.0326
36	0.400	-0.93	0.00037	-0.00371	0.0676	0.00060	-0.00596	0.1086
37	0.667	-0.93	-0.00057	0.00567	-0.1033	0.00038	-0.00378	0.0688
38	0.667	-0.87	0.00045	-0.00454	0.0827	0.00004	-0.00040	0.0072
39	0.667	-0.73	-0.00080	0.00800	-0.1458	-0.00036	0.00355	-0.0648
40	0.667	-0.40	-0.00101	0.01008	-0.1838	-0.00037	0.00372	-0.0678
41	0.667	0.	-0.00070	0.00705	-0.1284	-0.00061	0.00614	-0.1120
42	0.667	0.40	-0.00038	0.00382	-0.0696	-0.00097	0.00969	-0.1767
43	0.667	0.73	-0.00121	0.01208	-0.2201	0.00023	-0.00231	0.0421
44	0.667	0.87	-0.00059	0.00592	-0.1079	0.00055	-0.00545	0.0994
45	0.667	0.93	-0.00076	0.00758	-0.1382	-0.00129	0.01291	-0.2352
46	0.933	0.93	-	-	-	-	-	-
47	0.933	0.87	-	-	-	-	-	-
48	0.933	0.73	-	-	-	-	-	-
49	0.933	0.40	-	-	-	-	-	-
50	0.933	0.	-	-	-	-	-	-
51	0.933	-0.40	-	-	-	-	-	-
52	0.933	-0.73	-	-	-	-	-	-
53	0.933	-0.87	-	-	-	-	-	-
54	0.933	-0.93	-	-	-	-	-	-

Table 6.6 c). Reynolds shear stress distribution at section U-3 run no.3 Um = 0.09259 m/s

Loc. no.	η = z/h	2Y/B	Rey.s.s. formed by v' and w': $\overline{vw}$[m²/s²] [x100]	$-\rho\overline{vw}$[N/m²]	$\overline{vw}/Um^2$ [x100]	Rey.s.s. formed by v' and u': $\overline{vu}$[m²/s²] [x100]	$-\rho\overline{vu}$[N/m²]	$\overline{vu}/Um^2$ [x100]
1	0.033	-0.93	-	-	-	-	-	-
2	0.033	-0.87	-	-	-	-	-	-
3	0.033	-0.73	-	-	-	-	-	-
4	0.033	-0.40	-	-	-	-	-	-
5	0.033	0.	-	-	-	-	-	-
6	0.033	0.40	-	-	-	-	-	-
7	0.033	0.73	-	-	-	-	-	-
8	0.033	0.87	-	-	-	-	-	-
9	0.033	0.93	-	-	-	-	-	-
10	0.058	0.93	-	-	-	-	-	-
11	0.058	0.87	-	-	-	-	-	-
12	0.058	0.73	-	-	-	-	-	-
13	0.058	0.40	-	-	-	-	-	-
14	0.058	0.	-	-	-	-	-	-
15	0.058	-0.40	-	-	-	-	-	-
16	0.058	-0.73	-	-	-	-	-	-
17	0.058	-0.87	-	-	-	-	-	-
18	0.058	-0.93	-	-	-	-	-	-
19	0.133	-0.93	-0.00260	0.02604	-0.3038	-0.00053	0.00527	-0.0615
20	0.133	-0.87	-0.00286	0.02858	-0.3333	-0.00029	0.00286	-0.0334
21	0.133	-0.73	-0.00165	0.01652	-0.1927	0.00098	-0.00982	0.1145
22	0.133	-0.40	-0.00085	0.00850	-0.0991	0.00404	-0.04042	0.4715
23	0.133	0.	-0.00360	0.03598	-0.4196	0.00116	-0.01164	0.1358
24	0.133	0.40	-0.00298	0.02983	-0.3480	0.00384	-0.03842	0.4481
25	0.133	0.73	-0.00251	0.02507	-0.2925	0.00322	-0.03224	0.3761
26	0.133	0.87	-0.00238	0.02382	-0.2779	0.00240	-0.02396	0.2794
27	0.133	0.93	-0.00219	0.02194	-0.2559	0.00560	-0.05599	0.6531
28	0.400	0.93	-0.00210	0.02101	-0.2450	0.00467	-0.04670	0.5447
29	0.400	0.87	-0.00253	0.02534	-0.2955	0.00153	-0.01533	0.1788
30	0.400	0.73	-0.00276	0.02755	-0.3214	0.00107	-0.01075	0.1254
31	0.400	0.40	-0.00108	0.01077	-0.1256	0.00391	-0.03910	0.4561
32	0.400	0.	-0.00185	0.01852	-0.2161	0.00350	-0.03498	0.4080
33	0.400	-0.40	-0.00094	0.00939	-0.1096	0.00227	-0.02271	0.2649
34	0.400	-0.73	-0.00128	0.01275	-0.1488	0.00145	-0.01450	0.1691
35	0.400	-0.87	-0.00142	0.01418	-0.1654	0.00140	-0.01405	0.1638
36	0.400	-0.93	-0.00062	0.00618	-0.0721	0.00140	-0.01395	0.1627
37	0.667	-0.93	-0.00013	0.00127	-0.0148	0.00101	-0.01008	0.1175
38	0.667	-0.87	-0.00180	0.01800	-0.2099	0.00115	-0.01148	0.1339
39	0.667	-0.73	-0.00173	0.01728	-0.2015	0.00126	-0.01260	0.1469
40	0.667	-0.40	-0.00196	0.01964	-0.2291	0.00160	-0.01598	0.1863
41	0.667	0.	-0.00303	0.03028	-0.3532	0.00165	-0.01652	0.1927
42	0.667	0.40	-0.00607	0.06066	-0.7075	0.00081	-0.00809	0.0944
43	0.667	0.73	-0.00562	0.05624	-0.6560	0.00068	-0.00680	0.0793
44	0.667	0.87	-0.00385	0.03849	-0.4490	0.00131	-0.01305	0.1523
45	0.667	0.93	-0.00442	0.04424	-0.5161	0.00293	-0.02933	0.3421
46	0.933	0.93	-	-	-	-	-	-
47	0.933	0.87	-	-	-	-	-	-
48	0.933	0.73	-	-	-	-	-	-
49	0.933	0.40	-	-	-	-	-	-
50	0.933	0.	-	-	-	-	-	-
51	0.933	-0.40	-	-	-	-	-	-
52	0.933	-0.73	-	-	-	-	-	-
53	0.933	-0.87	-	-	-	-	-	-
54	0.933	-0.93	-	-	-	-	-	-

Table 6.7 *c). Reynolds shear stress distribution at section S-2 run no.1* Um = 0.04444 m/s

Loc. no.	η = z/h	2Y/B	Rey.s.s. formed by v' and w': $\overline{vw}$[m²/s²] [x100]	$-\rho\overline{vw}$[N/m²]	$\overline{vw}/Um^2$ [x100]	Rey.s.s. formed by v' and u': $\overline{vu}$[m²/s²] [x100]	$-\rho\overline{vu}$[N/m²]	$\overline{vu}/Um^2$ [x100]
1	0.044	-0.93	-	-	-	-	-	-
2	0.044	-0.87	-	-	-	-	-	-
3	0.044	-0.73	-	-	-	-	-	-
4	0.044	-0.40	-	-	-	-	-	-
5	0.044	0.	-	-	-	-	-	-
6	0.044	0.40	-	-	-	-	-	-
7	0.044	0.73	-	-	-	-	-	-
8	0.044	0.87	-	-	-	-	-	-
9	0.044	0.93	-	-	-	-	-	-
10	0.078	0.93	-	-	-	-	-	-
11	0.078	0.87	-	-	-	-	-	-
12	0.078	0.73	-	-	-	-	-	-
13	0.078	0.40	-	-	-	-	-	-
14	0.078	0.	-	-	-	-	-	-
15	0.078	-0.40	-	-	-	-	-	-
16	0.078	-0.73	-	-	-	-	-	-
17	0.078	-0.87	-	-	-	-	-	-
18	0.078	-0.93	-	-	-	-	-	-
19	0.178	-0.93	-0.00114	0.01139	-0.5765	-0.00022	0.00222	-0.1122
20	0.178	-0.87	0.00040	-0.00403	0.2039	-0.00100	0.01000	-0.5062
21	0.178	-0.73	0.00127	-0.01266	0.6409	-0.00067	0.00666	-0.3371
22	0.178	-0.40	0.00152	-0.01517	0.7680	-0.00144	0.01442	-0.7301
23	0.178	0.	0.00092	-0.00921	0.4663	-0.00191	0.01905	-0.9645
24	0.178	0.40	0.00000	-0.00005	0.0023	-0.00132	0.01321	-0.6688
25	0.178	0.73	0.00120	-0.01200	0.6074	-0.00014	0.00142	-0.0721
26	0.178	0.87	0.00202	-0.02017	1.0211	-0.00010	0.00098	-0.0495
27	0.178	0.93	-0.00259	0.02591	-1.3114	-0.00007	0.00075	-0.0379
28	0.422	0.93	0.00269	-0.02688	1.3610	-0.00152	0.01516	-0.7677
29	0.422	0.87	-0.00055	0.00553	-0.2798	-0.00189	0.01893	-0.9585
30	0.422	0.73	-0.00304	0.03037	-1.5377	-0.00090	0.00901	-0.4562
31	0.422	0.40	-0.00051	0.00514	-0.2600	-0.00158	0.01579	-0.7994
32	0.422	0.	0.00081	-0.00814	0.4119	-0.00109	0.01092	-0.5529
33	0.422	-0.40	0.00090	-0.00900	0.4555	0.00065	-0.00646	0.3272
34	0.422	-0.73	0.00092	-0.00918	0.4645	0.00093	-0.00934	0.4726
35	0.422	-0.87	0.00026	-0.00256	0.1294	0.00232	-0.02317	1.1728
36	0.422	-0.93	-0.00007	0.00072	-0.0366	0.00010	-0.00098	0.0496
37	0.667	-0.93	0.00027	-0.00265	0.1342	-0.00194	0.01939	-0.9817
38	0.667	-0.87	0.00042	-0.00420	0.2126	0.00087	-0.00874	0.4423
39	0.667	-0.73	0.00074	-0.00740	0.3746	-0.00012	0.00123	-0.0624
40	0.667	-0.40	0.00094	-0.00939	0.4756	0.00062	-0.00616	0.3116
41	0.667	0.	0.00062	-0.00623	0.3156	-0.00076	0.00762	-0.3857
42	0.667	0.40	-0.00045	0.00447	-0.2263	-0.00141	0.01413	-0.7154
43	0.667	0.73	-0.00062	0.00619	-0.3132	0.00008	-0.00078	0.0394
44	0.667	0.87	-0.00081	0.00805	-0.4077	-0.00099	0.00989	-0.5009
45	0.667	0.93	-0.00120	0.01196	-0.6055	-0.00059	0.00594	-0.3005

Table 6.8 *c). Reynolds shear stress distribution at section S-2 run no.2* Um = 0.07407 m/s

Loc. no.	η = z/h	2Y/B	Rey.s.s. formed by v' and w': $\overline{vw}$[m²/s²] [x100]	$-\rho\overline{vw}$[N/m²]	$\overline{vw}/Um^2$ [x100]	Rey.s.s. formed by v' and u': $\overline{vu}$[m²/s²] [x100]	$-\rho\overline{vu}$[N/m²]	$\overline{vu}/Um^2$ [x100]
1	0.033	-0.93	-	-	-	-	-	-
2	0.033	-0.87	-	-	-	-	-	-
3	0.033	-0.73	-	-	-	-	-	-
4	0.033	-0.40	-	-	-	-	-	-
5	0.033	0.	-	-	-	-	-	-
6	0.033	0.40	-	-	-	-	-	-
7	0.033	0.73	-	-	-	-	-	-
8	0.033	0.87	-	-	-	-	-	-
9	0.033	0.93	-	-	-	-	-	-
10	0.058	0.93	-	-	-	-	-	-
11	0.058	0.87	-	-	-	-	-	-
12	0.058	0.73	-	-	-	-	-	-
13	0.058	0.40	-	-	-	-	-	-
14	0.058	0.	-	-	-	-	-	-
15	0.058	-0.40	-	-	-	-	-	-
16	0.058	-0.73	-	-	-	-	-	-
17	0.058	-0.87	-	-	-	-	-	-
18	0.058	-0.93	-	-	-	-	-	-
19	0.133	-0.93	-0.00012	0.00123	-0.0224	0.00038	-0.00378	0.0688
20	0.133	-0.87	-0.00033	0.00334	-0.0609	-0.00175	0.01747	-0.3185
21	0.133	-0.73	-0.00095	0.00950	-0.1732	-0.00260	0.02600	-0.4738
22	0.133	-0.40	-0.00031	0.00312	-0.0569	-0.00318	0.03185	-0.5805
23	0.133	0.	-0.00041	0.00408	-0.0744	-0.00397	0.03973	-0.7240
24	0.133	0.40	0.00100	-0.00996	0.1816	-0.00288	0.02880	-0.5248
25	0.133	0.73	0.00066	-0.00664	0.1209	-0.00217	0.02173	-0.3959
26	0.133	0.87	0.00035	-0.00351	0.0640	-0.00212	0.02121	-0.3866
27	0.133	0.93	-0.00036	0.00360	-0.0656	-0.00256	0.02558	-0.4662
28	0.400	0.93	-0.00042	0.00422	-0.0769	-0.00192	0.01922	-0.3503
29	0.400	0.87	-0.00035	0.00348	-0.0634	-0.00139	0.01393	-0.2539
30	0.400	0.73	0.00020	-0.00203	0.0369	-0.00163	0.01633	-0.2976
31	0.400	0.40	-0.00081	0.00809	-0.1475	-0.00172	0.01723	-0.3140
32	0.400	0.	0.00089	-0.00887	0.1616	-0.00222	0.02218	-0.4042
33	0.400	-0.40	0.00039	-0.00385	0.0702	-0.00096	0.00963	-0.1755
34	0.400	-0.73	-0.00013	0.00135	-0.0246	-0.00194	0.01939	-0.3534
35	0.400	-0.87	-0.00101	0.01013	-0.1846	-0.00139	0.01395	-0.2542
36	0.400	-0.93	-0.00007	0.00075	-0.0136	0.00419	-0.04191	0.7638
37	0.667	-0.93	-0.00051	0.00508	-0.0925	-0.00267	0.02666	-0.4859
38	0.667	-0.87	-0.00017	0.00170	-0.0310	-0.00111	0.01110	-0.2023
39	0.667	-0.73	-0.00267	0.02666	-0.4859	-0.00181	0.01807	-0.3294
40	0.667	-0.40	-0.00000	0.00000	-0.0000	-0.00207	0.02073	-0.3779
41	0.667	0.	-0.00008	0.00079	-0.0143	-0.00334	0.03344	-0.6094
42	0.667	0.40	-0.00120	0.01200	-0.2187	-0.00085	0.00850	-0.1549
43	0.667	0.73	-0.00109	0.01089	-0.1984	-0.00169	0.01685	-0.3071
44	0.667	0.87	-0.00075	0.00753	-0.1372	-0.00133	0.01330	-0.2424
45	0.667	0.93	-0.00100	0.01001	-0.1824	-0.00161	0.01606	-0.2927
46	0.933	0.93	-	-	-	-	-	-
47	0.933	0.87	-	-	-	-	-	-
48	0.933	0.73	-	-	-	-	-	-
49	0.933	0.40	-	-	-	-	-	-
50	0.933	0.	-	-	-	-	-	-
51	0.933	-0.40	-	-	-	-	-	-
52	0.933	-0.73	-	-	-	-	-	-
53	0.933	-0.87	-	-	-	-	-	-
54	0.933	-0.93	-	-	-	-	-	-

Table 6.9 c). Reynolds shear stress distribution at section S-2 run no.3 Um = 0.09259 m/s

Loc. no.	η = z/h	2Y/B	Rey.s.s. formed by v' and w': $\overline{vw}[m^2/s^2]$ [x100]	$-\rho\overline{vw}[N/m^2]$	$\overline{vw}/Um^2$ [x100]	Rey.s.s. formed by v' and u': $\overline{vu}[m^2/s^2]$ [x100]	$-\rho\overline{vu}[N/m^2]$	$\overline{vu}/Um^2$ [x100]
1	0.033	-0.93	–	–	–	–	–	–
2	0.033	-0.87	–	–	–	–	–	–
3	0.033	-0.73	–	–	–	–	–	–
4	0.033	-0.40	–	–	–	–	–	–
5	0.033	0.	–	–	–	–	–	–
6	0.033	0.40	–	–	–	–	–	–
7	0.033	0.73	–	–	–	–	–	–
8	0.033	0.87	–	–	–	–	–	–
9	0.033	0.93	–	–	–	–	–	–
10	0.058	0.93	–	–	–	–	–	–
11	0.058	0.87	–	–	–	–	–	–
12	0.058	0.73	–	–	–	–	–	–
13	0.058	0.40	–	–	–	–	–	–
14	0.058	0.	–	–	–	–	–	–
15	0.058	-0.40	–	–	–	–	–	–
16	0.058	-0.73	–	–	–	–	–	–
17	0.058	-0.87	–	–	–	–	–	–
18	0.058	-0.93	–	–	–	–	–	–
19	0.133	-0.93	0.00044	-0.00444	0.0518	-0.00213	0.02130	-0.2484
20	0.133	-0.87	-0.00189	0.01887	-0.2201	-0.00558	0.05584	-0.6514
21	0.133	-0.73	-0.00213	0.02130	-0.2485	-0.00347	0.03470	-0.4047
22	0.133	-0.40	-0.00321	0.03208	-0.3742	-0.00673	0.06731	-0.7852
23	0.133	0.	-0.00209	0.02089	-0.2437	-0.00507	0.05066	-0.5909
24	0.133	0.40	-0.00212	0.02121	-0.2474	-0.00370	0.03697	-0.4312
25	0.133	0.73	-0.00245	0.02451	-0.2859	-0.00044	0.00441	-0.0514
26	0.133	0.87	0.00002	-0.00019	0.0022	-0.00142	0.01416	-0.1652
27	0.133	0.93	-0.00054	0.00544	-0.0635	-0.00050	0.00495	-0.0578
28	0.400	0.93	-0.00095	0.00951	-0.1109	-0.00370	0.03699	-0.4315
29	0.400	0.87	-0.00188	0.01875	-0.2187	-0.00168	0.01680	-0.1959
30	0.400	0.73	-0.00162	0.01617	-0.1887	-0.00277	0.02766	-0.3226
31	0.400	0.40	-0.00152	0.01523	-0.1776	-0.00310	0.03097	-0.3613
32	0.400	0.	0.00105	-0.01048	0.1222	-0.00272	0.02722	-0.3175
33	0.400	-0.40	-0.00077	0.00767	-0.0894	-0.00382	0.03823	-0.4459
34	0.400	-0.73	-0.00072	0.00718	-0.0837	-0.00313	0.03133	-0.3654
35	0.400	-0.87	-0.00034	0.00340	-0.0397	-0.00288	0.02880	-0.3359
36	0.400	-0.93	0.00054	-0.00542	0.0632	-0.00057	0.00574	-0.0670
37	0.667	-0.93	-0.00038	0.00380	-0.0444	-0.00265	0.02654	-0.3096
38	0.667	-0.87	-0.00238	0.02384	-0.2781	-0.00160	0.01598	-0.1864
39	0.667	-0.73	-0.00045	0.00455	-0.0531	-0.00295	0.02947	-0.3438
40	0.667	-0.40	-0.00018	0.00184	-0.0214	-0.00390	0.03903	-0.4552
41	0.667	0.	-0.00202	0.02022	-0.2358	-0.00236	0.02356	-0.2748
42	0.667	0.40	-0.00212	0.02119	-0.2472	-0.00587	0.05868	-0.6844
43	0.667	0.73	-0.00139	0.01393	-0.1624	-0.00211	0.02108	-0.2459
44	0.667	0.87	0.00087	-0.00866	0.1010	-0.00237	0.02369	-0.2763
45	0.667	0.93	0.00016	-0.00158	0.0184	-0.00283	0.02835	-0.3306
46	0.933	0.93		–	–	–	–	–
47	0.933	0.87	–	–	–	–	–	–
48	0.933	0.73	–	–	–	–	–	–
49	0.933	0.40	–	–	–	–	–	–
50	0.933	0.	–	–	–	–	–	–
51	0.933	-0.40	–	–	–	–	–	–
52	0.933	-0.73	–	–	–	–	–	–
53	0.933	-0.87	–	–	–	–	–	–
54	0.933	-0.93	–	–	–	–	–	–

Table 6.10 c). Reynolds shear stress distribution at section S-3 run no.1 Um = 0.04444 m/s

Loc. no.	η = z/h	2Y/B	Rey.s.s. formed by v' and w': $\overline{vw}[m^2/s^2]$ [x100]	$-\rho\overline{vw}[N/m^2]$	$\overline{vw}/Um^2$ [x100]	Rey.s.s. formed by v' and u': $\overline{vu}[m^2/s^2]$ [x100]	$-\rho\overline{vu}[N/m^2]$	$\overline{vu}/Um^2$ [x100]
1	0.044	-0.93	–	–	–	–	–	–
2	0.044	-0.87	–	–	–	–	–	–
3	0.044	-0.73	–	–	–	–	–	–
4	0.044	-0.40	–	–	–	–	–	–
5	0.044	0.	–	–	–	–	–	–
6	0.044	0.40	–	–	–	–	–	–
7	0.044	0.73	–	–	–	–	–	–
8	0.044	0.87	–	–	–	–	–	–
9	0.044	0.93	–	–	–	–	–	–
10	0.078	0.93	–	–	–	–	–	–
11	0.078	0.87	–	–	–	–	–	–
12	0.078	0.73	–	–	–	–	–	–
13	0.078	0.40	–	–	–	–	–	–
14	0.078	0.	–	–	–	–	–	–
15	0.078	-0.40	–	–	–	–	–	–
16	0.078	-0.73	–	–	–	–	–	–
17	0.078	-0.87	–	–	–	–	–	–
18	0.078	-0.93	–	–	–	–	–	–
19	0.178	-0.93	-0.00075	0.00752	-0.3805	-0.00059	0.00589	-0.2980
20	0.178	-0.87	0.00004	-0.00043	0.0219	0.00008	-0.00080	0.0405
21	0.178	-0.73	-0.00002	0.00025	-0.0124	0.00068	-0.00680	0.3445
22	0.178	-0.40	0.00014	-0.00142	0.0719	0.00038	-0.00375	0.1899
23	0.178	0.	-0.00006	0.00057	-0.0287	0.00113	-0.01133	0.5736
24	0.178	0.40	0.00090	-0.00899	0.4553	0.00114	-0.01135	0.5747
25	0.178	0.73	-0.00010	0.00095	-0.0482	0.00141	-0.01413	0.7154
26	0.178	0.87	-0.00009	0.00088	-0.0448	0.00203	-0.02033	1.0293
27	0.178	0.93	0.00000	-0.00000	0.0000	0.00177	-0.01773	0.8976
28	0.422	0.93	0.00028	-0.00282	0.1429	0.00273	-0.02725	1.3796
29	0.422	0.87	-0.00023	0.00227	-0.1147	0.00228	-0.02284	1.1561
30	0.422	0.73	0.00021	-0.00210	0.1063	0.00262	-0.02621	1.3266
31	0.422	0.40	0.00042	-0.00418	0.2115	0.00147	-0.01470	0.7441
32	0.422	0.	0.00036	-0.00356	0.1803	0.00101	-0.01006	0.5093
33	0.422	-0.40	0.00007	-0.00067	0.0340	0.00059	-0.00595	0.3012
34	0.422	-0.73	0.00028	-0.00283	0.1434	0.00064	-0.00642	0.3248
35	0.422	-0.87	0.00020	-0.00202	0.1024	0.00024	-0.00238	0.1206
36	0.422	-0.93	-0.00077	0.00773	-0.3912	0.00050	-0.00498	0.2520
37	0.667	-0.93	-0.00164	0.01637	-0.8290	-0.00004	0.00040	-0.0202
38	0.667	-0.87	-0.00053	0.00533	-0.2700	0.00035	-0.00349	0.1765
39	0.667	-0.73	0.00003	-0.00029	0.0147	0.00018	-0.00181	0.0917
40	0.667	-0.40	-0.00044	0.00437	-0.2214	0.00136	-0.01361	0.6892
41	0.667	0.	0.00068	-0.00675	0.3419	0.00077	-0.00767	0.3884
42	0.667	0.40	0.00056	-0.00559	0.2832	0.00123	-0.01226	0.6207
43	0.667	0.73	0.00027	-0.00272	0.1378	0.00153	-0.01530	0.7744
44	0.667	0.87	0.00003	-0.00028	0.0141	0.00195	-0.01946	0.9854
45	0.667	0.93	-0.00017	0.00171	-0.0868	0.00153	-0.01529	0.7741

Table 6.11 c). Reynolds shear stress distribution at section S-3 run no.2 Um = 0.07407 m/s

Loc. no.	η = z/h	2Y/B	Rey.s.s. formed by v' and w': $\overline{vw}$[m²/s²] [x100]	$-\rho\overline{vw}$[N/m²]	$\overline{vw}$/Um² [x100]	Rey.s.s. formed by v' and u': $\overline{vu}$[m²/s²] [x100]	$-\rho\overline{vu}$[N/m²]	$\overline{vu}$/Um² [x100]
1	0.033	-0.93	-	-	-	-	-	-
2	0.033	-0.87	-	-	-	-	-	-
3	0.033	-0.73	-	-	-	-	-	-
4	0.033	-0.40	-	-	-	-	-	-
5	0.033	0.	-	-	-	-	-	-
6	0.033	0.40	-	-	-	-	-	-
7	0.033	0.73	-	-	-	-	-	-
8	0.033	0.87	-	-	-	-	-	-
9	0.033	0.93	-	-	-	-	-	-
10	0.058	0.93	-	-	-	-	-	-
11	0.058	0.87	-	-	-	-	-	-
12	0.058	0.73	-	-	-	-	-	-
13	0.058	0.40	-	-	-	-	-	-
14	0.058	0.	-	-	-	-	-	-
15	0.058	-0.40	-	-	-	-	-	-
16	0.058	-0.73	-	-	-	-	-	-
17	0.058	-0.87	-	-	-	-	-	-
18	0.058	-0.93	-	-	-	-	-	-
19	0.133	-0.93	-0.00103	0.01025	-0.1868	-0.00049	0.00493	-0.0899
20	0.133	-0.87	-0.00173	0.01726	-0.3146	-0.00034	0.00338	-0.0615
21	0.133	-0.73	0.00026	-0.00260	0.0473	0.00006	-0.00056	0.0102
22	0.133	-0.40	0.00023	-0.00226	0.0411	-0.00116	0.01155	-0.2106
23	0.133	0.	-0.00024	0.00237	-0.0431	-0.00092	0.00918	-0.1672
24	0.133	0.40	-0.00090	0.00900	-0.1640	-0.00223	0.02231	-0.4066
25	0.133	0.73	-0.00057	0.00567	-0.1033	0.00011	-0.00108	0.0196
26	0.133	0.87	-0.00087	0.00870	-0.1585	0.00030	-0.00301	0.0548
27	0.133	0.93	-0.00017	0.00171	-0.0312	-0.00153	0.01533	-0.2794
28	0.400	0.93	0.00008	-0.00080	0.0146	-0.00032	0.00323	-0.0589
29	0.400	0.87	-0.00006	0.00060	-0.0110	0.00127	-0.01267	0.2309
30	0.400	0.73	0.00013	-0.00127	0.0232	-0.00064	0.00635	-0.1158
31	0.400	0.40	0.00012	-0.00120	0.0218	0.00027	-0.00267	0.0486
32	0.400	0.	0.00091	-0.00907	0.1653	-0.00048	0.00480	-0.0875
33	0.400	-0.40	-0.00038	0.00380	-0.0692	0.00185	-0.01850	0.3371
34	0.400	-0.73	-0.00008	0.00079	-0.0143	-0.00052	0.00519	-0.0947
35	0.400	-0.87	0.00007	-0.00069	0.0126	0.00024	-0.00243	0.0443
36	0.400	-0.93	-0.00040	0.00404	-0.0737	-0.00030	0.00303	-0.0553
37	0.667	-0.93	-0.00032	0.00319	-0.0582	-0.00019	0.00187	-0.0340
38	0.667	-0.87	-0.00075	0.00750	-0.1367	0.00088	-0.00878	0.1601
39	0.667	-0.73	-0.00056	0.00564	-0.1027	0.00093	-0.00932	0.1699
40	0.667	-0.40	-0.00097	0.00974	-0.1774	0.00052	-0.00524	0.0955
41	0.667	0.	-0.00027	0.00270	-0.0492	-0.00019	0.00185	-0.0337
42	0.667	0.40	0.00054	-0.00540	0.0984	0.00014	-0.00139	0.0253
43	0.667	0.73	0.00082	-0.00822	0.1498	-0.00035	0.00354	-0.0645
44	0.667	0.87	0.00023	-0.00226	0.0411	-0.00043	0.00427	-0.0777
45	0.667	0.93	0.00030	-0.00300	0.0547	-0.00052	0.00517	-0.0941
46	0.933	0.93	-	-	-	-	-	-
47	0.933	0.87	-	-	-	-	-	-
48	0.933	0.73	-	-	-	-	-	-
49	0.933	0.40	-	-	-	-	-	-
50	0.933	0.	-	-	-	-	-	-
51	0.933	-0.40	-	-	-	-	-	-
52	0.933	-0.73	-	-	-	-	-	-
53	0.933	-0.87	-	-	-	-	-	-
54	0.933	-0.93	-	-	-	-	-	-

Table 6.12 c). Reynolds shear stress distribution at section S-3 run no.3 Um = 0.09259 m/s

Loc. no.	η = z/h	2Y/B	Rey.s.s. formed by v' and w': $\overline{vw}$[m²/s²] [x100]	$-\rho\overline{vw}$[N/m²]	$\overline{vw}$/Um² [x100]	Rey.s.s. formed by v' and u': $\overline{vu}$[m²/s²] [x100]	$-\rho\overline{vu}$[N/m²]	$\overline{vu}$/Um² [x100]
1	0.033	-0.93	-	-	-	-	-	-
2	0.033	-0.87	-	-	-	-	-	-
3	0.033	-0.73	-	-	-	-	-	-
4	0.033	-0.40	-	-	-	-	-	-
5	0.033	0.	-	-	-	-	-	-
6	0.033	0.40	-	-	-	-	-	-
7	0.033	0.73	-	-	-	-	-	-
8	0.033	0.87	-	-	-	-	-	-
9	0.033	0.93	-	-	-	-	-	-
10	0.058	0.93	-	-	-	-	-	-
11	0.058	0.87	-	-	-	-	-	-
12	0.058	0.73	-	-	-	-	-	-
13	0.058	0.40	-	-	-	-	-	-
14	0.058	0.	-	-	-	-	-	-
15	0.058	-0.40	-	-	-	-	-	-
16	0.058	-0.73	-	-	-	-	-	-
17	0.058	-0.87	-	-	-	-	-	-
18	0.058	-0.93	-	-	-	-	-	-
19	0.133	-0.93	-0.00340	0.03399	-0.3965	0.00330	-0.03299	0.3848
20	0.133	-0.87	-0.00392	0.03916	-0.4567	0.00344	-0.03436	0.4008
21	0.133	-0.73	-0.00112	0.01120	-0.1306	-0.00377	0.03769	-0.4397
22	0.133	-0.40	-0.00057	0.00573	-0.0668	-0.00232	0.02323	-0.2710
23	0.133	0.	-0.00083	0.00827	-0.0965	-0.00079	0.00791	-0.0923
24	0.133	0.40	0.00085	-0.00848	0.0989	-0.00640	0.06399	-0.7464
25	0.133	0.73	0.00056	-0.00559	0.0652	-0.00135	0.01353	-0.1578
26	0.133	0.87	-0.00100	0.00995	-0.1161	0.00075	-0.00746	0.0871
27	0.133	0.93	-0.00073	0.00731	-0.0853	-0.00040	0.00400	-0.0467
28	0.400	0.93	-0.00020	0.00202	-0.0236	-0.00267	0.02672	-0.3116
29	0.400	0.87	0.00193	-0.01933	0.2255	0.00003	-0.00028	0.0032
30	0.400	0.73	0.00142	-0.01419	0.1655	0.00146	-0.01461	0.1704
31	0.400	0.40	0.00080	-0.00796	0.0929	-0.00424	0.04239	-0.4944
32	0.400	0.	0.00170	-0.01696	0.1978	-0.00028	0.00276	-0.0322
33	0.400	-0.40	0.00144	-0.01443	0.1684	0.00049	-0.00486	0.0567
34	0.400	-0.73	0.00182	-0.01820	0.2122	-0.00037	0.00366	-0.0427
35	0.400	-0.87	0.00040	-0.00397	0.0463	-0.00044	0.00440	-0.0514
36	0.400	-0.93	-0.00225	0.02248	-0.2622	0.00080	-0.00796	0.0929
37	0.667	-0.93	-0.00052	0.00518	-0.0604	0.00000	-0.00005	0.0006
38	0.667	-0.87	0.00042	-0.00422	0.0492	0.00078	-0.00777	0.0906
39	0.667	-0.73	0.00026	-0.00260	0.0304	0.00017	-0.00167	0.0194
40	0.667	-0.40	0.00144	-0.01439	0.1678	0.00078	-0.00782	0.0912
41	0.667	0.	0.00137	-0.01369	0.1597	0.00027	-0.00270	0.0315
42	0.667	0.40	0.00206	-0.02063	0.2406	-0.00115	0.01153	-0.1344
43	0.667	0.73	0.00244	-0.02444	0.2851	-0.00082	0.00819	-0.0955
44	0.667	0.87	0.00136	-0.01355	0.1581	0.00082	-0.00819	0.0956
45	0.667	0.93	0.00060	-0.00598	0.0697	-0.00204	0.02040	-0.2379
46	0.933	0.93	-	-	-	-	-	-
47	0.933	0.87	-	-	-	-	-	-
48	0.933	0.73	-	-	-	-	-	-
49	0.933	0.40	-	-	-	-	-	-
50	0.933	0.	-	-	-	-	-	-
51	0.933	-0.40	-	-	-	-	-	-
52	0.933	-0.73	-	-	-	-	-	-
53	0.933	-0.87	-	-	-	-	-	-
54	0.933	-0.93	-	-	-	-	-	-

Table 6.13 c). Reynolds shear stress distribution at section S-4 run no.1 Um = 0.04444 m/s

Loc. no.	η = z/h	2Y/B	Rey.s.s. formed by v' and w': $\overline{vw}$[m²/s²] [x100]	$-\rho\overline{vw}$[N/m²]	$\overline{vw}$/Um² [x100]	Rey.s.s. formed by v' and u': $\overline{vu}$[m²/s²] [x100]	$-\rho\overline{vu}$[N/m²]	$\overline{vu}$/Um² [x100]
1	0.044	-0.93	-	-	-	-	-	-
2	0.044	-0.87	-	-	-	-	-	-
3	0.044	-0.73	-	-	-	-	-	-
4	0.044	-0.40	-	-	-	-	-	-
5	0.044	0.	-	-	-	-	-	-
6	0.044	0.40	-	-	-	-	-	-
7	0.044	0.73	-	-	-	-	-	-
8	0.044	0.87	-	-	-	-	-	-
9	0.044	0.93	-	-	-	-	-	-
10	0.078	0.93	-	-	-	-	-	-
11	0.078	0.87	-	-	-	-	-	-
12	0.078	0.73	-	-	-	-	-	-
13	0.078	0.40	-	-	-	-	-	-
14	0.078	0.	-	-	-	-	-	-
15	0.078	-0.40	-	-	-	-	-	-
16	0.078	-0.73	-	-	-	-	-	-
17	0.078	-0.87	-	-	-	-	-	-
18	0.078	-0.93	-	-	-	-	-	-
19	0.178	-0.93	0.00025	-0.00254	0.1284	-0.00213	0.02126	-1.0764
20	0.178	-0.87	0.00006	-0.00061	0.0310	-0.00045	0.00455	-0.2302
21	0.178	-0.73	0.00003	-0.00027	0.0135	0.00036	-0.00355	0.1800
22	0.178	-0.40	0.00002	-0.00018	0.0090	-0.00002	0.00020	-0.0103
23	0.178	0.	0.00101	-0.01014	0.5134	-0.00029	0.00293	-0.1485
24	0.178	0.40	0.00005	-0.00050	0.0255	-0.00007	0.00067	-0.0337
25	0.178	0.73	0.00057	-0.00575	0.2910	-0.00003	0.00029	-0.0147
26	0.178	0.87	0.00150	-0.01505	0.7618	-0.00008	0.00082	-0.0416
27	0.178	0.93	0.00112	-0.01120	0.5669	-0.00022	0.00219	-0.1107
28	0.422	0.93	0.00037	-0.00365	0.1850	-0.00029	0.00288	-0.1460
29	0.422	0.87	0.00084	-0.00837	0.4237	-0.00026	0.00262	-0.1325
30	0.422	0.73	0.00141	-0.01409	0.7131	0.00020	-0.00205	0.1038
31	0.422	0.40	0.00132	-0.01320	0.6681	-0.00074	0.00737	-0.3729
32	0.422	0.	0.00118	-0.01182	0.5984	0.00014	-0.00137	0.0692
33	0.422	-0.40	0.00076	-0.00758	0.3836	0.00026	-0.00260	0.1318
34	0.422	-0.73	0.00167	-0.01671	0.8461	0.00035	-0.00355	0.1796
35	0.422	-0.87	0.00105	-0.01048	0.5306	0.00065	-0.00646	0.3272
36	0.422	-0.93	0.00006	-0.00061	0.0310	-0.00312	0.03121	-1.5800
37	0.667	-0.93	0.00003	-0.00034	0.0174	-0.00024	0.00244	-0.1237
38	0.667	-0.87	-0.00011	0.00111	-0.0562	-0.00049	0.00491	-0.2486
39	0.667	-0.73	-0.00035	0.00348	-0.1763	0.00055	-0.00545	0.2761
40	0.667	-0.40	-0.00002	0.00020	-0.0101	-0.00019	0.00190	-0.0962
41	0.667	0.	0.00147	-0.01475	0.7466	-0.00023	0.00229	-0.1159
42	0.667	0.40	0.00226	-0.02256	1.1421	-0.00017	0.00167	-0.0844
43	0.667	0.73	0.00249	-0.02488	1.2598	0.00011	-0.00105	0.0534
44	0.667	0.87	0.00273	-0.02735	1.3846	-0.00026	0.00263	-0.1329
45	0.667	0.93	0.00308	-0.03075	1.5568	-0.00032	0.00325	-0.1645

Table 6.14 c). Reynolds shear stress distribution at section S-4 run no.2 Um = 0.07407 m/s

Loc. no.	η = z/h	2Y/B	Rey.s.s. formed by v' and w': $\overline{vw}$[m²/s²] [x100]	$-\rho\overline{vw}$[N/m²]	$\overline{vw}$/Um² [x100]	Rey.s.s. formed by v' and u': $\overline{vu}$[m²/s²] [x100]	$-\rho\overline{vu}$[N/m²]	$\overline{vu}$/Um² [x100]
1	0.033	-0.93	-	-	-	-	-	-
2	0.033	-0.87	-	-	-	-	-	-
3	0.033	-0.73	-	-	-	-	-	-
4	0.033	-0.40	-	-	-	-	-	-
5	0.033	0.	-	-	-	-	-	-
6	0.033	0.40	-	-	-	-	-	-
7	0.033	0.73	-	-	-	-	-	-
8	0.033	0.87	-	-	-	-	-	-
9	0.033	0.93	-	-	-	-	-	-
10	0.058	0.93	-	-	-	-	-	-
11	0.058	0.87	-	-	-	-	-	-
12	0.058	0.73	-	-	-	-	-	-
13	0.058	0.40	-	-	-	-	-	-
14	0.058	0.	-	-	-	-	-	-
15	0.058	-0.40	-	-	-	-	-	-
16	0.058	-0.73	-	-	-	-	-	-
17	0.058	-0.87	-	-	-	-	-	-
18	0.058	-0.93	-	-	-	-	-	-
19	0.133	-0.93	-0.00008	0.00078	-0.0143	-0.00020	0.00202	-0.0368
20	0.133	-0.87	0.00005	-0.00055	0.0100	-0.00009	0.00089	-0.0162
21	0.133	-0.73	0.00089	-0.00888	0.1619	-0.00037	0.00365	-0.0666
22	0.133	-0.40	0.00068	-0.00683	0.1245	-0.00001	0.00015	-0.0027
23	0.133	0.	0.00166	-0.01662	0.3029	0.00012	-0.00119	0.0218
24	0.133	0.40	0.00235	-0.02346	0.4276	0.00018	-0.00180	0.0328
25	0.133	0.73	0.00214	-0.02135	0.3891	-0.00087	0.00872	-0.1590
26	0.133	0.87	0.00106	-0.01062	0.1935	-0.00059	0.00587	-0.1069
27	0.133	0.93	-0.00006	0.00058	-0.0105	-0.00048	0.00482	-0.0878
28	0.400	0.93	-0.00008	0.00081	-0.0148	-0.00052	0.00516	-0.0940
29	0.400	0.87	0.00218	-0.02175	0.3964	-0.00050	0.00503	-0.0916
30	0.400	0.73	0.00255	-0.02550	0.4647	0.00100	-0.01001	0.1824
31	0.400	0.40	0.00236	-0.02361	0.4302	-0.00005	0.00047	-0.0085
32	0.400	0.	0.00287	-0.02871	0.5232	0.00011	-0.00113	0.0207
33	0.400	-0.40	0.00247	-0.02475	0.4510	-0.00021	0.00214	-0.0389
34	0.400	-0.73	0.00064	-0.00642	0.1170	-0.00002	0.00017	-0.0031
35	0.400	-0.87	0.00041	-0.00412	0.0750	-0.00017	0.00172	-0.0314
36	0.400	-0.93	0.00051	-0.00511	0.0931	0.00001	-0.00009	0.0016
37	0.667	-0.93	0.00106	-0.01056	0.1925	0.00001	-0.00008	0.0015
38	0.667	-0.87	0.00154	-0.01541	0.2809	-0.00003	0.00030	-0.0055
39	0.667	-0.73	0.00189	-0.01887	0.3439	0.00013	-0.00125	0.0228
40	0.667	-0.40	0.00201	-0.02007	0.3658	-0.00029	0.00294	-0.0536
41	0.667	0.	0.00262	-0.02616	0.4767	-0.00053	0.00527	-0.0960
42	0.667	0.40	0.00337	-0.03371	0.6143	-0.00003	0.00026	-0.0047
43	0.667	0.73	0.00214	-0.02143	0.3905	0.00062	-0.00616	0.1123
44	0.667	0.87	0.00340	-0.03396	0.6189	0.00047	-0.00467	0.0851
45	0.667	0.93	0.00165	-0.01648	0.3003	0.00049	-0.00489	0.0892
46	0.933	0.93	-	-	-	-	-	-
47	0.933	0.87	-	-	-	-	-	-
48	0.933	0.73	-	-	-	-	-	-
49	0.933	0.40	-	-	-	-	-	-
50	0.933	0.	-	-	-	-	-	-
51	0.933	-0.40	-	-	-	-	-	-
52	0.933	-0.73	-	-	-	-	-	-
53	0.933	-0.87	-	-	-	-	-	-
54	0.933	-0.93	-	-	-	-	-	-

Table 6.15 c). Reynolds shear stress distribution at section S-4 run no.3 $U_m = 0.09259$ m/s

Loc. no.	η = z/h	2Y/B	Rey.s.s. formed by v' and w': $\overline{vw}$[m²/s²] [x100]	$-\rho\overline{vw}$[N/m²]	$\overline{vw}/U_m^2$ [x100]	Rey.s.s. formed by v' and u': $\overline{vu}$[m²/s²] [x100]	$-\rho\overline{vu}$[N/m²]	$\overline{vu}/U_m^2$ [x100]
1	0.033	-0.93	-	-	-	-	-	-
2	0.033	-0.87	-	-	-	-	-	-
3	0.033	-0.73	-	-	-	-	-	-
4	0.033	-0.40	-	-	-	-	-	-
5	0.033	0.	-	-	-	-	-	-
6	0.033	0.40	-	-	-	-	-	-
7	0.033	0.73	-	-	-	-	-	-
8	0.033	0.87	-	-	-	-	-	-
9	0.033	0.93	-	-	-	-	-	-
10	0.058	0.93	-	-	-	-	-	-
11	0.058	0.87	-	-	-	-	-	-
12	0.058	0.73	-	-	-	-	-	-
13	0.058	0.40	-	-	-	-	-	-
14	0.058	0.	-	-	-	-	-	-
15	0.058	-0.40	-	-	-	-	-	-
16	0.058	-0.73	-	-	-	-	-	-
17	0.058	-0.87	-	-	-	-	-	-
18	0.058	-0.93	-	-	-	-	-	-
19	0.133	-0.93	0.00006	-0.00060	0.0070	-0.00168	0.01684	-0.1964
20	0.133	-0.87	0.00119	-0.01193	0.1391	-0.00099	0.00994	-0.1159
21	0.133	-0.73	0.00076	-0.00757	0.0883	-0.00094	0.00942	-0.1099
22	0.133	-0.40	0.00091	-0.00914	0.1066	-0.00042	0.00418	-0.0487
23	0.133	0.	0.00194	-0.01940	0.2263	-0.00011	0.00111	-0.0129
24	0.133	0.40	0.00230	-0.02304	0.2687	-0.00004	0.00038	-0.0044
25	0.133	0.73	0.00337	-0.03374	0.3936	0.00035	-0.00354	0.0413
26	0.133	0.87	0.00362	-0.03624	0.4227	0.00027	-0.00267	0.0311
27	0.133	0.93	0.00132	-0.01320	0.1539	0.00017	-0.00167	0.0194
28	0.400	0.93	0.00187	-0.01866	0.2177	-0.00004	0.00040	-0.0046
29	0.400	0.87	0.00313	-0.03126	0.3646	-0.00026	0.00257	-0.0299
30	0.400	0.73	0.00417	-0.04166	0.4859	0.00017	-0.00175	0.0204
31	0.400	0.40	0.00346	-0.03461	0.4036	-0.00019	0.00195	-0.0227
32	0.400	0.	0.00296	-0.02959	0.3451	-0.00316	0.03157	-0.3683
33	0.400	-0.40	0.00212	-0.02118	0.2470	-0.00203	0.02033	-0.2371
34	0.400	-0.73	0.00227	-0.02273	0.2652	-0.00051	0.00512	-0.0598
35	0.400	-0.87	0.00207	-0.02074	0.2419	0.00046	-0.00463	0.0540
36	0.400	-0.93	0.00033	-0.00325	0.0379	0.00020	-0.00200	0.0233
37	0.667	-0.93	0.00084	-0.00845	0.0985	0.00147	-0.01468	0.1712
38	0.667	-0.87	0.00168	-0.01677	0.1956	-0.00017	0.00166	-0.0194
39	0.667	-0.73	0.00196	-0.01958	0.2284	0.00069	-0.00692	0.0807
40	0.667	-0.40	0.00243	-0.02427	0.2831	-0.00102	0.01022	-0.1192
41	0.667	0.	0.00347	-0.03466	0.4043	-0.00127	0.01269	-0.1480
42	0.667	0.40	0.00414	-0.04142	0.4831	-0.00161	0.01608	-0.1876
43	0.667	0.73	0.00316	-0.03163	0.3690	0.00123	-0.01233	0.1438
44	0.667	0.87	0.00338	-0.03383	0.3946	-0.00005	0.00052	-0.0061
45	0.667	0.93	0.00139	-0.01386	0.1617	-0.00018	0.00181	-0.0211
46	0.933	0.93	-	-	-	-	-	-
47	0.933	0.87	-	-	-	-	-	-
48	0.933	0.73	-	-	-	-	-	-
49	0.933	0.40	-	-	-	-	-	-
50	0.933	0.	-	-	-	-	-	-
51	0.933	-0.40	-	-	-	-	-	-
52	0.933	-0.73	-	-	-	-	-	-
53	0.933	-0.87	-	-	-	-	-	-
54	0.933	-0.93	-	-	-	-	-	-

Table 6.16 c). Reynolds shear stress distribution at section S-5 run no.1 $U_m = 0.04444$ m/s

Loc. no.	η = z/h	2Y/B	Rey.s.s. formed by v' and w': $\overline{vw}$[m²/s²] [x100]	$-\rho\overline{vw}$[N/m²]	$\overline{vw}/U_m^2$ [x100]	Rey.s.s. formed by v' and u': $\overline{vu}$[m²/s²] [x100]	$-\rho\overline{vu}$[N/m²]	$\overline{vu}/U_m^2$ [x100]
1	0.044	-0.93	-	-	-	-	-	-
2	0.044	-0.87	-	-	-	-	-	-
3	0.044	-0.73	-	-	-	-	-	-
4	0.044	-0.40	-	-	-	-	-	-
5	0.044	0.	-	-	-	-	-	-
6	0.044	0.40	-	-	-	-	-	-
7	0.044	0.73	-	-	-	-	-	-
8	0.044	0.87	-	-	-	-	-	-
9	0.044	0.93	-	-	-	-	-	-
10	0.078	0.93	-	-	-	-	-	-
11	0.078	0.87	-	-	-	-	-	-
12	0.078	0.73	-	-	-	-	-	-
13	0.078	0.40	-	-	-	-	-	-
14	0.078	0.	-	-	-	-	-	-
15	0.078	-0.40	-	-	-	-	-	-
16	0.078	-0.73	-	-	-	-	-	-
17	0.078	-0.87	-	-	-	-	-	-
18	0.078	-0.93	-	-	-	-	-	-
19	0.178	-0.93	-0.00061	0.00615	-0.3113	-0.00153	0.01529	-0.7739
20	0.178	-0.87	-0.00079	0.00785	-0.3975	-0.00098	0.00980	-0.4960
21	0.178	-0.73	-0.00097	0.00975	-0.4935	-0.00128	0.01278	-0.6468
22	0.178	-0.40	-0.00146	0.01461	-0.7395	-0.00173	0.01725	-0.8733
23	0.178	0.	-0.00186	0.01856	-0.9394	-0.00112	0.01116	-0.5652
24	0.178	0.40	-0.00123	0.01228	-0.6215	-0.00050	0.00498	-0.2522
25	0.178	0.73	-0.00109	0.01089	-0.5512	-0.00036	0.00359	-0.1817
26	0.178	0.87	-0.00067	0.00667	-0.3374	-0.00042	0.00415	-0.2103
27	0.178	0.93	0.00008	-0.00080	0.0405	-0.00015	0.00145	-0.0735
28	0.422	0.93	-0.00092	0.00918	-0.4645	-0.00042	0.00420	-0.2124
29	0.422	0.87	-0.00026	0.00258	-0.1305	-0.00045	0.00450	-0.2277
30	0.422	0.73	-0.00107	0.01069	-0.5410	-0.00076	0.00757	-0.3832
31	0.422	0.40	-0.00158	0.01582	-0.8009	-0.00129	0.01291	-0.6534
32	0.422	0.	-0.00203	0.02027	-1.0261	-0.00186	0.01861	-0.9420
33	0.422	-0.40	-0.00215	0.02150	-1.0885	-0.00165	0.01649	-0.8350
34	0.422	-0.73	-0.00313	0.03126	-1.5826	-0.00125	0.01249	-0.6321
35	0.422	-0.87	-0.00283	0.02830	-1.4329	-0.00141	0.01406	-0.7118
36	0.422	-0.93	-0.00073	0.00729	-0.3691	-0.00098	0.00979	-0.4954
37	0.667	-0.93	-0.00066	0.00657	-0.3326	-0.00044	0.00441	-0.2232
38	0.667	-0.87	-0.00272	0.02722	-1.3779	-0.00037	0.00374	-0.1892
39	0.667	-0.73	-0.00260	0.02603	-1.3178	-0.00073	0.00733	-0.3712
40	0.667	-0.40	-0.00316	0.03160	-1.5997	-0.00056	0.00555	-0.2811
41	0.667	0.	-0.00258	0.02581	-1.3065	-0.00116	0.01155	-0.5848
42	0.667	0.40	-0.00230	0.02297	-1.1630	-0.00064	0.00642	-0.3251
43	0.667	0.73	-0.00219	0.02193	-1.1102	-0.00068	0.00678	-0.3433
44	0.667	0.87	-0.00143	0.01433	-0.7255	-0.00070	0.00696	-0.3526
45	0.667	0.93	-0.00090	0.00900	-0.4555	-0.00056	0.00560	-0.2835

Table 6.17 c). Reynolds shear stress distribution at section S-5 run no.2 — Um = 0.07407 m/s

Loc. no.	η = z/h	2Y/B	Rey.s.s. formed by v' and w': $\overline{vw}$[m²/s²] [x100]	$-\rho\overline{vw}$[N/m²]	$\overline{vw}/Um^2$ [x100]	Rey.s.s. formed by v' and u': $\overline{vu}$[m²/s²] [x100]	$-\rho\overline{vu}$[N/m²]	$\overline{vu}/Um^2$ [x100]
1	0.033	-0.93	–	–	–	–	–	–
2	0.033	-0.87	–	–	–	–	–	–
3	0.033	-0.73	–	–	–	–	–	–
4	0.033	-0.40	–	–	–	–	–	–
5	0.033	0.	–	–	–	–	–	–
6	0.033	0.40	–	–	–	–	–	–
7	0.033	0.73	–	–	–	–	–	–
8	0.033	0.87	–	–	–	–	–	–
9	0.033	0.93	–	–	–	–	–	–
10	0.058	0.93	–	–	–	–	–	–
11	0.058	0.87	–	–	–	–	–	–
12	0.058	0.73	–	–	–	–	–	–
13	0.058	0.40	–	–	–	–	–	–
14	0.058	0.	–	–	–	–	–	–
15	0.058	-0.40	–	–	–	–	–	–
16	0.058	-0.73	–	–	–	–	–	–
17	0.058	-0.87	–	–	–	–	–	–
18	0.058	-0.93	–	–	–	–	–	–
19	0.133	-0.93	-0.00026	0.00257	-0.0468	-0.00160	0.01603	-0.2921
20	0.133	-0.87	-0.00085	0.00855	-0.1558	-0.00213	0.02132	-0.3885
21	0.133	-0.73	-0.00203	0.02033	-0.3704	-0.00218	0.02177	-0.3968
22	0.133	-0.40	-0.00217	0.02168	-0.3950	-0.00255	0.02551	-0.4649
23	0.133	0.	-0.00286	0.02859	-0.5210	-0.00226	0.02258	-0.4115
24	0.133	0.40	-0.00216	0.02164	-0.3945	-0.00137	0.01369	-0.2494
25	0.133	0.73	-0.00181	0.01809	-0.3296	-0.00039	0.00390	-0.0711
26	0.133	0.87	-0.00134	0.01341	-0.2445	-0.00061	0.00613	-0.1118
27	0.133	0.93	-0.00104	0.01044	-0.1903	-0.00048	0.00481	-0.0877
28	0.400	0.93	-0.00102	0.01016	-0.1851	-0.00064	0.00640	-0.1166
29	0.400	0.87	-0.00184	0.01837	-0.3349	-0.00056	0.00560	-0.1020
30	0.400	0.73	-0.00129	0.01293	-0.2357	-0.00059	0.00586	-0.1069
31	0.400	0.40	-0.00211	0.02108	-0.3842	-0.00128	0.01279	-0.2331
32	0.400	0.	-0.00197	0.01972	-0.3594	-0.00107	0.01073	-0.1956
33	0.400	-0.40	-0.00200	0.02004	-0.3652	-0.00090	0.00899	-0.1639
34	0.400	-0.73	-0.00109	0.01089	-0.1985	-0.00089	0.00886	-0.1615
35	0.400	-0.87	-0.00112	0.01121	-0.2043	-0.00064	0.00644	-0.1173
36	0.400	-0.93	0.00203	-0.02031	0.3701	-0.00061	0.00613	-0.1118
37	0.667	-0.93	-0.00055	0.00553	-0.1007	-0.00015	0.00146	-0.0266
38	0.667	-0.87	-0.00317	0.03171	-0.5779	-0.00021	0.00215	-0.0391
39	0.667	-0.73	-0.00373	0.03728	-0.6794	-0.00078	0.00778	-0.1417
40	0.667	-0.40	-0.00321	0.03206	-0.5843	-0.00004	0.00041	-0.0075
41	0.667	0.	-0.00373	0.03731	-0.6801	-0.00148	0.01480	-0.2698
42	0.667	0.40	-0.00241	0.02411	-0.4395	-0.00055	0.00548	-0.0998
43	0.667	0.73	-0.00192	0.01920	-0.3499	-0.00111	0.01114	-0.2029
44	0.667	0.87	-0.00153	0.01533	-0.2794	-0.00084	0.00838	-0.1527
45	0.667	0.93	-0.00128	0.01278	-0.2329	-0.00021	0.00211	-0.0384
46	0.933	0.93	–	–	–	–	–	–
47	0.933	0.87	–	–	–	–	–	–
48	0.933	0.73	–	–	–	–	–	–
49	0.933	0.40	–	–	–	–	–	–
50	0.933	0.	–	–	–	–	–	–
51	0.933	-0.40	–	–	–	–	–	–
52	0.933	-0.73	–	–	–	–	–	–
53	0.933	-0.87	–	–	–	–	–	–
54	0.933	-0.93	–	–	–	–	–	–

Table 6.18 c). Reynolds shear stress distribution at section S-5 run no.3 — Um = 0.09259 m/s

Loc. no.	η = z/h	2Y/B	Rey.s.s. formed by v' and w': $\overline{vw}$[m²/s²] [x100]	$-\rho\overline{vw}$[N/m²]	$\overline{vw}/Um^2$ [x100]	Rey.s.s. formed by v' and u': $\overline{vu}$[m²/s²] [x100]	$-\rho\overline{vu}$[N/m²]	$\overline{vu}/Um^2$ [x100]
1	0.033	-0.93	–	–	–	–	–	–
2	0.033	-0.87	–	–	–	–	–	–
3	0.033	-0.73	–	–	–	–	–	–
4	0.033	-0.40	–	–	–	–	–	–
5	0.033	0.	–	–	–	–	–	–
6	0.033	0.40	–	–	–	–	–	–
7	0.033	0.73	–	–	–	–	–	–
8	0.033	0.87	–	–	–	–	–	–
9	0.033	0.93	–	–	–	–	–	–
10	0.058	0.93	–	–	–	–	–	–
11	0.058	0.87	–	–	–	–	–	–
12	0.058	0.73	–	–	–	–	–	–
13	0.058	0.40	–	–	–	–	–	–
14	0.058	0.	–	–	–	–	–	–
15	0.058	-0.40	–	–	–	–	–	–
16	0.058	-0.73	–	–	–	–	–	–
17	0.058	-0.87	–	–	–	–	–	–
18	0.058	-0.93	–	–	–	–	–	–
19	0.133	-0.93	-0.00072	0.00722	-0.0842	-0.00046	0.00458	-0.0535
20	0.133	-0.87	-0.00249	0.02491	-0.2905	-0.00140	0.01401	-0.1634
21	0.133	-0.73	-0.00312	0.03116	-0.3635	-0.00045	0.00450	-0.0525
22	0.133	-0.40	-0.00323	0.03226	-0.3763	0.00029	-0.00293	0.0342
23	0.133	0.	-0.00359	0.03591	-0.4188	-0.00185	0.01845	-0.2152
24	0.133	0.40	-0.00303	0.03028	-0.3532	-0.00101	0.01011	-0.1179
25	0.133	0.73	-0.00204	0.02040	-0.2380	-0.00073	0.00733	-0.0855
26	0.133	0.87	-0.00182	0.01817	-0.2119	-0.00092	0.00919	-0.1071
27	0.133	0.93	-0.00178	0.01776	-0.2072	-0.00062	0.00621	-0.0724
28	0.400	0.93	-0.00167	0.01669	-0.1947	-0.00042	0.00416	-0.0485
29	0.400	0.87	-0.00281	0.02812	-0.3280	-0.00139	0.01389	-0.1620
30	0.400	0.73	-0.00245	0.02446	-0.2853	-0.00067	0.00667	-0.0777
31	0.400	0.40	-0.00301	0.03006	-0.3506	-0.00106	0.01064	-0.1241
32	0.400	0.	-0.00357	0.03573	-0.4167	-0.00268	0.02675	-0.3120
33	0.400	-0.40	-0.00319	0.03188	-0.3719	-0.00106	0.01055	-0.1231
34	0.400	-0.73	-0.00369	0.03695	-0.4310	0.00015	-0.00154	0.0179
35	0.400	-0.87	-0.00320	0.03203	-0.3736	-0.00066	0.00661	-0.0771
36	0.400	-0.93	-0.00086	0.00856	-0.0999	-0.00022	0.00221	-0.0258
37	0.667	-0.93	0.00101	-0.01014	0.1183	-0.00183	0.01833	-0.2139
38	0.667	-0.87	-0.00276	0.02756	-0.3214	-0.00216	0.02161	-0.2521
39	0.667	-0.73	-0.00319	0.03185	-0.3715	-0.00166	0.01656	-0.1932
40	0.667	-0.40	-0.00340	0.03403	-0.3969	-0.00130	0.01296	-0.1511
41	0.667	0.	-0.00325	0.03250	-0.3791	-0.00193	0.01931	-0.2252
42	0.667	0.40	-0.00199	0.01986	-0.2316	-0.00178	0.01777	-0.2073
43	0.667	0.73	-0.00106	0.01060	-0.1236	-0.00114	0.01145	-0.1335
44	0.667	0.87	-0.00159	0.01595	-0.1860	-0.00146	0.01459	-0.1702
45	0.667	0.93	-0.00203	0.02026	-0.2363	-0.00016	0.00160	-0.0187
46	0.933	0.93	–	–	–	–	–	–
47	0.933	0.87	–	–	–	–	–	–
48	0.933	0.73	–	–	–	–	–	–
49	0.933	0.40	–	–	–	–	–	–
50	0.933	0.	–	–	–	–	–	–
51	0.933	-0.40	–	–	–	–	–	–
52	0.933	-0.73	–	–	–	–	–	–
53	0.933	-0.87	–	–	–	–	–	–
54	0.933	-0.93	–	–	–	–	–	–

Table 6.19 c). *Reynolds shear stress distribution at section S-6 run no.1* Um = 0.04444 m/s

Loc. no.	η = z/h	2Y/B	Rey.s.s. formed by v' and w': $\overline{vw}$[m²/s²] [x100]	$-\rho\overline{vw}$[N/m²]	$\overline{vw}/Um^2$ [x100]	Rey.s.s. formed by v' and u': $\overline{vu}$[m²/s²] [x100]	$-\rho\overline{vu}$[N/m²]	$\overline{vu}/Um^2$ [x100]
1	0.044	-0.93	-	-	-	-	-	-
2	0.044	-0.87	-	-	-	-	-	-
3	0.044	-0.73	-	-	-	-	-	-
4	0.044	-0.40	-	-	-	-	-	-
5	0.044	0.	-	-	-	-	-	-
6	0.044	0.40	-	-	-	-	-	-
7	0.044	0.73	-	-	-	-	-	-
8	0.044	0.87	-	-	-	-	-	-
9	0.044	0.93	-	-	-	-	-	-
10	0.078	0.93	-	-	-	-	-	-
11	0.078	0.87	-	-	-	-	-	-
12	0.078	0.73	-	-	-	-	-	-
13	0.078	0.40	-	-	-	-	-	-
14	0.078	0.	-	-	-	-	-	-
15	0.078	-0.40	-	-	-	-	-	-
16	0.078	-0.73	-	-	-	-	-	-
17	0.078	-0.87	-	-	-	-	-	-
18	0.078	-0.93	-	-	-	-	-	-
19	0.178	-0.93	-0.00079	0.00795	-0.4024	0.00028	-0.00276	0.1398
20	0.178	-0.87	-0.00106	0.01059	-0.5359	0.00044	-0.00437	0.2211
21	0.178	-0.73	-0.00132	0.01320	-0.6681	0.00046	-0.00463	0.2342
22	0.178	-0.40	-0.00236	0.02356	-1.1926	0.00119	-0.01191	0.6032
23	0.178	0.	-0.00148	0.01482	-0.7502	0.00174	-0.01743	0.8822
24	0.178	0.40	-0.00101	0.01010	-0.5115	0.00139	-0.01389	0.7031
25	0.178	0.73	-0.00123	0.01229	-0.6222	0.00064	-0.00644	0.3263
26	0.178	0.87	-0.00135	0.01347	-0.6820	0.00031	-0.00313	0.1586
27	0.178	0.93	-0.00088	0.00884	-0.4473	0.00087	-0.00868	0.4394
28	0.422	0.93	-0.00156	0.01560	-0.7898	0.00019	-0.00193	0.0975
29	0.422	0.87	-0.00066	0.00663	-0.3357	0.00021	-0.00214	0.1082
30	0.422	0.73	-0.00092	0.00918	-0.4648	0.00053	-0.00525	0.2659
31	0.422	0.40	-0.00183	0.01833	-0.9279	0.00057	-0.00568	0.2875
32	0.422	0.	-0.00174	0.01740	-0.8808	0.00111	-0.01110	0.5618
33	0.422	-0.40	-0.00170	0.01698	-0.8598	0.00077	-0.00774	0.3920
34	0.422	-0.73	-0.00107	0.01069	-0.5413	0.00082	-0.00823	0.4168
35	0.422	-0.87	-0.00091	0.00909	-0.4601	0.00056	-0.00564	0.2853
36	0.422	-0.93	0.00016	-0.00160	0.0812	0.00088	-0.00879	0.4448
37	0.667	-0.93	-0.00043	0.00432	-0.2185	0.00024	-0.00236	0.1196
38	0.667	-0.87	-0.00114	0.01136	-0.5753	0.00023	-0.00231	0.1170
39	0.667	-0.73	-0.00078	0.00779	-0.3945	0.00032	-0.00323	0.1634
40	0.667	-0.40	-0.00154	0.01541	-0.7801	0.00063	-0.00626	0.3169
41	0.667	0.	-0.00203	0.02030	-1.0274	0.00106	-0.01063	0.5382
42	0.667	0.40	-0.00170	0.01705	-0.8630	0.00134	-0.01344	0.6802
43	0.667	0.73	-0.00143	0.01433	-0.7255	0.00066	-0.00660	0.3341
44	0.667	0.87	-0.00142	0.01417	-0.7174	0.00048	-0.00478	0.2419
45	0.667	0.93	-0.00167	0.01671	-0.8461	0.00041	-0.00406	0.2055

Table 6.20 c). *Reynolds shear stress distribution at section S-6 run no.2* Um = 0.07407 m/s

Loc. no.	η = z/h	2Y/B	Rey.s.s. formed by v' and w': $\overline{vw}$[m²/s²] [x100]	$-\rho\overline{vw}$[N/m²]	$\overline{vw}/Um^2$ [x100]	Rey.s.s. formed by v' and u': $\overline{vu}$[m²/s²] [x100]	$-\rho\overline{vu}$[N/m²]	$\overline{vu}/Um^2$ [x100]
1	0.033	-0.93	-	-	-	-	-	-
2	0.033	-0.87	-	-	-	-	-	-
3	0.033	-0.73	-	-	-	-	-	-
4	0.033	-0.40	-	-	-	-	-	-
5	0.033	0.	-	-	-	-	-	-
6	0.033	0.40	-	-	-	-	-	-
7	0.033	0.73	-	-	-	-	-	-
8	0.033	0.87	-	-	-	-	-	-
9	0.033	0.93	-	-	-	-	-	-
10	0.058	0.93	-	-	-	-	-	-
11	0.056	0.87	-	-	-	-	-	-
12	0.058	0.73	-	-	-	-	-	-
13	0.058	0.40	-	-	-	-	-	-
14	0.058	0.	-	-	-	-	-	-
15	0.058	-0.40	-	-	-	-	-	-
16	0.058	-0.73	-	-	-	-	-	-
17	0.058	-0.87	-	-	-	-	-	-
18	0.058	-0.93	-	-	-	-	-	-
19	0.133	-0.93	-0.00095	0.00950	-0.1731	0.00176	-0.01762	0.3211
20	0.133	-0.87	-0.00212	0.02121	-0.3866	0.00174	-0.01740	0.3171
21	0.133	-0.73	-0.00307	0.03065	-0.5586	0.00220	-0.02202	0.4013
22	0.133	-0.40	-0.00307	0.03069	-0.5593	0.00272	-0.02717	0.4951
23	0.133	0.	-0.00226	0.02259	-0.4117	0.00206	-0.02056	0.3746
24	0.133	0.40	-0.00203	0.02027	-0.3695	0.00200	-0.01998	0.3641
25	0.133	0.73	-0.00180	0.01796	-0.3274	0.00031	-0.00307	0.0559
26	0.133	0.87	-0.00172	0.01721	-0.3136	0.00021	-0.00211	0.0385
27	0.133	0.93	-0.00153	0.01533	-0.2794	0.00017	-0.00173	0.0316
28	0.400	0.93	-0.00177	0.01773	-0.3231	0.00066	-0.00663	0.1208
29	0.400	0.87	-0.00142	0.01423	-0.2594	0.00128	-0.01275	0.2324
30	0.400	0.73	-0.00196	0.01959	-0.3570	0.00121	-0.01213	0.2211
31	0.400	0.40	-0.00256	0.02565	-0.4674	0.00143	-0.01435	0.2615
32	0.400	0.	-0.00298	0.02980	-0.5432	0.00231	-0.02310	0.4209
33	0.400	-0.40	-0.00373	0.03731	-0.6801	0.00308	-0.03084	0.5621
34	0.400	-0.73	-0.00305	0.03051	-0.5560	0.00249	-0.02487	0.4532
35	0.400	-0.87	-0.00257	0.02566	-0.4677	0.00182	-0.01818	0.3314
36	0.400	-0.93	-0.00120	0.01198	-0.2183	0.00189	-0.01890	0.3444
37	0.667	-0.93	-0.00031	0.00306	-0.0557	0.00051	-0.00508	0.0925
38	0.667	-0.87	-0.00248	0.02475	-0.4511	0.00055	-0.00551	0.1004
39	0.667	-0.73	-0.00276	0.02760	-0.5030	0.00074	-0.00744	0.1355
40	0.667	-0.40	-0.00360	0.03599	-0.6560	0.00180	-0.01805	0.3289
41	0.667	0.	-0.00361	0.03610	-0.6578	0.00192	-0.01922	0.3503
42	0.667	0.40	-0.00297	0.02968	-0.5410	0.00117	-0.01171	0.2134
43	0.667	0.73	-0.00203	0.02035	-0.3708	0.00132	-0.01321	0.2408
44	0.667	0.87	-0.00160	0.01602	-0.2920	0.00204	-0.02041	0.3720
45	0.667	0.93	-0.00085	0.00854	-0.1556	0.00088	-0.00877	0.1598
46	0.933	0.93	-	-	-	-	-	-
47	0.933	0.87	-	-	-	-	-	-
48	0.933	0.73	-	-	-	-	-	-
49	0.933	0.40	-	-	-	-	-	-
50	0.933	0.	-	-	-	-	-	-
51	0.933	-0.40	-	-	-	-	-	-
52	0.933	-0.73	-	-	-	-	-	-
53	0.933	-0.87	-	-	-	-	-	-
54	0.933	-0.93	-	-	-	-	-	-

Table 6.21 c). *Reynolds shear stress distribution at section S-6 run no.3* Um = 0.09259 m/s

Loc. no.	η = z/h	2Y/B	Rey.s.s. formed by v' and w': $\overline{vw}$[m²/s²] [x100]	Rey.s.s. formed by v' and w': $-\rho\overline{vw}$[N/m²]	Rey.s.s. formed by v' and w': $\overline{vw}/Um^2$ [x100]	Rey.s.s. formed by v' and u': $\overline{vu}$[m²/s²] [x100]	Rey.s.s. formed by v' and u': $-\rho\overline{vu}$[N/m²]	Rey.s.s. formed by v' and u': $\overline{vu}/Um^2$ [x100]
1	0.033	-0.93	-	-	-	-	-	-
2	0.033	-0.87	-	-	-	-	-	-
3	0.033	-0.73	-	-	-	-	-	-
4	0.033	-0.40	-	-	-	-	-	-
5	0.033	0.	-	-	-	-	-	-
6	0.033	0.40	-	-	-	-	-	-
7	0.033	0.73	-	-	-	-	-	-
8	0.033	0.87	-	-	-	-	-	-
9	0.033	0.93	-	-	-	-	-	-
10	0.058	0.93	-	-	-	-	-	-
11	0.058	0.87	-	-	-	-	-	-
12	0.058	0.73	-	-	-	-	-	-
13	0.058	0.40	-	-	-	-	-	-
14	0.058	0.	-	-	-	-	-	-
15	0.058	-0.40	-	-	-	-	-	-
16	0.058	-0.73	-	-	-	-	-	-
17	0.058	-0.87	-	-	-	-	-	-
18	0.058	-0.93	-	-	-	-	-	-
19	0.133	-0.93	0.00019	-0.00186	0.0217	-0.00030	0.00302	-0.0352
20	0.133	-0.87	-0.00096	0.00961	-0.1121	-0.00015	0.00150	-0.0175
21	0.133	-0.73	-0.00308	0.03083	-0.3596	0.00000	-0.00000	0.0000
22	0.133	-0.40	-0.00304	0.03043	-0.3549	0.00062	-0.00623	0.0726
23	0.133	0.	-0.00324	0.03238	-0.3777	0.00091	-0.00907	0.1057
24	0.133	0.40	-0.00274	0.02737	-0.3193	0.00056	-0.00564	0.0658
25	0.133	0.73	-0.00180	0.01801	-0.2101	-0.00002	0.00024	-0.0028
26	0.133	0.87	-0.00177	0.01773	-0.2068	0.00002	-0.00025	0.0029
27	0.133	0.93	-0.00281	0.02812	-0.3280	-0.00002	0.00023	-0.0027
28	0.400	0.93	-0.00238	0.02385	-0.2781	0.00046	-0.00455	0.0531
29	0.400	0.87	-0.00270	0.02702	-0.3151	0.00001	-0.00007	0.0008
30	0.400	0.73	-0.00287	0.02872	-0.3349	0.00015	-0.00149	0.0174
31	0.400	0.40	-0.00323	0.03228	-0.3765	0.00058	-0.00575	0.0671
32	0.400	0.	-0.00308	0.03079	-0.3592	-0.00037	0.00373	-0.0435
33	0.400	-0.40	-0.00339	0.03394	-0.3959	0.00024	-0.00236	0.0276
34	0.400	-0.73	-0.00328	0.03284	-0.3831	0.00065	-0.00649	0.0757
35	0.400	-0.87	-0.00199	0.01993	-0.2325	0.00117	-0.01174	0.1369
36	0.400	-0.93	-0.00015	0.00153	-0.0178	0.00127	-0.01267	0.1478
37	0.667	-0.93	-0.00047	0.00470	-0.0548	0.00041	-0.00406	0.0473
38	0.667	-0.87	-0.00121	0.01210	-0.1412	-0.00011	0.00110	-0.0128
39	0.667	-0.73	-0.00150	0.01501	-0.1750	0.00114	-0.01144	0.1334
40	0.667	-0.40	-0.00381	0.03810	-0.4444	0.00148	-0.01480	0.1726
41	0.667	0.	-0.00323	0.03231	-0.3768	-0.00027	0.00274	-0.0319
42	0.667	0.40	-0.00280	0.02799	-0.3265	-0.00002	0.00020	-0.0023
43	0.667	0.73	-0.00234	0.02340	-0.2729	-0.00001	0.00006	-0.0007
44	0.667	0.87	-0.00217	0.02166	-0.2527	0.00017	-0.00170	0.0198
45	0.667	0.93	-0.00143	0.01430	-0.1668	0.00045	-0.00451	0.0526
46	0.933	0.93	-	-	-	-	-	-
47	0.933	0.87	-	-	-	-	-	-
48	0.933	0.73	-	-	-	-	-	-
49	0.933	0.40	-	-	-	-	-	-
50	0.933	0.	-	-	-	-	-	-
51	0.933	-0.40	-	-	-	-	-	-
52	0.933	-0.73	-	-	-	-	-	-
53	0.933	-0.87	-	-	-	-	-	-
54	0.933	-0.93	-	-	-	-	-	-

Table 6.22 c). *Reynolds shear stress distribution at section S-7 run no.1* Um = 0.04444 m/s

Loc. no.	η = z/h	2Y/B	Rey.s.s. formed by v' and w': $\overline{vw}$[m²/s²] [x100]	Rey.s.s. formed by v' and w': $-\rho\overline{vw}$[N/m²]	Rey.s.s. formed by v' and w': $\overline{vw}/Um^2$ [x100]	Rey.s.s. formed by v' and u': $\overline{vu}$[m²/s²] [x100]	Rey.s.s. formed by v' and u': $-\rho\overline{vu}$[N/m²]	Rey.s.s. formed by v' and u': $\overline{vu}/Um^2$ [x100]
1	0.044	-0.93	-	-	-	-	-	-
2	0.044	-0.87	-	-	-	-	-	-
3	0.044	-0.73	-	-	-	-	-	-
4	0.044	-0.40	-	-	-	-	-	-
5	0.044	0.	-	-	-	-	-	-
6	0.044	0.40	-	-	-	-	-	-
7	0.044	0.73	-	-	-	-	-	-
8	0.044	0.87	-	-	-	-	-	-
9	0.044	0.93	-	-	-	-	-	-
10	0.078	0.93	-	-	-	-	-	-
11	0.078	0.87	-	-	-	-	-	-
12	0.078	0.73	-	-	-	-	-	-
13	0.078	0.40	-	-	-	-	-	-
14	0.078	0.	-	-	-	-	-	-
15	0.078	-0.40	-	-	-	-	-	-
16	0.078	-0.73	-	-	-	-	-	-
17	0.078	-0.87	-	-	-	-	-	-
18	0.078	-0.93	-	-	-	-	-	-
19	0.178	-0.93	-0.00021	0.00208	-0.1051	0.00049	-0.00486	0.2461
20	0.178	-0.87	-0.00102	0.01020	-0.5164	0.00043	-0.00428	0.2165
21	0.178	-0.73	-0.00176	0.01760	-0.8908	0.00091	-0.00911	0.4612
22	0.178	-0.40	-0.00173	0.01725	-0.8735	0.00058	-0.00584	0.2959
23	0.178	0.	-0.00221	0.02213	-1.1203	0.00135	-0.01349	0.6827
24	0.178	0.40	-0.00256	0.02558	-1.2952	0.00115	-0.01150	0.5821
25	0.178	0.73	-0.00255	0.02550	-1.2907	0.00086	-0.00855	0.4330
26	0.178	0.87	-0.00234	0.02338	-1.1835	0.00124	-0.01237	0.6260
27	0.178	0.93	-0.00213	0.02130	-1.0784	0.00074	-0.00740	0.3748
28	0.422	0.93	-0.00158	0.01578	-0.7986	0.00016	-0.00159	0.0804
29	0.422	0.87	-0.00222	0.02222	-1.1248	0.00085	-0.00852	0.4314
30	0.422	0.73	-0.00191	0.01906	-0.9649	0.00203	-0.02030	1.0274
31	0.422	0.40	-0.00249	0.02490	-1.2603	0.00134	-0.01338	0.6771
32	0.422	0.	-0.00199	0.01993	-1.0092	0.00083	-0.00833	0.4218
33	0.422	-0.40	-0.00158	0.01581	-0.8006	0.00021	-0.00211	0.1069
34	0.422	-0.73	-0.00072	0.00724	-0.3668	0.00007	-0.00071	0.0360
35	0.422	-0.87	-0.00076	0.00760	-0.3847	-0.00000	0.00000	-0.0002
36	0.422	-0.93	-0.00084	0.00836	-0.4232	0.00004	-0.00044	0.0221
37	0.667	-0.93	-0.00064	0.00644	-0.3258	0.00002	-0.00021	0.0107
38	0.667	-0.87	-0.00020	0.00200	-0.1012	0.00025	-0.00247	0.1249
39	0.667	-0.73	-0.00099	0.00989	-0.5005	0.00040	-0.00398	0.2016
40	0.667	-0.40	-0.00148	0.01480	-0.7494	0.00055	-0.00546	0.2765
41	0.667	0.	-0.00184	0.01840	-0.9313	0.00031	-0.00306	0.1547
42	0.667	0.40	-0.00197	0.01973	-0.9988	0.00103	-0.01031	0.5220
43	0.667	0.73	-0.00181	0.01807	-0.9150	0.00187	-0.01865	0.9443
44	0.667	0.87	-0.00168	0.01675	-0.8482	0.00037	-0.00375	0.1898
45	0.667	0.93	-0.00113	0.01133	-0.5736	-0.00008	0.00080	-0.0405

Table 6.23 *c). Reynolds shear stress distribution at section S-7 run no.2* Um = 0.07407 m/s

Loc. no.	η = z/h	2Y/B	Rey.s.s. formed by v' and w': $\overline{vw}$[m^2/s^2] [x100]	$-\rho\overline{vw}$[N/m^2]	$\overline{vw}$/Um^2 [x100]	Rey.s.s. formed by v' and u': $\overline{vu}$[m^2/s^2] [x100]	$-\rho\overline{vu}$[N/m^2]	$\overline{vu}$/Um^2 [x100]
1	0.033	-0.93	-	-	-	-	-	-
2	0.033	-0.87	-	-	-	-	-	-
3	0.033	-0.73	-	-	-	-	-	-
4	0.033	-0.40	-	-	-	-	-	-
5	0.033	0.	-	-	-	-	-	-
6	0.033	0.40	-	-	-	-	-	-
7	0.033	0.73	-	-	-	-	-	-
8	0.033	0.87	-	-	-	-	-	-
9	0.033	0.93	-	-	-	-	-	-
10	0.058	0.93	-	-	-	-	-	-
11	0.058	0.87	-	-	-	-	-	-
12	0.058	0.73	-	-	-	-	-	-
13	0.058	0.40	-	-	-	-	-	-
14	0.058	0.	-	-	-	-	-	-
15	0.058	-0.40	-	-	-	-	-	-
16	0.058	-0.73	-	-	-	-	-	-
17	0.058	-0.87	-	-	-	-	-	-
18	0.058	-0.93	-	-	-	-	-	-
19	0.133	-0.93	-0.00179	0.01791	-0.3265	-0.00017	0.00175	-0.0319
20	0.133	-0.87	-0.00197	0.01966	-0.3583	-0.00143	0.01431	-0.2608
21	0.133	-0.73	-0.00237	0.02370	-0.4319	-0.00207	0.02066	-0.3766
22	0.133	-0.40	-0.00238	0.02378	-0.4335	-0.00248	0.02485	-0.4528
23	0.133	0.	-0.00371	0.03713	-0.6768	-0.00224	0.02244	-0.4090
24	0.133	0.40	-0.00354	0.03538	-0.6448	-0.00235	0.02352	-0.4287
25	0.133	0.73	-0.00370	0.03697	-0.6738	-0.00254	0.02537	-0.4624
26	0.133	0.87	-0.00312	0.03118	-0.5682	-0.00288	0.02880	-0.5249
27	0.133	0.93	-0.00176	0.01759	-0.3206	-0.00282	0.02820	-0.5139
28	0.400	0.93	-0.00115	0.01155	-0.2105	-0.00230	0.02297	-0.4186
29	0.400	0.87	-0.00357	0.03572	-0.6510	-0.00260	0.02604	-0.4746
30	0.400	0.73	-0.00392	0.03919	-0.7142	-0.00259	0.02589	-0.4718
31	0.400	0.40	-0.00363	0.03630	-0.6617	-0.00253	0.02530	-0.4611
32	0.400	0.	-0.00355	0.03549	-0.6469	-0.00285	0.02852	-0.5198
33	0.400	-0.40	-0.00280	0.02804	-0.5110	-0.00245	0.02447	-0.4461
34	0.400	-0.73	-0.00290	0.02904	-0.5293	-0.00173	0.01731	-0.3154
35	0.400	-0.87	-0.00264	0.02643	-0.4817	-0.00131	0.01305	-0.2379
36	0.400	-0.93	-0.00217	0.02166	-0.3948	-0.00124	0.01239	-0.2259
37	0.667	-0.93	-0.00121	0.01210	-0.2205	-0.00142	0.01421	-0.2590
38	0.667	-0.87	-0.00219	0.02188	-0.3987	-0.00089	0.00889	-0.1621
39	0.667	-0.73	-0.00214	0.02142	-0.3903	-0.00120	0.01198	-0.2183
40	0.667	-0.40	-0.00385	0.03846	-0.7009	-0.00240	0.02397	-0.4369
41	0.667	0.	-0.00406	0.04058	-0.7396	-0.00179	0.01791	-0.3265
42	0.667	0.40	-0.00356	0.03565	-0.6497	-0.00140	0.01398	-0.2547
43	0.667	0.73	-0.00315	0.03149	-0.5740	-0.00174	0.01740	-0.3171
44	0.667	0.87	-0.00281	0.02808	-0.5118	-0.00144	0.01441	-0.2627
45	0.667	0.93	-0.00242	0.02420	-0.4410	-0.00020	0.00203	-0.0371
46	0.933	0.93	-	-	-	-	-	-
47	0.933	0.87	-	-	-	-	-	-
48	0.933	0.73	-	-	-	-	-	-
49	0.933	0.40	-	-	-	-	-	-
50	0.933	0.	-	-	-	-	-	-
51	0.933	-0.40	-	-	-	-	-	-
52	0.933	-0.73	-	-	-	-	-	-
53	0.933	-0.87	-	-	-	-	-	-
54	0.933	-0.93	-	-	-	-	-	-

Table 6.24 *c). Reynolds shear stress distribution at section S-7 run no.3* Um = 0.09259 m/s

Loc. no.	η = z/h	2Y/B	Rey.s.s. formed by v' and w': $\overline{vw}$[m^2/s^2] [x100]	$-\rho\overline{vw}$[N/m^2]	$\overline{vw}$/Um^2 [x100]	Rey.s.s. formed by v' and u': $\overline{vu}$[m^2/s^2] [x100]	$-\rho\overline{vu}$[N/m^2]	$\overline{vu}$/Um^2 [x100]
1	0.033	-0.93	-	-	-	-	-	-
2	0.033	-0.87	-	-	-	-	-	-
3	0.033	-0.73	-	-	-	-	-	-
4	0.033	-0.40	-	-	-	-	-	-
5	0.033	0.	-	-	-	-	-	-
6	0.033	0.40	-	-	-	-	-	-
7	0.033	0.73	-	-	-	-	-	-
8	0.033	0.87	-	-	-	-	-	-
9	0.033	0.93	-	-	-	-	-	-
10	0.058	0.93	-	-	-	-	-	-
11	0.058	0.87	-	-	-	-	-	-
12	0.058	0.73	-	-	-	-	-	-
13	0.058	0.40	-	-	-	-	-	-
14	0.058	0.	-	-	-	-	-	-
15	0.058	-0.40	-	-	-	-	-	-
16	0.058	-0.73	-	-	-	-	-	-
17	0.058	-0.87	-	-	-	-	-	-
18	0.058	-0.93	-	-	-	-	-	-
19	0.133	-0.93	-0.00071	0.00708	-0.0825	0.00045	-0.00450	0.0525
20	0.133	-0.87	-0.00139	0.01385	-0.1616	-0.00001	0.00014	-0.0016
21	0.133	-0.73	-0.00250	0.02501	-0.2917	-0.00014	0.00144	-0.0168
22	0.133	-0.40	-0.00303	0.03028	-0.3532	-0.00082	0.00817	-0.0952
23	0.133	0.	-0.00300	0.02999	-0.3497	-0.00089	0.00891	-0.1039
24	0.133	0.40	-0.00234	0.02336	-0.2724	-0.00162	0.01618	-0.1888
25	0.133	0.73	-0.00342	0.03423	-0.3992	-0.00241	0.02407	-0.2807
26	0.133	0.87	-0.00318	0.03181	-0.3710	-0.00274	0.02739	-0.3195
27	0.133	0.93	-0.00110	0.01095	-0.1278	-0.00262	0.02625	-0.3061
28	0.400	0.93	-0.00216	0.02156	-0.2515	-0.00255	0.02545	-0.2969
29	0.400	0.87	-0.00368	0.03683	-0.4295	-0.00249	0.02487	-0.2900
30	0.400	0.73	-0.00429	0.04288	-0.5001	-0.00241	0.02406	-0.2807
31	0.400	0.40	-0.00392	0.03917	-0.4569	-0.00095	0.00953	-0.1111
32	0.400	0.	-0.00404	0.04044	-0.4717	-0.00053	0.00534	-0.0623
33	0.400	-0.40	-0.00371	0.03708	-0.4325	0.00008	-0.00080	0.0093
34	0.400	-0.73	-0.00292	0.02922	-0.3409	-0.00016	0.00157	-0.0184
35	0.400	-0.87	-0.00205	0.02048	-0.2389	-0.00004	0.00041	-0.0048
36	0.400	-0.93	-0.00209	0.02090	-0.2438	0.00002	-0.00020	0.0023
37	0.667	-0.93	-0.00200	0.02004	-0.2338	-0.00018	0.00178	-0.0207
38	0.667	-0.87	-0.00250	0.02495	-0.2910	-0.00004	0.00037	-0.0043
39	0.667	-0.73	-0.00358	0.03581	-0.4176	-0.00006	0.00061	-0.0071
40	0.667	-0.40	-0.00364	0.03644	-0.4251	-0.00045	0.00450	-0.0524
41	0.667	0.	-0.00341	0.03411	-0.3979	-0.00034	0.00335	-0.0391
42	0.667	0.40	-0.00366	0.03663	-0.4272	-0.00139	0.01389	-0.1620
43	0.667	0.73	-0.00368	0.03676	-0.4287	-0.00275	0.02747	-0.3204
44	0.667	0.87	-0.00324	0.03242	-0.3781	-0.00253	0.02530	-0.2951
45	0.667	0.93	-0.00045	0.00453	-0.0529	-0.00284	0.02840	-0.3312
46	0.933	0.93	-	-	-	-	-	-
47	0.933	0.87	-	-	-	-	-	-
48	0.933	0.73	-	-	-	-	-	-
49	0.933	0.40	-	-	-	-	-	-
50	0.933	0.	-	-	-	-	-	-
51	0.933	-0.40	-	-	-	-	-	-
52	0.933	-0.73	-	-	-	-	-	-
53	0.933	-0.87	-	-	-	-	-	-
54	0.933	-0.93	-	-	-	-	-	-

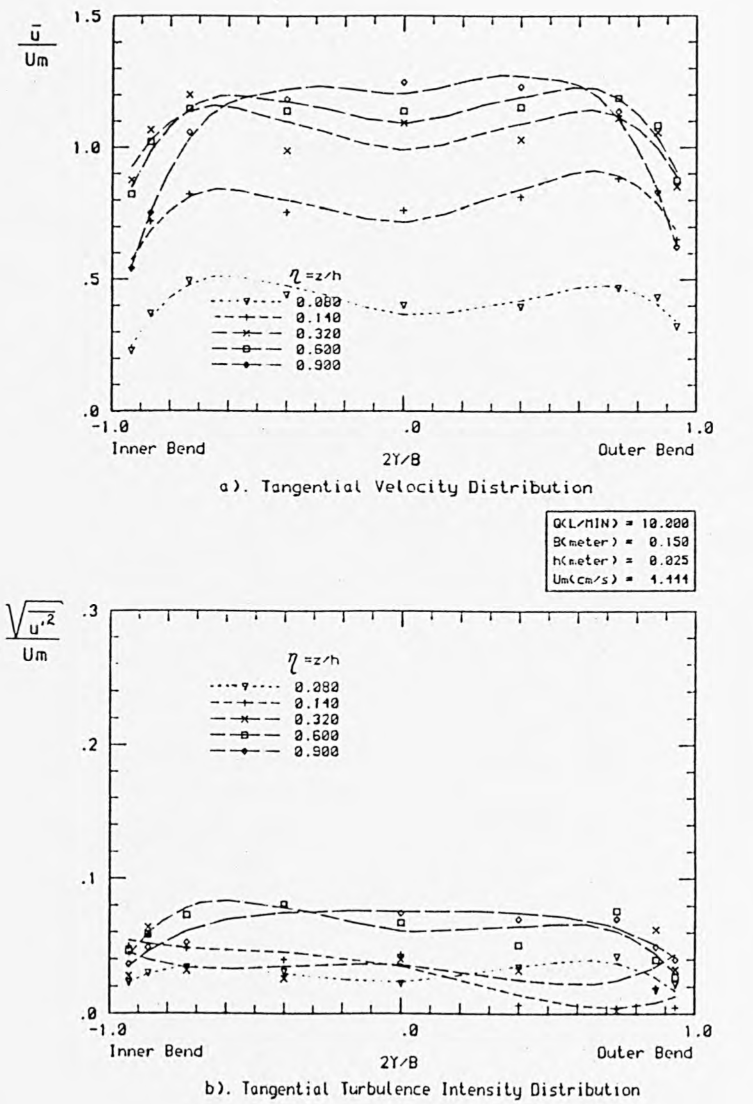

Fig. 6. 1 Tangential velocity and tangential turbulence intensity distribution at section U-1, run no.1

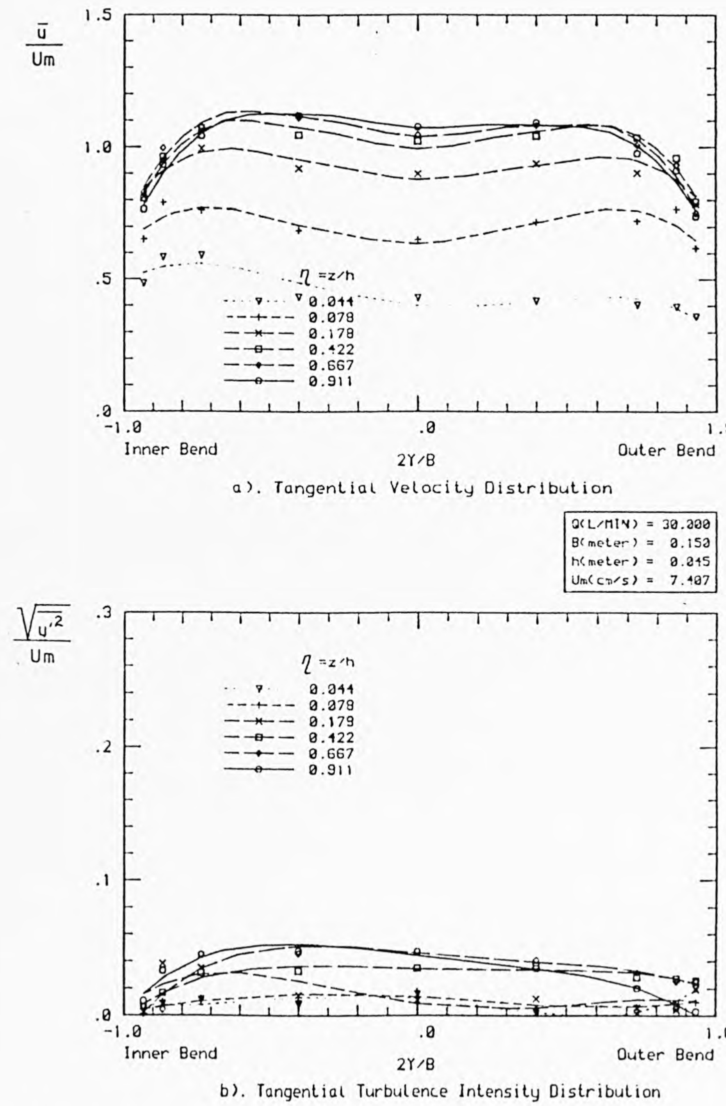

Fig. 6. 2 Tangential velocity and tangential turbulence intensity distribution at section U-1, run no.2

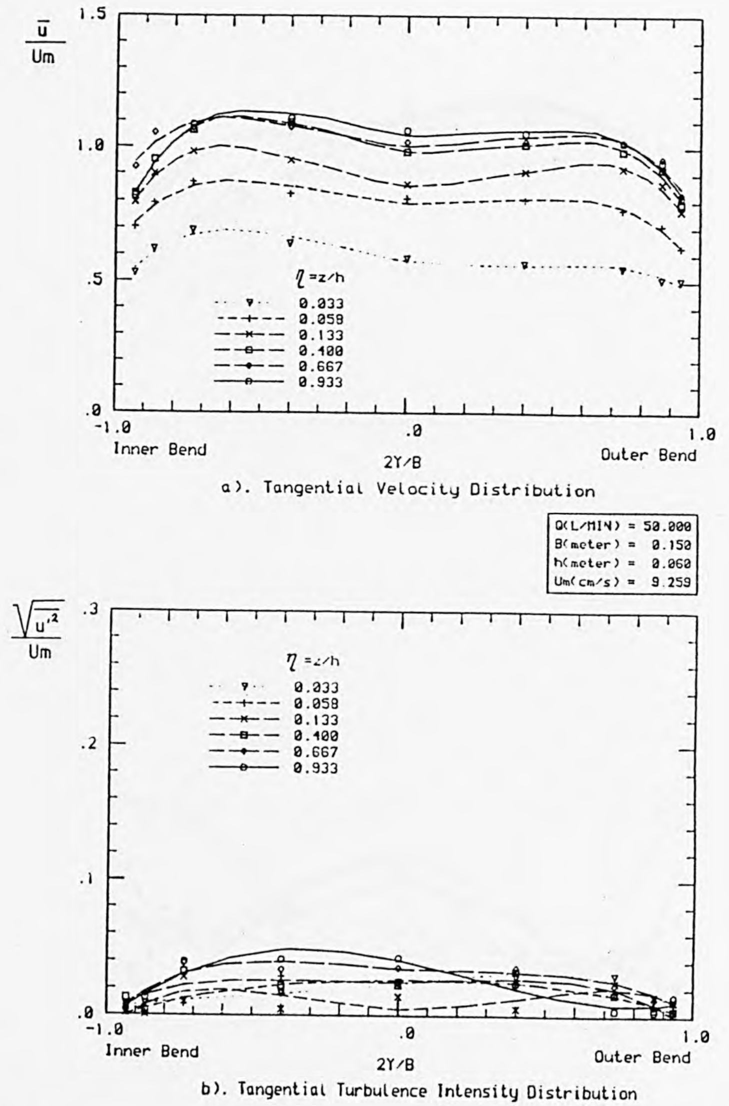

Fig. 6. 3 Tangential velocity and tangential turbulence intensity distribution at section U-1, run no.3

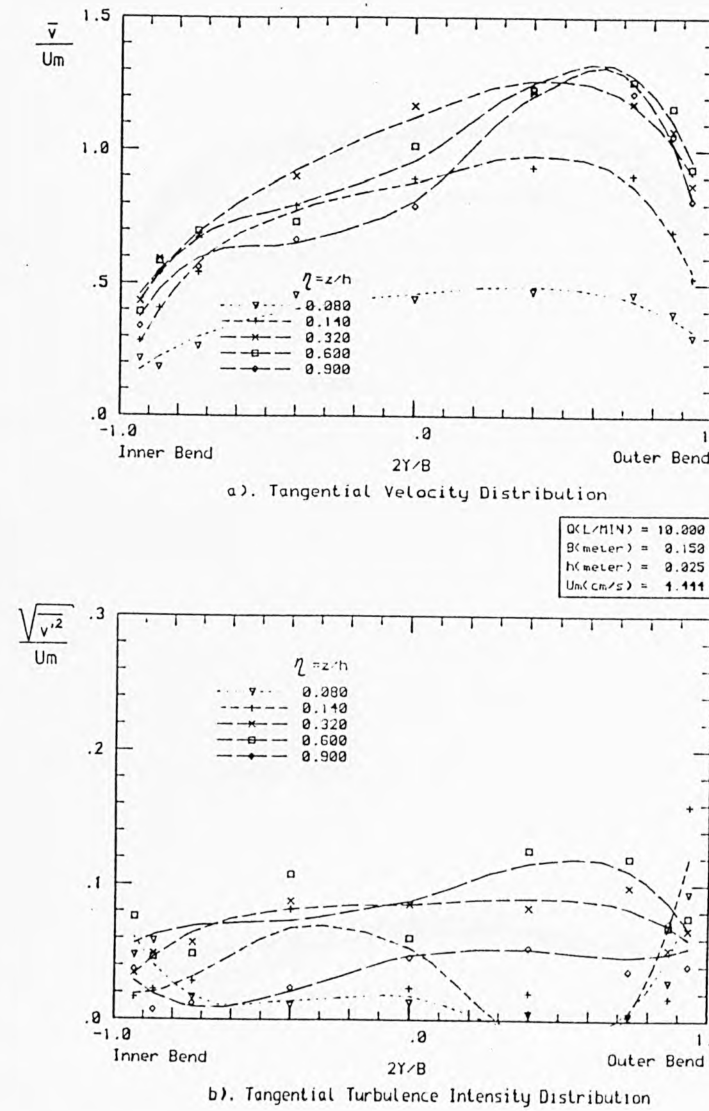

Fig. 6. 4 Tangential velocity and tangential turbulence intensity distribution at section U-2, run no.1

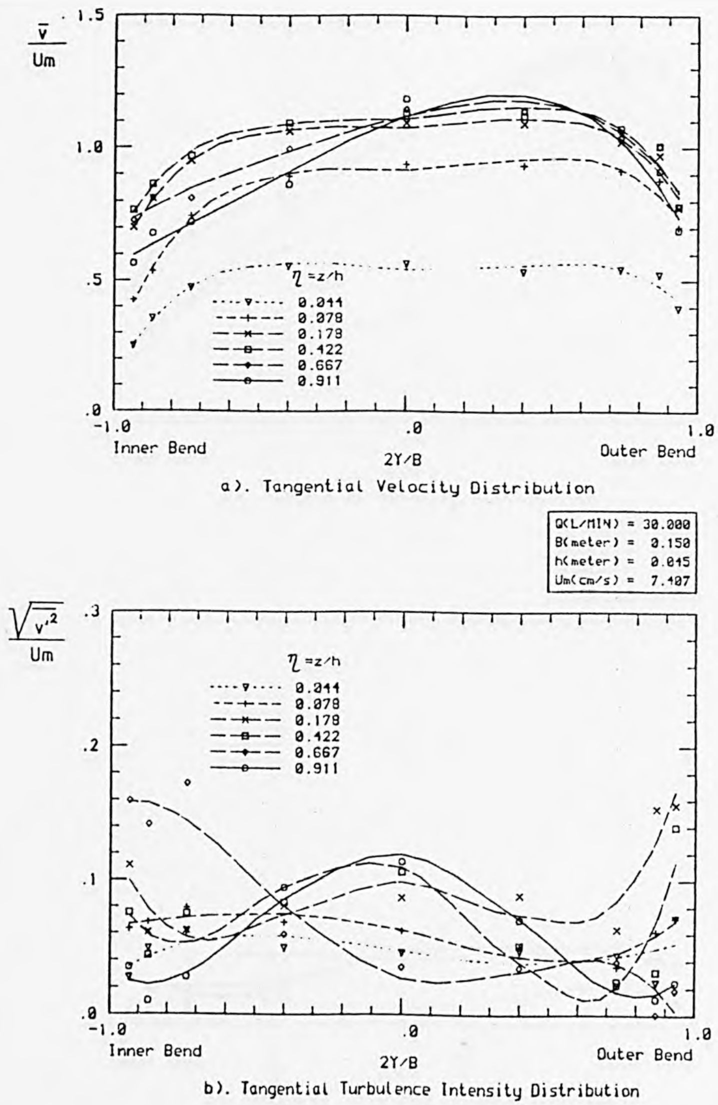

Fig. 6. 5 Tangential velocity and tangential turbulence intensity distribution at section U-2, run no.2

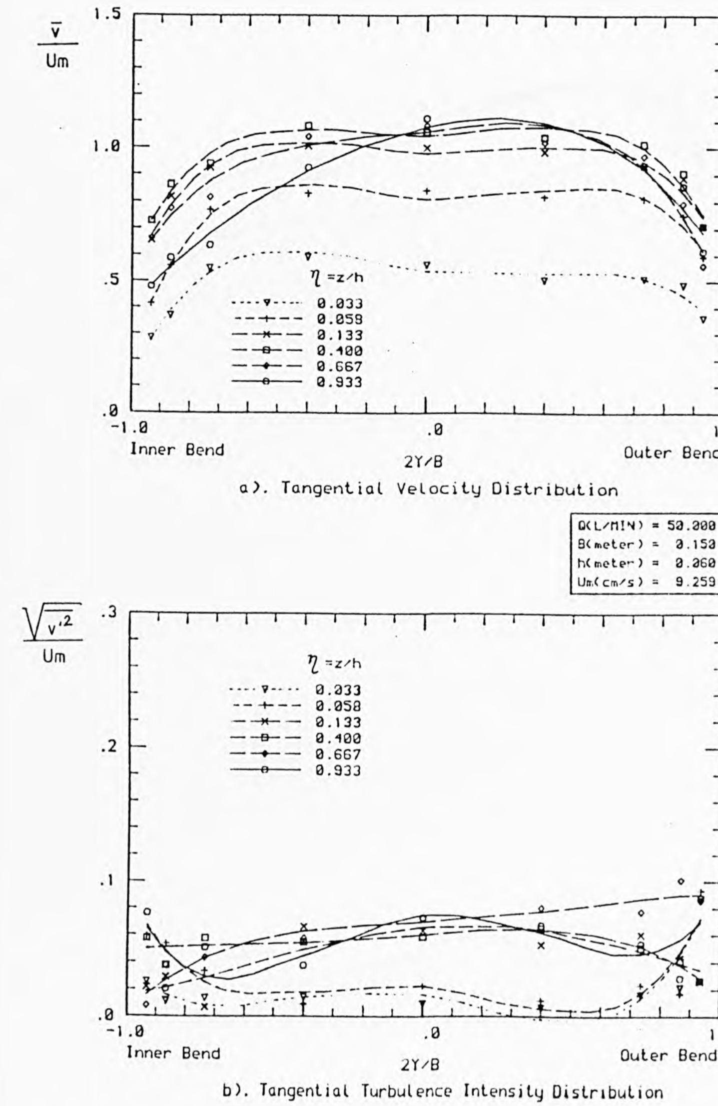

Fig. 6. 6 Tangential velocity and tangential turbulence intensity distribution at section U-2, run no.3

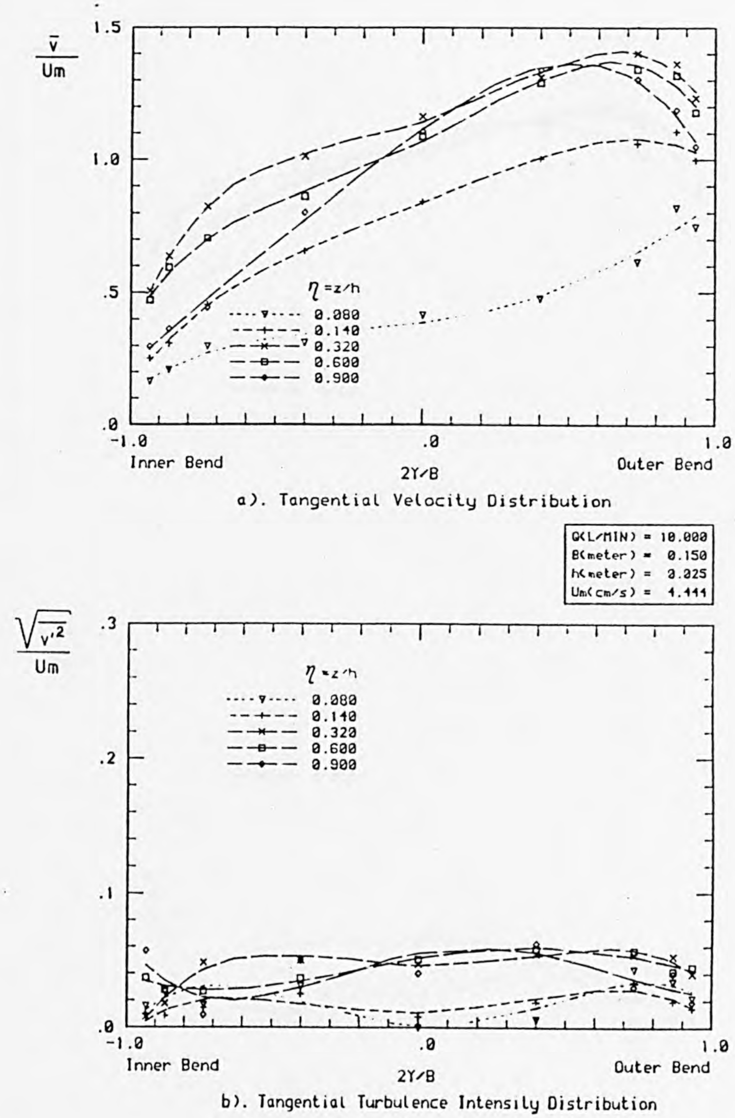

Fig. 6. 7 Tangential velocity and tangential turbulence intensity distribution at section U-3, run no.1

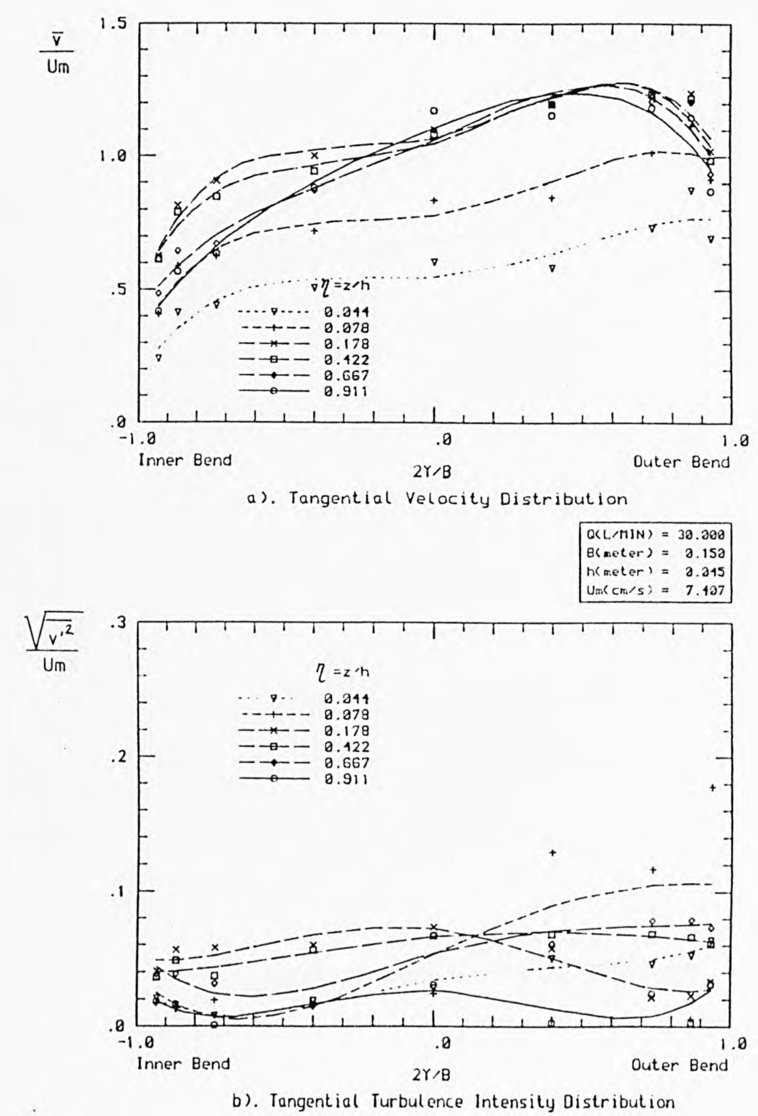

Fig. 6. 8 Tangential velocity and tangential turbulence intensity distribution at section U-3, run no.2

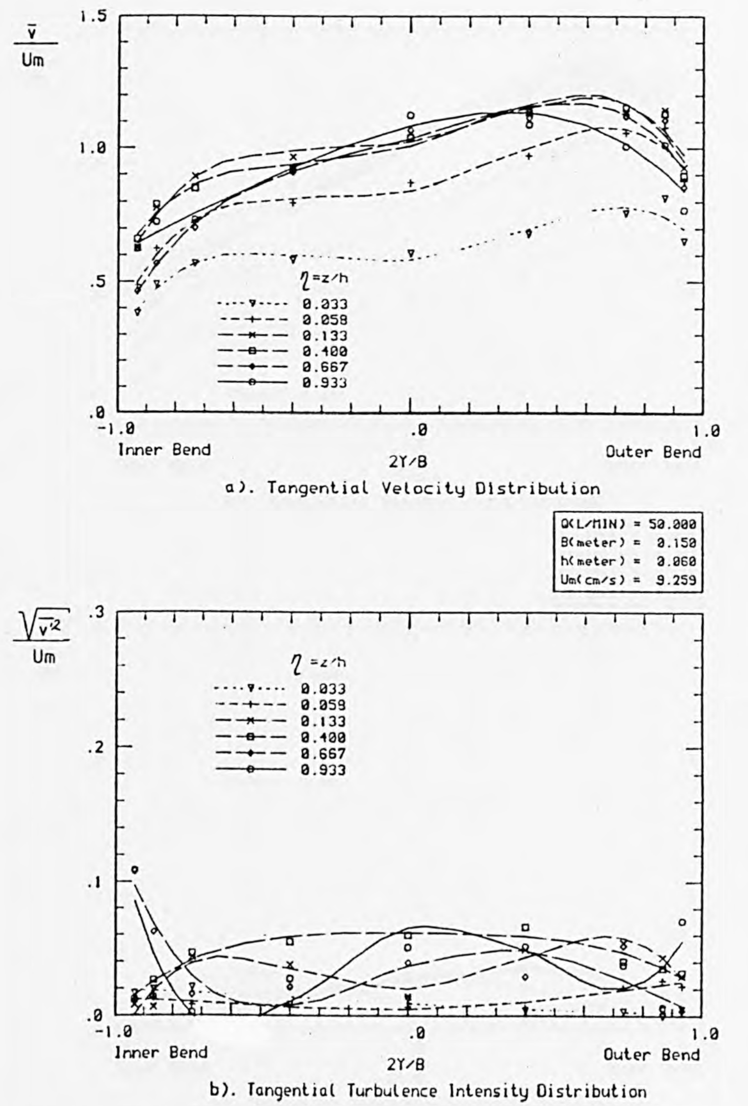

Fig. 6. 9 Tangential velocity and tangential turbulence intensity distribution at section U-3, run no.3

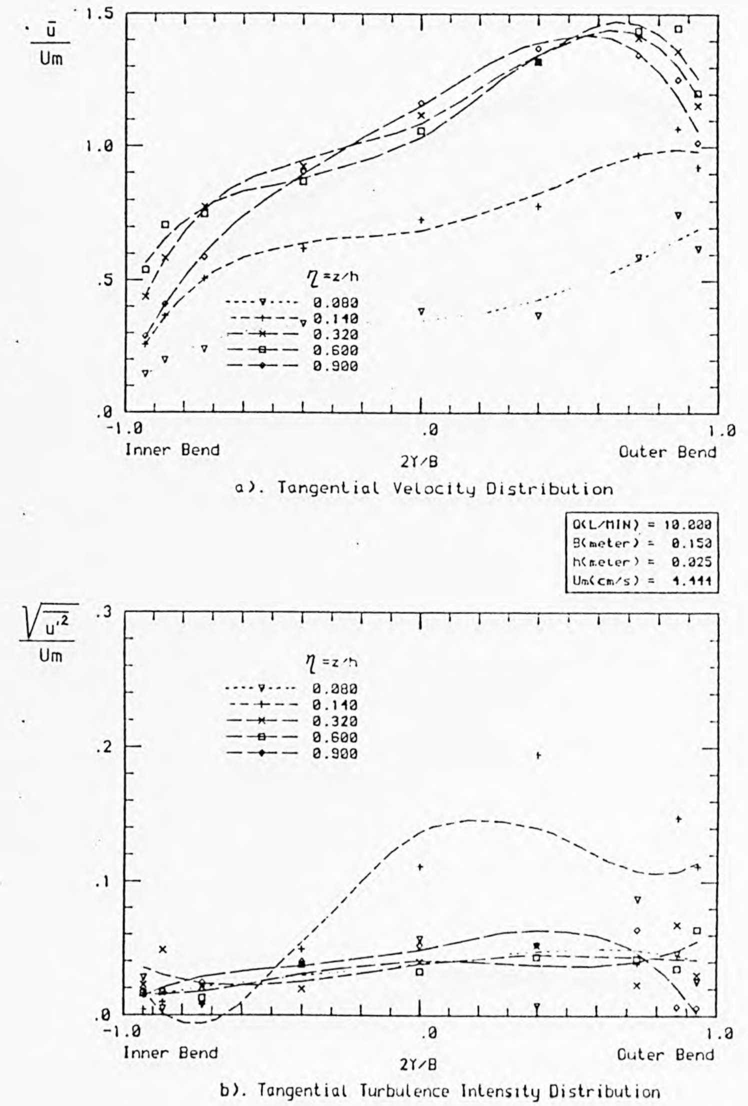

Fig. 6.10 Tangential velocity and tangential turbulence intensity distribution at section U-4, run no.1

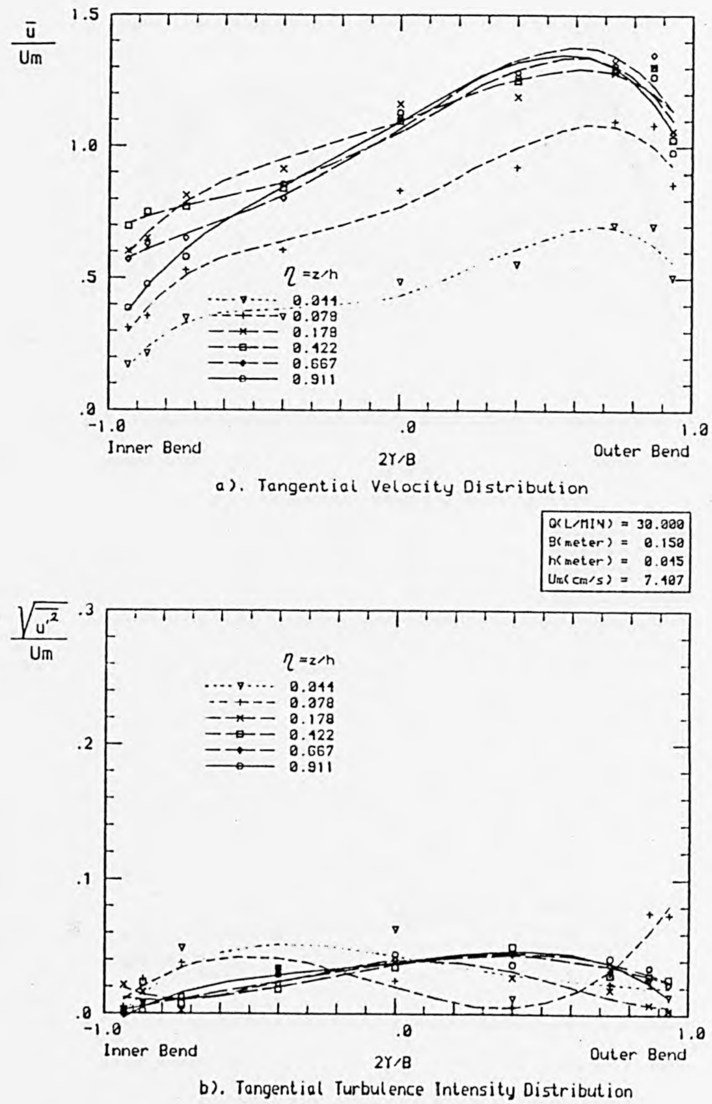

Fig. 6.11 Tangential velocity and tangential turbulence intensity distribution at section U-4, run no.2

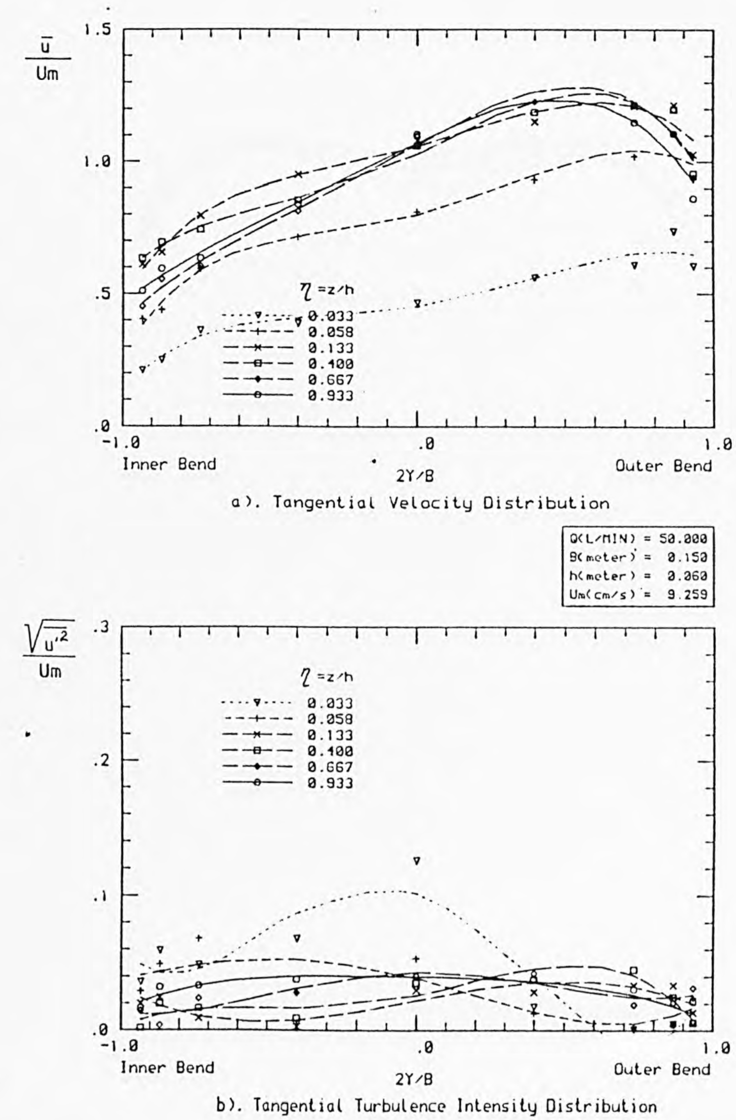

Fig. 6.12 Tangential velocity and tangential turbulence intensity distribution at section U-4, run no.3

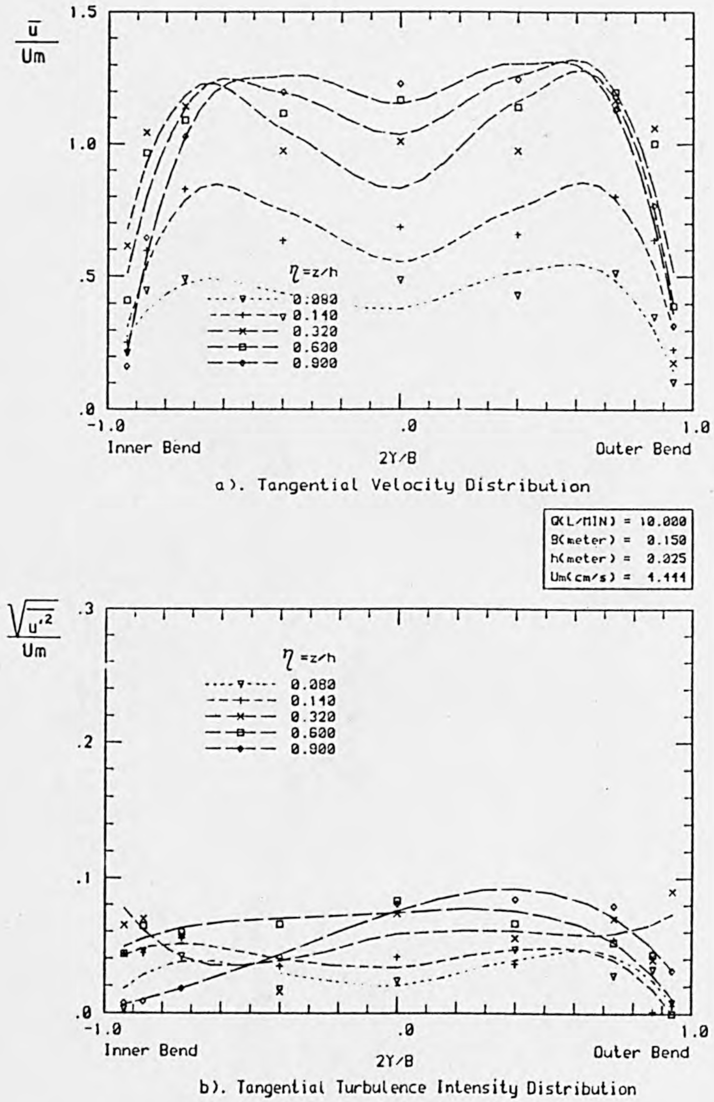

Fig. 6.13 Tangential velocity and tangential turbulence intensity distribution at section S-1, run no.1

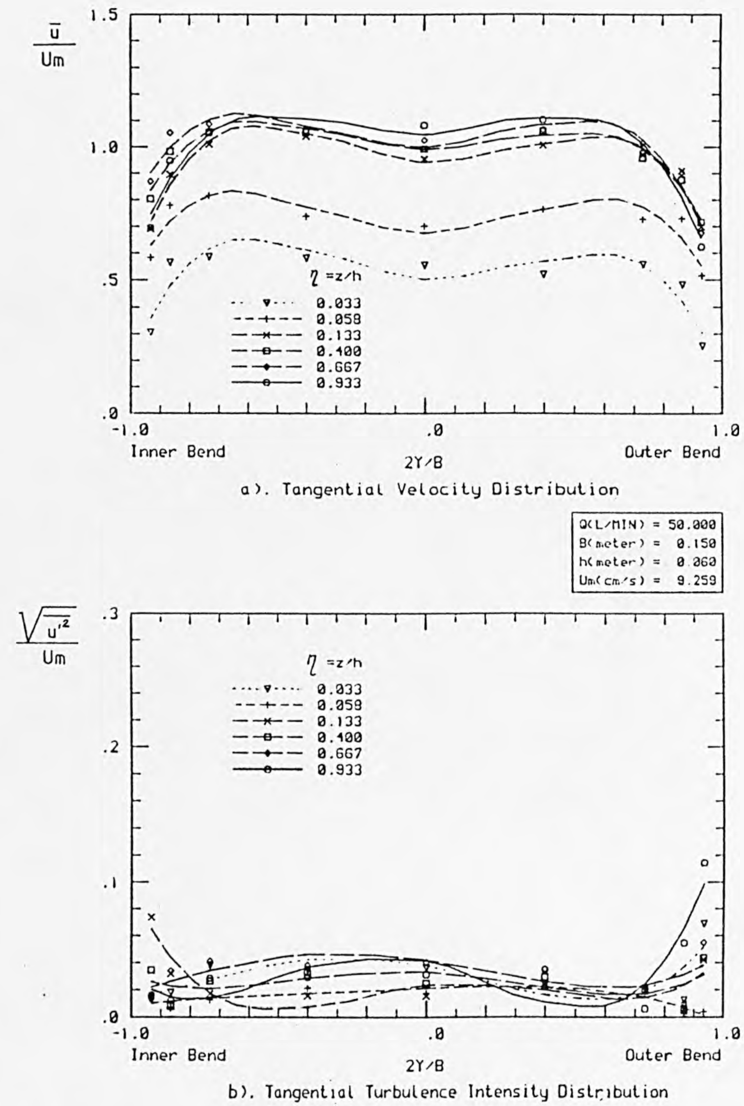

Fig. 6.14 Tangential velocity and tangential turbulence intensity distribution at section S-1, run no.2

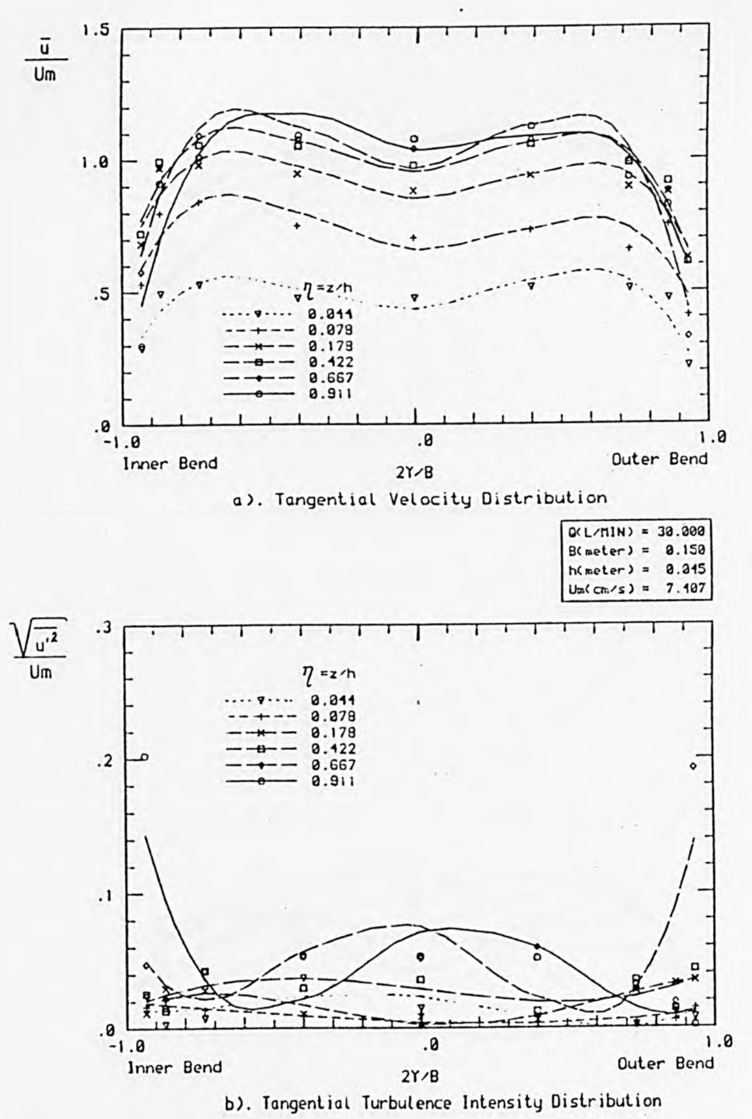

Fig. 6.15 Tangential velocity and tangential turbulence intensity distribution at section S-1, run no.3

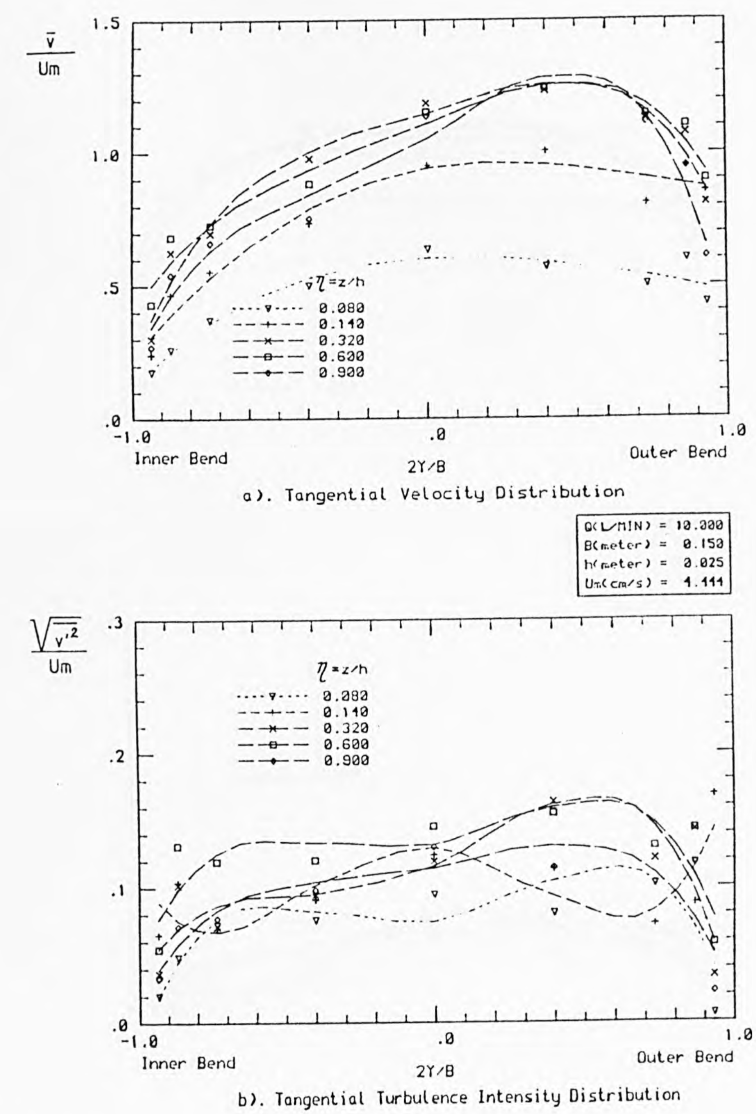

Fig. 6.16 Tangential velocity and tangential turbulence intensity distribution at section S-2, run no.1

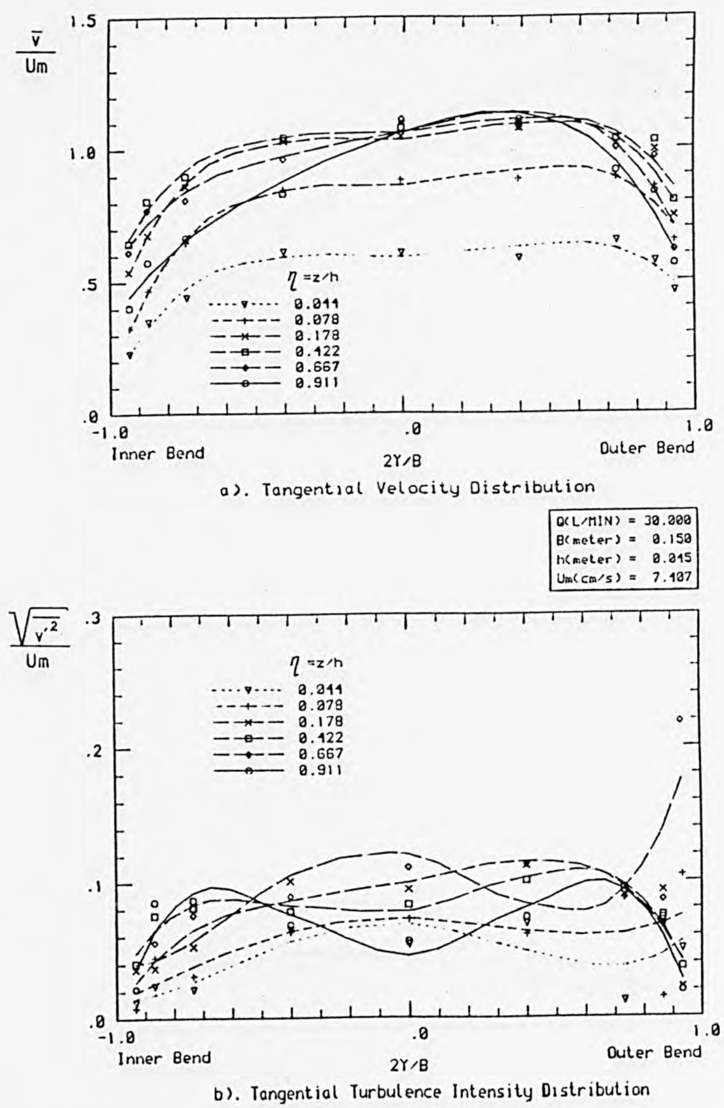

Fig. 6.17 Tangential velocity and tangential turbulence intensity distribution at section S-2, run no.2

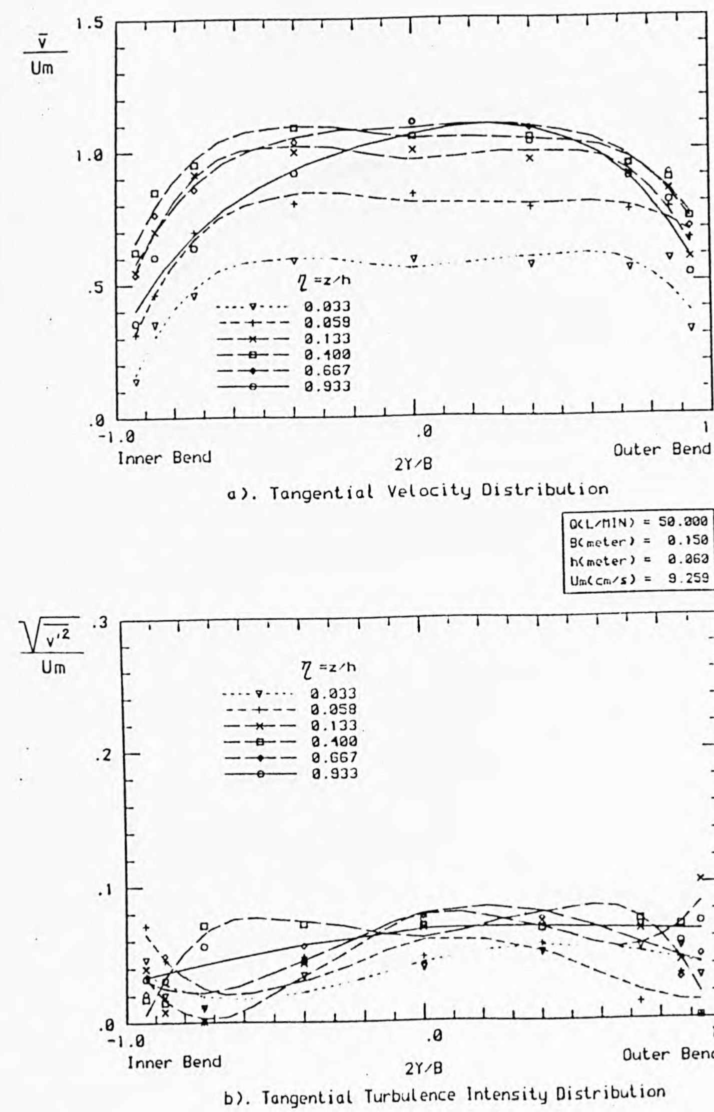

Fig. 6.18 Tangential velocity and tangential turbulence intensity distribution at section S-2, run no.3

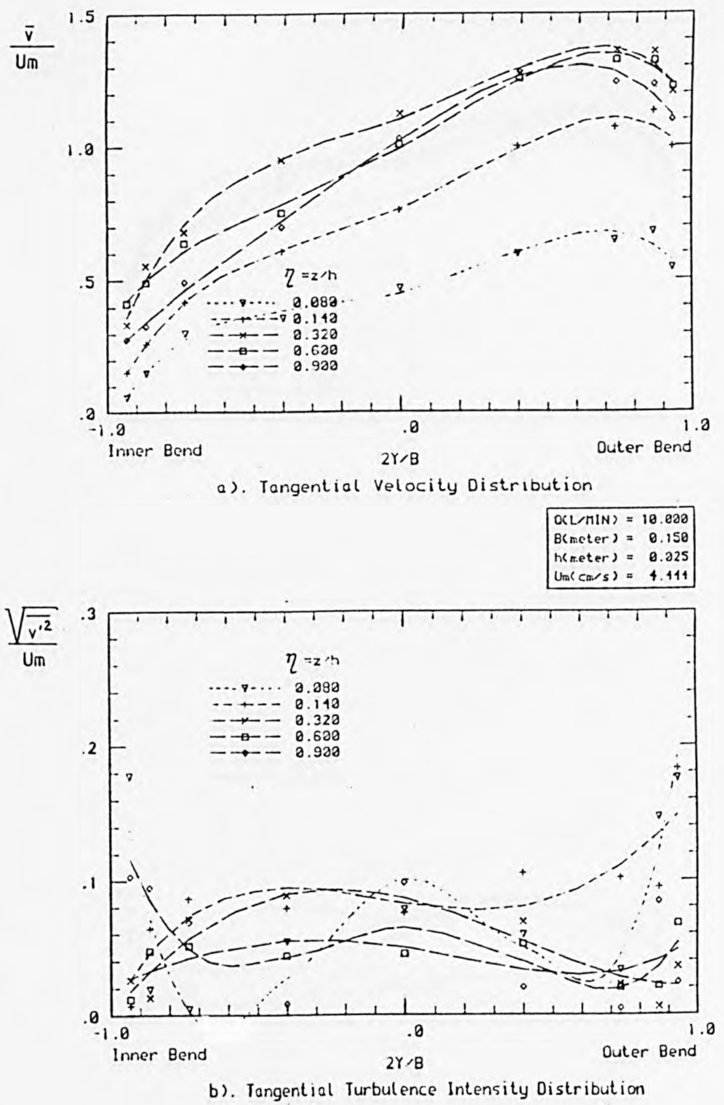

Fig. 6.19 Tangential velocity and tangential turbulence intensity distribution at section S-3, run no.1

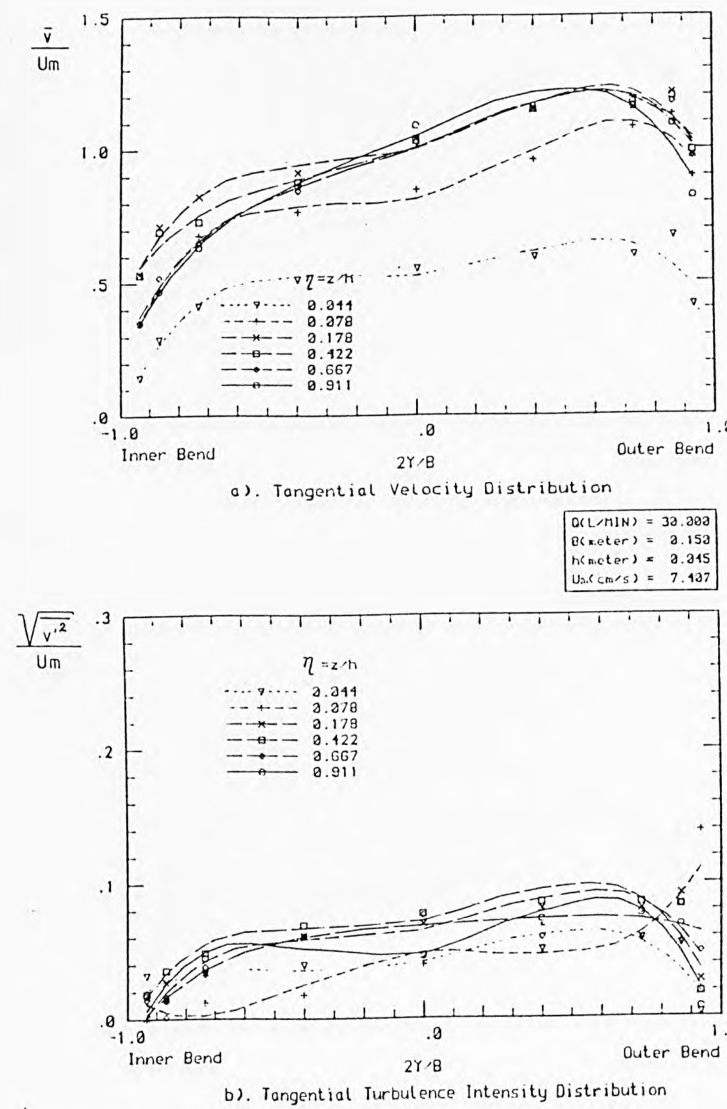

Fig. 6.20 Tangential velocity and tangential turbulence intensity distribution at section S-3, run no.2

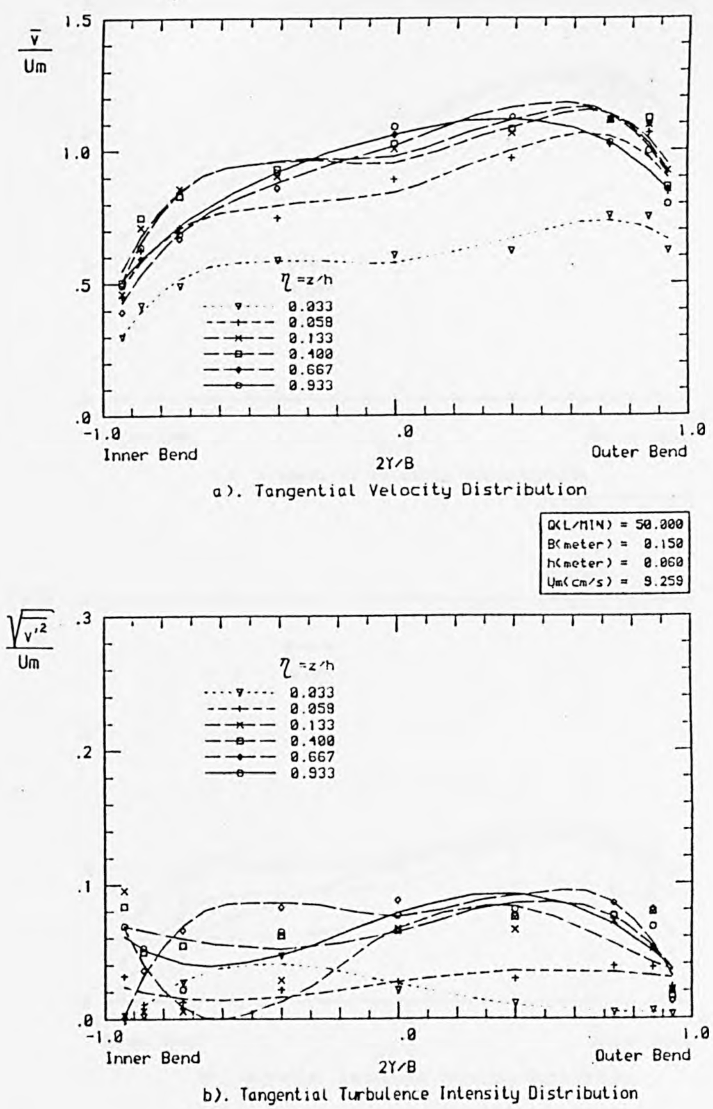

Fig. 6.21 Tangential velocity and tangential turbulence intensity distribution at section S-3, run no.3

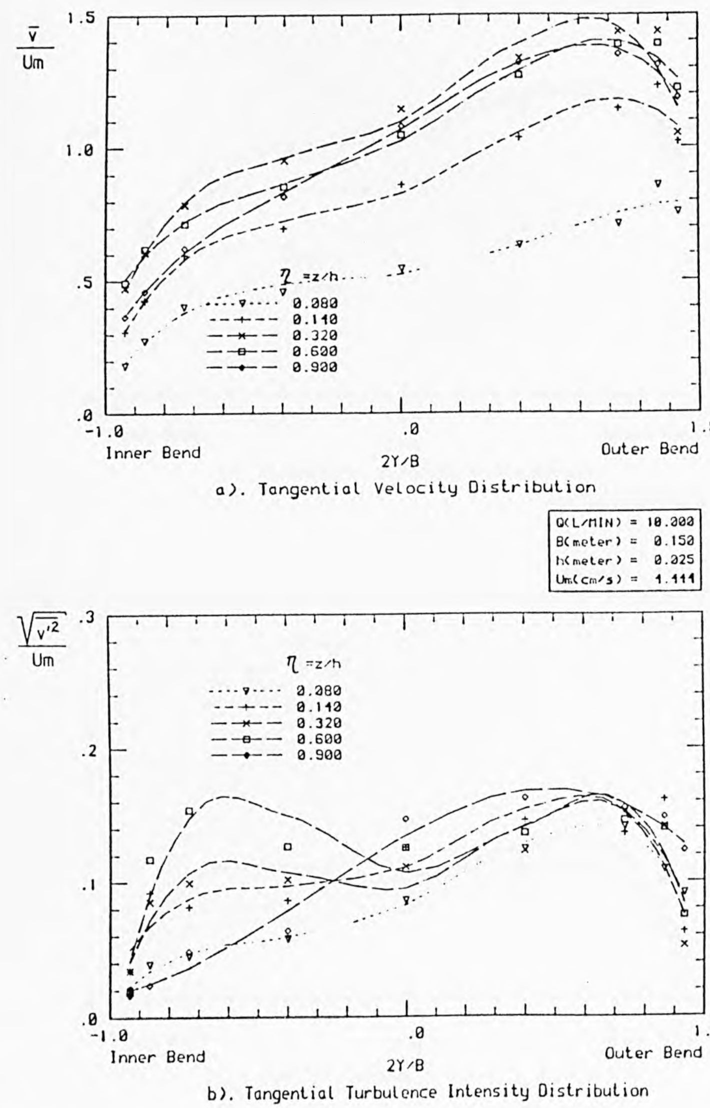

Fig. 6.22 Tangential velocity and tangential turbulence intensity distribution at section S-4, run no.1

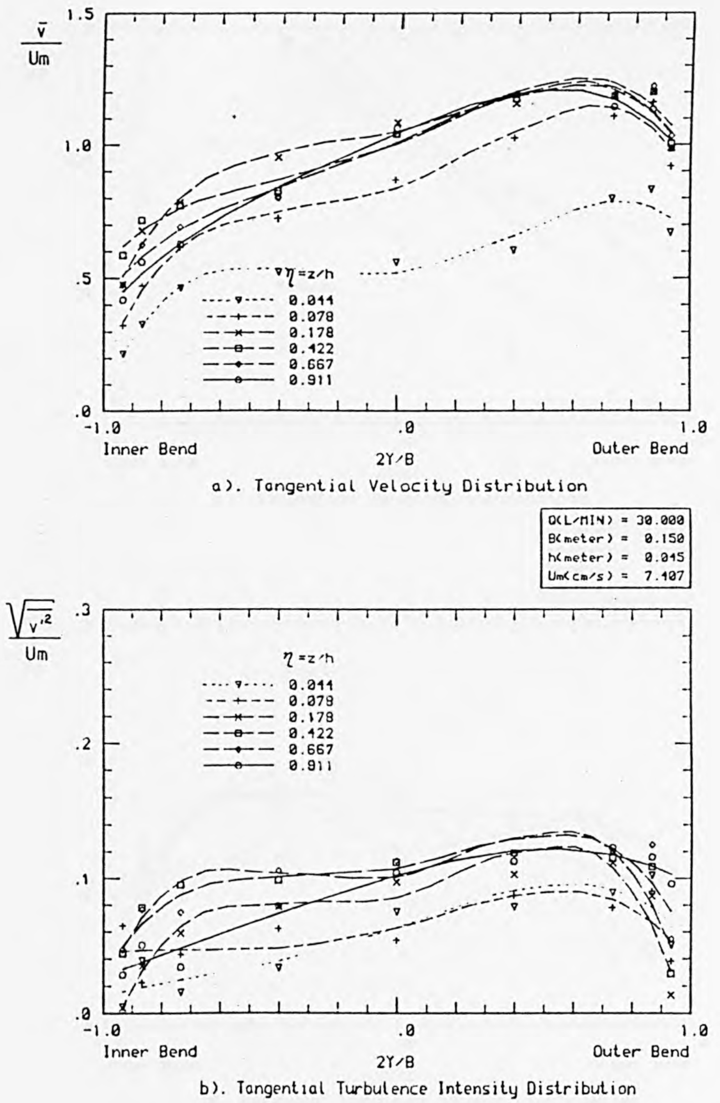

Fig. 6.23 Tangential velocity and tangential turbulence intensity distribution at section S-4, run no.2

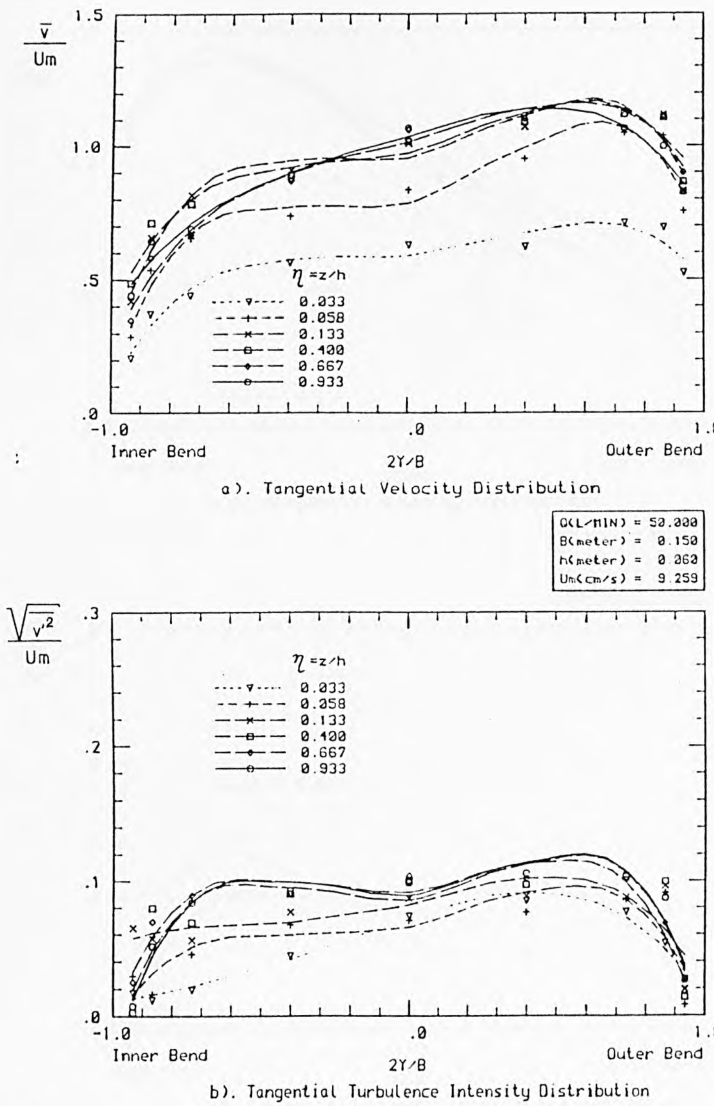

Fig. 6.24 Tangential velocity and tangential turbulence intensity distribution at section S-4, run no.3

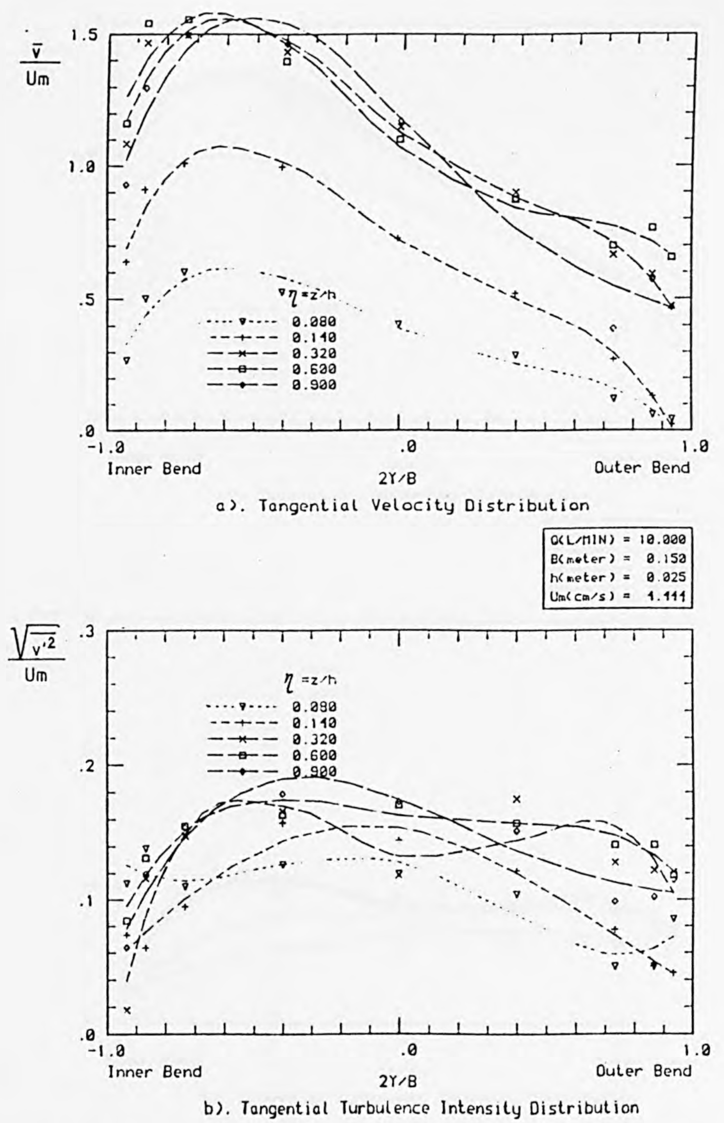

Fig. 6.25 Tangential velocity and tangential turbulence intensity distribution at section S-5, run no.1

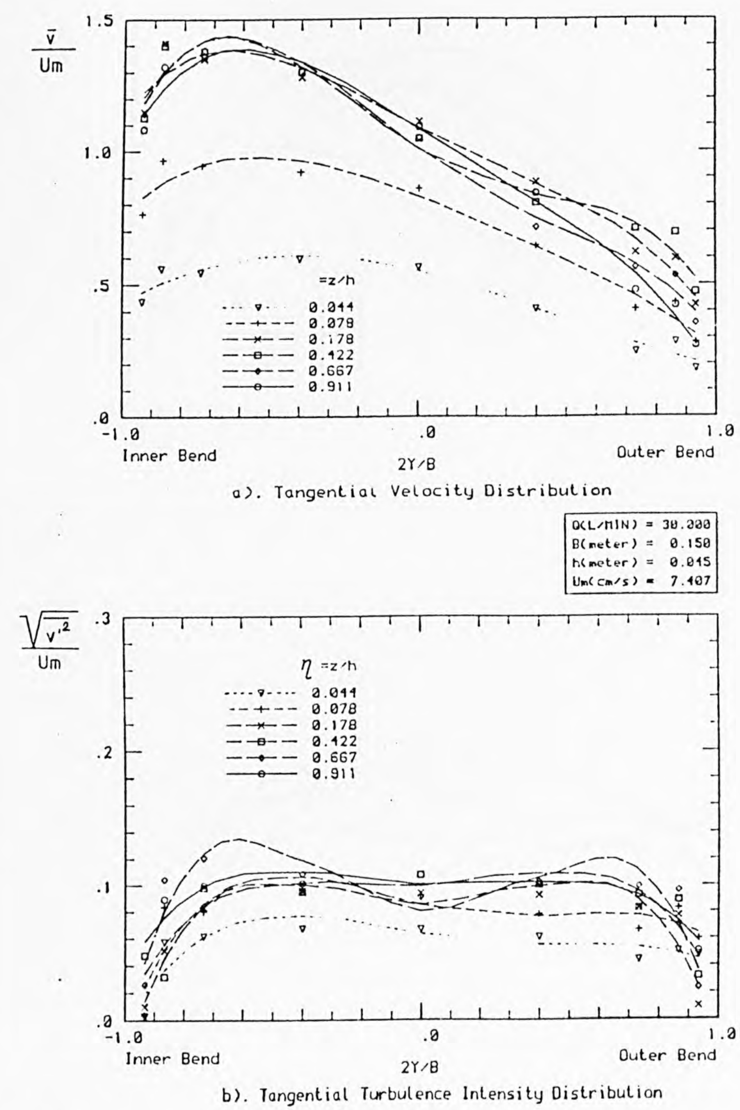

Fig. 6.26 Tangential velocity and tangential turbulence intensity distribution at section S-5, run no.2

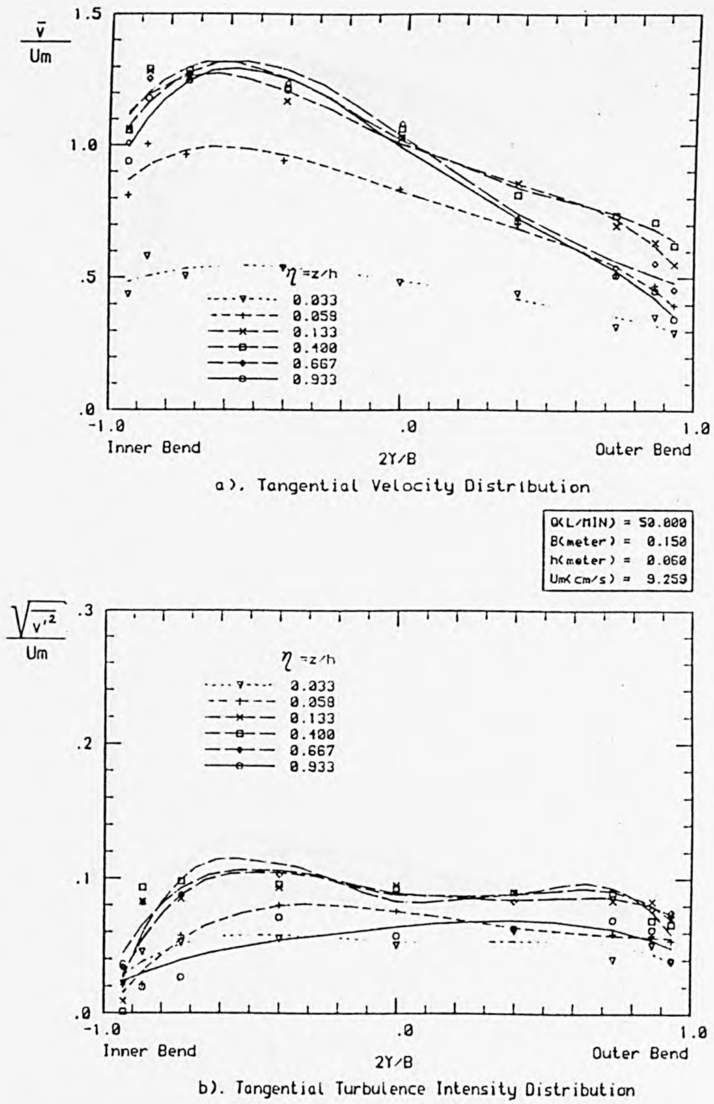

Fig. 6.27 Tangential velocity and tangential turbulence intensity distribution at section S-5, run no.3

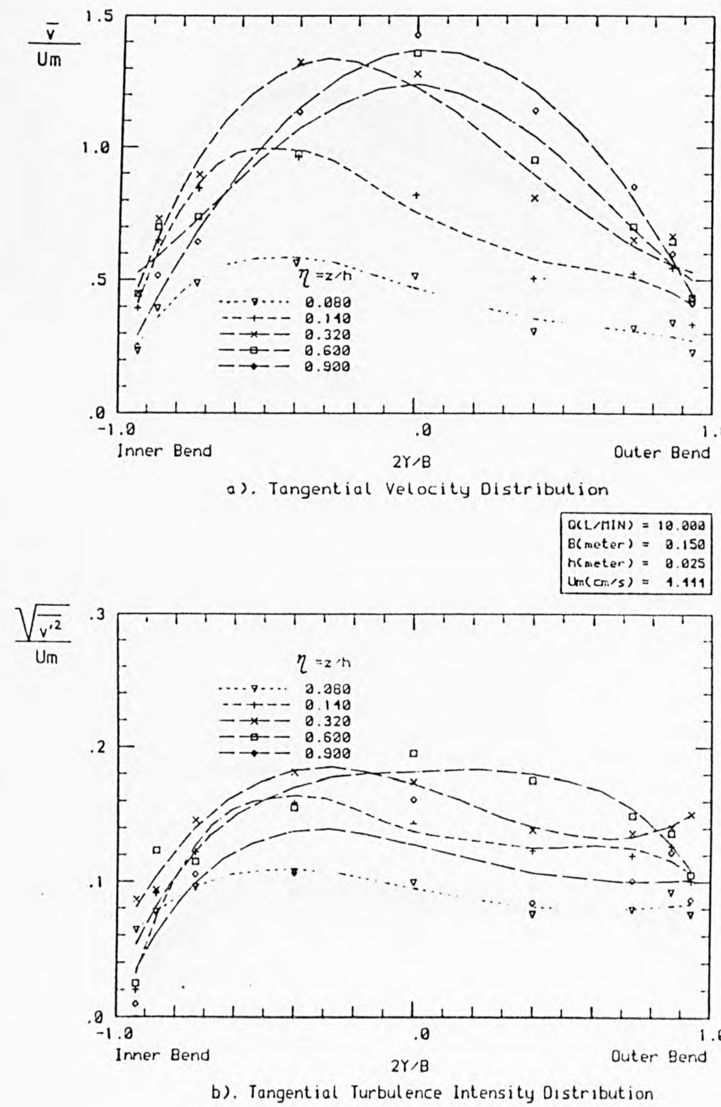

Fig. 6.28 Tangential velocity and tangential turbulence intensity distribution at section S-6, run no.1

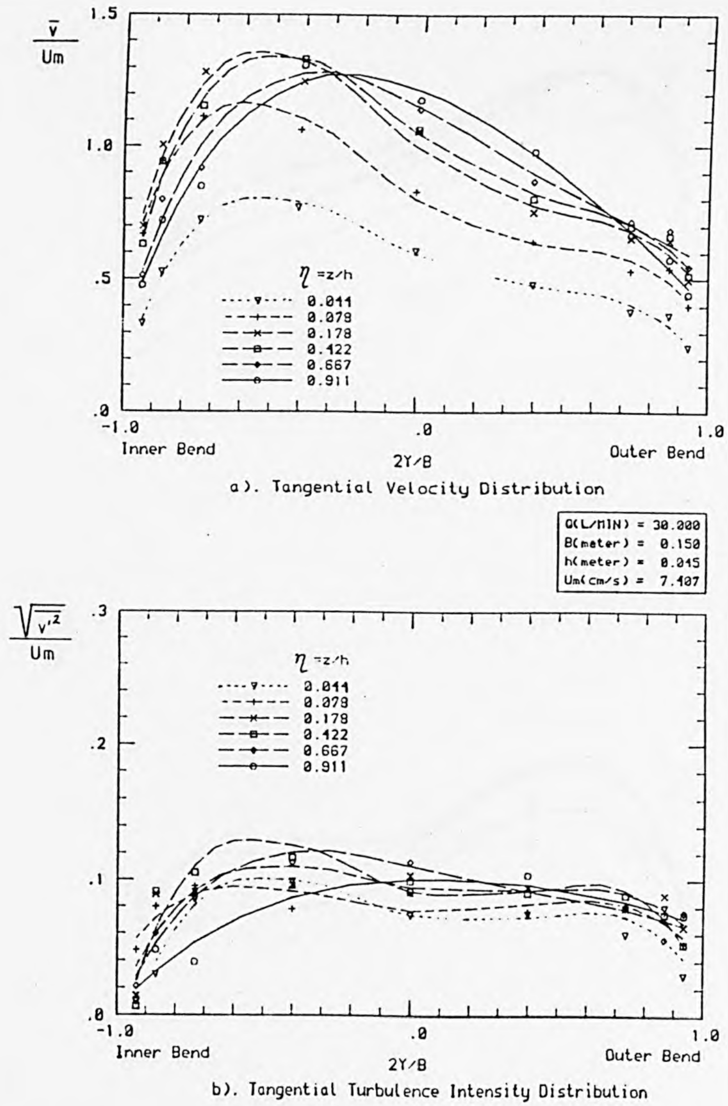

Fig. 6.29 Tangential velocity and tangential turbulence intensity distribution at section S-6, run no.2

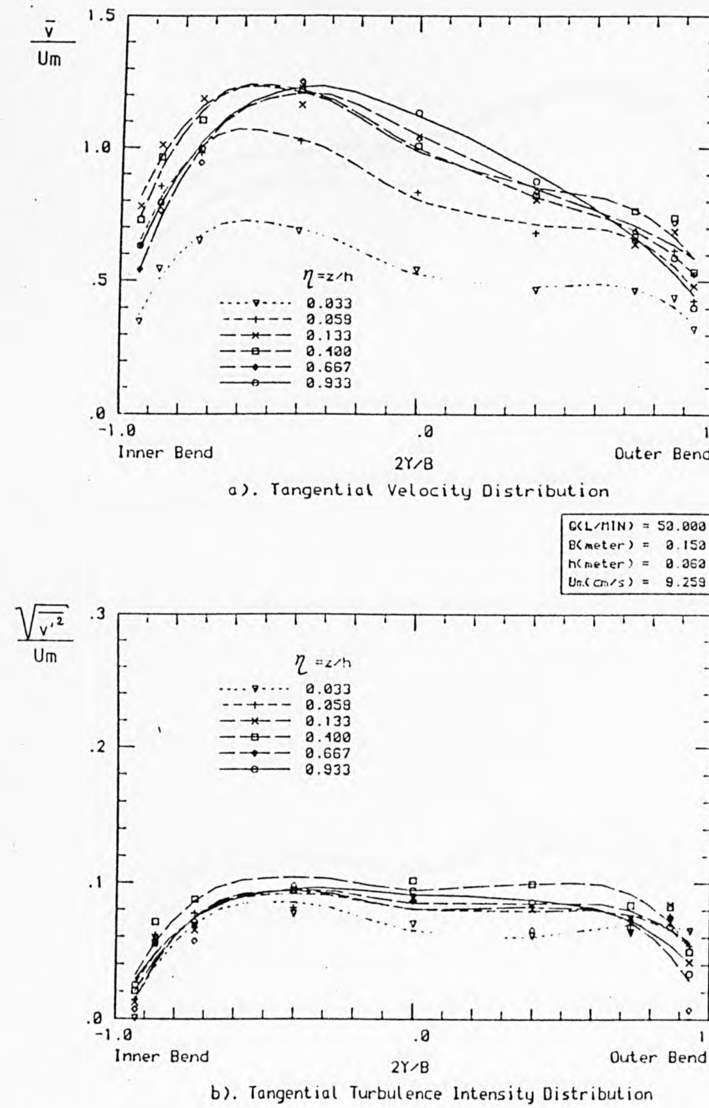

Fig. 6.30 Tangential velocity and tangential turbulence intensity distribution at section S-6, run no.3

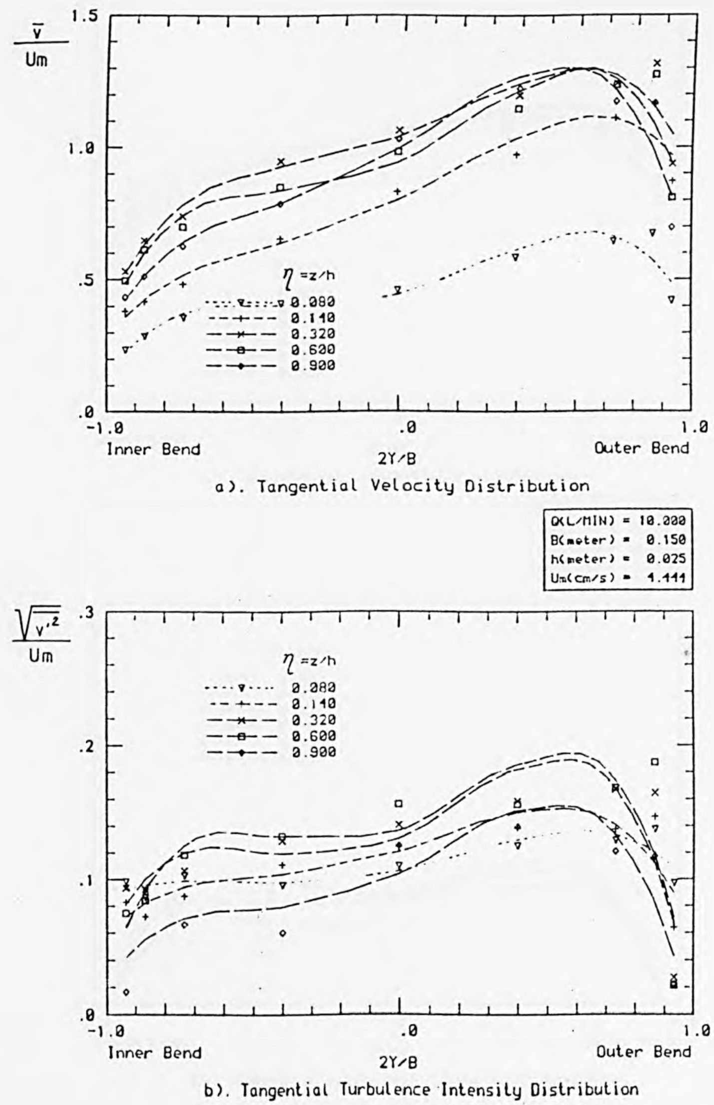

Fig. 6.31 Tangential velocity and tangential turbulence intensity distribution at section S-7, run no.1

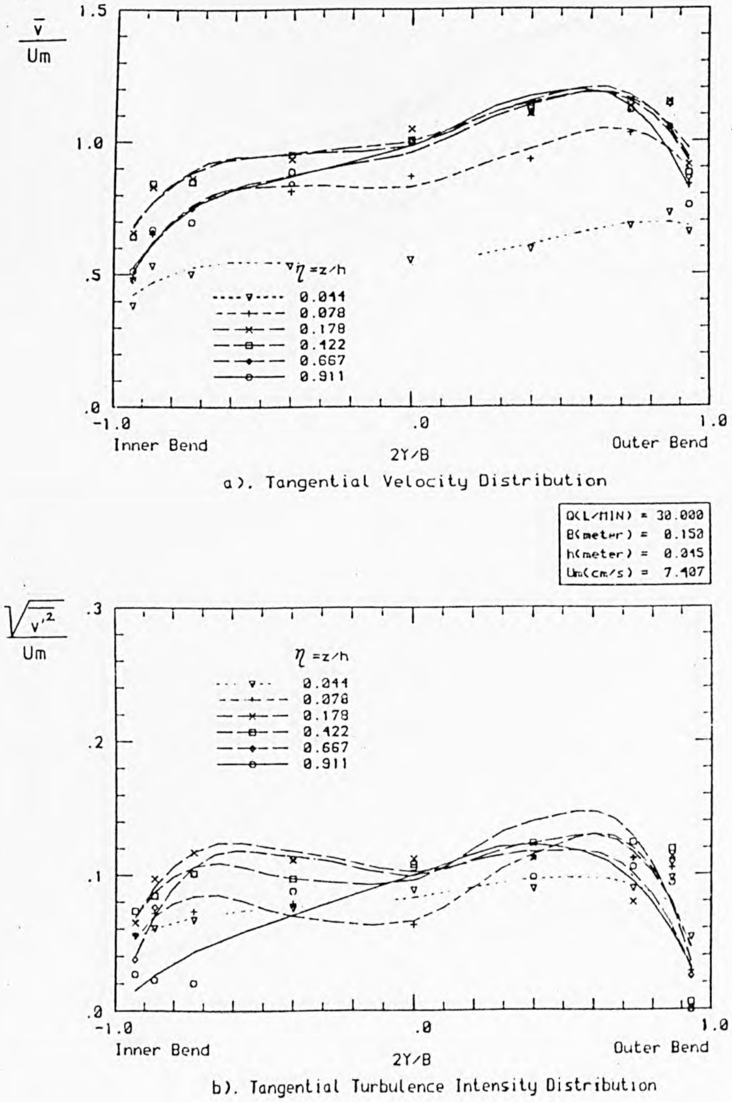

Fig. 6.32 Tangential velocity and tangential turbulence intensity distribution at section S-7, run no.2

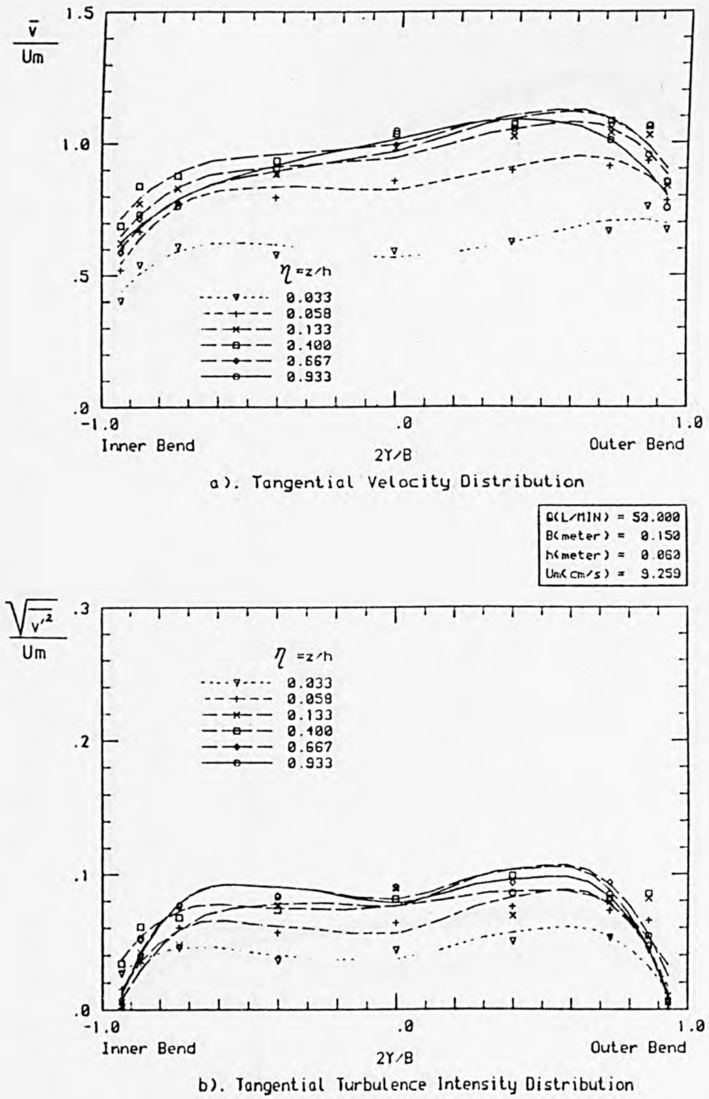

Fig. 6.33 Tangential velocity and tangential turbulence intensity distribution at section S-7, run no.3

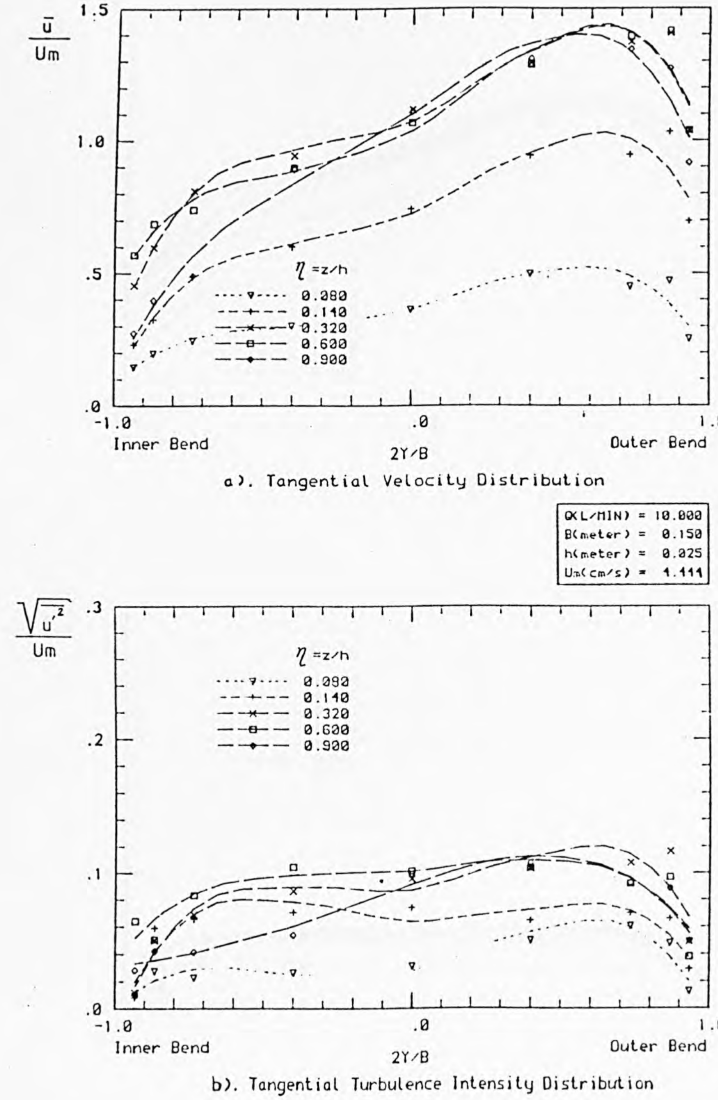

Fig. 6.34 Tangential velocity and tangential turbulence intensity distribution at section S-8, run no.1

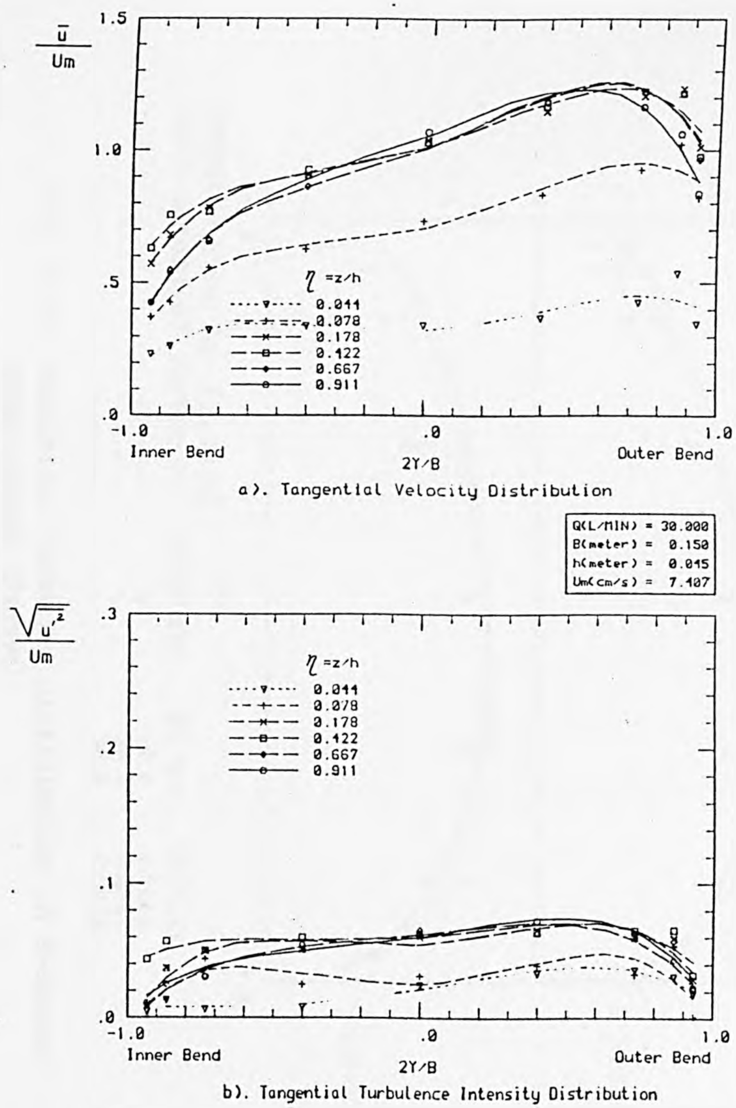

a). Tangential Velocity Distribution

b). Tangential Turbulence Intensity Distribution

Fig. 6.35 Tangential velocity and tangential turbulence intensity distribution at section S-8, run no.2

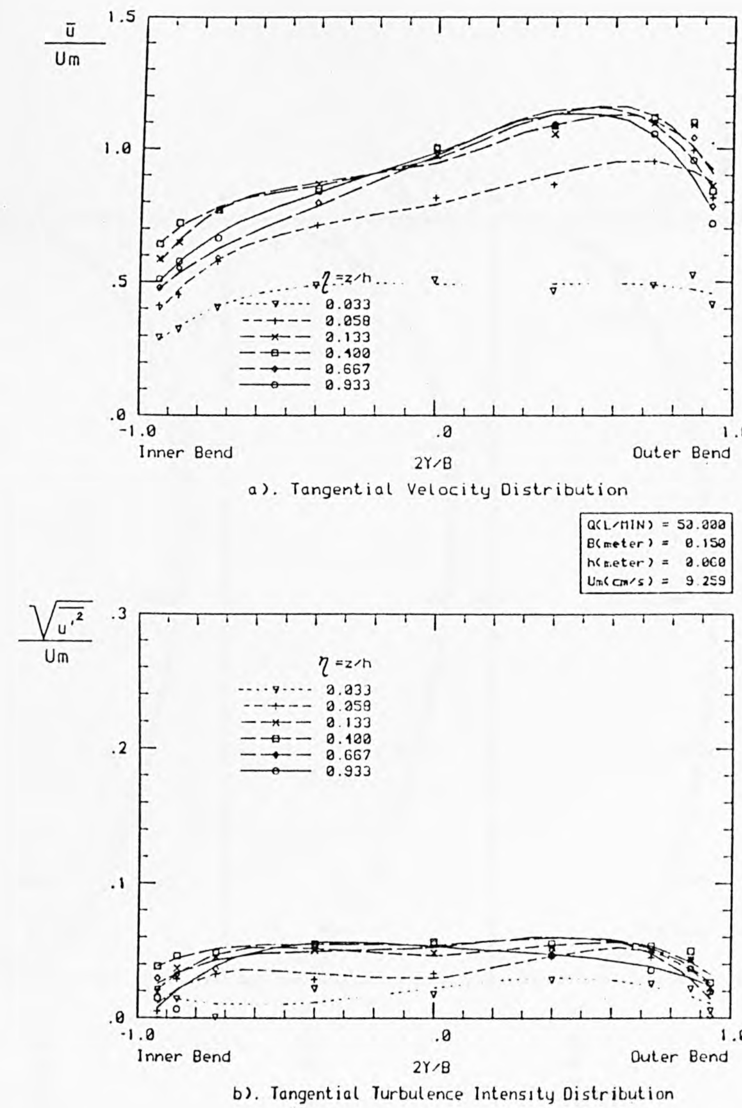

a). Tangential Velocity Distribution

b). Tangential Turbulence Intensity Distribution

Fig. 6.36 Tangential velocity and tangential turbulence intensity distribution at section S-8, run no.3

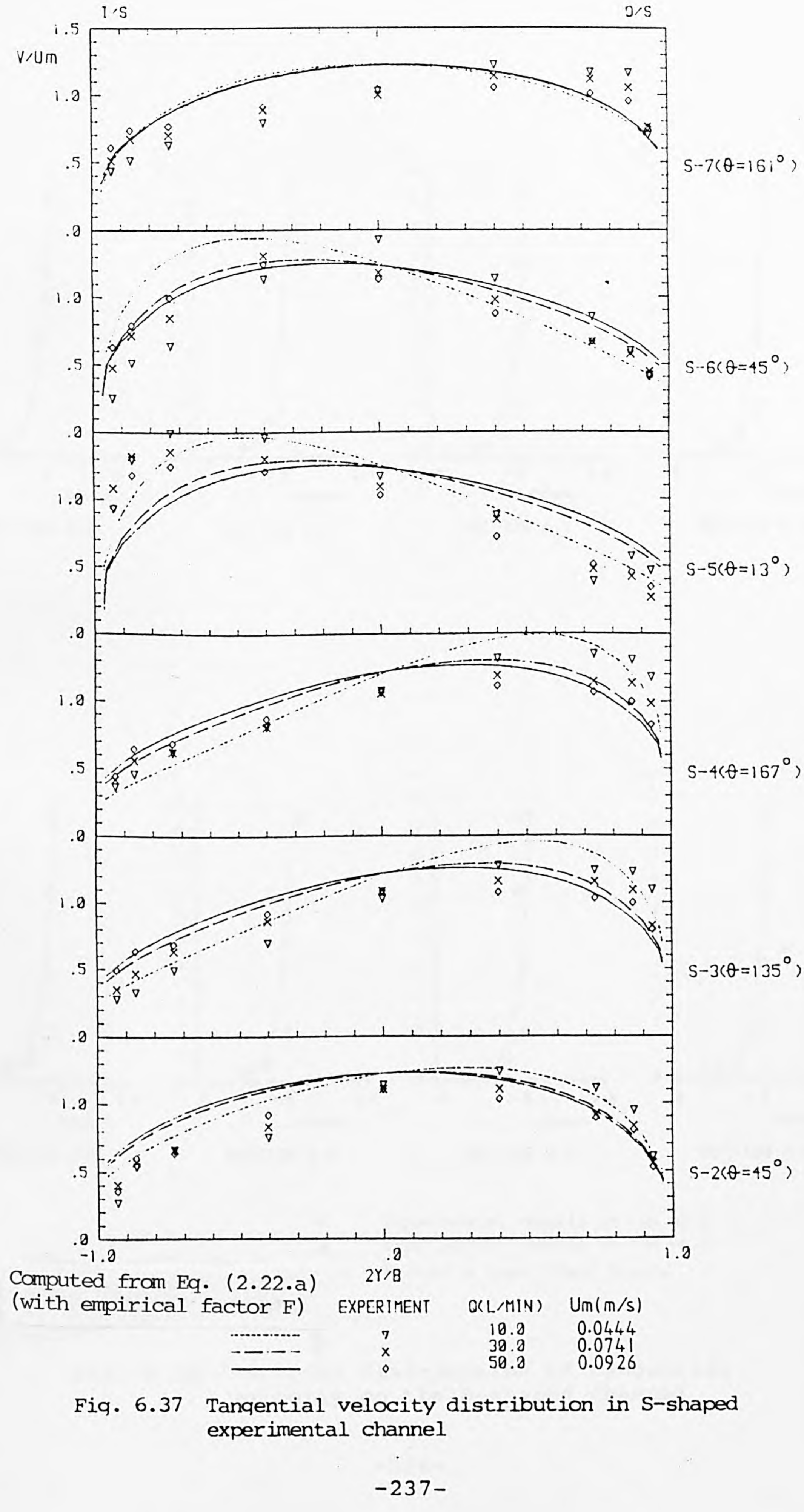

Fig. 6.37 Tangential velocity distribution in S-shaped experimental channel

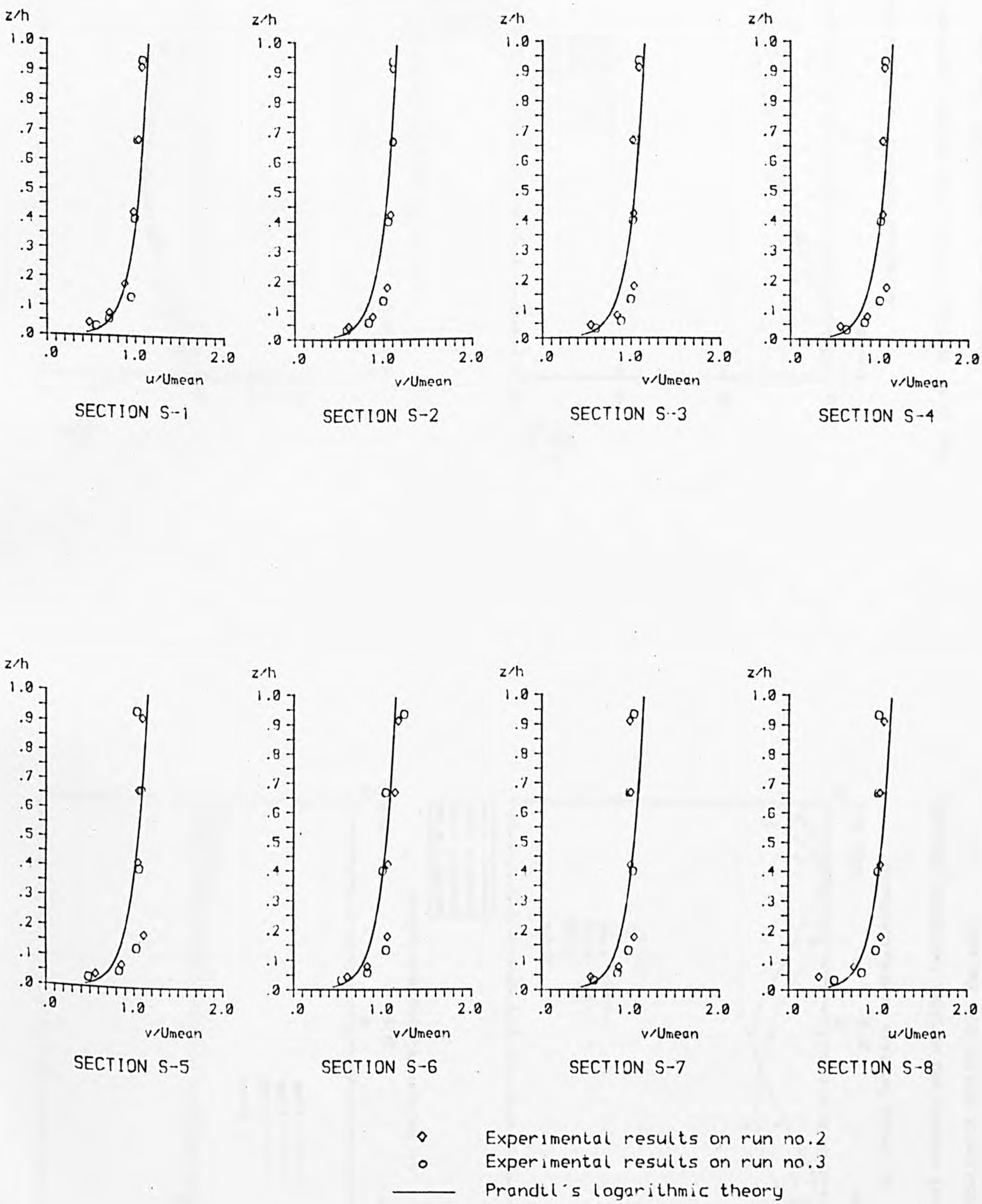

Fig. 6.38 Vertical distribution of tangential velocity on the S-shaped channel

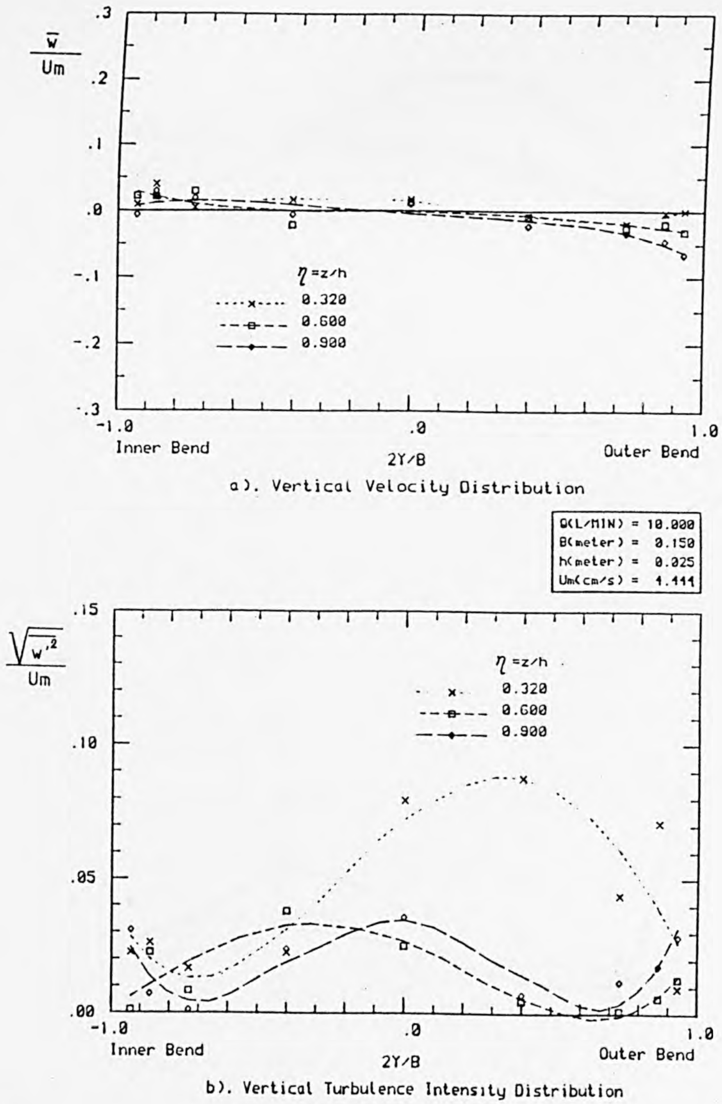

Fig. 6.39 Vertical velocity and vertical turbulence intensity distribution at section U-2, run no.1

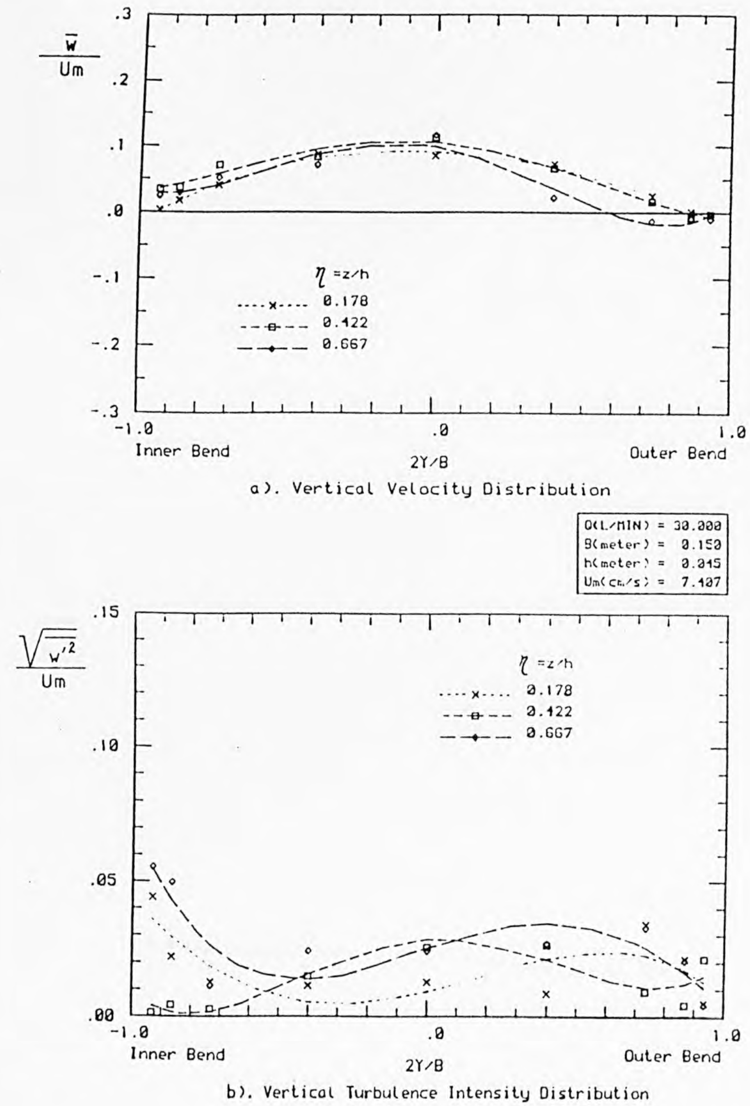

Fig. 6.40 Vertical velocity and vertical turbulence intensity distribution at section U-2, run no.2

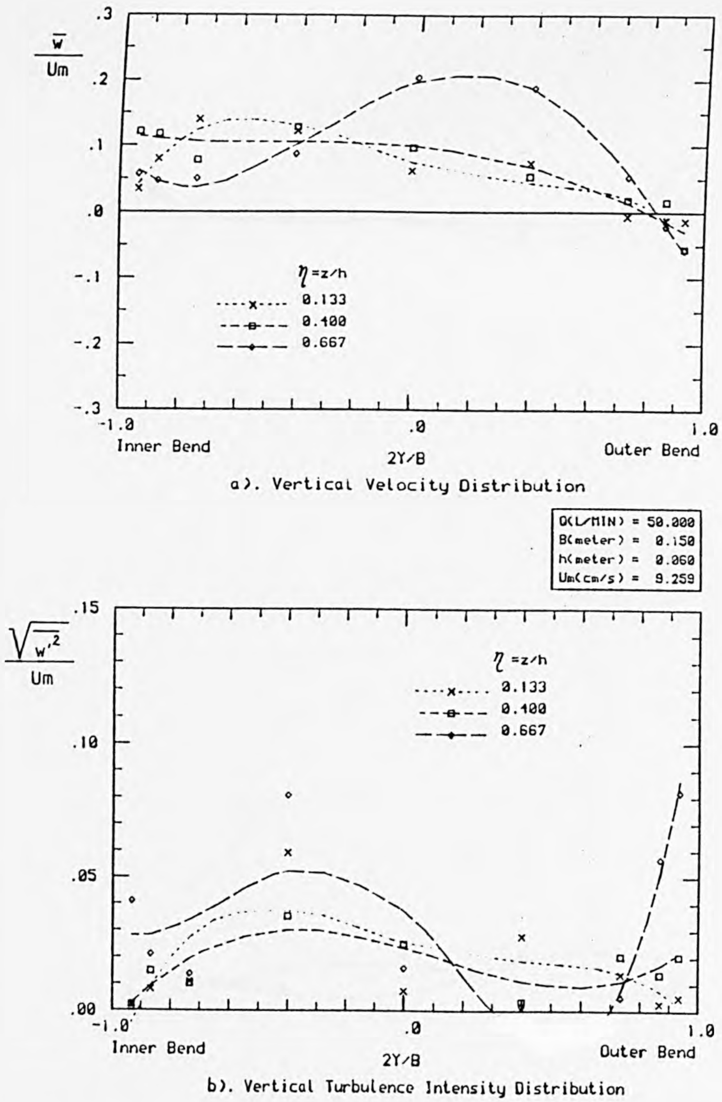

Fig. 6.41 Vertical velocity and vertical turbulence intensity distribution at section U-2, run no.3

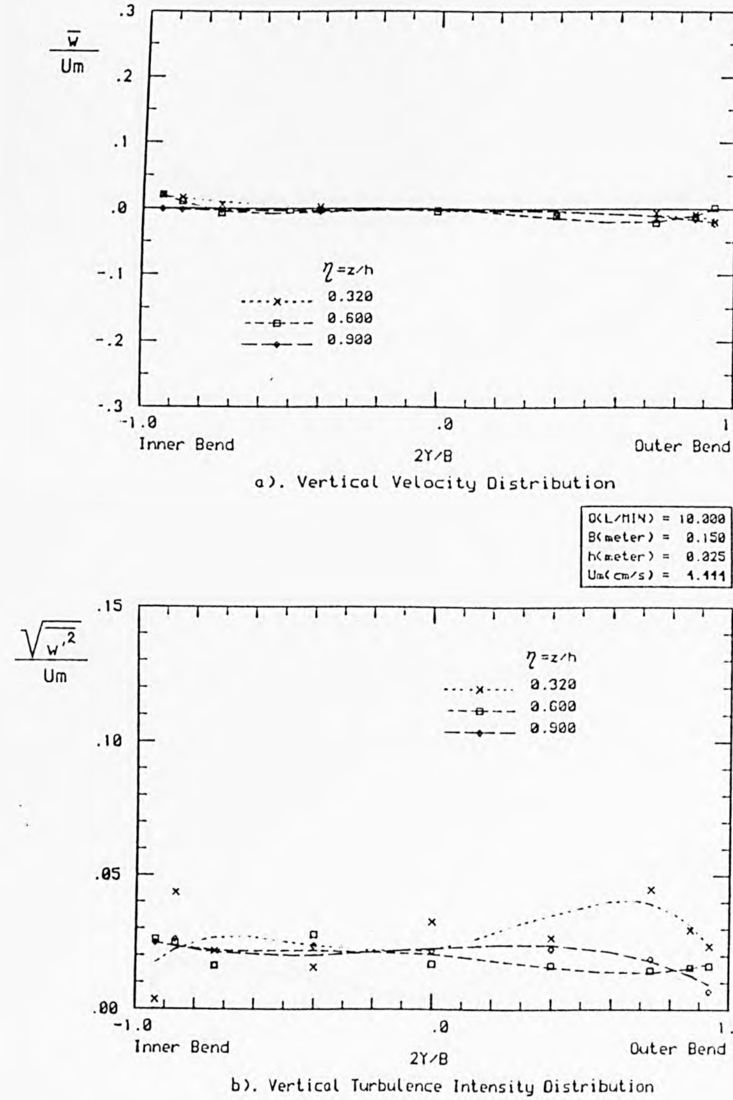

Fig. 6.42 Vertical velocity and vertical turbulence intensity distribution at section U-3, run no.1

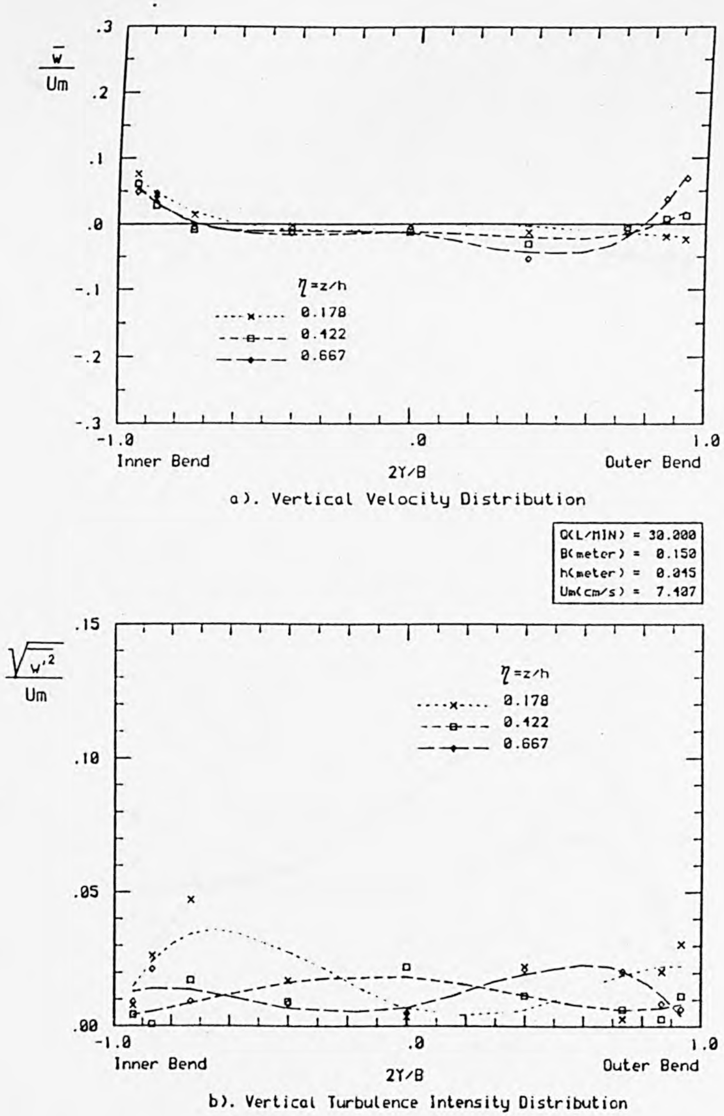

Fig. 6.43 Vertical velocity and vertical turbulence intensity distribution at section U-3, run no.2

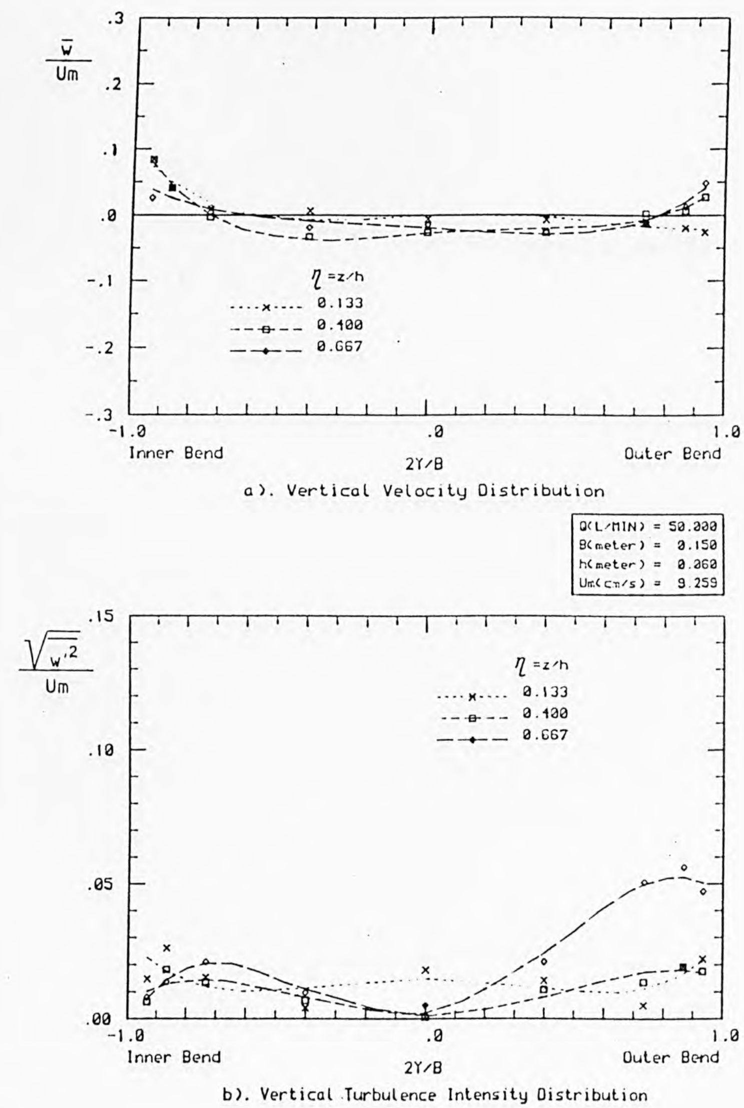

Fig. 6.44 Vertical velocity and vertical turbulence intensity distribution at section U-3, run no.3

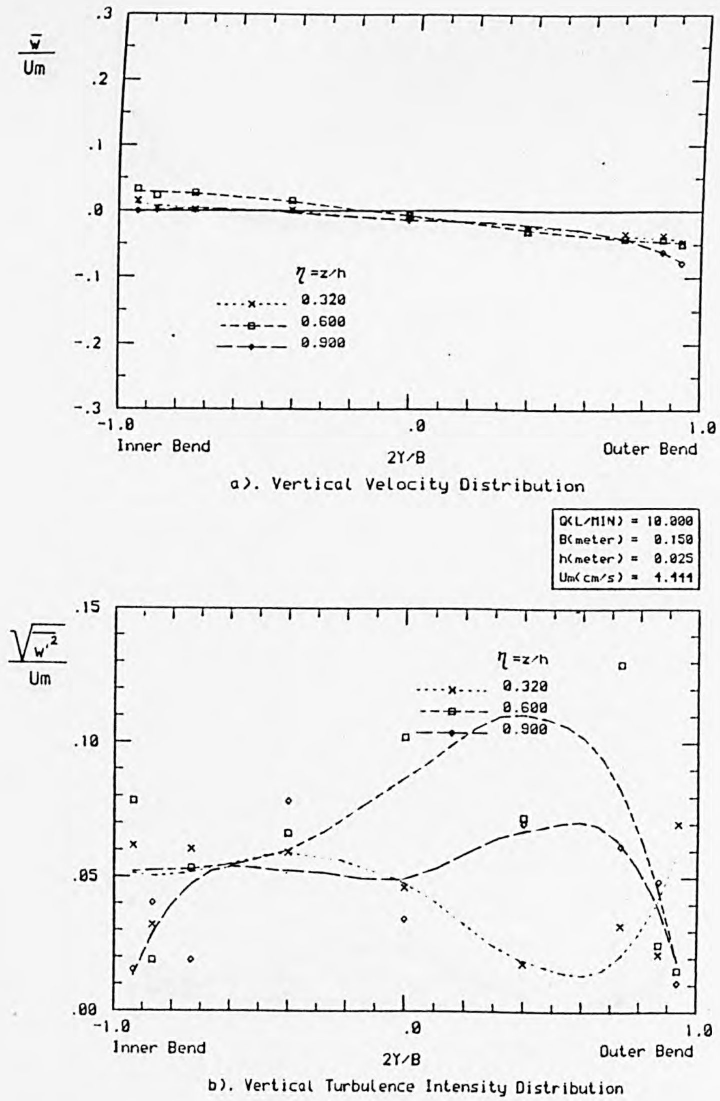

Fig. 6.45 Vertical velocity and vertical turbulence intensity distribution at section S-2, run no.1

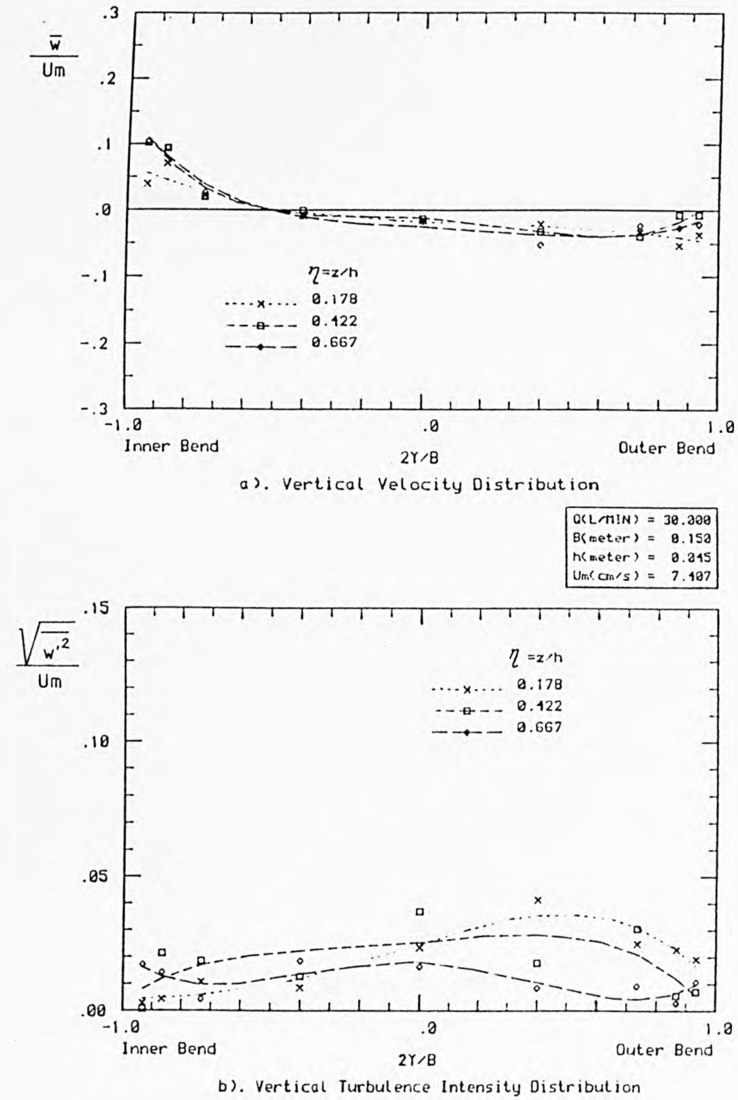

Fig. 6.46 Vertical velocity and vertical turbulence intensity distribution at section S-2, run no.2

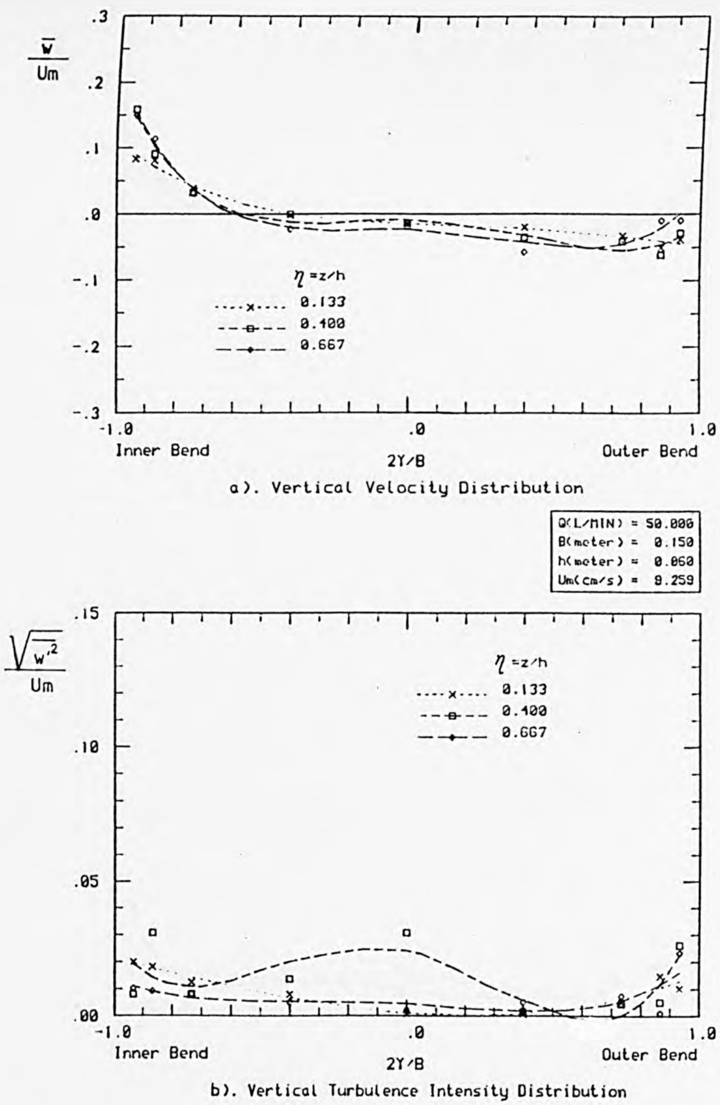

Fig. 6.47 Vertical velocity and vertical turbulence intensity distribution at section S-2, run no.3

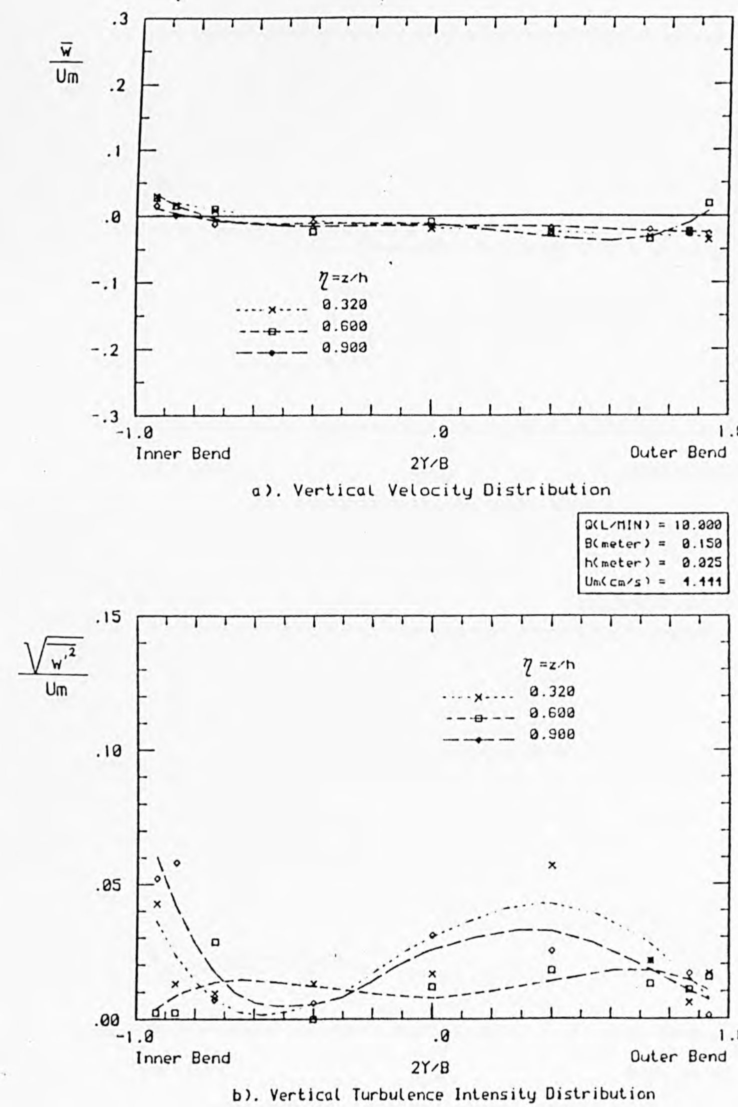

Fig. 6.48 Vertical velocity and vertical turbulence intensity distribution at section S-3, run no.1

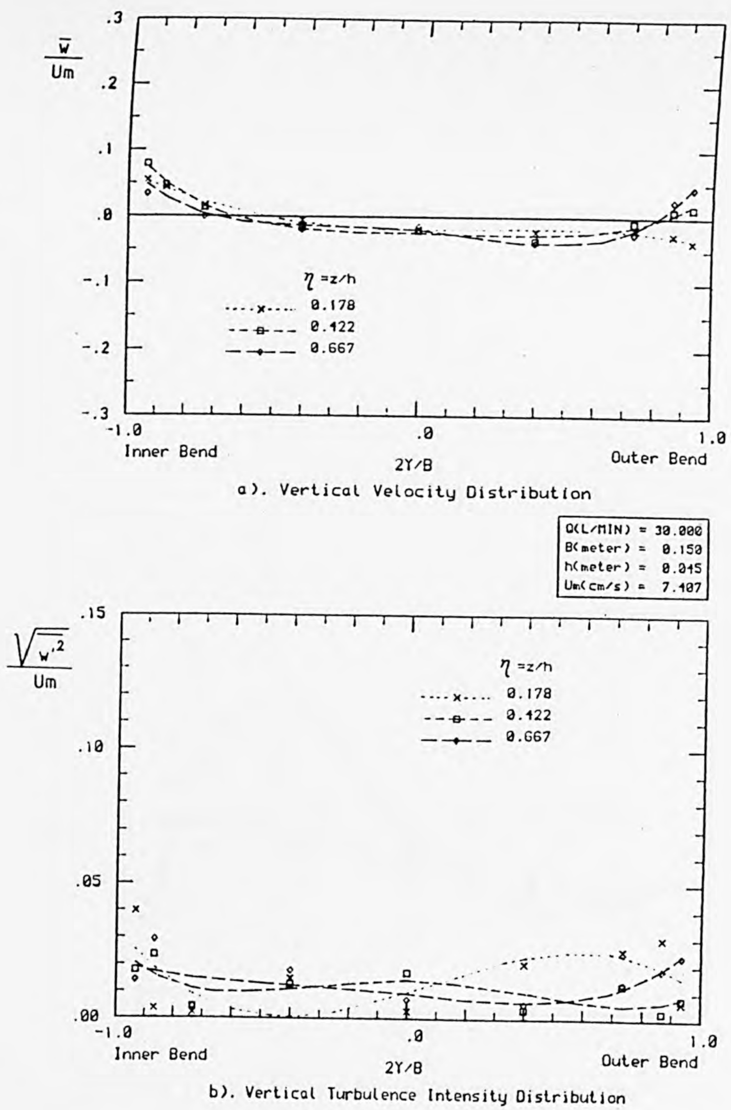

Fig. 6.49 Vertical velocity and vertical turbulence intensity distribution at section S-3, run no.2

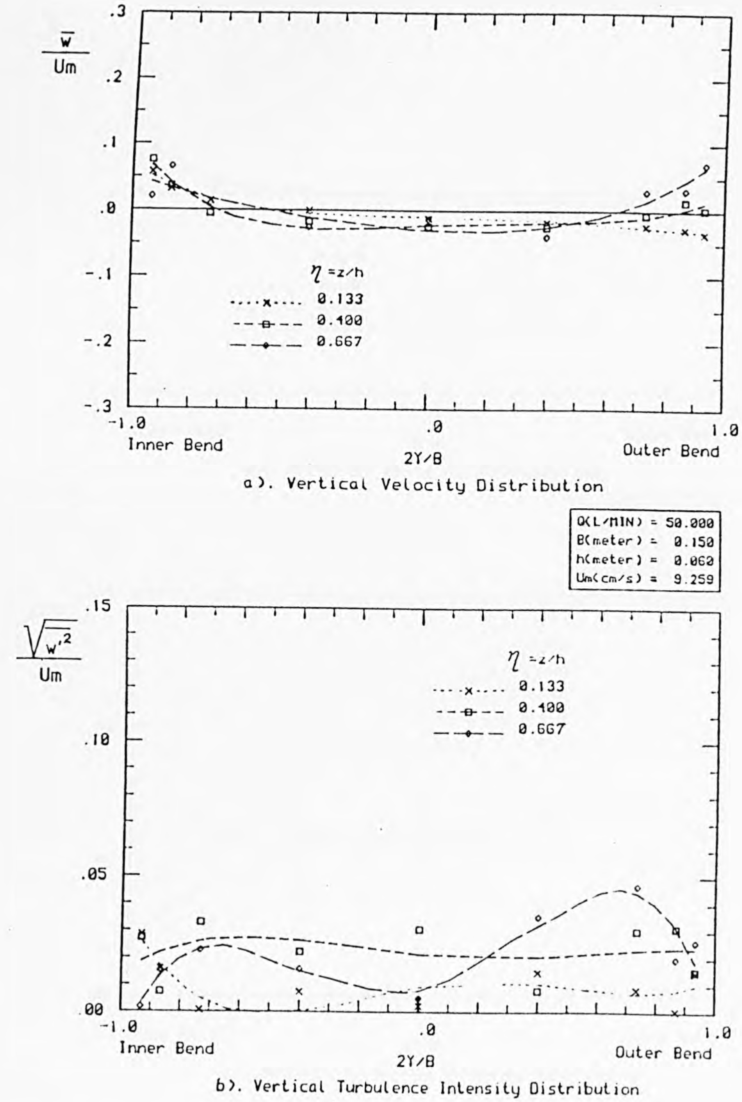

Fig. 6.50 Vertical velocity and vertical turbulence intensity distribution at section S-3, run no.3

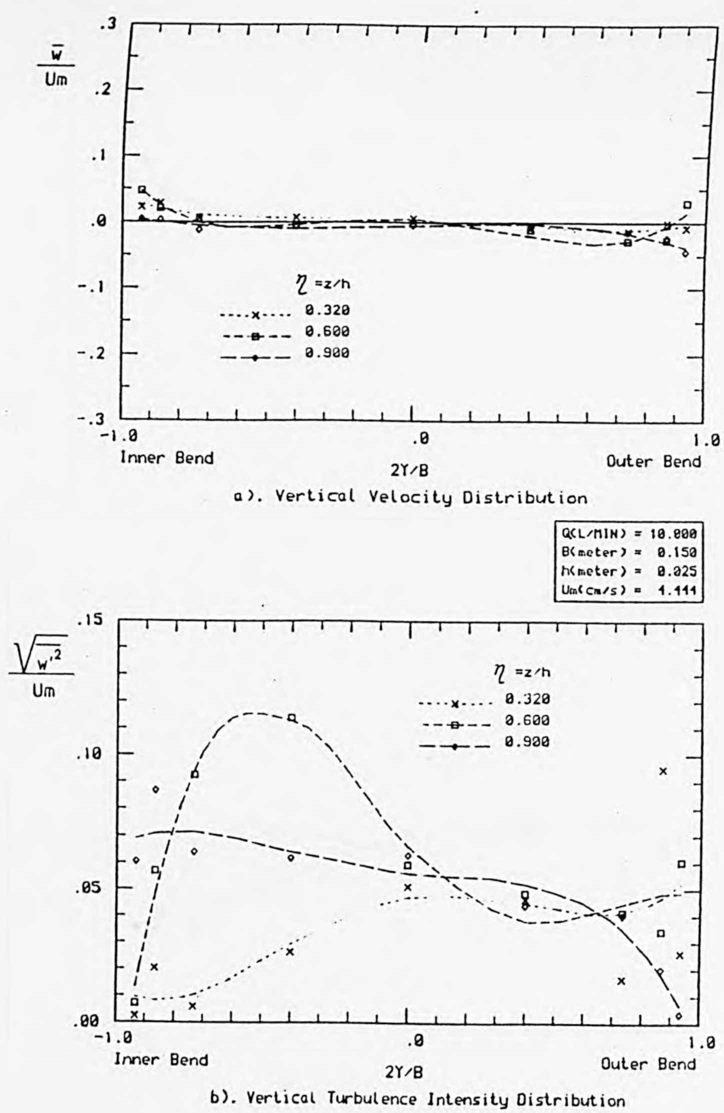

Fig. 6.51 Vertical velocity and vertical turbulence intensity distribution at section S-4, run no.1

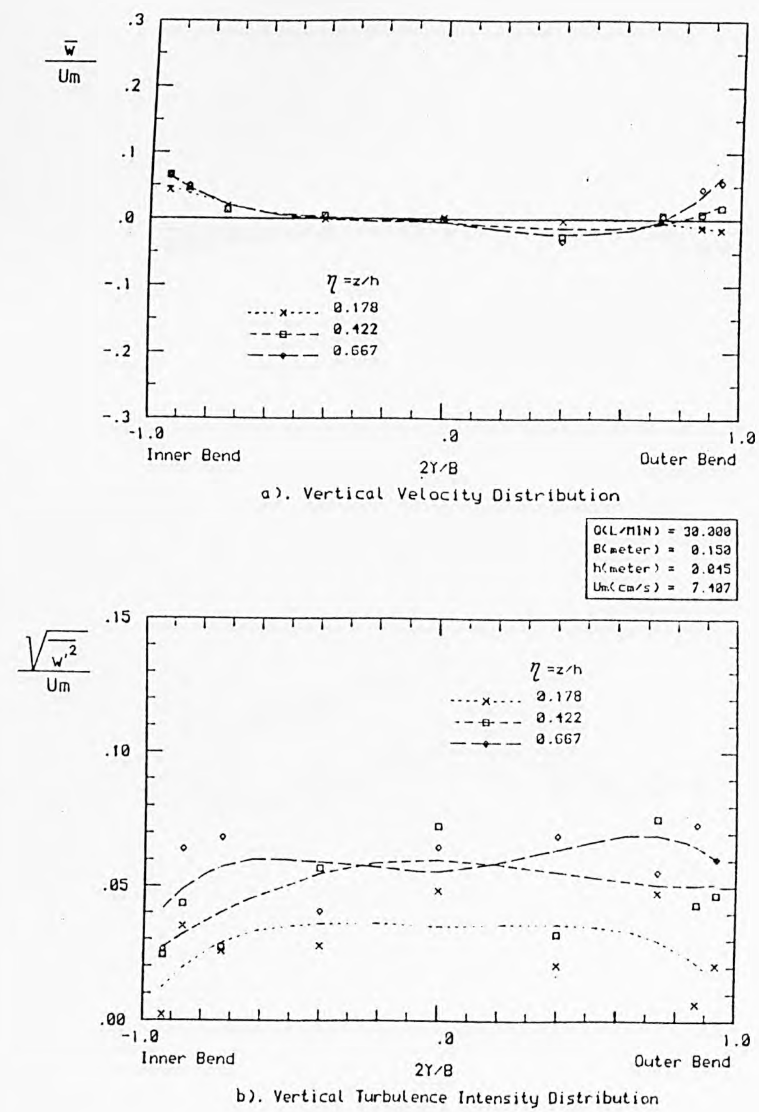

Fig. 6.52 Vertical velocity and vertical turbulence intensity distribution at section S-4, run no.2

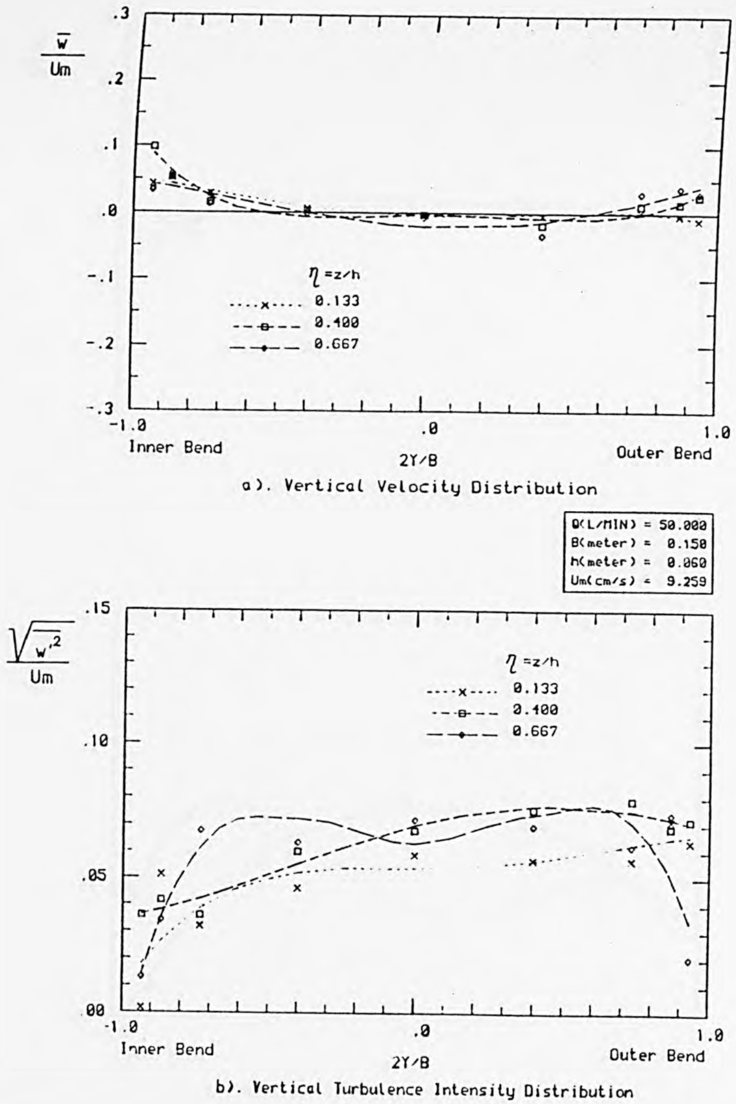

Fig. 6.53 Vertical velocity and vertical turbulence intensity distribution at section S-4, run no.3

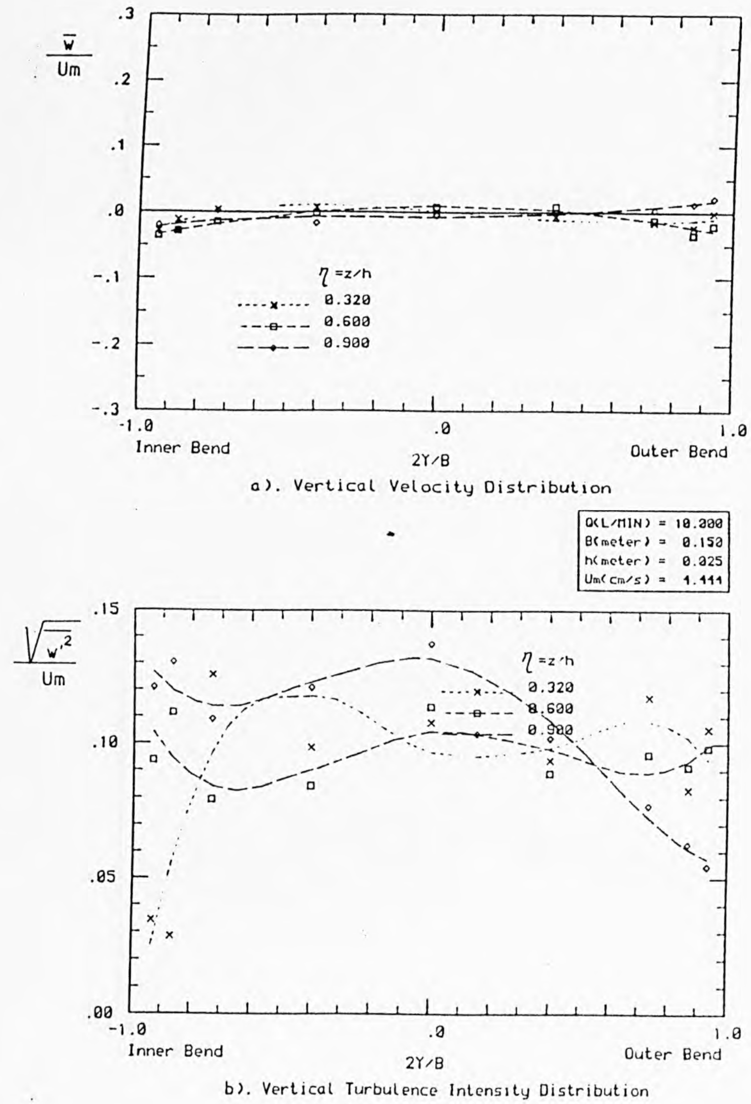

Fig. 6.54 Vertical velocity and vertical turbulence intensity distribution at section S-5, run no.1

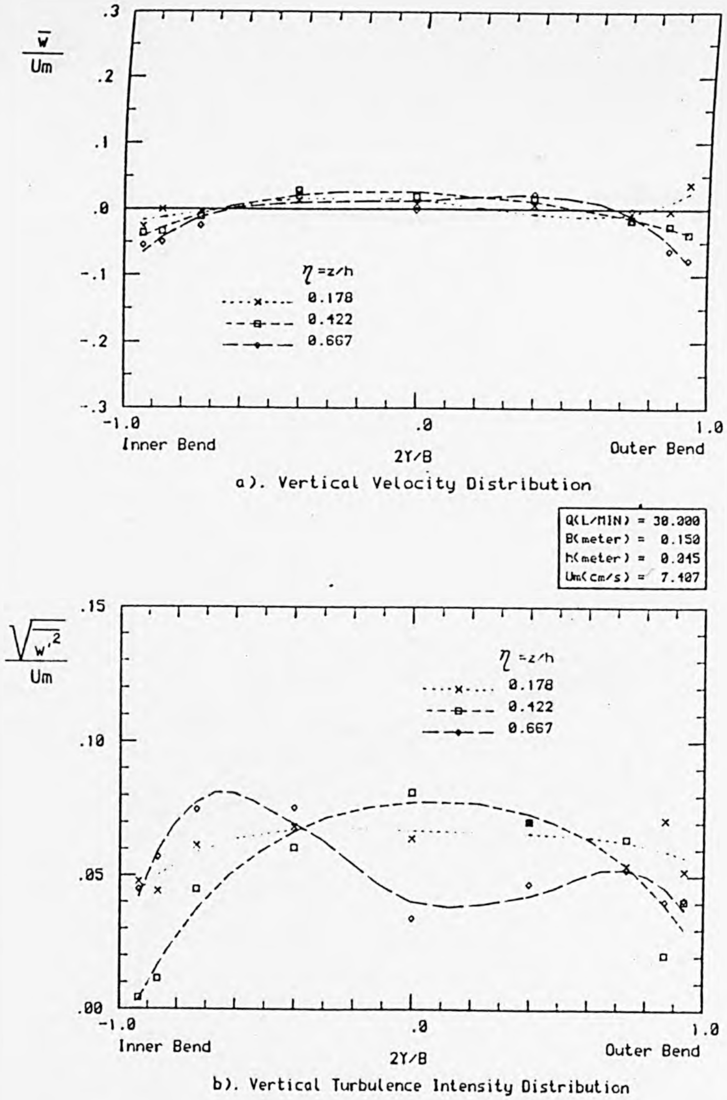

Fig. 6.55 Vertical velocity and vertical turbulence intensity distribution at section S-5, run no.2

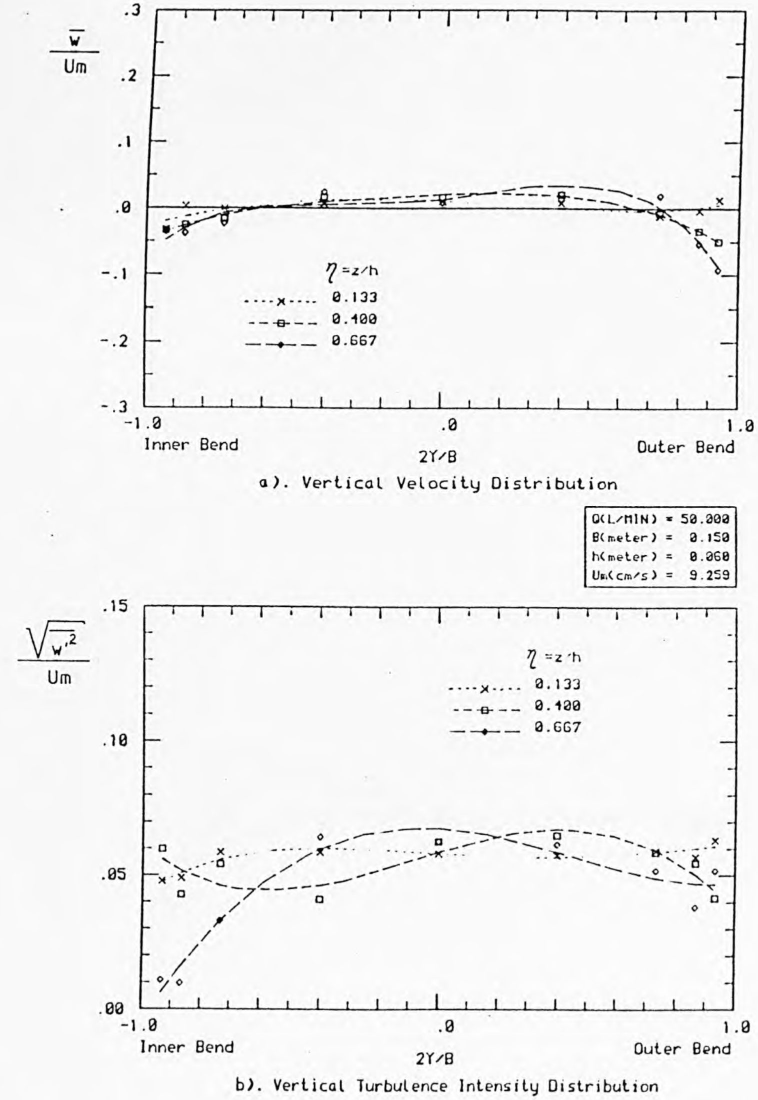

Fig. 6.56 Vertical velocity and vertical turbulence intensity distribution at section S-5, run no.3

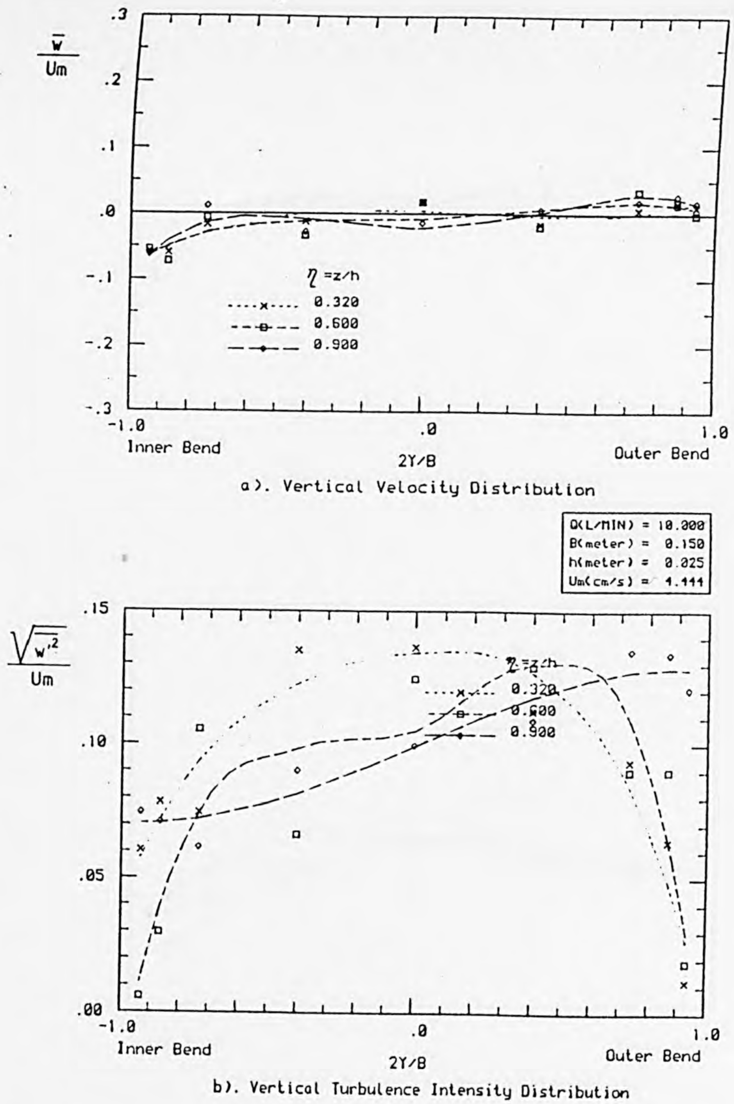

Fig. 6.57 Vertical velocity and vertical turbulence intensity distribution at section S-6, run no.1

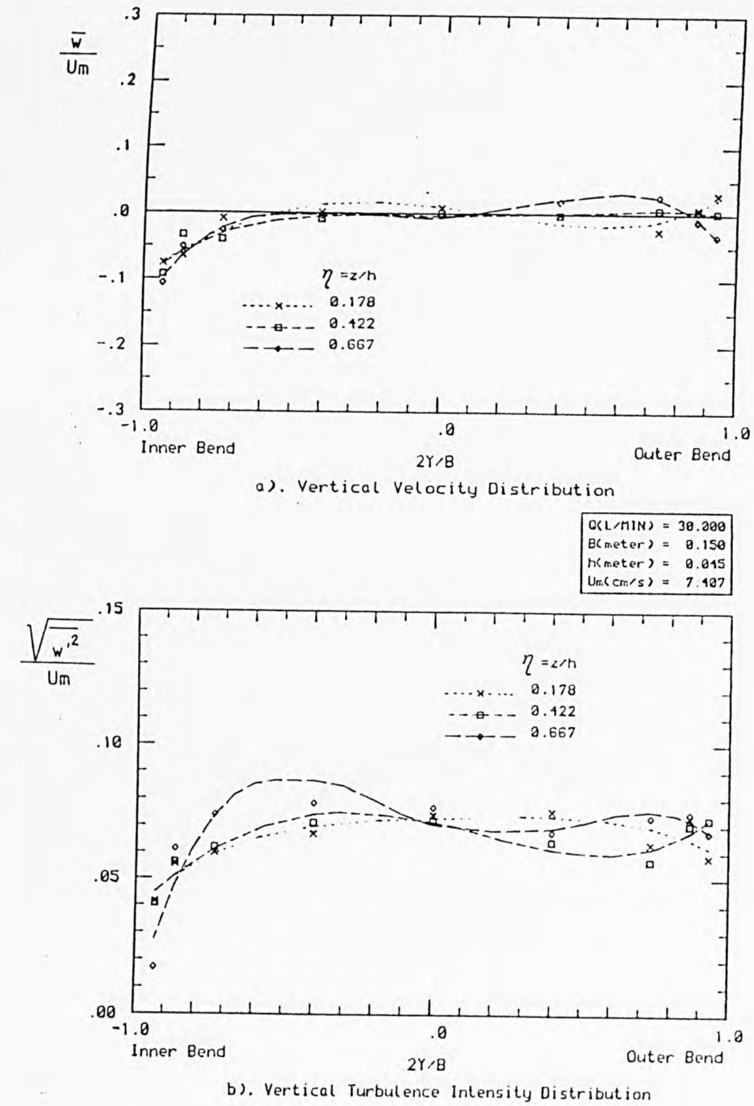

Fig. 6.58 Vertical velocity and vertical turbulence intensity distribution at section S-6, run no.2

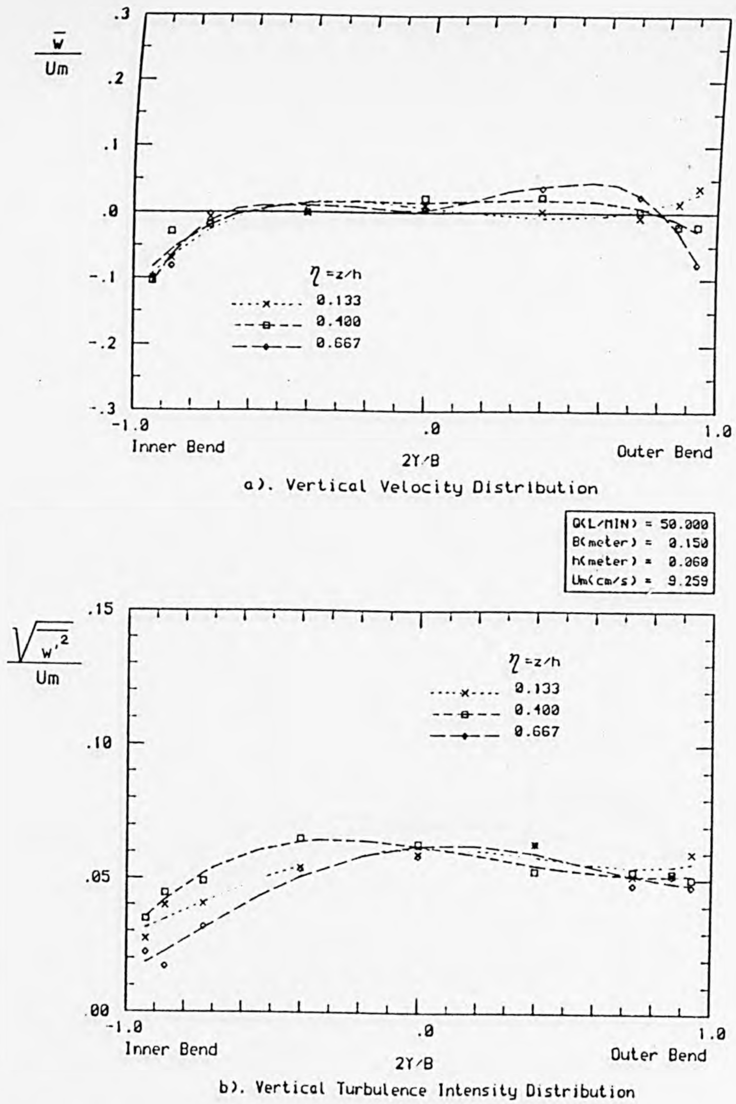

Fig. 6.59 Vertical velocity and vertical turbulence intensity distribution at section S-6, run no.3

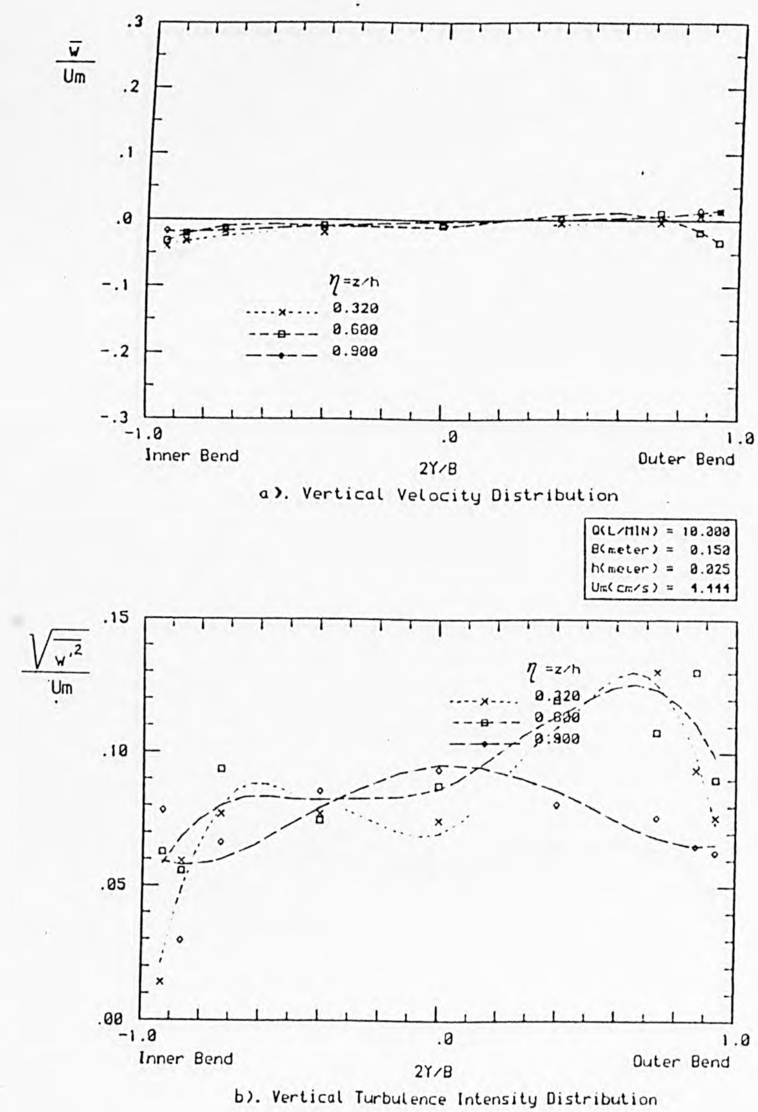

Fig. 6.60 Vertical velocity and vertical turbulence intensity distribution at section S-7, run no.1

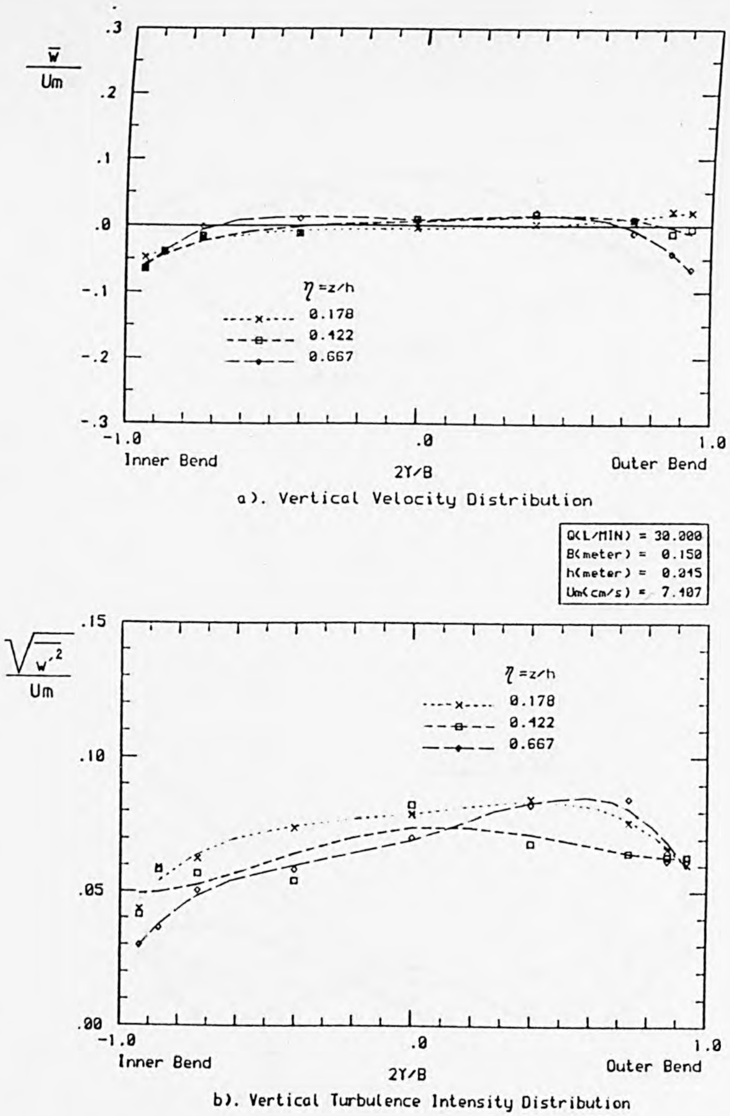

Fig. 6.61 Vertical velocity and vertical turbulence intensity distribution at section S-7, run no.2

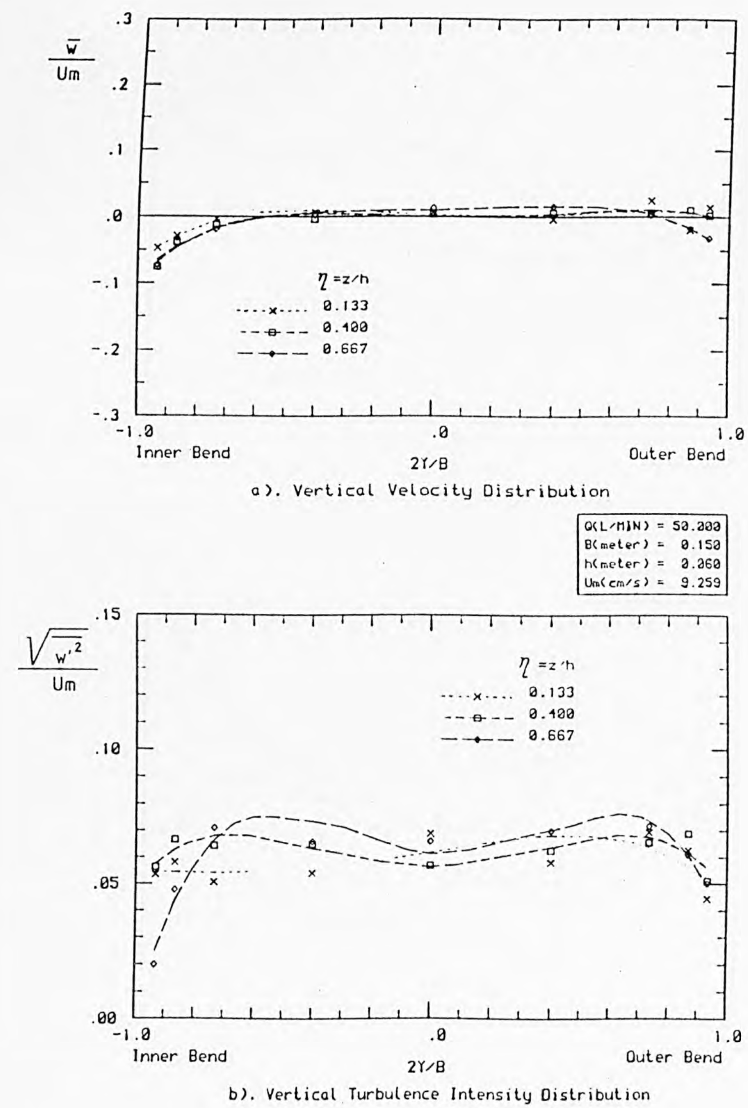

Fig. 6.62 Vertical velocity and vertical turbulence intensity distribution at section S-7, run no.3

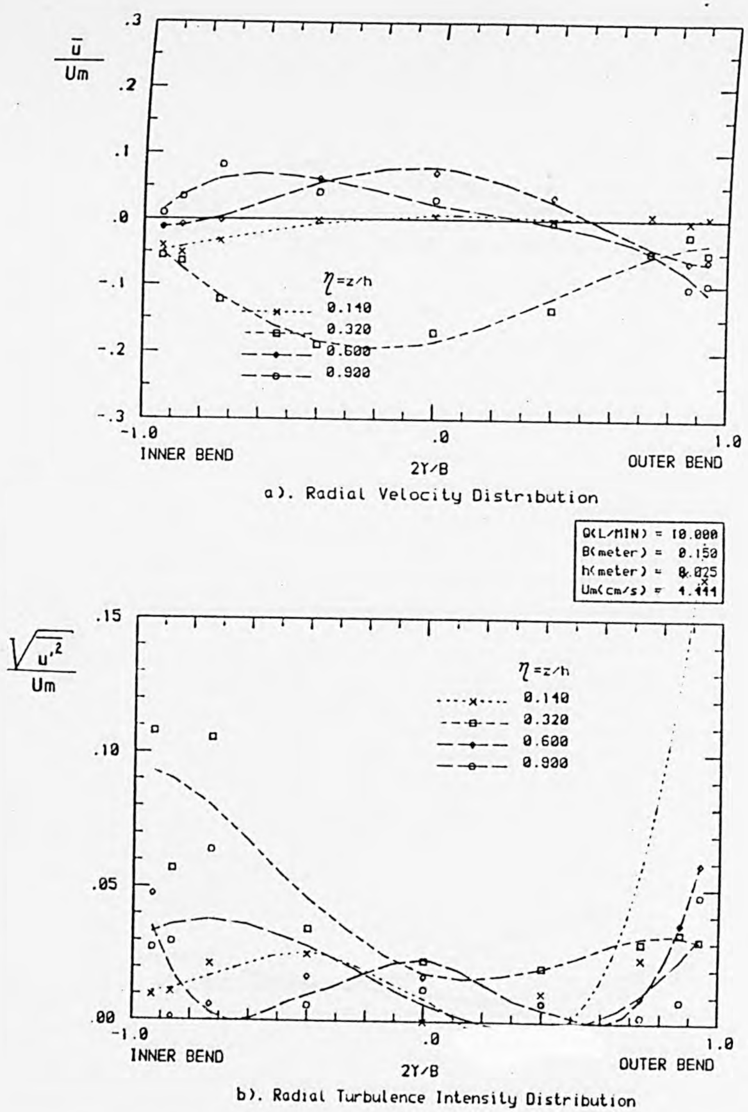

Fig. 6.63 Radial velocity and radial turbulence intensity distribution at section U-2, run no.1

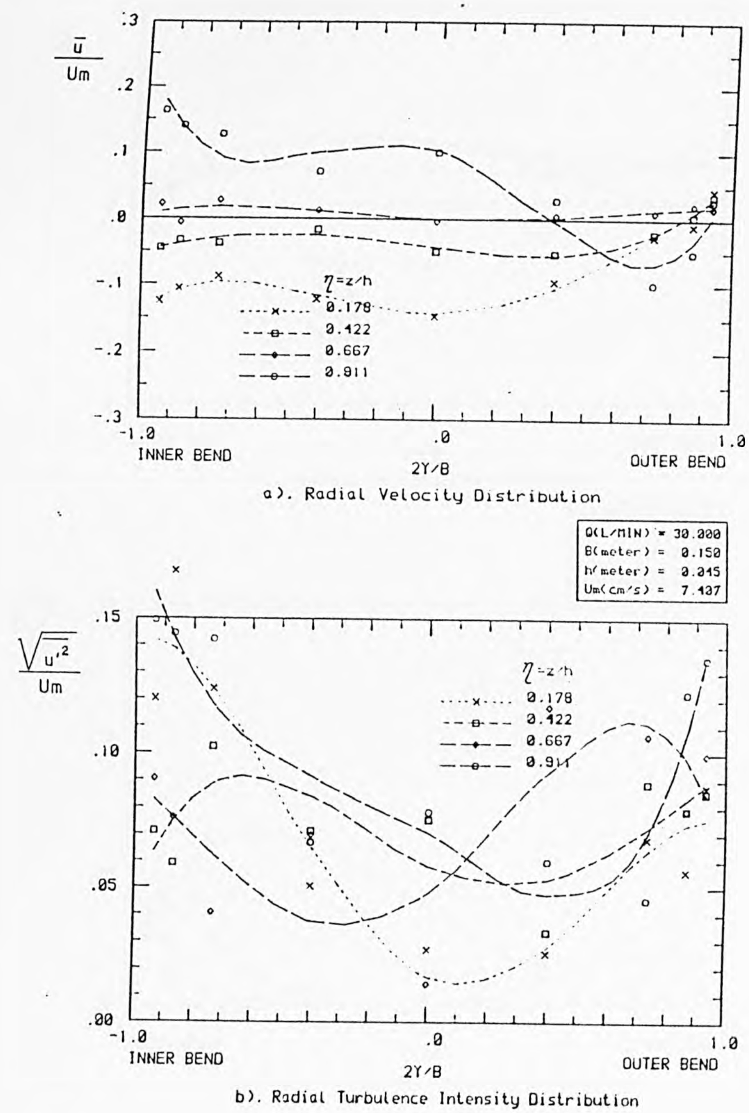

Fig. 6.64 Radial velocity and radial turbulence intensity distribution at section U-2, run no.2

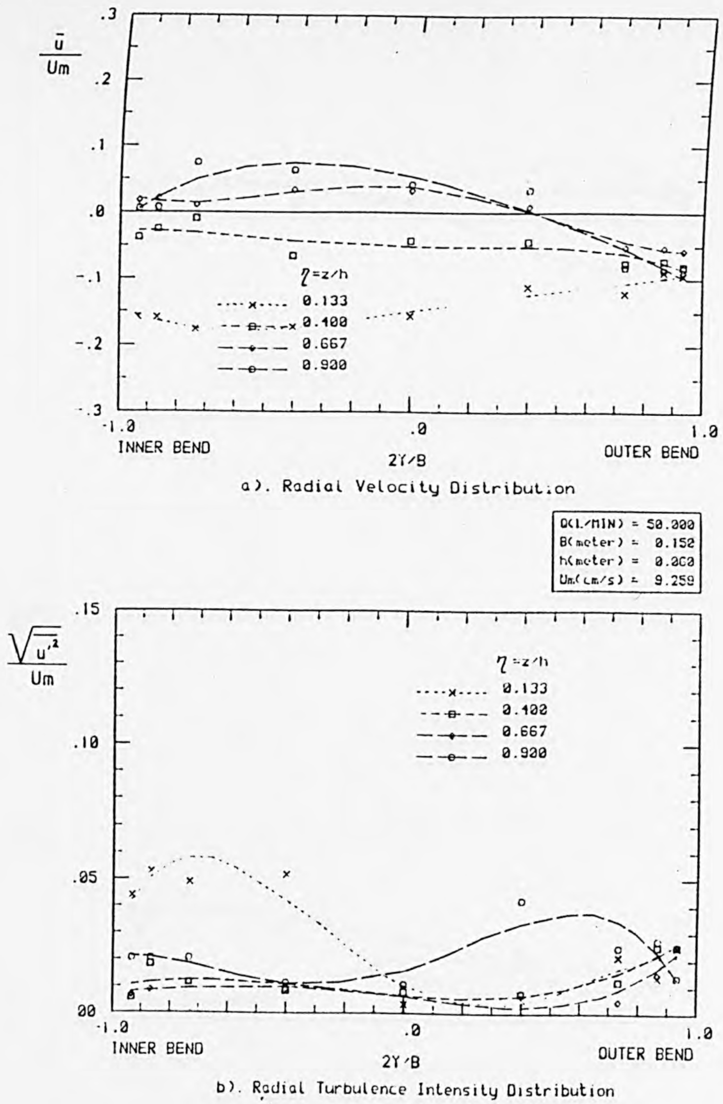

Fig. 6.65 Radial velocity and radial turbulence intensity distribution at section U-2, run no.3

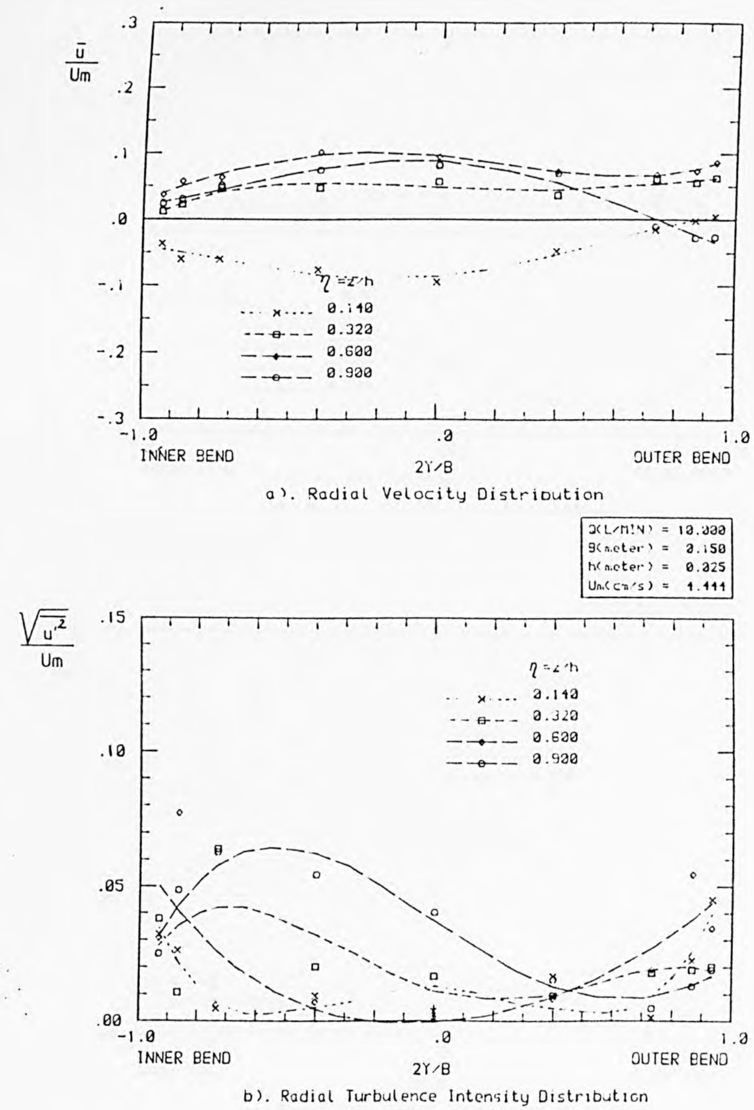

Fig. 6.66 Radial velocity and radial turbulence intensity distribution at section U-3, run no.1

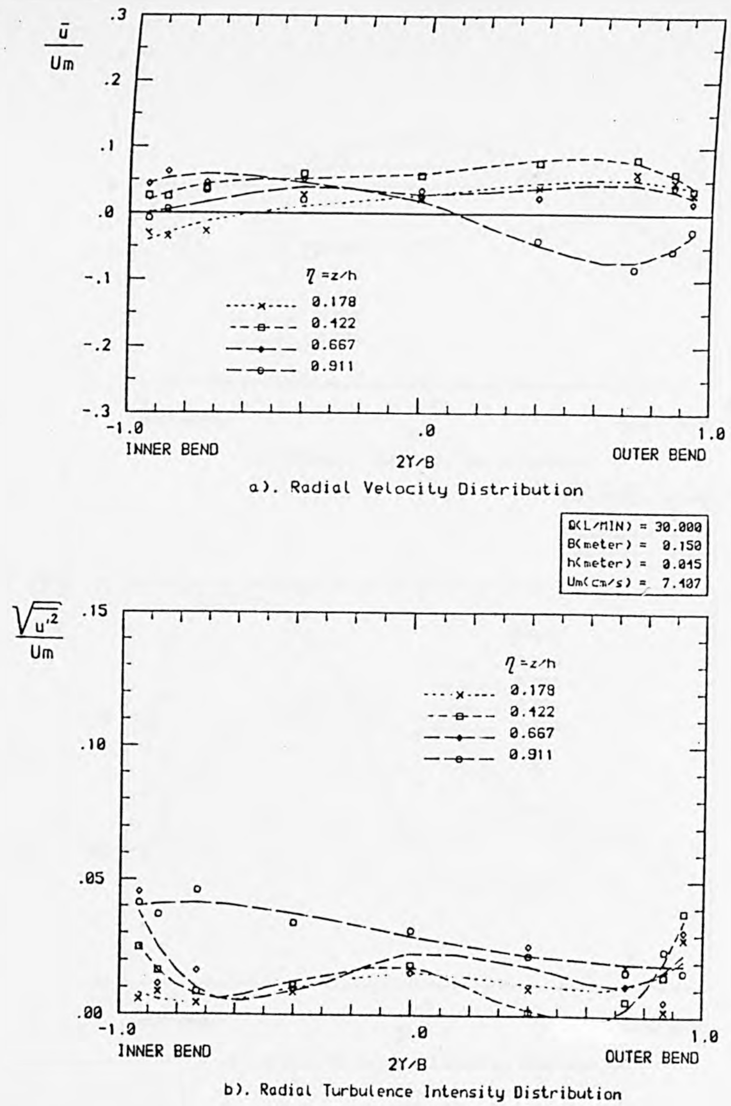

Fig. 6.67 Radial velocity and radial turbulence intensity distribution at section U-3, run no.2

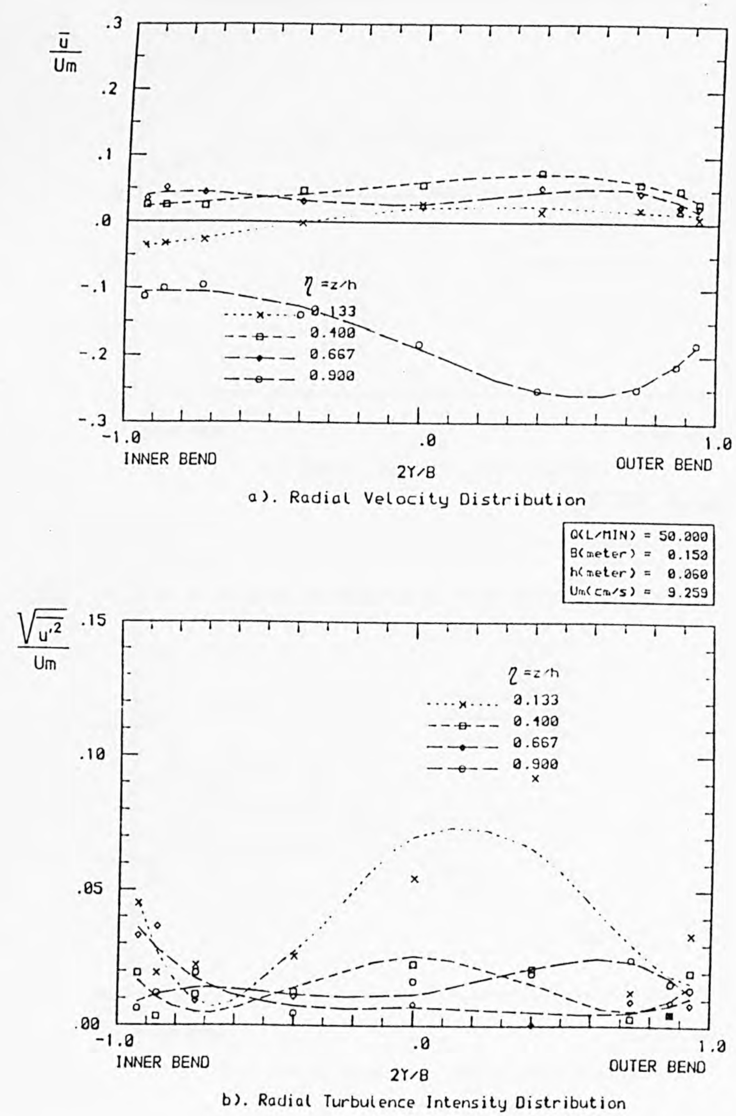

Fig. 6.68 Radial velocity and radial turbulence intensity distribution at section U-3, run no.3

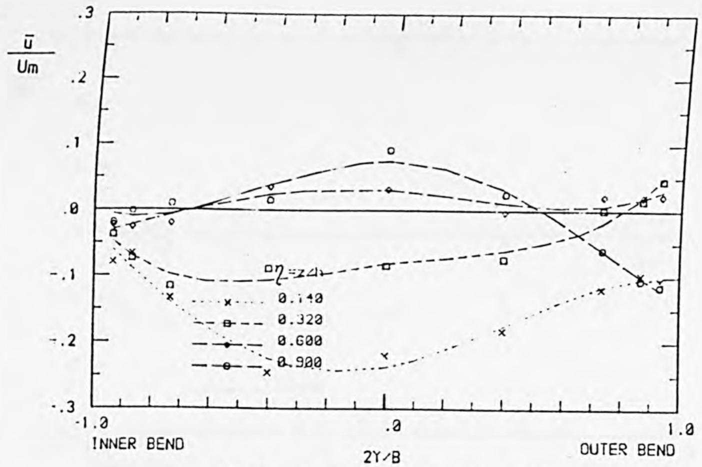

a). Radial Velocity Distribution

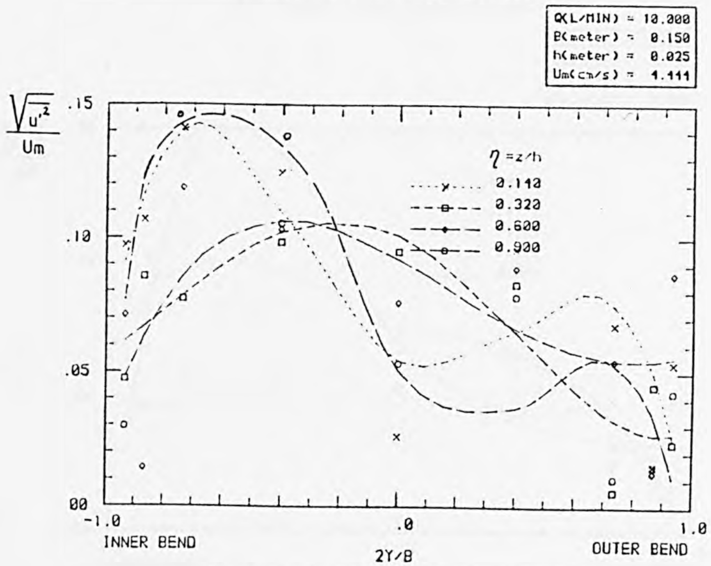

b). Radial Turbulence Intensity Distribution

Fig. 6.69 Radial velocity and radial turbulence intensity distribution at section S-2, run no.1

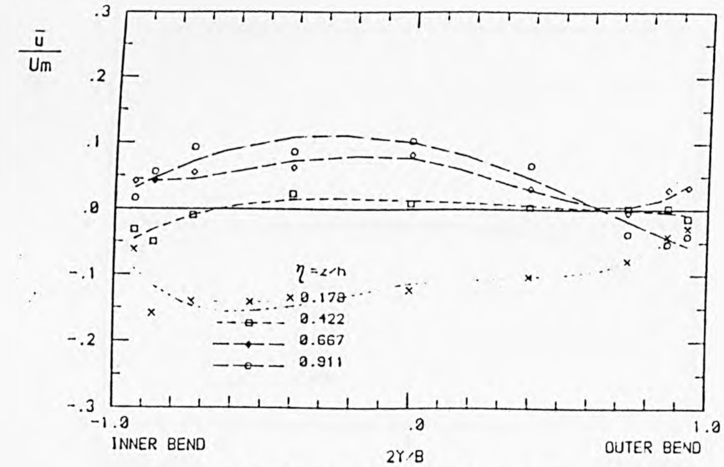

a). Radial Velocity Distribution

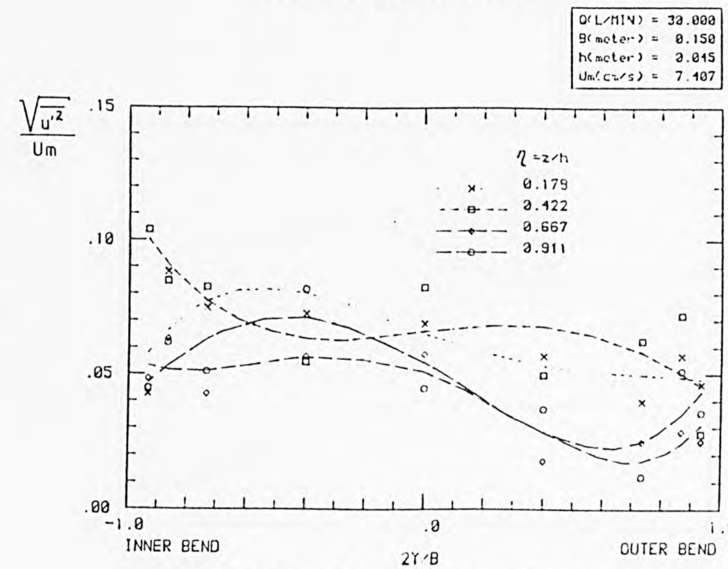

b). Radial Turbulence Intensity Distribution

Fig. 6.70 Radial velocity and radial turbulence intensity distribution at section S-2, run no.2

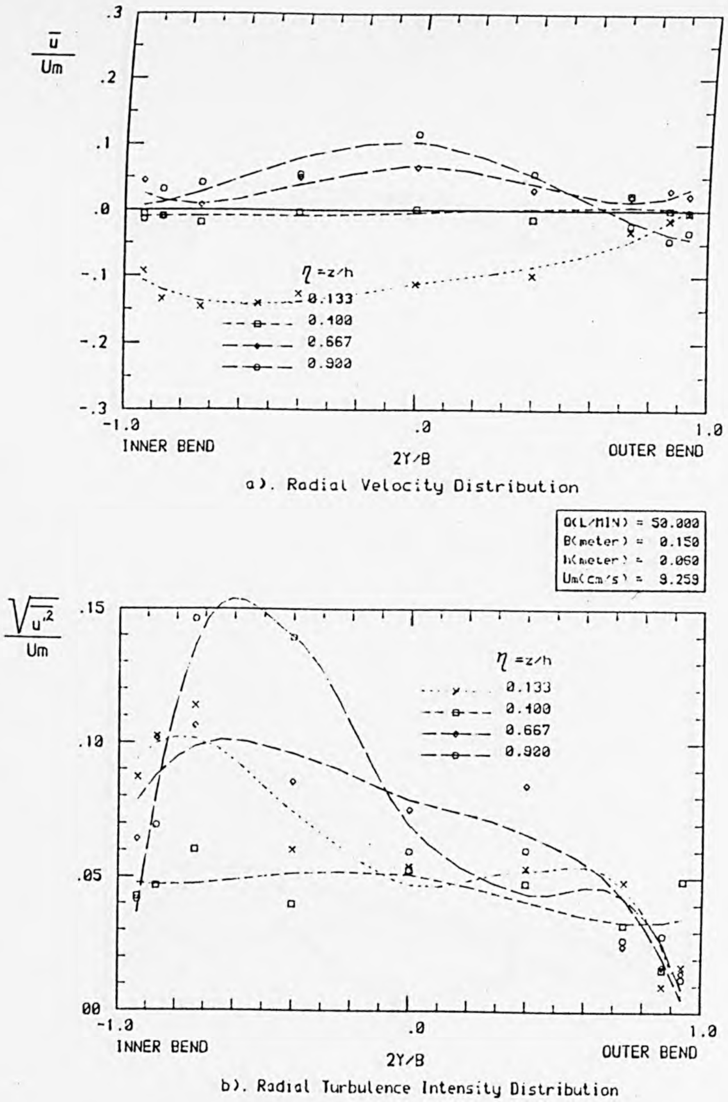

Fig. 6.71 Radial velocity and radial turbulence intensity distribution at section S-2, run no.3

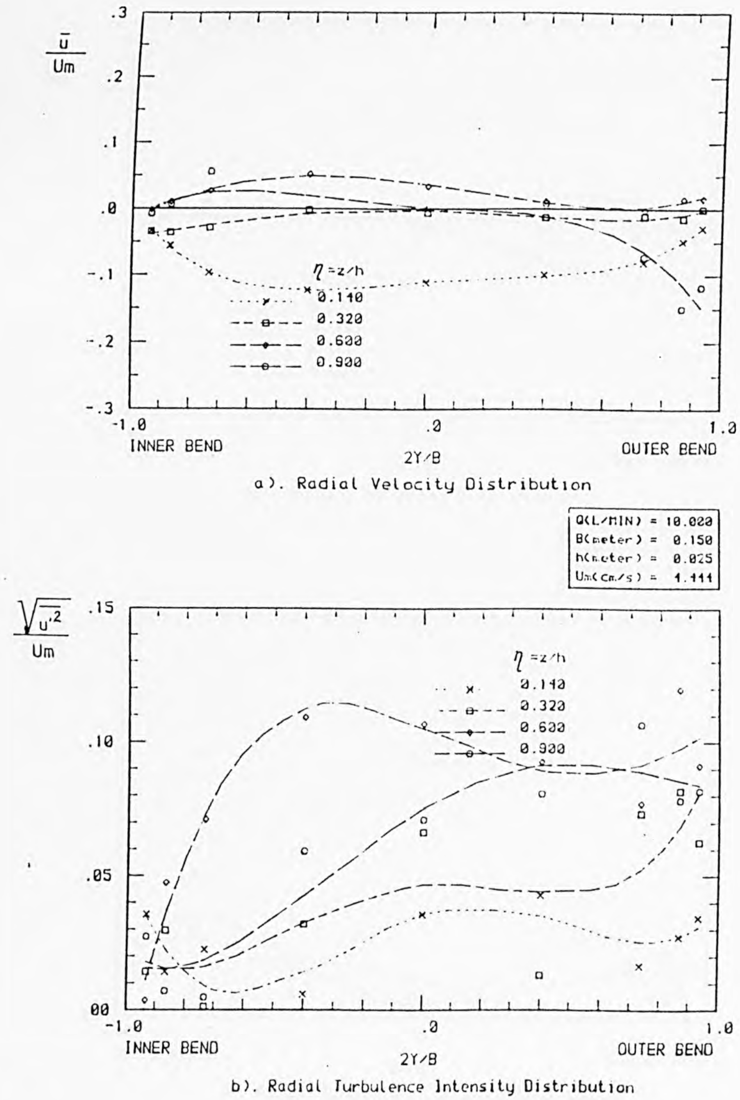

Fig. 6.72 Radial velocity and radial turbulence intensity distribution at section S-3, run no.1

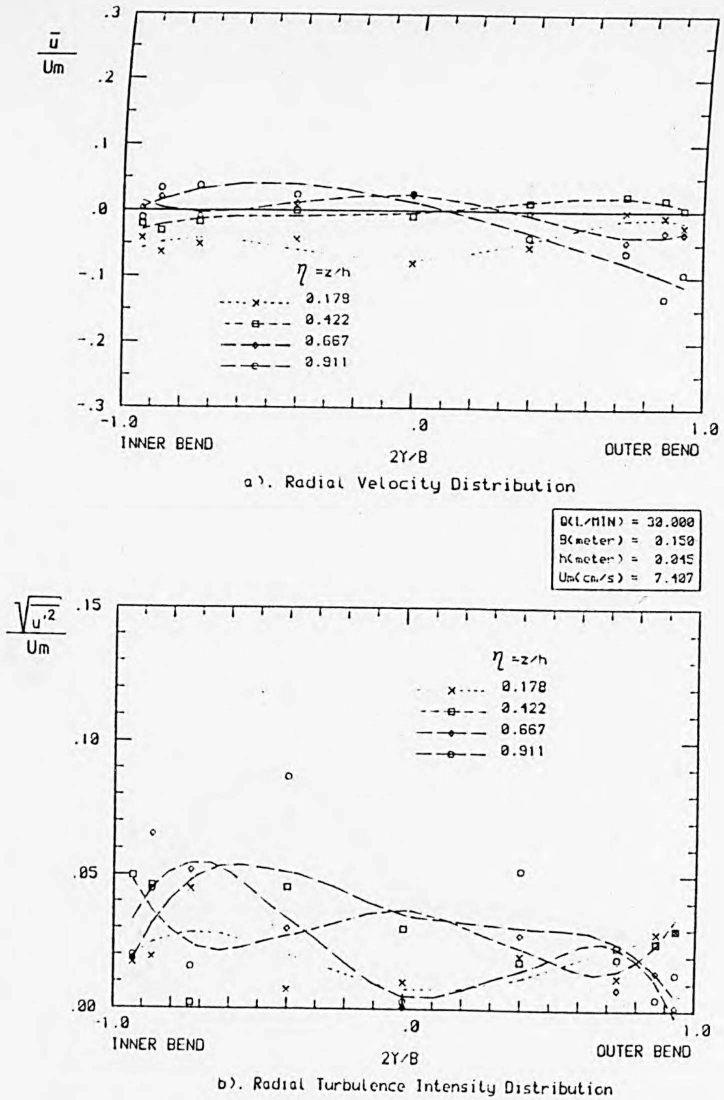

Fig. 6.73 Radial velocity and radial turbulence intensity distribution at section S-3, run no.2

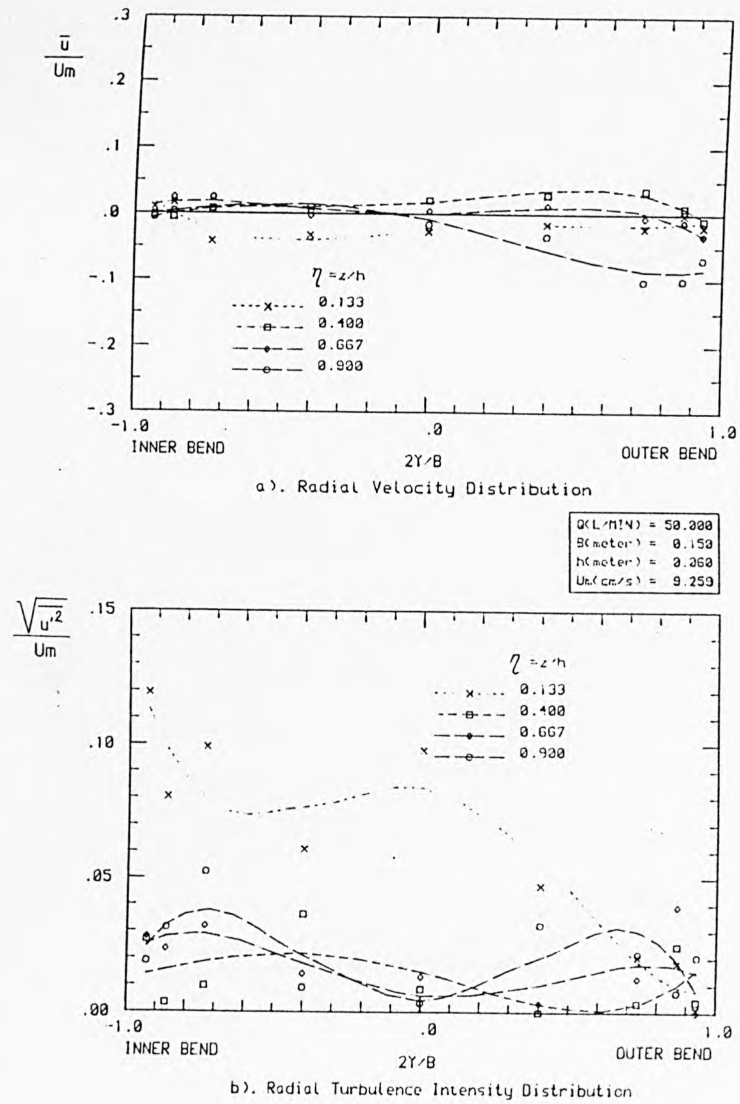

Fig. 6.74 Radial velocity and radial turbulence intensity distribution at section S-3, run no.3

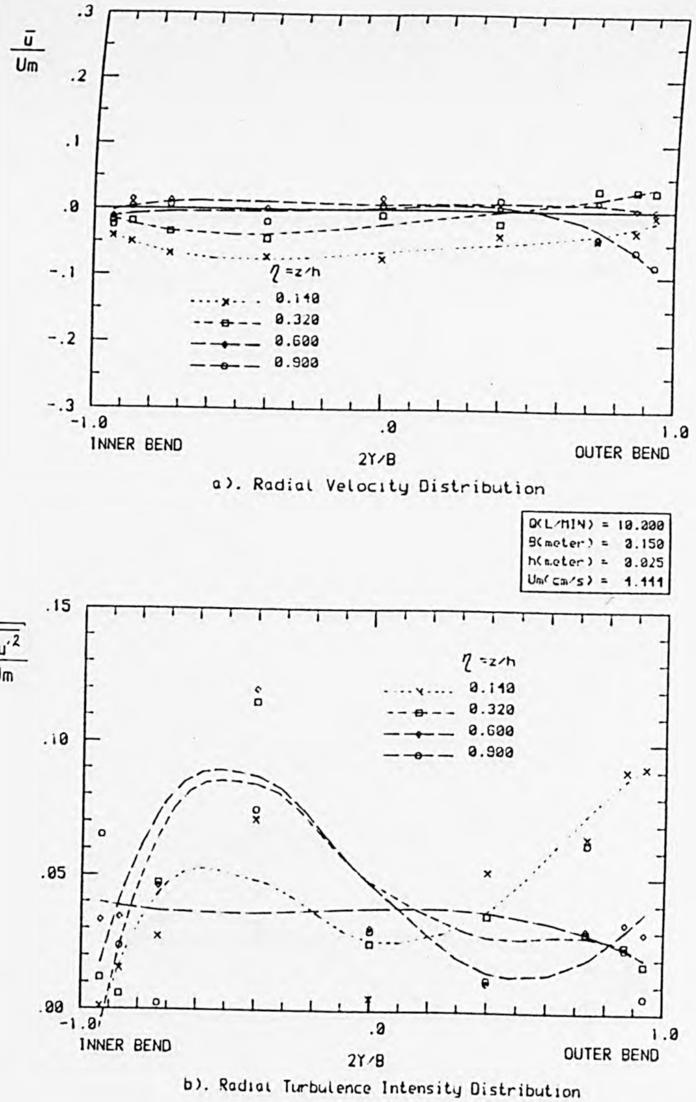

Fig. 6.75 Radial velocity and radial turbulence intensity distribution at section S-4, run no.1

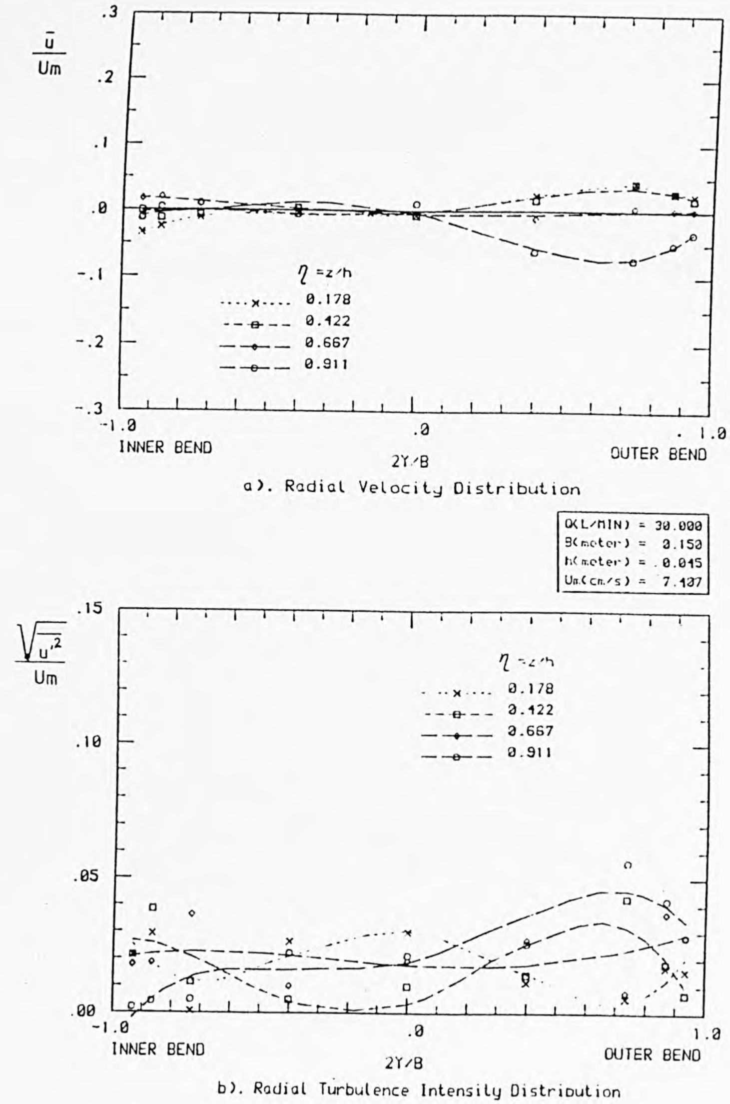

Fig. 6.76 Radial velocity and radial turbulence intensity distribution at section S-4, run no.2

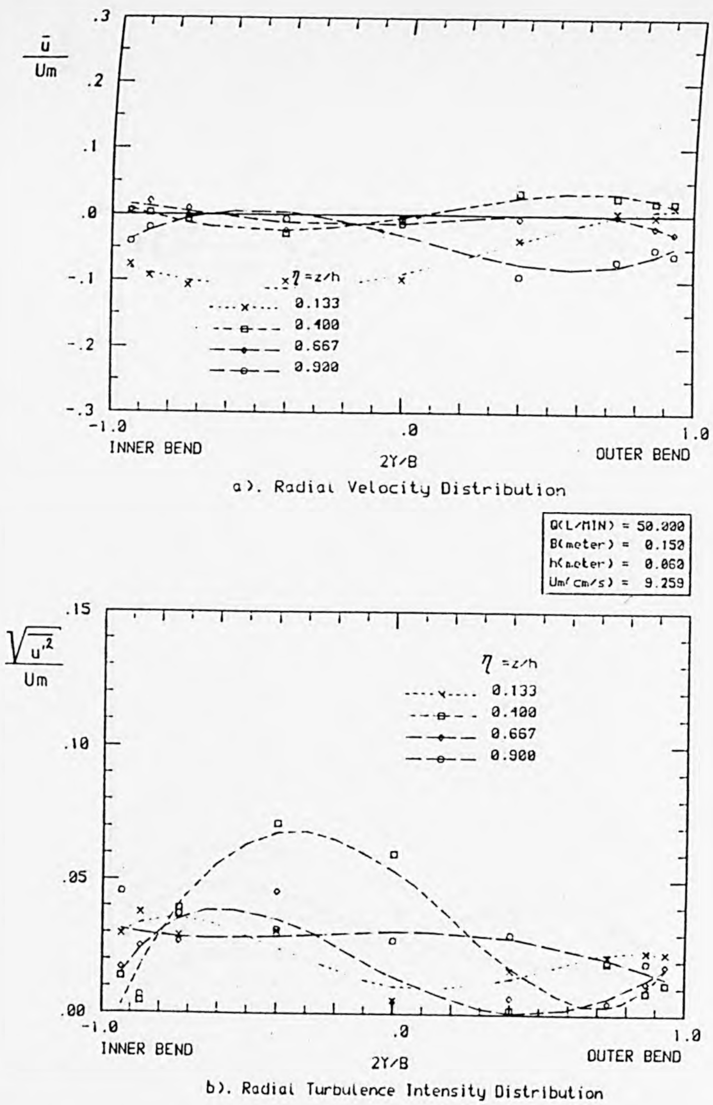

Fig. 6.77 Radial velocity and radial turbulence intensity distribution at section S-4, run no.3

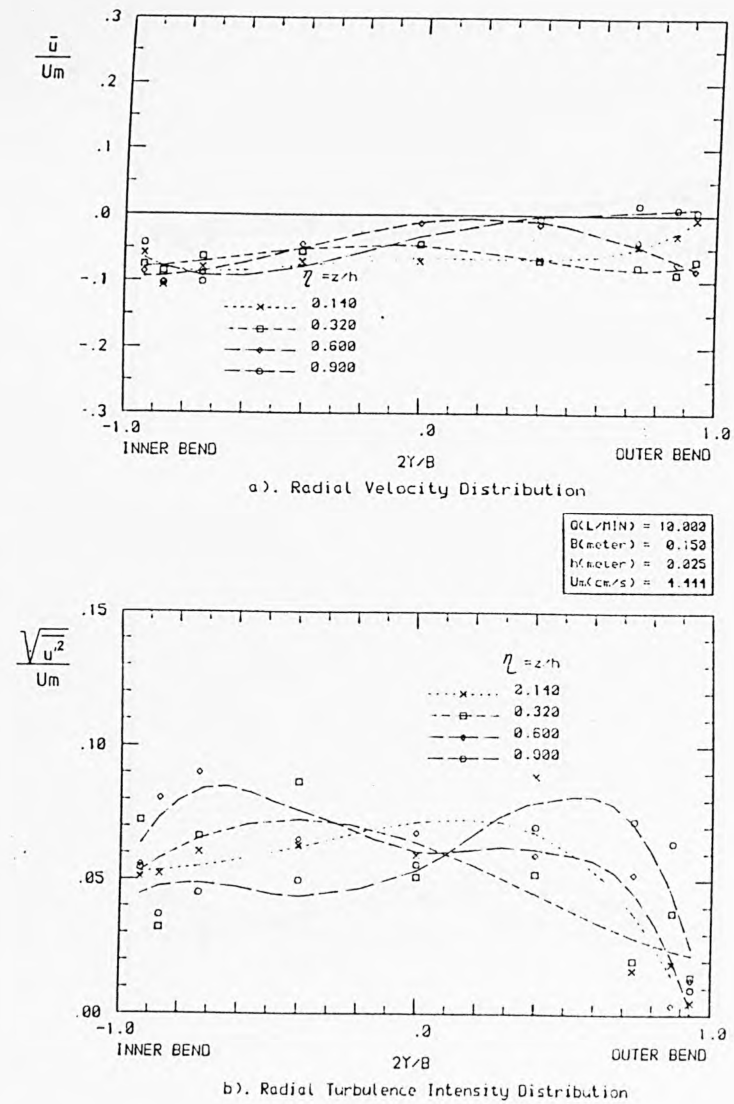

Fig. 6.78 Radial velocity and radial turbulence intensity distribution at section S-5, run no.1

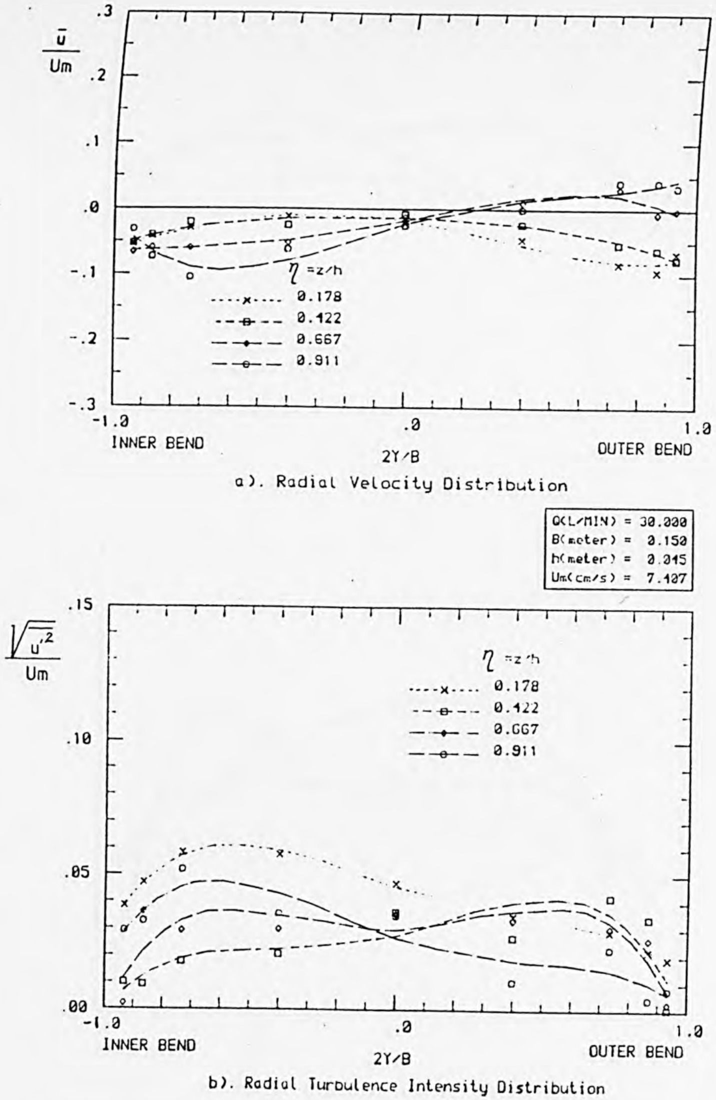

Fig. 6.79 Radial velocity and radial turbulence intensity distribution at section S-5, run no.2

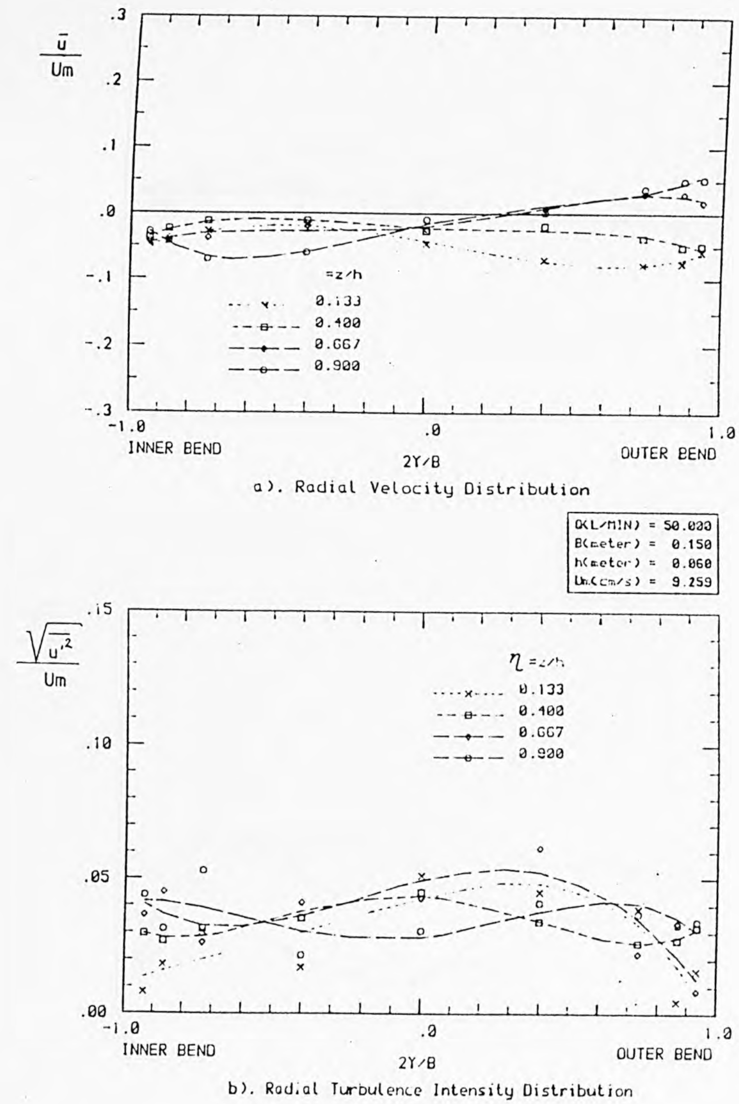

Fig. 6.80 Radial velocity and radial turbulence intensity distribution at section S-5, run no.3

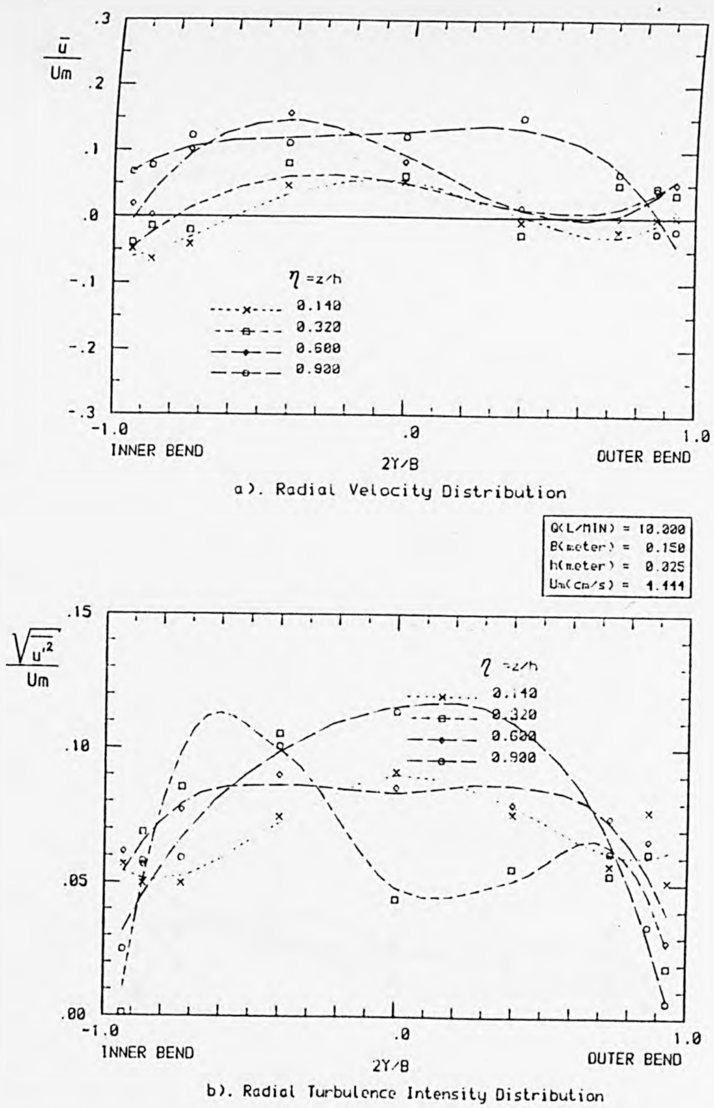

Fig. 6.81 Radial velocity and radial turbulence intensity distribution at section S-6, run no.1

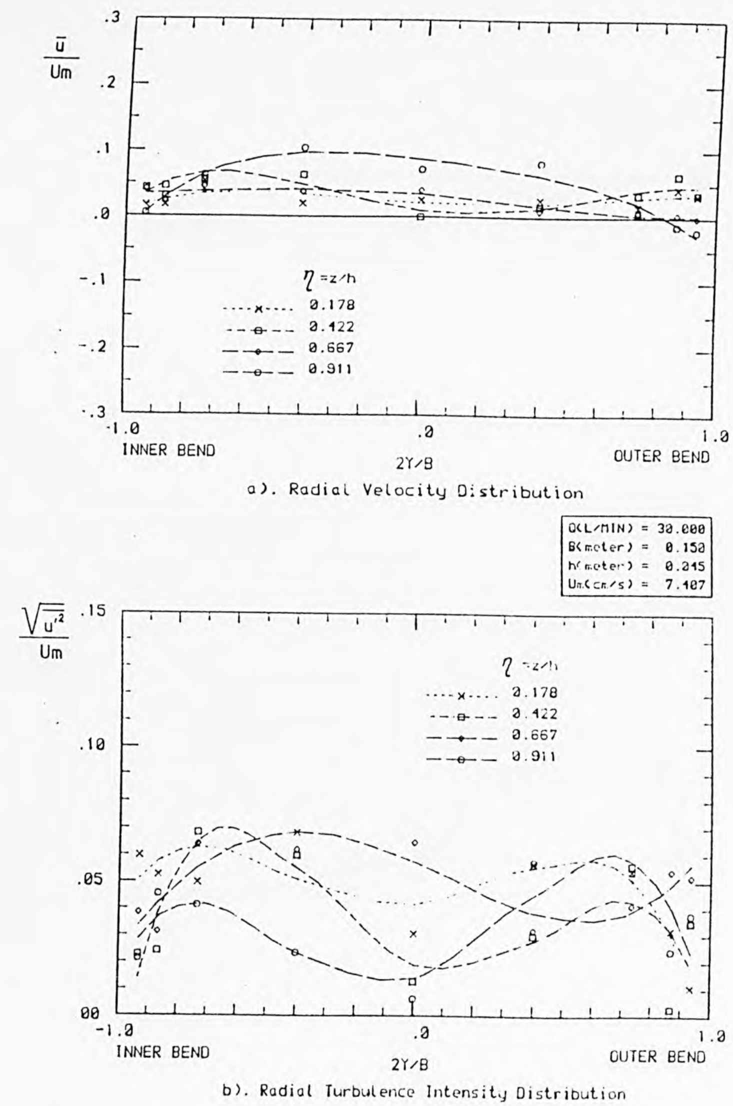

Fig. 6.82 Radial velocity and radial turbulence intensity distribution at section S-6, run no.2

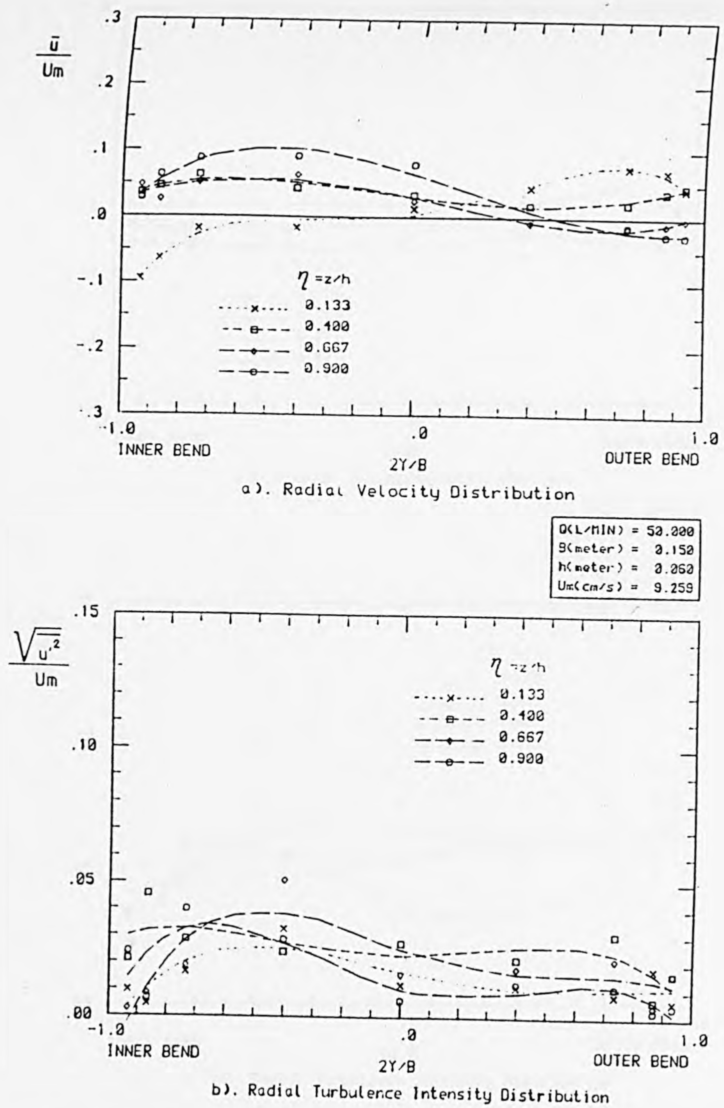

Fig. 6.83 Radial velocity and radial turbulence intensity distribution at section S-6, run no.3

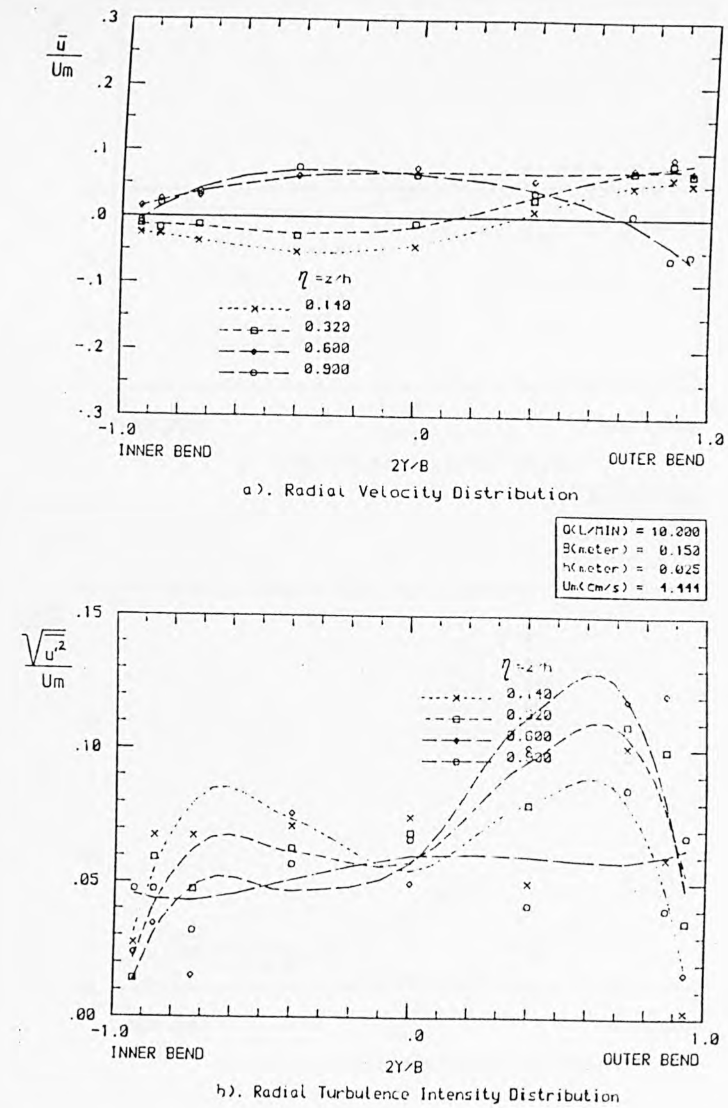

Fig. 6.84 Radial velocity and radial turbulence intensity distribution at section S-7, run no.1

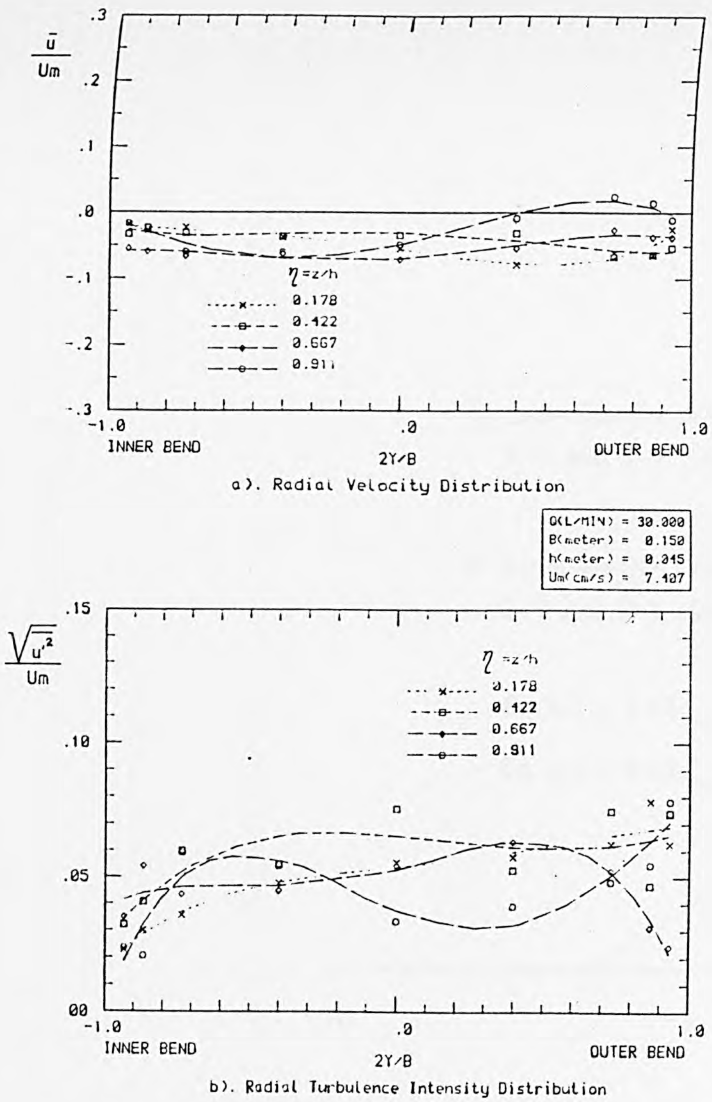

Fig. 6.85 Radial velocity and radial turbulence intensity distribution at section S-7, run no.2

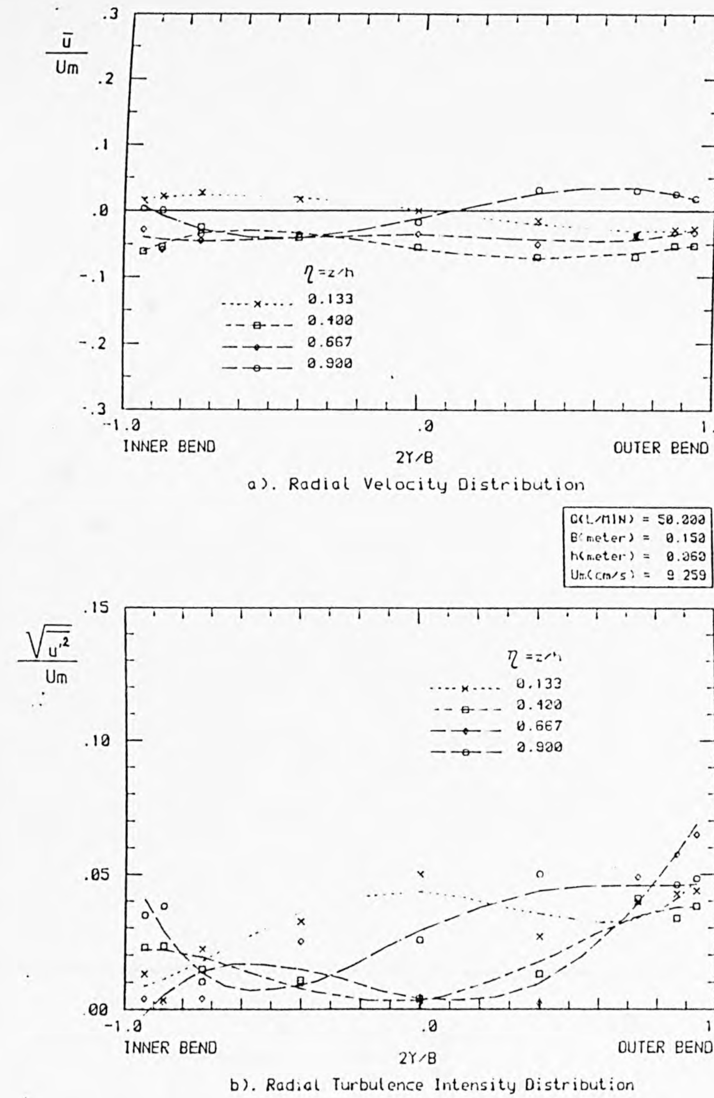

Fig. 6.86 Radial velocity and radial turbulence intensity distribution at section S-7, run no.3

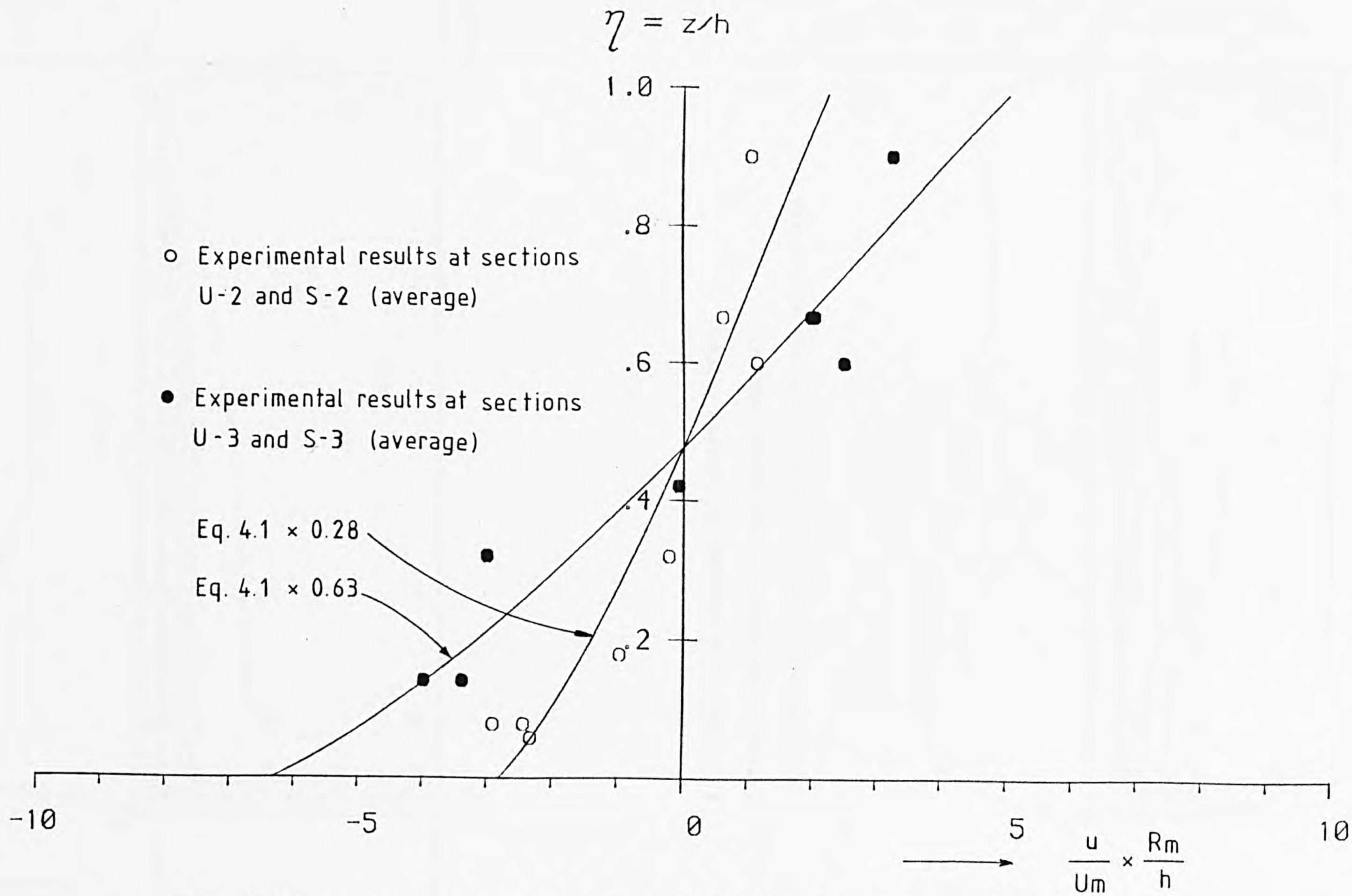

Fig. 6.87 Comparison between theoretical and experimental result of radial velocity component on a vertical at the centre of the channel

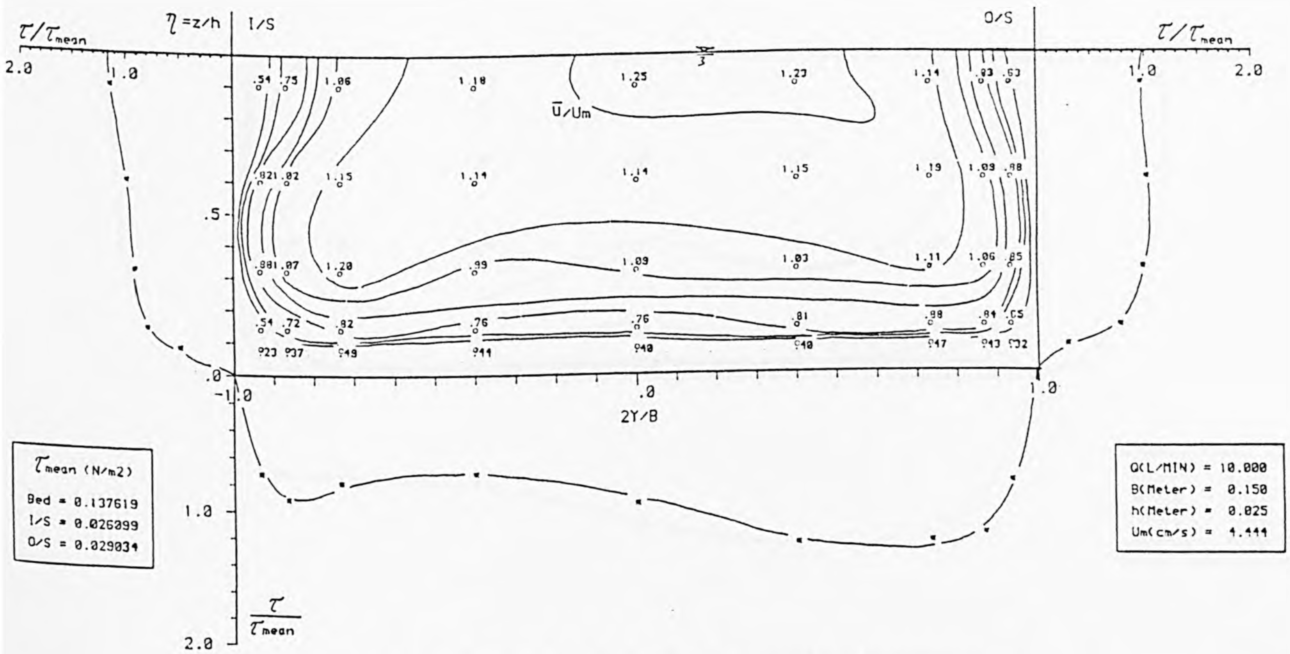

Fig. 6.88 Isovels of the velocity distribution in the direction of flow and boundary shear stress at section U-1, run no.1

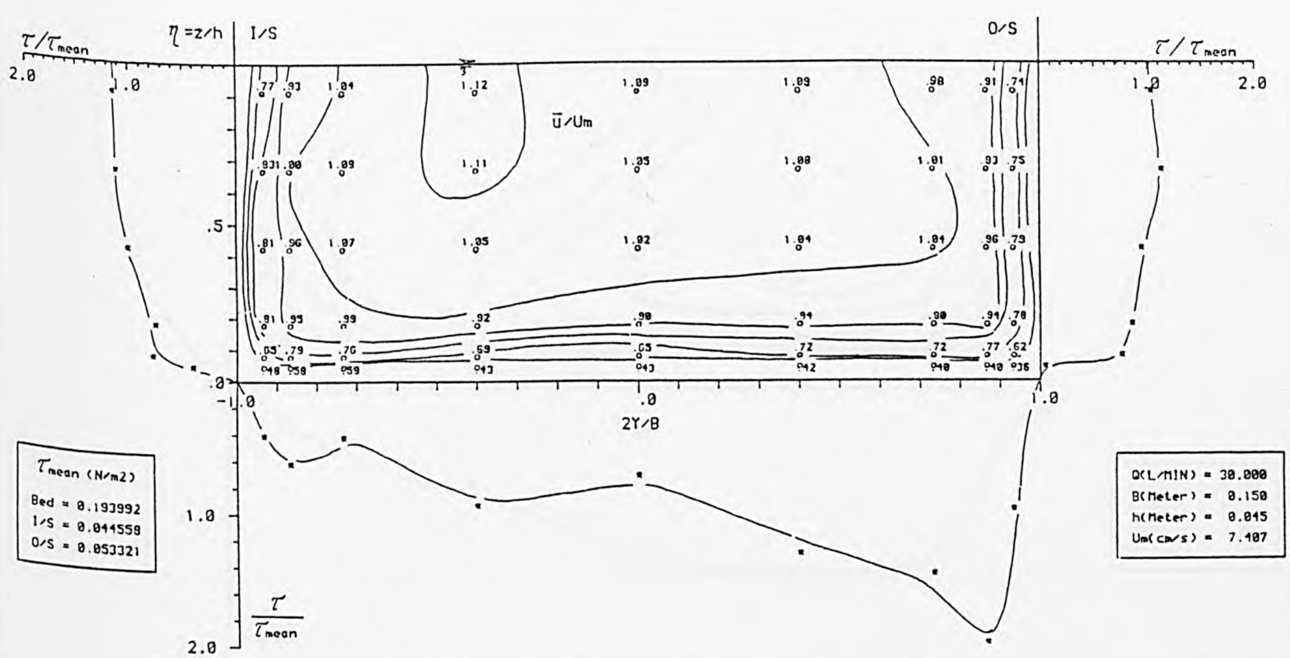

Fig. 6.89 Isovels of the velocity distribution in the direction of flow and boundary shear stress at section U-1, run no.2

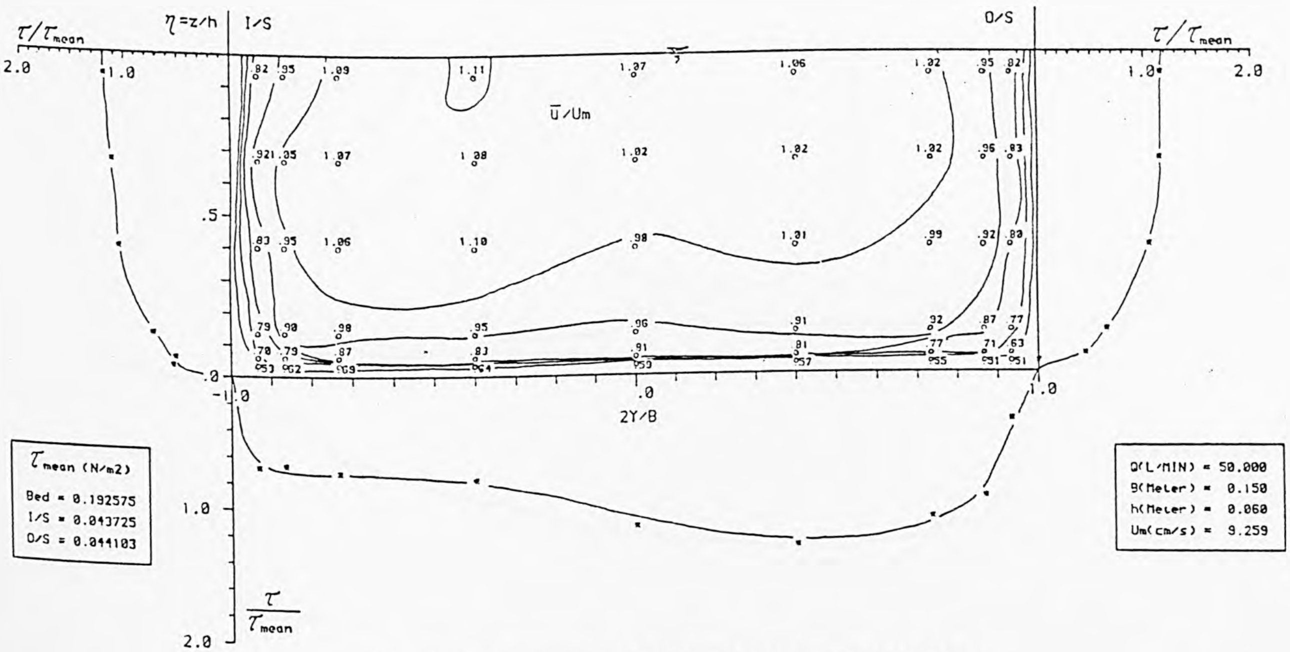

Fig. 6.90 Isovels of the velocity distribution in the direction of flow and boundary shear stress at section U-1, run no.3

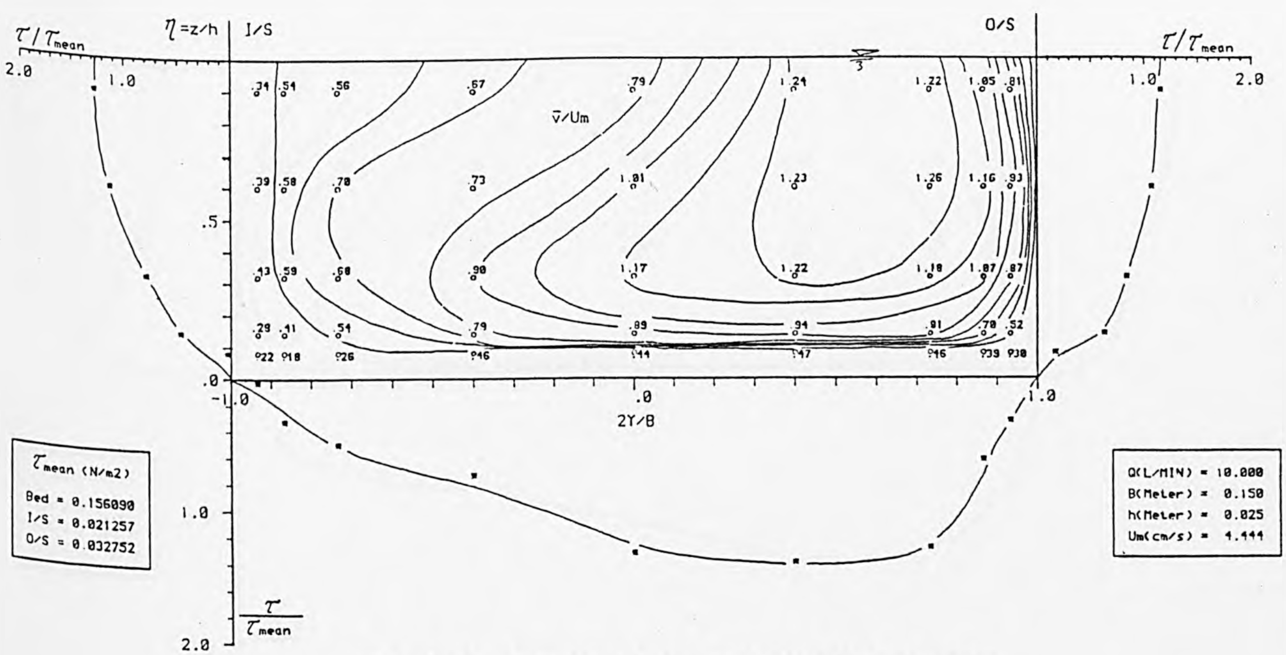

Fig. 6.91 Isovels of the velocity distribution in the direction of flow and boundary shear stress at section U-2, run no.1

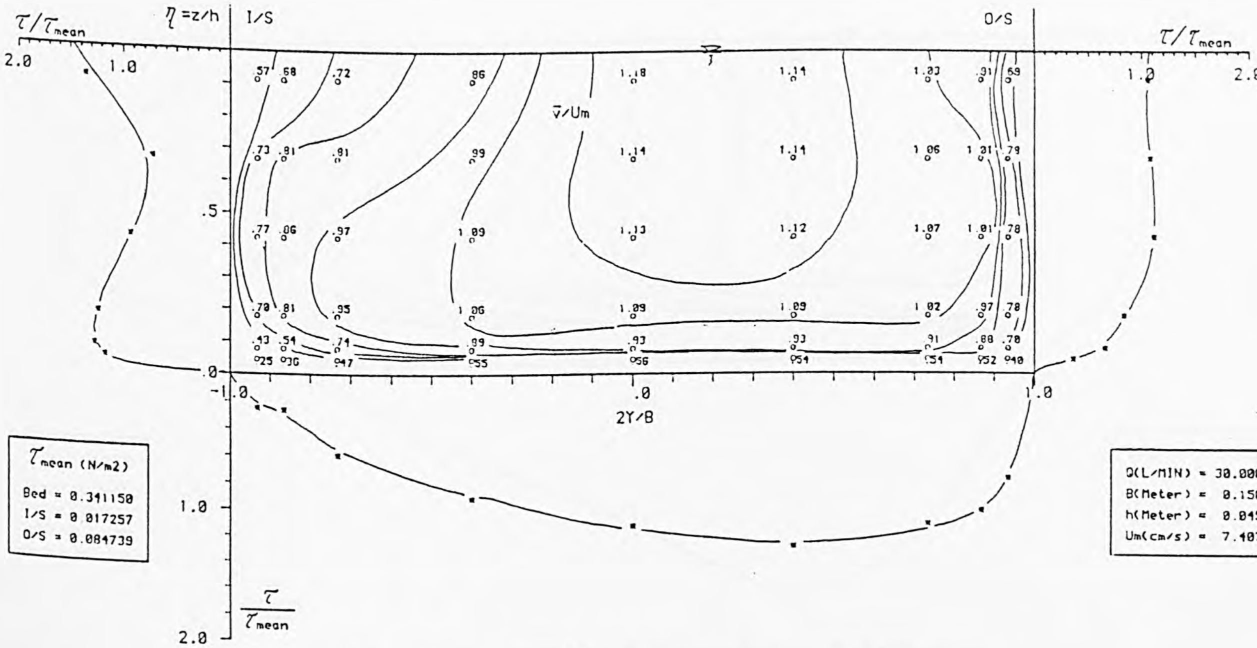

Fig. 6.92 Isovels of the velocity distribution in the direction of flow and boundary shear stress at section U-2, run no.2

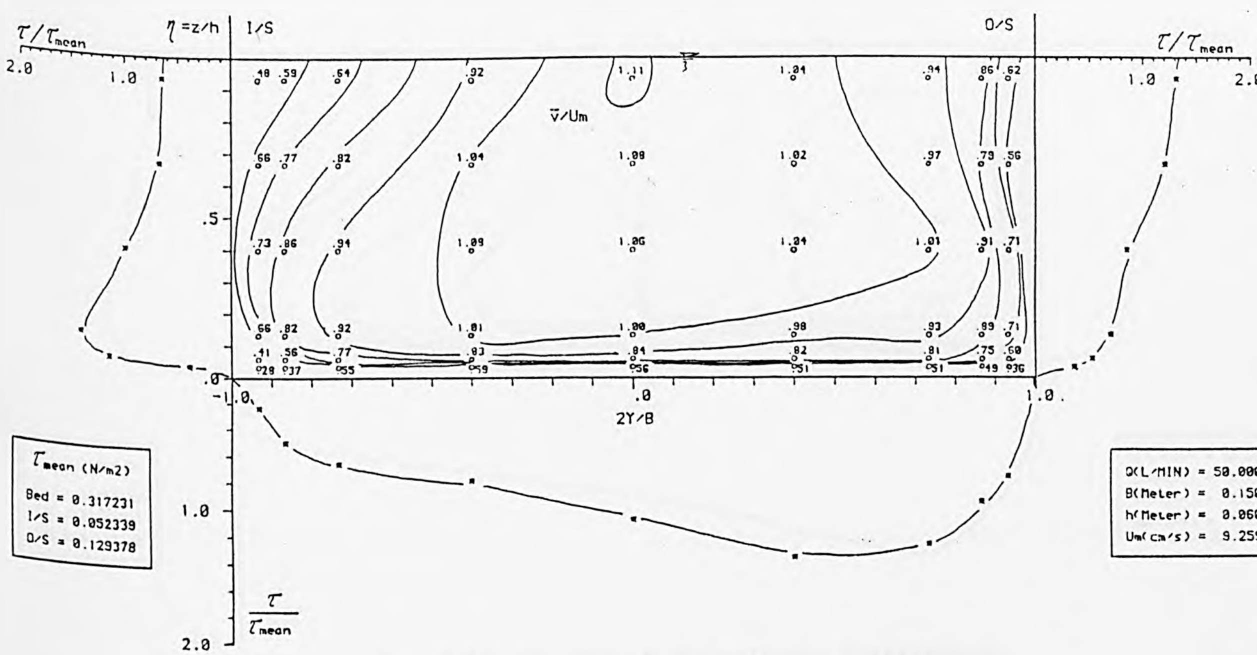

Fig. 6.93 Isovels of the velocity distribution in the direction of flow and boundary shear stress at section U-2, run no.3

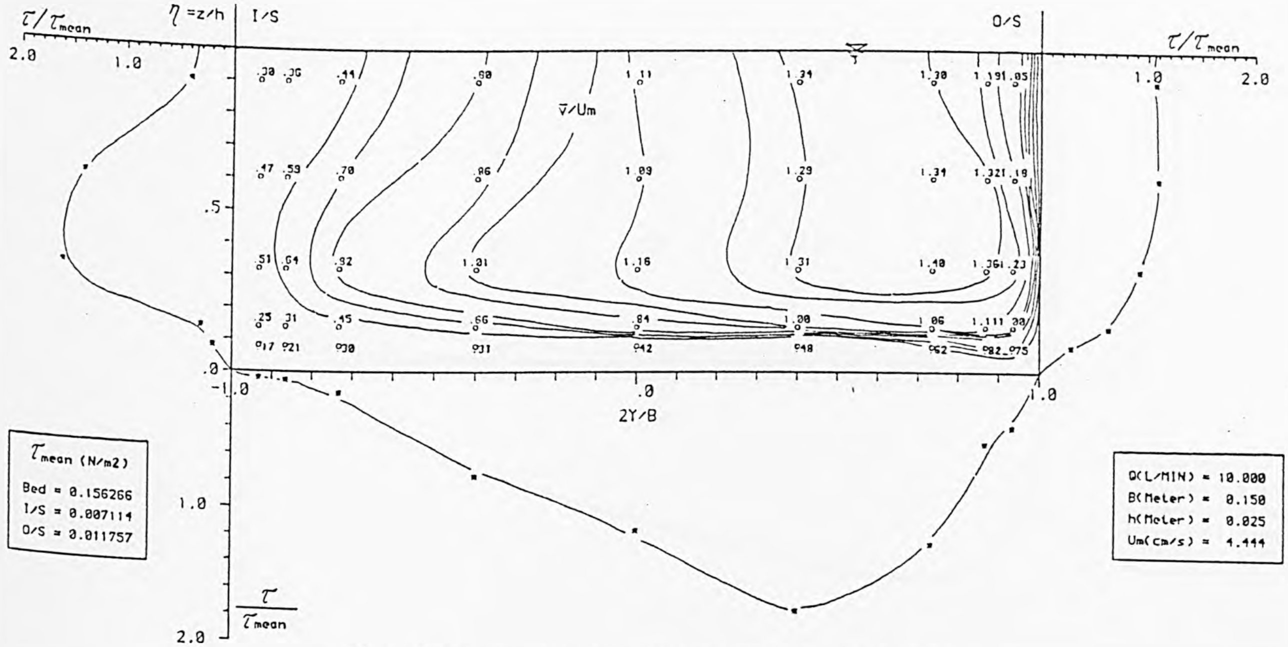

Fig. 6.94 Isovels of the velocity distribution in the direction of flow and boundary shear stress at section U-3, run no.1

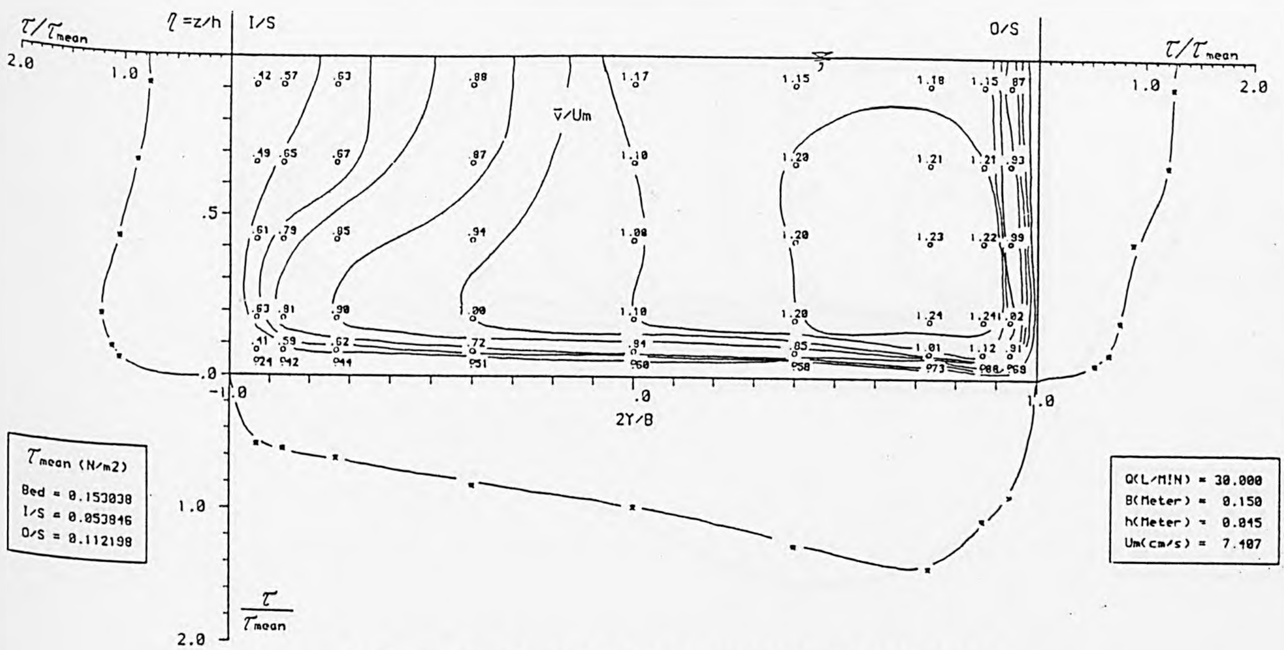

Fig. 6.95 Isovels of the velocity distribution in the direction of flow and boundary shear stress at section U-3, run no.2

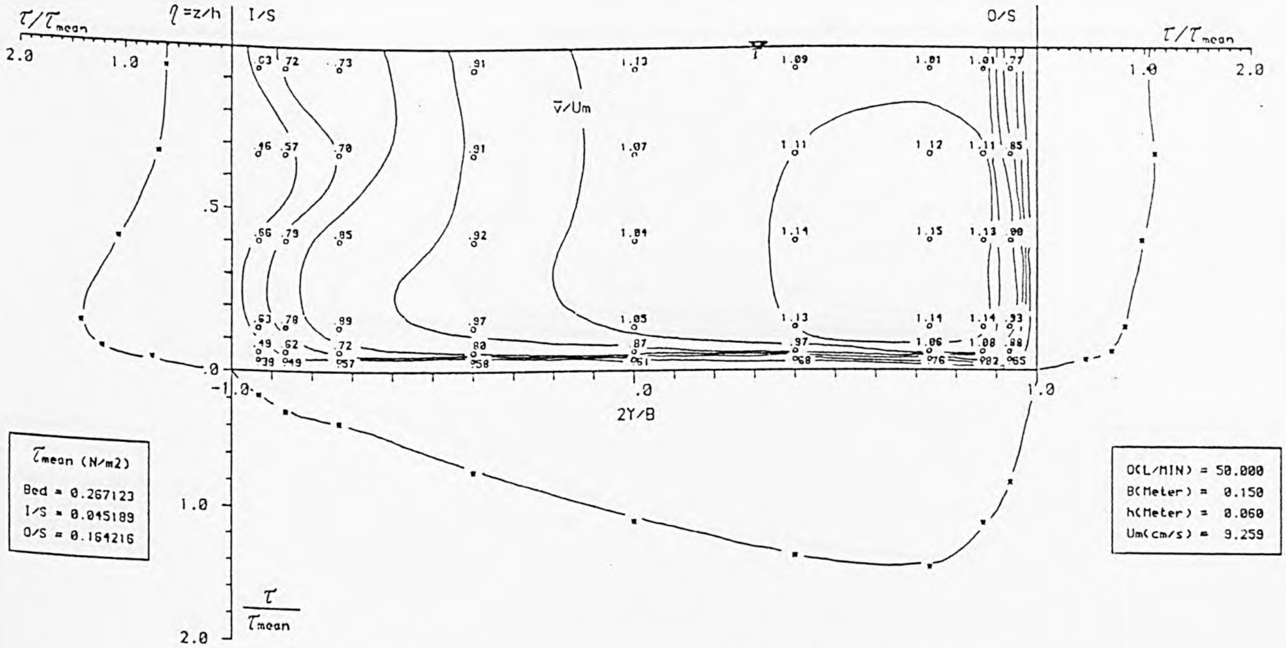

Fig. 6.96 Isovels of the velocity distribution in the direction of flow and boundary shear stress at section U-3, run no.3

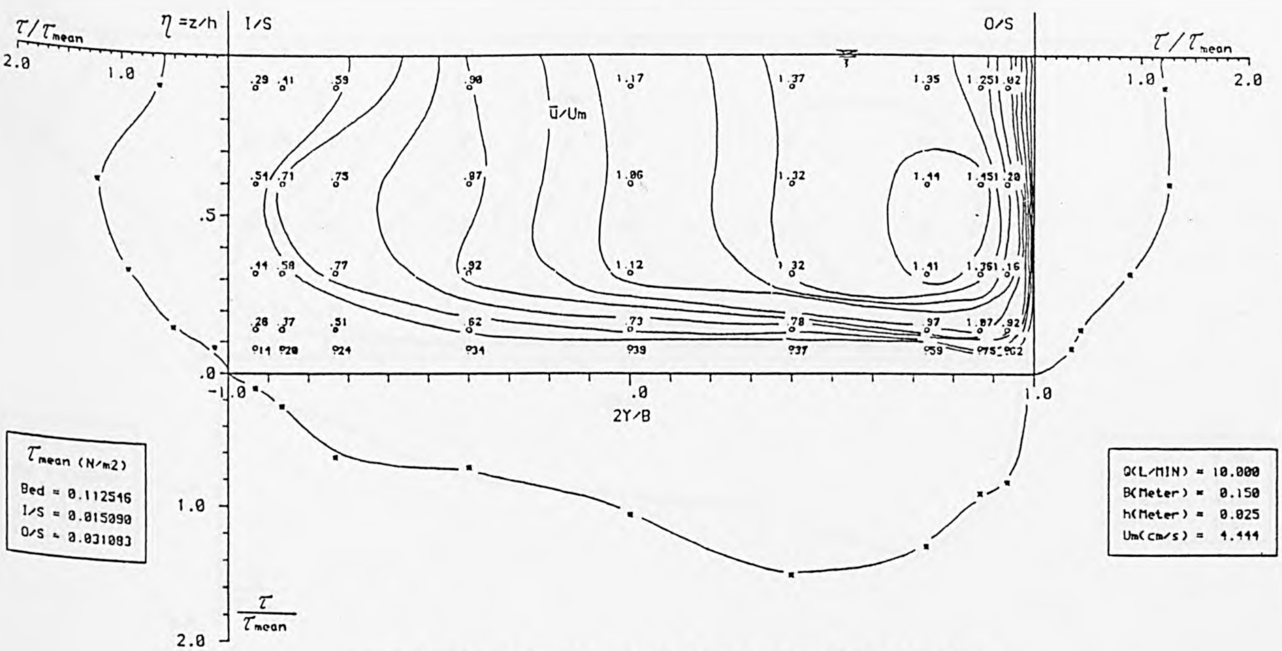

Fig. 6.97 Isovels of the velocity distribution in the direction of flow and boundary shear stress at section U-4, run no.1

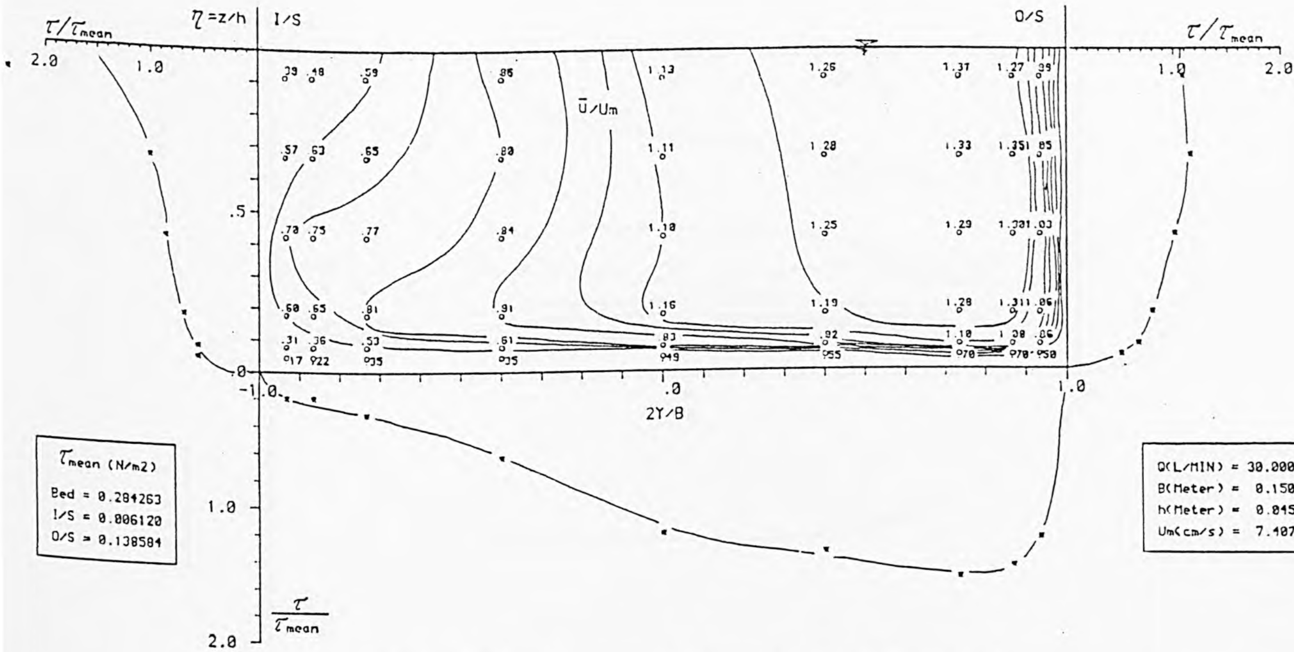

Fig. 6.98 Isovels of the velocity distribution in the direction of flow and boundary shear stress at section U-4, run no.2

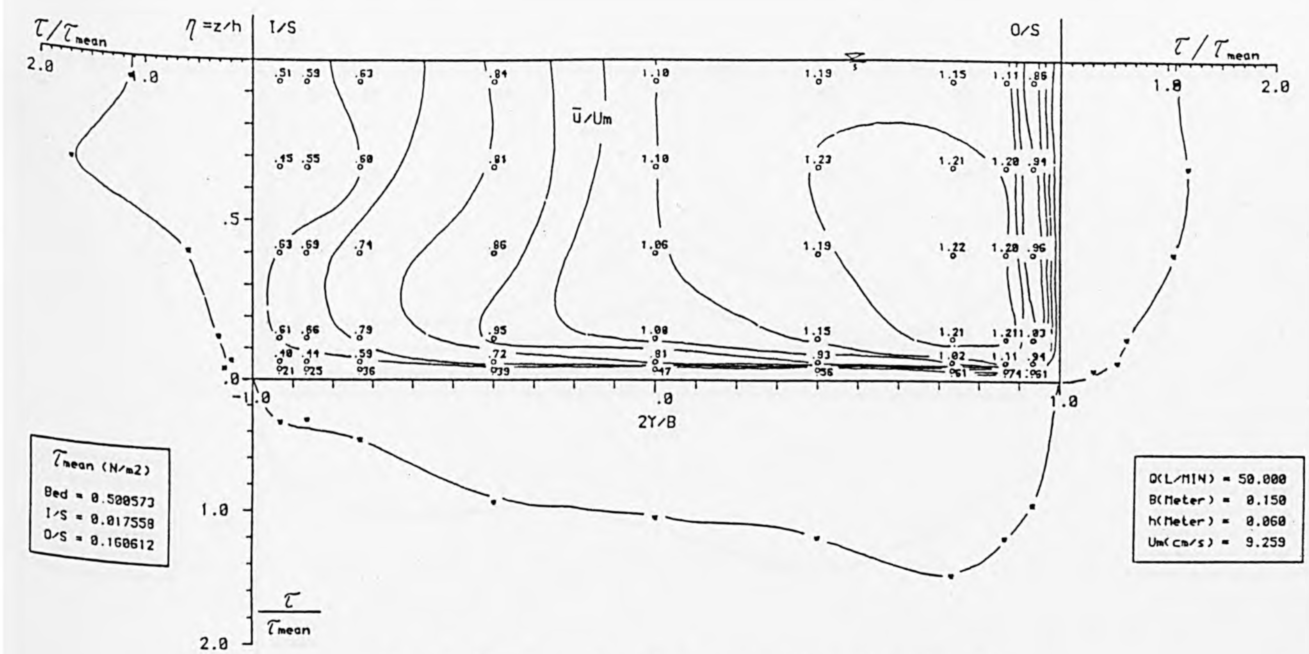

Fig. 6.99 Isovels of the velocity distribution in the direction of flow and boundary shear stress at section U-4, run no.3

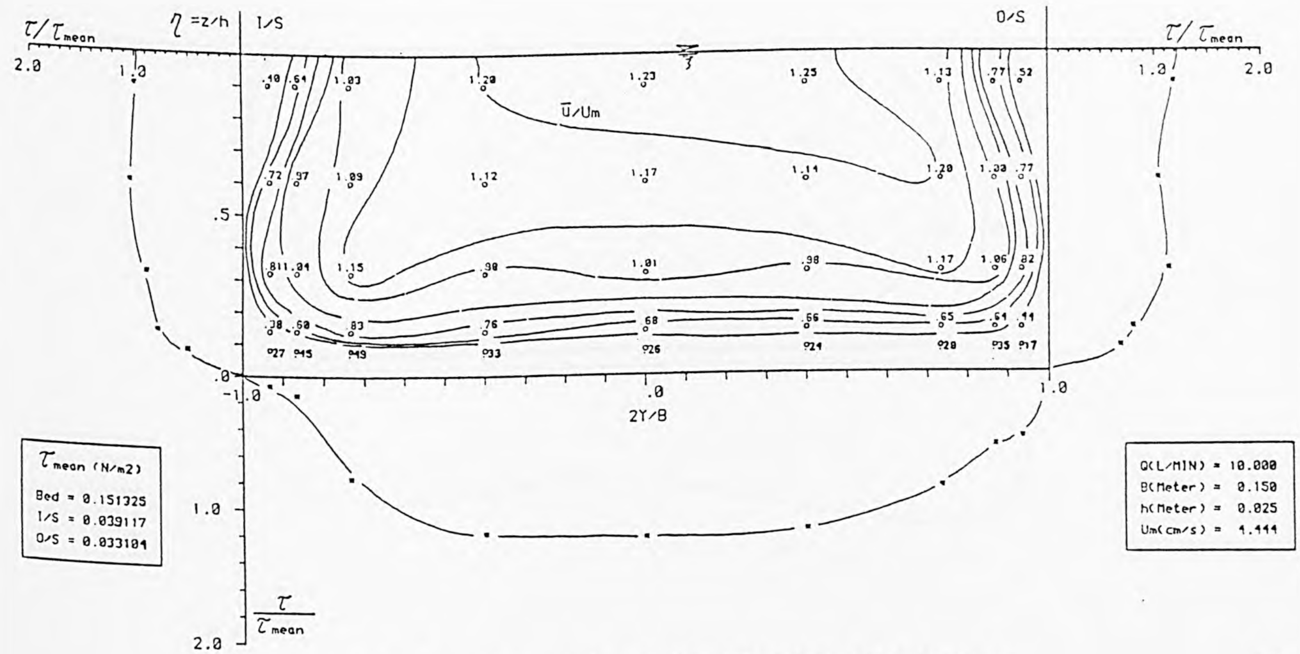

Fig. 6.100 Isovels of the velocity distribution in the direction of flow and boundary shear stress at section S-1, run no.1

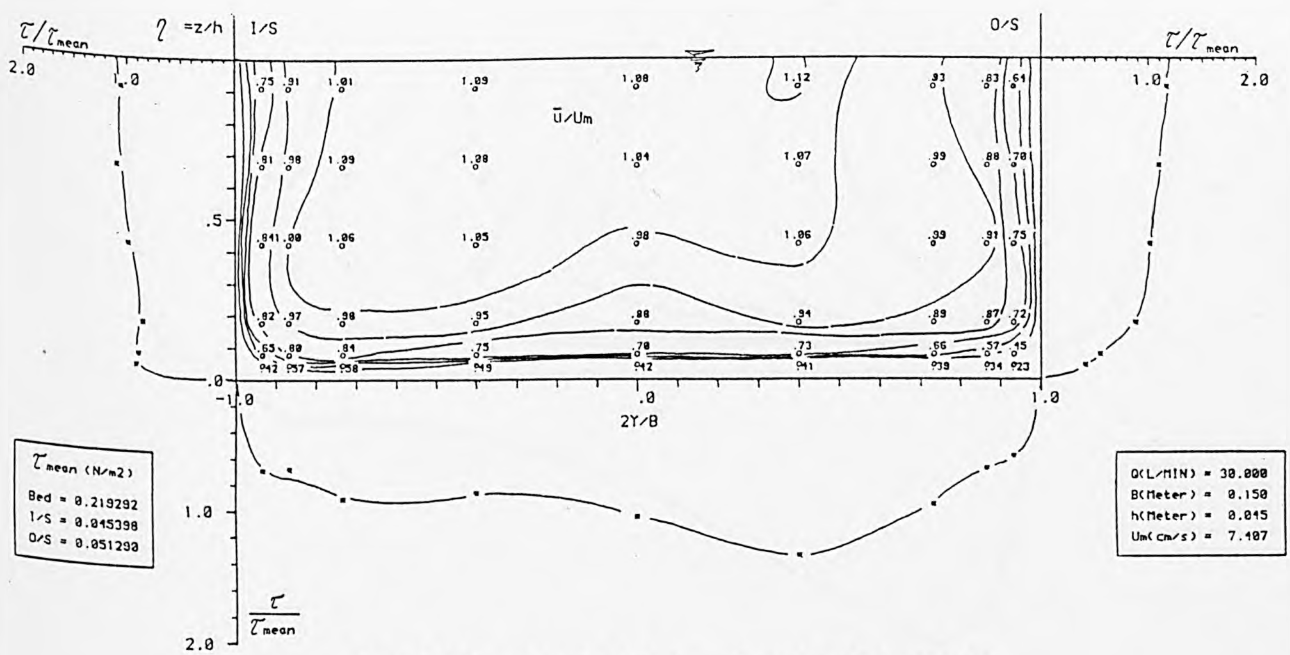

Fig. 6.101 Isovels of the velocity distribution in the direction of flow and boundary shear stress at section S-1, run no.2

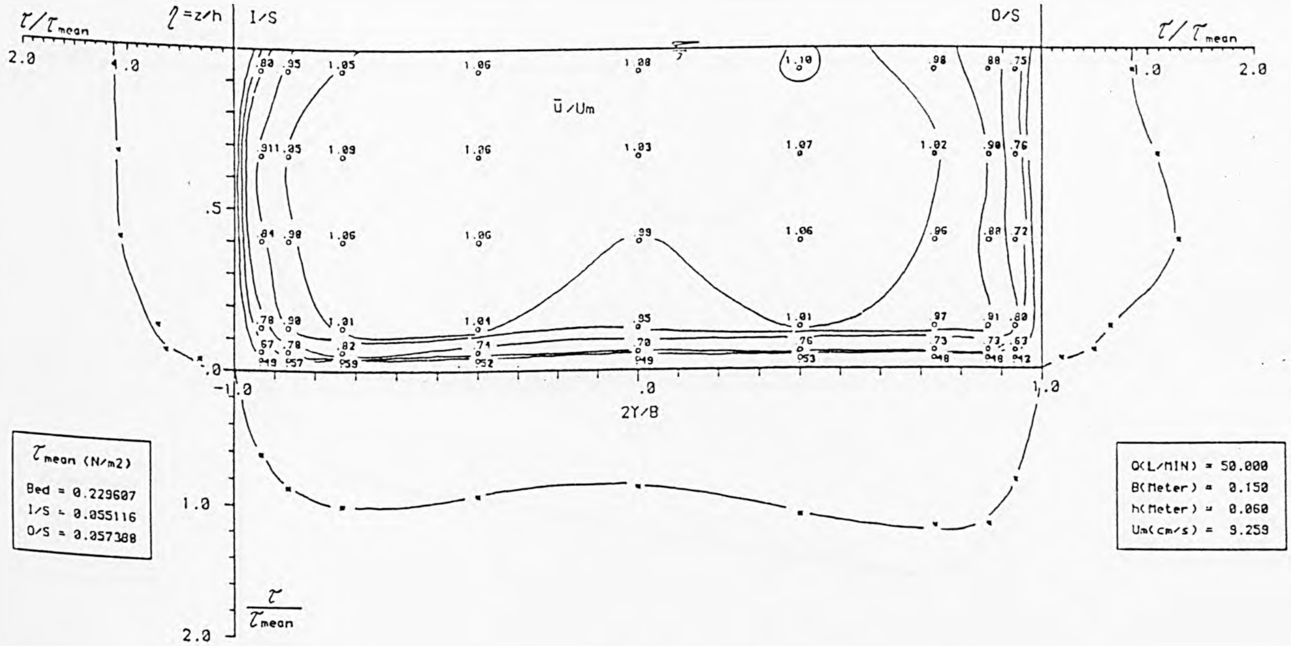

Fig. 6.102 Isovels of the velocity distribution in the direction of flow and boundary shear stress at section S-1, run no.3

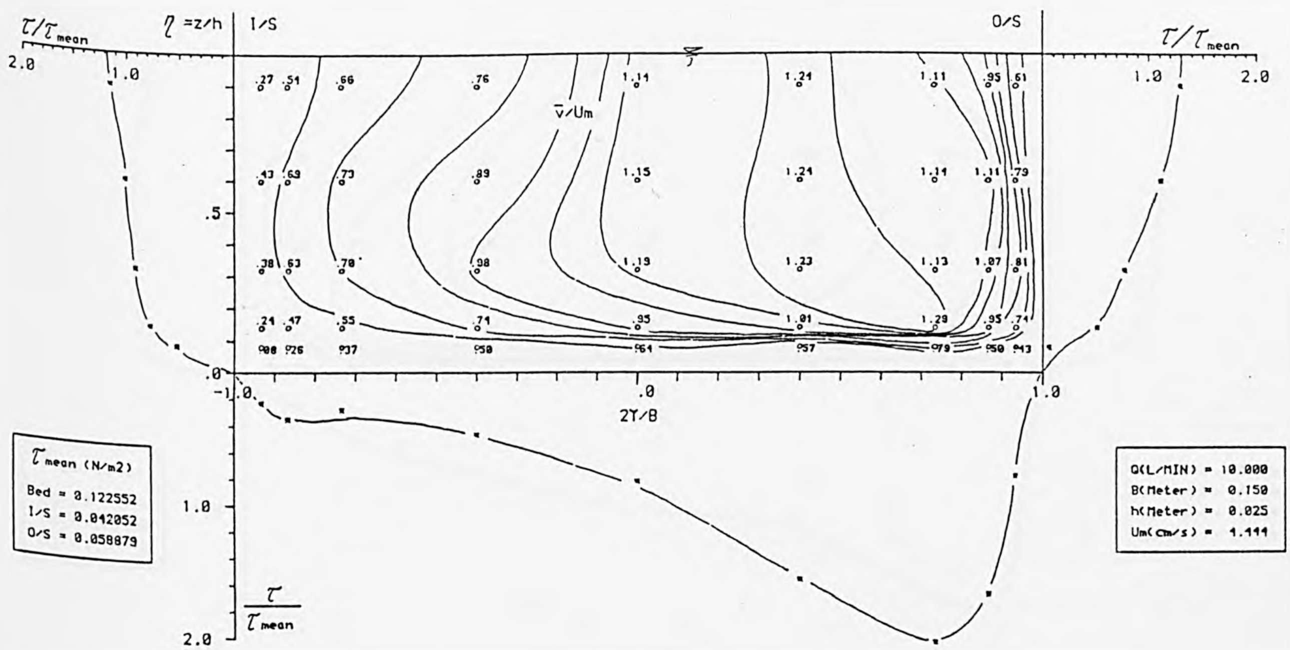

Fig. 6.103 Isovels of the velocity distribution in the direction of flow and boundary shear stress at section S-2, run no.1

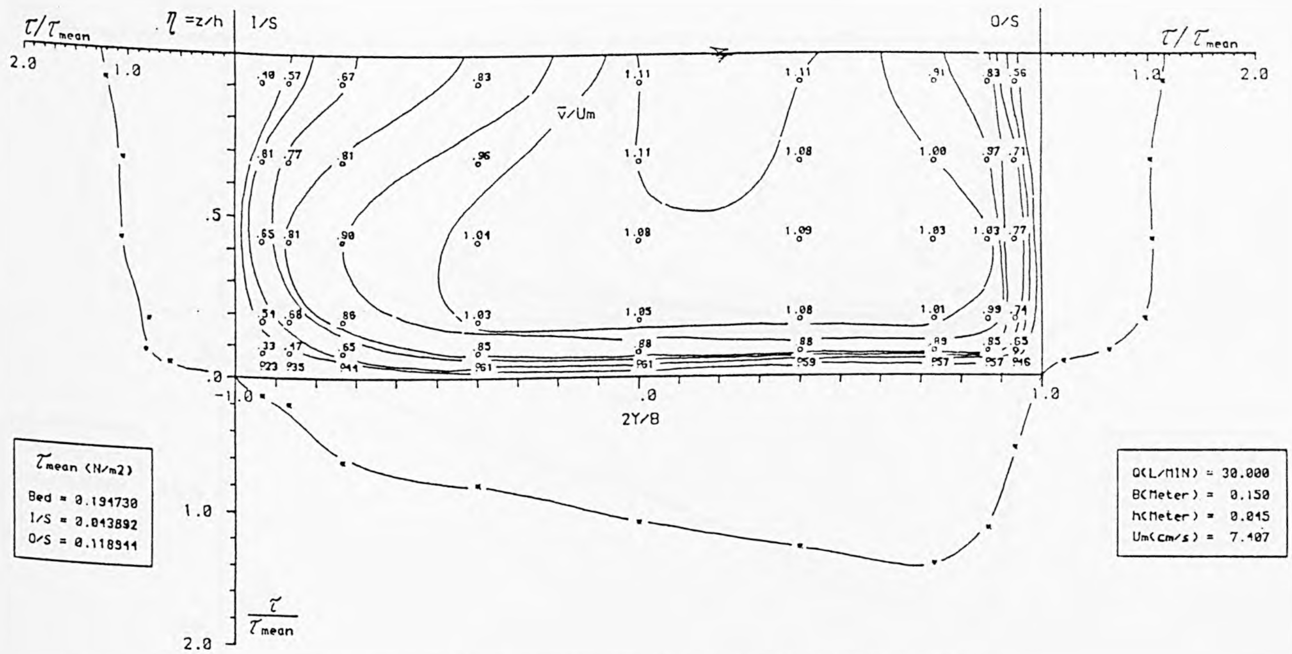

Fig. 6.104 Isovels of the velocity distribution in the direction of flow and boundary shear stress at section S-2, run no.2

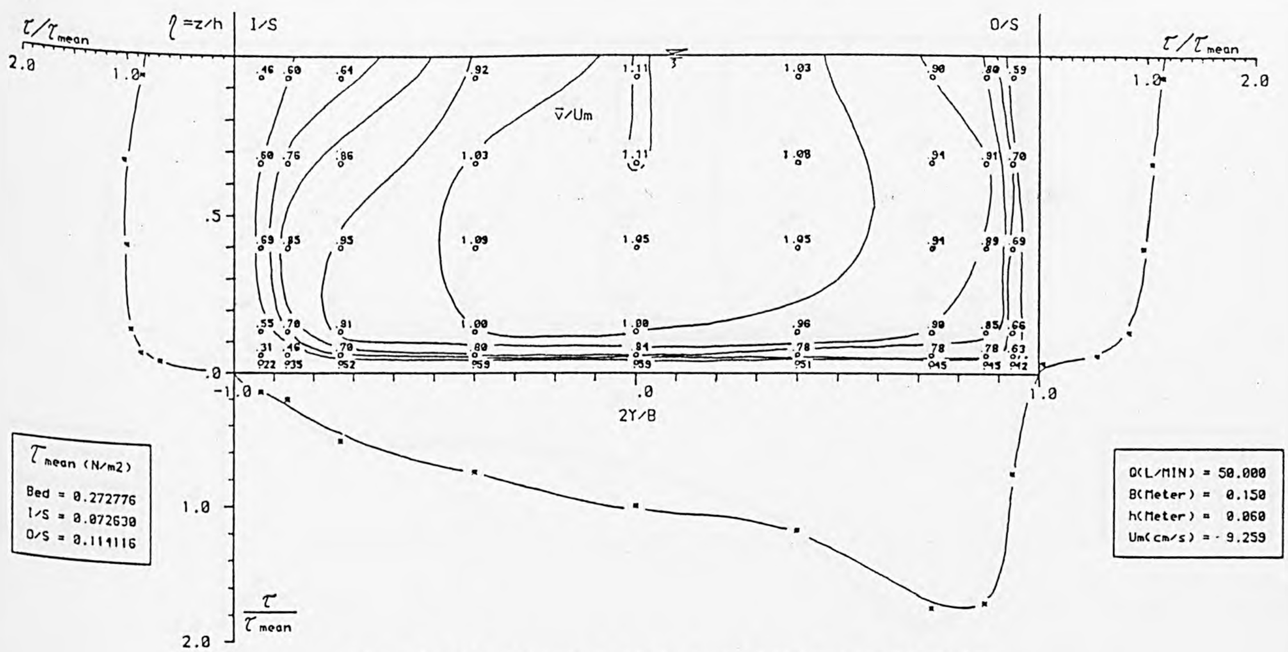

Fig. 6.105 Isovels of the velocity distribution in the direction of flow and boundary shear stress at section S-2, run no.3

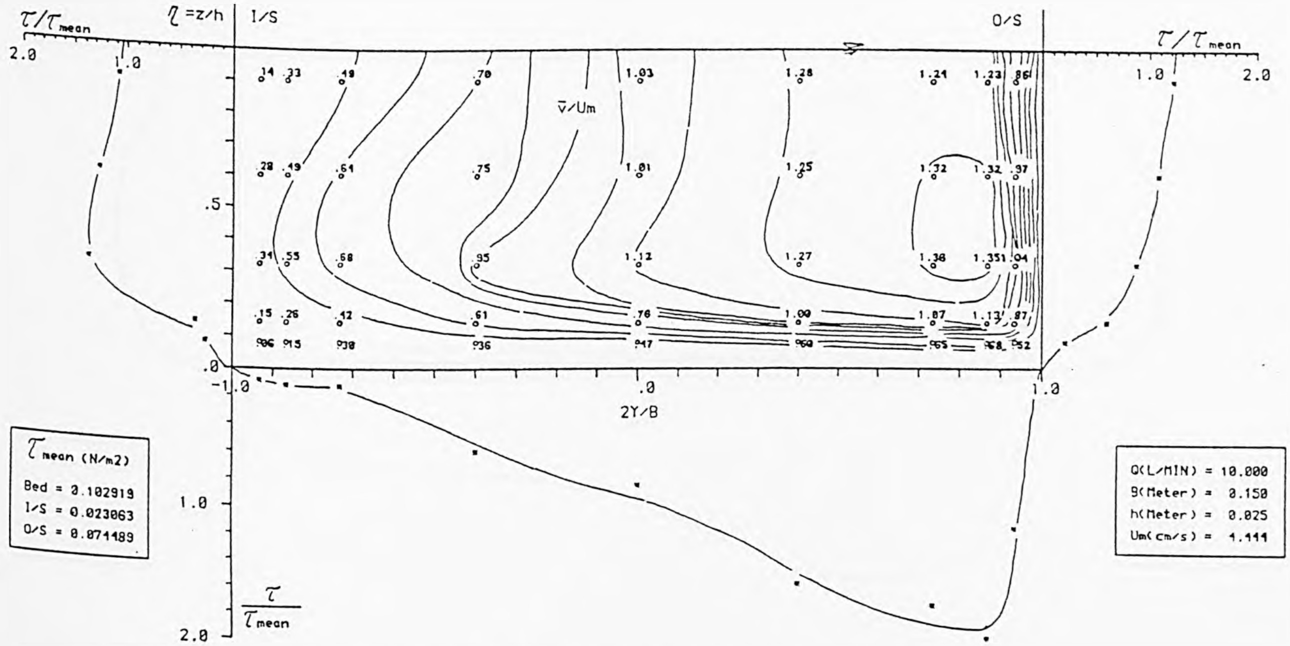

Fig. 6.106 Isovels of the velocity distribution in the direction of flow and boundary shear stress at section S-3, run no.1

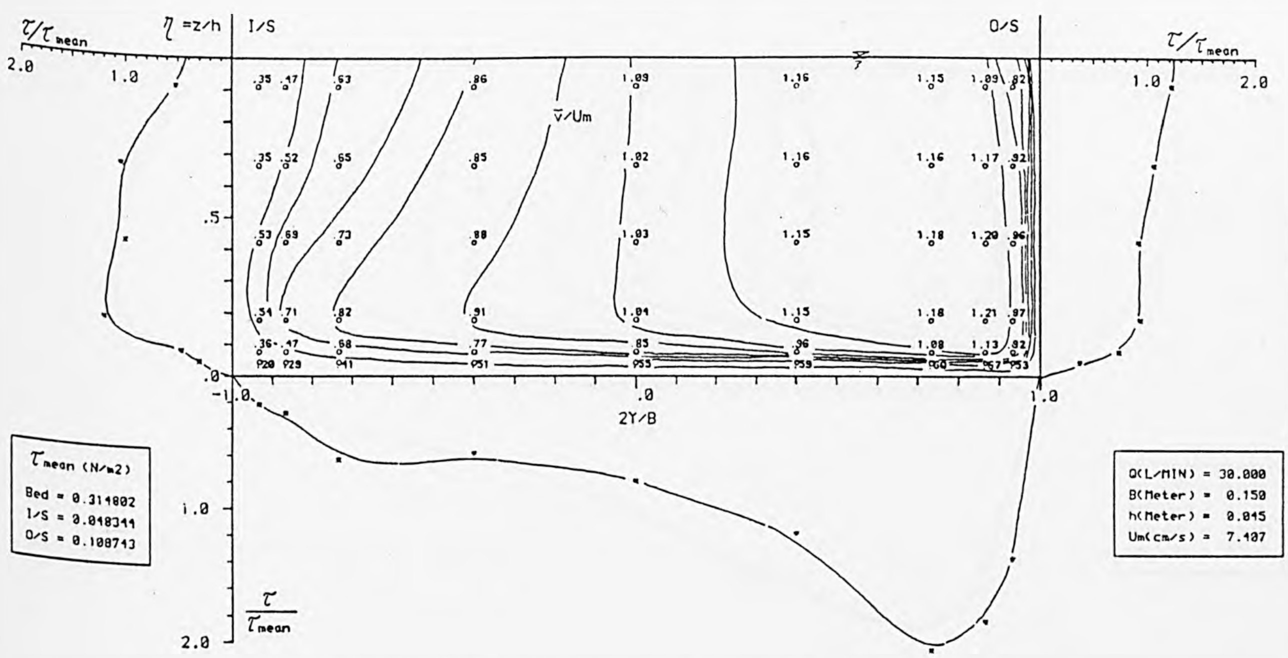

Fig. 6.107 Isovels of the velocity distribution in the direction of flow and boundary shear stress at section S-3, run no.2

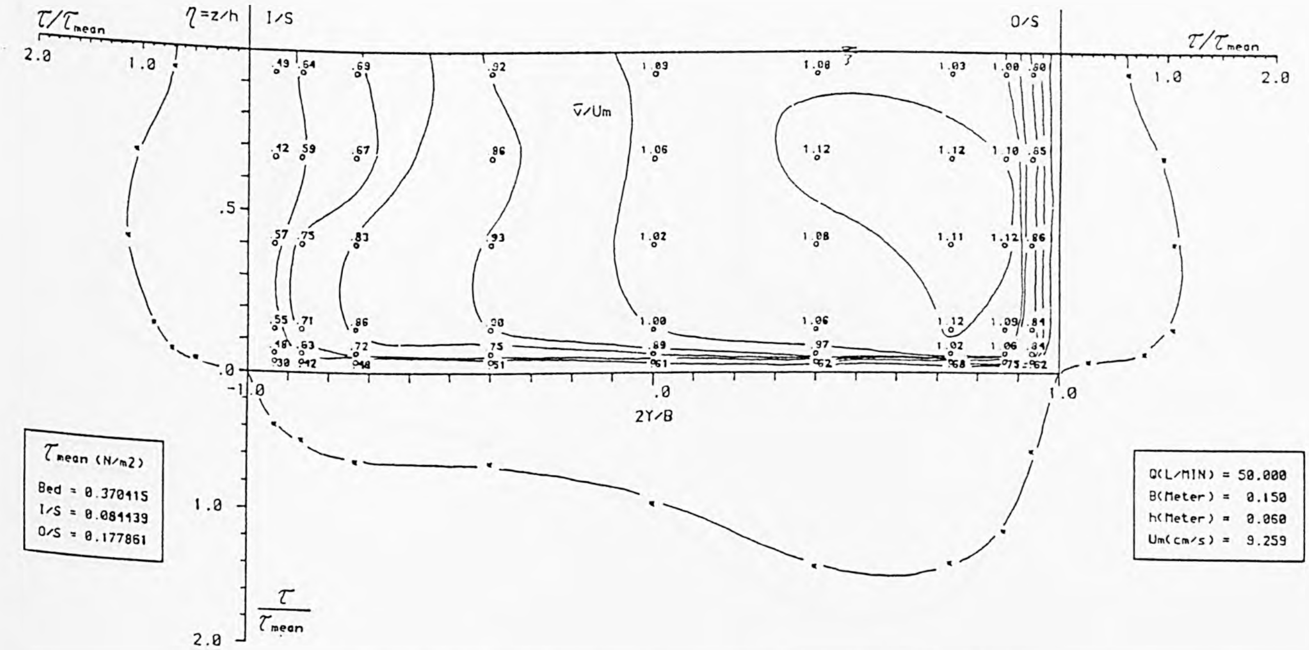

Fig. 6.108 Isovels of the velocity distribution in the direction of flow and boundary shear stress at section S-3, run no.3

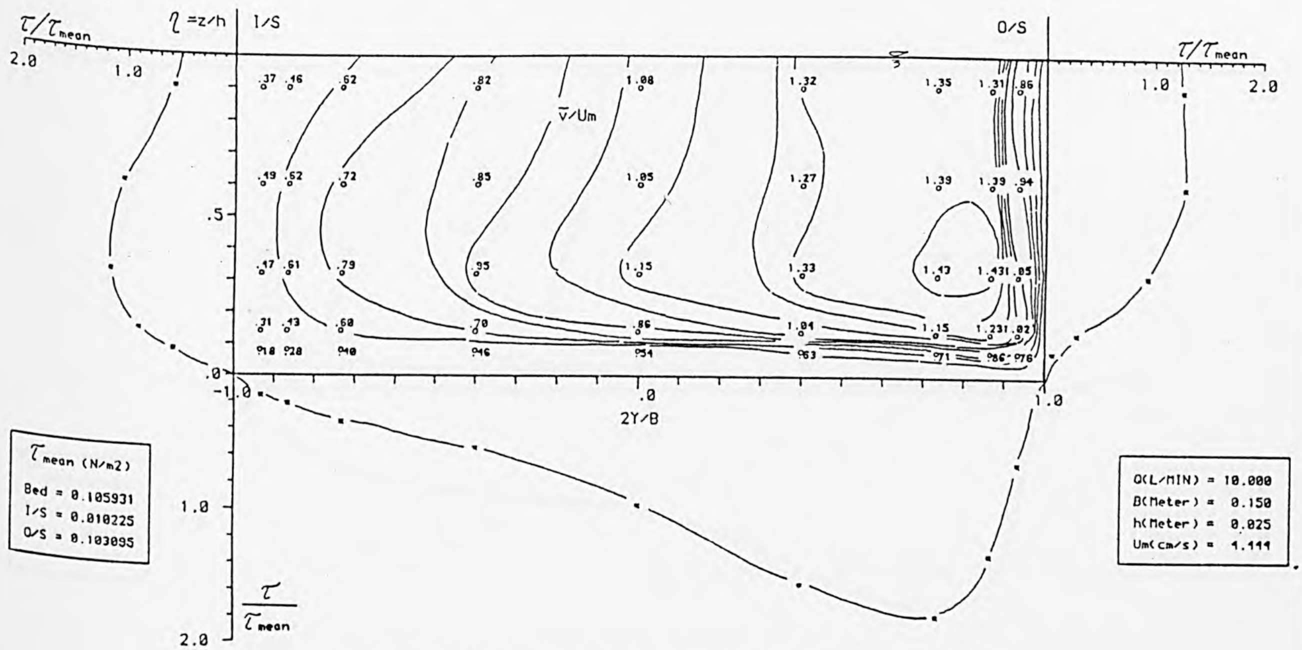

Fig. 6.109 Isovels of the velocity distribution in the direction of flow and boundary shear stress at section S-4, run no.1

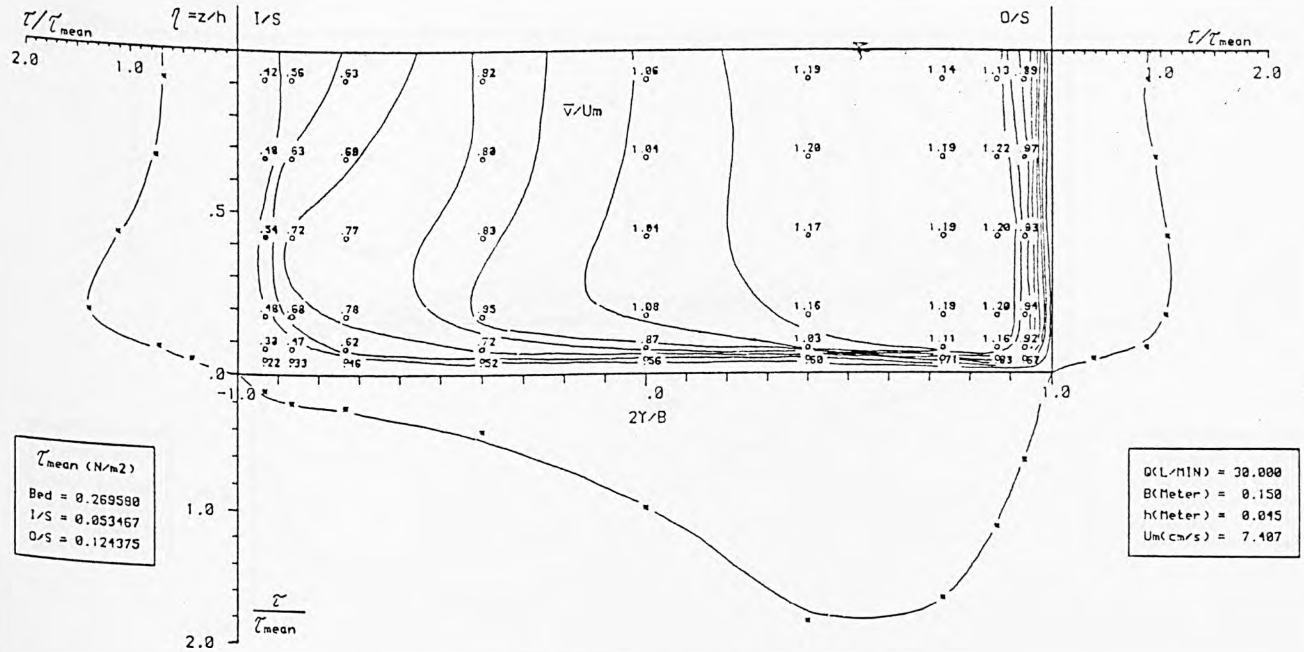

Fig. 6.110 Isovels of the velocity distribution in the direction of flow and boundary shear stress at section S-4, run no.2

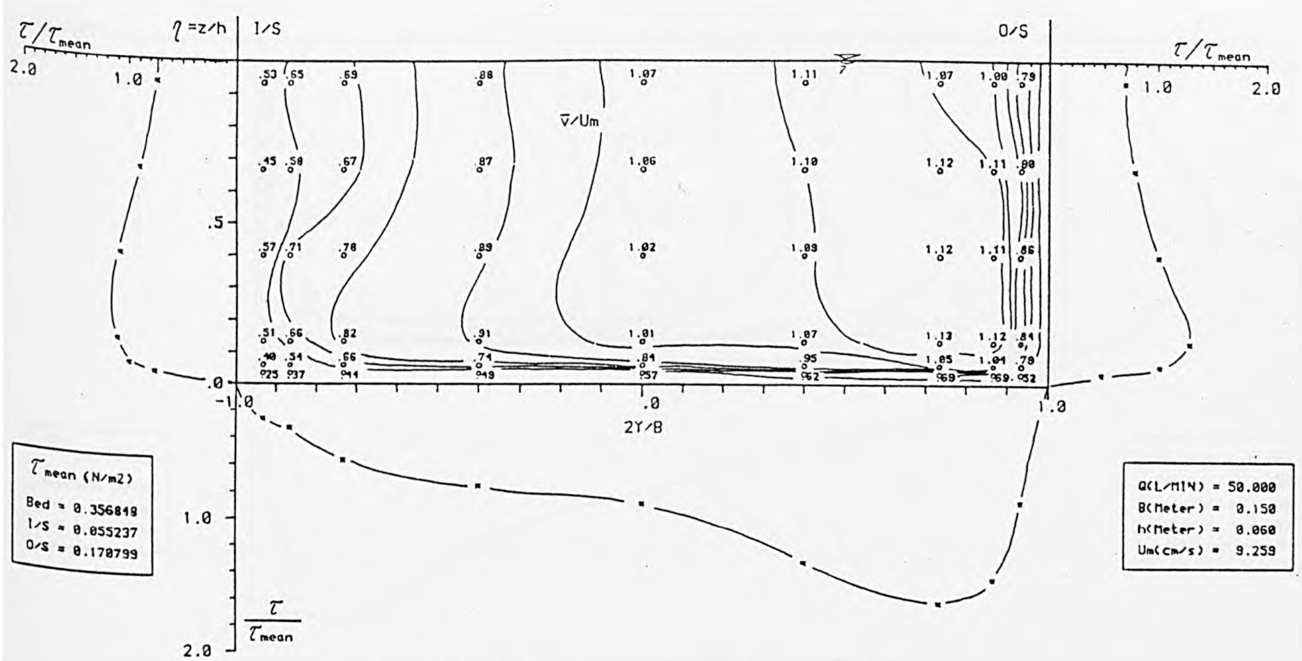

Fig. 6.111 Isovels of the velocity distribution in the direction of flow and boundary shear stress at section S-4, run no.3

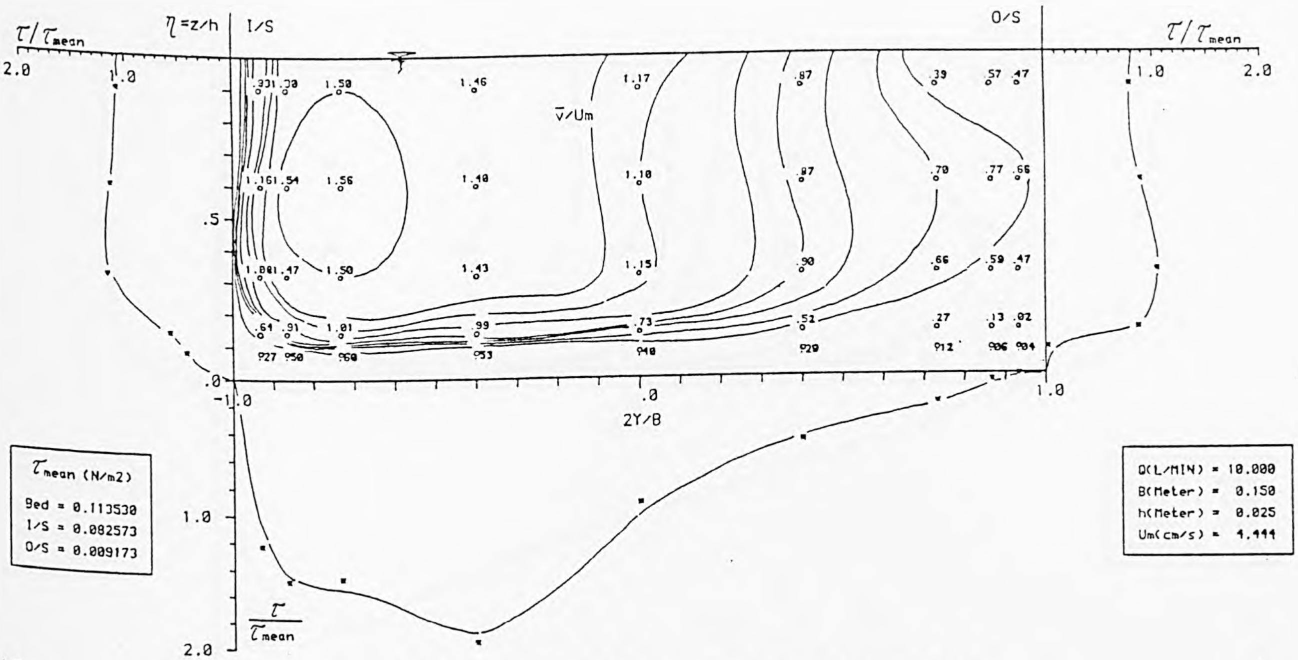

Fig. 6.112 Isovels of the velocity distribution in the direction of flow and boundary shear stress at section S-5, run no.1

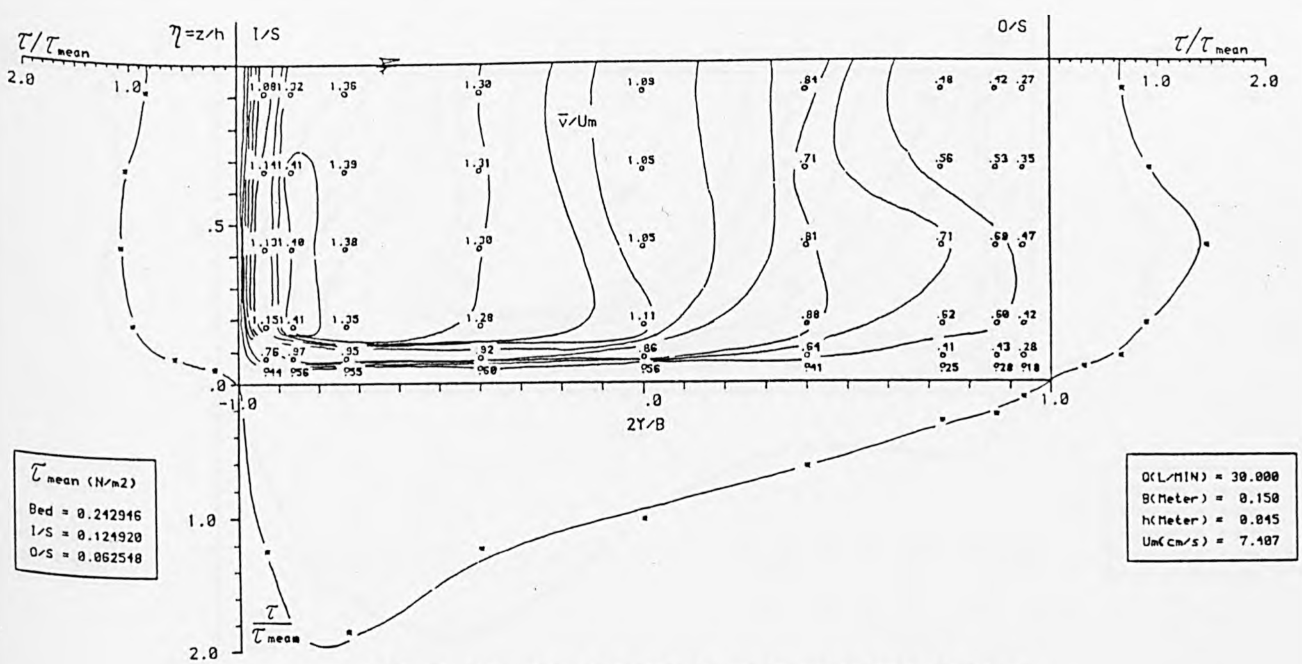

Fig. 6.113 Isovels of the velocity distribution in the direction of flow and boundary shear stress at section S-5, run no.2

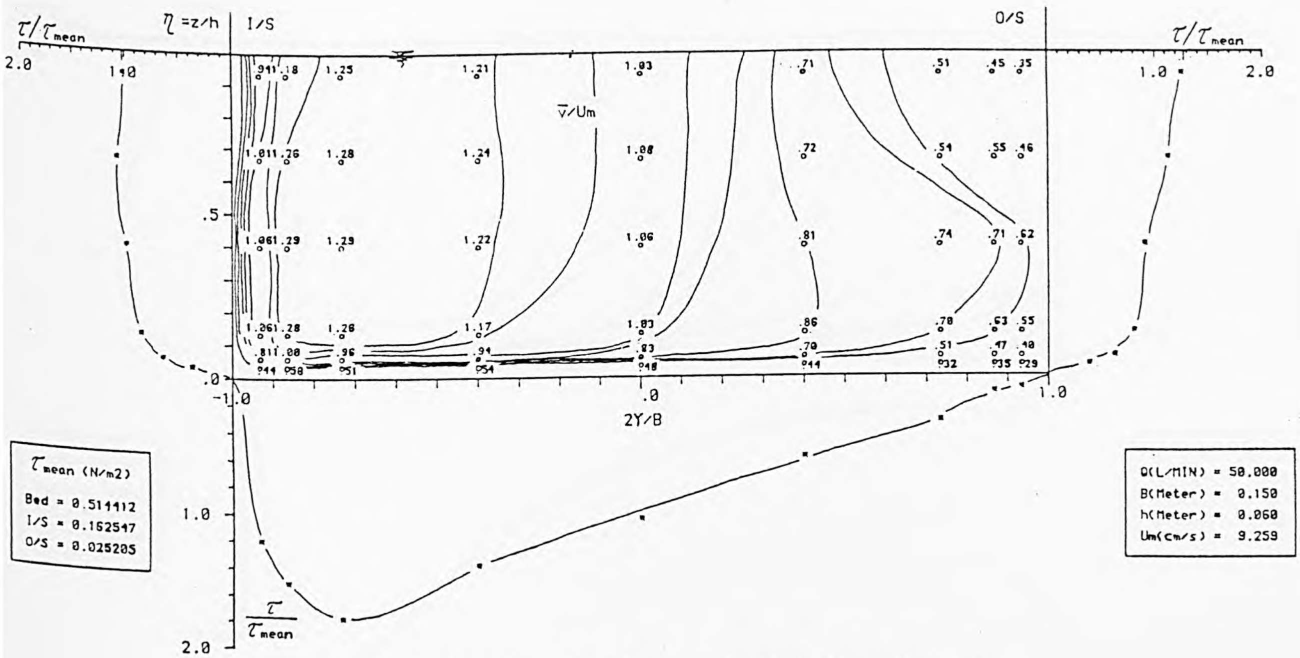

Fig. 6.114 Isovels of the velocity distribution in the direction of flow and boundary shear stress at section S-5, run no.3

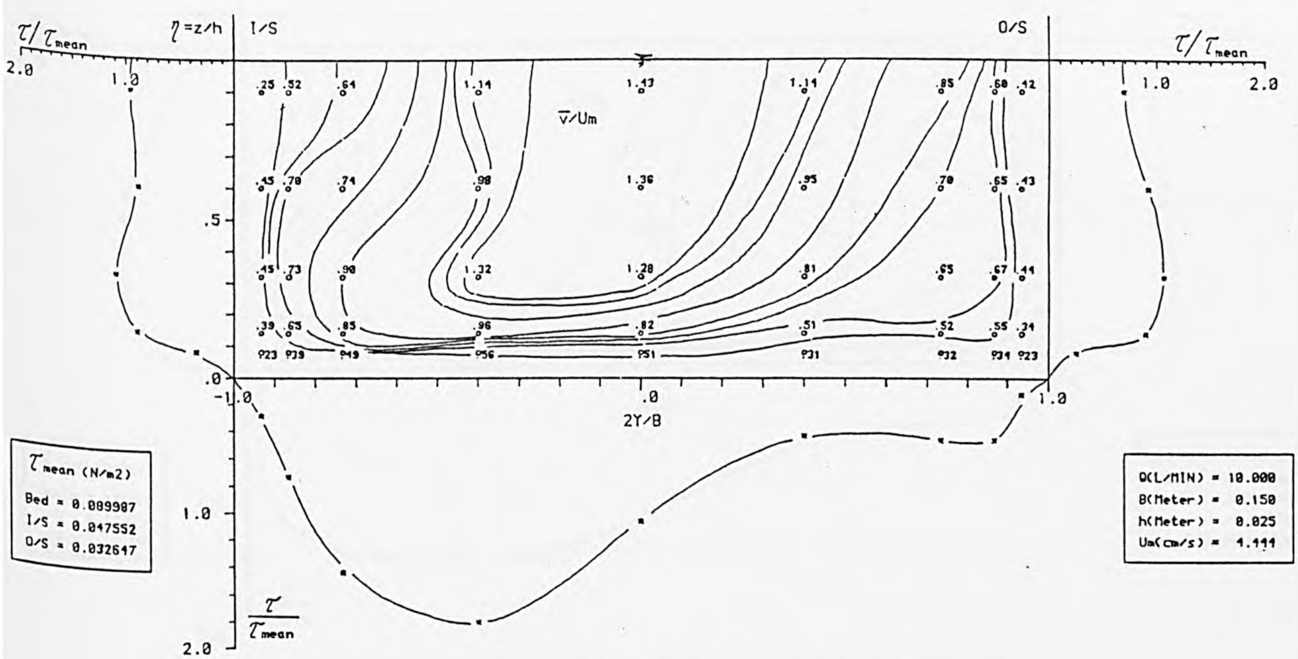

Fig. 6.115 Isovels of the velocity distribution in the direction of flow and boundary shear stress at section S-6, run no.1

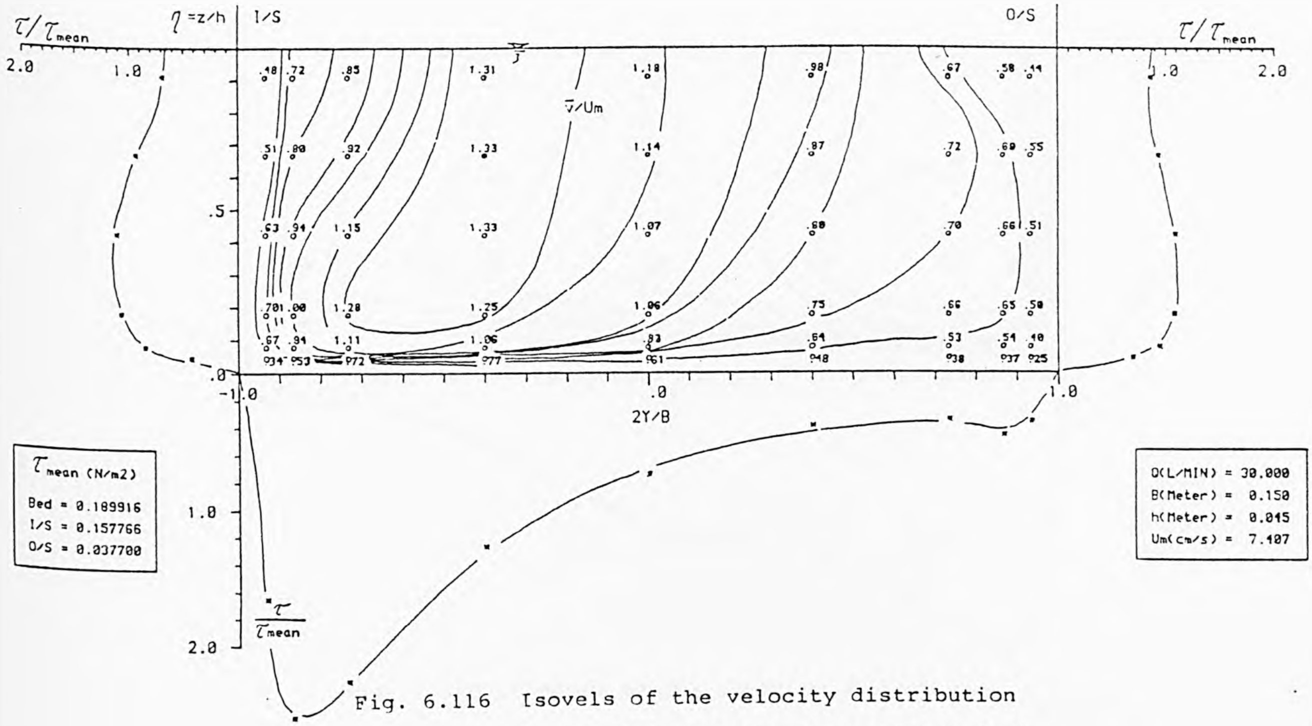

Fig. 6.116 Isovels of the velocity distribution in the direction of flow and boundary shear stress at section S-6, run no.2

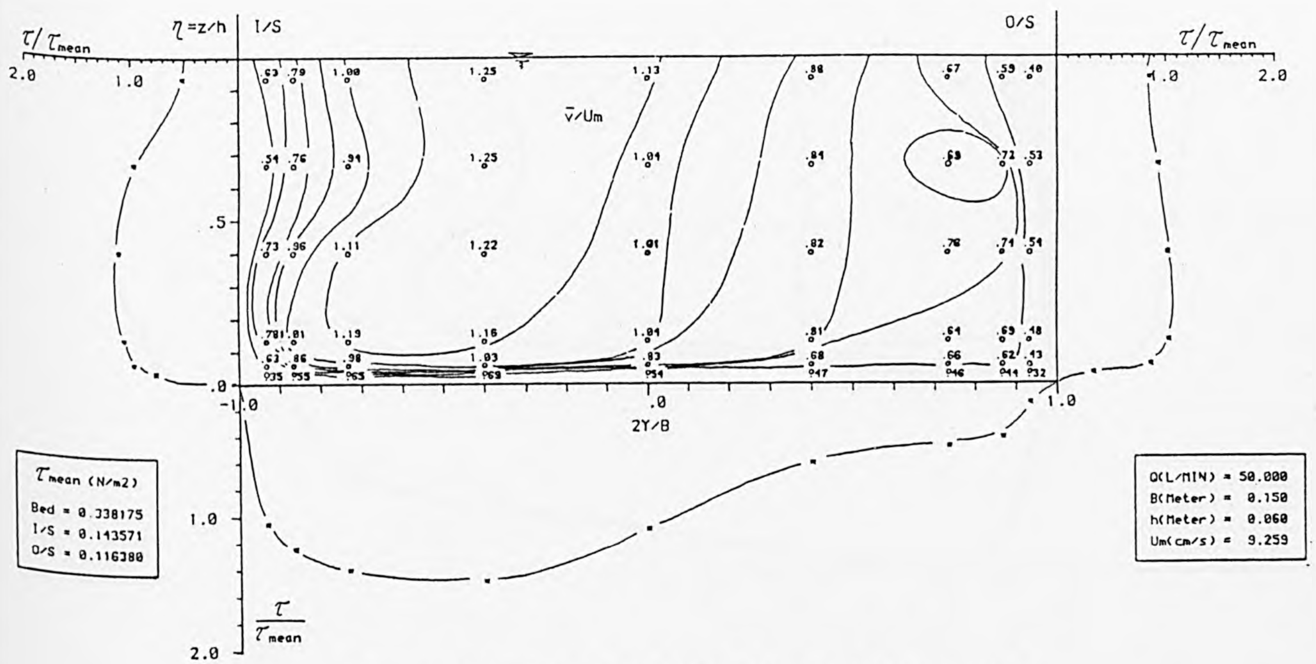

Fig. 6.117 Isovels of the velocity distribution in the direction of flow and boundary shear stress at section S-6, run no.3

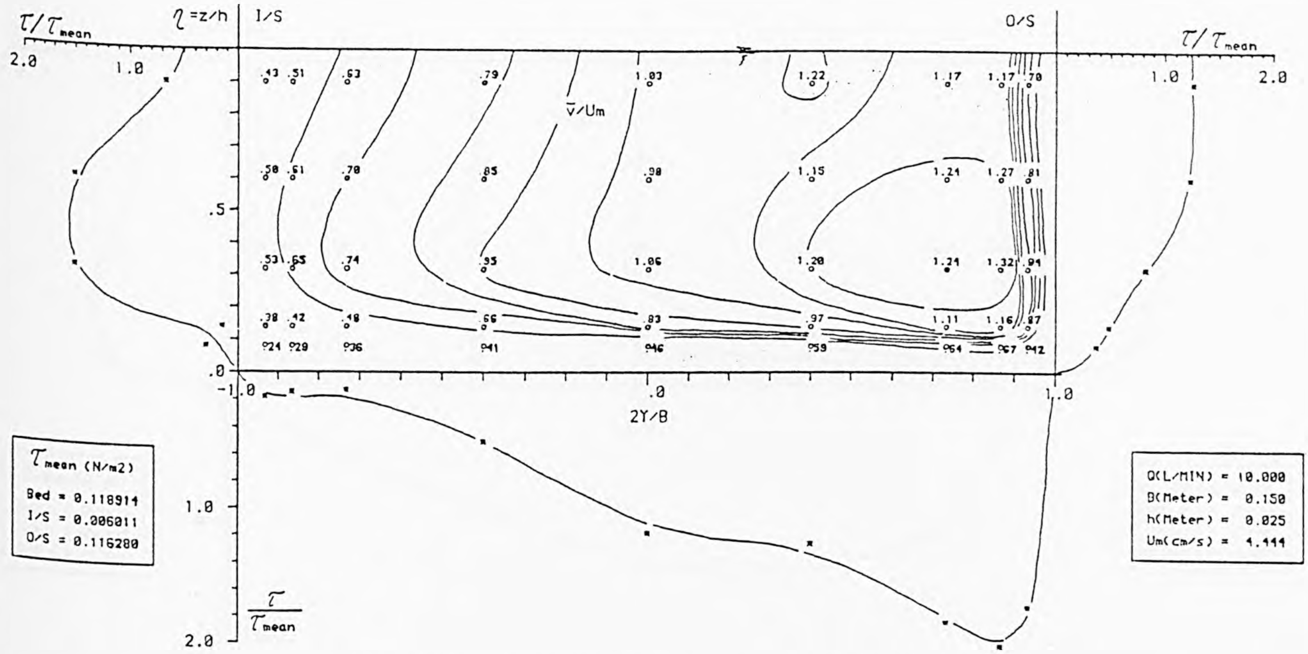

Fig. 6.118 Isovels of the velocity distribution in the direction of flow and boundary shear stress at section S-7, run no.1

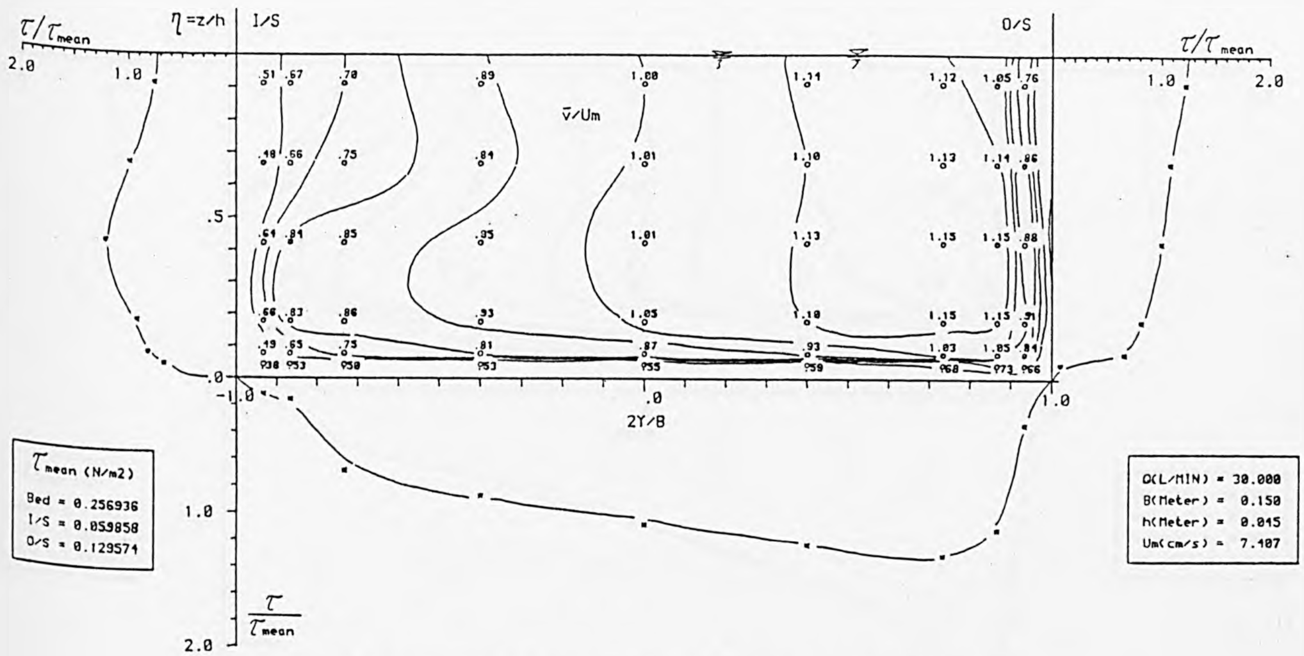

Fig. 6.119 Isovels of the velocity distribution in the direction of flow and boundary shear stress at section S-7, run no.2

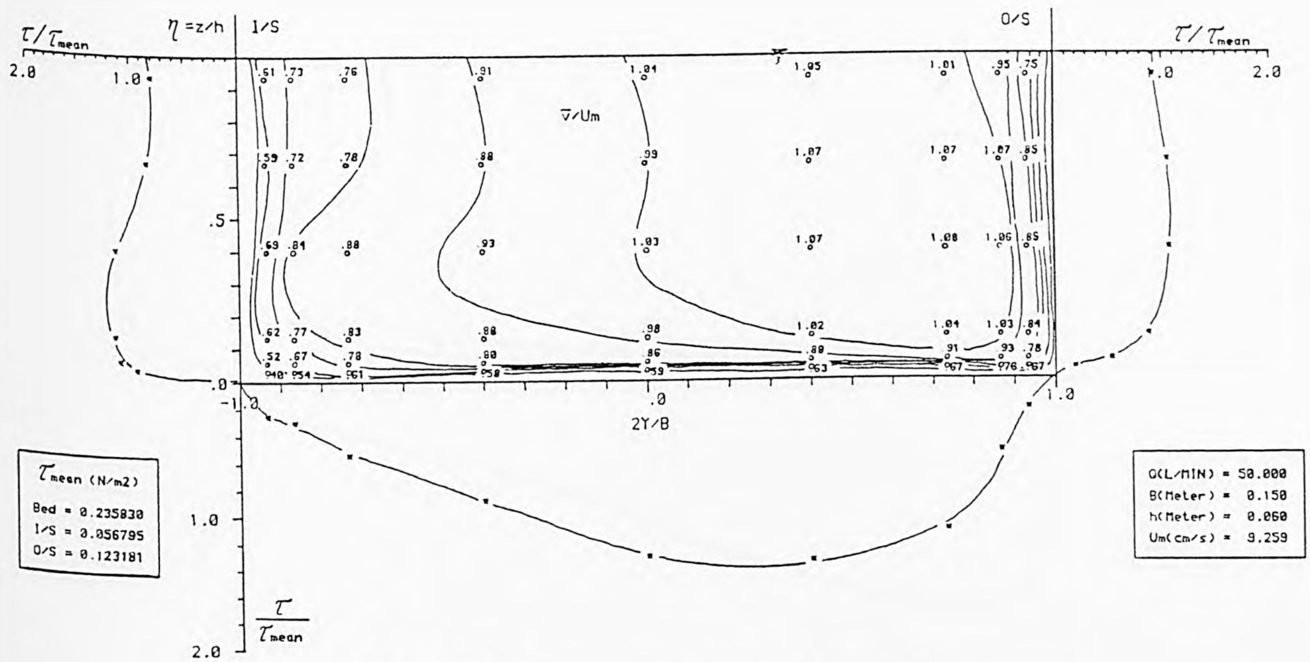

Fig. 6.120 Isovels of the velocity distribution in the direction of flow and boundary shear stress at section S-7, run no.3

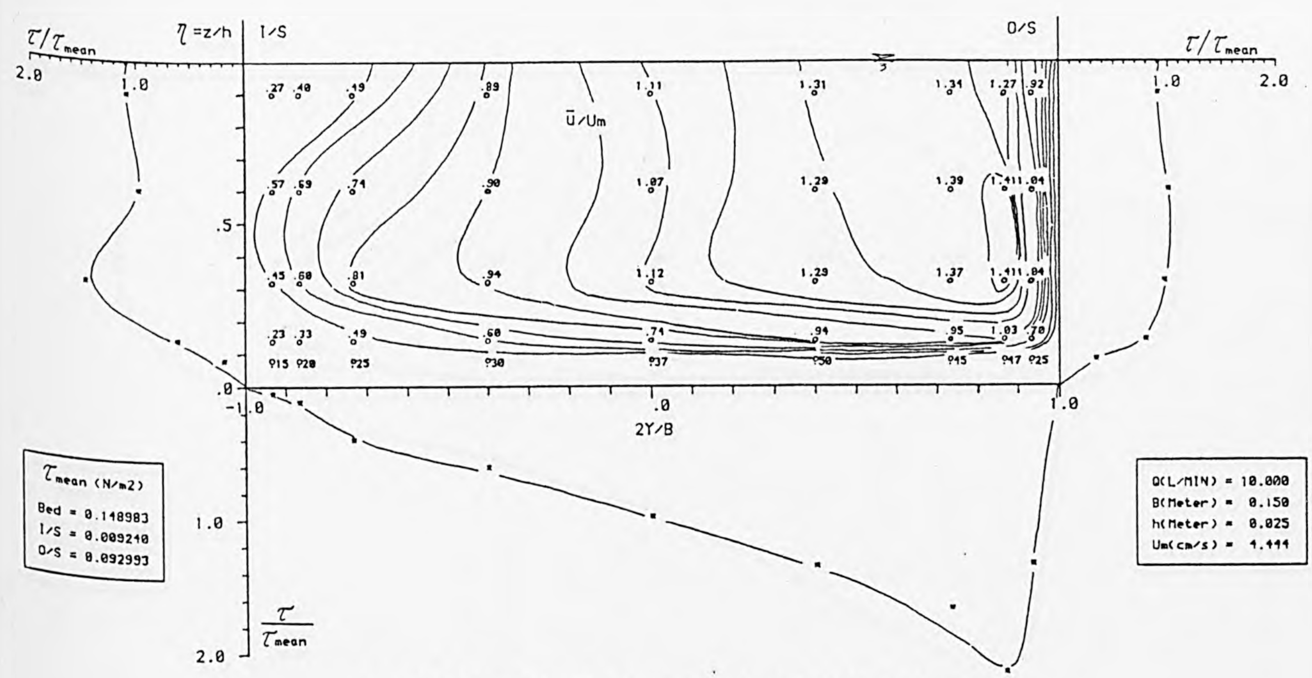

Fig. 6.121 Isovels of the velocity distribution in the direction of flow and boundary shear stress at section S-8, run no.1

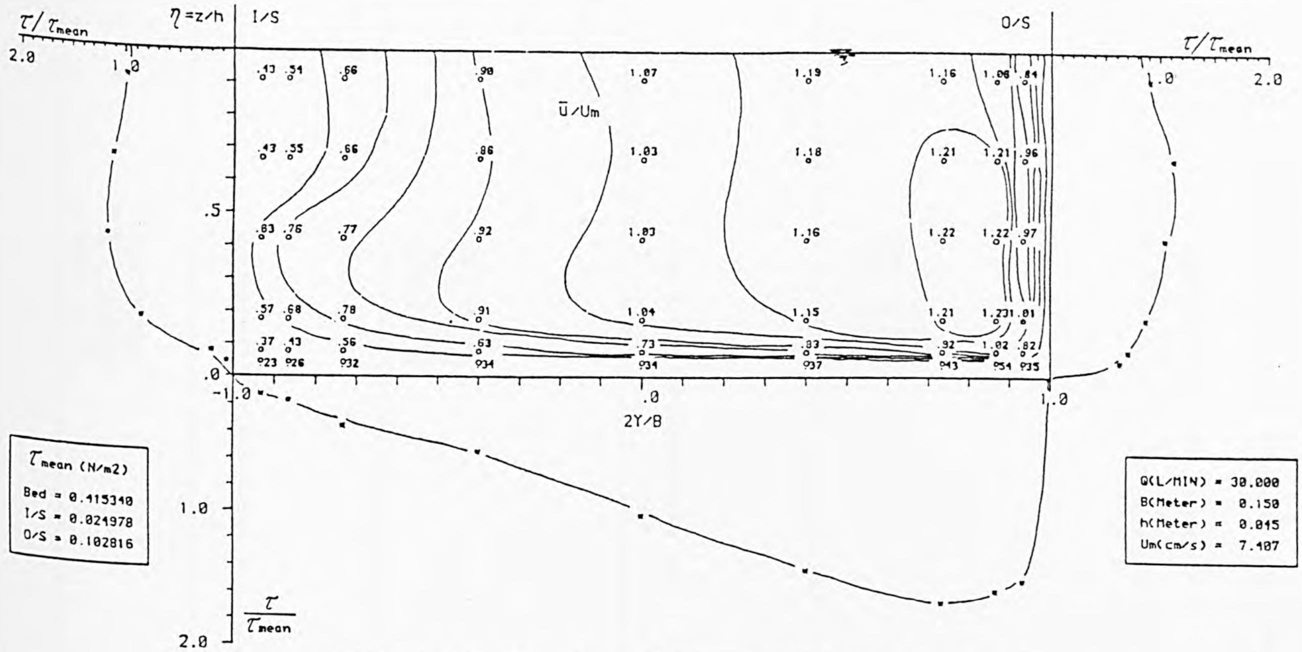

Fig. 6.122 Isovels of the velocity distribution in the direction of flow and boundary shear stress at section S-8, run no.2

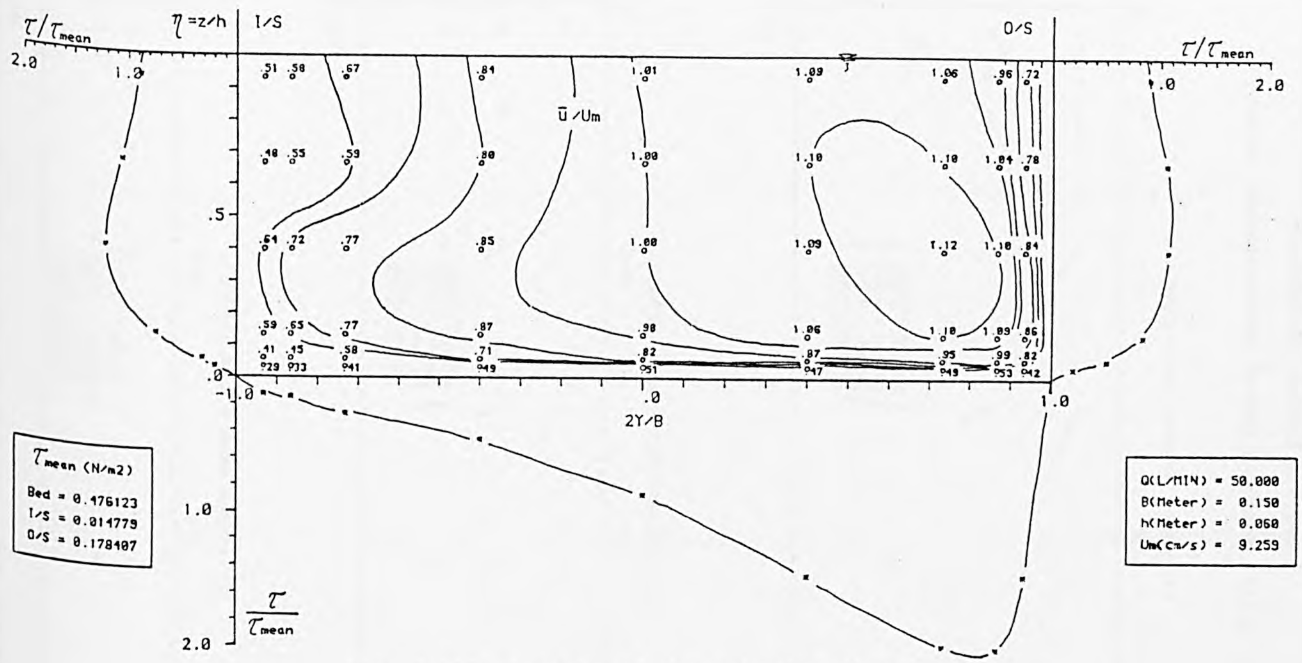

Fig. 6.123 Isovels of the velocity distribution in the direction of flow and boundary shear stress at section S-8, run no.3

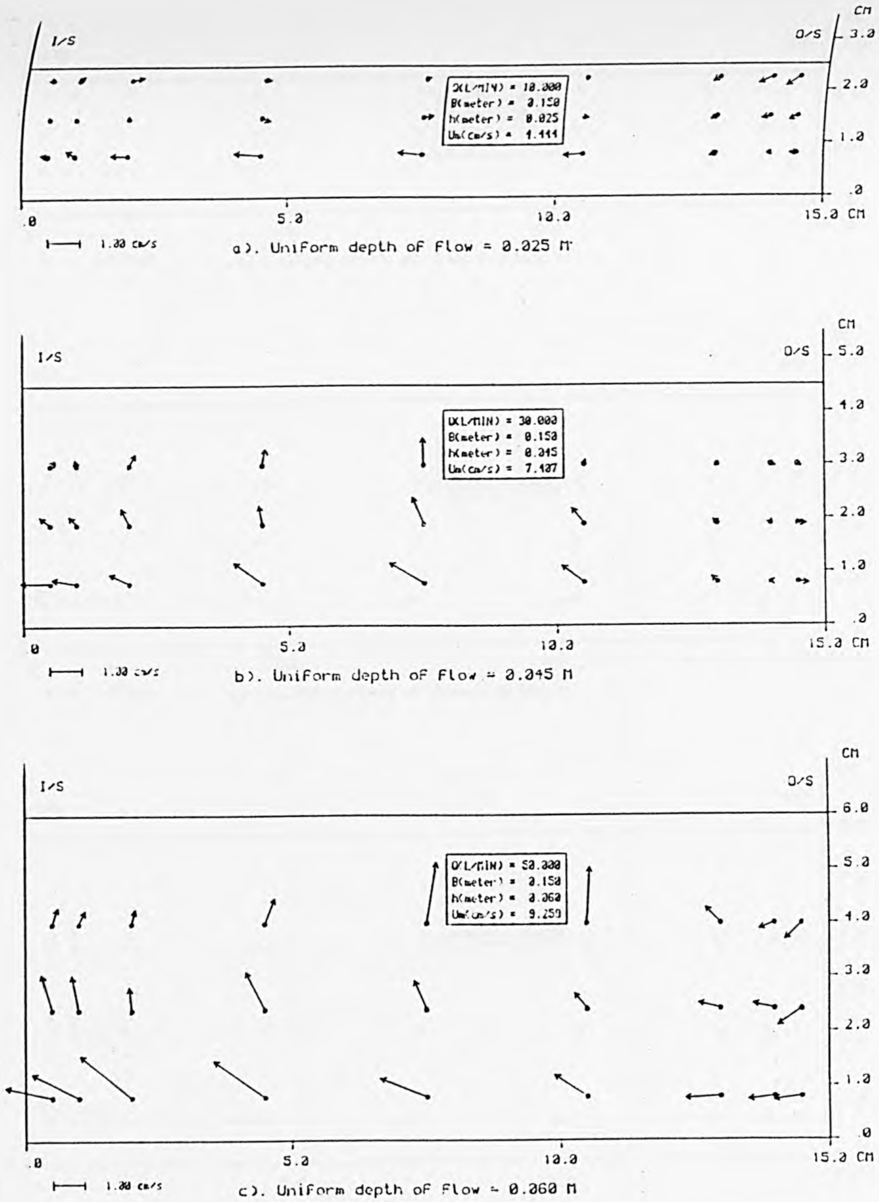

Fig. 6.124 Secondary flow at three different uniform depth of flows at section U-2

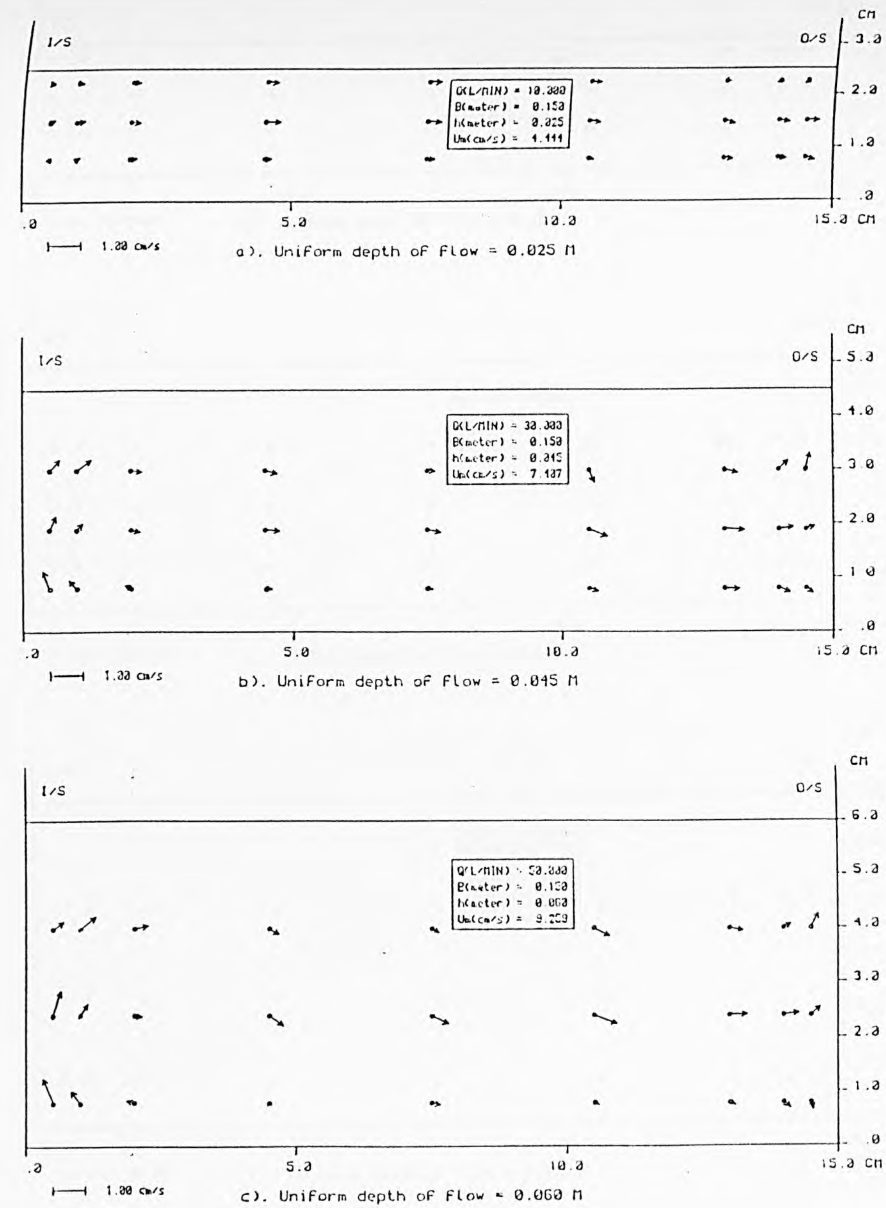

Fig. 6.125 Secondary flow at three different uniform depth of flows at section U-3

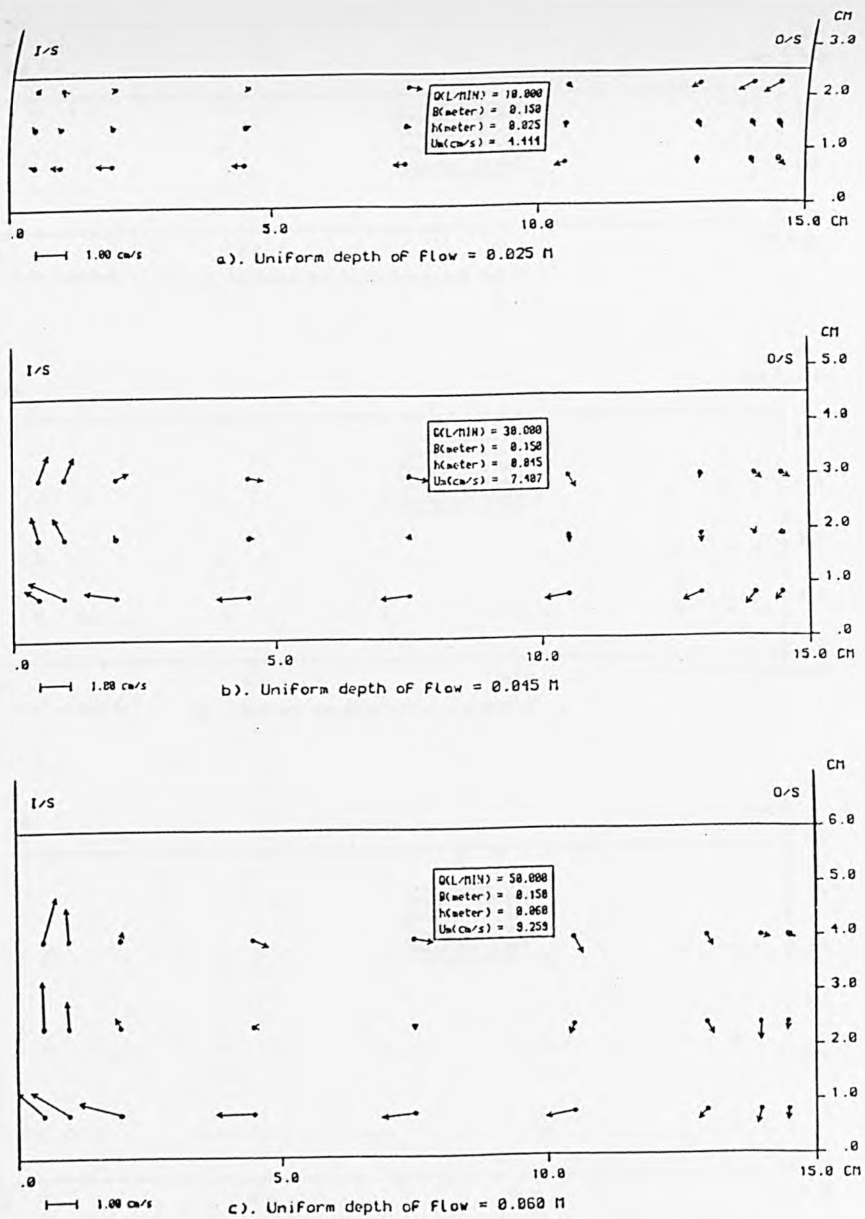

Fig. 6.126 Secondary flow at three different uniform depth of flows at section S-2

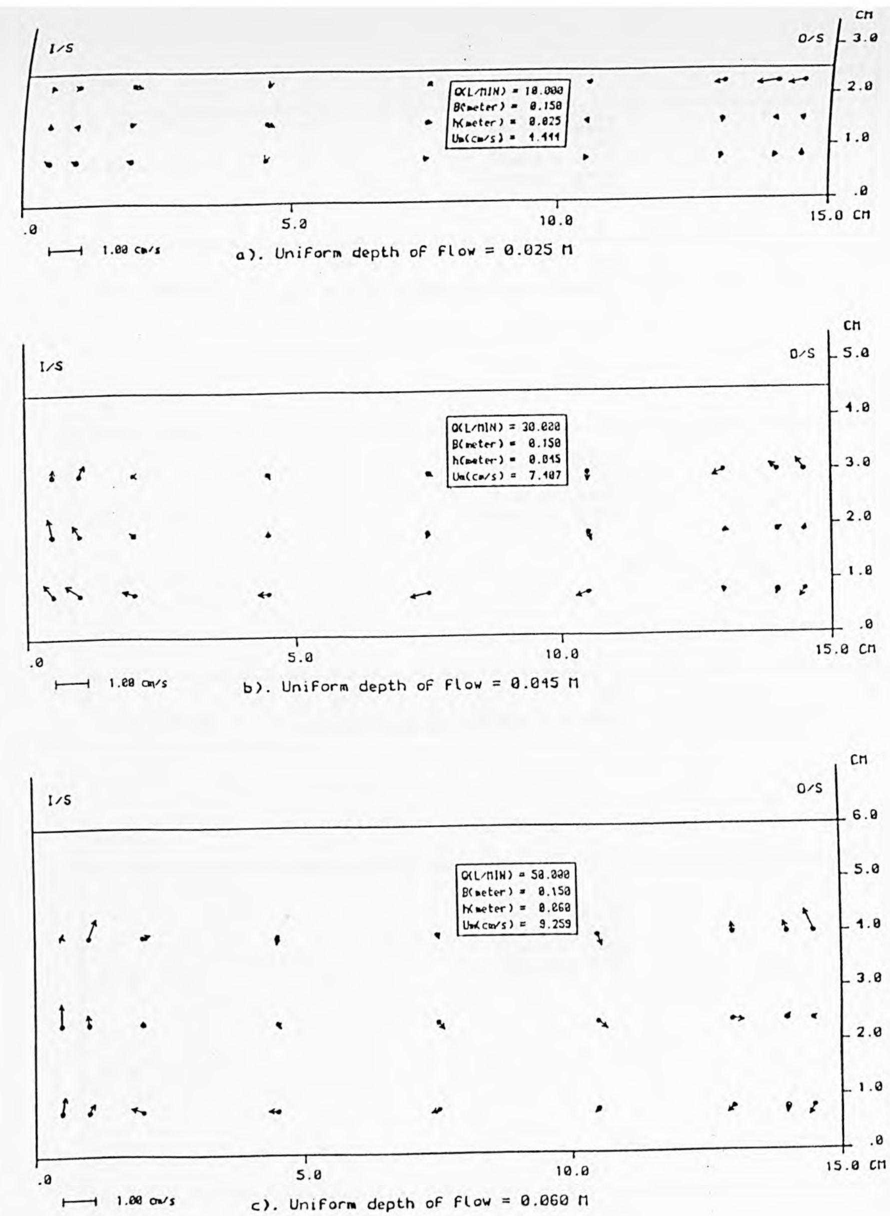

Fig. 6.127 Secondary flow at three different uniform depth of flows at section S-3

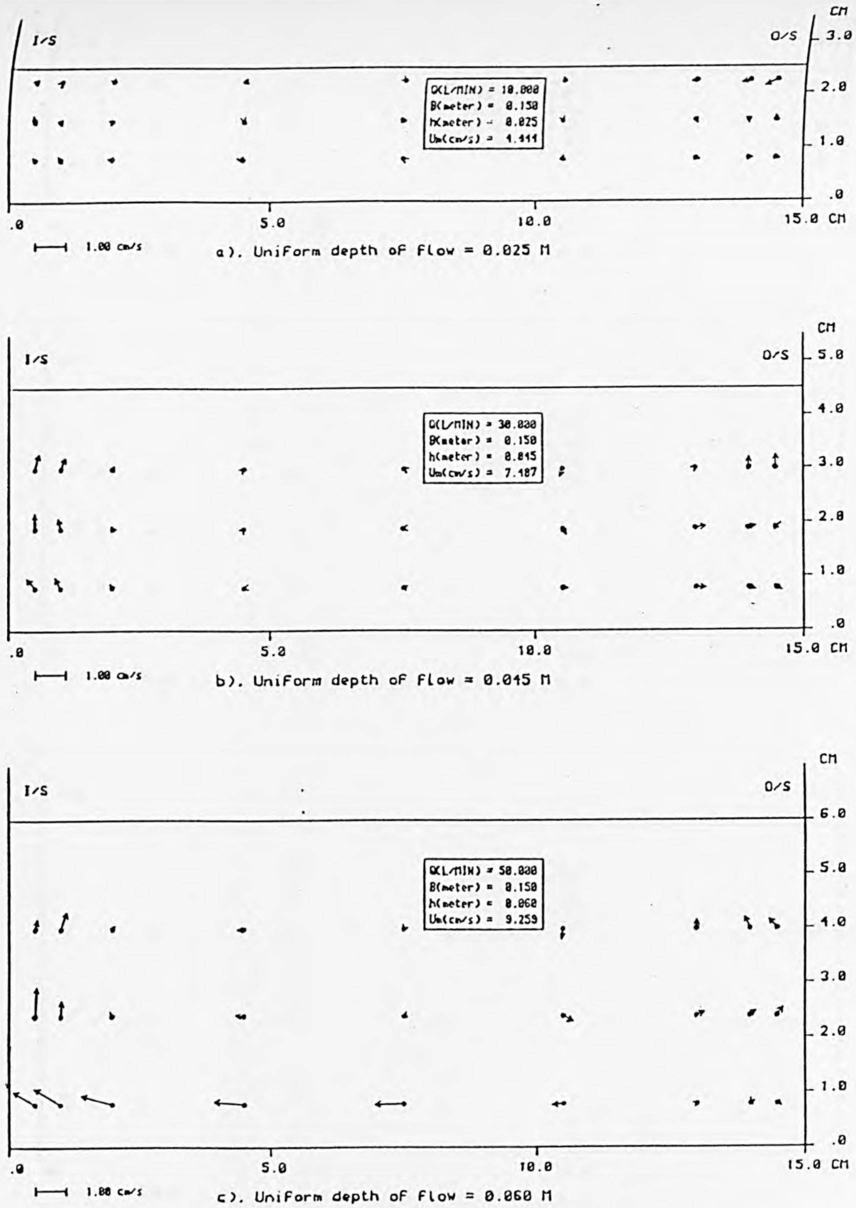

Fig. 6.128 Secondary flow at three different uniform depth of flows at section S-4

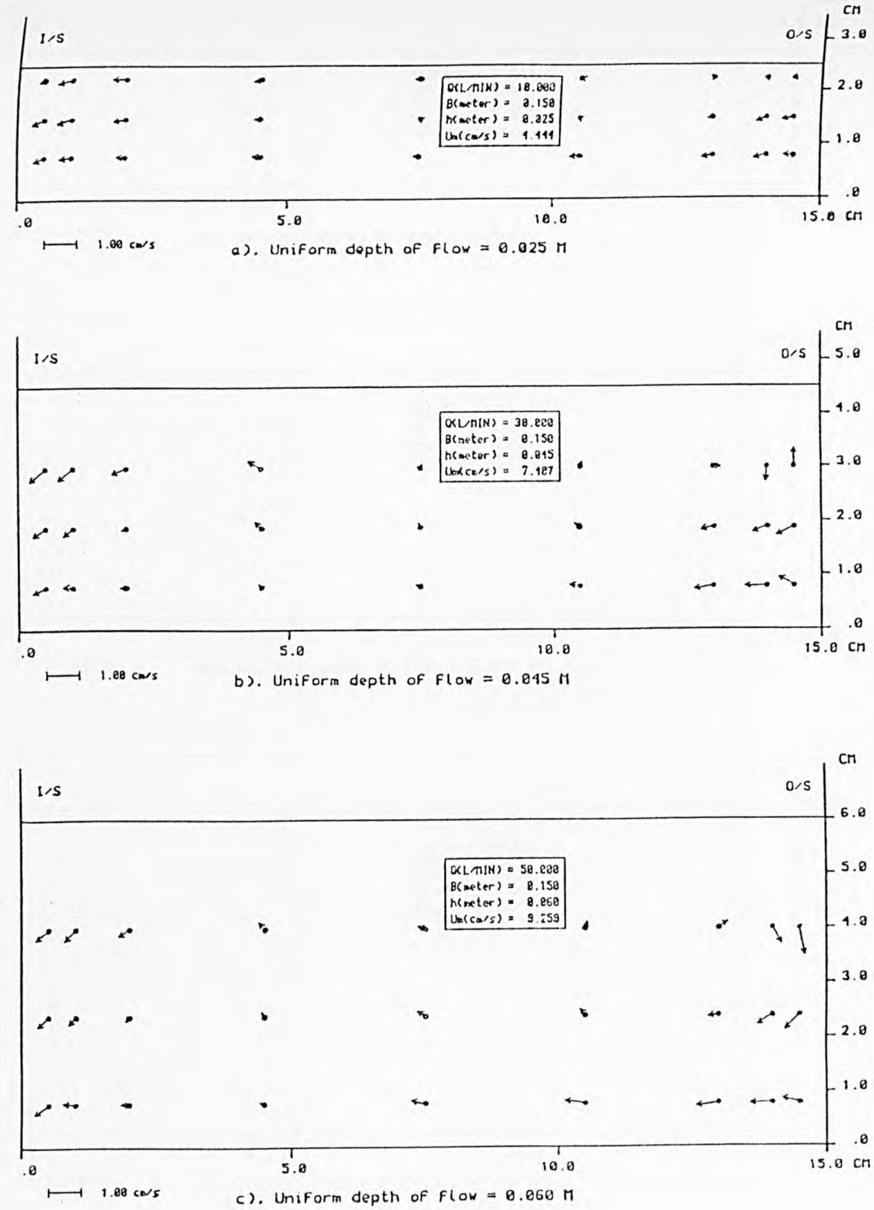

Fig. 6.129 Secondary flow at three different uniform depth of flows at section S-5

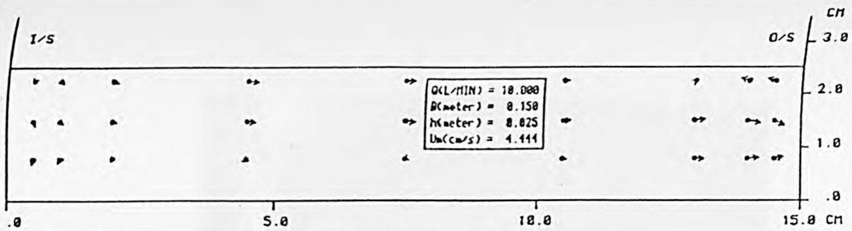

a). Uniform depth of Flow = 0.025 M

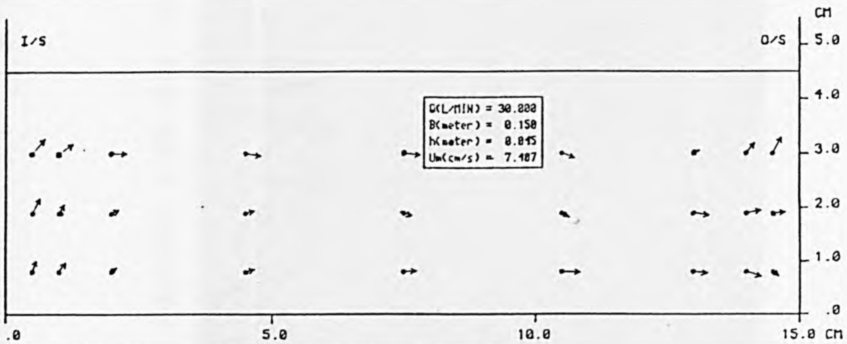

b). Uniform depth of Flow = 0.045 M

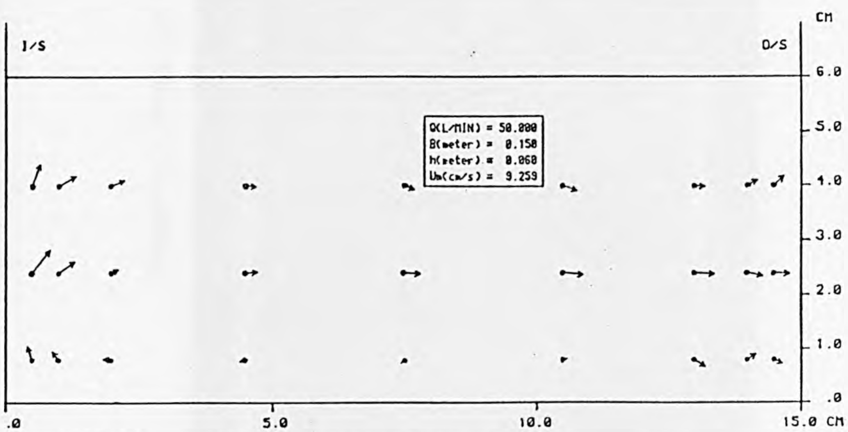

c). Uniform depth of Flow = 0.060 M

Fig. 6.131 Secondary flow at three different uniform depth of flows at section S-7

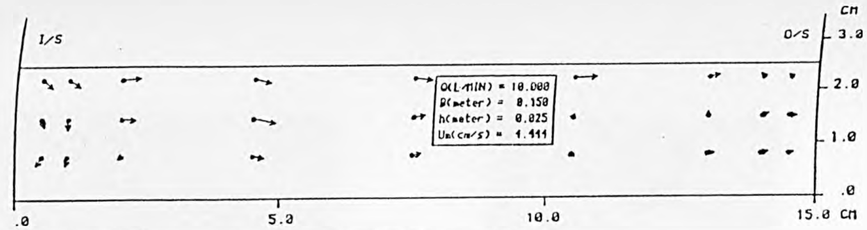

a). Uniform depth of Flow = 0.025 M

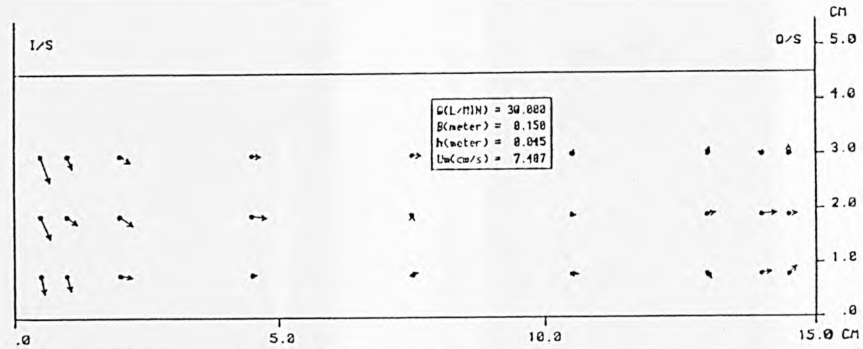

b). Uniform depth of Flow = 0.045 M

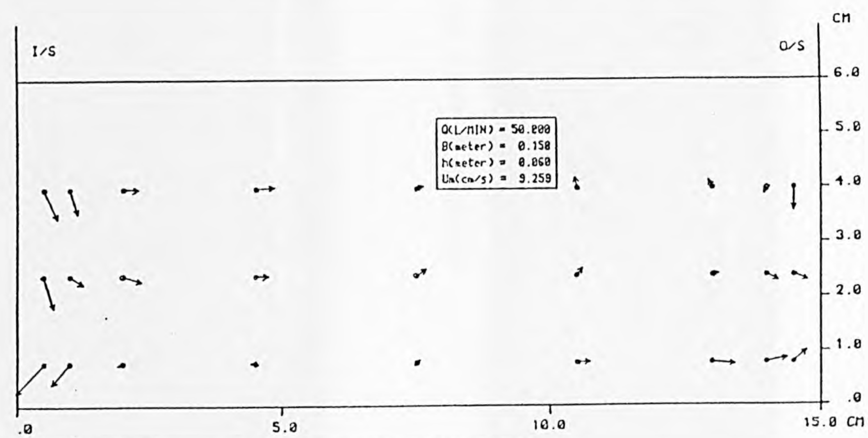

c). Uniform depth of Flow = 0.060 M

Fig. 6.130 Secondary flow at three different uniform depth of flows at section S-6

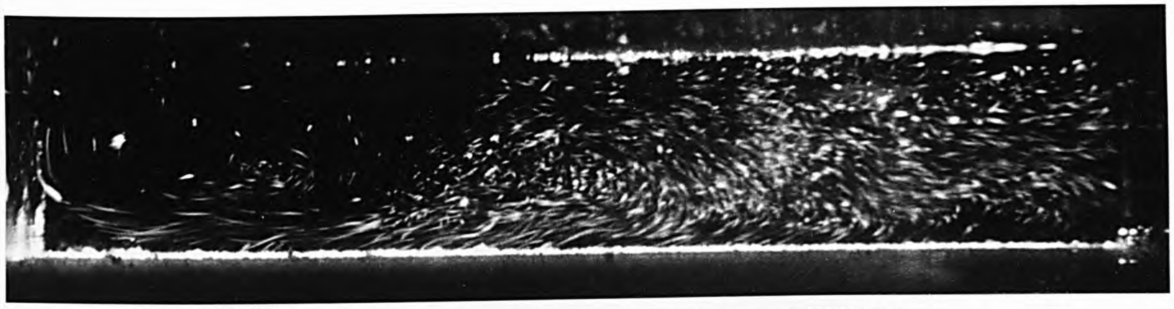

a). Run no.1 (uniform depth of flow = 0.025m)

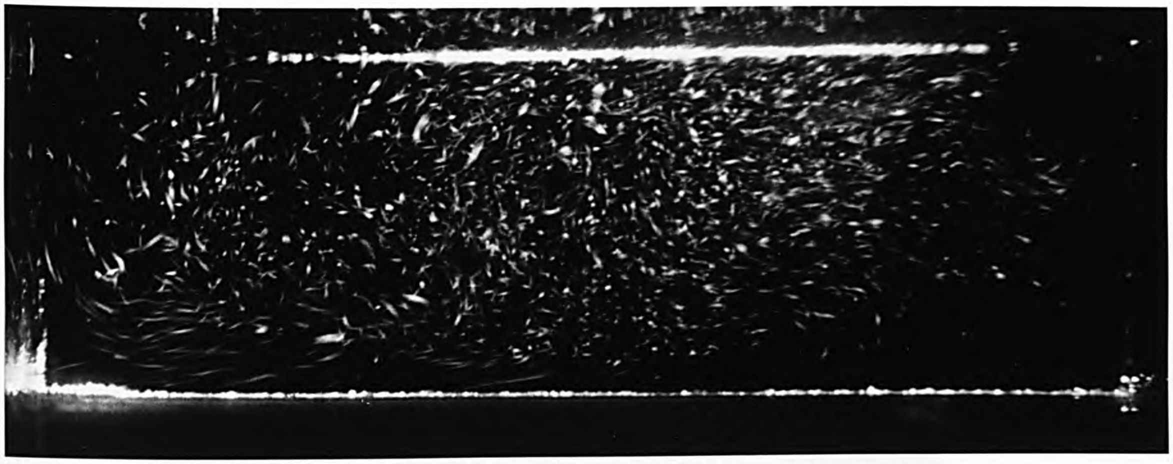

b). Run no.2 (uniform depth of flow = 0.045m)

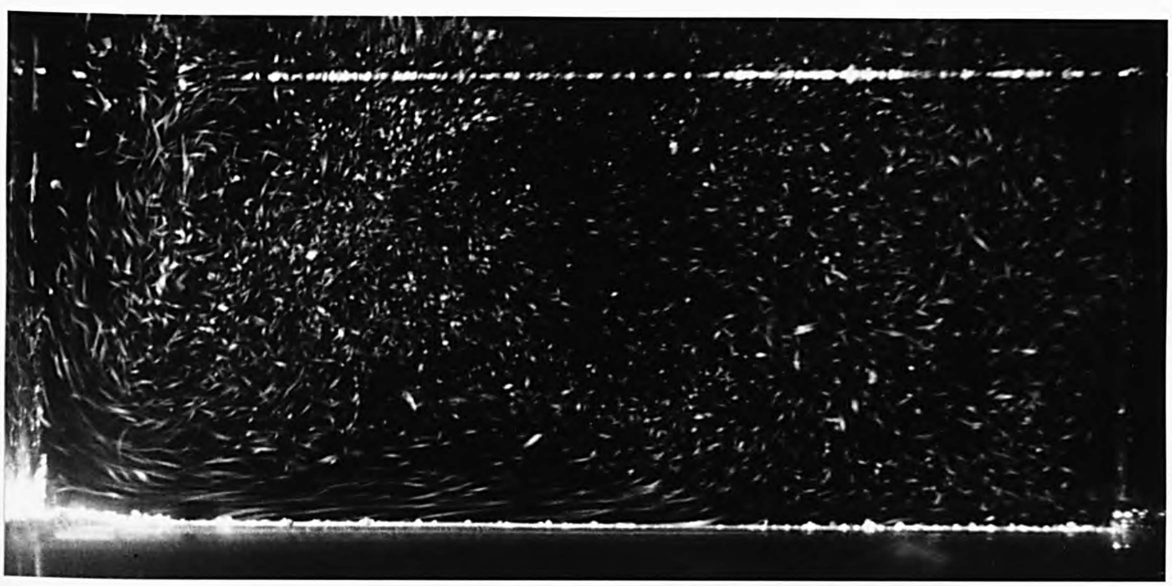

c). Run no.3 (uniform depth of flow = 0.060m)

Plate 6.1 Secondary flow pattern at section U-2 run no.1, run no.2 and run no.3

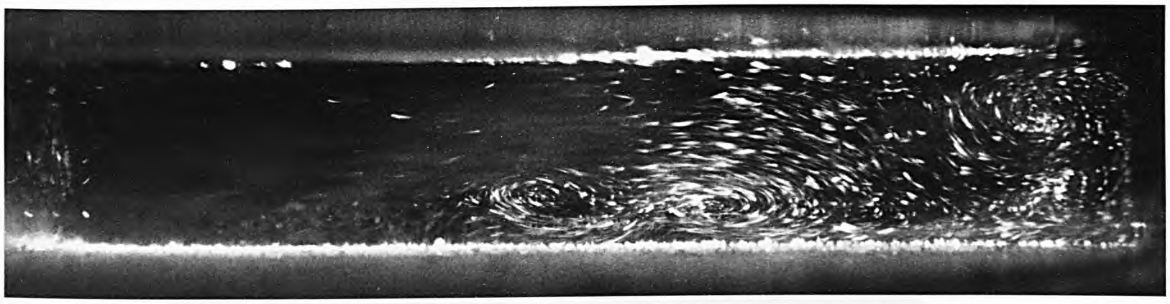

a). Run no.1 (uniform depth of flow = 0.025m)

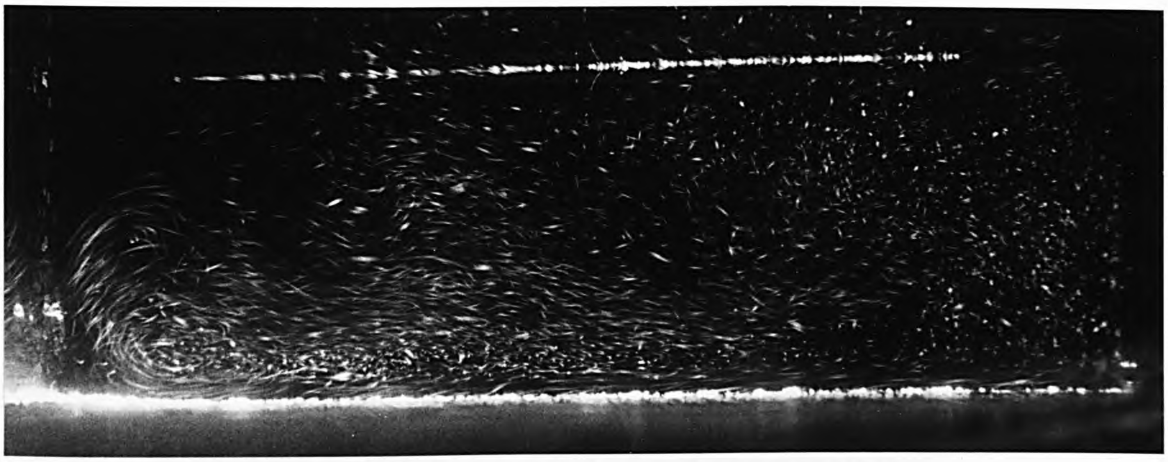

b). Run no.2 (uniform depth of flow = 0.045m)

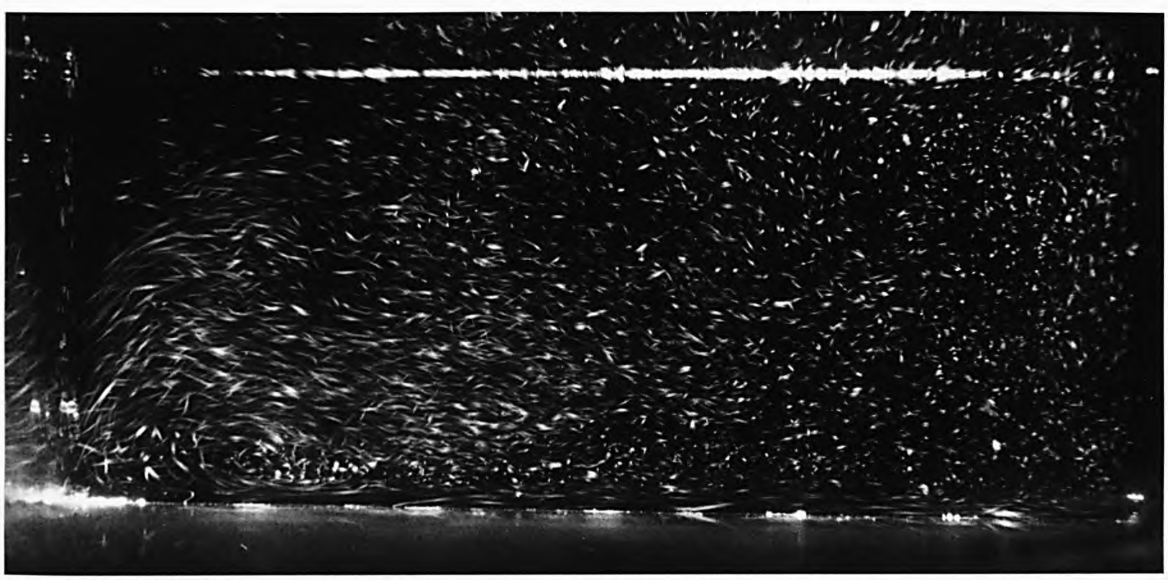

c). Run no.3 (uniform depth of flow = 0.060m)

Plate 6.2 Secondary flow pattern at section U-3 run no.1, run no.2 and run no.3

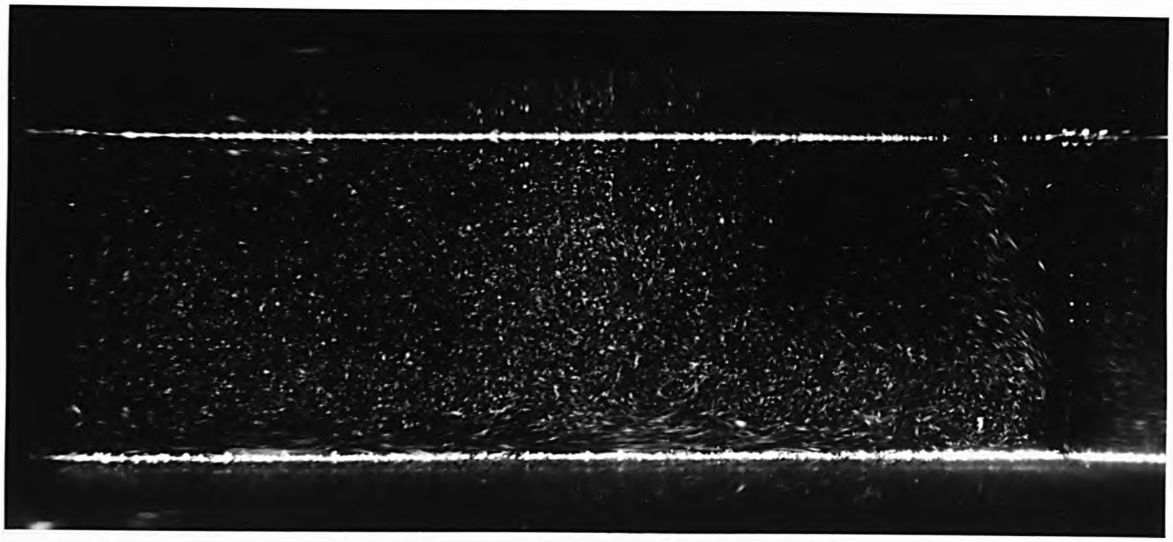

a). Run no.2 of section S-6 (uniform depth of flow = 0.045m)

b). Run no.1 of section S-7 (uniform depth of flow = 0.025m)

Plate 6.3 Secondary flow pattern at section S-6 run no.2, and section S-7 run no.1

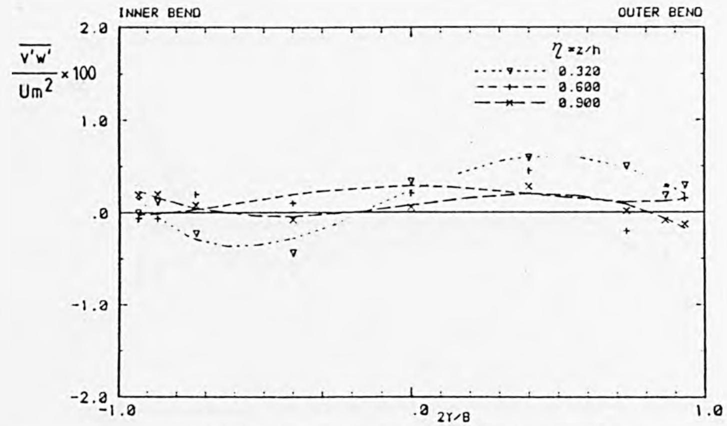

a). Reynolds Shear Stress Formed by Tangential and Vertical Velocity Fluctuations

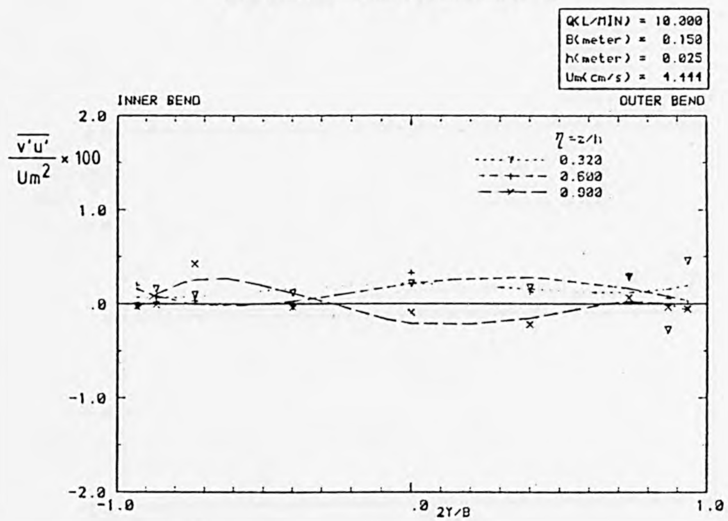

b). Reynolds Shear Stress Formed by Tangential and Radial Velocity Fluctuations

Fig. 6.132 Reynolds shear stress at section U-2, run no.1

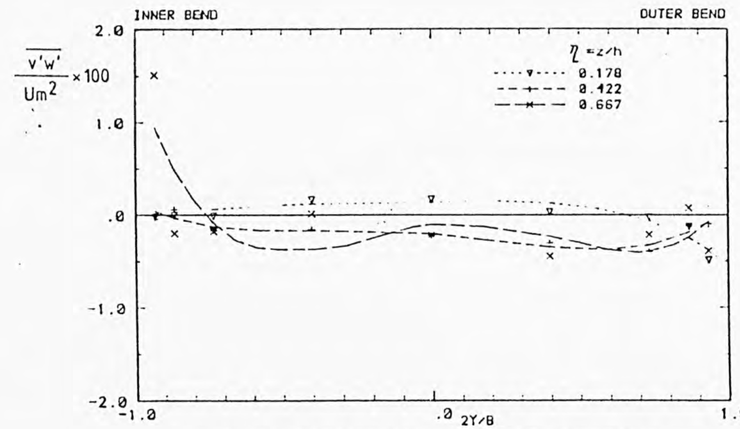

a). Reynolds Shear Stress Formed by Tangential and Vertical Velocity Fluctuations

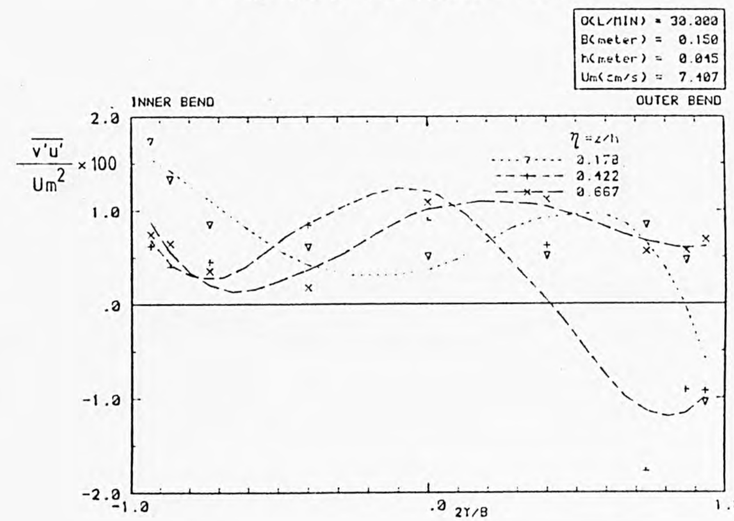

b). Reynolds Shear Stress Formed by Tangential and Radial Velocity Fluctuations

Fig. 6.133 Reynolds shear stress at section U-2, run no.2

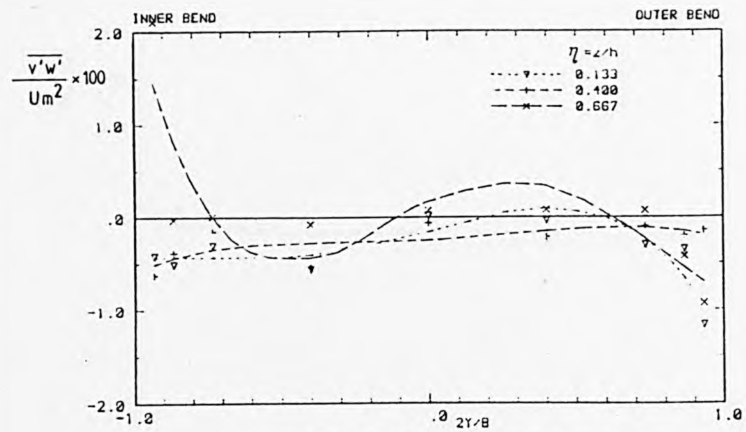

a). Reynolds Shear Stress Formed by Tangential and Vertical Velocity Fluctuations

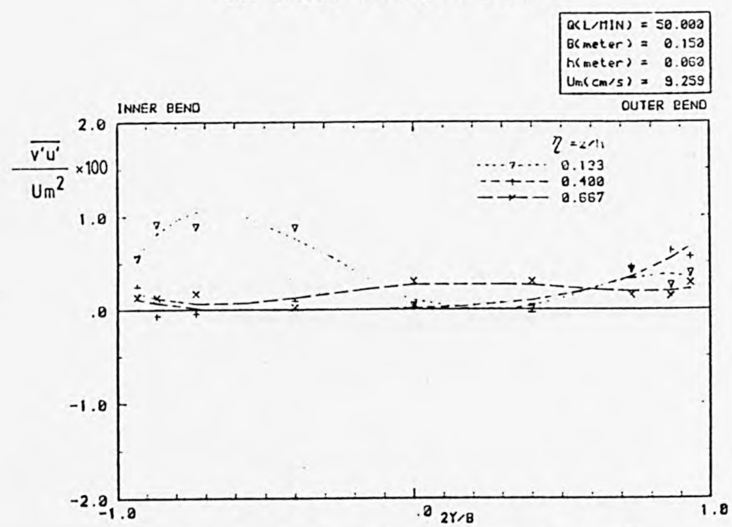

b). Reynolds Shear Stress Formed by Tangential and Radial Velocity Fluctuations

Fig. 6.134 Reynolds shear stress at section U-2, run no.3

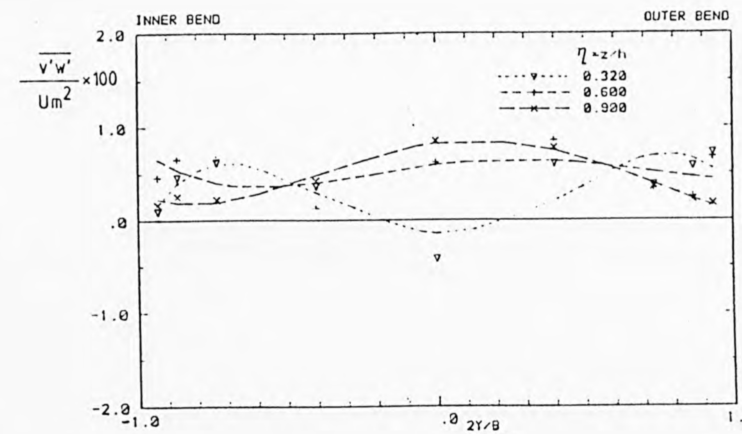

a). Reynolds Shear Stress Formed by Tangential and Vertical Velocity Fluctuations

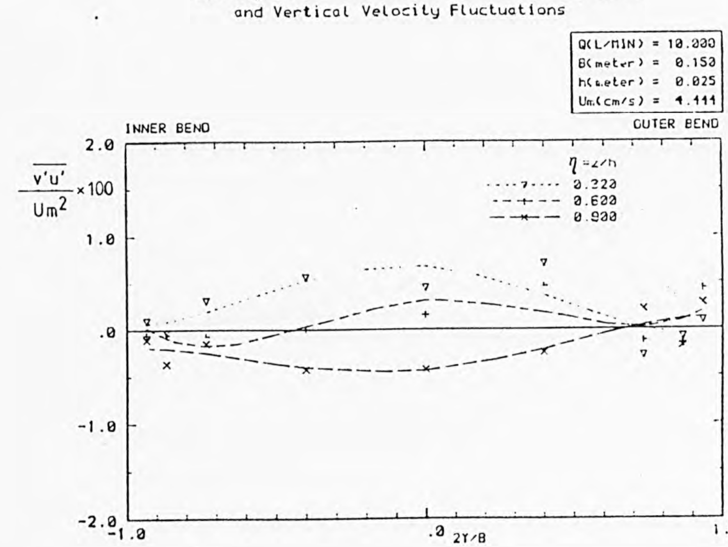

b). Reynolds Shear Stress Formed by Tangential and Radial Velocity Fluctuations

Fig. 6.135 Reynolds shear stress at section U-3, run no.1

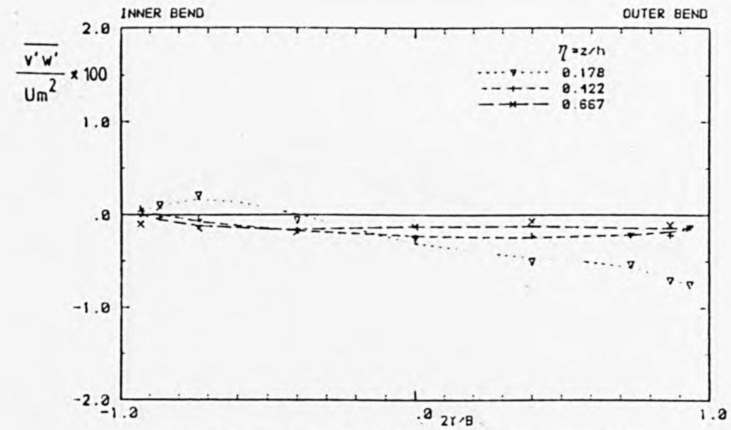

a). Reynolds Shear Stress Formed by Tangential and Vertical Velocity Fluctuations

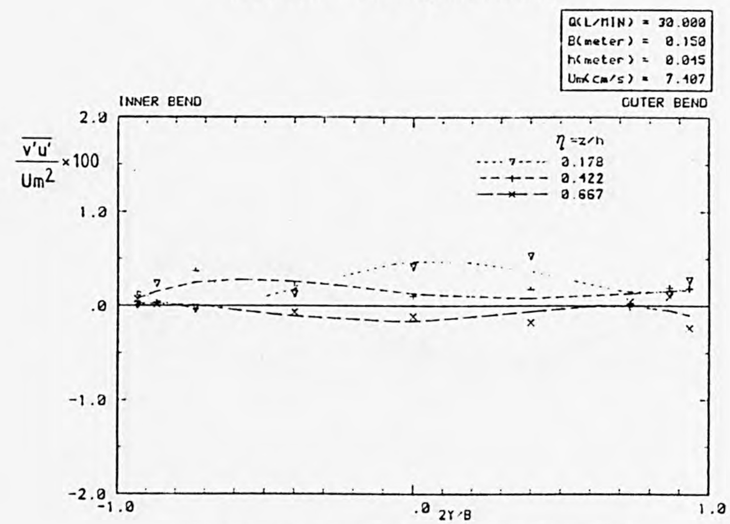

b). Reynolds Shear Stress Formed by Tangential and Radial Velocity Fluctuations

Fig. 6.136 Reynolds shear stress at section U-3, run no.2

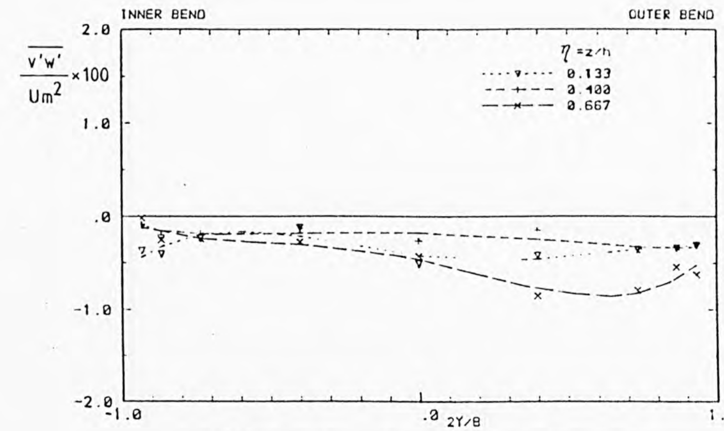

a). Reynolds Shear Stress Formed by Tangential and Vertical Velocity Fluctuations

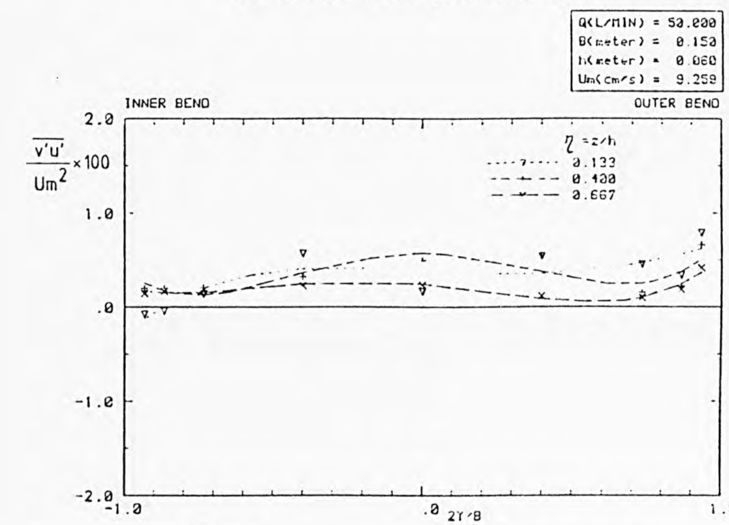

b). Reynolds Shear Stress Formed by Tangential and Radial Velocity Fluctuations

Fig. 6.137 Reynolds shear stress at section U-3, run no.3

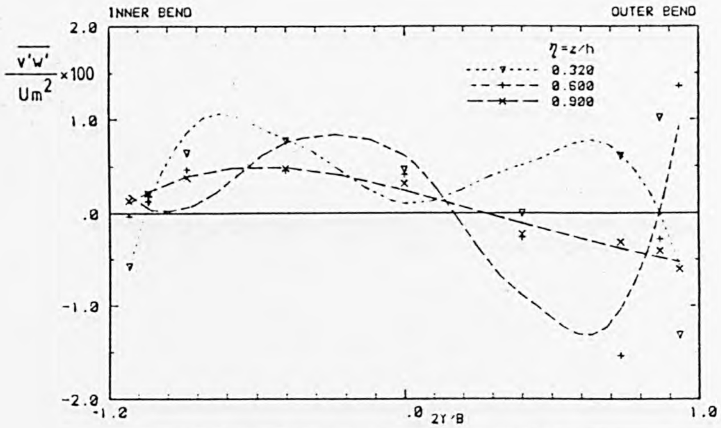

a). Reynolds Shear Stress Formed by Tangential and Vertical Velocity Fluctuations

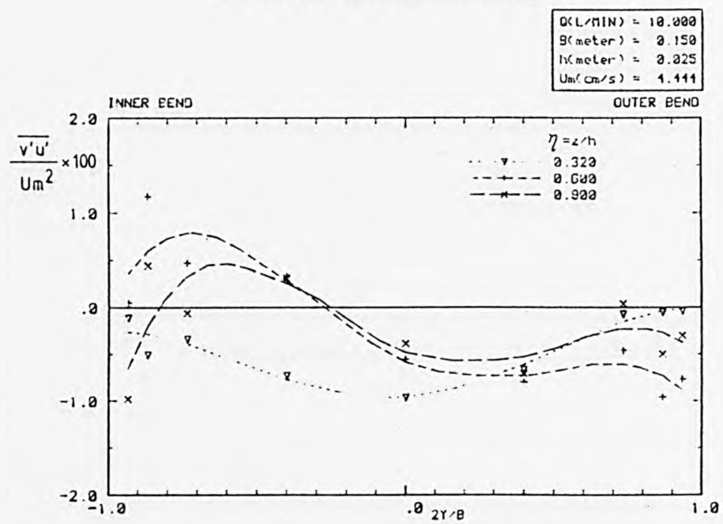

b). Reynolds Shear Stress Formed by Tangential and Radial Velocity Fluctuations

Fig. 6.138 Reynolds shear stress at section S-2, run no.1

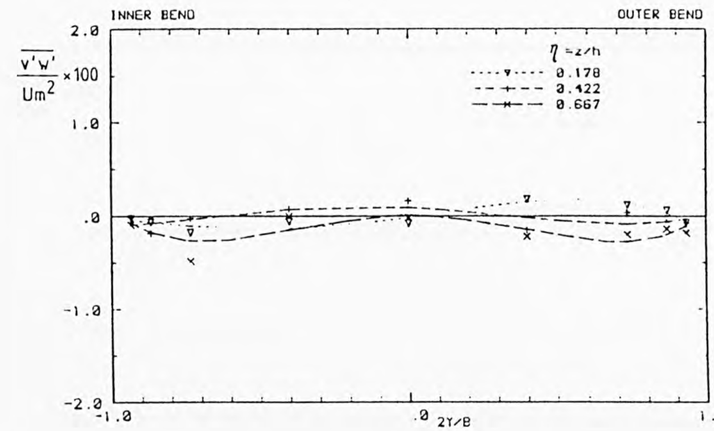

a). Reynolds Shear Stress Formed by Tangential and Vertical Velocity Fluctuations

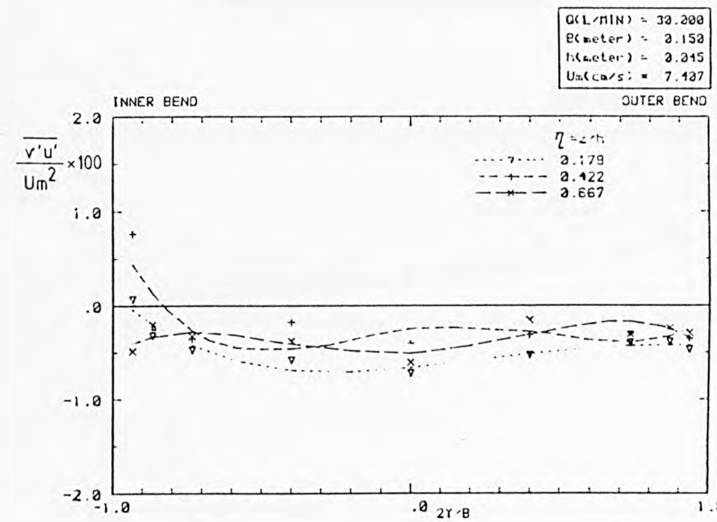

b). Reynolds Shear Stress Formed by Tangential and Radial Velocity Fluctuations

Fig. 6.139 Reynolds shear stress at section S-2, run no.2

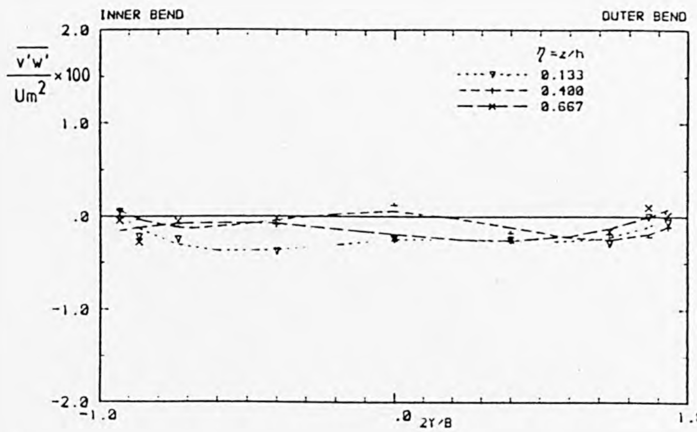

a). Reynolds Shear Stress Formed by Tangential and Vertical Velocity Fluctuations

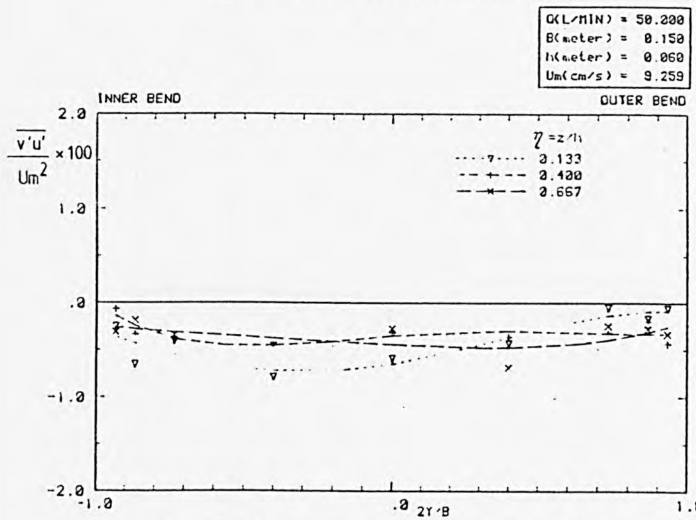

b). Reynolds Shear Stress Formed by Tangential and Radial Velocity Fluctuations

Fig. 6.140 Reynolds shear stress at section S-2, run no.3

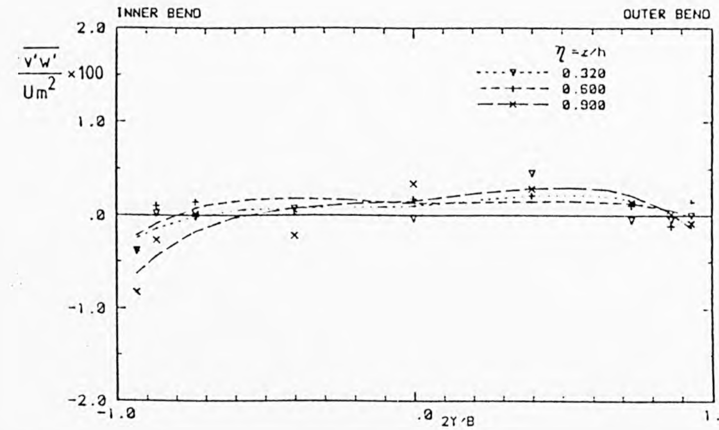

a). Reynolds Shear Stress Formed by Tangential and Vertical Velocity Fluctuations

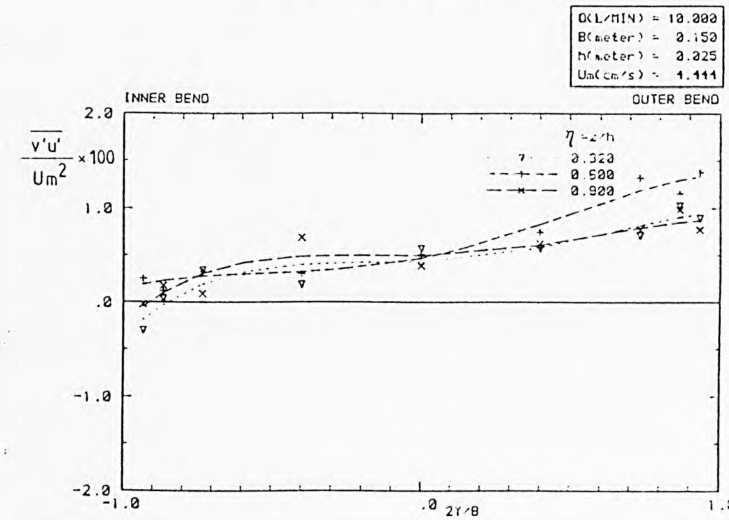

b). Reynolds Shear Stress Formed by Tangential and Radial Velocity Fluctuations

Fig. 6.141 Reynolds shear stress at section S-3, run no.1

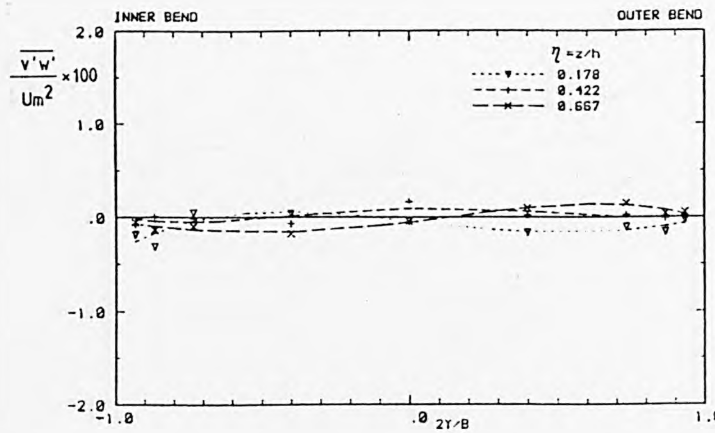

a). Reynolds Shear Stress Formed by Tangential and Vertical Velocity Fluctuations

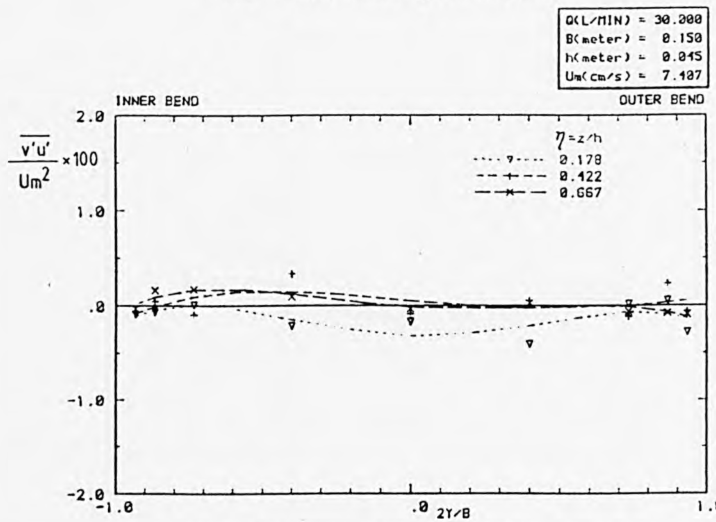

b). Reynolds Shear Stress Formed by Tangential and Radial Velocity Fluctuations

Fig. 6.142 Reynolds shear stress at section S-3, run no.2

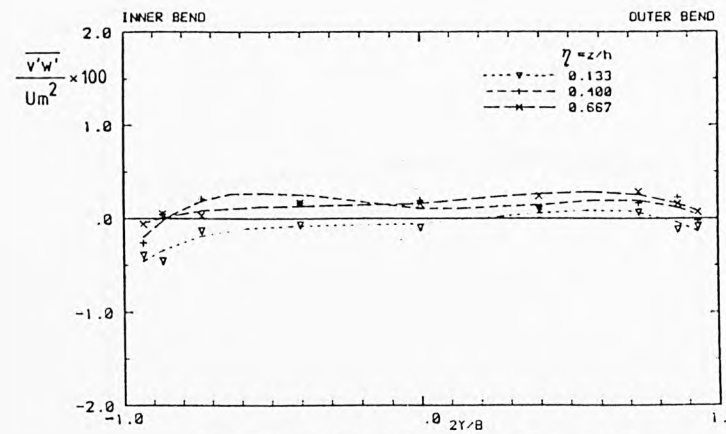

a). Reynolds Shear Stress Formed by Tangential and Vertical Velocity Fluctuations

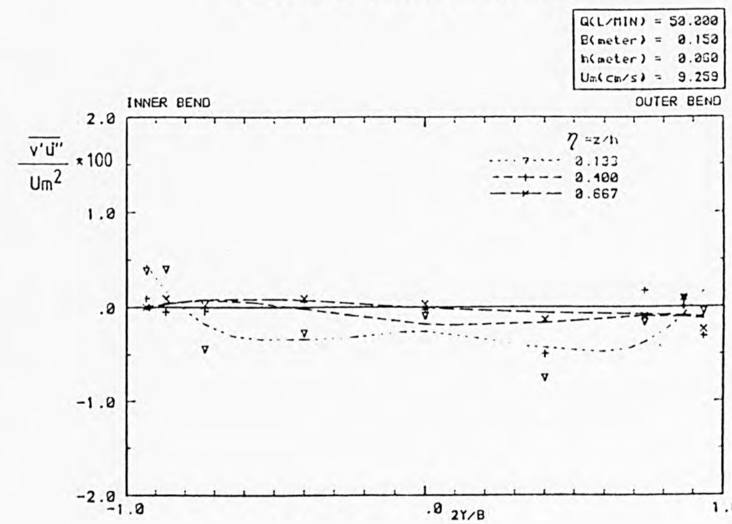

b). Reynolds Shear Stress Formed by Tangential and Radial Velocity Fluctuations

Fig. 6.143 Reynolds shear stress at section S-3, run no.3

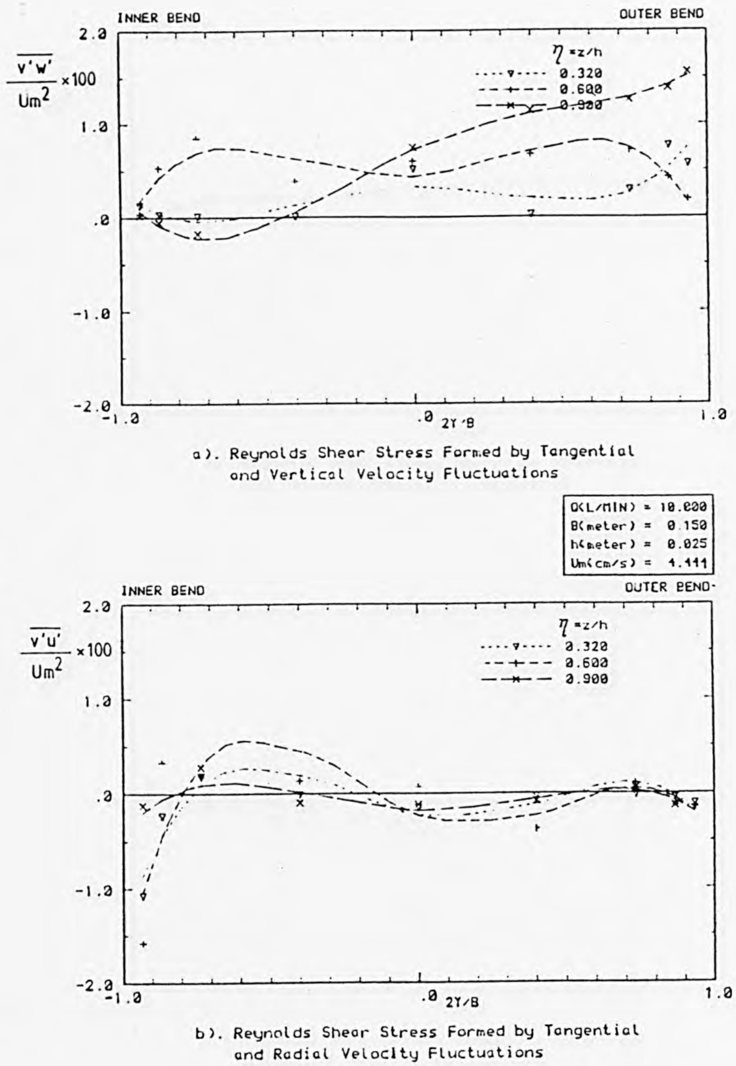

Fig. 6.144 Reynolds shear stress at section S-4, run no.1

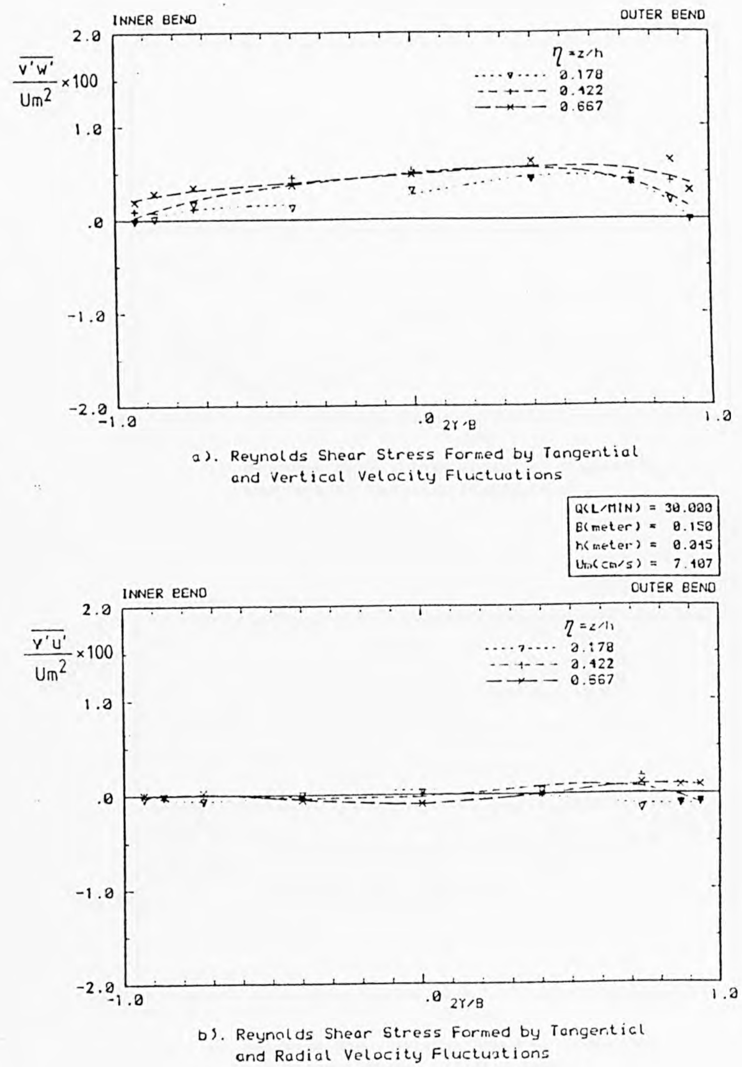

Fig. 6.145 Reynolds shear stress at section S-4, run no.2

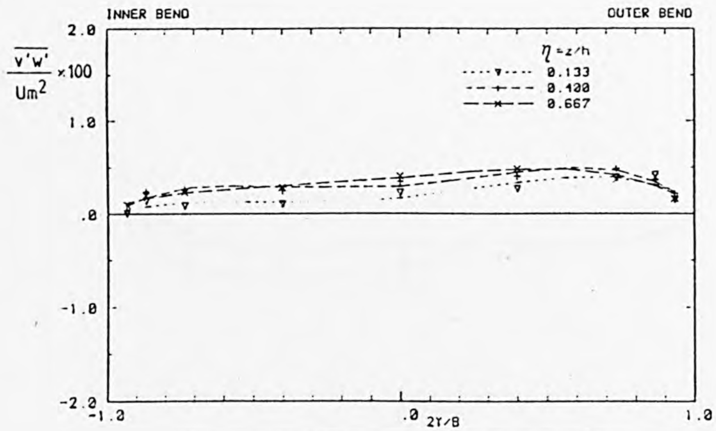

a). Reynolds Shear Stress Formed by Tangential and Vertical Velocity Fluctuations

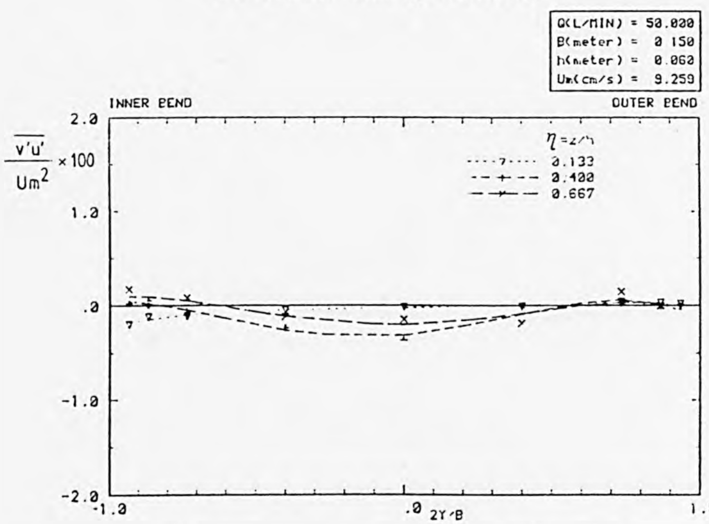

b). Reynolds Shear Stress Formed by Tangential and Radial Velocity Fluctuations

Fig. 6.146 Reynolds shear stress at section S-4, run no.3

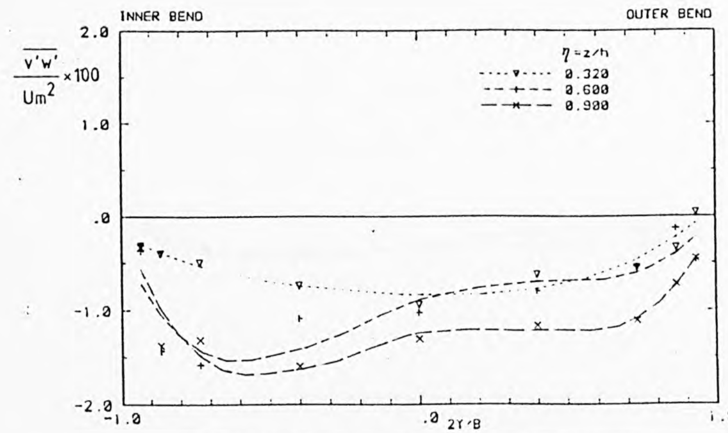

a). Reynolds Shear Stress Formed by Tangential and Vertical Velocity Fluctuations

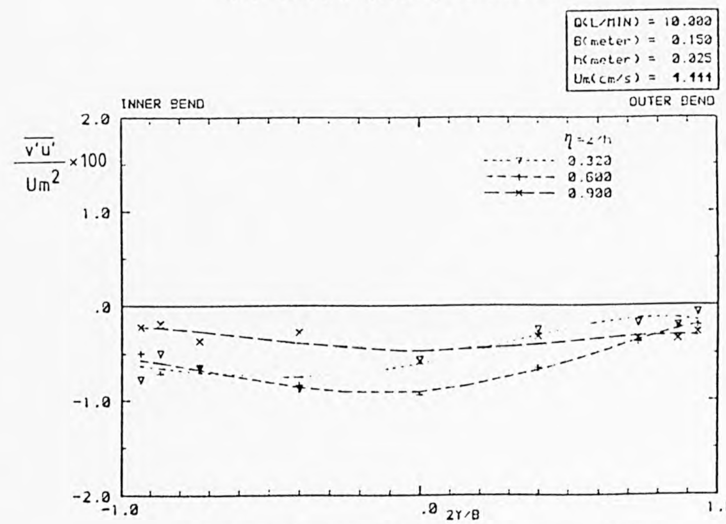

b). Reynolds Shear Stress Formed by Tangential and Radial Velocity Fluctuations

Fig. 6.147 Reynolds shear stress at section S-5, run no.1

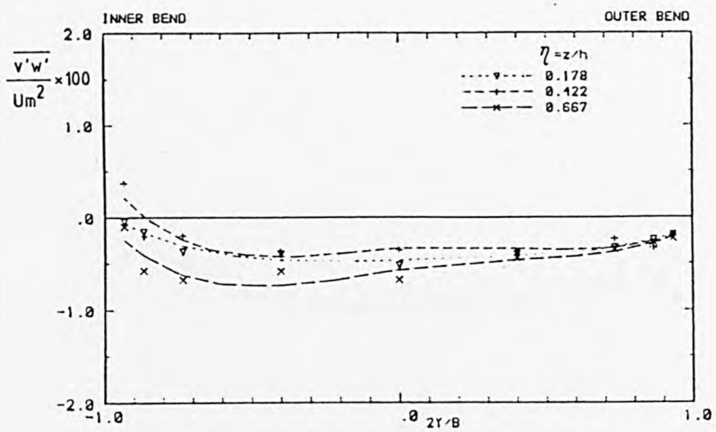

a). Reynolds Shear Stress Formed by Tangential and Vertical Velocity Fluctuations

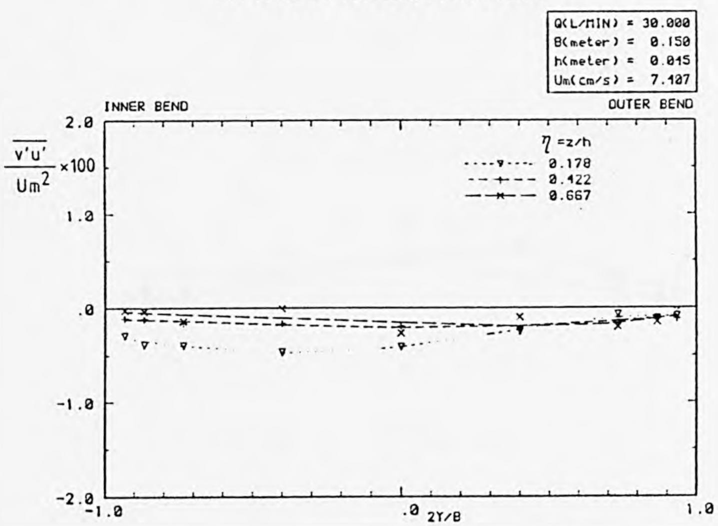

b). Reynolds Shear Stress Formed by Tangential and Radial Velocity Fluctuations

Fig. 6.148 Reynolds shear stress at section S-5, run no.2

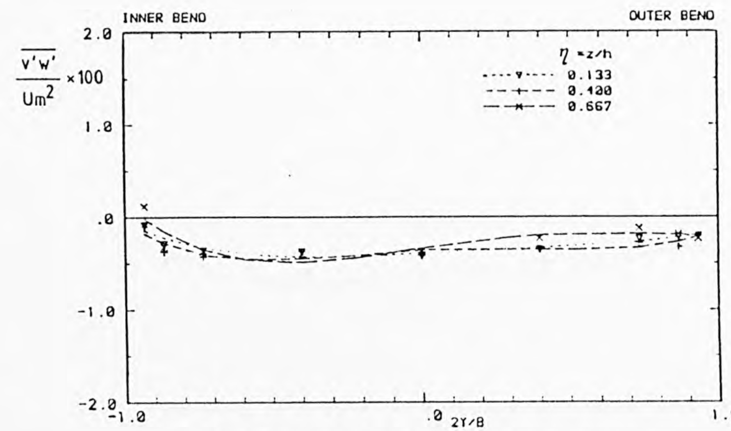

a). Reynolds Shear Stress Formed by Tangential and Vertical Velocity Fluctuations

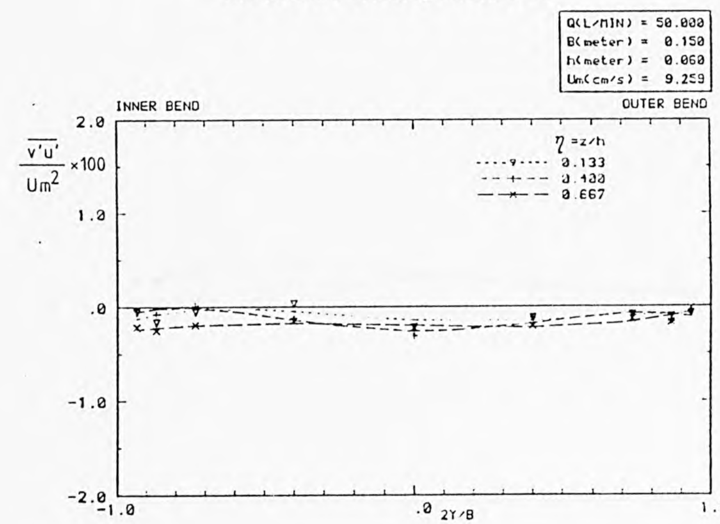

b). Reynolds Shear Stress Formed by Tangential and Radial Velocity Fluctuations

Fig. 6.149 Reynolds shear stress at section S-5, run no.3

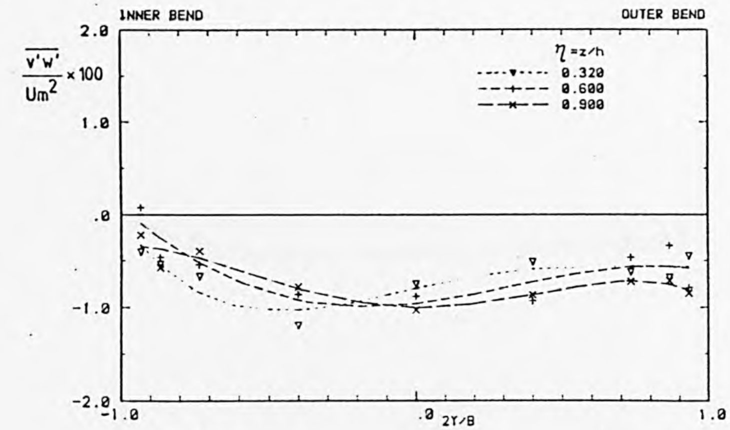

a). Reynolds Shear Stress Formed by Tangential and Vertical Velocity Fluctuations

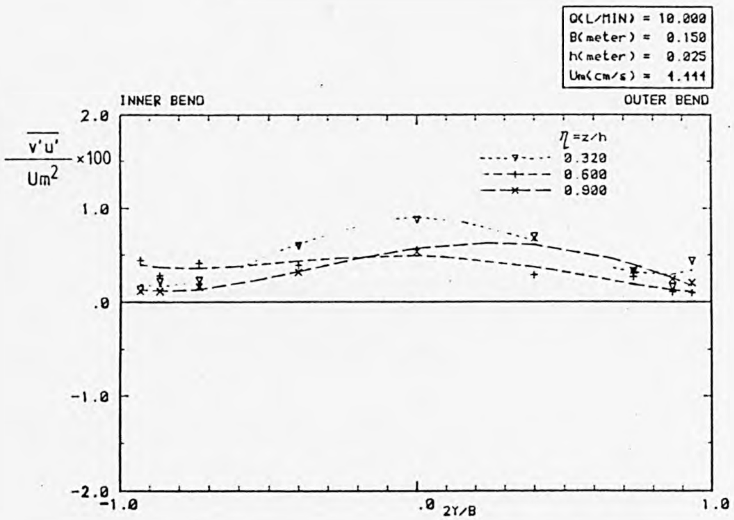

b). Reynolds Shear Stress Formed by Tangential and Radial Velocity Fluctuations

Fig. 6.150 Reynolds shear stress at section S-6, run no.1

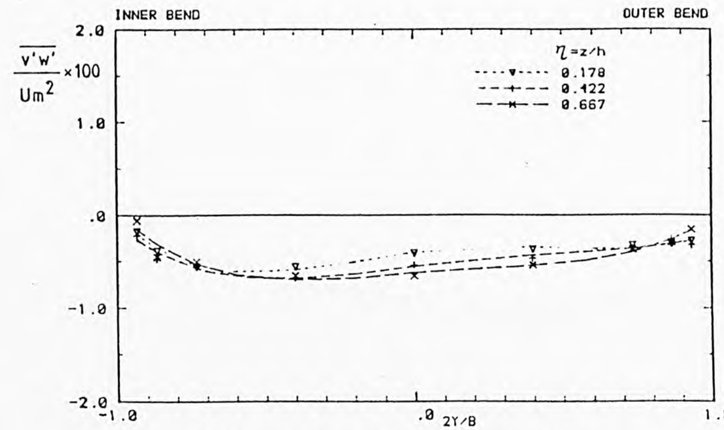

a). Reynolds Shear Stress Formed by Tangential and Vertical Velocity Fluctuations

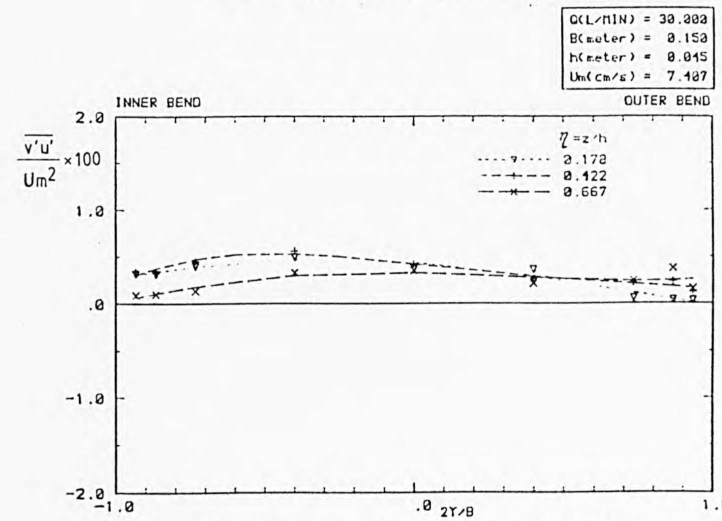

b). Reynolds Shear Stress Formed by Tangential and Radial Velocity Fluctuations

Fig. 6.151 Reynolds shear stress at section S-6, run no.2

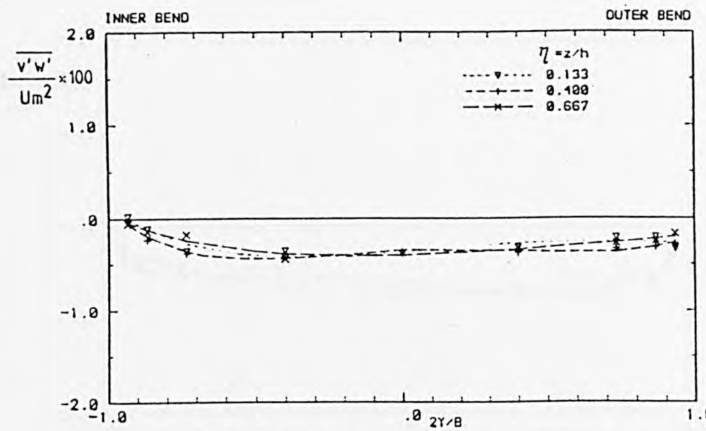

a). Reynolds Shear Stress Formed by Tangential and Vertical Velocity Fluctuations

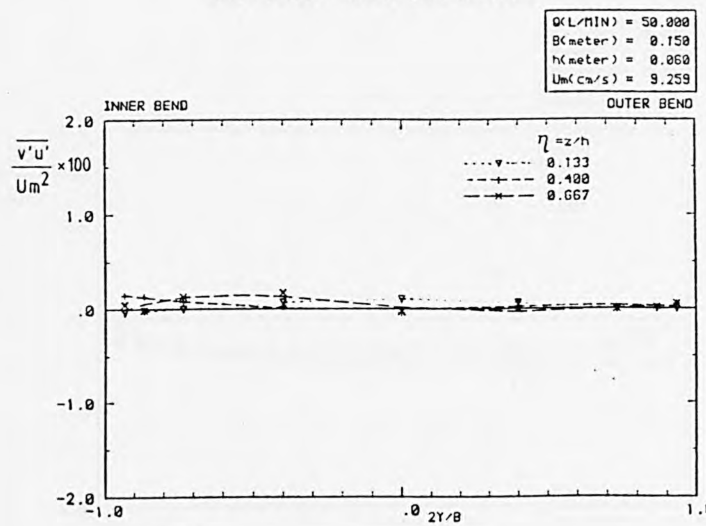

b). Reynolds Shear Stress Formed by Tangential and Radial Velocity Fluctuations

Fig. 6.152 Reynolds shear stress at section S-6, run no.3

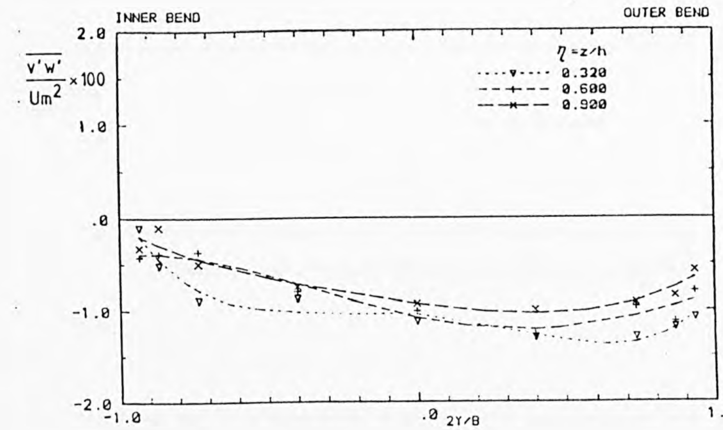

a). Reynolds Shear Stress Formed by Tangential and Vertical Velocity Fluctuations

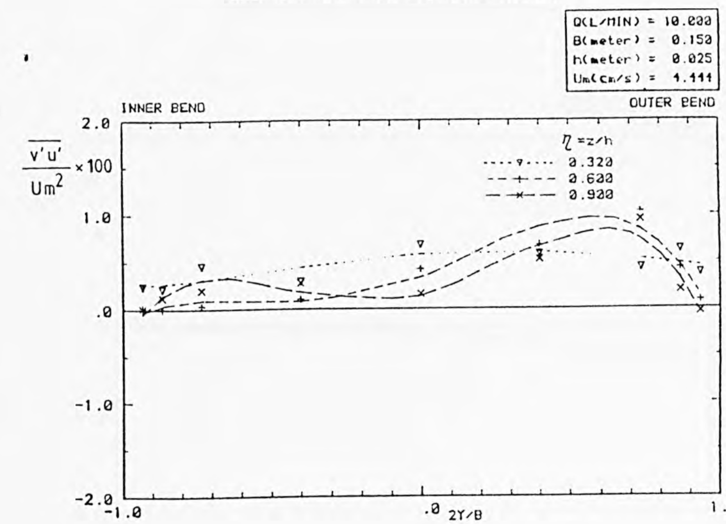

b). Reynolds Shear Stress Formed by Tangential and Radial Velocity Fluctuations

Fig. 6.153 Reynolds shear stress at section S-7, run no.1

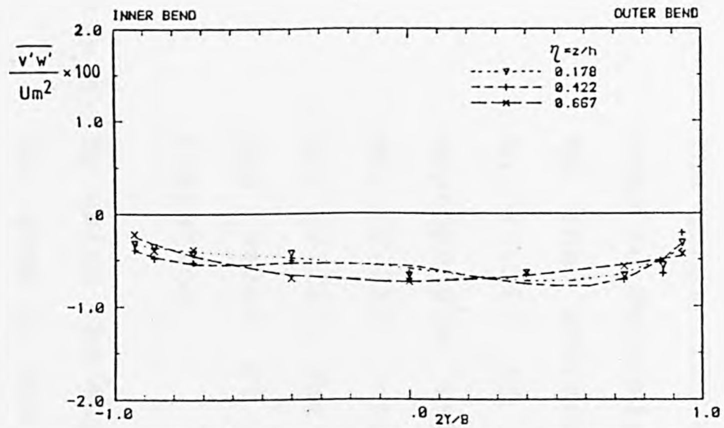

a). Reynolds Shear Stress Formed by Tangential and Vertical Velocity Fluctuations

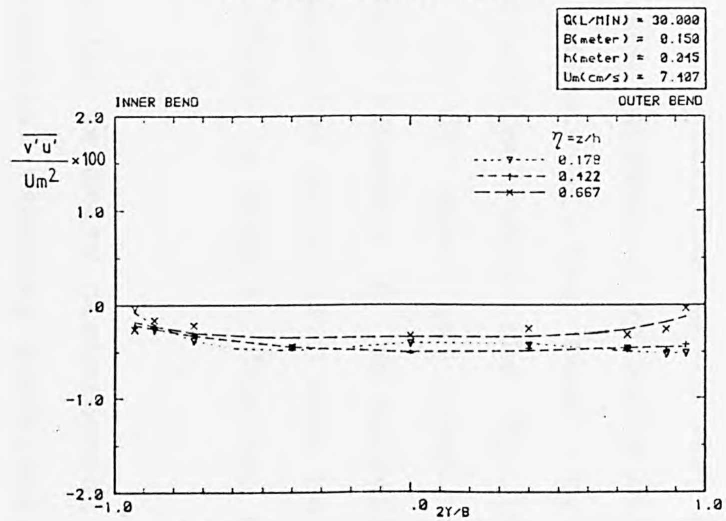

b). Reynolds Shear Stress Formed by Tangential and Radial Velocity Fluctuations

Fig. 6.154 Reynolds shear stress at section S-7, run no.2

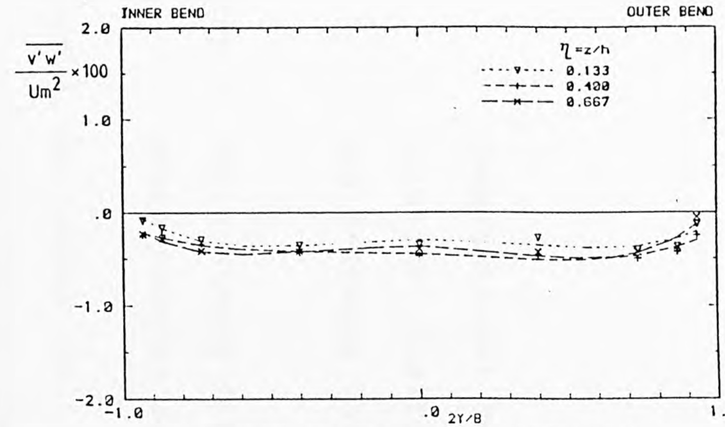

a). Reynolds Shear Stress Formed by Tangential and Vertical Velocity Fluctuations

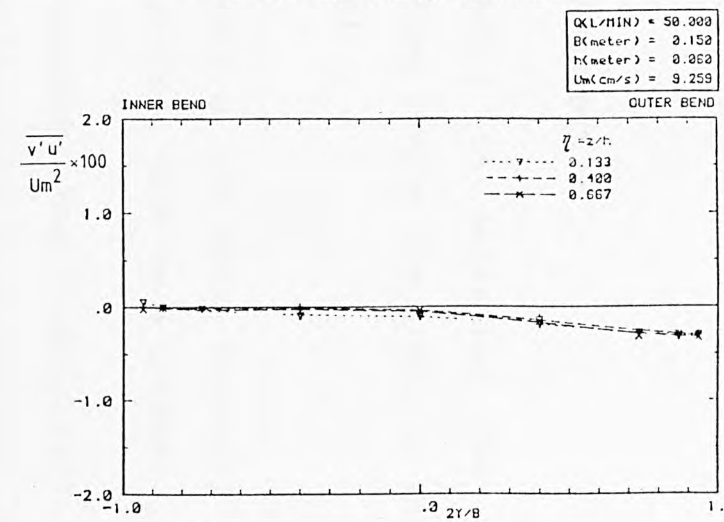

b). Reynolds Shear Stress Formed by Tangential and Radial Velocity Fluctuations

Fig. 6.155 Reynolds shear stress at section S-7, run no.3

APPENDIX 1

Computational Procedure to determine the tangential velocity distribution across the width in the U-shaped and S-shaped channel

Step 1. For a steady flow rate Q, the mean velocity over the cross section is obtained from Um = Q/(BxH).

Step 2. In order to determine the tangential velocity distribution across the width in a straight channel, an appropriate value of Umax in Eq. (2.16) must be found. The mean velocity Um is then calculated by computing the area under the curve of the velocity distribution, and this must be equal to the value of Um defined in step 1. This can be done by iteration.

Step 3. The tangential velocity distribution in step 2 is then used to determined the tangential velocity distribution in the entrance region of the bend by solving Eq. (2.21) in conjunction with the Eq. (2.22). An appropriate value of C2 must be found to solve Eq. (2.21), and the flowrate Q is calculated using Eq. (2.22). The calculated value of Q must be equal to the value of Q given in step 1. This can be done by iteration.

Step 4. By using the tangential velocity distribution obtained in step 3, the tangential velocity distribution within the bend at the first increment $\partial\theta$ is calculated by solving Eq. (2.23.a) in conjunction with Eq. (2.23.b). An appropriate value of I must be found to solve the Eq. (2.23.a), then the flow rate Q is calculated by solving Eq. (2.23.b). The calculated value of Q must be equal to the value of Q given in step 1. This can again be achieved by iteration.

Similar procedure is continued to calculate the tangential velocity distribution within the bend for the next increment $\partial\theta$, and so on. It must be noted that the sign convention of $\partial\theta$ must be changed when the flow enters downstream bend of the S-shaped channel.

Step 5. Finally, the tangential velocity distribution at the exit region of the bend can be obtained by solving Eq. (2.24) in conjunction with Eq. (2.25). The tangential velocity distribution within the bend near to the exit region obtained from step 4 and the appropriate value of C2 are used to solve the Eq. (2.24), the the flow rate Q is calculated by solving the Eq. (2.25). The calculated value of Q must again be equal to the value of Q given in step 1. This is also done by iteration.

The Newton-Raphson method of iteration is used in the above five steps and the rate of convergence is found to be satisfactory.

Computer programs
(Appendices 2-8, pp. 304-321)
have been deleted for
copyright reasons

APPENDIX 2

Program 'MFAD1'

A computer program to determine the main flow distribution across the width of a rectangular U-shaped and S-shaped channels using the method of Finite Difference

APPENDIX 3

Program 'DECGROW'

A computer program to solve the growth of transverse circulation within the bend and the decay of transverse circulation beyond the bend of a channel

APPENDIX 4

Program 'UROZO'

A computer program to solve the radial velocity distribution according to Eq. (2.16)

APPENDIX 5

Program 'UROZ1'

A computer program to solve the radial velocity distribution according to Eq. (4.1)

APPENDIX 6

Program 'UROZ2'

A computer program to solve the radial velocity distribution according to Eq. (4.5)

APPENDIX 7

Program 'UBOUW'

A computer program to solve the radial velocity distribution according to Eq. (4.6)

APPENDIX 8

Program 'UKEN'

A computer program to solve the radial velocity distribution according to Eq. (4.9)

APPENDIX 9

Paper presented at the 21st IAHR Congress,

August, 1985, Melbourne, Australia

"Velocity Distribution Across the Width of a Rectangular Open Channel as Revealed by the Laser Doppler Anemometer"

APPENDIX 9 (pp. 323-326)
Paper presented at the 21st IAHR Congress, August, 1985, Melbourne, Australia
"Velocity Distribution Across the Width of a Rectangular Open Channel as Revealed by the Laser Doppler Anemometer"
has been deleted for copyright reasons